Funktion und Evolution pflanzlicher B-Chromosomen

Habilitationsschrift
zur Erlangung des akademischen Grades
doctor agriculturarum habilitatus
(Dr. agr. habil.)

verteidigt am 14.12.2009 an der
Naturwissenschaftlichen Fakultät III
der Martin-Luther-Universität Halle-Wittenberg

von
Dr. agr. Andreas Houben
geb. am 06.05.1963 in Magdeburg

Gutachter:
Prof. Dr. Klaus Pillen (Martin-Luther Universität Halle-Wittenber)
Prof. Dr. Thomas Schmidt (Technische Universität Dresden)
Prof. Dr. Christian Jung (Christian-Albrechts-Universität zu Kiel)

Dekan der Naturwissenschaftlichen Fakultät III
Prof. Dr. Peter Wycisk

Inhaltsverzeichnis

Abkürzungsverzeichnis

bp	Basenpaar
Bs	B-Chromosomen
2C	DNA-Gehalt des diploiden, unreplizierten Chromosomensatzes
DAPI	4’,6’-Diamidino-2-Phenylindol
FISH	Fluoreszenz-*in-situ*-Hybridisierung
G1	Zellzyklusphase G1
G2	Zellzyklusphase G2
ITS2	Internal-Transcribed-Spacer 2
K4	Lysin 4
K9	Lysin 9
K20	Lysin 20
K27	Lysin 27
H3	Histon H3
H4	Histon H4
mB	Mikro-B-Chromosomen
Mbp	Megabasenpaare
me	methyliert
me1	monomethyliert
me2	dimethyliert
me3	trimethyliert
nB	Standard-B-Chromosomen
NOR	Nukleolusorganisatorregion
rDNA	ribosomale DNA
rRNA	ribosomale RNA
PCR	Polymerase-Kettenreaktion
ph	Phorphorylierung
RT-PCR	Reverse-Transcriptase-PCR
S10	Serin 10
S28	Serin 28
T3	Threonin 3,
T11	Threonin 11
T32	Threonin 32

1. Einleitung und Fragestellung

Chromosomen portionieren das Genom und ermöglichen die korrekte Weitergabe der Zellkern-lokalisierten Erbinformation. Die Genomgröße und Anzahl der Chromosomen innerhalb einer Spezies sind weitgehend konstant. Häufig ist aber die Artenevolution mit einer numerischen und strukturellen Karyotypveränderung verbunden, wodurch sich die Genomgröße und Anzahl von Chromosomen einzelner Individuen einer Art unterscheiden kann.

Eine Vielzahl von pflanzlichen und tierischen Arten besitzen neben den normalen Standardchromosomen oder auch A-Chromosomen genannt, überzählige sogenannte B-Chromosomen. Diese Zusatzchromosomen unterscheiden sich von den A-Chromosomen dadurch, dass diese keine essentiellen Erbinformationen besitzen, ein nicht-mendelndes Segregationsverhalten zeigen und auch nicht mit den A-Chromosomen während der Meiose paaren (Jones and Rees, 1982; Jones, 1991a; Jones and Puertas, 1993; Beukeboom, 1994; Jones, 1993; Bougourd and Jones, 1997; Covert, 1998; Camacho et al., 2000; Puertas, 2002; Jones et al., 2008). Sie treten gewöhnlich nur in einigen Individuen einer Art auf (Jones, 2004). Außerdem kann ihre Anzahl innerhalb und zwischen Individuen variieren. B-Chromosomen können extrem hohe Zahlen in natürlichen Populationen erreichen, abhängig davon, wie viele zusätzliche Chromosomen eine bestimmte Art tolerieren kann (Camacho et al., 2000). Durch diese unikalen Eigenschaften kann sich die Evolution beider Chromosomentypen unterscheiden. Da in der überwiegenden Mehrzahl die Gegenwart von B-Chromosomen, vor allem in höherer Kopienzahl, sich negativ auf die Vitalität und Fruchtbarkeit des Trägerorganismus auswirken kann, werden B-Chromosomen oftmals als parasitäre Bestandteile des Genoms eingestuft.

Die Verteilung von B-Chromosomen innerhalb der Angiospermen ist nicht zufällig. Fremdbefruchtende Arten mit großen Genomen und wenigen Chromosomen besitzen bevorzugt diesen Chromosomentyp. Die Auswertung der B-Chromosomen-Verteilung zeigte auch, dass B-Chromosomen gleich oft in polyploiden und diploiden Arten auftreten (Palestis et al., 2004; Trivers et al., 2004; Levin et al., 2005). Die positive Korrelation zwischen Genomgröße und der Gegenwart von B-Chromosomen kann evtl. dadurch erklärt werden, dass großgenomige Arten

zusätzliche Chromosomen leichter tolerieren können (Puertas, 2002) oder, da das Genom großgenomiger Arten hauptsächlich aus nicht-kodierender DNA besteht, diese Genomkomponente die Formierung von B-Chromosomen unterstützt (Levin et al., 2005). Die Auswertung von 23.652 Angiospermen (rund 9% der geschätzten 260.000 Arten) zeigte, dass zirka 8% der Monokotyledonen und 3% der Eudicots Träger von B-Chromosomen sind. In den besonders artenreichen Poaceae und Asteraceae wurden am häufigsten Zusatzchromosomen nachgewiesen. Dagegen besitzen Liliales und Commelinales besonders viele Arten mit B-Chromosomen (Palestis et al., 2004; Levin et al., 2005).

Obwohl seit der Erstbeschreibung von B-Chromosomen durch Wilson (1907) die rätselhaften Eigenschaften dieser Genomkomponente das Interesse einer Vielzahl von Forschern geweckt haben, sind noch viele Fragen zur Evolution und Funktionsweise von B-Chromosomen unbeantwortet. Insgesamt liegen dieser Habilitationsarbeit 20 Originalarbeiten zugrunde.

Ziel meiner Arbeit war es:
(A) den Ursprung und die Evolution von B-Chromosomen zu erkunden;

(B) die Chromatinzusammensetzung von A- und B-Chromosomen zu vergleichen und chromosomale Verteilung von Eu- und Heterochromatin-typischen Histonveränderungen zu bestimmen.

(C) B-Chromosomen zur Funktionsbestimmung von Zellzyklus-abhängigen Histon H3 Phosphorylierungen einzusetzen.

(D) die Transkriptionsaktivität, der sogenannten „genetisch inaktiven“ B-Chromosomen erstmals molekulargenetisch zu charakterisieren.

(E) *Brachycome dichromosomatica* als Modellart für die Analyse von B-Chromosomen zu etablieren.

Zur Bearbeitung der aufgelisteten Themen wurden von mir bevorzugt B-Chromosomen des Roggens (*Secale cereale* L., 2n= 14 +0-8 Bs), der Australischen

Gänseblume (*Brachycome dichromosomatica*, Synonym: *Brachyscome dichromosomatica,* 2n= 4 +0-3 Standard Bs + 0-9 Mikro Bs), der Puschkinie (*Puschkinia libanotica,* 2n= ? + 0-7 Bs), und des Kleinköpfigen Pippau (*Crepis capillaris,* 2n= 6 +0-4 Bs) experimentell untersucht.

Die B-Chromosomen des Roggens wurden untersucht, da bereits viele Vorarbeiten an diesen Chromosomen durchgeführt worden waren (Jones und Puertas, 1993) und somit die DNA-Zusammensetzung der Roggen Bs teilweise bekannt war. Aufgrund der geringen A-Chromosomenanzahl (2n = 4) und der Existenz von zwei B-Chromosomentypen war *B. dichromosomatica* prädestiniert, um die Evolution, DNA und Chromatinzusammensetzung von Bs zu erkunden. *C. capillaris* wurde ausgewählt, da diese Art B-lokalisierte rDNA Sequenzen besitzt, welche zur Analyse der Transkription und Phylogenie von B-Chromosomen geeignet sind.

2. Eigene Arbeiten (A1-A20)

A1 Carchilan, M., Delgado, M., Ribeiro, T., Costa-Nunes, P., Caperta, A., Morais-Cecilio, L., Jones, R.N., Viegas, W., and Houben, A. (2007). Transcriptionally active heterochromatin in rye B chromosomes. Plant Cell 19, 1738-1749.

A2 Cohen, S., Houben, A., and Segal, D. (2008). Extrachromosomal circular DNA derived from tandemly repeated genomic sequences in plants. Plant Journal 53, 1027-1034.

A3 Gernand, D., Demidov, D., and Houben, A. (2003). The temporal and spatial pattern of histone H3 phosphorylation at serine 28 and serine 10 is similar in plants but differs between mono- and polycentric chromosomes. Cytogenet Genome Res 101, 172-176.

A4 Gernand, D., Rutten, T., Varshney, A., Rubtsova, M., Prodanovic, S., Bruss, C., Kumlehn, J., Matzk, F., and Houben, A. (2005). Uniparental chromosome elimination at mitosis and interphase in wheat and pearl millet crosses involves micronucleus formation, progressive heterochromatinization, and DNA fragmentation. Plant Cell 17, 2431-2438.

A5 Houben, A., and Schubert, I. (2007). Engineered plant minichromosomes: a resurrection of B chromosomes? Plant Cell 19, 2323-2327.

A6 Houben, A., Demidov, D., Caperta, A.D., Karimi, R., Agueci, F., and Vlasenko, L. (2007). Phosphorylation of histone H3 in plants - A dynamic affair. Biochim Biophys Acta.

A7 Houben, A., Demidov, D., Rutten, T., and Scheidtmann, K.H. (2005). Novel phosphorylation of histone H3 at threonine 11 that temporally correlates with condensation of mitotic and meiotic chromosomes in plant cells. Cytogenet Genome Res 109, 148-155.

A8 Houben, A., Demidov, D., Gernand, D., Meister, A., Leach, C.R., and Schubert, I. (2003). Methylation of histone H3 in euchromatin of plant chromosomes depends on basic nuclear DNA content. Plant Journal 33, 967-973.

A9 Houben, A., Verlin, D., Leach, C.R., and Timmis, J.N. (2001). The genomic complexity of micro B chromosomes of *Brachycome dichromosomatica*. Chromosoma 110, 451-459.

A10 Houben, A., Wanner, G., Hanson, L., Verlin, D., Leach, C.R., and Timmis, J.N. (2000). Cloning and characterisation of polymorphic heterochromatic segments of *Brachycome dichromosomatica*. Chromosoma 109, 433-433.

A11 Houben, A., Thompson, N., Ahne, R., Leach, C.R., Verlin, D., and Timmis, J.N. (1999). A monophyletic origin of the B chromosomes of *Brachycome dichromosomatica* (Asteraceae). Plant Syst Evol 219, 127-135.

A12 Houben, A., Belyaev, N.D., Leach, C.R., and Timmis, J.N. (1997a). Differences of histone H4 acetylation and replication timing between A and B chromosomes of *Brachycome dichromosomatica*. Chromosome Res 5, 233-237.

A13 Houben, A., Leach, C.R., Verlin, D., Rofe, R., and Timmis, J.N. (1997b). A repetitive DNA sequence common to the different B chromosomes of the genus *Brachycome*. Chromosoma 106, 513-519.

A14 Houben, A., Kynast, R.G., Heim, U., Hermann, H., Jones, R.N., and Forster, J.W. (1996). Molecular cytogenetic characterisation of the terminal heterochromatic segment of the B-chromosome of rye (*Secale cereale*). Chromosoma 105, 97-103.

A15 Jones, N., and Houben, A. (2003). B chromosomes in plants: escapees from the A chromosome genome? Trends Plant Sci 8, 417-423.

A16 Kumke, K., Jones, R.N., and Houben, A. (2008). B chromosomes of *Puschkinia libanotica* are characterized by a reduced level of euchromatic histone H3 methylation marks. Cytogenet Genome Res 121, 266-270.

A17 Leach, C.R., Houben, A., Field, B., Pistrick, K., Demidov, D., Timmis, J.N. (2005). Molecular evidence for transcription of genes on a B chromosome in *Crepis capillaris*. Genetics 171, 269-278.

A18 Manzanero, S., Arana, P., Puertas, M.J., and Houben, A. (2000). The chromosomal distribution of phosphorylated histone H3 differs between plants and animals at meiosis. Chromosoma 109, 308-317.

A19 Marschner, S., Kumke, K., and Houben, A. (2007a). B chromosomes of *B. dichromosomatica* show a reduced level of euchromatic histone H3 methylation marks. Chromosome Res 15, 215-222.

A20 Marschner, S., Meister, A., Blattner, F.R., and Houben, A. (2007b). Evolution and function of B chromosome 45S rDNA sequences in *Brachycome dichromosomatica*. Genome 50, 638-644.

A1 Carchilan, M., Delgado, M., Ribeiro, T., Costa-Nunes, P., Caperta, A., Morais-Cecilio, L., Jones, R.N., Viegas, W., and Houben, A. (2007). Transcriptionally active heterochromatin in rye B chromosomes. Plant Cell 19, 1738-1749.

This article is published in *The Plant Cell* Online, *The Plant Cell* Preview Section, which publishes manuscripts accepted for publication after they have been edited and the authors have corrected proofs, but before the final, complete issue is published online. Early posting of articles reduces normal time to publication by several weeks.

Transcriptionally Active Heterochromatin in Rye B Chromosomes [W]

Mariana Carchilan,[a,1] Margarida Delgado,[b,1] Teresa Ribeiro,[b] Pedro Costa-Nunes,[b] Ana Caperta,[b] Leonor Morais-Cecílio,[b] R. Neil Jones,[c] Wanda Viegas,[b] and Andreas Houben[a,2]

[a] Leibniz Institute of Plant Genetics and Crop Plant Research, 06466 Gatersleben, Germany
[b] Secção de Genética, Centro de Botânica Aplicada à Agricultura, Instituto Superior de Agronomia, Technical University of Lisbon, Tapada da Ajuda, 1349-017 Lisboa, Portugal
[c] Institute of Biological Sciences, University of Wales, Aberystwyth SY23 3DD, Wales, United Kingdom

B chromosomes (Bs) are dispensable components of the genomes of numerous species. Thus far, there is a lack of evidence for any transcripts of Bs in plants, with the exception of some rDNA sequences. Here, we show that the Giemsa banding-positive heterochromatic subterminal domain of rye (*Secale cereale*) Bs undergoes decondensation during interphase. Contrary to the heterochromatic regions of A chromosomes, this domain is simultaneously marked by trimethylated H3K4 and by trimethylated H3K27, an unusual combination of apparently conflicting histone modifications. Notably, both types of B-specific high copy repeat families (E3900 and D1100) of the subterminal domain are transcriptionally active, although with different tissue type–dependent activity. No small RNAs were detected specifically for the presence of Bs. The lack of any significant open reading frame and the highly heterogeneous size of mainly polyadenylated transcripts indicate that the noncoding RNA may function as structural or catalytic RNA.

INTRODUCTION

B chromosomes (Bs) are dispensable components of the genomes of numerous species of both plants and animals. They do not pair with any of the standard A chromosomes at meiosis, by definition, and have irregular modes of inheritance (reviewed in Jones and Houben, 2003). In rye (*Secale cereale*), there is a widespread polymorphism for Bs across all geographic regions where this species grows as wild or semiwild populations (Jones and Puertas, 1993), and the Bs are structurally identical at the cytological level among geographically distinct populations. The absence of Bs from some individuals, by definition, and their presence in variable numbers in others provide a unique experimental system to investigate their apparent genetic emptiness. A unique feature of the rye B is that it undergoes a directed nondisjunction at both the first pollen grain and first egg cell mitosis, based on sticking of sensitive sites on either side of the centromere, which delay separation of sister chromatids, and then directs them into the cells destined to become gametes. The accumulation process is controlled by a *trans*-acting genetic element located in the distal part of the long arm of the B chromosome. This is known because deficient Bs, which lack this terminal region of the long arm, undergo normal disjunction, unless a standard form of the B chromosome is present in the same cell. Numerical accumulation is counterbalanced by loss of unpaired Bs at meiosis and by the deleterious effects of the Bs on physiological and reproductive fitness (Jones, 1995).

This particular aspect of the transmission of the rye B has triggered a number of investigations aiming to identify and isolate the genetic element controlling nondisjunction in gametophytes, but thus far no nondisjunction element has been identified (Langdon et al., 2000).

In terms of structural organization, the rye B is mainly composed of DNA sequences in common with those of the A chromosomes (As) (Rimpau and Flavell, 1975; Timmis et al., 1975), with the exception of the terminal part of the long arm (Tsujimoto and Niwa, 1992; Wilkes et al., 1995; Houben et al., 1996). Two B-specific families of high-copy repetitive DNA, D1100 (Sandery et al., 1990) and E3900 (Blunden et al., 1993), have been isolated and mapped to this terminal domain. Both families are organized in a complex manner, and neither represents a simple monotonous array of tandem repeats (Langdon et al., 2000). In situ hybridization shows that at c-metaphase the D1100 displays two adjacent clusters with a small gap between them, with the more homogeneous E3900 positioned toward the telomere (Wilkes et al., 1995; Langdon et al., 2000). This B-specific domain is characterized as the B heterochromatic block, which replicates late in S phase and also corresponds to the most prominent and conserved Giemsa-banding positive band discriminated by 4′,6-diamidino-2-phenylindole (DAPI) staining at metaphase (Jones and Puertas, 1993; Houben et al., 1996; Langdon et al., 2000) (Figure 1A). Thus far, there is a lack of evidence for any active genes in the Bs of rye, or of maize (*Zea mays*) or other plants, with the exception of some rDNA sequences of *Crepis capillaris* (Leach et al., 2005).

[1] These authors contributed equally to this work.
[2] To whom correspondence should be addressed. E-mail houben@ipk-gatersleben.de; fax 49-39482-5137.
The author responsible for distribution of materials integral to the findings presented in this article in accordance with the policy described in the Instructions for Authors (www.plantcell.org) is: Andreas Houben (houben@ipk-gatersleben.de).
[W] Online version contains Web-only data.
www.plantcell.org/cgi/doi/10.1105/tpc.106.046946

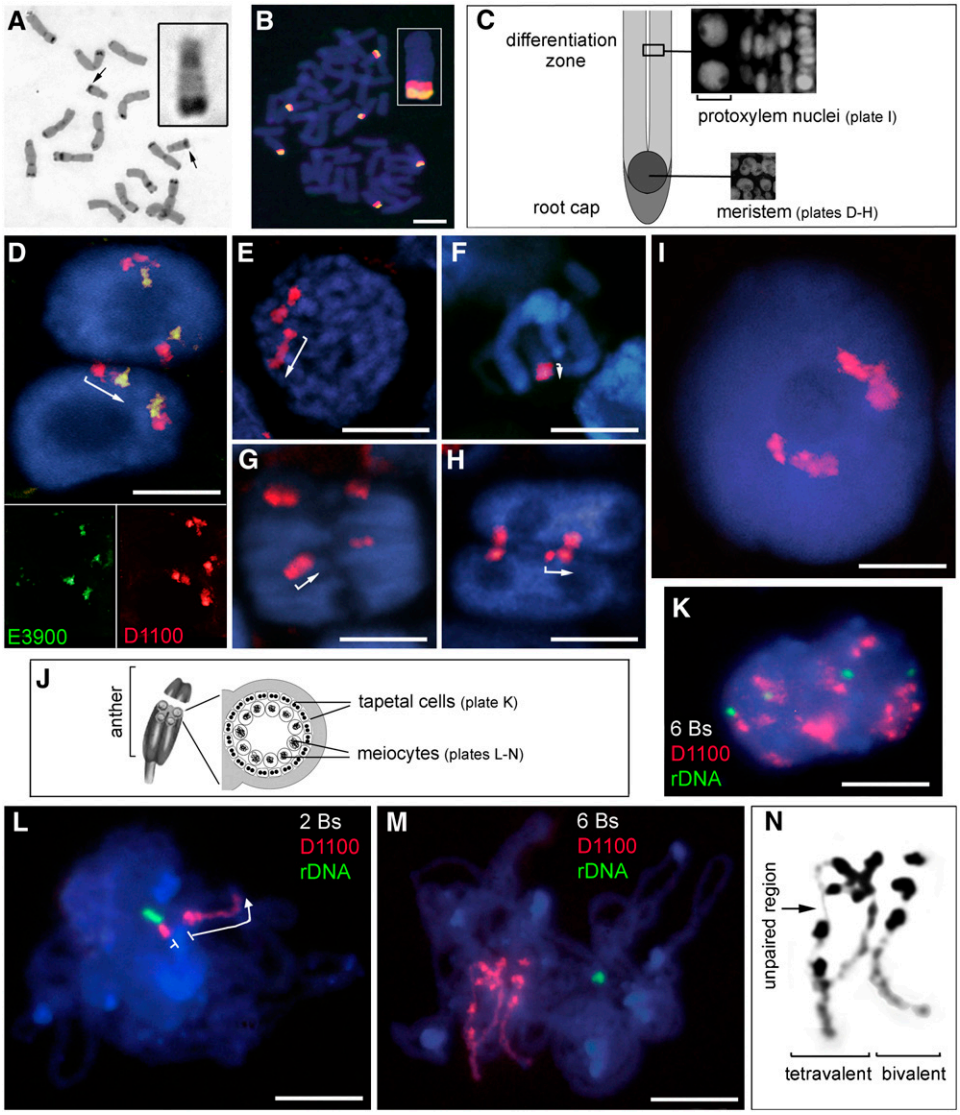

Figure 1. Cytological Organization of the B-Specific Domain during Development.

(A) Giemsa C-banded metaphase chromosomes of rye with Bs (arrows and inset).
(B) Root tip meristematic c-metaphase cell of Lindström wheat with six Bs hybridized with D1100 (red) and E3900 (green) probes. At this stage, the D1100 terminal domain displays a high level of condensation, and the B-specific domain is defined as two contiguous blocks (one centromere-proximal and the other distal); E3900 labels only the distal block (yellow signal due to superimposition of red and green channels).
(C) Organization of the root tip showing the location of meristematic and protoxylem nuclei.
(D) and **(E)** Heterogeneous organization of the B-specific domain defined by D1100 (red), showing condensed and diffuse regions in 2B meristematic cells. The start of the arrow indicates the start of the B domain, and the end of the arrow indicates the telomeric end of the domain.
(D) Two interphase nuclei hybridized with D1100 and E3900 (green; yellow signal is due to superimposition with D1100 red signal). An unlabeled gap frequently separates the condensed and decondensed regions. The bottom of the figure shows the single channel images of the same nuclei for E3900 (left) and D1100 (right).
(E) to **(H)** B-specific domain during mitoses in meristematic cells with two Bs: **(E)** at prophase, **(F)** at metaphase showing the B-specific domain fully condensed (only one B is visible), **(G)** at anaphase, and **(H)** at telophase (only one of the Bs is visible over its full length due to the orientation of projection).
(I) D1100 pattern in a nucleus from a developing xylem cell (see **[C]** for location of cell type).
(J) to **(N)** organization of the B-specific domain in anther tissues: **(J)** location of meiocytes and tapetal cells, **(K)** binucleate tapetal nuclei, **(L)** and **(M)** pachytene nuclei with two Bs fully paired **(L)** and six Bs with irregular pairing **(M)**. The curved arrow in **(L)** indicates the full length of B-specific domain, and the intercalary cut shows the extended gap in D1100 labeling. **(N)** shows the magnification of the B-specific domain from the six B pachytene cells in **(M)**, showing two fully paired Bs forming a bivalent (right) and four Bs with irregular pairing forming a tetravalent. DAPI staining for DNA is in blue. Bars = 10 μm.

Heterochromatin was first defined cytologically by Heitz (1928) as the genome fraction that maintains a high level of condensation throughout the cell cycle. It was later associated with genome regions that replicate late in the S phase and are mainly composed of repetitive DNA sequences with low gene density. More recent advances in chromatin characterization, in terms of epigenetic marks, showed the involvement of DNA methylation and posttranslational histone modifications (reviewed in Richards and Elgin, 2002; Craig, 2005; Kouzarides, 2007). Although there has been great progress in the discovery of several residue-specific histone methylations and other histone modifiers involved in chromatin packaging (reviewed in Martin and Zhang, 2005), methylation of histone H3 at Lys residues 4, 9, and 27 has become the best studied. Whereas the euchromatin-specific methylation of H3K4 is highly conserved among eukaryotes, heterochromatin indexing by methylation marks at H3K9/27 and H4K20 is more variable (Fuchs et al., 2006). Several studies have shown that modification of the histone H3 tail by methylation of Lys residues 9 (H3K9me) and 27 (H3K27me) negatively regulate transcription by promoting a compact chromatin structure (Bannister et al., 2001; Jacobs et al., 2001; Cao et al., 2002; Czermin et al., 2002; Francis et al., 2004). By contrast, euchromatin is marked by the same type of modification at Lys residue 4 (H3K4me) (Noma et al., 2001; Santos-Rosa et al., 2002; Zegerman et al., 2002). The identification of a H3K4-specific histone demethylase (Shi et al., 2004) challenged the view that histone methylations are permanent and nonreversible.

In this study, through in situ localization of rye B-specific repetitive DNA families D1100 and E3900, we disclose that the B heterochromatic domain is consistently decondensed at interphase in two distinct genomic backgrounds of rye and also in a wheat (*Triticum aestivum*)–rye B addition line. Furthermore, we show that this chromatin conformation is maintained in different cell types, namely meristematic, differentiated, and meiocytes. Immunodetection of epigenetic marks revealed that the atypical behavior of this B-specific heterochromatic domain is accompanied by enrichment in the euchromatic mark H3K4me3, but no distinctive features were obtained for the heterochromatic marks H3methylK9/K27 and H4K20me or for methylated cytosine residues. In addition, transcriptional activity of the E3900 and D1100 repeats in somatic and meiotic tissue has been demonstrated.

RESULTS

The Heterogeneous Organization of the B-Specific Domain Is Maintained in Different Genomic Environments and Distinct Cell Types

At c-metaphase the B-specific domain is characterized by a condensed Giemsa-banding positive region (Figure 1A, arrows) that corresponds to the location of the two B-specific sequences D1100 and E3900. D1100 occupies the entire domain, and E3900 is restricted to a more terminal position (Figure 1B). In meristematic interphase cells, the organization of the domain, defined by the presence of the D1100 repeat family, was evaluated in both rye and wheat root meristematic cells through confocal microscopy after in situ hybridization, using structurally preserved root tip tissue sections (Figure 1C). The B domain forms a well-defined region displaying a heterogeneous internal organization. There are two distinct regions: one is tightly condensed and the other is more diffuse (Figure 1D), as previously described (Morais-Cecílio et al., 1996; Langdon et al., 2000). Simultaneous labeling with the E3900 repeat reveals that the decondensed D1100 region is the more distal of the two since it colocalizes with the E3900 region, which is subterminal (Figures 1B and 1D). Decondensation in the subterminal part of the domain is observed not only at interphase but also at prophase and to a lesser extent in anaphase and telophase of mitosis, but no decondensation was observed in metaphase (Figures 1E to 1H). A gap in D1100-positive regions (Figure 1D) is frequently observed separating the condensed from the decondensed regions. In untreated metaphases (Figure 1F) the B-terminal domain has a condensed appearance, likewise observed in c-metaphases (Figures 1A and 1B). Although no major differences in the B domain organization were detected between rye and wheat, the level of decondensation of the subterminal region at interphase is higher in rye than in wheat (data not shown) and increases with the number of Bs present (Table 1). The D1100 *Dra*I restriction pattern shows six identical bands, for B-carrying wheat and rye (see Supplemental Figure 1 online), although two additional bands (1.6 and 0.65 kb) were revealed in this analysis that were not seen previously (Sandery et al., 1990). The *Eco*RI restriction pattern for the E3900 sequence in both rye and wheat gave the same results (data not shown) as previously obtained by Blunden et al. (1993) in rye.

To establish whether the decondensed interphase structure of the B-specific domain is a general feature, further cell types were analyzed, such as differentiated root cells and anther cells (meiocytes at pachytene and tapetal cells) (Figures 1C and 1I to 1N).

Structurally preserved sections of roots in the differentiation zone allowed the analysis of two distinct cell types: parenchyma and developing xylem vessel cells. Protoxylem vessels are easily recognized as a central row of large cells due to endoreduplication that occurs as part of the differentiation process, and, as expected, they present enlarged nuclei accompanied by a correspondingly extended D1100 domain (Figures 1C and 1I). In these endopolyploid cells, as in parenchyma (data not shown), the same basic organization of the B-specific domain is maintained, with a condensed region in the centromere proximal end and a pronounced decondensation toward the telomeric end. In anther cells (Figures 1J to 1N), the level of decondensation is

Table 1. Average Length (μm) of D1100- and E3900-Labeled Regions in Interphase Nuclei from JNK Rye Plants with 2Bs or 4Bs

Domain	2Bs	4Bs	*t* Test[a]
D1100	2.37	3.53	P = 0.0026
E3900	1.30	1.66	P = 0.0030

The measurements were performed in the longitudinal axis of the B-specific domain defined by the centromere proximal condensed D1100 block and by the distal region labeled by both D1100 and E3900. Mean values were obtained from at least 30 nuclei from three different plants.

[a] P is the probability associated with a two-tailed Student's *t* test.

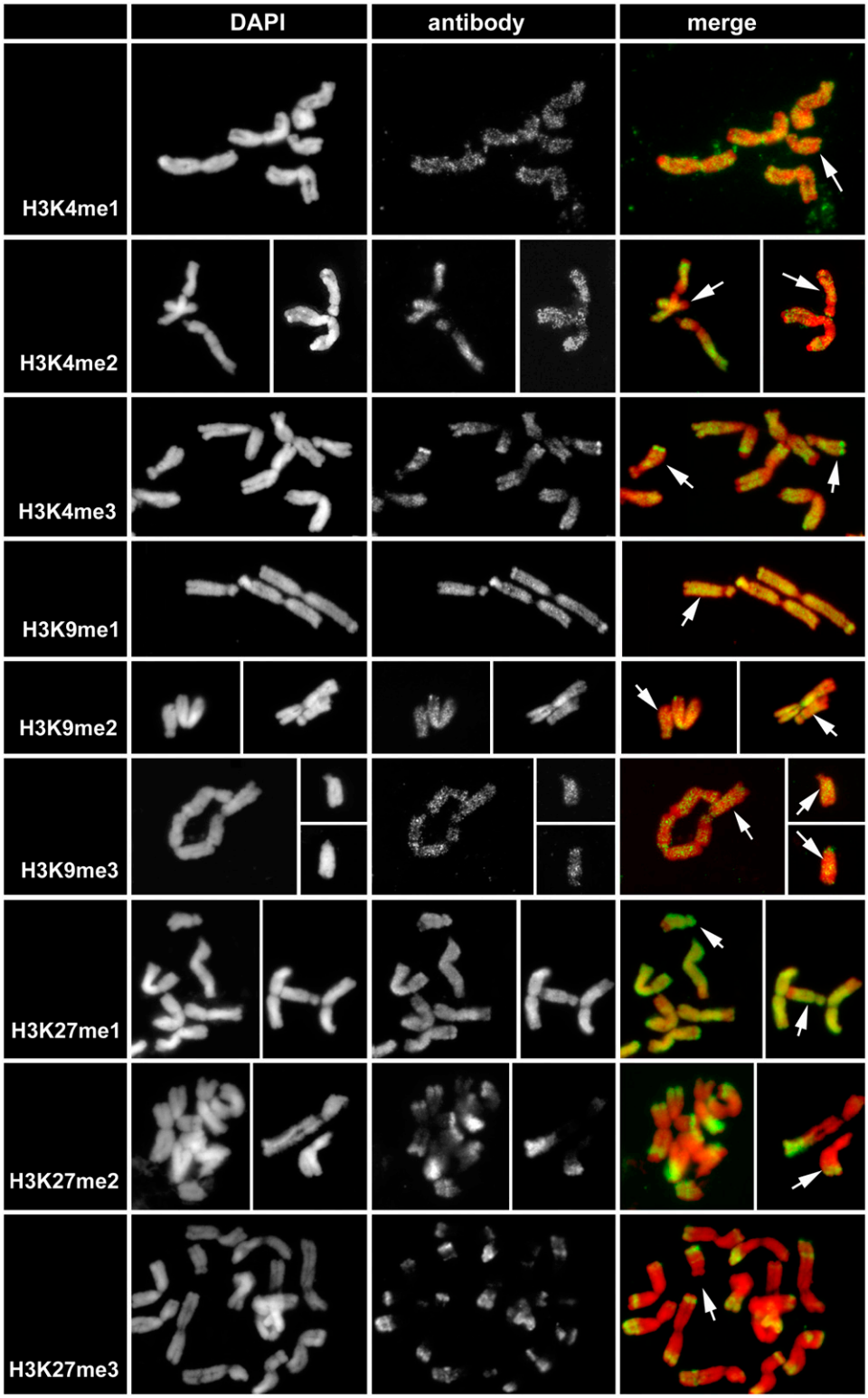

Figure 2. Histone Marks of As and Bs.

Metaphase cells of rye with Bs (arrows) after immunostaining with antibodies specific for H3K4me1,2,3; H3K9me1,2,3; and H3K27me1,2,3.

greatly increased. In binucleated tapetal cells (Figure 1K), the distal region of the domain assumes a cloudy appearance. At pachytene, the D1100 domain is particularly extended, although a more condensed zone toward the centromere is still recognized (Figures 1L to 1N). In this cell type, however, the decondensed distal region is particularly extensive relative to the condensed proximal block, which was always detected and usually far apart from the rest of the domain, leaving a very pronounced gap (Figure 1L). This high level of decondensation contrasts with strong condensation observed in the 45S rDNA cluster visualized as a single block due to chromosome pairing. The pairing pattern of the B-specific region varies with B number: in most 2B meiocytes, only one D1100 domain was observed, indicating close association of these domains (Figure 1L). Conversely, a more complex arrangement was detected in 6B meiocytes (Figures 1M and 1N). Although the structural organization of the B-specific domain is maintained, various configurations were detected with both incomplete pairing and multivalent formation (Figure 1N). The more decondensed organization of the B-specific domain is, however, a generalized feature of meiocytes, and it is not directly related with levels of chromosome pairing since it is observed both in cells with regular or abnormal paring at this region.

The B-Specific Domain Has a Unique Distribution of Histone H3 Trimethylated at Lys Residues 4 and 27

As the B-specific heterochromatic domain undergoes a cell cycle–dependent decondensation process, we characterized its structure in terms of epigenetic marks by examining the methylation status of certain Lys residues in the N-terminal tails of histones H3 and H4. Cells were stained with antisera that discriminated between mono-, di-, and trimethylated Lys residues (Lys-4, Lys-9, and Lys-27 of H3 and Lys-20 of H4; Figure 2, Table 2).

Table 2. Spatial Relationship of a Variety of Histone H3/H4 and DNA Modifications with the Mitotic Rye B Chromosome

	B-Terminal Domain	B without Terminal Domain
H3K4me1	Dispersed	Dispersed, except pericentromere
H3K4me2	Dispersed	Dispersed, except pericentromere
H3K4me3	Strongly increased	Dispersed, except pericentromere
H3K9me1	Dispersed	Dispersed, except pericentromere
H3K9me2	Dispersed	Dispersed
H3K9me3	Weakly dispersed	Weakly dispersed
H3K27me1	Deficient	Dispersed
H3K27me2	Dispersed	Deficient
H3K27me3	Dispersed	Deficient
H4K20me1	Weakly dispersed	Weakly dispersed
H4K20me2	Weakly dispersed	Weakly dispersed
H4K20me3	Weakly dispersed	Weakly dispersed
DNA methylation	Dispersed	Dispersed

The chromosomal distribution patterns observed for the heterochromatin marks H3K9me1 and 3 were as reported for H3K9me2, which is characteristic for plants with large genomes (Houben et al., 2003), for both As and Bs, with a uniform distribution throughout chromosome arms. While the terminal heterochromatic regions of As and Bs were H3K27me1 deficient, the same chromosomal regions were enriched in di- and trimethylated H3K27. Staining specific for H4K20me1,2,3 resulted in a weak and disperse labeling (see Supplemental Figure 2 online). The distribution pattern of 5-methylcytosine DNA residues showed a punctuated and uniform pattern along both the As and Bs, without any particular sites of accumulation (see Supplemental Figure 3 online). These patterns are independent of the number of Bs present.

The highly conserved euchromatin-specific methylation mark at Lys-4 of H3 revealed a B domain–specific distribution pattern. H3K4me1,2 preferentially mark euchromatin of A and B chromosomes, although the heterochromatic B subterminal domain displays some level of labeling. Immunodetection of histone H3 trimethylated at Lys-4 revealed the same distribution pattern of signals for the As both in rye (Figures 3A and 3B) and wheat (Figures 3C and 3D). There is a higher density of labeling in chromosome arms, a decrease in pericentromeric regions, and an absence of signal in heterochromatin. This is particularly evident in the telomeric heterochromatic blocks of rye As that are brightly stained with DAPI (Figure 3A). Surprisingly, the largest signal of H3K4me3 was seen in the terminal part of the long arm of the Bs. To be more precise, it superimposes with the distal block of the D1100/E3900-positive region that forms the most prominent DAPI-stained region in these chromosomes (Figures 3B and 3G). This immunostaining pattern is dependent on the presence of the B-specific domain, since morphological variants of the B chromosome that lack the terminal part of the long arm do not show any particular enrichment in H3K4me3 (Figure 3G). At interphase, no pronounced H3K4me3 labeling was found, most likely due to decondensation and therefore reduced intensity of immunosignals (Figures 3E and 3F). Alternatively, but less likely, a cell cycle–dependent B domain–specific demethylation of H3K4me3 occurs. This H3K4me3 distribution pattern is identical for plants with different numbers of Bs in rye and wheat.

The E3900 and D1100 B-Specific Repeats Are Transcriptionally Active

The abundance of trimethylated Lys-4 of histone H3 and the decondensed structure at interphase of the B subtelomeric domain prompted us to investigate whether transcriptional activity of this region could be detected. The B-terminal region is mainly composed of arrays of E3900 and D1100 repeats (Langdon et al., 2000), and these were used as probes in an RNA gel blot analysis of total RNAs prepared from plants with and without Bs. As shown in Figure 4A, probe E3900-0N, which covers the entire length of E3900, detected a continuum of transcripts ranging in size from 6.5 to <0.2 kb that were mainly present in plants containing Bs. In addition, bands of 2, 3, and 5 kb were detected over the smear. Weak hybridizing bands in 0B material could be explained by cross-hybridization with homologous transcribed

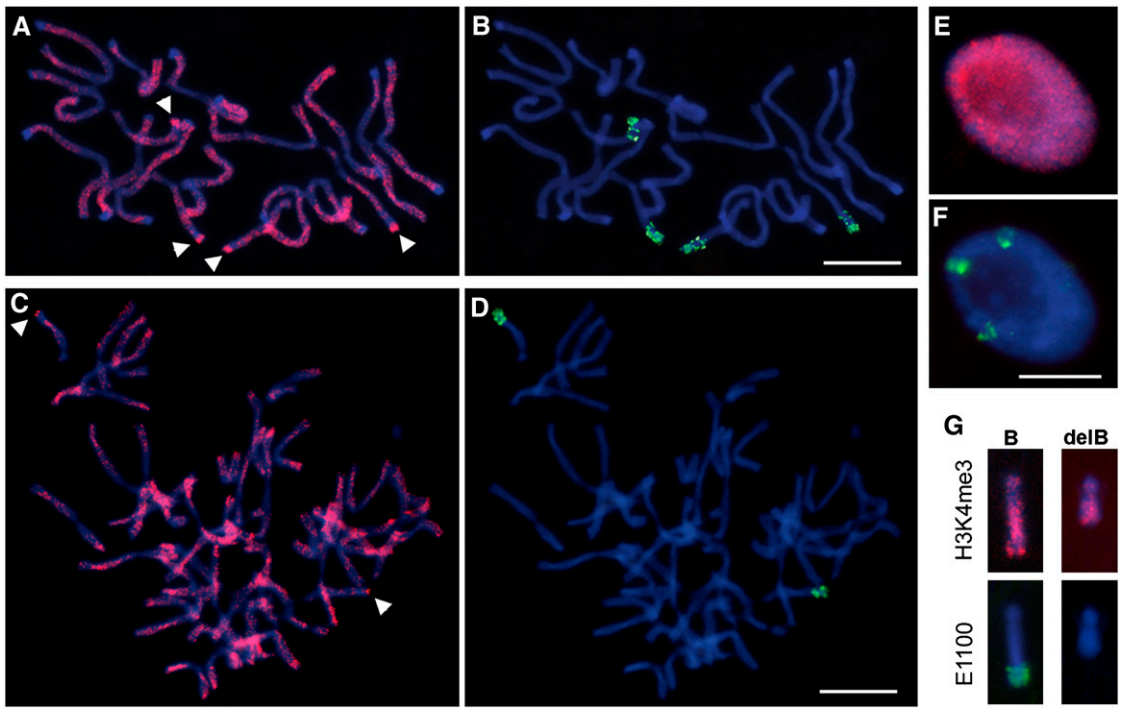

Figure 3. Comparative Analysis of B Variants.

(A) to **(F)** Root tip meristematic metaphase cells of JNK rye (**[A]** and **[B]**) with four Bs (arrowheads) and of Lindström wheat (**[C]** and **[D]**) with two Bs (arrowheads) and an interphase nucleus of JNK rye with three Bs (**[E]** and **[F]**) after immunodetection of H3K4me3 (**[A]**, **[C]**, **[E]** in red) following in situ hybridization with the B-specific D1100 repeat (**[B]**, **[D]**, and **[F]** in green). In **(A)**, note the absence of H3K4me3 in the heterochromatic subtelomeric blocks of rye As. Bars = 10 μm.

(G) Individual standard B and deleted B (delB) after immunodetection of H3K4me3 (red) and in situ hybridization of D1100 (green). DNA is stained with DAPI (blue).

A sequences. To analyze whether the entire E3900 repeat is transcriptionally active in total, or only parts of it, five subregions of E3900 were used as RNA gel blot probes. All regions revealed cross-hybridization with RNAs of small size (<200 bases; Figure 4A, arrows) derived from anthers with Bs, with the highest level of transcription at the end of the 3900 repeat (region 5N). Weak hybridizing bands in 0B material could be explained by cross-hybridization of short microsatellite sequences located within the 3′-region of E3900 (region 5N) (Langdon et al., 2000). Anther- and B-specific hybridization of small size transcripts were also found for D1100 (Figure 4B, arrow).

Therefore, to further characterize the transcribed sequences, RT-PCR experiments were conducted on total RNA isolated from roots, leaves, and anthers of 0B and +B rye and wheat Lindström plants. E3900 transcripts were amplified from all subregions of the repeat (Figure 5A). The primer pair D1100-1RT allows the amplification of a D1100-specific fragment of expected size (Figure 5B). In each cDNA sample derived from RNA of B-containing plants, a product of the expected size, which was not present in any sample derived from the RNA of plants lacking Bs, was amplified. As indicated by RNA gel blot hybridization (Figure 4), there were differences in yield in many cases, mostly showing a higher abundance of B transcripts in anthers rather than in roots and leaves.

As control, RT-PCR with primers specific for the elongation factor eEF1-α showed a comparable yield in all three tissues, and the differences were not due to unequal RNA loading. Notably, although the same number of PCR cycles were used to amplify the different E3900 subregions, as was demonstrated by RNA gel blot hybridization (Figure 4), regions RT4 to RT6 revealed the highest level of transcription with less tissue type specificity.

Control experiments (Figure 5C) with RNA of all samples without an initial reverse transcription step (lanes -RT) and on genomic template DNA (lane g) confirmed that the PCR products are unequivocally dependent on reverse transcription of RNA molecules originating from transcribed E3900/D1100 repeats on the Bs. This result confirms that the B-located E3900/D1100 repeats are transcribed. Hence, both types of B-specific repeats are transcriptionally active, although with different tissue type–dependent activity.

RT-PCR products amplified from anthers were sequenced. All of the sequences obtained shared a high similarity (92 to 99%) with either D1100 or E3900 repeats (see Supplemental Table 2 online). Both repeat transcripts are at least partly polyadenylated, since all D1100/E3900 RT-PCR products were obtained from cDNA synthesized with poly(dT) primers. In addition, RNA gel blot hybridization of both repeats showed cross-hybridization with fractions enriched for polyadenylated RNA, although the

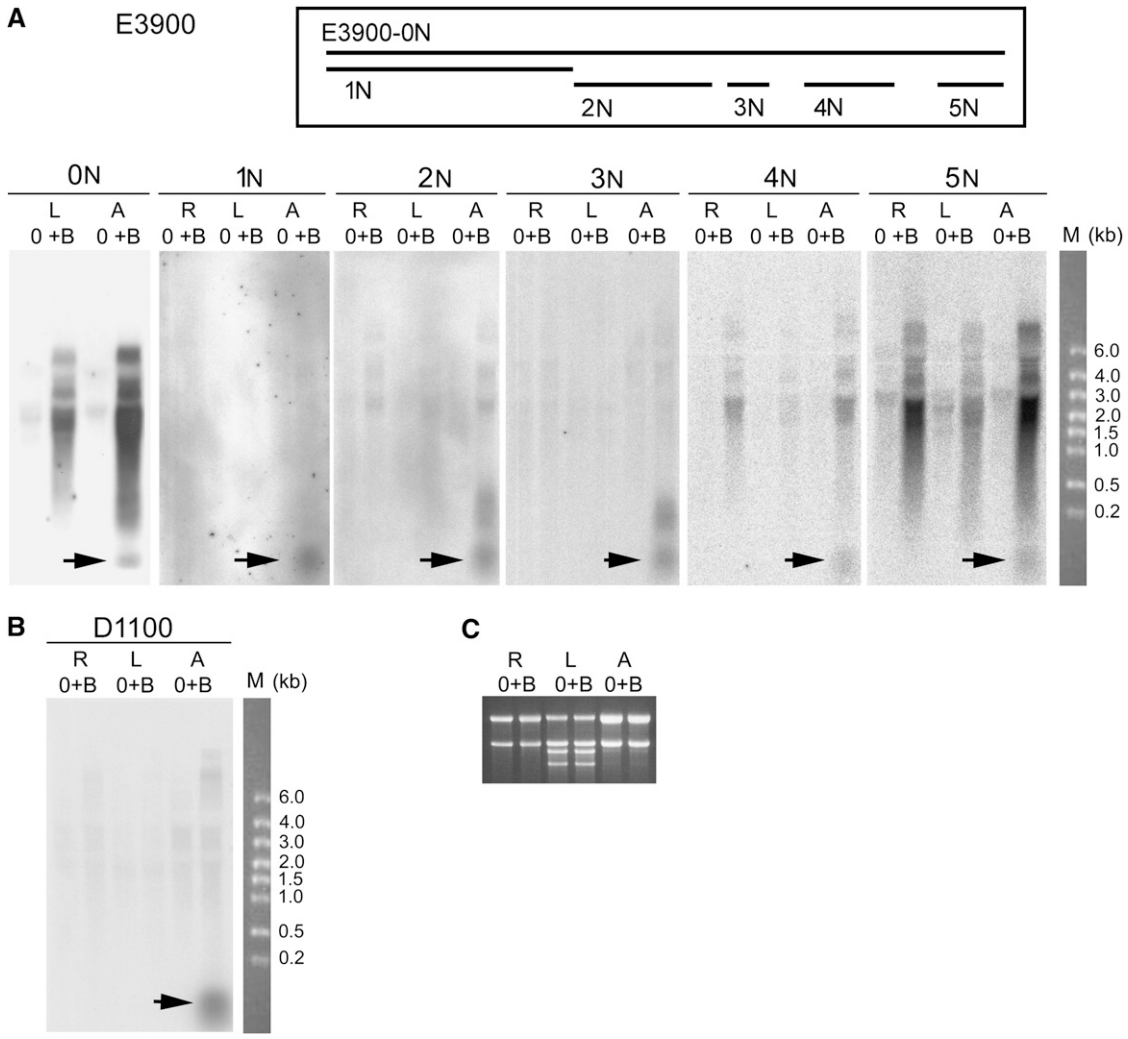

Figure 4. Transcriptional Analysis of E3900 and D1100.

(A) and **(B)** RNA gel blot analysis of E3900 **(A)** and D1100 **(B)** transcripts isolated from roots (R), leaves (L), and anthers (A) of 0B/+B rye. Schemata indicates the different regions (0N to 5N) of E3900 used as hybridization probes. Arrows indicate B-specific signals of small size (<200 bases).
(C) Ethidium bromide–stained RNA gel that was used as a loading control. Size marker is the RiboRuler RNA ladder (Fermentas).

E3900 revealed a significantly stronger signal in the polyadenylated fraction than the D1100 (Figure 6).

To determine whether the D1100 and E3900 transcripts are processed into small RNA (smRNA), we conducted RNA gel blot hybridizations using low molecular weight RNA isolated from anther and leaf tissue of plants with and without Bs. The blots were hybridized with the E3900-specific probe 3N and the cloned RT-PCR product of D1100. Neither probe detected any B-specific smRNAs but gave hybridization signals in the size range of 21 to 24 nucleotides in RNA from anthers, compared with leaves, and independent of the presence or absence of Bs (see Supplemental Figure 4 online). This result implies that the majority of D1100 and E3900 transcripts escaped processing by the RNA interference machinery in leaf and anther tissue. To check probe quality, the D1100 probe was hybridized with artificially generated smRNAs, and hybridization of 21 nucleotides in length was found, depending of the amount of control smRNA loaded (see Supplemental Figure 4A online, arrow).

DISCUSSION

In the two genomic backgrounds analyzed, both meristematic nuclei and those from differentiated and meiotic cells showed cell cycle–dependent decondensation of the distal zone of the B-terminal region, whereas the proximal zone remains condensed, as previously described (Morais-Cecílio et al., 1996; Langdon et al., 2000). The level of decondensation of the distal zone increases with the number of Bs, although to a greater extent in rye than in wheat. These genome-associated differences may be related with the availability of chromatin remodeling factors. Notwithstanding some variation, decondensation of the subterminal domain is a consistent feature, independent of

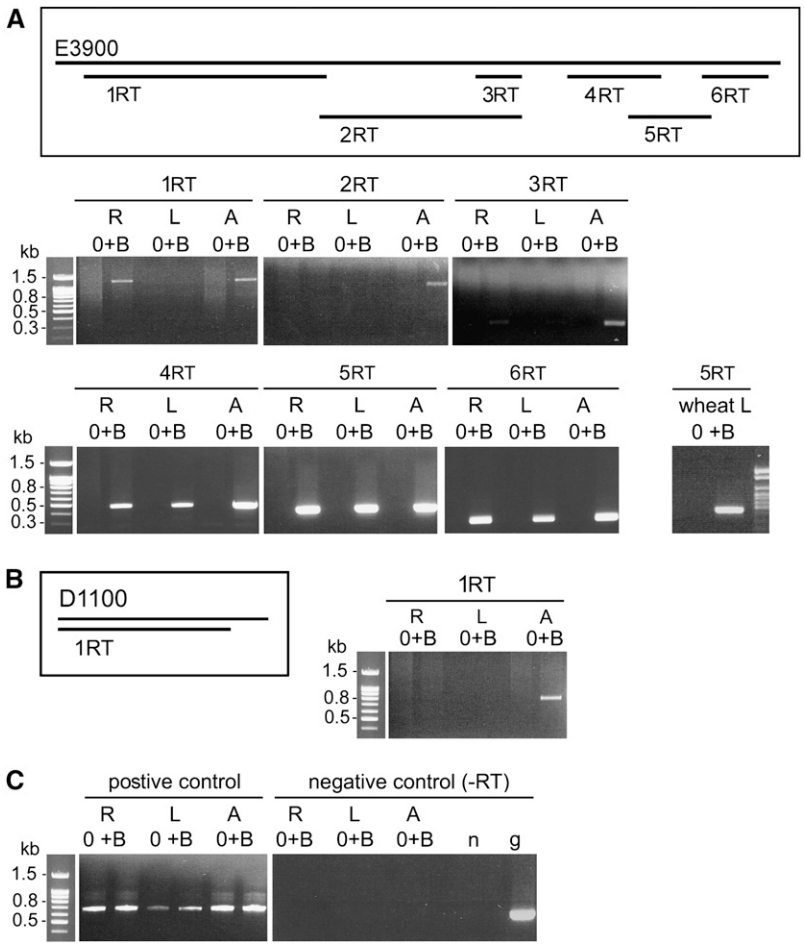

Figure 5. Transcriptional Analysis of E3900 and D1100 Reveals Tissue Type–Specific Activity.

(A) and **(B)** E3900 and D1100 RNA abundance assessed by semiquantitative RT-PCR on root (R), leaf (L), and anther (A) tissue of 0B/+B rye and 0B/+B wheat. Schematas indicate the different regions of E3900 and D1100 amplified by RT-PCR.

(C) Controls: positive control using B-independent primers (eEF1-α elongation factor). Negative control using RNA of all samples without an initial reverse transcription step to demonstrate the absence of genomic DNA contamination, (n) PCR without template DNA and (g) PCR on genomic +B DNA. Each sample contained approximately the same amount of RNA.

genotype and cell type, which is an unexpected result since this domain represents otherwise classic constitutive heterochromatin. C-banding procedures reveal that at mitosis rye Bs have a large heterochromatic band in the distal part of their long arm, where the two B-specific repetitive DNA families are clustered. This segment was also found to replicate later than the rest of the B, in the last part of the S-phase (Lima-de-Faria and Jaworska, 1972), but our results are in conflict with the established knowledge about the heterochromatic nature of the distal end of the rye B. Based on our findings, we propose that the B-subterminal domain forms inconsistent heterochromatin. We also note that the meristematic metaphase pattern of the B-specific domain matches perfectly between rye and wheat, indicating that chromosome location of that fraction is maintained after the introgression of the B into an alien species. This is further confirmed by the identical restriction patterns obtained in both species for the D1100 and for E3900 repeat families. The restriction pattern obtained here for the D1100 sequence in wheat and rye differs slightly from the one found by Sandery et al. (1990), with two additional *Dra*I fragments of 1.6 and 0.650 kb. The fact that the cloned D1100 fragment used as probe belongs to a DNA family that displays heterogeneity between its members (Sandery et al., 1990; Langdon et al., 2000) may account for the differences observed between the two sets of results.

H3K27 methylation shows a species-specific chromosomal distribution. The euchromatic regions of rye As and Bs are uniformly H3K27me1 labeled. By contrast, the same modification in *Arabidopsis thaliana* and barley (*Hordeum vulgare*) seems to be a heterochromatin mark (Fuchs et al., 2006). H3K27me2 is typical for heterochromatin in *Arabidopsis* and rye but characteristic of euchromatin in barley, while H3K27me3 is euchromatin specific in *Arabidopsis* and barley but clusters at a certain heterochromatic position in *Vicia faba* (Fuchs et al., 2006) and rye As and Bs.

The peculiarity of the terminal B region lies in the fact that, contrary to the Giemsa-positive telomeric heterochromatic regions

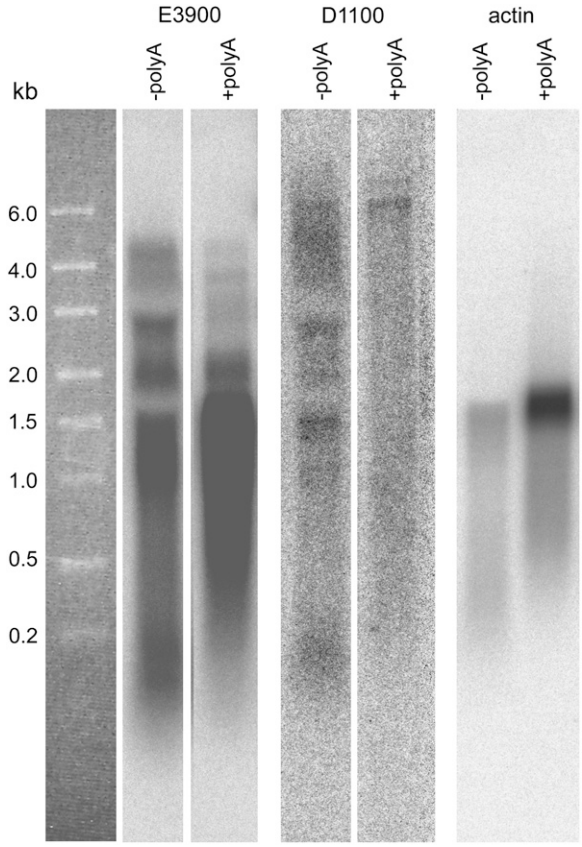

Figure 6. D1100 and E3900 Undergo Polyadenylation.

RNA gel blot hybridization of D1100 and E3900 with total RNA separated into poly(A)$^+$ and poly(A)$^-$ fractions. A probe specific for actin was used as a poly(A)$^+$ positive probe.

of As, this domain is simultaneously marked by trimethylated H3K4 and methylated H3K27, an unusual combination of apparently conflicting chromatin modifications. Conversely, detection of mono-, di-, or trimethylated H3K9, H4K20, and methylated cytosine residues show no discrimination for the B-terminal domain. Methylation of histone H3 at Lys residues 4, 9, and 27 has become one of the most consistent epigenetic marks to differentiate euchromatin and heterochromatin across a wide range of species (reviewed in Martin and Zhang, 2005). Histone Lys residues may be mono-, di-, or trimethylated in vivo, and the fully functional significance of these three states remains unclear (Rice et al., 2003). Both dimethyl and trimethyl states of H3K4 have been described as being associated with active euchromatic regions, although the trimethylated, rather than the dimethylated, form of K4 in H3 marks the transcription start site of eukaryotic genes. However, only the H3K4 trimethylated state has been related to gene transcription in yeast (Santos-Rosa et al., 2002) and mammals (Miao and Natarajan, 2005). The presence of H3K4me3 in a chromatin fraction enriched in heterochromatic histone modifications and DNA methylation was only recently reported for the first time in the urochordate *Oikopleura dioica* (Spada et al., 2005). The occurrence of H3K4me3 in domains with heterochromatic features might therefore be a more common situation than hitherto realized. Moreover, the terminal domain of the rye B seems to have a high specificity for the trimethylation status of H3K4, since no enhanced labeling was found with antibodies directed against the mono- and dimethylated states of H3K4.

Further work is required to resolve whether nonrepressive (H3K4me) and repressive (H3K27me) histone modifications coexist within the same nucleosome or whether they occupy alternate nucleosomes of the terminal heterochromatic, but transcriptionally active, B region.

The fact that only the subtelomeric domain is highly enriched in trimethylated H3K4 shows a direct correlation with dynamic chromatin decondensation. The decondensation of that chromosome domain was consistently observed in all cell types analyzed and is particularly striking in pachytene cells in contrast with the behavior of other repetitive DNA sequences observed in the same cells, namely, the subtelomeric heterochromatic blocks in the As and the rDNA cluster, that remain tightly condensed at this stage (Cunado et al., 2000). The maintenance of a condensed state during meiotic prophase and low levels of recombination are general features of repetitive DNA sequences (Schwarzacher, 2003). Interestingly, an extensive analysis at the molecular level revealed a high degree of instability in this region and a potential for amplification especially associated with the E3900 sequence (Langdon et al., 2000). These authors suggest that sequence polymorphism may be involved in the B transmission equilibrium, since small changes in relative sequence amount may alter the balance between condensed and decondensed forms affecting meiotic pairing. Variation in the B ability for forming bivalents at metaphase I is one of the main features modulating their transmission rate (M.M. Jiménez et al., 1997; G. Jiménez et al., 2000), since the mitotic drive affected by nondisjunction occurs at a constant and high frequency. This strongly supports the hypothesis that the chromatin conformation of the B-terminal domain is a crucial feature for B transmission and for the maintenance of rye Bs in natural populations.

An intriguing result of our analyses is the identification of transcripts arising from the B-specific tandem repeats in the terminal region. Satellite DNA is generally considered not to be transcribed. However, various examples of transcribed tandem repeats have recently been reported in several organisms, including plants (May et al., 2005; Zhang et al., 2005). These examples suggest an active role for tandem repeat transcripts in several regulatory layers from chromatin modulation to transcription, RNA maturation, and translation (reviewed in Ugarkovic, 2005) and even to centromere function (Bouzinba-Segard et al., 2006).

The function of B transcripts and the mechanism of transcription of B-tandem repeats are unknown at present. Their transcription may be due to readthrough from other active sequences, such as mobile elements. It has been shown that transcription of centromeric satellite DNA (May et al., 2005), or heterochromatin-located genes, is driven by adjacent regulatory elements of retroelements (Dimitri et al., 2005). Both B repeats undergo polyadenylation, at least in part, as also shown for noncoding RNA transcribed in stressed human cells (Rizzi et al., 2004), and the highest transcription activity was found in anthers.

The size heterogeneity and the lack of any significant open frame is compatible with the idea that these molecules are in fact composed partly of a variable number of repeats of E3900 and D1100 sequences, arguing against a possible coding function. The size heterogeneity of B transcripts could also be explained by the fact that the members of the E3900 and D1100 sequence families are not organized as a simple monotonous array. Members of the two B repeat families are often contiguous, and more than one size class of *Eco*RI fragments was identified as derived from D1100 and E3900 families (Langdon et al., 2000). We hypothesize that these transcripts could serve some structural function in the organization and regulation of Bs. It is tempting to speculate that the unique chromatin conformation and transcription activity of the B-terminal region could be involved in the *trans*-acting mechanism of directed nondisjunction of the rye B at pollen mitosis. Although no controlling element for this process has been identified in the B-specific domain, the deletion of this region leads to a loss of the nondisjunction, indicating its direct involvement in chromatid nondisjunction (reviewed in Jones, 1995). The process of nondisjunction is highly regulated and only occurs in the gametophytes, but we cannot exclude the hypothesis that it might be related with the presence of a unique combination of chromatin marks and noncoding RNA in diploid cells.

METHODS

Plant Material

Seeds of rye (*Secale cereale* cv JNK; 2n = 2x = 14 + Bs) and wheat (*Triticum aestivum* cv Lindström; 2n = 6x = 42 + Bs), both known to carry rye Bs, and a JNK rye line selected for the presence of deleted Bs (structural variants that lack the terminal part of the long arm (Ribeiro et al., 2004), were germinated on moist filter paper at 24°C.

Some of the primary root tips were immersed in ice-cold water for 24 h to induce c-metaphases, while others were without this treatment to avoid metaphase chromosome condensation. All root tips were fixed in 4% (w/v) formaldehyde. For meiotic preparations, immature spikes were collected, and anthers selected for the pachytene stage were fixed in fresh ethanol:glacial acetic acid (3:1 [v/v]).

Indirect Immunostaining, Giemsa C-Banding, and Fluorescence in Situ Hybridization

Chromosome preparation and immunolocalization of modified histones were done according to published methods (Houben et al., 1996). The primary antibodies (Abcam and Upstate Biotechnology) were used in the following dilutions: 1:2000 (anti-H3K4me3), 1:500 (anti-H3K9me2), 1:200 (anti-H3K4me1,2, anti-H3K9me1,3, and anti-H3K27me1,2,3), and 1:100 (anti-H4K20me1,2,3) in PBS and 1% BSA. Secondary antibodies were conjugated to Cy3, and DNA was counterstained with DAPI. Immunolocalization of 5-methylcytosine residues and Giemsa C-banding were performed according to published methods (Schlegel and Gill, 1984; Castilho et al., 1999). Following histone immunostaining, fluorescence in situ hybridization was performed on chromosome spreads according to (Schwarzacher and Heslop-Harrison, 2000). Meiotic pachytene spreads and root tip longitudinal sections (~30 μm) obtained with a vibratome (Santos et al., 2002) were also used for fluorescence in situ hybridization. The rye-specific probes pJRB1100, containing an *Eco*RI fragment of 1.1 kb from the repetitive family D1100 (Sandery et al., 1990); pTZE3900, containing an *Eco*RI fragment of 3.9 kb from the repetitive family E3900 (Blunden et al., 1993); and pTa71, containing 45S rDNA gene sequences, were labeled using a nick-translation kit (Roche).

Cell Analysis

The number of Bs (from 0 to 6) was determined in squashed c-metaphases. Mitotic and meiotic cell spreads were analyzed with epifluorescence microscopy (Zeiss Axioskop 2; Olympus BX61). Root sections were observed by confocal microscopy (Bio-Rad MRC-1000 UV). Optical section images were assembled as composite images using Photoshop (Adobe Systems) and Confocal Assistant 4.02 (Bio-Rad).

RNA Extraction, RT-PCR, and RNA Gel Blot Hybridization

Total RNA was isolated from young roots, young leaves, and anthers (microscopically staged between meiosis and development of mature pollen) using the Trizol method (Chomczynski and Sacchi, 1987). To remove genomic DNA contamination, DNase (Roche) digestion was performed. DNase was inactivated by heating for 10 min at 70°C and then removed by phenol:chloroform treatment. The absence of genomic DNA contamination was confirmed by PCR with specific primers for a region of E3900 on DNase-treated RNA. cDNA was synthesized from 1 μg RNA (Clontech). Separation of total RNA into poly(A)$^+$ and poly(A)$^-$ fractions was performed with the Dynabeads mRNA purification kit (Invitrogen).

The RT-PCR mix contained 75 ng of cDNA from rye and wheat Lindström material with and without Bs, 1 μM of each primer (see Supplemental Table 1 online), buffer, deoxynucleotide triphosphate, and 1 unit of *Taq* polymerase. Thirty amplification cycles (45 s at 95°C, 1 min at 64°C, and 2 min at 72°C) were run for the amplification of E3900 and D1100 transcripts. Sequences of cloned RT-PCR products were deposited in the GenBank database under accession numbers EF566937, EF566938, EF566939, EF566940, and EF538668.

For RNA gel blot experiments, 20 μg of RNA was blotted onto a Hybond-N$^+$ membrane (Amersham). Prehybridization and hybridization were performed in Church buffer (7% SDS, 10 mM EDTA, and 0.5 M phosphate buffer, pH 7.2) at 64°C. Equal loading of RNA samples after spectrophotometric measurement was monitored by gel electrophoresis and ethidium bromide staining. The probes either generated from the clones D1100 and E3900 or by PCR amplification using primer pairs specific for E3900 regions 1N-5N (see Supplemental Table 1 online) were labeled using the HexaLabel DNA labeling kit (Fermentas).

After overnight hybridization, the membranes were washed twice in 40 mM phosphate buffer, pH 7.0, containing 1% SDS and 2 mM EDTA at 65°C; they were then exposed for 1 h for probes 3900-4 and -5 or 48 h for all other probes. The barley actin EST clone (BU 990587; Zhang et al., 2004) was used as hybridization control.

Analysis of smRNA

RNA was isolated from leaf or anthers using the Trizol method (Chomczynski and Sacchi, 1987). smRNAs were enriched and analyzed according to Mette et al. (2005). RNA (60 μg) was resolved on denaturing 15% acrylamide gel and then transferred to a Zeta-Probe nylon membrane (Bio-Rad). Decade RNA markers (Ambion) were used as size markers. To equalize the migration speed of markers and probes, 60 μg of *Escherichia coli* tRNA was added to markers. RNA probes were synthesized according to an RNA in vitro transcription kit (Fermentas) and labeled with [α-^{32}P]UTP (Amersham). The hybridization was performed overnight in 125 mM sodium phosphate buffer, pH 7.2, containing 250 mM NaCl, 7% SDS, and 50% deionized formamide. After hybridization, the membranes were washed two times for 30 min in 2× SSC and 0.2% SDS at 42°C.

To remove any unspecific hybridization, membranes were treated with RNase A and then exposed to an x-ray film for 5 d. smRNA of D1100 as a hybridization positive control was prepared using the ShortCut RNAi kit (New England Biolabs).

Accession Numbers

Sequence data from this article can be found in the GenBank/EMBL data libraries under accession numbers EF566937, EF566938, EF566939, EF566940, and EF538668.

Supplemental Data

The following materials are available in the online version of this article.

Supplemental Figure 1. Metaphase Cells of Rye with Bs after Immunostaining with Antibodies Specific for H4K20me1,2,3.

Supplemental Figure 2. DNA Gel Blot Hybridization Showing *Dra*I Restriction Patterns.

Supplemental Figure 3. Metaphase Cell of Rye with Bs after Immunostaining with Antibody Specific for 5-Methylcytosine DNA Residues.

Supplemental Figure 4. Small RNA Analysis.

Supplemental Table 1. List of Primers.

Supplemental Table 2. Sequence Comparison between Genomic DNA and Transcribed Sequences.

ACKNOWLEDGMENTS

We thank Katrin Kumke (Leibniz Institute of Plant Genetics and Crop Plant Research) and Augusta Barão (Centro de Botânica Aplicada à Agricultura) for excellent technical assistance and Michael Florian Mette for critically reading the manuscript. M.C. was supported by grants of the German Academic Exchange Service and the Leibniz Institute of Plant Genetics and Crop Plant Research. M.D. and T.R. were supported by Fundação Ciência Tecnologia, Portugal (Grants SFRH/BPD/14607/2003 and SFRH/BD/13319/2004). We also acknowledge the support of a Leverhulme Trust Emeritus Fellowship (R.N.J.).

Received August 29, 2006; revised May 23, 2007; accepted May 31, 2007; published June 22, 2007.

REFERENCES

Bannister, A.J., Zegerman, P., Partridge, J.F., Miska, E.A., Thomas, J.O., Allshire, R.C., and Kouzarides, T. (2001). Selective recognition of methylated lysine 9 on histone H3 by the HP1 chromo domain. Nature **410:** 120–124.

Blunden, R., Wilkes, T.J., Forster, J.W., Jiménez, M.M., Sandery, M.J., Karp, A., and Jones, R.N. (1993). Identification of the E3900 family, a 2nd family of rye chromosome B-specific repeated sequences. Genome **36:** 706–711.

Bouzinba-Segard, H., Guais, A., and Francastel, C. (2006). Accumulation of small murine minor satellite transcripts leads to impaired centromeric architecture and function. Proc. Natl. Acad. Sci. USA **103:** 8709–8714.

Cao, R., Wang, L.J., Wang, H.B., Xia, L., Erdjument-Bromage, H., Tempst, P., Jones, R.S., and Zhang, Y. (2002). Role of histone H3 lysine 27 methylation in polycomb-group silencing. Science **298:** 1039–1043.

Castilho, A., Neves, N., Rufini-Castiglione, M., Viegas, W., and Heslop-Harrison, J.S. (1999). 5-Methylcytosine distribution and genome organization in Triticale before and after treatment with 5-azacytidine. J. Cell Sci. **112:** 4397–4404.

Chomczynski, P., and Sacchi, N. (1987). Single-step method of RNA isolation by acid guanidinium thiocyanate phenol chloroform extraction. Anal. Biochem. **162:** 156–159.

Craig, J.M. (2005). Heterochromatin - Many flavours, common themes. Bioessays **27:** 17–28.

Cunado, N., Barrios, J., and Santos, J.L. (2000). Organization of highly repeated sequences in surface-spread pachytene chromosomes of rye. Genome **43:** 945–948.

Czermin, B., Melfi, R., McCabe, D., Seitz, V., Imhof, A., and Pirrotta, V. (2002). Drosophila enhancer of Zeste/ESC complexes have a histone H3 methyltransferase activity that marks chromosomal polycomb sites. Cell **111:** 185–196.

Dimitri, P., Corradini, N., Rossi, F., and Verni, F. (2005). The paradox of functional heterochromatin. Bioessays **27:** 29–41.

Francis, N.J., Kingston, R.E., and Woodcock, C.L. (2004). Chromatin compaction by a polycomb group protein complex. Science **306:** 1574–1577.

Fuchs, J., Demidov, D., Houben, A., and Schubert, I. (2006). Chromosomal histone modification patterns - From conservation to diversity. Trends Plant Sci. **11:** 199–208.

Heitz, E. (1928). Das Heterochromatin der Moose. Jahrb. Wiss Bot. **69:** 762–818.

Houben, A., Demidov, D., Gernand, D., Meister, A., Leach, C.R., and Schubert, I. (2003). Methylation of histone H3 in euchromatin of plant chromosomes depends on basic nuclear DNA content. Plant J. **33:** 967–973.

Houben, A., Kynast, R.G., Heim, U., Hermann, H., Jones, R.N., and Forster, J.W. (1996). Molecular cytogenetic characterisation of the terminal heterochromatic segment of the B-chromosome of rye (*Secale cereale*). Chromosoma **105:** 97–103.

Jacobs, S.A., Taverna, S.D., Zhang, Y.N., Briggs, S.D., Li, J.M., Eissenberg, J.C., Allis, C.D., and Khorasanizadeh, S. (2001). Specificity of the HP1 chromo domain for the methylated N-terminus of histone H3. EMBO J. **20:** 5232–5241.

Jiménez, G., Manzanero, S., and Puertas, M. (2000). Relationship between pachytene synapsis, metaphase I associations, and transmission of 2B and 4B chromosomes in rye. Genome **43:** 232–239.

Jiménez, M.M., Romera, F., González Sáanchez, M., and Puertas, M.J. (1997). Genetic control of the rate of transmission of rye B chromosomes. 3. Male meiosis and gametogenesis. Heredity **78:** 636–644.

Jones, N., and Houben, A. (2003). B chromosomes in plants: Escapees from the A chromosome genome? Trends Plant Sci. **8:** 417–423.

Jones, R.N. (1995). Tansley review no 85 - B chromosomes in plants. New Phytol. **131:** 411–434.

Jones, R.N., and Puertas, M.J. (1993). The B chromosomes of rye (*Secale cereale* L.). In Frontiers in Plant Science Research, K.K. Dhir and T.S. Sareen, eds (Delhi, India: Bhagwati Enterprises), pp. 81–112.

Kouzarides, T. (2007). Chromatin modifications and their function. Cell **128:** 693–705.

Langdon, T., Seago, C., Jones, R.N., Ougham, H., Thomas, H., Forster, J.W., and Jenkins, G. (2000). De novo evolution of satellite DNA on the rye B chromosome. Genetics **154:** 869–884.

Leach, C.R., Houben, A., Field, B., Pistrick, K., Demidov, D., and Timmis, J.N. (2005). Molecular evidence for transcription of B chromosome ribosomal RNA genes in *Crepis capillaris*. Genetics **171:** 269–278.

Lima-de-Faria, M., and Jaworska, H. (1972). The relation between the chromosome size gradient and the sequence of DNA replication in rye. Hereditas **70:** 39–58.

Martin, C., and Zhang, Y. (2005). The diverse functions of histone lysine methylation. Nat. Rev. Mol. Cell Biol. **6:** 838–849.

May, B.P., Lippman, Z.B., Fang, Y., Spector, D.L., and Martienssen, R.A. (2005). Differential regulation of strand-specific transcripts from Arabidopsis centromeric satellite repeats. PLoS Genet **1:** e79.

Mette, M.F., Aufsatz, W., Kanno, T., Daxinger, L., Rovina, P., Matzke, M., and Matzke, A.J. (2005). Analysis of double-stranded RNA and small RNAs involved in RNA-mediated transcriptional gene silencing. Methods Mol. Biol. **309:** 61–82.

Miao, F., and Natarajan, R. (2005). Mapping global histone methylation patterns in the coding regions of human genes. Mol. Cell. Biol. **25:** 4650–4661.

Morais-Cecílio, L., Delgado, M., Jones, R.N., and Viegas, W. (1996). Painting rye B chromosomes in wheat: Interphase chromatin organization, nuclear disposition and association in plants with two, three or four Bs. Chromosome Res. **4:** 195–200.

Noma, K., Allis, C.D., and Grewal, S.I.S. (2001). Transitions in distinct histone H3 methylation patterns at the heterochromatin domain boundaries. Science **293:** 1150–1155.

Ribeiro, T., Pires, B., Delgado, M., Viegas, W., Jones, N., and Morais-Cecílio, L. (2004). Evidence for 'cross-talk' between A and B chromosomes of rye. Proc. R. Soc. Lond. B Biol. Sci. **271:** S482–S484.

Rice, J.C., Briggs, S.D., Ueberheide, B., Barber, C.M., Shabanowitz, J., Hunt, D.F., Shinkai, Y., and Allis, C.D. (2003). Histone methyltransferases direct different degrees of methylation to define distinct chromatin domains. Mol. Cell **12:** 1591–1598.

Richards, E.J., and Elgin, S.C.R. (2002). Epigenetic codes for heterochromatin formation and silencing: Rounding up the usual suspects. Cell **108:** 489–500.

Rimpau, J., and Flavell, R.B. (1975). Characterization of rye B chromosome DNA by DNA-DNA hybridization. Chromosoma **52:** 207–217.

Rizzi, N., Denegri, M., Chiodi, I., Corioni, M., Valgardsdottir, R., Cobianchi, F., Riva, S., and Biamonti, G. (2004). Transcriptional activation of a constitutive heterochromatic domain of the human genome in response to heat shock. Mol. Biol. Cell **15:** 543–551.

Sandery, M.J., Forster, J.W., Blunden, R., and Jones, R.N. (1990). Identification of a family of repeated sequences on the rye B-chromosome. Genome **33:** 908–913.

Santos, A.P., Abranches, R., Stoger, E., Beven, A., Viegas, W., and Shaw, P.J. (2002). The architecture of interphase chromosomes and gene positioning are altered by changes in DNA methylation and histone acetylation. J. Cell Sci. **115:** 4597–4605.

Santos-Rosa, H., Schneider, R., Bannister, A.J., Sherriff, J., Bernstein, B.E., Emre, N.C.T., Schreiber, S.L., Mellor, J., and Kouzarides, T. (2002). Active genes are tri-methylated at K4 of histone H3. Nature **419:** 407–411.

Schlegel, R., and Gill, B.S. (1984). N-banding analysis of rye chromosomes and the relationship between N-banded and C-banded heterochromatin. Can. J. Genet. Cytol. **26:** 765–769.

Schwarzacher, T. (2003). DNA, chromosomes, and in situ hybridization. Genome **46:** 953–962.

Schwarzacher, T., and Heslop-Harrison, J.S. (2000). Practical in Situ Hybridisation. (Oxford, UK: Bios).

Shi, Y.J., Lan, F., Matson, C., Mulligan, P., Whetstine, J.R., Cole, P.A., Casero, R.A., and Shi, Y. (2004). Histone demethylation mediated by the nuclear arnine oxidase homolog LSD1. Cell **119:** 941–953.

Spada, F., Vincent, M., and Thompson, E.M. (2005). Plasticity of histone modifications across the invertebrate to vertebrate transition: Histone H3 lysine 4 trimethylation in heterochromatin. Chromosome Res. **13:** 57–72.

Timmis, J.N., Ingle, J., Sinclair, J., and Jones, R.N. (1975). Genomic quality of rye B chromosomes. J. Exp. Bot. **26:** 367–378.

Tsujimoto, H., and Niwa, K. (1992). DNA-structure of the B-chromosome of rye revealed by in situ hybridization using repetitive sequences. Jpn. J. Genet. **67:** 233–241.

Ugarkovic, D. (2005). Functional elements residing within satellite DNAs. EMBO Rep. **6:** 1035–1039.

Wilkes, T.M., Francki, M.G., Langridge, P., Karp, A., Jones, R.N., and Forster, J.W. (1995). Analysis of rye B-chromosome structure using fluorescence insitu hybridization (FISH). Chromosome Res. **3:** 466–472.

Zegerman, P., Canas, B., Pappin, D., and Kouzarides, T. (2002). Histone H3 lysine 4 methylation disrupts binding of nucleosome remodeling and deacetylase (NuRD) repressor complex. J. Biol. Chem. **277:** 11621–11624.

Zhang, H., et al. (2004). Large-scale analysis of the barley transcriptome based on expressed sequence tags. Plant J. **40:** 276–290.

Zhang, W., Yi, C., Bao, W., Liu, B., Cui, J., Yu, H., Cao, X., Gu, M., Liu, M., and Cheng, Z. (2005). The transcribed 165-bp CentO satellite is the major functional centromeric element in the wild rice species *Oryza punctata.* Plant Physiol. **139:** 306–315.

A2 Cohen, S., Houben, A., and Segal, D. (2008). Extrachromosomal circular DNA derived from tandemly repeated genomic sequences in plants. Plant Journal 53, 1027-1034.

The Plant Journal (2008) **53**, 1027–1034 doi: 10.1111/j.1365-313X.2007.03394.x

Extrachromosomal circular DNA derived from tandemly repeated genomic sequences in plants

Sarit Cohen[1,*], Andreas Houben[2] and Daniel Segal[1]
[1]*Department of Molecular Microbiology and Biotechnology, Tel Aviv University, Tel Aviv, Israel, and*
[2]*Leibniz-Institute of Plant Genetics and Crop Plant Research (IPK), Gatersleben, Germany*

Received 20 November 2007; accepted 3 December 2007.
[*]For correspondence (fax +972 36409407; e-mail scohen@post.tau.ac.il).

Summary

Extrachromosomal circular DNA (eccDNA) is one characteristic of the plasticity of the eukaryotic genome. It was found in various non-plant organisms from yeast to humans. EccDNA is heterogeneous in size and contains sequences derived primarily from repetitive chromosomal DNA. Here, we report the occurrence of eccDNA in small and large genome plant species, as identified using two-dimensional gel electrophoresis. We show that eccDNA is readily detected in both *Arabidopsis thaliana* and *Brachycome dichromosomatica*, reflecting a normal phenomenon that occurs in wild-type plants. The size of plant eccDNA ranges from > 2 kb to < 20 kb, which is similar to the sizes found in other organisms. These DNA molecules correspond to 5S ribosomal DNA (rDNA), non-coding chromosomal high-copy tandem repeats and telomeric DNA of both species. Circular multimers of the repeating unit of 5S rDNA were identified in both species. In addition, similar multimers were also demonstrated with the *B. dichromosomatica* repetitive element Bdm29. Such circular multimers of tandem repeats were found in animal models, suggesting a common mechanism for eccDNA formation among eukaryotes. This mechanism may involve looping-out via intrachromosomal homologous recombination. The implications of these results on genome plasticity and evolutionary processes are discussed.

Keywords: extrachromosomal circular DNA, genome evolution, tandem repeats, ribosomal DNA, copy number polymorphisms.

Introduction

For a long time the genome of eukaryotic species has been considered as relatively stable. However, in the last few decades many phenomena have been described that exhibit plasticity of the genome. Yet most of these remain unexplained at the molecular and genetic levels. These include the expansion, contraction and homogenization of chromosomal tandem repeats (Ugarkovic and Plohl, 2002), the occurrence of B chromosomes (Jones and Houben, 2003), the mobility of ribosomal genes (Schubert and Wobus, 1985; Shishido *et al*., 2000), DNA elimination during the development of several organisms in the plant and animal kingdoms (Kloc and Zagrodzinska, 2001) and the elimination of DNA in response of a 'genomic shock' after interspecies hybridization in plants (Leitch and Bennett, 2004; Levy and Feldman, 2002; Ma *et al*., 2004).

Extrachromosomal circular DNA (eccDNA) is another hallmark of genome plasticity, which appears to be involved in various phenomena of genome dynamics. EccDNA has been detected in every eukaryotic genome tested so far (reviewed in Kuttler and Mai, 2007). Although the population of eccDNA may include intermediates of mobile elements or viral genomes (Hirochika and Otsuki, 1995), we refer to the circular molecules that are derived from the entire genome, primarily from chromosomal repetitive sequences, as eccDNA. These sequences do not appear to harbor an intrinsic 'jumping' or excision mechanism mediated by specific sequences (Gaubatz, 1990). In plants, eccDNA was detected, by electron microscopy, in nuclear fractions from wheat and tobacco (Kinoshita *et al*., 1985), and as a single chromosomal sequence that was amplified as an extrachromosomal circle in cultured cells of rice (Cuzzoni *et al*., 1990). However, the heterogeneous population of eccDNA molecules has never been characterized in detail at the molecular level.

A two-dimensional (2D) gel electrophoresis technique facilitates the characterization of eccDNA by separation of DNA molecules according to their size and structure (Figure 1a) (Cohen and Lavi, 1996). This technique enables the identification of circular molecules within a relatively small sample of total DNA, and, following hybridization with specific probes, allows the characterization of its size distribution, molecular organization and sequence content. Using the 2D gel, eccDNA was characterized in humans (Cohen *et al.*, 1997), rodents (Cohen and Lavi, 1996), *Xenopus* (Cohen and Mechali, 2001, 2002; Cohen *et al.*, 1999) and *Drosophila* (Cohen *et al.*, 2003). The population of eccDNA comprises multimers of tandemly repeated, coding as well as non-coding, sequences, including ribosomal genes. The formation of eccDNA is independent of chromosomal DNA replication (Cohen and Mechali, 2001), but may be enhanced upon chemical stress by DNA-damaging agents (Cohen and Lavi, 1996; Cohen *et al.*, 1997, 2003), and is likely to involve intrachromosomal homologous recombination and looping-out. Furthermore, rolling circle replication of eccDNA appears to occur in *Drosophila*, irrespectively of the expression of the replicated genes (Cohen *et al.*, 2005). This finding has wide implications on the evolution of chromosomal tandem repeats, including processes such as repeat expansion, homogenization and mobility of tandem genes.

The possible involvement of eccDNA in the evolution of genomes is of particular interest for plants. This is because the size of the genome among angiosperms varies by 1000-fold (Bennett and Leitch, 1995), and large genomes are composed mainly of repetitive elements, including tandemly organized sequences (Britten and Kohne, 1968). Tandemly repeated DNA (satellite DNA) can increase in copy number in a relatively short evolutionary time, by replication slippage, rolling circle replication, conversion-like events or by some other unexplained mechanisms (Charlesworth *et al.*, 1994). The outcome of all the processes affecting satellite DNA arrays is a high turnover of this part of the eukaryotic genome.

In this work we asked whether eccDNA can be detected in plants using the 2D gel technique, and we chose known tandem repeats as probes. We show that eccDNA is readily detected in both the small genome species *Arabidopsis thaliana* (genome size, 1C = 170 Mbp) and in the large genome dicot *Brachycome dichromosomatica* (1C = 1510 Mbp). These eccDNA molecules correspond to 5S ribosomal DNA (rDNA), non-coding chromosomal tandem repeats and telomeric DNA. The implications of these results on genome plasticity and evolutionary processes are discussed.

Results

Although a previous report suggested the presence of eccDNA in plants, based on electron microscope observations (Kinoshita *et al.*, 1985), molecular analysis of these molecules has never been preformed. We therefore asked whether the 2D gel technique could be used to detect eccDNA in plants. Our previous results from animal models (Cohen *et al.*, 1999, 2003), showed that chromosomal tandem repeats are over-represented in populations of

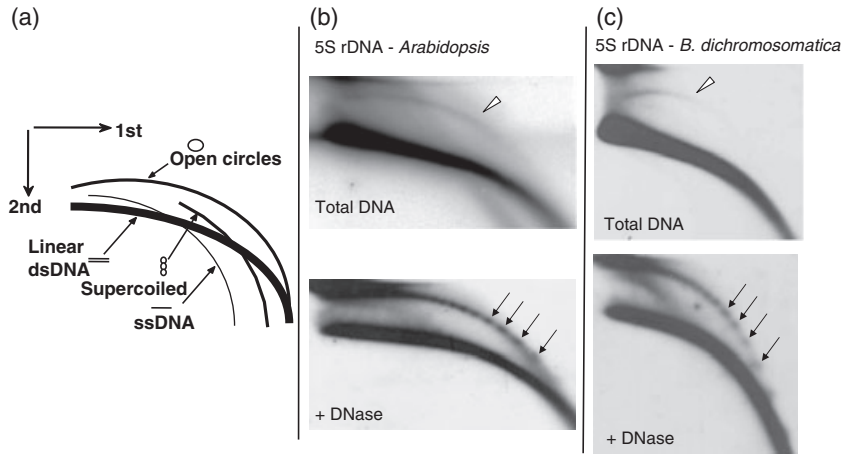

Figure 1. Two-dimensional (2D) gel electrophoresis for the analysis of extrachromosomal circles of 5S ribosomal DNA (rDNA).
(a) A diagram of 2D gel electrophoretic patterns of genomic DNA generated by populations of linear and circular molecules of heterogeneous sizes. Each arc consists of molecules sharing the same structure, but differing in mass (Cohen and Lavi, 1996). This analysis identifies double-stranded linear DNA (linear dsDNA), single-stranded linear DNA (ssDNA), open circular molecules and supercoiled molecules.
(b, c) The extrachromosomal circular DNA (eccDNA) of 5S rDNA in Arabidopsis and *Brachycome dichromosomatica* is organized in multimers. Total DNA from Arabidopsis (b) and *B. dichromosomatica* (c) was cleaved with *Xba*I, analyzed on 2D gel, blotted and hybridized with a cloned copy of the Arabidopsis and *B. dichromsomatica* 5S rDNA, respectively (total DNA). Open circles are indicated by arrowheads. To enrich for eccDNA and improve the 2D gel resolution, genomic DNA of both species was first digested with *Xba*I and then cleaved with 'Plasmid-Safe' DNase prior to its 2D gel analysis (+DNase). Hybridization with the corresponding 5S rDNA probes reveals a pattern of discrete spots formed by the circular multimers of the repeated unit (arrows).

eccDNA. Therefore, known high-copy tandem repeats were chosen to serve as probes for detecting eccDNA in Arabidopsis and *B. dichromosomatica*.

A most intriguing sequence to begin our analysis is the 5S rDNA. It is a coding gene and is organized in tandem repeats. Moreover, we and others have demonstrated that 5S rDNA is present in the population of eccDNA from *Drosophila* (Cohen *et al.*, 2003; Pont *et al.*, 1987) and *Xenopus* embryos (Cohen *et al.*, 1999).

In Arabidopsis about 1000 copies of 5S rDNA genes are organized in tandem arrays localized in heterochromatic pericentromeric regions of chromosomes 3, 4 and 5. Each 5S rDNA unit (~ 500 bp) contains a 120-bp transcribed region and a non-transcribed spacer (Campell *et al.*, 1992).

Total genomic DNA from leaves of Arabidopsis was cleaved with *Xba*I, which cuts outside of the 5S rDNA repeat, and were analyzed by 2D gel electrophoresis. Using the 5S rDNA probe we detected a clear arc corresponding to open circles, as well as a massive arc that corresponds to the linear double-stranded DNA (Figure 1b). Thus, eccDNA homologous to the 5S rDNA repeat does exist in Arabidopsis.

The continuous arc of eccDNA indicates the presence of a heterogeneous population of circular molecules of variable masses. The size of 5S rDNA circles in Arabidopsis ranges from less than 2 kb to over 20 kb, based on our estimation of eccDNA size using circular size markers (Cohen *et al.*, 1999, 2003, 2005). Longer exposures revealed evidence for the presence of circular multimers of 500 bp at a poor resolution (data not shown). To facilitate the migration of eccDNA on the 2D gel, and to improve its resolution, we enriched our DNA sample for circular molecules prior to its loading on the gel. 'Plasmid-Safe' DNase selectively hydrolyzes double-stranded linear DNA, and has no activity on circular DNA. Although the linear DNA was not completely removed by the DNase (Figure 1b, +DNase), a clear pattern of spots, corresponding to multimers of 500 bp, is visible upon DNase treatment. We previously reported similar patterns of spots in *Drosophila*, using different probes including the 5S rDNA (Cohen *et al.*, 2003), and in *Xenopus* embryos (Cohen *et al.*, 1999).

We next asked whether eccDNA corresponding to 5S rDNA could be detected in other plant species, such as the large genome species *B. dichromosomatica*. The 5S rDNA genes in this species are present in a cluster estimated to be at least 21-kb long (Houben *et al.*, 2001), but their organization within the cluster has never been investigated. To verify whether 5S rDNA in *B. dichromosomatica* is organized in tandem repeats, as is the case in many other organisms, we performed a partial digest of genomic DNA with *Bam*HI, which cleaves within the 5S gene. A ladder pattern, typical for tandem organization of a repeated unit, was obtained (Figure S1). We estimate the size of the repeating unit to be ca 500-bp long.

To test for the presence of eccDNA homologous to 5S rDNA, we performed a similar analysis to that described above for 5S rDNA in Arabidopsis. Total genomic DNA of *B. dichromosomatica* was cleaved with *Xba*I, migrated on a 2D gel and hybridized with a 5S rDNA probe of *B. dichromosomatica* (Figure 2c, total DNA) . As in Arabidopsis, an arc consisting of circular multimers of the 5S rDNA was identified upon DNase treatment (Figure 1c, +DNase).

The detection of 5S rDNA in a circular form in both Arabidopsis and *B. dichromosomatica* implies that similar circles may occur in other plant species.

EccDNA homologous to arrays of high-copy tandem repeats including non-coding satellite DNA, was reported in various animals (reviewed in Gaubatz, 1990; Kuttler and Mai, 2007), and was identified by us using 2D gels in *Drosophila* (Cohen *et al.*, 2003), *Xenopus* embryos (Cohen and Mechali, 2002; Cohen *et al.*, 1999) and in mammalian cultured cells (Cohen and Lavi, 1996; Cohen *et al.*, 1997). We therefore predicted that the centromeric 180-bp repeat of Arabidopsis would be present in the eccDNA population. Indeed, 2D gel analysis identified eccDNA homologous to this sequence (Figure 2a). The possible organization of these circles as multimers of the repeating unit could not be demonstrated because of the resolution limitations of our technique.

In *B. dichromosomatica*, a set of tandemly repeated sequences were identified that reside in the A chromosomes and/or in the B chromosomes (Leach *et al.*, 2004). For example, Bds1 is a tandemly repeated 91-bp element that is a main component of a supernumerary A-chromosome segment (Houben *et al.*, 2000). EccDNA homologous to this repeat was readily detected (Figure 2b).

We used circular size markers, as previously described (Cohen and Mechali, 2002; Cohen *et al.*, 1999), to estimate the size range of the eccDNA reported in this work. For example, we mixed genomic DNA with the relaxed form of three plasmids of 3.2, 9.4 and 11.2 kb, and analyzed them on 2D gel. Hybridization with both Bds1 and a plasmid probe revealed the spots of the plasmid DNA on the arc of eccDNA (Figure 2c). This arc continues towards the high-molecular-weight region of the gel, beyond the 11.2-kb marker. Longer exposures (not shown, but see Figure 2e) demonstrate that the arc of eccDNA can continue towards the low-molecular-weight region, below the 3.2-kb marker. These results indicate a population of eccDNA of a heterogeneous mass, which can be smaller than 2 kb and larger than 20 kb. This size range was found for every probe tested throughout this work, and is similar to the size range of eccDNA in other organisms (Cohen *et al.*, 1999, 2003, 2005).

Bdm29 is a 300-bp high-copy tandem repeat that is specific to micro B chromosomes (Houben *et al.*, 1997). Indeed, in plants containing micro B chromosomes we detected the circular form of this sequence (Figure 2d).

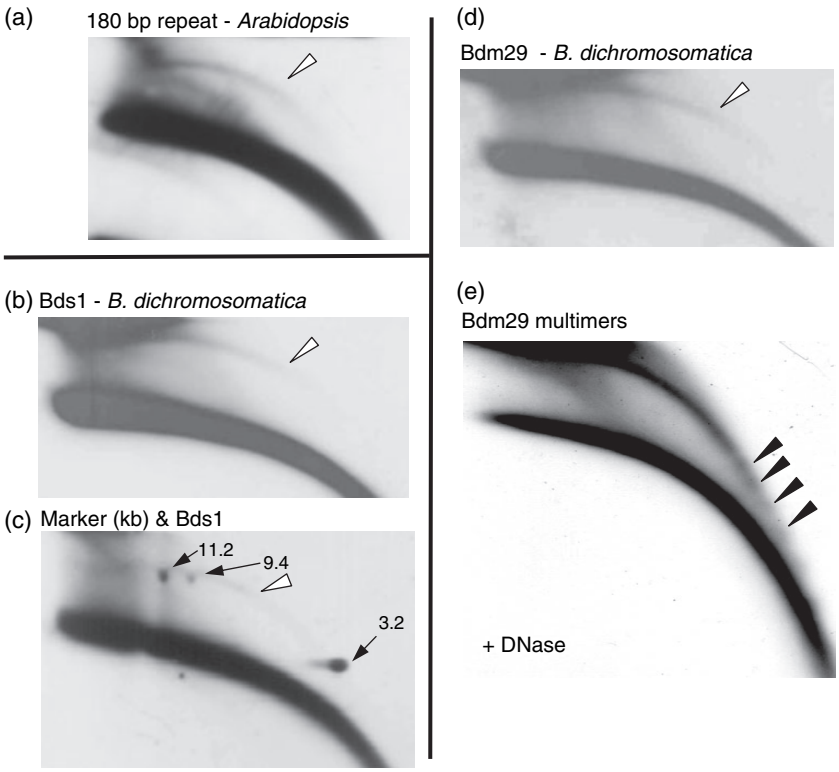

Figure 2. Extrachromosomal circular DNA (eccDNA) of non-coding high-copy tandem repeats.
(a) Genomic DNA of Arabidopsis was digested with *Xba*I, analyzed on 2D gel and hybridized with the Arabidopsis 180-bp pericentric repeat.
(b) Genomic DNA of *Brachycome dichromosomatica* was cleaved with *Bgl*II, analyzed on 2D gel and hybridized with the 91-bp repetitive element Bds1.
(c) Size estimation of eccDNA. Genomic DNA of *B. dichromosomatica* (cleaved with *Xba*I) was mixed with the relaxed form of three plasmids of 3.2, 9.4 and 11.2 kb, and was then analyzed on 2D gel. The blot was hybridized with Bds1 and plasmid probes. Arrows indicate relaxed plasmid markers, and white arrowheads indicate open circles (eccDNA).
(d) The blot shown in (b) was rehybridized with the 300-bp repetitive element Bdm29.
(e) To visualize circular multimers, genomic DNA from *B. dichromosomatica* was digested with *Xba*I and then cleaved with 'Plasmid-Safe' DNase prior to its 2D gel analysis. Hybridization with Bdm29 probe reveals the spot pattern of circular multimers (black arrowheads).

Pre-treatment with 'Plasmid-Safe' DNase enabled the identification of circular multimers of Bdm29 (Figure 2e).

To assess the relative levels of eccDNA within the total DNA, we used PHOSPHORIMAGER to quantify the signal of the arc corresponding to eccDNA and the signal of the arc corresponding to the linear DNA in various blots. The percentage of the eccDNA signal was calculated in several different gels made from independent DNA preparations. We found, for example, that the percentage of Bdm29 eccDNA could range from 0.2 to 2% of its linear DNA signal in different wild-type strains (Figure 3a,b, respectively). Similar values were obtained for the other repeats described above in both Arabidopsis and *B. dichromosomatica*.

Over-representation of repetitive DNA in the population of eccDNA was previously reported in various organisms (Cohen *et al.*, 2003; and references therein). To test whether this is the case in plants, the same membrane was probed with Bdm29 (Figure 3c) and then reprobed with total genomic DNA of *B. dichromosomatica* (Figure 3d). The arc of eccDNA obtained with total genomic probe was clearly weaker than that of Bdm29, indicating that Bdm29 is over-represented in eccDNA compared with random genomic sequences. Hence, as found in many animal organisms, and now also found in *B. dichromosomatica*, we demonstrate that a tandemly repetitive element is over-represented in eccDNA.

Telomeric repeats are organized in tandem arrays, and if they behave as other chromosomal tandem repeats, they should be prone to circle formation in wild-type plants. EccDNA homologous to telomeric repeats was identified, using 2D gels, by others and by us in human

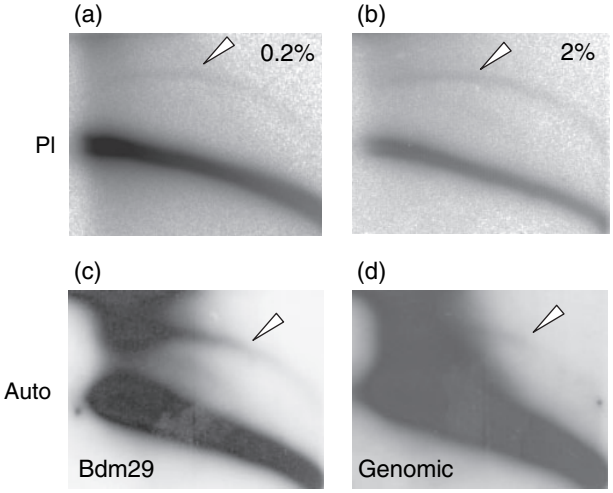

Figure 3. Over-representation and variable levels of Bdm29 in the population of *Brachycome dichromosomatica* extrachromosomal circular DNA (eccDNA).
(a, b) Genomic DNA from two different plants was cleaved with *Pvu*II, and analyzed on the same 2D gel. The blot was hybridized with Bdm29 probe, and the signal of the eccDNA was quantified by PHOSPHORIMAGER (PI). The percentage of eccDNA in each DNA sample is indicated. The autoradiogram of (b) is shown in (c) (auto). Panel (c) was rehybridized with total *B. dichromosomatica* genomic DNA (d, genomic). Arrowheads indicate open circles.

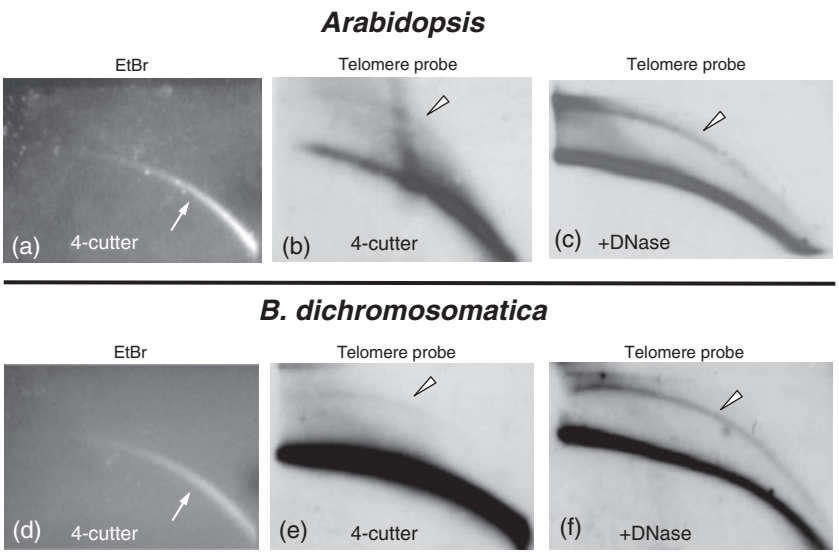

Figure 4. Arabidopsis-type telomere circles in plants. Four-cutter analysis: genomic DNA from Arabidopsis (a, b) and *Brachycome dichromosomatica* (d, e) was digested with the four-cutters *Hae*III (a, b) or *Hae*III and *Msp*I (d, e), and then analyzed on 2D gel. Ethidium bromide staining shows the massive degradation of most of the genomic DNA (arrows), whereas hybridization with telomere probe reveals circular telomeric molecules (arrowheads). DNase analysis (c, f): genomic DNA from Arabidopsis (c) and *B. dichromosomatica* (e) was digested with *Xba*I and then cleaved with 'Plasmid-Safe' DNase prior to its 2D gel analysis. Hybridization with telomere probe reveals circular telomeric molecules (arrowheads).

cells (Regev *et al.*, 1998; Wang *et al.*, 2004), in normal *Xenopus* embryos (Cohen and Mechali, 2002) and in yeast (Larrivee and Wellinger, 2006). To search for telomere circles in wild-type plants, we examined the total genomic DNA from both Arabidopsis and the Arabidopsis telomere-type-positive Asteracea *B. dichromosomatica*. The DNA was digested with four cutters (*Hae*III and/or *Msp*I) prior to its 2D gel analysis, so as to cleave most of the genomic DNA. Indeed, the ethidium bromide staining indicates that most of the DNA was of low-molecular weight (Figure 4a,d). Hybridization with an Arabidopsis telomere probe revealed an arc of eccDNA, corresponding to telomeric DNA in both Arabidopsis and *B. dichromosomatica* (Figure 4b,e, respectively). In a complementary experiment, the DNA samples were treated with 'Plasmid-Safe' DNase prior to the 2D gel analysis. Our results indicate a clear arc of eccDNA homologous to the telomere repeats in both species (Figure 4c,f).

Note that telomere circles in both species can be at least several kb long. In Arabidopsis, the length of the chromosomal telomeric DNA is up to 8 kb (Watson and Shippen, 2007), suggesting that in this species telomere circles could reach the size of an entire telomere cluster.

Discussion

Our results indicate that, as in animal systems, eccDNA exists in the plant kingdom and can be easily detected by 2D gels. These molecules are heterogeneous in size and consist mainly of sequences homologous to chromosomal tandem repeats.

The presence of various tandem repeats within the population of eccDNA in both Arabidopsis and *B. dichromosomatica* is consistent with a recent publication by Zellinger *et al.* (2007), which demonstrated eccDNA that is homologous to the same Arabidopsis probes reported here. These authors also showed that the DNA repair factor Ku70/80 inhibits the production of telomeric circles, but not those of the other repeats. However, in contrast to Zellinger *et al.* (2007) our 2D analysis also detected telomeric eccDNA in wild-type Arabidopsis.

eccDNA molecules in plants are estimated to comprise up to several percent of their linear counterparts, similarly to the levels estimated in *Drosophila* (Cohen *et al.*, 2003). The relative level of eccDNA homologous to a specific sequence (e.g. Bdm29) may vary in different wild-type strains of *B. dichromosomatica* (Figure 3a,b). Variation in the levels of eccDNA was also observed in different wild-type strains of *Drosophila* (Cohen *et al.*, 2003), and we speculate that it results from variations in the efficiency of the machinery that forms eccDNA.

The occurrence of a spot-like pattern in the 5S rDNA and the 300-bp repetitive element Bdm29 (Figures 1 and 2), suggests that eccDNA is composed of circular multimers of the tandemly repeated units. In addition, six or seven multiples of a chromosomal tandemly repeated unit of 7.2 kb were amplified as an extrachromosomal circle in cultured rice cells (Cuzzoni *et al.*, 1990). Organization of eccDNA in multimers was found in various organisms, including humans (Kiyama *et al.*, 1986, 1987), mouse (Cohen *et al.*, 2006), *Xenopus* embryos (Cohen and Mechali, 2001; Cohen *et al.*, 1999) and *Drosophila* (Cohen *et al.*, 2003; Degroote *et al.*, 1989; Pont *et al.*, 1987).

The exact multimer organization of eccDNA in all organisms tested suggests a mechanism of eccDNA formation, which would involve intrachromosomal homologous recombination and looping-out of circular molecules (for a detailed discussion, see Cohen *et al.*, 2003). Thus, the machinery of eccDNA formation appears to be universal among eukaryotes. Furthermore, we reported evidence for

rolling circle replication (RCR) of eccDNA in *Drosophila* (Cohen *et al.*, 2005). In addition, eccDNA molecules harboring a sigmoid form (circles with hanging tails) from mung bean were observed by electron microscopy (Bhattachyryya and Roy, 1986), suggesting that RCR may also occur in plants. RCR may contribute to the accumulation of the extra copies of sequences that are included in the eccDNA. However, it is not clear whether these eccDNA replication products can reintegrate into the chromosome.

Hence, we suggest that eccDNA might be involved in contraction and expansion of chromosomal arrays of tandem repeats via excision, and integration, respectively, as described here.

Does eccDNA contribute to the evolution and plasticity of plant genomes? Rapid elimination of DNA sequences has frequently been found as a result of the allopolyploidization that occurs in interspecific crosses (reviewed in Levy and Feldman, 2002). Several studies have shown that DNA elimination in both diploids and polyploids can occur by a variety of recombinational mechanisms, such as intrachromosomal unequal homologous recombination and double-strand break (DSB) repair (Kirik *et al.*, 2000). In addition, homologous recombination between long terminal repeats of adjacent retrotransposal elements, and 'looping out' of the genomic region between them, has been demonstrated to contribute to genome reduction in Arabidopsis. This suggests a role for DNA circle formation as a mechanism that counteracts genome expansion in plants (Devos *et al.*, 2002). An attractive possibility is that elimination of DNA occurs via formation of eccDNA.

Genome sequencing has revealed the presence of organellar, relic viral, transposon and retroelement DNAs, providing clear evidence that nuclear genomes of plants, like those of other eukaryotes, are promiscuous in integrating DNA. Whether eccDNA can reintegrate into the nuclear genome is unknown. However, given that the circular plasmid constructs commonly used for plant transformation readily integrate into the nuclear genome, via illegitimate recombination (Somers and Makarevitch, 2004), it is likely that a similar process could operate to reintegrate eccDNA. Therefore, eccDNA could serve as a DNA reservoir contributing to the genetic variability of plant genomes.

Although no direct experimental evidence is currently available, it is tempting to speculate that eccDNA is involved in the evolution of B chromosomes and also might explain the mobility of rDNA. The origin of B chromosomes has remained a mystery, but spontaneous amplification of coding and non-coding tandem repeat sequences derived from standard A chromosomes appears to be strongly associated with their origin and evolution (Jones and Houben, 2003). Indeed, it should be noted that B chromosomes contain coding and non-coding repeats, as found in the eccDNA of various organisms (Cohen *et al.*, 2003). Furthermore, the present work shows that at least three sequences that are found in B chromosomes of *B. dichromosomatica*, i.e. Bdm29, Bds1 and telomeric repeats, are represented in the population of eccDNA from this species (Figures 2 and 4). EccDNA integration into B chromosomes may be favored because the transcriptionally less active B chromosomes are likely to be subjected to reduced negative selection.

There is increasing evidence that ribosomal genes are able to change position within the genome without corresponding changes in the surrounding sequences. The mechanism of rDNA transposition is not known. Yet, known mechanisms, such as chromosomal translocations, homologous recombination and transposon mobility, seem insufficient to explain the variability in the position of rDNA loci in genomes (Shishido *et al.*, 2000). The previously reported eccDNA, consisting of rDNA sequences in non-plant species (Cohen *et al.*, 1999, 2003; Degroote *et al.*, 1989; Pont *et al.*, 1987), and our finding of 5S rDNA in the eccDNA of Arabidopsis and *B. dichromosomatica*, raise the possibility that *de novo* formation of rDNA loci is mediated by rDNA-containing eccDNA.

The existence of eccDNA in eukaryotic genomes also has implications for the data analysis of copy number polymorphisms of tandem repeats, conducted by comparative genomic hybridization, or other hybridization techniques. As most of the DNA samples used for hybridization are isolated from total genomic DNA, it is likely that because of the coexistence of eccDNA, the copy number assessments of nuclear genome localized repeats are somewhat overestimated.

Our identification of eccDNA in plants has opened up a new research area that could potentially uncover mechanisms underlying complex behaviors of large genomes. Further research will provide insight into the contribution of eccDNA to genome function and dynamics, in particular with respect to genome instability, function of satellite sequences and evolution of chromosomes.

Experimental procedures

Plant material

Genomic DNA of *A. thaliana* (ecotype Columbia) and *B. dichromosomatica* (cytodeme A2) was isolated from leaf material, using the procedure described by Wienand and Feix (1980), and was then digested with different restriction enzymes according to the manufacturer's recommendations. Prior to its analysis on 2D gels, DNA was digested with restriction enzymes that do not cleave within each of the specific tested sequences. 'Plasmid-Safe' ATP-dependent DNase (Epicentre Biotechnologies, http://www.epibio.com) was used to enrich DNA samples for circular molecules using its specific affinity for double-stranded linear DNA. Restriction-digested DNA samples were extracted with phenol:chloroform and were ethanol precipitated prior to 'Plasmid-Safe' digestion, which was carried out according to the manufacture's protocol.

DNA probe preparation

The Arabidopis 5S rDNA probe was a purified 500-bp insert of the 5S rDNA unit subcloned into Bluescript SK plasmid (obtained from S. Tourmente (Unité Mixte de Recherche CNRS 6547 BIOMOVE, Université Blaise Pascal, France). A *B. dichromosomatica* 5S rDNA-specific probe was amplified from genomic DNA of *B. dichromosomatica* using primers designed according to the 5S rDNA sequence of the *Glycine* species (Gottlobmchugh *et al.*, 1990). An Arabidopsis-type telomere probe and the Arabidopsis-specific centromeric 180-bp repeat probe were synthesized by thermal cycling according to the method described by Ijdo *et al.* (1991) and Kawabe and Nasuda (2005), respectively. The inserts of the clones Bdm29 and Bds1 were used as *Brachycome*-specific probes (Leach *et al.*, 2004).

Neutral–neutral 2D gel electrophoresis, blotting and hybridization

These were performed as previously described (Cohen *et al.*, 2003). Briefly, the DNA was separated on the first dimension in 0.4% agarose at 0.7 V cm^{-1} in 1× TBE (Tris–Borate–EDTA) overnight, and the second dimension was separated in 1% agarose containing 0.3 μg ml^{-1} Ethidium bromide at 4 V cm^{-1} in 1 × TBE for 4 h. The gels were blotted onto positively charged nylon membrane (Zeta-probe; Bio-Rad, http://www.bio-rad.com). Probes were labeled by a random priming kit (Biological Industries, http://www.bioind.com). Radiolabeled DNA was detected by autoradiography, and the signal was quantified with a Phosphorimager (FLA 2000; Fuji, http://www.fujifilm.com) by using the TINA 2.10g software.

Acknowledgements

We are grateful to K. Kumke and S. Marschner for excellent technical assistance. We also thank S. Tourmente (Unité Mixte de Recherche CNRS 6547 BIOMOVE, Université Blaise Pascal, France) for the 5S rDNA probe of Arabidopsis.

Supplementary Material

The following supplementary material is available for this article online:

Figure S1. Tandem organization of 5S ribosomal DNA (rDNA) genes in *Brachycome dichromosomatica*.

This material is available as part of the online article from http://www.blackwell-synergy.com

Please note: Blackwell Publishing are not responsible for the content or functionality of any supplementary materials supplied by the authors. Any queries (other than missing material) should be directed to the corresponding author for the article.

References

Bennett, M.D. and Leitch, I.J. (1995) Nuclear DNA amounts in angiosperms. *Ann. Bot.* **76**, 113–176.

Bhattachyryya, N. and Roy, P. (1986) Extrachromosomal DNA from a dicot plant *Vigna radiata*. *FEBS Lett.* **208**, 386–390.

Britten, R.J. and Kohne, D.E. (1968) Repeated sequences in DNA. *Science*, **161**, 529.

Campell, B.R., Song, Y.G., Posch, T.E., Cullis, C.A. and Town, C.D. (1992) Sequence and organization of 5s ribosomal RNA encoding genes of *Arabidopsis thaliana*. *Gene*, **112**, 225–228.

Charlesworth, B., Sniegowski, P. and Stephan, W. (1994) The evolutionary dynamics of repetitive DNA in eukaryotes. *Nature*, **371**, 215–220.

Cohen, S. and Lavi, S. (1996) Induction of circles of heterogeneous sizes in carcinogen-treated cells: two-dimensional gel analysis of circular DNA molecules. *Mol. Cell. Biol.* **16**, 2002–2014.

Cohen, S. and Mechali, M. (2001) A novel cell-free system reveals a mechanism of circular DNA formation from tandem repeats. *Nucleic Acids Res.* **29**, 2542–2548.

Cohen, S. and Mechali, M. (2002) Formation of extrachromosomal circles from telomeric DNA in *Xenopus laevis*. *EMBO Rep.* **3**, 1168–1174.

Cohen, S., Regev, A. and Lavi, S. (1997) Small polydispersed circular DNA (spcDNA) in human cells: association with genomic instability. *Oncogene*, **14**, 977–985.

Cohen, S., Menut, S. and Mechali, M. (1999) Regulated formation of extrachromosomal circular DNA molecules during development in *Xenopus laevis*. *Mol. Cell. Biol.* **19**, 6682–6689.

Cohen, S., Yacobi, K. and Segal, D. (2003) Extrachromosomal circular DNA of tandemly repeated genomic sequences in Drosophila. *Genome Res.* **13**, 1133–1145.

Cohen, S., Agmon, N., Yacobi, K., Mislovati, M. and Segal, D. (2005) Evidence for rolling circle replication of tandem genes in Drosophila. *Nucleic Acids Res.* **33**, 4519–4526.

Cohen, Z., Bacharach, E. and Lavi, S. (2006) Mouse major satellite DNA is prone to eccDNA formation via DNA ligase IV-dependent pathway. *Oncogene*, **25**, 4515–4524.

Cuzzoni, E., Ferretti, L., Giordani, C., Castiglione, S. and Sala, F. (1990) A repeated chromosomal DNA sequence is amplified as a circular extrachromosomal molecule in rice (*Oryza sativa* L.). *Mol. Gen. Genet.* **222**, 58–64.

Degroote, F., Pont, G., Micard, D. and Picard, G. (1989) Extrachromosomal circular DNAs in *Drosophila melanogaster*: comparison between embryos and Kc0% cells. *Chromosoma*, **98**, 201–206.

Devos, K.M., Brown, J.K. and Bennetzen, J.L. (2002) Genome size reduction through illegitimate recombination counteracts genome expansion in Arabidopsis. *Genome Res.* **12**, 1075–1079.

Gaubatz, J.W. (1990) Extrachromosomal circular DNAs and genomic sequence plasticity in eukaryotic cells. *Mutat. Res.* **237**, 271–292.

Gottlobmchugh, S.G., Levesque, M., Mackenzie, K., Olson, M., Yarosh, O. and Johnson, D.A. (1990) Organization of the 5s ribosomal-RNA genes in the soybean *Glycine max* (L) Merrill and conservation of the 5s rDNA repeat structure in higher plants. *Genome*, **33**, 486–494.

Hirochika, H. and Otsuki, H. (1995) Extrachromosomal circular forms of the tobacco retrotransposon Tto1. *Gene*, **165**, 229–232.

Houben, A., Leach, C.R., Verlin, D., Rofe, R. and Timmis, J.N. (1997) A repetitive DNA sequence common to the different B chromosomes of the genus Brachycome. *Chromosoma*, **106**, 513–519.

Houben, A., Wanner, G., Hanson, L., Verlin, D., Leach, C.R. and Timmis, J.N. (2000) Cloning and characterisation of polymorphic heterochromatic segments of *Brachycome dichromosomatica*. *Chromosoma*, **109**, 206–213.

Houben, A., Verlin, D., Leach, C.R. and Timmis, J.N. (2001) The genomic complexity of micro B chromosomes of *Brachycome dichromosomatica*. *Chromosoma*, **110**, 451–459.

Ijdo, J.W., Wells, R.A., Baldini, A. and Reeders, S.T. (1991) Improved telomere detection using a telomere repeat probe (TTAGGG)n generated by PCR. *Nucleic Acids Res.* **19**, 4780.

Jones, N. and Houben, A. (2003) B chromosomes in plants: escapees from the A chromosome genome? *Trends Plant Sci.* **8**, 417–423.

Kawabe, A. and Nasuda, S. (2005) Structure and genomic organization of centromeric repeats in Arabidopsis species. *Mol. Genet. Genomics*, **272**, 593–602.

Kinoshita, Y., Ohnishi, N., Yamada, Y., Kunisada, T. and Yamagishi, H. (1985) Extrachromosomal circular DNA from nuclear fraction of higher plants. *Plant Cell Physiol.*, **26**, 1401–1409.

Kirik, A., Salomon, S. and Puchta, H. (2000) Species-specific double-strand break repair and genome evolution in plants. *EMBO J.* **19**, 5562–5566.

Kiyama, R., Matsui, H. and Oishi, M. (1986) A repetitive DNA family (Sau3A family) in human chromosomes: extrachromosomal DNA and DNA polymorphism. *Proc. Natl Acad. Sci. USA*, **83**, 4665–4669.

Kiyama, R., Matsui, H., Okumura, K. and Oishi, M. (1987) A group of repetitive human DNA families that is characterized by extrachromosomal oligomers and restriction-fragment length polymorphism. *J. Mol. Biol.* **193**, 591–597.

Kloc, M. and Zagrodzinska, B. (2001) Chromatin elimination – an oddity or a common mechanism in differentiation and development? *Differentiation*, **68**, 84–91.

Kuttler, F. and Mai, S. (2007) Formation of non-random extrachromosomal elements during development, differentiation and oncogenesis. *Semin. Cancer Biol.* **17**, 56–64.

Larrivee, M. and Wellinger, R.J. (2006) Telomerase- and capping-independent yeast survivors with alternate telomere states. *Nat. Cell Biol.* **8**, 741–747.

Leach, C.R., Houben, A. and Timmis, J.N. (2004) The B chromosomes in Brachycome. *Cytogenet. Genome Res.* **106**, 199–209.

Leitch, I.J. and Bennett, M.D. (2004) Genome downsizing in polyploid plants. *Biol. J. Linn. Soc.* **82**, 651–663.

Levy, A.A. and Feldman, M. (2002) The impact of polyploidy on grass genome evolution. *Plant Physiol.* **130**, 1587–1593.

Ma, X.F., Fang, P. and Gustafson, J.P. (2004) Polyploidization-induced genome variation in Triticale. *Genome*, **47**, 839–848.

Pont, G., Degroote, F. and Picard, G. (1987) Some extrachromosomal circular DNAs from Drosophila embryos are homologous to tandemly repeated genes. *J. Mol. Biol.* **195**, 447–451.

Regev, A., Cohen, S., Cohen, E., Bar-Am, I. and Lavi, S. (1998) Telomeric repeats on small polydisperse circular DNA (spcDNA) and genomic instability. *Oncogene*, **17**, 3455–3461.

Schubert, I. and Wobus, U. (1985) In situ hybridization confirms jumping nucleolus organizing regions in Allium. *Chromosoma*, **92**, 143–148.

Shishido, R., Sano, Y. and Fukui, K. (2000) Ribosomal DNAs: an exception to the conservation of gene order in rice genomes. *Mol. Gen. Genet.* **263**, 586–591.

Somers, D.A. and Makarevitch, I. (2004) Transgene intergration in plants: poking or patching holes in promiscuous genomes? *Curr. Opin. Biotechnol.* **15**, 126–131.

Ugarkovic, D. and Plohl, M. (2002) Variation in satellite DNA profiles–causes and effects. *EMBO J.* **21**, 5955–5959.

Wang, R.C., Smogorzewska, A. and de Lange, T. (2004) Homologous recombination generates T-loop-sized deletions at human telomeres. *Cell*, **119**, 355–368.

Watson, J.M. and Shippen, D.E. (2007) Telomere rapid deletion regulates telomere length in *Arabidopsis thaliana*. *Mol. Cell. Biol.* **27**, 1706–1715.

Wienand, U. and Feix, G. (1980) Zein specific restriction enzyme fragments of maize DNA. *FEBS Lett.* **116**, 14–16.

Zellinger, B., Akimcheva, S., Puizina, J., Schirato, M. and Riha, K. (2007) Ku suppresses formation of telomeric circles and alternative telomere lengthening in Arabidopsis. *Mol. Cell*, **27**, 163–169.

A3 Gernand, D., Demidov, D., and Houben, A. (2003). The temporal and spatial pattern of histone H3 phosphorylation at serine 28 and serine 10 is similar in plants but differs between mono- and polycentric chromosomes. Cytogenet Genome Res 101, 172-176.

Cytogenet Genome Res 101:172–176 (2003)
DOI: 10.1159/000074175

Cytogenetic and Genome Research

The temporal and spatial pattern of histone H3 phosphorylation at serine 28 and serine 10 is similar in plants but differs between mono- and polycentric chromosomes

D. Gernand, D. Demidov and A. Houben

Institute of Plant Genetics and Crop Plant Research (IPK), Gatersleben (Germany)

Abstract. Immunolabeling using site-specific antibodies against phosphorylated histone H3 at serine 10 or serine 28 revealed in plants an almost similar temporal and spatial pattern of both post-translational modification sites at mitosis and meiosis. During the first meiotic division the entire chromosomes are highly H3 phosphorylated. In the second meiotic division, like in mitosis, the chromosomes contain high phosphorylation levels in the pericentromeric region and very little H3 phosphorylation along the arms of monocentric species. In the polycentric plant *Luzula luzuloides* phosphorylation at both serine positions occurs along the whole chromosomes, whereas in monocentric species, only the pericentromeric regions showed strong signals from mitotic prophase to telophase. No phosphorylated serine 10 or serine 28 was detectable on single chromatids at anaphase II resulting from equational segregation of rye B chromosome univalents during the preceding anaphase I. In addition, we found a high level of serine 28 as well as of serine 10 phosphorylation along the entire mitotic monocentric chromosomes after treatment of mitotic cells using the phosphatase inhibitor cantharidin. These observations suggest that histone H3 phosphorylation at serine 10 and 28 is an evolutionarily conserved event and both sites are likely to be involved in the same process, such as sister chromatid cohesion.

The cell cycle-dependent phosphorylation of histone H3 at serine 10 is conserved in eukaryotes. This dynamic post-translational modification has been linked to transcription activation (reviewed in Thomson et al., 1999) and to chromosome condensation and segregation (reviewed in Fabienne and Dimitrov, 2001). Observations in several organisms have shown that the levels of H3 phosphorylation, which are very low at interphase, increase substantially at the beginning of cell division and decrease again during telophase (Gurley et al., 1975, Wei and Allis, 1998). Using a site- and phosphorylation state-specific antibody (Hendzel et al., 1997) it was shown that in protozoa, nematodes, insects and mammals phosphorylated H3 at serine position 10 is distributed homogeneously throughout the chromosomes both in mitosis and meiosis. In plants, phosphorylation levels are high in pericentromeric regions but very low along the chromosome arms during mitosis (Houben et al., 1999). The pericentromere-specific distribution of phosphorylated (Ser10)H3 is altered by cold treatment and exposure to the phosphatase inhibitor cantharidin (Manzanero et al., 2002).

In plants the distribution of (Ser10)H3 phosphorylation varies at first and second meiotic division (Manzanero et al., 2000). During the first meiotic division the entire chromosomes are highly phosphorylated, whereas at the second meiotic division the H3 phosphorylation is restricted to the pericentromeric regions. At the same time single chromatids, resulting from equational division of univalents at anaphase I, show low levels of phosphorylation all over. These results led to the hypothesis that H3 phosphorylation is involved in sister chromatid cohesion, supported by the observation of Kaszás and Cande (2000) who showed that in a maize mutant defective in sister chromatid cohesion, univalents at metaphase I showed

D.D. and A.H. were supported by Deutsche Forschungsgemeinschaft, grant Ho 1779/2-2.

Received 25 March 2003; manuscript accepted 13 May 2003.

Request reprints from Andreas Houben
Institute of Plant Genetics and Crop Plant Research (IPK)
DE–06466 Gatersleben (Germany); telephone: +49 394825486
fax: +49 394825136; e-mail: houben@ipk-gatersleben.de

0301–0171/03/1012–0172$19.50/0

Accessible online at:
www.karger.com/cgr

high phosphorylation only in the pericentromeric regions. The genes involved in this post-translational modification of histone H3 in plants are still unknown.

Goto et al. (1999) have reported that in mammals during mitosis histone H3 is phosphorylated not only at Ser10, but also at Ser28 and that Aurora-B kinase directly phosphorylates H3 at both serine positions (Goto et al., 2002; Sugiyama et al., 2002). Immunocytochemical studies with antibodies against phosphorylated (Ser28)H3 and biochemical analysis showed that in mammals (Ser28)H3 phosphorylation occurs predominantly during early mitosis coinciding with the initiation of mitotic chromosome condensation. Only limited information is available on the function of H3 serine 28 phosphorylation. It is unknown whether this modification occurs during cell divisions in plants.

In the present study we compared the chromosomal distribution of phosphorylated histone H3 at serine positions 10 and 28 during mitotic and meiotic divisions in several plant species. To investigate whether the dynamics of histone H3 phosphorylation differs between chromosomes with different types of centromeres or in dependence on the mode of segregation, we included mono- and polycentric chromosomes and studied also meiotic cells of individuals forming bivalents and univalents (B chromosomes). In addition, we used the protein phosphatase inhibitor – cantharidin to compare the response of dividing plant cells with regard to H3 phosphorylation at Ser10 and Ser28.

Materials and methods

Plant material

The following plant species have been used: (i) *Arabidopsis thaliana*, (ii) *Luzula luzuloides* (kindly provided by the Botanical Garden of the Martin Luther University, Halle-Wittenberg), (iii) barley *(Hordeum vulgare)* and (iiii) rye *(Secale cereale)* from the Korean population Paldang which contains B chromosomes in 20 % of the individuals (Manzanero et al., 2000).

Cantharidin treatment

Seedlings of barley were transferred to filter paper soaked in 50 μM cantharidin (CALBIOCHEM) dissolved in 0.1 % dimethyl sulfoxide (DMSO) in water, for 3 h, prior to fixation according Manzanero et al. (2002). Cantharidin is a specific inhibitor of both PP2A and PP1, inhibiting PP2A at lower concentrations than necessary for PP1 (MacKintosh and MacKintosh, 1994).

Chromosome preparation and indirect immunofluorescence

Preparation of mitotic and meiotic chromosomes and immunostaining were carried out following the method described by Manzanero et al. (2000). To avoid non-specific antibody binding, slides were blocked for 30 min in 4 % (w/v) bovine serum albumine (BSA), 0.1 % Triton X100 in phosphate-buffered saline (PBS) at room temperature prior to two washes in PBS for 5 min each, and incubated with the primary antibodies in a humid chamber. Polyclonal rabbit antibody against histone H3 phosphorylated at serine 10 (ph(Ser10)H3, Upstate Biotechnology, USA) and a rat monoclonal antibody against H3 phosphorylated at serine 28 (ph(Ser10)H3), Goto et al., 1999) were diluted 1:400 in PBS with 3 % BSA. After a 12 h incubation at 4 °C and washing for 15 min in PBS, the slides were incubated in rhodamine-conjugated anti-rabbit IgG (Dianova) and FITC-conjugated anti-rat IgG (Dianova) diluted 1:200 in PBS, 3 % BSA for 1 h at 37 °C. After final washes in PBS, the preparations were mounted in antifade containing 4′,6-diamidino-2-phenylindole (DAPI) as counterstain.

Imaging of immunofluorescence was performed using an Olympus BX61 microscope and an ORCA-ER CCD camera (Hamamatsu). Deconvolution microscopy was employed for superior optical resolution of globular structures. Thus each photograph was collected as sequential image along the Z-axis with approximately 11 slices per specimen. All images were collected in grey scale and pseudocoloured with Adobe Photoshop, and projections (maximum intensity) were done with the program AnalySIS (Soft Imaging System).

Results

The histone H3 serine 28 phosphorylation revealed an immunofluorescence pattern similar but not identical to that observed for histone H3 serine 10 phosphorylation

Mitotic cells of the monocentric species *A. thaliana* (Fig. 1a–c), *H. vulgare* (Fig. 1d) and *T. aestivum* (Fig. 1e) were simultaneously labelled with antibodies recognizing histone H3 phosphorylated at serine 10 and serine 28. In all species examined, no immunostaining of interphase nuclei was observed. Distinct ph(Ser10)H3-immunofluorescence signal clusters became visible first at the beginning of chromosome condensation at early prophase, while ph(Ser28)H3 distribution was more diffuse at that stage (Fig. 1a). Distinct ph(Ser28)H3-signals become detectable at a later phase of prophase (Fig. 1b). At meta- and anaphase, the pericentromeric region is H3 serine 10 hyperphosphorylated, whereas ph(Ser28)H3-signals were confined strictly to the central part of the pericentromeric region (Fig. 1c–e). With the decondensation of the chromosomes at telophase, the phosphorylated serine 28 immunoreactivity disappears towards interphase faster than that of serine 10. These results suggest that the temporal and spatial phosphorylation pattern of H3 at both serine positions is generally similar but at serine 28 phosphorylation starts later and disappears earlier.

The distribution of phosphorylated histone H3 differs between mono- and polycentric chromosomes

To investigate whether the type of centromeres affects the distribution of histone H3 phosphorylated at serine 10 or serine 28, the mitotic chromosomes of *L. luzuloides* were investigated. The kinetochores of the polycentric Juncaceae *L. luzuloides* have a continuous distribution along the length of the chromosomes (Braselton, 1971). Such chromosomes bind to microtubules along their entire length and sister chromatids move in parallel position to the poles (Madej et al., 1998). The temporal pattern of H3 phosphorylation at both serine positions was the same for mitotic mono- and polycentric species. However, in contrast to chromosomes of monocentric species (Fig. 1a–e), the rod-shaped chromosomes of *L. luzuloides* were uniformly ph(Ser10/28)H3-immunolabeled (Fig. 1f). This implies that the distribution of phosphorylated histone H3 correlates with the chromosomal distribution of active centromeres.

The protein phosphatase inhibitor cantharidin increases the level of histone H3 phosphorylation at serine 10 as well as at serine 28 along mitotic chromosomes

The phosphatase inhibitor cantharidin perturbs the balance between phosphorylation and dephosphorylation of histone H3 at serine 10 (Manzanero et al., 2002). To assess the effects of cantharidin on the phosphorylation of histone H3 at position serine 28, we treated barley seedlings with 50 μM cantharidin, for 3 h. Cantharidin-treated interphase cells were only weakly

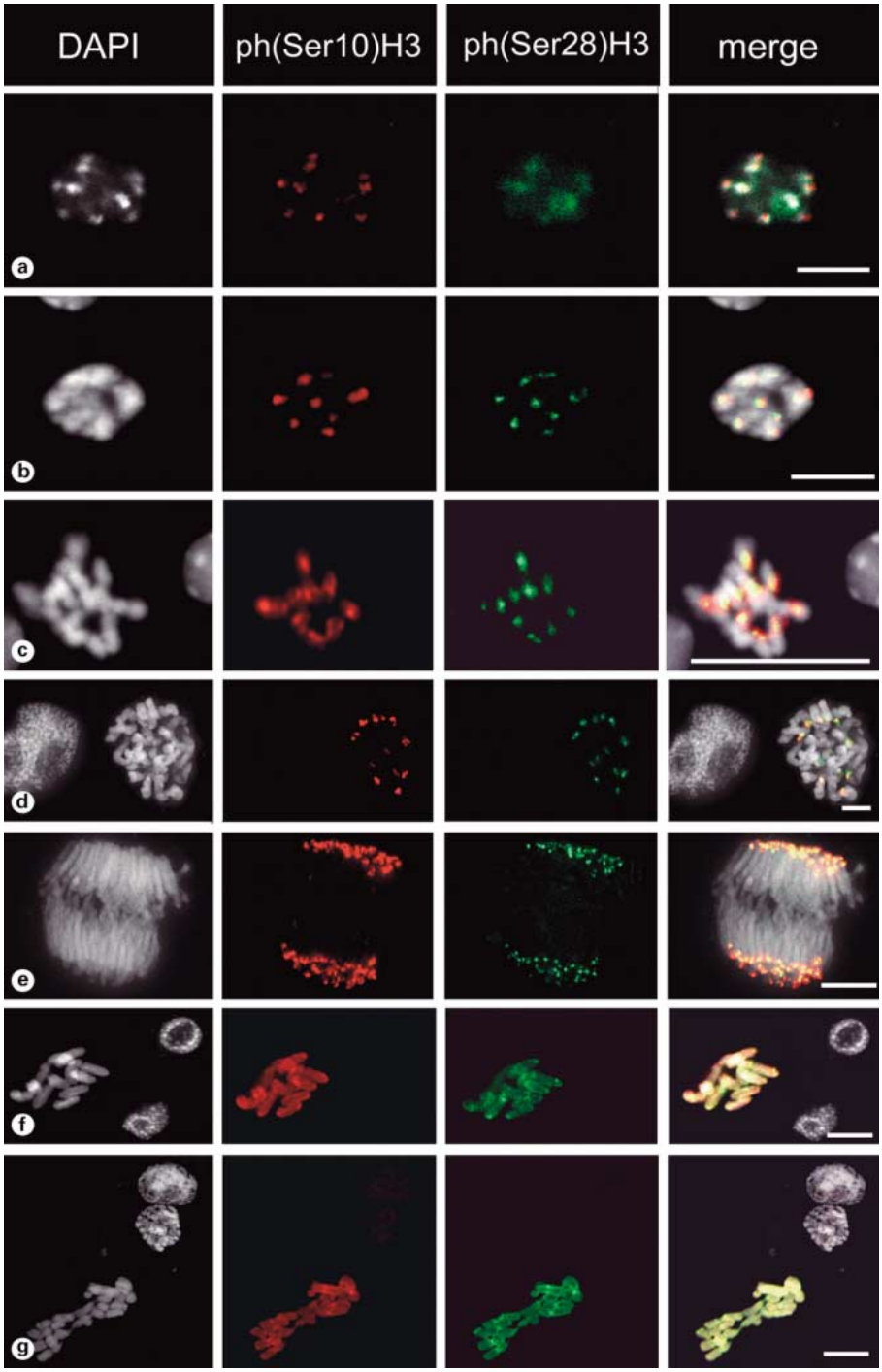

Fig. 1. Immunolabelling of phosphorylated histone H3 at serine 10 (ph(Ser10)H3) or serine 28 (ph(Ser28)H3) during mitosis of the monocentric species *Arabidopsis thaliana* (**a–c**), *Hordeum vulgare* (**d**, **g**), *Triticum aestivum* (**e**) and the polycentric species *Luzula luzuloides* (**f**). In (**g**) *Hordeum vulgare* after 3 h treatment with 50 µM of the protein phosphatase inhibitor cantharidin. DNA counterstained with DAPI (grey scale); phosphorylated (Ser10)H3 in red; phosphorylated (Ser28)H3 in green. Bars represent 10 µm.

immunolabelled, comparable to untreated cells (Fig. 1g). However in mitosis, cantharidin modified the chromosomal distribution of phosphorylated H3 at both serine positions. As described by Manzanero et al. (2002) for serine 10, almost all chromosomes (Fig. 1g) displayed uniform distribution of phosphorylated H3 at serine 28. Thus, cantharidin may disturb directly or indirectly an ordered sequence of phosphorylation and dephosphorylation of serine residues 10 and 28 of histone H3.

The histone H3 phosphorylation pattern of serine 28 differs between formerly reductionally and equationally divided univalents during the second meiotic division

The immunolabelling patterns for the different stages of meiosis were studied for *S. cereale*. The first diffuse ph(Ser10)H3-immunosignals were detectable during the transition from leptotene to zygotene as reported by Manzanero et al. (2000). With the further compaction of chromosomes during diakinesis, immunosignals specific for phosphorylated H3 at

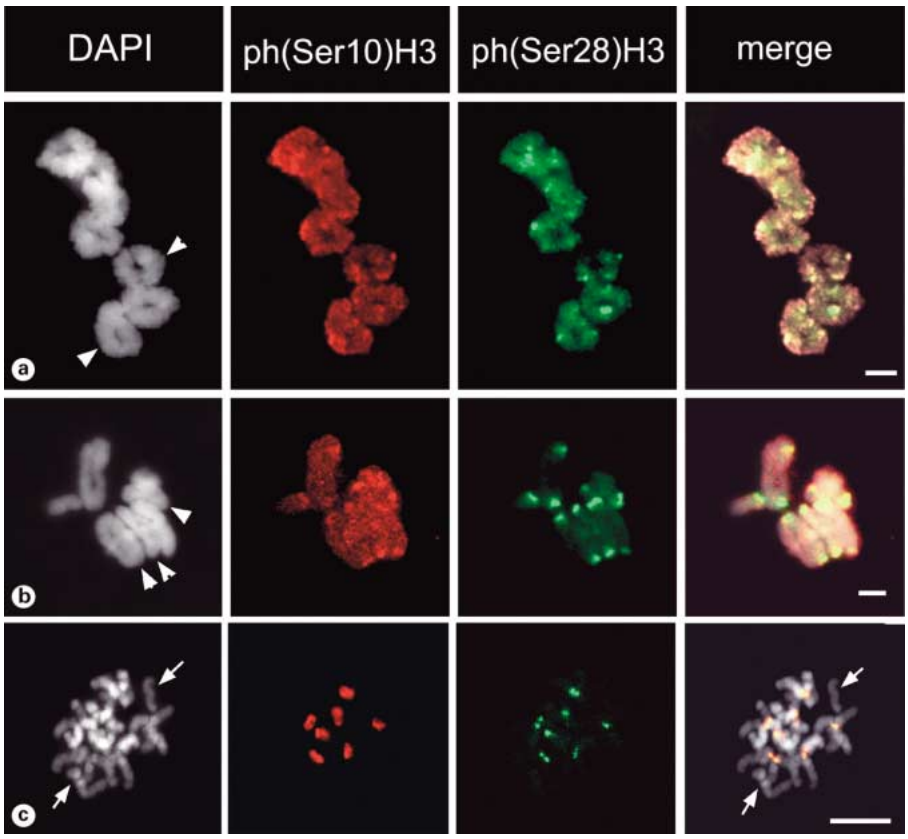

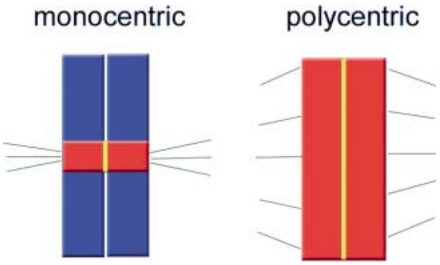

Fig. 3. Model of mitotic monocentric and polycentric chromosomes. Distribution of phosphorylated (Ser10/Ser28) H3 (in red) correlates with the distribution of pericentromeric chromatin in mono- and polycentric species and the assumed positions of sister chromatid cohesion (in yellow). Microtubules are indicated as green lines.

Fig. 2. Immunolocalization of phosphorylated histone H3 at serine 10 (ph(Ser10)H3) or serine 28 (ph(Ser28)H3) during meiosis of *Secale cereale.* Diakinesis (**a**), metaphase I (**b**) and metaphase II with prematurely separated (arrowed) B chromosome chromatids (**c**). DNA counterstained with DAPI (grey scale); phosphorylated (Ser10)H3 in red; phosphorylated (Ser28)H3 in green. A number of centromere positions are indicated by arrow heads. Bars represent 10 µm.

serine 10 and 28 were scattered over the chromosomes (Fig. 2a). At this stage histone H3 of the centromeric regions appeared to be slightly stronger phosphorylated at both serine positions than the rest of the chromosomes. At metaphase I, congressed bivalents were entirely and strongly ph(Ser10)H3-immunolabeled (Fig. 2b), whereas phosphorylation of serine 28 was mainly confined to the pericentromeric regions. At telophase I (not shown), the phosphorylation of histone H3 at both serine positions gradually disappeared towards interkinesis. During the second meiotic divisions the phosphorylation patterns were similar to those observed during mitosis, where mainly the pericentromeric regions are immunolabeled at metaphase and anaphase. Chromosomes were H3 hyperphosphorylated at both serine positions only in the centromeric regions (Fig. 2c).

To investigate whether the dynamics of histone H3 phosphorylation at both serine positions differs between chromosomes with different modes of segregation at meiosis, we included meiotic cells of individuals forming bivalents plus univalents. B chromosomes of rye form up to 66 % univalents at metaphase I (Manzanero et al., 2000). A high proportion of B chromosome univalents were syntelically oriented and migrated reductionally to the poles at anaphase I. The amphitelically oriented univalents divided equationally at anaphase I, with sister chromatids separating to different poles. During the first meiotic division, H3 phosphorylation at both serine positions was identical for equationally and reductionally dividing chromosomes. Single B chromosome chromatids are easily detected by their centromere position at the metaphase II plate of the second meiotic division (arrowed in Fig. 2c). They were condensed in a similar manner as the sister chromatids of reductionally divided chromosomes. However, the immunostaining revealed that, within the same metaphase II cell, only the seven chromosomes consisting of two sister chromatids had strong signals at their pericentromeric regions, whereas single B chromatids showed no immunosignal at either serine position 10 or 28 (Fig. 2c).

Discussion

The novel finding of this study is that histone H3 is phosphorylated not only at serine 10 but also at serine 28 during mitosis and meiosis of plants, similarly as described for mammals (Goto et al., 1999, 2002). Thus, this post-translational modification must be conserved during the evolution of plants and animals. While in mammals the entire chromosomes undergo H3 phosphorylation at both serine positions (Goto et al., 1999, 2002) in all monocentric plants analysed, these histone modifications are confined to the pericentromeric regions during mitosis. Also in plants, the degree and duration of serine 28 phosphorylation was less than that of serine 10 phosphorylation. However only in plants the treatment of dividing cells with the protein phosphatase inhibitor cantharidin caused similarly high phosphorylation of serine 10 and 28 along whole chromosome arms, as opposed to just the pericentromeric area

in control cells. In mammals, phosphorylated serine 28 is much more sensitive to phosphatases than serine 10 (Goto et al., 1999, 2002). After treatment with calyculin A, a phosphatase inhibitor of PP1 and PP2A, serine 28 phosphorylation emerges in late G_2 cells. This was not observed in plants after treatment with cantharidin. This may be partly due to the different phosphatase inhibitors used or due to differences between the species analysed.

The distribution of phosphorylated histone H3 correlates with the position of centromeres in mono- and polycentric species. In monocentric species the phosphorylation of H3 occurs only at the defined pericentromeric regions and in the polycentric *L. luzuloides* histone H3 phosphorylation occurs along the entire length of the chromosomes. The present and our previous results (Houben et al., 1999; Manzanero et al., 2000, 2002) support the hypothesis that H3 phosphorylation is involved in sister chromatid cohesion rather than in chromosome condensation. Phosphorylation of histone H3 occurs where sister chromatids cohere until the onset of anaphase – in polycentric chromosomes cohesion occurs along the entire chromatid arms, in monocentrics only at a single chromosome region (Fig. 3). Single chromatids that result from equational segregation of univalents during the first meiotic division lack immunosignals during meiosis II but show the same degree of condensation as chromatids resulting from bivalents. Since no reduplication of chromosomes occurs at interkinesis, such chromatids have no sister with which to cohere and therefore need not, or cannot, be H3 phosphorylated at the pericentromeric chromatin.

Acknowledgments

We are grateful to Margit Hantschmann and Katrin Kumke for excellent technical assistance. The antibody against H3 phosphorylated at serine 28 was kindly provided by Dr. M. Inagaki.

References

Braselton JT: The ultrastructure of non-localized kinetochores of *Luzula* and *Cyperus*. Chromosoma 36:89–99 (1971).

Fabienne H, Dimitrov S: Histone H3 phosphorylation and cell division. Oncogene 20:3021–3027 (2001).

Goto H, Tomono Y, Ajiro K, Kosako H, Fujita M, Sakurai M, Okawa K, Iwamatsu A, Okigaki T, Takahashi T, Inagaki M: Identification of a novel phosphorylation site on histone H3 coupled with mitotic chromosome condensation. J biol Chem 274:25543–25549 (1999).

Goto H, Yasui Y, Nigg EA, Inagaki M: Aurora-B phosphorylates Histone H3 at serine 28 with regard to the mitotic chromosome condensation. Genes Cells 7:11–17 (2002).

Gurtley LR, Walters RA, Tobey RA: Sequential phosphorylation of histone subfractions in the Chinese hamster cell cycle. J biol Chem 250:43936–43944 (1975).

Hendzel MJ, Wei Y, Mancini A, Van Hooser A, Ranalli T, Brinkley BR, Bazett-Jones DP, Allis CD: Mitosis-specific phosphorylation of histone H3 initiates primarily within pericentromeric heterochromatin during G_2 and spreads in an ordered fashion coincident with mitotic chromosome condensation. Chromosoma 106:348–360 (1997).

Houben A, Wako T, Furushima-Shimogawara R, Presting G, Künzel G, Schubert I, Fukui, K: The cell cycle dependent phosphorylation of histone H3 is correlated with the condensation of plant mitotic chromosomes. Plant J 18:675–679 (1999).

MacKintosh C, MacKintosh RW: Inhibitors of protein kinases and phosphatases. Trends Biochem Sci 19:444–448 (1994).

Madej A: Spindle microtubules and chromosome behavior in mitosis of *Luzula luzuloides*, a species with holokinetic chromosomes. Acta biol Cracov Ser Bot 40:61–67 (1998).

Manzanero S, Rutten T, Kotseruba V, Houben A: Alterations in the distribution of histone H3 phosphorylation in mitotic plant chromosomes in response to cold treatment and the protein phosphatase inhibitor cantharidin. Chrom Res 10:467–476 (2002).

Manzanero S, Arana P, Puertas MJ, Houben A: The chromosomal distribution of phosphorylated histone H3 differs between plants and animals at meiosis. Chromosoma 109:308–317 (2000).

Kaszás E, Cande WZ: Phosphorylation of histone H3 is correlated with changes in the maintenance of sister chromatid cohesion during meiosis in maize, rather than the condensation of the chromatin. J Cell Sci 113:3217–3226 (2000).

Sugiyama K, Sugiura K, Hara T, Sugimoto K, Shima H, Honda K, Furukawa K, Yamashita S, Urano T: Aurora-B associated protein phosphatases as negative regulators of kinase activation. Oncogene 21:3103–3111 (2002).

Thomson S, Mahadevan LC, Clayton AL: MAP kinase-mediated signalling to nucleosomes and immediate-early gene induction. Semin Cell Dev Biol 10:205–214 (1999).

Wei Y, Allis CD: A new marker for mitosis. Trends Cell Biol 8:266 (1998).

A4 Gernand, D., Rutten, T., Varshney, A., Rubtsova, M., Prodanovic, S., Bruss, C., Kumlehn, J., Matzk, F., and Houben, A. (2005). Uniparental chromosome elimination at mitosis and interphase in wheat and pearl millet crosses involves micronucleus formation, progressive heterochromatinization, and DNA fragmentation. Plant Cell 17, 2431-2438.

This article is published in *The Plant Cell* Online, *The Plant Cell* Preview Section, which publishes manuscripts accepted for publication after they have been edited and the authors have corrected proofs, but before the final, complete issue is published online. Early posting of articles reduces normal time to publication by several weeks.

Uniparental Chromosome Elimination at Mitosis and Interphase in Wheat and Pearl Millet Crosses Involves Micronucleus Formation, Progressive Heterochromatinization, and DNA Fragmentation

Dorota Gernand, Twan Rutten, Alok Varshney, Myroslava Rubtsova,[1] Slaven Prodanovic,[2] Cornelia Brüß, Jochen Kumlehn, Fritz Matzk, and Andreas Houben[3]

Institute of Plant Genetics and Crop Plant Research, D-06466 Gatersleben, Germany

Complete uniparental chromosome elimination occurs in several interspecific hybrids of plants. We studied the mechanisms underlying selective elimination of the paternal chromosomes during the development of wheat (*Triticum aestivum*) × pearl millet (*Pennisetum glaucum*) hybrid embryos. All pearl millet chromosomes were eliminated in a random sequence between 6 and 23 d after pollination. Parental genomes were spatially separated within the hybrid nucleus, and pearl millet chromatin destined for elimination occupied peripheral interphase positions. Structural reorganization of the paternal chromosomes occurred, and mitotic behavior differed between the parental chromosomes. We provide evidence for a novel chromosome elimination pathway that involves the formation of nuclear extrusions during interphase in addition to postmitotically formed micronuclei. The chromatin structure of nuclei and micronuclei is different, and heterochromatinization and DNA fragmentation of micronucleated pearl millet chromatin is the final step during haploidization.

INTRODUCTION

After interspecific fertilization, two different parental genomes are combined within one nucleus, which, in most cases, is embedded within the maternal cytoplasm. Such a novel genomic constitution may result in intergenomic conflicts leading to genetic and epigenetic reorganization (Riddle and Birchler, 2003). Even if in most cases the parental genomes remain combined after a successful fertilization, an elimination of specific DNA sequences frequently follows in the early stages of allopolyploidization (Liu et al., 1996; Feldman et al., 1997). In grasses, a partial somatic elimination of chromosomes from one parental species may occur, for example, in wide crosses of *Hordeum lechleri* × *H. vulgare* (Linde-Laursen and von Bothmer, 1999), *Avena sativa* × *Zea mays* (Riera Lizarazu et al., 1996), or *Triticum aestivum* × *H. vulgare* (Barclay, 1975). Complete uniparental chromosome elimination also occurs in some interspecific hybrids between closely related species (as *H. vulgare* or *H. parodii* × *H. bulbosum* and *H. marinum* × *H. vulgare*; Kasha and Kao, 1970; Subrahmanyam, 1977; Finch, 1983) as well as between remotely related parental species (*Aegilops* spp, ryegrass [*Lolium multiflorum*], barley, oat, rye [*Secale cereale*], or wheat × *Pennisetum glaucum*, *Sorghum bicolor*, *Tripsacum dactyloides*, or *Z. mays*; Zenkteler and Nitzsche, 1984; Laurie and Bennett, 1986, 1988; Rines and Dahleen, 1990; Chen and Hayes, 1991; Matzk and Mahn, 1994; Matzk, 1996; Matzk et al., 1997).

Crosses between wheat and maize and between *H. vulgare* × *H. bulbosum* are used for generating homozygous doubled haploid wheat and barley plants, respectively, from heterozygous maternal plants. The elimination rate of *H. bulbosum* chromosomes in *H. vulgare* × *H. bulbosum* hybrid embryos is affected by temperature (Pickering, 1985; Pickering and Morgan, 1985) and by the ploidy level of the *H. bulbosum* genome (Ho and Kasha, 1975). A tissue-specific elimination of alternative whole parental genomes was observed in the embryo and endosperm of *H. marinum* × *H. vulgare* crosses (Finch, 1983). Elimination of parental chromosomes has also been observed in somatically produced wide hybrids. In these cases, the elimination tends to be irregular and incomplete, leading to asymmetric hybrids or cybrids (Liu et al., 2005). In several metazoa, such as nematodes, copepods, sciarid flies (Goday and Ruiz, 2002), hagfish, and marsupials, chromatin/chromosome elimination is part of normal cell differentiation and/or sex determination (Kloc and Zagrodzinska, 2001).

Several hypotheses have been presented to explain uniparental chromosome elimination during hybrid embryo development in plants, for example, differences in timing of essential mitotic processes due to asynchronous cell cycles (Gupta, 1969) or asynchrony in nucleoprotein synthesis leading to a loss of the most retarded chromosomes (Bennett et al., 1976; Laurie and Bennett, 1989). Other hypotheses propose the formation of multipolar spindles (Subrahmanyam and Kasha, 1973), spatial

[1] Current address: ICON Genetics GmbH, 06120 Halle, Germany.
[2] Current address: Faculty of Agriculture, 11080 Belgrade, Serbia and Montenegro.
[3] To whom correspondence should be addressed. E-mail houben@ipk-gatersleben.de; fax 49-039482-5137.
The author responsible for distribution of materials integral to the findings presented in this article in accordance with the policy described in the Instructions for Authors (www.plantcell.org) is: Andreas Houben (houben@ipk-gatersleben.de).
Article, publication date, and citation information can be found at www.plantcell.org/cgi/doi/10.1105/tpc.105.034249.

separation of genomes during interphase (Finch and Bennett, 1983; Linde-Laursen and von Bothmer, 1999) and metaphase (Schwarzacher-Robinson et al., 1987), parent-specific inactivation of centromeres (Finch, 1983; Kim et al., 2002; Jin et al., 2004; Mochida et al., 2004), and by analogy with the host-restriction and modification systems of bacteria (Boyer, 1971), degradation of alien chromosomes by host-specific nuclease activity (Davies, 1974).

Initial cytological studies revealed a rapid preferential uniparental chromosome loss by formation of micronuclei during mitosis in early hybrid embryos (Kasha and Kao, 1970). Chromosomes destined for elimination often did not congregate properly at metaphase and lagged behind other chromosomes at anaphase (Laurie and Bennett, 1989). These observations are consistent with the classical mechanism of micronucleus formation, which involves the enclosure of lagging chromosome fragments during reformation of nuclear membranes at the end of mitosis (Heddle and Carrano, 1977; Schubert and Oud, 1997). It is not yet clear how the micronucleated paternal genome is finally eliminated.

This work provides a more detailed insight into the processes of selective elimination of paternal chromosomes during the development of wheat × pearl millet hybrid embryos. The selective elimination of pearl millet chromosomes was found to consist of consecutive steps: parental interphase chromatin separation, micronucleus formation, heterochromatinization, and DNA fragmentation of micronucleated chromatin. In addition to mitotic micronucleus formation by nonsegregating chromatids, pearl millet chromatin-containing micronuclei are extruded directly from interphase nuclei.

RESULTS

The Elimination of Pearl Millet Chromatin in Developing Hybrid Embryos Is Sequential

First, we studied the distribution of pearl millet chromatin in morphologically well preserved 6-d-old wheat × pearl millet embryos by whole-mount genomic in situ hybridization (GISH) (Figures 1A and 1B). Wheat line S6, the female parent, carries a translocation (1B/1R) with the short arm of the rye chromosome 1R (Matzk et al., 1997). Therefore, as an internal control, GISH with differently labeled genomic DNA probes of pearl millet and rye yielded a rye-specific hybridization signal in almost all nuclei of the embryos independent of the developmental stage (Figures 1E and 1F). By contrast, the percentage of cells with a pearl millet–specific signal varied between embryos at different stages as well as between embryos at the same stage and between

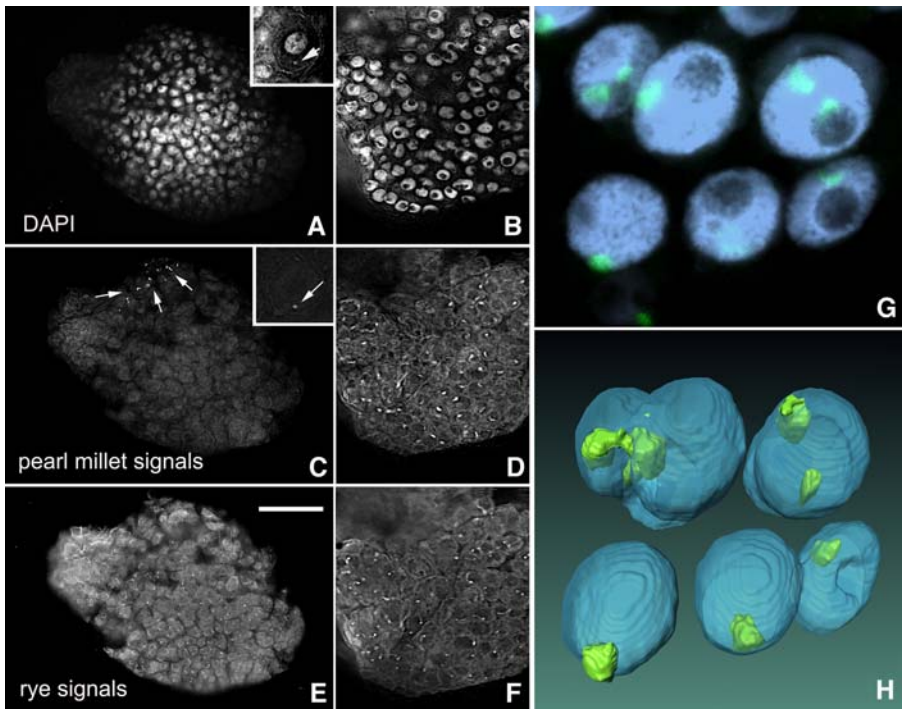

Figure 1. Distribution of Pearl Millet Chromatin in Wheat × Pearl Millet Embryos.

(A) to **(F)** Whole-mount GISH on two 4′,6-diamidino-2-phenylindole (DAPI)-stained 6-d-old wheat × pearl hybrid embryos (**[A]** and **[B]**) with pearl millet DNA (**[C]** and **[D]**) and rye DNA (**[E]** and **[F]**). Note that the proportion of cells with pearl millet chromatin varies between embryos of the same age. Pearl millet chromatin was within small (**[C]**, arrows) or large **(D)** cell clusters. Further enlarged cells with a pearl millet DNA-positive micronucleus (arrows) are shown in the insets in **(A)** and **(C)**. Rye-specific hybridization signals are clearly visible in almost all embryonic nuclei (**[E]** and **[F]**). Bar in **(E)** = 50 μm. **(G)** and **(H)** Selected interphase nuclei after whole-mount GISH with labeled pearl millet DNA before **(G)** and after **(H)** three-dimensional modeling. Pearl millet chromatin (in green) occupies a predominantly peripheral position. The DAPI-stained wheat chromatin is indicated in blue.

different regions of individual embryos. Irrespective of the region within the embryo, the pearl millet–specific signals were detected in small (Figure 1C) or large (Figure 1D) cell clusters. Pearl millet–positive chromatin was observed inside and/or outside the major nucleus during interphase. The external hybridization signals coincided with the positions of one or more additional micronuclei (Figures 1A and 1C, insets). Inside the nucleus, the pearl millet chromatin usually occupied one or two spherical or spindle shaped territories (Figures 1G and 1H). Three-dimensional reconstruction of interphase nuclei clearly demonstrated that the parental genomes were spatially separated and tended to occupy distinct domains within the interphase nuclei. Pearl millet chromatin destined for elimination was found to occupy peripheral positions (Figure 1H). In contrast with the more condensed pearl millet chromatin, the rye chromatin revealed a partly decondensed string-like appearance.

To analyze the temporal progression of chromosome elimination during embryo development, GISH was performed on 83 squash preparations made from embryos 6 to 23 d after pollination (DAP). The number of pearl millet chromatin-containing nuclei decreased during embryo development in a manner that varied among embryos of the same stage (Figure 2). The highest percentage (30%) of cells containing pearl millet–positive micronuclei was observed in embryos 6 to 8 DAP. In embryos 17 to 23 DAP, micronuclei were only occasionally observed. Pearl millet–specific signals were detected only in a few cell clusters of embryos older than 19 d, suggesting that a minority of pearl millet chromatin undergoes a slow rate of elimination that allows it to be retained for a long period. To test whether or not elimination was completed, DNA gel blot hybridization with a pearl millet centromere-specific repeat as a probe was performed on DNA from potted plants. Eight out of 178 young plantlets still revealed weak pearl millet–specific signals. When the same plants were reanalyzed at the mature stage, no signals remained.

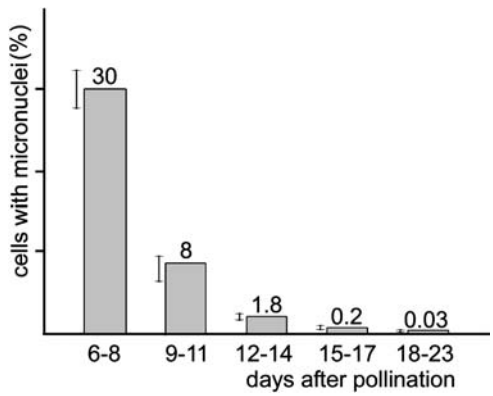

Figure 2. The Percentage of Cells Containing Micronuclei in Wheat × Pearl Millet Hybrid Embryos at Different Developmental Stages.

The histogram is based on the analysis of 1337 cells from 19 embryos 6 to 8 DAP, of 1573 cells from 10 embryos 9 to 11 DAP, of 4691 cells from 16 embryos 12 to 14 DAP, of 11,349 cells from 19 embryos 15 to 17 DAP, and of 12,858 cells from 19 embryos 18 to 23 DAP. The 95% confidence intervals are indicated as a bar to the left of each column.

Pearl Millet Chromosomes Are Structurally Rearranged and Become Reduced in Size in Hybrid Embryos

At mitosis, besides the standard type of metaphase chromosomes, dicentric pearl millet chromosomes of unusual size were identified after simultaneous hybridization with labeled genomic DNA and the pearl millet centromere-specific probe (Figures 3A and 3B). The additional centromere could result from a centric translocation or a chromosome fusion event. In interphase nuclei older than 17 DAP, most of the pearl millet chromosomes were reduced in size and displayed centromere-specific signals with no, or only minor, traces of chromosome arm-specific signals (Figures 3C and 3D). Pearl millet–specific chromatin without centromeric signals was observed in <1% of embryos. These observations indicate that pearl millet chromosomes are eliminated in portions with the centromere region remaining until last.

Pearl Millet Chromosomes Form Micronuclei during Cell Division as well as during Interphase

The mitotic behavior of pearl millet chromosomes was analyzed to determine whether micronuclei are formed exclusively by nonsegregating chromosomes as is usually assumed (Ford and Correll, 1992). The segregation behavior differed between pearl millet and wheat chromosomes. At anaphase, some pearl millet chromosomes lagged behind wheat chromosomes, and the sister chromatids segregated asymmetrically (Figure 3F). The level of chromosome condensation also partially differed between the parental genomes, with chromosomes of pearl millet often less condensed (Figure 3F, arrows). This observation is consistent with a loss of paternal chromosomes during cell division via lagging chromosomes that form micronuclei (Laurie, 1989; Mochida et al., 2004). In addition, pearl millet chromatin bodies similar to micronuclei in shape and size were found attached to the main interphase nuclei (Figures 3G and 3H), suggesting that they are extruded directly at interphase. Hence, budding of pearl millet chromatin seems to be another pathway of micronucleus formation and specific genome exclusion.

Alternatively, buds of pearl millet chromatin might represent micronuclei fusing with the main nucleus, but this would reverse the process of elimination. The size of micronuclei containing chromatin of pearl millet varied considerably (Figures 3I to 3L). To determine the number of pearl millet chromosomes per micronucleus, pearl millet centromere-specific probes were hybridized in situ together with labeled pearl millet genomic DNA. In >80% of micronuclei, one to three pearl millet centromeres were counted (Figure 3I), and in the early stages of embryo development (6 DAP), large micronuclei with up to seven pearl millet centromeres occurred (Figure 3J). Hence, the entire haploid pearl millet genome can either be eliminated concomitantly, either as individual chromosomes, or fused together prior to exclusion.

Micronuclei without centromeric sequences of pearl millet were rarely observed (0.5% of micronuclei; Figure 3L). Only 5% of the micronuclei also contained traces of maternal chromatin (Figure 3K), and those containing wheat chromatin alone were extremely rare (0.2% of micronuclei; data not shown). This indicates that the majority of micronuclei contained at least one pearl millet chromosome and possibly acentric chromosome fragments.

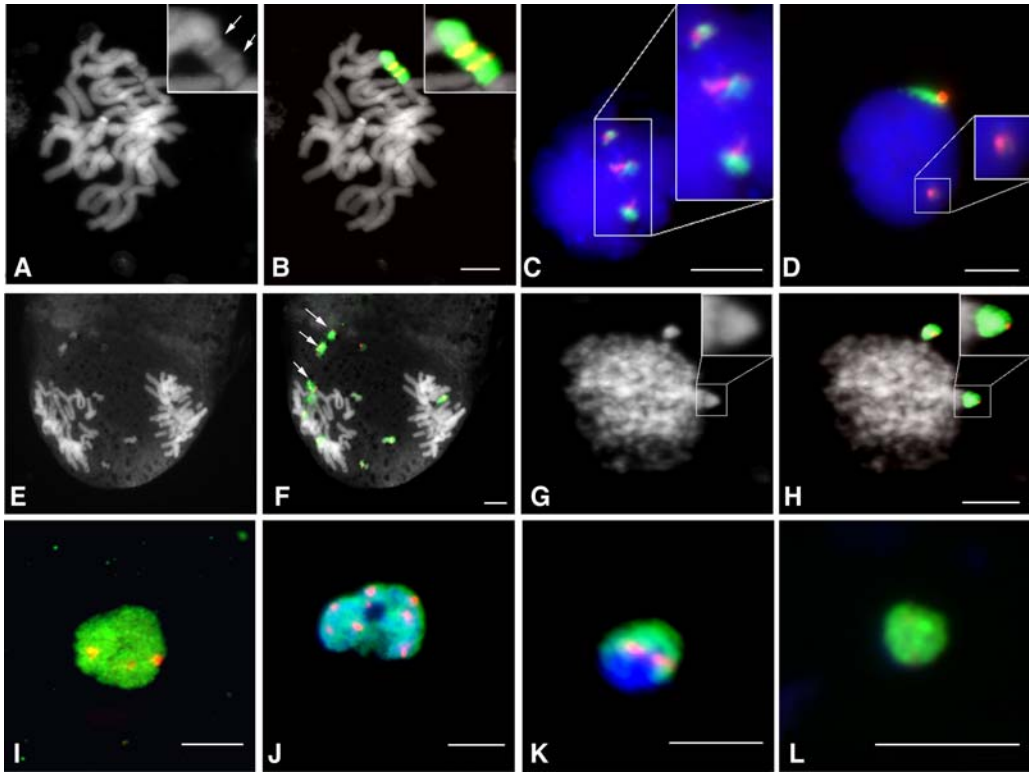

Figure 3. Elimination Process of Pearl Millet Chromosomes during Cell Division as well as during Interphase.

Dividing cells (**[A]**, **[E]**, and **[F]**), interphase nuclei (**[C]**, **[D]**, **[G]**, and **[H]**), and micronuclei (**[I]** to **[L]**) of wheat × pearl millet embryos after in situ hybridization with pearl millet genomic DNA (green) and pearl millet centromeric sequences (red). Note dicentric pearl millet chromosomes (**[A]** and **[B]**, arrows), exclusively labeled pearl millet centromeric signals **(D)**, and centromeric signals associated with very small amounts of pearl millet chromatin **(C)**. Anaphase with lagging asymmetric pearl millet chromosomes (**[E]** and **[F]**). Interphase nuclei with budding pearl millet chromatin (**[G]** and **[H]**). Centromere-containing micronuclei (**[I]** to **[K]**); centromere-free micronucleus **(L)**. The micronucleus in **(K)** contains traces of unlabeled wheat chromatin. Bars = 5 μm.

Chromatin Structure Differs between Nuclei and Micronuclei, and Degradation of Micronucleated DNA Is the Final Step in Chromosome Elimination

Ultrastructural studies showed that micronuclei are surrounded by a double membrane with nuclear pores like normal nuclei (Figures 4C and 4D, arrowheads). However, the different staining intensities of the heterochromatin between nuclei and micronuclei indicate a different degree of chromatin condensation. Micronuclei contained either exclusively heterochromatin (Figures 4A and 4C) or a mixture of euchromatin and heterochromatin (Figures 4B and 4D). The latter micronuclei resembled the normal nucleus of the same cell except that the heterochromatin was more dense (Figure 4B). These micronuclei were significantly larger than those that were predominantly heterochromatic (cf. Figures 4C and 4D).

To analyze the final step of elimination, the integrity of pearl millet DNA in micronuclei was tested by combining GISH with terminal dUTP nick end-labeling (TUNEL) assays. Some micronuclei with pearl millet chromatin displayed strong TUNEL signals (Figure 5), indicating that their DNA was strongly fragmented. No DNA cleavage was found in wheat chromatin-containing major nuclei. Apparently, pearl millet chromatin initially undergoes extensive fragmentation immediately prior to haploidization of the maternal genome. Together, the experimental results suggested a multistep model for pearl millet chromatin elimination from hybrid embryos (Figure 6).

DISCUSSION

The combined analyses of wheat × pearl millet crosses indicate that uniparental chromosome elimination in developing hybrid embryos occurs in a complex stepwise manner. We confirmed that mitotic chromosome elimination starts immediately after fertilization (Laurie and Bennett, 1989; Mochida et al., 2004), but contrary to previous reports, we found chromatin of both parental species still present in mature embryos. We show that heterochromatinization and DNA fragmentation in micronuclei formed by extrusion of paternal chromatin from interphase nuclei is involved in the pathway of haploidization, in addition to the formation of micronuclei after nonsegregation of paternal chromosomes or fragments during karyokinesis (Subrahmanyam and Kasha, 1973; Bennett et al., 1976; Thomas, 1988; Mochida and Tsujimoto, 2001; Mochida et al., 2004). On the one hand, the

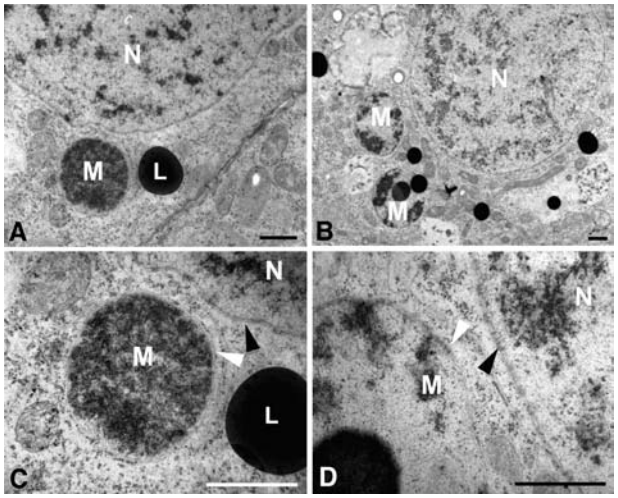

Figure 4. The Morphology of Nuclei and Micronuclei in Wheat × Pearl Millet Hybrid Embryos.

(A) The electron density of the small micronucleus (M) indicates a high content of heterochromatin compared with the nucleus (N). L, lipid droplet.
(B) Cell with two large micronuclei each containing a substantial amount of euchromatin.
(C) Higher magnification reveals double membranes surrounding the nucleus (black arrowhead) and the micronucleus (white arrowhead).
(D) Double membranes of nucleus and micronucleus with nuclear pores (black and white arrowheads); note that the heterochromatin of the micronucleus is more electron dense than that of the nucleus.
Bars = 1 μm.

elimination of pearl millet chromosomes was complete in adult plants, which is an important prerequisite for the generation of homozygous doubled haploid wheat plants. On the other hand, the observed late completion of elimination might increase the potential for chromatin introgression from pearl millet into wheat.

The distinct peripheral localization of the pearl millet chromatin during interphase may indicate that the interphase arrangement of both parental genomes differs. While wheat chromosomes follow the Rabl-orientation with centromeres clustered at one pole and telomeres at the opposite one (Dong and Jiang, 1998), chromosomes of pearl millet do not (our unpublished data). However, this difference cannot be a general reason for uniparental elimination of chromosomes in hybrids since chromosomes of both *H. vulgare* and *H. bulbosum* show Rabl-orientation, albeit that *H. bulbosum* chromosomes disposed at the periphery are often excluded from the daughter cells (Finch, 1983; Kim et al., 2002).

The selective degradation of pearl millet chromosomes could be triggered by asynchronous DNA replication of the two parental genomes. Inhibition of DNA replication induces DNA double strand breaks and genome rearrangements (Michel, 2000). Assuming that the timing of DNA replication differs between wheat and pearl millet as reported for the parental genomes of *Nicotiana tabacum* hybrids (Gupta, 1969), asynchrony of DNA replication may lead to breakages of pearl millet chromosomes. Subsequent rearrangements of the paternal genome might result in the observed dicentric or shortened pearl millet chromosomes. Alternatively, a hybridization-mediated genomic shock (McClintock, 1984) might trigger a genome-specific activation of mobile elements and thus cause structural chromosome aberrations as reported for artificial allopolyploids of *Arabidopsis thaliana* (Comai et al., 2000) and wheat (Kashkush et al., 2002) as well as for mammalian hybrids (O'Neill et al., 1998).

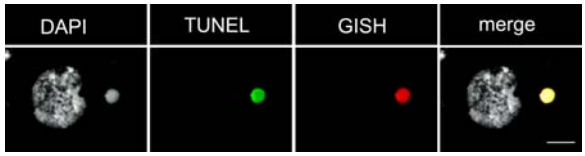

Figure 5. Interphase Nucleus of a Wheat × Pearl Millet Hybrid Embryo with a Micronucleus-Containing Pearl Millet Chromatin after TUNEL (Green) and GISH (Red) Experiments.

The TUNEL signal indicates fragmentation of micronucleated pearl millet DNA. Bar = 5 μm.

The centromere regions of pearl millet chromosomes are eliminated last. This might be due to its mobile and heterochromatic nature or to the absolute requirement for mitotic competence of surviving chromatin. If such a centric fragment is retained rather than lost during elimination of parental chromosomes, a subsequent spontaneous chromosome doubling could provide an ideal prerequisite for the de novo formation of supernumerary chromosomes, a scenario similar to that described in *Coix* (Sapre and Deshpande, 1987), where a B chromosome was generated spontaneously as a result of the crossing of two species.

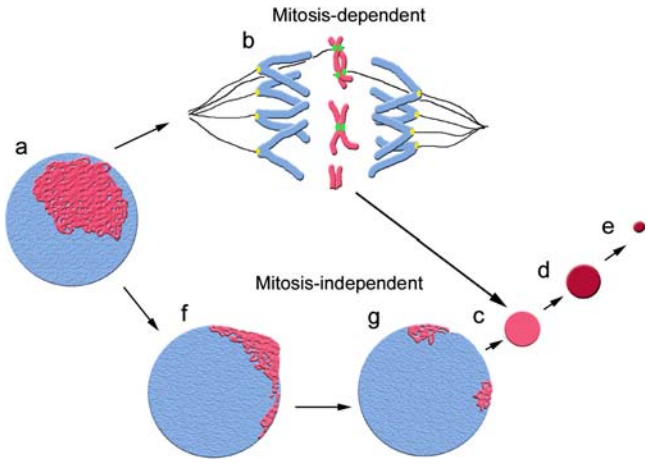

Figure 6. Schematic for the Mitotic and Interphase Elimination of Pearl Millet Chromosomes from Wheat × Pearl Millet Hybrid Embryos.

Mitotic elimination: (a) spatial separation of parental genomes; (b) imperfect segregation of pearl millet chromosomes caused by (1) faulty kinetochore/spindle fiber interaction, (2) the presence of an additional centromere, or (3) absence of a centromere; (c) formation of micronucleus; (d) heterochromatinization and DNA fragmentation of micronucleus; (e) disintegration of micronucleus. Interphase elimination: (a) spatial separation of parental genomes; (f) budding of pearl millet chromatin; (g) release of pearl millet chromatin-containing micronucleus; (c) formation of micronucleus; (d) heterochromatinization and DNA fragmentation of micronucleus; (e) disintegration of micronucleus.

Our finding of a selective elimination of pearl millet chromatin through extrusion from hybrid nuclei during interphase and subsequent micronucleation is consistent with the interpretation that nuclear buds containing extrachromosomal elements, such as double minutes, may form micronuclei in mammalian tumor cells during interphase (Shimizu et al., 1998; Tanaka and Shimizu, 2000). The striking similarities to a mechanism for formation of micronuclei in mammals may indicate an evolutionarily conserved process that allows intact maternal chromatin/DNA and alien chromatin/DNA to be distinguished and the latter to be removed from the nucleus. The detailed mechanism by which pearl millet chromatin is extruded through the nuclear double membrane remains unclear. In *Sciara* flies, the selective extrusion of chromosomes during interphase is accompanied by a local accumulation of rough endoplasmatic reticulum and mitochondria at the potential site of chromosome elimination. This is compatible with the idea of a localized membrane synthesis necessary to produce a nuclear bulge (Perondini and Ribeiro, 1997).

Our ultrastructural data indicate an increased condensation level of micronucleated chromatin and reveal a correlation between the size of micronuclei and the ratio of euchromatin and heterochromatin. Large micronuclei always contain a large amount of euchromatin, whereas small micronuclei are almost completely heterochromatic. It is tempting to speculate that these variations in ultrastructure reflect the gradual degradation of micronuclei from relatively large, euchromatin-containing structures into small strongly heterochromatic ones.

The process of elimination of micronuclei is similar, and partly analogous, to the events observed during programmed cell death. Nuclei undergoing an apoptosis-like death (Fukuda, 2000) and micronuclei with pearl millet chromatin exhibit similar features, such as chromatin condensation, nuclear shrinkage, and DNA fragmentation. The recognition and consecutive elimination of pearl millet DNA via micronuclei seem to be regulated processes. A specific chromatin topology possibly dictates endonuclease activation and genome-specific fragmentation. The drastic changes in the integrity of DNA and chromatin compaction during uniparental genome elimination suggest that posttranslational histone modification might play a role in promoting and directing these changes. Heterochromatinization and compaction of chromatin is associated with developmentally determined chromosome elimination in *Sciara*. Differential acetylation of histones H3 and H4 and methylation of histone H3 are candidate drivers of chromosome elimination in sciarid flies (Goday and Ruiz, 2002) and in the programmed DNA elimination process that accompanies macronuclear development in *Tetrahymena* (Taverna et al., 2002). For wheat × pearl millet embryos, it remains to be seen whether modification of histones or other chromatin proteins differs between the parental genomes.

METHODS

Plant Material, in Vitro Culture of Hybrid Zygotes, and Preparation of Embryos

The Salmon line (S6) of hexaploid wheat (*Triticum aestivum*, $2n = 6x = 42$) was used as female parent (Matzk et al., 1997). S6 carries a translocation of the short arm of rye (*Secale cereale*) chromosome 1R into wheat chromosome 1B (1B/1R). The accession PEN 5/78 (Institute of Plant Genetics and Crop Plant Research) of pearl millet (*Pennisetum glaucum*, $2n = 2x = 14$) was used as pollen donor. Wheat spikes were emasculated 1 to 2 d before anthesis and pollinated 1 d later with fresh pearl millet pollen or with dehiscing anthers (Kumlehn et al., 1997). In order to minimize the complexity of steps involved in the process of chromosome elimination, we kept the plant growing conditions constant at 16 h light with ~20°C and 8 h dark with ~14°C.

For isolation of hybrid zygotes, 2 to 4 h after hand-pollination, spikes were cut off and surface-sterilized for 10 min in 2.5% NaOCl solution supplemented with 0.01% Tween 20. Zygote isolation was performed as described (Kumlehn et al., 1997). Immature wheat pistils used for conditioning zygote cultures were isolated under sterile conditions from spikes that had emerged 2 to 4 cm from the flag leaf sheath. Zygotes were cultured in 12-mm Millicell inserts (Millipore); each zygote was placed into a 35-mm Petri dish containing 3 mL of N6Z medium (Kumlehn et al., 1998). Half of the medium used had been preconditioned for 2 weeks by culturing four immature wheat pistils per milliliter. Prior to zygote transfer, 200 μL of the culture medium was transferred from the Petri dish to the Millicell insert. Zygotes were taken up with a glass capillary with an opening diameter of 100 μm. The capillary was interfaced to a Cell Tram Vario (Eppendorf) by Teflon tubing filled with 0.55 M mannitol. Liquid uptake and release were regulated by manually operating the Cell Tram. The zygotes were released onto the semipermeable membrane of a Millicell insert. For further conditioning, six precultured wheat pistils were added per Petri dish outside the Millicell insert. All cultures were incubated in the dark at 24°C for 2 to 4 d.

Embryo development was stimulated by dipping the spikes into an aqueous solution of 50 ppm Dicamba (Sigma-Aldrich) 2 DAP. Embryo rescue was necessary to generate plants from mature embryos. Therefore, embryos were excised ~18 DAP and placed on Kruse medium under sterile conditions (Matzk and Mahn, 1994).

For in situ hybridization of in vivo–grown embryos, ovaries were dissected 6 to 23 DAP, fixed in ethanol:acetic acid (3:1), and stored at 4°C. To isolate the embryos, ovaries were stained with acetocarmine. Embryos were dissected in distilled water with fine needles under a stereomicroscope. For preparation of plant specimens, isolated embryos were squashed in 45% acetic acid between slide and cover slip.

Fluorescence in Situ Hybridization on Squashed and Whole-Mount Embryos and Construction of a Three-Dimensional Image

A member of the pearl millet centromere-specific sequence repeat family, pPgKB1 (Kamm et al., 1994), and total genomic DNA of pearl millet and rye were used as probes for fluorescence in situ hybridization (FISH) after labeling by nick translation with biotin-16-dUTP or digoxigenin-11-dUTP.

FISH on squashed embryos was performed as previously described (Houben et al., 2001). Briefly, 80 ng biotin/digoxigenin-labeled genomic DNA, 50 ng digoxigenin-labeled pearl millet centromere-specific sequence, and 800 ng of sonicated, unlabeled total wheat genomic DNA (used as competitor to suppress nonspecific hybridization) were applied per slide. Hybridization sites of digoxigenin- or biotin-labeled probes were detected using sheep antidigoxigenin-rhodamine, rhodamine anti-sheep antibody, or the streptavidin Alexa 488 system, respectively. Epifluorescence signals were recorded with a cooled CCD camera (ORCA-ER; Hamamatsu). The images were optimized for contrast and brightness with Adobe Photoshop 7.0.

For whole-mount GISH (Caperta et al., 2002; Santos et al., 2002), embryos were isolated and fixed in 4% (w/v) formaldehyde freshly prepared from paraformaldehyde (PFA) in MTSB buffer (50 mM PIPES, 5 mM $MgSO_4$, and 5 mM EGTA, pH 6.9) under vacuum for 20 min at room temperature prior to washing in MTSB for 10 min. Tissues were made permeable by incubating with 2% (w/v) cellulase Onozuka R10 (Serva)

and 2% (w/v) pectinase (Sigma-Aldrich) in citrate buffer for 70 min at 37°C. Embryos were subsequently washed in 2 × SSC (standard saline citrate) for 10 min and allowed to dry on multiwell slides. GISH was performed as described for squashed embryos.

A three-dimensional model of in situ–hybridized interphase nuclei was reconstructed using high-level image processing techniques. First, optical section stacks were collected with a Zeiss 510 meta confocal laser scanning microscope. Automatic procedures for the segmentation of the nuclei and the paternal DNA have been implemented with MATLAB (The MathWorks). This was mainly achieved by combining a priori knowledge, principal component analysis, three-dimensional watershed segmentation, and thresholding. Finally, the resulting two-dimensional gray-tone image stack containing the segmentation information was transformed into a three-dimensional model with the visualization and modeling software AMIRA (TGS Europe).

TUNEL Assay Combined with GISH

The TUNEL assay was conducted according to the manufacturer's instructions of the ApopTag apoptosis detection kit manual (S7110; Serological Corporation) with some modifications. Freshly dissected embryos were fixed for 20 min in ice-cold 4% PFA in PBS. After washing in cold PBS, embryos were made permeable by incubating with 2.5% cellulase Onozuka R10 (w/v) Serva, 2.5% (w/v) pectinase (Sigma-Aldrich), and 2.5% pectolyase Y-23 (Sigma-Aldrich) in PBS for 30 min at 37°C. The embryos were squashed in PBS between glass slide and cover slip. The cover slips were removed after freezing in liquid nitrogen. Air-dried specimens were postfixed in 4% PFA for 10 min at room temperature and then incubated in TUNEL-equilibration buffer for 5 min at room temperature. The end-labeling reaction was done by incubating the slides in terminal deoxynucleotidyl transferase in reaction buffer for 60 min at 37°C. Slides were then incubated in stop/wash buffer for 30 min at 37°C, washed three times for 3 min in PBS at room temperature, and stored in 70% ethanol at −20°C. After the TUNEL reaction, GISH was performed as described above. The transferase-incorporated digoxigenin-dUTP was detected with fluorescein isothiocyanate–conjugated sheep antidigoxigenin antibodies amplified by fluorescein-5-isothiocyanate–conjugated rabbit anti-sheep antibodies. In situ–hybridized pearl millet DNA labeled with biotin was detected with avidin-conjugated Texas red. Finally, slides were mounted with DAPI/Vectashield and analyzed under the conditions used for FISH. TUNEL-negative controls were performed without terminal deoxynucleotidyl transferase enzyme and positive controls with additional DNase I treatment as recommended by the manufacturers.

Transmission Electron Microscopy

Three-day-old embryos originated from in vitro–cultivated zygotes were fixed with 2% glutaraldehyde and 2% formaldehyde in cacodylate buffer (50 mM, pH 7.0) for 2 h. After three 15-min washes with the same buffer, the embryos were postfixed with 1% OsO_4 for 2 h and then washed again with buffer and distilled water before embedding in 1.5% low melting point agarose. Small blocks of 1 × 1 mm were cut, each containing a single embryo. These blocks were dehydrated in a graded ethanol series followed by embedding in Spurr's low viscosity resin. After thin sectioning, samples were stained with 4% uranyl acetate and lead citrate. Digital recordings were made on a Zeiss 902 electron microscope at 80 kV.

ACKNOWLEDGMENTS

We thank Ingo Schubert (Institute of Plant Genetics and Crop Plant Research), Richard Pickering (New Zealand Institute for Crop and Food Research, Christchurch, New Zealand), and Jeremy Timmis (University of Adelaide, Australia) for critical reading of the manuscript and anonymous reviewers for helpful comments. We are grateful to Katrin Kumke, Heike Büchner, Mechthild Pürschel, and Bernhard Claus (Institute of Plant Genetics and Crop Plant Research) for excellent technical assistance. This work was supported by the Bundesministerium für Bildung und Forschung (Berlin, Germany) and Icon Genetics GmbH (Halle, Germany).

Received May 12, 2005; revised July 1, 2005; accepted July 1, 2005; published July 29, 2005.

REFERENCES

Barclay, I.R. (1975). High-frequencies of haploid production in wheat (*Triticum aestivum*) by chromosome elimination. Nature **256,** 410–411.

Bennett, M.D., Finch, R.A., and Barclay, I.R. (1976). The time rate and mechanism of chromosome elimination in *Hordeum* hybrids. Chromosoma **54,** 175–200.

Boyer, H.W. (1971). DNA restriction and modification mechanisms in bacteria. Annu. Rev. Microbiol. **25,** 153–176.

Caperta, A.D., Neves, N., Morais-Cecilio, L., Malho, R., and Viegas, W. (2002). Genome restructuring in rye affects the expression, organization and disposition of homologous rDNA loci. J. Cell Sci. **115,** 2839–2846.

Chen, F.Q., and Hayes, P.M. (1991). Wide hybridization of *Hordeum vulgare* x *Zea mays.* Genome **34,** 603–605.

Comai, L., Tyagi, A.P., Winter, K., Holmes-Davis, R., Reynolds, S.H., Stevens, Y., and Byers, B. (2000). Phenotypic instability and rapid gene silencing in newly formed Arabidopsis allotetraploids. Plant Cell **12,** 1551–1567.

Davies, D.R. (1974). Chromosome elimination in inter-specific hybrids. Heredity **32,** 267–270.

Dong, F.G., and Jiang, J.M. (1998). Non-RabI patterns of centromere and telomere distribution in the interphase nuclei of plant cells. Chromosome Res. **6,** 551–558.

Feldman, M., Liu, B., Segal, G., Abbo, S., Levy, A.A., and Vega, J.M. (1997). Rapid elimination of low-copy DNA sequences in polyploid wheat: A possible mechanism for differentiation of homoeologous chromosomes. Genetics **147,** 1381–1387.

Finch, R.A. (1983). Tissue-specific elimination of alternative whole parental genomes in one barley hybrid. Chromosoma **88,** 386–393.

Finch, R.A., and Bennett, M.D. (1983). The mechanism of somatic chromosome elimination in *Hordeum*. In Kew Chromosome Conference II: Proceedings of the Second Chromosome Conference, P.E. Brandham, ed (London: Allen & Unwin), pp. 146–153.

Ford, J.H., and Correll, A.T. (1992). Chromosome errors at mitotic anaphase. Genome **35,** 702–705.

Fukuda, H. (2000). Programmed cell death of tracheary elements as paradigm in plants. Plant Mol. Biol. **44,** 245–253.

Goday, C., and Ruiz, M.F. (2002). Differential acetylation of histones H3 and H4 in paternal and maternal germline chromosomes during development of sciarid flies. J. Cell Sci. **115,** 4765–4775.

Gupta, S.B. (1969). Duration of mitotic cycle and regulation of DNA replication in *Nicotiana plumbaginifolia* and a hybrid derivative of *N. tabacum* showing chromosome instability. Can. J. Genet. Cytol. **11,** 133–142.

Heddle, J.A., and Carrano, A.V. (1977). The DNA content of micronuclei induced in mouse bone marrow by gamma-irradation: Evidence that miconulcei arise from acentric chromsomal fragments. Mutat. Res. **44,** 63–69.

Ho, K.M., and Kasha, K.J. (1975). Genetic control of chromosome elimination during haploid formation in barley. Genetics **81,** 263–275.

Houben, A., Field, B.L., and Saunders, V. (2001). Microdissection and chromosome painting of plant B chromosomes. Methods Cell Sci. **23,** 115–124.

Jin, W.W., Melo, J.R., Nagaki, K., Talbert, P.B., Henikoff, S., Dawe, R.K., and Jiang, J.M. (2004). Maize centromeres: Organization and functional adaptation in the genetic background of oat. Plant Cell **16,** 571–581.

Kamm, A., Schmidt, T., and Heslop-Harrison, J.S. (1994). Molecular and physical organization of highly repetitive, undermethylated DNA from *Pennisetum glaucum.* Mol. Gen. Genet. **244,** 420–425.

Kasha, K.J., and Kao, K.N. (1970). High frequency haploid production in barley (*Hordeum vulgare* L.). Nature **225,** 874–875.

Kashkush, K., Feldman, M., and Levy, A.A. (2002). Gene loss, silencing and activation in a newly synthesized wheat allotetraploid. Genetics **160,** 1651–1659.

Kim, N.S., Armstrong, K.C., Fedak, G., Ho, K., and Park, N.I. (2002). A microsatellite sequence from the rice blast fungus (*Magnaporthe grisea*) distinguishes between the centromeres of *Hordeum vulgare* and *H. bulbosum* in hybrid plants. Genome **45,** 165–174.

Kloc, M., and Zagrodzinska, B. (2001). Chromatin elimination—An oddity or a common mechanism in differentiation and development? Differentiation **68,** 84–91.

Kumlehn, J., Brettschneider, R., Lörz, H., and Kranz, E. (1997). Zygote implantation to cultured ovules leads to direct embryogenesis and plant regeneration of wheat. Plant J. **12,** 1473–1479.

Kumlehn, J., Lorz, H., and Kranz, E. (1998). Differentiation of isolated wheat zygotes into embryos and normal plants. Planta **205,** 327–333.

Laurie, D.A. (1989). The frequency of fertilization in wheat x pearl millet crosses. Genome **32,** 1063–1067.

Laurie, D.A., and Bennett, M.D. (1986). Wheat x maize hybridization. Can. J. Genet. Cytol. **28,** 313–316.

Laurie, D.A., and Bennett, M.D. (1988). Cytological evidence for fertilization in hexaploid wheat x sorghum crosses. Plant Breed. **100,** 73–82.

Laurie, D.A., and Bennett, M.D. (1989). The timing of chromosome elimination in hexaploid wheat x maize crosses. Genome **32,** 953–961.

Linde-Laursen, I., and von Bothmer, R. (1999). Orderly arrangement of the chromosomes within barley genomes of chromosome-eliminating *Hordeum lechleri* x barley hybrids. Genome **42,** 225–236.

Liu, J.H., Xu, X.Y., and Deng, X.X. (2005). Intergeneric somatic hybridization and its application to crop genetic improvement. Plant Cell Tissue Organ Cult. **82,** 19–44.

Liu, S.C., Kowalski, S.P., Lan, T.H., Feldmann, K.A., and Paterson, A.H. (1996). Genome-wide high-resolution mapping by recurrent intermating using *Arabidopsis thaliana* as a model. Genetics **142,** 247–258.

Matzk, F. (1996). Hybrids of crosses between oat and *Andropogene* or *Paniceae* species. Crop Sci. **36,** 17–21.

Matzk, F., and Mahn, A. (1994). Improved techniques for haploid production in wheat using chromosome elimination. Plant Breed. **113,** 125–129.

Matzk, F., Oertel, C., Altenhofer, P., and Schubert, I. (1997). Manipulation of reproductive systems in *Poaceae* to increase the efficiency in crop breeding and production. Trends Agron. **1,** 19–34.

McClintock, B. (1984). The significance of response of the genomes to challenge. Science **226,** 792–810.

Michel, B. (2000). Replication fork arrest and DNA recombination. Trends Biochem. Sci. **25,** 173–178.

Mochida, K., and Tsujimoto, J. (2001). Development of a genomic in situ hybridization method using Technovit 7100 sections of early wheat embryo. Biotech. Histochem. **76,** 257–260.

Mochida, K., Tsujimoto, H., and Sasakuma, T. (2004). Confocal analysis of chromosome behavior in wheat x maize zygotes. Genome **47**, 199–205.

O'Neill, R.J., O'Neill, M.J., and Graves, J.A. (1998). Undermethylation associated with retroelement activation and chromosome remodelling in an interspecific mammalian hybrid. Nature **393,** 68–72.

Perondini, A.L.P., and Ribeiro, A.F. (1997). Chromosome elimination in germ cells of Sciara embryos: Involvement of the nuclear envelope. Invertebr. Reprod. Dev. **32,** 131–141.

Pickering, R.A. (1985). Partial control of chromosome elimination by temperature in immature embryos of *Hordeum vulgare* L. x *H. bulbosum.* Euphytica **14,** 869–874.

Pickering, R.A., and Morgan, P.W. (1985). The influence of temperature on chromosome elimination during embryo development in crosses involving *Hordeum* spp., wheat (*Triticum aestivum* L.) and rye (*Secale cereale* L). Theor. Appl. Genet. **70,** 199–206.

Riddle, N.C., and Birchler, J.A. (2003). Effects of reunited diverged regulatory hierarchies in allopolyploids and species hybrids. Trends Genet. **19,** 597–600.

Riera Lizarazu, O., Rines, H.W., and Phillips, R.L. (1996). Cytological and molecular characterization of oat x maize partial hybrids. Theor. Appl. Genet. **93,** 123–135.

Rines, H.W., and Dahleen, L.S. (1990). Haploids of plants produced by application of maize pollen to emasculated oat florets. Crop Sci. **30,** 1073–1078.

Santos, A.P., Abranches, R., Stoger, E., Beven, A., Viegas, W., and Shaw, P.J. (2002). The architecture of interphase chromosomes and gene positioning are altered by changes in DNA methylation and histone acetylation. J. Cell Sci. **115,** 4597–4605.

Sapre, B., and Deshpande, S. (1987). Origin of B chromosomes in Coix L. through spontaneous interspecific hybridisation. J. Hered. **78,** 191–196.

Schubert, I., and Oud, J.L. (1997). There is an upper limit of chromosome size for normal development of an organism. Cell **88,** 515–520.

Schwarzacher-Robinson, T., Finch, R.A., Smith, J.B., and Bennett, M.D. (1987). Genotypic control of centromere positions of parental genomes in *Hordeum* x *Secale* hybrid metaphases. J. Cell Sci. **87,** 291–304.

Shimizu, N., Itoh, N., Utiyama, H., and Wahl, G.M. (1998). Selective entrapment of extrachromosomally amplified DNA by nuclear budding and micronucleation during S phase. J. Cell Biol. **140,** 1307–1320.

Subrahmanyam, N.C. (1977). Haploidy from *Hordeum* interspecific crosses. I. Polyhaploids of *H. parodii* and *H. procerum.* Theor. Appl. Genet. **49,** 209–217.

Subrahmanyam, N.C., and Kasha, K.J. (1973). Selective chromosomal elimination during haploid formation in barley following interspecific hybridization. Chromosoma **42,** 111–125.

Tanaka, T., and Shimizu, N. (2000). Induced detachment of acentric chromatin from mitotic chromosomes leads to their cytoplasmic localization at G(1) and the micronucleation by lamin reorganization at S phase. J. Cell Sci. **113,** 697–707.

Taverna, S.D., Coyne, R.S., and Allis, C.D. (2002). Methylation of histone H3 at lysine 9 targets programmed DNA elimination in *Tetrahymena.* Cell **110,** 701–711.

Thomas, H.M. (1988). Chromosome elimination and chromosome pairing in tetraploid hybrids of *Hordeum vulgare* x *H. bulbosum.* Theor. Appl. Genet. **76,** 118–124.

Zenkteler, M., and Nitzsche, W. (1984). Wide hybridization experiments in cereals. Theor. Appl. Genet. **68,** 311–315.

A5 Houben, A., and Schubert, I. (2007). Engineered plant minichromosomes: a resurrection of B chromosomes? Plant Cell 19, 2323-2327.

The Plant Cell, Vol. 19: 2323–2327, August 2007, www.plantcell.org

CURRENT PERSPECTIVE ESSAY

Engineered Plant Minichromosomes: A Resurrection of B Chromosomes?

A number of crop species of commercial interest have been transformed using either *Agrobacterium*-mediated, biolistic, or other systems. However, these methods have several limitations. For example, they allow insertion of single or a few genes at random genomic positions, but complex traits cannot be transferred in a coordinated manner. Furthermore, the integrity of the host genome can be disturbed by transgene insertion. These limitations stimulated the development of a chromosome-based vector system suitable for transferring large genes, gene complexes, and/or multiple genes together with regulatory elements for safe, controlled, and persistent expression, avoiding rearrangements that are often linked with insertion events. Additionally, engineered chromosomes could be used to address questions concerning the function of specific chromosomal domains (e.g., centromeric regions). Chromosome engineering has been applied successfully in mammals and yeasts but has lagged in plants. Recent efforts to generate maize minichromosomes by J. Birchler and colleagues from the University of Missouri (Yu et al., 2006, 2007) open new venues for plant biotechnology and chromosome biology.

TOP-DOWN VERSUS BOTTOM-UP APPROACHES

Considerable progress has been made in developing mammalian chromosome-based vector systems either by engineering endogenous chromosomes (top-down approach) or by artificial composition of cloned chromosomal constituents into functional chromosomes (bottom-up approach). The bottom-up strategy relies on cell-mediated chromosome assembly after transfection of a cell line with cloned centromeric sequences and a selectable marker gene, with or without telomeric and genomic DNA (Harrington et al., 1997; Ikeno et al., 1998). However, the process of de novo chromosome assembly within cells is hard to control and has been achieved only in a limited number of mammalian cell lines (Irvine et al., 2005). For plants, the bottom-up strategy has not yet yielded artificial chromosomes.

Our limited understanding of centromere function and maintenance is one of the obstacles on the way to generating artificial chromosomes. In one study, transformation of rice with Mb-sized centromeric repeat arrays from either maize or rice did not result in stable de novo formation of centromeres (Phan et al., 2007). Also, transformation of the fungus *Candida albicans* with naked homologous centromeric DNA (85 kb) was unable to recruit the centromeric histone variant CENH3 and to form functionally active centromeric chromatin (Baum et al., 2006). Although plant centromeres can be very large (Jin et al., 2004), more recent data suggest that the size of a functional centromere might be only a few hundred kilobases (Nagaki et al., 2004). It has been shown that barley centromeric repeats are neither necessary nor sufficient to establish a centromere (Nasuda et al., 2005). Rapid inactivation of the second centromere of dicentric maize chromosomes with two sequence identical centromeres (Han et al., 2006) supports the idea that the primary DNA sequence alone does not determine centromere identity. Rather, a specific epigenetic mark seems to be responsible for centromere specification (Vig, 1994; Karpen and Allshire, 1997). Although substitution of the histone H3 by CENH3 in centromeric nucleosomes is crucial for kinetochore formation, we do not know what originally triggers this substitution when a new centromere is initiated, or why and how CENH3 gets lost when a centromere becomes inactive.

To circumvent the necessity of de novo centromere formation, modification of existing chromosomes to generate a chromosome-based vector can be achieved by at least two different routes. As shown first by Farr et al. (1991), cloned telomeric repeats introduced into cells may truncate the distal portion of a chromosome by the formation of a new telomere at the integration site (Figure 1). This elegant in vivo approach was an important step toward constructing a gene delivery system based on engineered human chromosomes (Lim and Farr, 2004).

A second in vivo approach of engineering endogenous mammalian chromosomes is based on the generation of dicentric chromosomes by amplification of (peri)centromeric satellite DNA and other host sequences, such as rDNA, together with the transgenes after transfection with plasmids (Keresö et al., 1996). Although the generation of a second centromere within transgenic mouse and hamster cell lines seems to be reproducible, the underlying mechanism is not well understood. Nevertheless, the breakage products of such dicentrics can be stabilized by healing the ends via telomere addition. The resulting engineered chromosomes (satellite DNA–based artificial chromosomes) are composed mainly of amplified satellite repeats and ribosomal DNA, interspersed with coamplified transfected foreign DNA (Csonka et al., 2000). A similar process has been associated with the formation of a naturally occurring B chromosome of the plant *Plantago lagopus* (Dhar et al., 2002). This supernumerary chromosome, which originated from a trisomic A chromosome, underwent a number of structural changes combined with rDNA amplification.

www.plantcell.org/cgi/doi/10.1105/tpc.107.053603

CURRENT PERSPECTIVE ESSAY

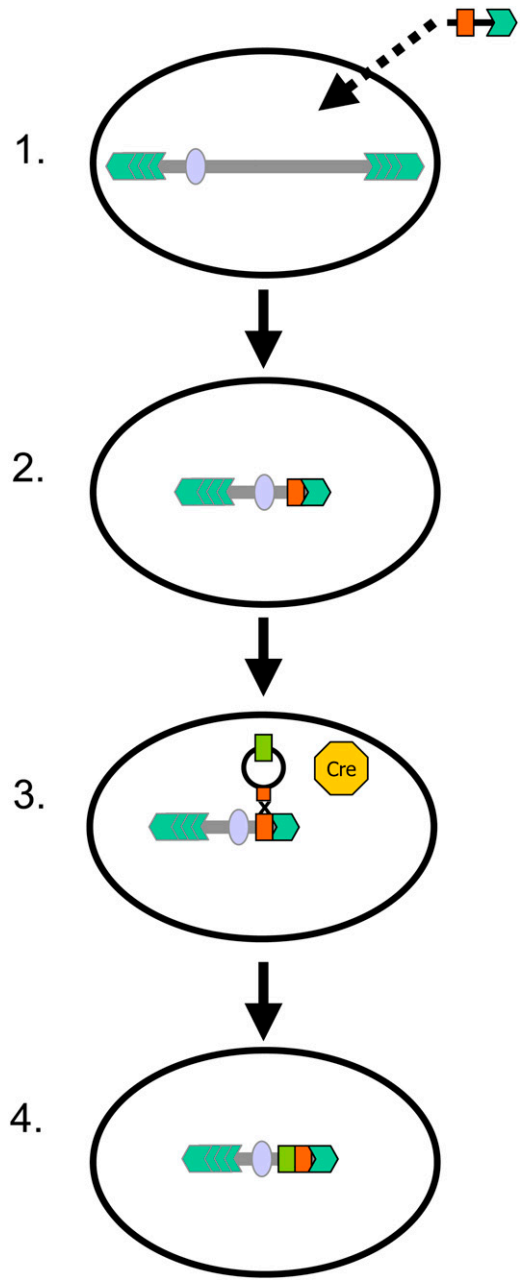

Figure 1. Telomere-Associated Chromosome Fragmentation: A Strategy to Generate Minichromosomes by Truncation of Natural Chromosomes.

A vector containing *Arabidopsis*-type telomere repeats, a selectable marker, and a homologous recombination site is used to fragment recipient chromosomes (Yu et al., 2006, 2007). The transformation occurs via *Agrobacterium*-mediated or biolistic transformation of immature embryos prior to selection of cells for antibiotic or herbicide resistance (1 and 2). To add genes onto an engineered minichromosome, targeted transgenes are integrated via site-specific recombinase, as provided by the Cre/lox system, after biolistic transformation (Srivastava and Ow, 2001) of a construct carrying a recombination site that activates a selection marker (3 and 4). The Cre recombinase could be expressed transiently.

RECENT PROGRESS IN MAIZE

Telomere-mediated chromosome truncation technology recently has been adapted for maize (Figure 2; Yu et al., 2006, 2007). An array of 2.6 kb of *Arabidopsis*-type telomeric repeats was used for *Agrobacterium*-mediated or biolistic transformation of immature maize embryos. Because sequence targeting by homologous recombination is inefficient in seed plants (Reiss, 2003), a targeted introgression of cloned telomeres as used in mammals (Lim and Farr, 2004) was not yet possible. Therefore, the sites of chromosomal truncations are random, and in situ hybridization with chromosome-specific marker sequences is required for identifying the origin of the truncated chromosomes.

The presence of telomeric sequences at the double-stranded ends of the transgene insertion sites might be considered as telomere seeding (Yu et al., 2006). The transgenic telomeric sequences might recruit telomerase and telomere binding proteins, thus mediating chromosome healing rather than nonhomologous end joining (Yu et al., 2006). The frequency of chromosomal truncation is low in plants compared with mammalian cells, but testing different constructs and genetic backgrounds might result in an improved truncation efficiency. Because the truncation efficiency of mammalian chromosomes is highest in a hyperrecombinogenic chicken cell line (Buerstedde and Takeda, 1991), plant accessions or mutants with a high somatic recombination frequency might be preferable host organisms.

The lack of meiotic pairing of the derived maize minichromosome with its progenitors suggests that such small chromosomes have a minimal chance of recombination with the normal chromosome and therefore can be used as starting material for plant-engineered chromosomes. The generation of even smaller minichromosomes might be prevented by the requirement of a minimal chromosome size for stable inheritance. While too large chromosomes (with arms longer than half of the average spindle axis) often are not correctly transmitted through mitotic division (Schubert and Oud, 1997), the bottleneck for transmission of too small chromosomes seems to be meiosis. Lower limits of chromosome size for correct transmission seem to vary between species, from ~50 kb in yeast to <5% of genome size in field bean (Schubert, 2001), while microchromosomes of birds show stable inheritance (Burt, 2002). At present, we do not know whether the lack of meiotic pairing and recombination, the absence of a lateral support for centromeres to maintain centromeric cohesion, or other reasons are responsible for impaired transmission of very small chromosomes.

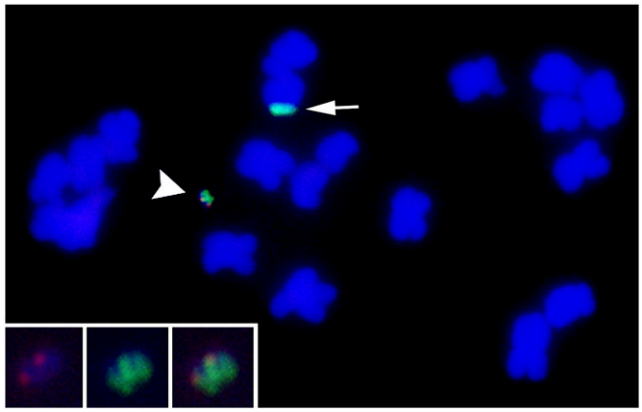

Figure 2. A Chromosome Spread of Maize Is Shown with a Minichromosome Produced by Truncating a B Chromosome of Maize.

The truncated B chromosome has a specific centromeric DNA sequence that is labeled in green. A normal B chromosome is shown for comparison (arrow). The arrowhead denotes the minichromosome produced by telomere-mediated truncation. The addition of telomeres to the chromosome by genetic transformation fractures the chromosome at that site and leaves the added genes (red) at the tip of the chromosome. The insets (enlarged below) show the added genes in red, the specific centromere region of the minichromosome in green, and the merged image. The chromosomes are stained blue. Modified from Yu et al. (2007).

A VERSUS B CHROMOSOMES

B chromosomes, the often neglected components of the karyotypes of numerous plant and animal species, could become a major player for the generation of engineered chromosomes because of their unique features. B chromosomes are dispensable and do not pair with any of the standard A chromosomes at meiosis by definition. They have irregular modes of inheritance (Jones and Houben, 2003). With respect to the possible use of mini-B chromosomes as a vector, it is important that B chromosomes have little effect on an individual's phenotype. Only in the case of a high number, B chromosomes can reduce vigor (Puertas, 2002). Thus, engineered mini-Bs allow the study of gene dosage effects. Except for the B chromosome–located 45S rRNA gene of *Crepis capillaris* (Leach et al., 2005) and for transcriptionally active B-specific repetitive sequences (Carchilan et al., 2007; Lamb et al., 2007), there has been no direct molecular evidence for transcription of genes from plant Bs.

The survival rate after telomere-associated truncation was higher for B than for A chromosomes (Yu et al., 2007), most likely because most Bs are genetically inert. Constitutive transgene expression from A and B chromosome–derived minichromosomes suggests that inactivation of genes on B chromosomes, if it occurs, it is at least not a rapid process. It is of interest to compare transgene expression on A and B chromosomes over several generations.

To achieve viability of plants with an A chromosome–derived minichromosome, the truncation event should take place in a polyploid or (for the target chromosome) aneuploid background. Maize A-derived minichromosomes were faithfully transmitted from one generation to the next, whereas the meiotic transmission rate of B-type minichromosomes varied from 12 to 39% via the male parent (Yu et al., 2007), comparable to the transmission rate of mini-B chromosomes generated by breakage-fusion-bridge cycles (Kato et al., 2005). However, due to the intrinsic postmeiotic drive of intact B chromosomes (which includes specific nondisjunction at pollen mitosis and preferential fertilization of the egg by the sperm containing the B chromosomes; Carlson, 1978) a B chromosome–derived vector might potentially reveal an increase of transmission frequency above Mendelian expectation. The truncation of the B eliminates nondisjunction of the mini-B and confers inheritance characteristics equal to any normal A chromosome. However, the nondisjunction process can be restored by the addition of normal B chromosomes to the genotype, which would supply the required *trans*-acting factor for nondisjunction that is located at the very tip of the chromosome. Early studies indicated that the drive mechanisms for B chromosomes are independent of the background genotype and mitotic nondisjunction is controlled by the B itself (Müntzing, 1970).

Since most of the engineered mammalian chromosomes have been generated and maintained in cell culture, our knowledge on their meiotic transmissibility is rather limited. Studies in transchromosomal animals and nonhuman mammalian tissues suggest a high variability as to the stability of engineered human chromosomes between tissue types and between genetic backgrounds. The meiotic transmission is clearly below that of endogenous chromosomes (Irvine et al., 2005). It remains to be tested whether microinjection or microcell-mediated transfer will broaden the application of engineered chromosomes in cases where the transfer of plant minichromosomes via sexual crossing is not feasible.

THE NEXT STEP: MAKING USE OF ENGINEERED PLANT MINICHROMOSOMES

How are genes of interest introduced onto engineered minichromosomes? Targeted transgene integration into unique chromosomal loci might be achieved using gene constructs in combination with a site-specific recombinase cassette as provided by the Cre/lox system. The proof of principle has been demonstrated by Yu et al. (2007). The engineered maize chromosome R2 provides a defined recipient locus for site-specific integration of transgenes, enabling genetic manipulation via site-specific recombination. After crossing a transgenic plant supplying the Cre recombinase and a *lox* recombination site at the terminus of chromosome 3 with a plant carrying the minichromosome R2 with a defined recipient site, composition of two complementary parts at the recipient locus led to activation of the DsRed reporter gene in some tissues, indicating

CURRENT PERSPECTIVE ESSAY

reciprocal translocation between *lox* sites. Although the recombination efficiency is not as high as in many nonplant organisms, this approach offers a possible way of adding transgenes to a minichromosome. Ayabe et al. (2005) used an engineered human chromosome to introduce the native human *HPRT* gene together with ~40 kb upstream and ~10 kb downstream regions that include all regulatory elements needed for correct expression in *Hprt*-deficient cells and demonstrated functional complementation. To harness targeted gene loading onto the engineered chromosome, an elegant combination of transformation-associated recombination cloning of the gene-containing genomic fragment into a YAC vector (Kouprina et al., 1998) and Cre/loxP-based site-specific recombination of the circular YAC-DNA into the recipient loxP site of the engineered human minichromosome has been developed (Ayabe et al., 2005) and might be adapted for plants as well.

In summary, the future for engineered plant chromosomes as a fascinating new tool for basic research on chromosomes and biotechnology is promising. The initial demonstration of their construction and behavior provides the foundation for this technology in plants, onto which further developments can be built. However, an increase of truncation efficiency, the introduction of multiple site-specific recombination systems, and a demonstration of full meiotic transmissibility of site-specific recombination products are required before engineered plant chromosomes will enter commercial application.

ACKNOWLEDGMENTS

We thank James Birchler and colleagues (University of Missouri) for providing the image of the maize minichromosome and for comments on the manuscript.

Andreas Houben and Ingo Schubert
Leibniz-Institute of Plant Genetics and Crop Plant Research
D-06466 Gatersleben, Germany
schubert@ipk-gatersleben.de

REFERENCES

Ayabe, F., Katoh, M., Inoue, T., Kouprina, N., Larionov, V., and Oshimura, M. (2005). A novel expression system for genomic DNA loci using a human artificial chromosome vector with transformation-associated recombination cloning. J. Hum. Genet. **50:** 592–599.

Baum, M., Sanyal, K., Mishra, P.K., Thaler, N., and Carbon, J. (2006). Formation of functional centromeric chromatin is specified epigenetically in *Candida albicans*. Proc. Natl. Acad. Sci. USA **103:** 14877–14882.

Buerstedde, J.M., and Takeda, S. (1991). Increased ratio of targeted to random integration after transfection of chicken B cell lines. Cell **67:** 179–188.

Burt, D.W. (2002). Origin and evolution of avian microchromosomes. Cytogenet. Genome Res. **96:** 97–112.

Carchilan, M., Delgado, M., Ribeiro, T., Costa-Nunes, P., Caperta, A., Morais-Cecílio, L., Jones, R.N., Viegas, W., and Houben, A. (2007). Transcriptionally active heterochromatin in rye B chromosomes. Plant Cell **19:** 1738–1749.

Carlson, W.R. (1978). B-chromosome of corn. Annu. Rev. Genet. **12:** 5–23.

Csonka, E., Cserpan, I., Fodor, K., Hollo, G., Katona, R., Keresö, J., Praznovszky, T., Szakal, B., Telenius, A., deJong, G., Udvardy, A., and Hadlaczky, G. (2000). Novel generation of human satellite DNA-based artificial chromosomes in mammalian cells. J. Cell Sci. **113:** 3207–3216.

Dhar, M.K., Friebe, B., Koul, A.K., and Gill, B.S. (2002). Origin of an apparent B chromosome by mutation, chromosome fragmentation and specific DNA sequence amplification. Chromosoma **111:** 332–340.

Farr, C., Fantes, J., Goodfellow, P., and Cooke, H. (1991). Functional reintroduction of human telomeres into mammalian cells. Proc. Natl. Acad. Sci. USA **88:** 7006–7010.

Han, F., Lamb, J.C., and Birchler, J.A. (2006). High frequency of centromere inactivation resulting in stable dicentric chromosomes of maize. Proc. Natl. Acad. Sci. USA **103:** 3238–3243.

Harrington, J.J., Van Bokkelen, G., Mays, R.W., Gustashaw, K., and Willard, H.F. (1997). Formation of de novo centromeres and construction of first-generation human artificial microchromosomes. Nat. Genet. **15:** 345–355.

Ikeno, M., Grimes, B., Okazaki, T., Nakano, M., Saitoh, K., Hoshino, H., McGill, N.I., Cooke, H., and Masumoto, H. (1998). Construction of YAC-based mammalian artificial chromosomes. Nat. Biotechnol. **16:** 431–439.

Irvine, D.V., Shaw, M.L., Choo, K.H., and Saffery, R. (2005). Engineering chromosomes for delivery of therapeutic genes. Trends Biotechnol. **23:** 575–583.

Jin, W., Melo, J.R., Nagaki, K., Talbert, P., Henikoff, S., Dawe, R.K., and Jiang, J. (2004). Maize centromeres: Organization and functional adaptation in the genetic background of oat. Plant Cell **16:** 571–581.

Jones, N., and Houben, A. (2003). B chromosomes in plants: Escapees from the A chromosome genome? Trends Plant Sci. **8:** 417–423.

Karpen, G.H., and Allshire, R.C. (1997). The case for epigenetic effects on centromere identity and function. Trends Genet. **13:** 489–496.

Kato, A., Zheng, Y.Z., Auger, D.L., Phelps-Durr, T., Bauer, M.J., Lamb, J.C., and Birchler, J.A. (2005). Minichromosomes derived from the B chromosome of maize. Cytogenet. Genome Res. **109:** 156–165.

Keresö, J., et al. (1996). De novo chromosome formations by large-scale amplification of the centromeric region of mouse chromosomes. Chromosome Res. **4:** 226–239.

Kouprina, N., Annab, L., Graves, J., Afshari, C., Barrett, J.C., Resnick, M.A., and Larionov, V. (1998). Functional copies of a human gene can be directly isolated by transformation-associated recombination cloning with a small 3′ end target sequence. Proc. Natl. Acad. Sci. USA **95:** 4469–4474.

Lamb, J.C., Riddle, N.C., Cheng, Y.M., Theuri, J., and Birchler, J.A. (2007). Localization and transcription of a retrotransposon-derived element on the maize B chromosome. Chromosome Res. **15:** 383–398.

Leach, C.R., Houben, A., Field, B., Pistrick, K., Demidov, D., and Timmis, J.N. (2005). Molecular evidence for transcription of genes on a B chromosome in *Crepis capillaris*. Genetics **171:** 269–278.

CURRENT PERSPECTIVE ESSAY

Lim, H.N., and Farr, C.J. (2004). Chromosome-based vectors for Mammalian cells: An overview. Methods Mol. Biol. **240:** 167–186.

Müntzing, A. (1970). Chromosomal variation in the Lindström strain of wheat carrying accessory chromosomes in rye. Hereditas **66:** 279–286.

Nagaki, K., Cheng, Z.K., Ouyang, S., Talbert, P.B., Kim, M., Jones, K.M., Henikoff, S., Buell, C.R., and Jiang, J.M. (2004). Sequencing of a rice centromere uncovers active genes. Nat. Genet. **36:** 138–145.

Nasuda, S., Hudakova, S., Schubert, I., Houben, A., and Endo, T.R. (2005). Stable barley chromosomes without centromeric repeats. Proc. Natl. Acad. Sci. USA **102:** 9842–9847.

Phan, B.H., Jin, W., Topp, C.N., Zhong, C.X., Jiang, J., Dawe, R.K., and Parrott, W.A. (2007). Transformation of rice with long DNA-segments consisting of random genomic DNA or centromere-specific DNA. Transgenic Res. **16:** 341–351.

Puertas, M.J. (2002). Nature and evolution of B chromosomes in plants: A non-coding but information-rich part of plant genomes. Cytogenet. Genome Res. **96:** 198–205.

Reiss, B. (2003). Homologous recombination and gene targeting in plant cells. Int. Rev. Cytol. **228:** 85–139.

Schubert, I. (2001). Alteration of chromosome numbers by generation of minichromosomes - Is there a lower limit of chromosome size for stable segregation? Cytogenet. Cell Genet. **93:** 175–181.

Schubert, I., and Oud, J.L. (1997). There is an upper limit of chromosome size for normal development of an organism. Cell **88:** 515–520.

Srivastava, V., and Ow, D.W. (2001). Biolistic mediated site-specific integration in rice. Mol. Breed. **8:** 345–350.

Vig, B.K. (1994). Do specific nucleotide bases constitute the centromere? Mutat. Res. **309:** 1–10.

Yu, W., Han, F., Gao, Z., Vega, J.M., and Birchler, J. (2007). Construction and behavior of engineered mini-chromosomes in maize. Proc. Natl. Acad. Sci. USA **104:** 8924–8929.

Yu, W., Lamb, J.C., Han, F., and Birchler, J.A. (2006). Telomere-mediated chromosomal truncation in maize. Proc. Natl. Acad. Sci. USA **103:** 17331–17336.

A6 Houben, A., Demidov, D., Caperta, A.D., Karimi, R., Agueci, F., and Vlasenko, L. (2007). Phosphorylation of histone H3 in plants - A dynamic affair. Biochim Biophys Acta.

Available online at www.sciencedirect.com
ScienceDirect
Biochimica et Biophysica Acta 1769 (2007) 308–315
Biochimica et Biophysica Acta
BBA
www.elsevier.com/locate/bbaexp

Review

Phosphorylation of histone H3 in plants—A dynamic affair

Andreas Houben [a,*], Dmitri Demidov [a], Ana D. Caperta [b], Raheleh Karimi [a], Francesco Agueci [a], Liudmila Vlasenko [a]

[a] Leibniz-Institute of Plant Genetics and Crop Plant Research, Chromosome Structure and Function Group, Corrensstrasse 3, D-06466 Gatersleben, Germany
[b] Centro de Botânica Aplicada à Agricultura, Secção de Genética, Instituto Superior de Agronomia, Tapada da Ajuda, 1349-017, Lisboa, Portugal

Received 28 September 2006; received in revised form 8 January 2007; accepted 11 January 2007
Available online 19 January 2007

Abstract

Histones are the main protein components of chromatin: they undergo extensive post-translational modifications, particularly acetylation, methylation, phosphorylation, ubiquitination and ADP-ribosylation which modify the structural/functional properties of chromatin. Post-translational modifications of the N-terminal tails of the core histones within the nucleosome particle are thought to act as signals from the chromatin to the cell, for various processes. Thus, in many ways histone tails can be viewed as complex protein–protein interaction surfaces that are regulated by numerous post-translational modifications. Histone phosphorylation has been linked to chromosome condensation/segregation, activation of transcription, apoptosis and DNA damage repair. In plants, the cell cycle dependent phosphorylation of histone H3 has been described; it is hyperphosphorylated at serines 10/28 and at threonines 3/11 during both mitosis and meiosis in patterns that are specifically coordinated in both space and time. Although this post-translational modification is highly conserved, data show that the chromosomal distribution of individual modifications can differ between groups of eukaryotes. Initial results indicate that members of the plant Aurora kinase family have the capacity to control cell cycle regulated histone H3 phosphorylation, and in addition we describe other potential H3 kinases and discuss their functions.

Keywords: Histone phosphorylation; Chromosomes; Centromeres; Cell cycle; Aurora kinases

1. Cell-cycle dependent histone phosphorylation

The cell cycle dependent transition from decondensed interphase chromatin to condensed metaphase chromatin, and vice versa, is the most obvious dynamic change in chromatin structure. Histones are among numerous DNA-binding proteins that control the level of DNA condensation, and post-translational modifications of histone tails play a critical role in the dynamic condensation/decondensation process. Early observations in several eukaryotes have shown that the level of H3 phosphorylation, which is minimal in interphase, increases during mitosis [1]. With the development of an antibody specific for histone H3 phosphorylated at S10 Hendzel and colleagues [2] were able to demonstrate, *in vivo*, a precise spatial and temporal pattern of H3 phosphorylation in mammalian cells. They found that phosphorylation of H3 is initiated in late G2, and then spreads throughout the chromatin as it undergoes condensation, up to the end of mitosis. The same cell-cycle dependent histone modification was later demonstrated in plants [3]. It is noteworthy that although the process of H3 phosphorylation is highly conserved, its significance and chromosomal distribution may differ to some extent among different species groups. In mammals the cell-cycle dependent phosphorylation of H3 at serine positions 10 and 28, that originates in the pericentromere [4] and spreads throughout the chromosomes during the G2-M transition phase, is most likely to be interlinked with the initiation of chromosome condensation [5]. In yeast on the other hand, phosphorylation of S10 in H3 is not required for cell-cycle progression, where phosphorylation of histone H2B might replace the function of H3 phosphorylation [6]. Similarly, mitotic cells in *Drosophila borr* mutant embryos display only a slight undercondensation of their dividing chromosomes despite a substantial reduction of H3S10 phosphorylation [7].

* Corresponding author. Tel.: +49 39482 5486; fax: +49 39482 5137.
E-mail address: houben@ipk-gatersleben.de (A. Houben).

0167-4781/$ - see front matter © 2007 Elsevier B.V. All rights reserved.
doi:10.1016/j.bbaexp.2007.01.002

In plants, the distribution of phosphorylated histone H3 at serine 10 [3,8,9], and serine 28 [10,11], correlates with the position of the pericentromere during mitosis and meiosis II (Figs. 1a, 2). Immunogold scanning electron microscopy supports the view that during the progression through the mitotic stages phosphorylation of histone H3 at serine 10 accumulates in the pericentromeric chromatin at metaphase [12]. The immunosignal gap observed by high resolution scanning electron microscopy represents the core centromere [12] , characterised by parallel chromatin fibres, reduced DNA and enriched protein amounts compared to the chromosome arms [13]. This agrees with the observation that histone H3 is replaced by the evolutionarily conserved centromere-specific histone H3-variant CENP-A within the core centromere [14].

Interestingly, during meiosis in monocentric plants the distribution of S10 and S28 phosphorylation varies between the two meiotic divisions [8–10] (Fig. 2). During the first division the chromosomes are highly phosphorylated throughout their entire length, while in the second division the H3 phosphorylation is restricted to the pericentromeric regions, as in mitotic chromosomes (Fig. 2a, c) . Surprisingly, at the same time, single chromatids resulting from equational division of univalents at anaphase I show no H3 phosphorylation (Fig. 2c). Irrespective of their low level of H3 phosphorylation, however, prematurely separated chromatids show normal condensation and their kinetochores interact with the microtubules. These observations led to the hypothesis that in plants pericentromeric H3 phosphorylation at both serine positions is required for cohesion of sister chromatids during metaphase I, and for sister chromatid pericentromeres during mitosis and metaphase II, respectively [9,10] (Fig. 3). This hypothesis was further supported by the observation that in a maize mutant (*afdI*) defective in sister chromatid cohesion the univalents at metaphase I showed strong phosphorylation only at the pericentromeric regions [8], and that a dicentric chromosome revealed hyperphosphorylated H3 only at the functional centromere [3,15]. In contrast the polycentric chromosomes of *Rhynchospora tenuis* [16] and of the genus *Luzula* [10,17] (Fig. 1c), were labelled along the entire length of chromosomes during mitosis. The fact that histone H3, at the positions described, becomes dephosphorylated at interkinesis and phosphorylated again during prophase II indicates that this post-translational modification is reversible, and it can occur independent of the DNA replication process.

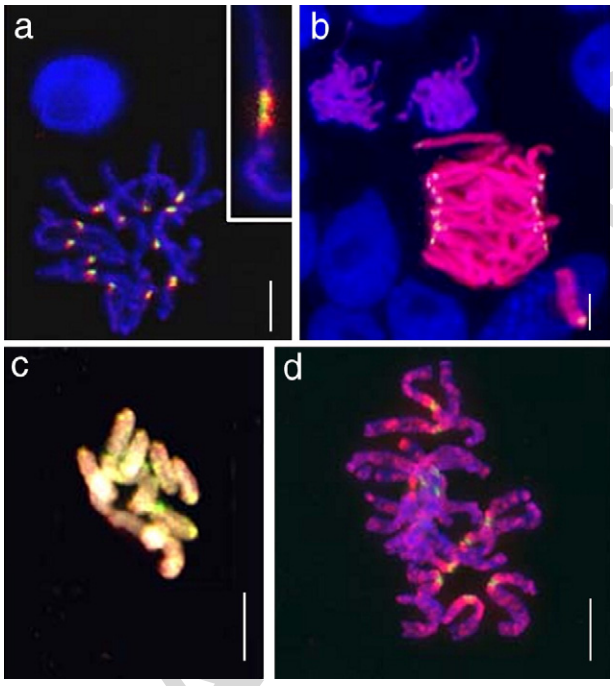

Fig. 1. Mitotic cell cycle regulated histone H3 phosphorylation in plants (a: *Hordeum vulgare,* b: *Vicia faba*, c: *Luzula luzuloides*, d: *Secale cereale*). (a) On monocentric chromosomes the pericentromeric regions show H3S10ph (red), whereas H3S28ph (yellow) is confined to the central part of the pericentromeric region (inset). DAPI-stained interphase nuclei (blue) display no detectable H3 phosphorylation. (b) H3T11ph (red) correlates with condensation of metaphase chromosomes [18]. (c) The polycentric chromosomes of *L. luzuloides* are entirely labelled with H3 phosphorylated at both serine positions (red/yellow) [10]. (d) H3T3ph (red) correlates with condensation of metaphase chromosomes. H3S28ph (yellow) is confined to the pericentromeric region [10]. Bars represent 5 μm.

Compared to serine phosphorylation there are fewer reports for histone threonine phosphorylation. Phosphorylation at T3 (Fig. 1d) and T11 [18] (Fig. 1b) in plants occurs along entire chromosome arms, and correlates with the condensation of mitotic and meiotic chromosomes (Fig. 3). In mammals, in contrast, where phosphorylation of T3 and T11 is most abundant in the centromere [19–21], it may instead serve as a recognition code for centromere assembly. The reverse may be true for S10/28 modifications, which may provide a label for the pericentromere region in plants (Fig. 1a, d), but has a function in chromosome condensation in mammals.

The coincidence of H3 phosphorylation (at S10/28) with chromosome condensation in animal cells had led to the proposal of a causal relationship [2,4]. However, since this correlation does not exist in plants and other organisms this proposal has been modified to the “ready production hypothesis” [22,23], meaning that H3 phosphorylation during mitosis simply serves as a ‘memory’ that chromosomes are ready for separation. With the finding that in plant cells phosphorylation at T3/11, rather than S10/28, correlates with chromosome condensation the original proposal by Hendzel et al. [2] may well be valid, due to species-specific differences in the biological significance of the histone code.

The dynamics of histone H3 phosphorylation has been artificially altered by the application of phosphatase and kinase inhibitors. The protein phosphatase inhibitor cantharidin increases histone H3S10/28 phosphorylation along chromosome arms from prophase to telophase in plants [10,24]. Unlike the situation in mammals, where phosphatase inhibitors induced premature chromosome condensation and stimulate H3 phosphorylation in interphase nuclei [25], no such severe effect of interphase histone H3 phosphorylation could be found in plants. The H3S10 phosphorylation pattern after *in vitro* treatment with cantharidin resembles that of the chromosomes at first meiotic division in plants. It could be that the phosphorylation of the pericentric chromatin, and of chromosome arms, is controlled by different kinases. Alternatively, there might only be one

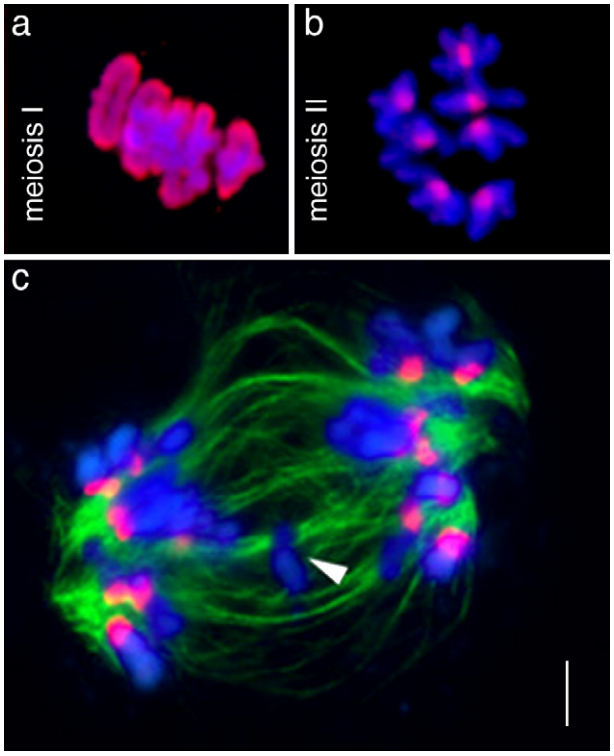

Fig. 2. Distribution of phosphorylated H3S10 differs between the first and second meiotic division [9]. At the first division (a) entire *Secale cereale* chromosomes are labelled with H3S10ph-specific signals (red), whereas at second division (b) H3S10ph is confined to the pericentromeric regions. (c) Histone H3 of chromatids that are condensed prematurely and of separated chromatids (arrowed) are not S10-phosphorylated at the pericentromeric regin. Note: irrespective of their low level of H3 phosphorylation prematurely separated chromatids are normally condensed and their kinetochores interact with microtubules (green). Bar represents 5 μm.

kinase whose activity along the chromosome is regulated differently in mitosis and meiosis. Following cantharidin treatment the observed meta/anaphase cells appeared normal, with the exception of very rare lagging chromatids at anaphase, and a delayed transition from metaphase to anaphase (Manzanero, A. and Houben, A., unpublished data). Inhibition of histone deacetylation by trichostatin in *Nicotiana sylvestris* protoplasts during mitosis induces the accumulation of metaphase cells and reduces H3S10ph at anaphase and telophase [26], which suggests a direct or indirect interaction between H3 phosphorylation and acetylation.

For threonine 11 of histone H3 a different response to cantharidin has been reported [18]. T11 became phosphorylated during interphase, but this phosphorylation was restricted to pericentromeric regions. The simplest explanation for this finding is that phosphorylation takes place in interphase as well, but remains undetected because the rate of dephosphorylation exceeds that of phosphorylation. Alternatively, the kinase phosphorylating T11 may be inactivated by dephosphorylation during interphase. Thus, inhibition of phosphatase activity could result in activation of this kinase. Since cantharidin affects a number of different PP2A and PP1 phosphatases [27] the specific enzyme involved cannot be deduced. It could be however, that the artificially induced H3T11 phosphorylation of the pericentric interphase chromatin and the phosphorylation of the chromosome arms is controlled by different kinases/phosphatases.

A reduced level of H3S10/28 phosphorylation and an aberrant segregation of mitotic chromosomes have been revealed by varying the Aurora kinase activity of cultured tobacco cells with the inhibitor Hesperadin [28]. Hesperadin, which has been developed as potential anticancer drug [29], is a small molecule that inhibits Aurora B activity. Because the Hesperadin binding sites of Aurora B are conserved between human and *Arabidopsis*, Hesperadin potentially inhibits plant Aurora kinases in the same manner as ATP competitive inhibitors in animals [28]. Since chromatids were normally condensed without H3S10/S28 phosphorylation, and a high frequency of lagging anaphase chromosomes in Hesperadin-treated tobacco cells were found, it is likely that H3S10/S28 phosphorylation is required for the dissociation of mitotic sister chromatid cohesion in plants. Further experiments will be necessary to clarify the interrelationship between a reduction in H3S10/S28ph staining and defects in chromatid segregation.

2. Proposed functions of histone H3 phosphorylation during cell cycle

Given the varied and often conflicting data on histone H3 phosphorylation its function remains controversial. The primary function of the cell cycle dependent histone phosphorylation may be to identify different domains of the chromosomes, and to mark their progress through the cell cycle [23]. Older models proposed that histone modifications may directly influence either the structure or the folding dynamics of nucleosomal arrays, but there is little evidence for such models [30]. Analysing the folding patterns of synthetic *in vitro* assembled nucleosomal arrays has demonstrated that arrays assembled with homogeneously phosphorylated H3S10 do not behave any differently from unmodified H3S10, indicating that H3S10 phosphorylation has no direct effect on inter-nucleosomal tail interactions which are important for higher-order folding [32]. It seems to be more likely that histone modifications control the binding of non-histone proteins to the chromatin fibre. For example, some chromodomains bind to methylated lysines, whereas bromodomains specify binds to acetylated lysines (reviewed in [30–32]. Also phosphorylation of H3S10 in *S. cerevisiae*, facilitates the sequential acetylation of lysine 14 by directly enhancing the binding of the GCN5 acetyltransferase [33,34].

The reversible cycle of histone phosphorylation/dephosphorylation may govern the capacity of chromatin-binding proteins to bind methylated lysines, and to re-release these binding factors at the appropriate stage of the cell cycle. To date, however, no protein has yet been described that could ‘read’ and interact with the phosphorylated histone. Rather, evidence exists that in mammals phosphorylation of H3S10 is responsible for the dissociation of the methyl H3K9-binding protein HP1 during mitosis [35,36]. Mass spectrometry data provided some *in vivo* support for the ‘methyl/phos’ binary switch hypothesis [35,37], since phosphopeptides containing lysine

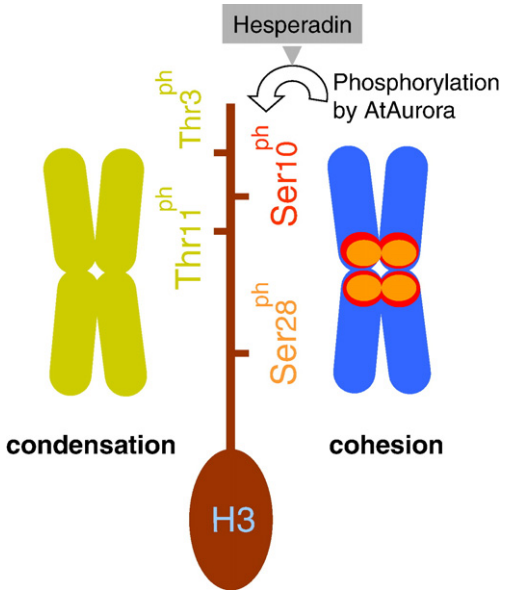

Fig. 3. Model: In plants the cell cycle dependent phosphorylation at H3T11/3 may serve as a signal for other proteins involved in chromosome condensation, while H3S10/28ph is involved sister chromatid cohesion at the pericentromeres of metaphase chromosomes during mitosis and meiosis II. Aurora-like kinase phosphorylates H3 at S10/28, and Hesperadin inhibits phosphorylation activity of Aurora.

methylation were often found. This suggests that these binary switches could also possibly extended to K27/S28 and T3/K4 [38]. This finding is in contrast to earlier reports suggesting that the coexistence of H3K9 methylation and S10 phosphorylation was unlikely [39]. A reduction in the levels of the JIL-1 histone H3S10 kinase resulted in the spreading of the major heterochromatin markers H3K9me2 and HP1 to ectopic locations on the chromosome arms, with the most pronounced increase on the X chromosomes [40]. Whether a similar 'methyl/phos binary switch' exists in plants remains to be studied. However, the finding that the subnuclear localisation of HP1-like protein was unaffected in Arabidopsis mutants displaying a significant reduction in H3K9 methylation raises some doubt about the role of H3-K9 methylation in HP1 recruitment to chromocentres in plants [41]. In the same way, Arabidopsis DNA methylation mutants (DDM1 and MET1) did not reveal any altered H3S10 phosphorylation sites at the microscopical level (Houben, A., unpublished data).

3. Candidate kinases involved in cell cycle-dependent histone phosphorylation

Genetic and biochemical data indicate that members of the Aurora kinase family, in particular Ipl1p of *Saccharomyces cerevisiae* and the B-type Aurora of *Caenorhabditis elegans, Drosophila* and mammals, can control cell cycle regulated histone H3 phosphorylation at serine 10 and 28, as opposed to a type 1 phosphatase (Glc7p in *S. cerevisiae*) [6,42–44]. At the same time several other kinases, have also been reported to be involved in the phosphorylation of H3 after mitogenic stimulation or stress (listed in [45]). Thus many kinases, which appear to be involved in histone H3 phosphorylation, may be stimulus- and cell type-dependent. The first plant type Aurora kinases have recently been characterised [46,47]. Consistent with the mitotic function of Aurora kinases described in other systems, transcripts and proteins of Arabidopsis Auroras are most abundant in tissues containing actively dividing cells. Localisation of GFP-tagged AtAuroras revealed that AtAuroras primarily associate with mitotic structures such as microtubule spindles, centromeres and with the emerging cell plate of dividing BY-2 culture cells of tobacco. All three members of the Arabidopsis *Aurora*-like gene family (*At4g32830, At2g25880, At2g45490*) phosphorylate histone H3 at serine 10 *in vitro*. At Aurora-specific immunosignals at the pericentromeres that are coincident with histone H3 that is phosphorylated at serine position S10 further supports histone H3 substrate specificity. But in contrast to the mammalian B-type Aurora [44] recombinant AtAurora1 of Arabidopsis reveals no *in vitro* kinase activity towards H3 at position serine 28. Overexpression data of [47] indicate that AtAurora3 also acts on gamma-tubulin disposition or recruitment to promote spindle formation. The generation of knockdown mutants will help to further define the mitotic and meiotic function of plant Aurora kinases.

Evolutionary analysis shows that Aurora kinases, while having a consistent sequence theme throughout eukaryotes, have undergone lineage-specific expansions and functional specialization in metazoans. The occurrence of two subclades in plants raises the interesting possibility that plants possess two different isoforms of Aurora, called plant Aurora α and Aurora β [46].

In animals, Aurora B is an enzymatic core of chromosomal passenger complex, which also includes the inner centromere protein INCENP, survivin, and borealin/DasraB. The complex localises to the centromere during prometaphase and metaphase [48]. Members of the Aurora B complex in fission yeast and budding yeast have been characterised and shown to have similar functions to their animal-cell orthologues (reviewed in [49]). However, homologues of INCENP, survivin, and borealin/DasraB could not be found in the Arabidopsis genome and other plant proteins using NCBI conserved domain database and blastp [47]. Whether the plant kinetochore-localised histone H3 variant CENH3 (CENPA) undergoes phosphorylation by an Aurora kinase, as reported for other organisms, remains to be answered. In human S7 of CENH3 is phosphorylated in a temporal pattern that is similar to H3S10 [50]. In plants it is noteworthy that CENH3-S50 and H3S28 are phosphorylated with virtually identical kinetics [11]. Based on the temporal coordination of CENH3 and H3S28 phosphorylation Zhang et al. [11] suggest that one signal for centromere-mediated cohesion accumulation is a histone kinase, which binds first at CENH3 and then diffuses outwards over histone H3 to define the boundaries of the pericentromeric domains. Identification of additional plant Aurora kinase substrates will be very fruitful in determining details of their molecular function.

NIMA kinase (never in mitosis, [51]) activity is required for both phosphorylation of histone H3 Serine 10 and chromo-

some condensation in *Aspergillus nidulans* [52]. The fission yeast NIMA homologue, Fin1p, can induce profound chromosome condensation in the absence of condensin and topoisomerase II, indicating that Fin1p-induced condensation differs from mitotic condensation [53]. Yet, despite similarity to NIMA of *Aspergillus*, no evidence for histone H3-specific kinase activity has been found for Fin1p [51]; although *in vitro* evidence exists that the human NIMA-like kinase Nek6 has potential histone H3 substrate specificity [54]. While yeast and filamentous fungi have only a single NIMA-like kinase, *Caenorhabditis elegans* encodes four [55], humans encode at least 11 [56] and Arabidopsis encodes a *NIMA*-related gene family with 7 members (*At1g54510*, *At3g04810, At5g28290*, *At3g63280*, *At3g20860*, *At3g44200*, *At3g12200*) [56]. The first plant NIMA-like kinases were described in *Antirrhinum majus* [57], tomato [58] and poplar [56]; but whether histone H3 is the substrate for any of these plant NIMA-like proteins remains to be analysed.

The human haspin kinase (haploid germ cell-specific nuclear protein [59]) phosphorylates histone H3 on T3 *in vitro*, and probably also *in vivo* in human cultured cells. Haspin RNA interference in mammals causes misalignment of metaphase chromosomes, and overexpression delays progression through early mitosis [60]. Genes encoding *haspin* homologues are present in all major eukaryotic phyla, but not in any of the sequenced prokaryotic or archaea genomes [61]. In mammals haspin localises to the nucleus, to condensed chromosomes throughout mitosis, to the centrosomes and spindle microtubules during metaphase and to the midbody in telophase [19]. Despite its crucial role in mitosis, a cell cycle dependent kinase activity could not be detected for haspin [19]. Similarly, based on publicly available microarray datasets [62] the expression profile of the *haspin*-like gene of Arabidopsis (*At1g09450*) does not change during mitosis. *In vitro* kinase assays testing histone substrate specificity of the *Saccharomyces cerevisiae* haspin-related proteins Alk1 and Alk2 failed to identify histones as putative substrates [63].

The potential kinase(s) involved in phosphorylation of H3T11 in plants remain to be identified. In mammals, Dlk/ZIP kinase seems to be a likely candidate since it phosphorylates H3 at T11 *in vitro* and its association with centromeres parallels precisely the appearance of T11 phosphorylation [21]. A BLAST search of the Arabidopsis databank for homologues of DAP kinase family members [64] only revealed protein kinases with low similarity.

The identification of different kinases with H3 substrate specificity suggests that various kinases could function as mitotic H3 kinases in different organisms. It is also conceivable that within any single organism many kinases can phosphorylate histones during cell division.

4. Histone phosphorylation in the activation of transcription, apoptosis and DNA damage repair

Histone phosphorylation, like other post-translational histone modifications, has also been linked to the activation of transcription, apoptosis, DNA damage repair and even sex chromosome dosage compensation (reviewed in [23,65,66]); although our knowledge of its involvement in these processes in plants is limited.

Recent transcriptome analysis in yeast demonstrated that H3S10 phosphorylation is not a general requirement for transcription at all promoters, but it may play a role tailored to specific promoters [67]. In addition diverse stimuli, including salt stress [68] or treatment of cells with growth factors [69], elicit rapid and transient phosphorylation of different serine/threonine positions on histones. Probably H3 phosphorylation also has a role in the transcriptional activation of plant genes [70]. Its involvement in stress response of plants is indirectly supported by the observation that cold, salt or hormone stress enhances the activity of the Arabidopsis MSK homologues ATPK6/19 kinases [71]. MSK kinases are enzymes involved in the process of histone phosphorylation during stress conditions [72]. In the same way, the treatment of cultured BY-2 cells of tobacco with different concentrations of sucrose, or of NaCl, can lead to an increase in phosphorylation of histone H3 at S10 and T3, particularly at intermediate concentrations, independently of any increase in the rate of cell division (Fig. 4, Demidov, D., unpublished data). Similar changes in the modifications of histone H3 after salt stress were reported for a tobacco cell culture [73]. We assume that the treatment with sucrose and NaCl might induce in a time and concentration dependent manner the chromatin environment of genes involved in the processes of energy and carbohydrates metabolism and osmotic-salt stress responsive pathway, respectively.

The correlation of H3S10 phosphorylation with gene transcription received further support after increased phospho H3S10-specific immunolabelling was observed in actively transcribing shock puffs in *Drosophila* polytene chromosomes following heat shock [74]. Cold treatment of plant root meristems has also been found to result in additional chromosomal sites (45S rDNA loci and heterochromatic sites) of H3S10 phosphorylation, besides that in the centromeres [24]; although

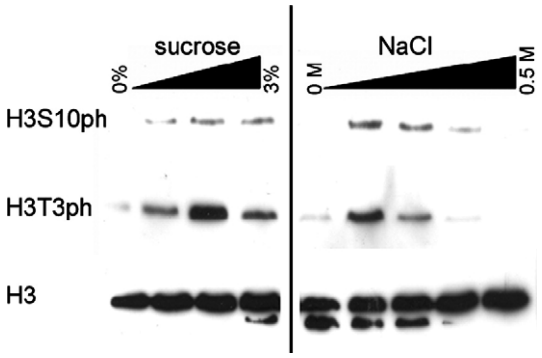

Fig. 4. Western blot analysis of histone H3 phosphorylation on total protein extracts from tobacco BY-2 cells after treatment with different concentrations of sucrose (0, 0.1, 1 and 3%) and NaCl (0, 0.1, 0.1, 0.25 and 0.5 M). Cell suspension was cultivated in a basic medium [87] and the treatment was performed for 1 h. Total protein isolation and immunodetection by Western blot was performed according [47]. Left: BY-2 suspension after treatment with 0–3% sucrose and subjected for Western blot analysis with antibodies against H3S10ph, H3T3ph and unmodified histone H3, respectively. Right: The same antibodies as above were used for the Western blot on protein extracts isolated from BY-2 cells treated with 0–0.5 M NaCl.

it is not clear whether chromosomal cold-sensitive regions are indirectly correlated with cold-stress activated genes.

Histone phosphorylation has also been observed in association with the apoptosis-induced chromatin condensation process (reviewed in [75]). Besides histone H3, there is also evidence for a correlation between histone H2A.X phosphorylation [76] and H2B phosphorylated at serine 14 [77] with the onset of apoptotic chromatin condensation and DNA fragmentation in human cells. In contrast with S10/28 phosphorylation of H3, the H2BS14 phosphorylation mark is not detected in mitotic chromosomes. This has led to the hypothesis of a non-overlapping set of phosphorylation marks discriminating mitotic from apoptotic chromatin, a 'life versus death histone code' [77]. Chromatin apoptotic-like features partly similar to mammalian cells have been observed in plants (reviewed in [78]) but a relationship between H3 phosphorylation and apoptosis is not yet established for plants.

In yeast and in metazoa the histone variant H2A.X becomes phosphorylated (known as gamma-H2A.X) at its C-terminal S139 on either side of a DNA double-strand break, induced by ionising radiation, meiosis, replication and recombination, at a distance of 1 to 50 kb by specific kinases (ATM, ATR). Phosphorylated H2A.X reversibly triggers the accumulation of components involved in DNA recombination repair, and in cell cycle checkpoint activation including histone acetyltransferase and cohesin (for review see [79]). In plants, phosphorylation of H2A.X is induced by gamma-irradiation at only one third the rate observed in yeast and mammals, suggesting that plants are more resistant than mammals to the induction of DNA lesions [80]. It is possible that in plants, fewer DNA lesions are formed in response to ionising radiation, or plants possess a greater capacity for DNA repair and/or damage tolerance than mammals do [80].

5. Outlook

Except for centromeric histone CENPA of maize [11], plant histone H3 investigations have not yet looked specifically at individual H3 isoform phosphorylation. It is known however, that Arabidopsis encodes 15 histone H3 genes, including five H3.1, three *H3.3* and five *H3.3* like genes [81]. Amongst them are H3 variants with highly similar protein sequences, but different function, suggesting that phospho-specific antibodies are insufficient to distinguish between the phosphorylation status of different H3 isoforms. As mentioned by [39], future work on histone H3 phosphorylation cannot overlook the fact that modification differences in H3 variants may exist and should be taken into account. Complementary approaches, combining mass spectrometry with immunological assays, will be necessary to decipher the meaning of the diverse combinations of histone H3 modifications. Besides further research on H3 and isoforms, the functional analysis of phosphorylation of the other core histones including linker histones will improve our knowledge on the complex interplay of post-translational histone modifications in plants. Recently, chromatin condensation has been linked to phosphorylation of histone H4 [82,83], H2A [82], H2B [84] and H1 [76] in non-plant species.

Although the components of the chromatin code are fairly well conserved throughout eukaryotes, evidence is growing that the interpretation of the code has diverged in different organisms, particular in plants versus animals [85,86]. We look forward to further exciting insights that are certain to arise as researchers continue to investigate the function and regulation of histone modifications in diverse model systems.

Acknowledgments

AH, DD, RK, FA and LV were supported by grants from the Land Sachsen-Anhalt and from the DFG. We apologize to all our colleagues who contributed to the field but could not be cited due to space limitation.

References

[1] L.R. Gurtley, R.A. Walters, R.A. Tobey, Sequential phosphorylation of histone subfractions in the Chinese hamster cell cycle, J. Biol. Chem. 250 (1975) 3936–3944.
[2] M.J. Hendzel, Y. Wei, M.A. Mancini, A. Van Hooser, T. Ranalli, B.R. Brinkley, D.P. Bazett-Jones, C.D. Allis, Mitosis-specific phosphorylation of histone H3 initiates primarily within pericentromeric heterochromatin during G2 and spreads in an ordered fashion coincident with mitotic chromosome condensation, Chromosoma 106 (1997) 348–360.
[3] A. Houben, T. Wako, R. Furushima-Shimogawara, G. Presting, G. Kunzel, I. Schubert, K. Fukui, The cell cycle dependent phosphorylation of histone H3 is correlated with the condensation of plant mitotic chromosomes, Plant J. 18 (1999) 675–679.
[4] H. Goto, Y. Tomono, K. Ajiro, H. Kosako, M. Fujita, M. Sakurai, K. Okawa, A. Iwamatsu, T. Okigaki, T. Takahashi, M. Inagaki, Identification of a novel phosphorylation site on histone H3 coupled with mitotic chromosome condensation, J. Biol. Chem. 274 (1999) 25543–25549.
[5] A. Van Hooser, D.W. Goodrich, C.D. Allis, B.R. Brinkley, M.A. Mancini, Histone H3 phosphorylation is required for the initiation, but not maintenance, of mammalian chromosome condensation, J. Cell Sci. 111 (1998) 3497–3506.
[6] J.Y. Hsu, Z.W. Sun, X. Li, M. Reuben, K. Tatchell, D.K. Bishop, J.M. Grushcow, C.J. Brame, J.A. Caldwell, D.F. Hunt, R. Lin, M.M. Smith, C. D. Allis, Mitotic phosphorylation of histone H3 is governed by Ipl1/aurora kinase and Glc7/PP1 phosphatase in budding yeast and nematodes, Cell 102 (2000) 279–291.
[7] K.K. Hanson, A.C. Kelley, M. Bienz, Loss of *Drosophila borealin* causes polyploidy, delayed apoptosis and abnormal tissue development, Development 132 (2005) 4777–4787.
[8] E. Kaszas, W.Z. Cande, Phosphorylation of histone H3 is correlated with changes in the maintenance of sister chromatid cohesion during meiosis in maize, rather than the condensation of the chromatin, J. Cell. Sci. 113 (2000) 3217–3226.
[9] S. Manzanero, P. Arana, M.J. Puertas, A. Houben, The chromosomal distribution of phosphorylated histone H3 differs between plants and animals at meiosis, Chromosoma 109 (2000) 308–317.
[10] D. Gernand, D. Demidov, A. Houben, The temporal and spatial pattern of histone H3 phosphorylation at serine 28 and serine 10 is similar in plants but differs between mono- and polycentric chromosomes, Cytogenet. Genome Res. 101 (2003) 172–176.
[11] X.L. Zhang, X.X. Li, J.B. Marshall, C.X. Zhong, R.K. Dawe, Phosphoserines on maize CENTROMERIC HISTONE H3 and histone H3 demarcate the centromere and pericentromere during chromosome segregation, Plant Cell 17 (2005) 572–583.
[12] E. Schroeder-Reiter, A. Houben, G. Wanner, Immunogold labeling of chromosomes for scanning electron microscopy: a closer look at phosphorylated histone H3 in mitotic metaphase chromosomes of *Hordeum vulgare*, Chromosome Res. 11 (2003) 585–596.

[13] G. Wanner, H. Formanek, A new chromosome model, J. Struct. Biol. 132 (2000) 147–161.
[14] A.A. Van Hooser, I.I. Ouspenski, H.C. Gregson, D.A. Starr, T.J. Yen, M.L. Goldberg, K. Yokomori, W.C. Earnshaw, K.F. Sullivan, B.R. Brinkley, Specification of kinetochore-forming chromatin by the histone H3 variant CENP-A, J. Cell. Sci. 114 (2001) 3529–3542.
[15] F. Han, J.C. Lamb, J.A. Birchler, High frequency of centromere inactivation resulting in stable dicentric chromosomes of maize, Proc. Natl. Acad. Sci. U. S. A. 103 (2006) 3238–3243.
[16] M. Guerra, A.C. Brasileiro-Vidal, P. Arana, M.J. Puertas, Mitotic micortubule development and histone H3 phosphorylation in the holocentric chromosomes of *Rhynchospora tenuis* (Cyperaceae), Genetica 126 (2006) 33–41.
[17] K. Nagaki, K. Kashihara, M. Murata, Visualization of diffuse centromeres with centromere-specific histone H3 in the holocentric plant *Luzula nivea*, Plant Cell 17 (2005) 1886–1893.
[18] A. Houben, D. Demidov, T. Rutten, K.H. Scheidtmann, Novel phosphorylation of histone H3 at threonine 11 that temporally correlates with condensation of mitotic and meiotic chromosomes in plant cells, Cytogenet. Genome Res. 109 (2005) 148–155.
[19] J. Dai, J.M.G. Higgins, Haspin—A mitotic histone kinase required for metaphase chromosome alignment, Cell Cycle 4 (2005) 665–668.
[20] H. Polioudaki, Y. Markaki, N. Kourmouli, G. Dialynas, P.A. Theodoropoulos, P.B. Singh, S.D. Georgatos, Mitotic phosphorylation of histone H3 at threonine 3, FEBS Lett. 560 (2004) 39–44.
[21] U. Preuss, G. Landsberg, K.H. Scheidtmann, Novel mitosis-specific phosphorylation of histone H3 at Thr11 mediated by Dlk/ZIP kinase, Nucleic Acids Res. 31 (2003) 878–885.
[22] F. Hans, S. Dimitrov, Histone H3 phosphorylation and cell division, Oncogene 20 (24) (2001) 3021–3027.
[23] C. Prigent, S. Dimitrov, Phosphorylation of serine 10 in histone H3, what for? J. Cell Sci. 116 (2003) 3677–3685.
[24] S. Manzanero, T. Rutten, V. Kotseruba, A. Houben, Alterations in the distribution of histone H3 phosphorylation in mitotic plant chromosomes in response to cold treatment and the protein phosphatase inhibitor cantharidin, Chromosome Res. 10 (2002) 467–476.
[25] K. Ajiro, K. Yoda, K. Utsumi, Y. Nishikawa, Alteration of cell cycle-dependent histone phosphorylations by okadaic acid. Induction of mitosis-specific H3 phosphorylation and chromatin condensation in mammalian interphase cells, J. Biol. Chem. 271 (1996) 13197–13201.
[26] Y. Li, Y. Butenko, G. Grafi, Histone deacetylation is required for progression through mitosis in tobacco cells, Plant J. 41 (2005) 346–352.
[27] C. MacKintosh, R.M. MacKintosh, Inhibitors of protein kinases and phosphatases, Trends Biochem. Sci. 19 (1994) 444–448.
[28] D. Kurihara, S. Matsunaga, A. Kawabe, S. Fujimoto, M. Noda, S. Uchiyama, K. Fukui, Aurora kinase is required for chromosome segregation in tobacco BY-2 cells, Plant J. 48 (2006) 572–580.
[29] S. Hauf, R.W. Cole, S. LaTerra, C. Zimmer, G. Schnapp, R. Walter, A. Heckel, J. van Meel, C.L. Rieder, J.M. Peters, The small molecule Hesperadin reveals a role for Aurora B in correcting kinetochore-microtubule attachment and in maintaining the spindle assembly checkpoint, J. Cell Biol. 161 (2003) 281–294.
[30] C.L. Peterson, M.A. Laniel, Histones and histone modifications, Curr. Biol. 14 (2004) R546–R551.
[31] C.J. Fry, M.A. Shogren-Knaak, C.L. Peterson, Histone H3 amino-terminal tail phosphorylation and acetylation: synergistic or independent transcriptional regulatory marks? Cold Spring Harbor Symposia on Quantitative Biology 69 (2004) 219–226.
[32] W. Fischle, Y. Wang, C.D. Allis, Histone and chromatin cross-talk, Curr. Opin. Cell Biol. 15 (2003) 172–183.
[33] A. Clements, A.N. Poux, W.S. Lo, L. Pillus, S.L. Berger, R. Marmorstein, Structural basis for histone and phosphohistone binding by the GCN5 histone acetyltransferase, Mol. Cell 12 (2003) 461–473.
[34] W.S. Lo, R.C. Trievel, J.R. Rojas, L. Duggan, J.Y. Hsu, C.D. Allis, R. Marmorstein, S.L. Berger, Phosphorylation of serine 10 in histone H3 is functionally linked in vitro and in vivo to Gcn5-mediated acetylation at lysine 14, Mol. Cell 5 (2000) 826–917.
[35] W. Fischle, B.S. Tseng, H.L. Dormann, B.M. Ueberheide, B.A. Garcia, J. Shabanowitz, D.F. Hunt, H. Funabiki, C.D. Allis, Regulation of HP1-chromatin binding by histone H3 methylation and phosphorylation, Nature 438 (2005) 1116–1122.
[36] T. Hirota, J.J. Lipp, B.H. Toh, J.M. Peters, Histone H3 serine 10 phosphorylation by Aurora B causes HP1 dissociation from heterochromatin, Nature 438 (2005) 1176–1180.
[37] W. Fischle, Y. Wang, C.D. Allis, Binary switches and modification cassettes in histone biology and beyond, Nature 425 (2003) 475–479.
[38] B.A. Garcia, C.M. Barber, S.B. Hake, C. Ptak, F.B. Turner, S.A. Busby, J. Shabanowitz, R.G. Moran, C.D. Allis, D.F. Hunt, Modifications of human histone H3 variants during mitosis, Biochemistry 44 (2005) 13202–13213.
[39] S. Rea, F. Eisenhaber, D. O'Carroll, B.D. Strahl, Z.W. Sun, M. Schmid, S. Opravil, K. Mechtler, C.P. Ponting, C.D. Allis, T. Jenuwein, Regulation of chromatin structure by site-specific histone H3 methyltransferases, Nature 406 (2000) 593–599.
[40] W. Zhang, H. Deng, X. Bao, S. Lerach, J. Girton, J. Johansen, K.M. Johansen, The JIL-1 histone H3S10 kinase regulates dimethyl H3K9 modifications and heterochromatic spreading in *Drosophila*, Development 133 (2006) 229–235.
[41] A. Zemach, Y. Li, H. Ben-Meir, M. Oliva, A. Mosquna, V. Kiss, Y. Avivi, N. Ohad, G. Grafi, Different domains control the localization and mobility of LIKE HETEROCHROMATIN PROTEIN1 in Arabidopsis nuclei, Plant Cell 18 (2006) 133–145.
[42] C. Crosio, G.M. Fimia, R. Loury, M. Kimura, Y. Okano, H. Zhou, S. Sen, C.D. Allis, P. Sassone-Corsi, Mitotic phosphorylation of histone H3: spatio-temporal regulation by mammalian Aurora kinases, Mol. Cell. Biol. 22 (2002) 874–885.
[43] R. Giet, D.M. Glover, *Drosophila* aurora B kinase is required for histone H3 phosphorylation and condensin recruitment during chromosome condensation and to organize the central spindle during cytokinesis, J. Cell Biol. 152 (2001) 669–682.
[44] H. Goto, Y. Yasui, E.A. Nigg, M. Inagaki, Aurora-B phosphorylates histone H3 at serine28 with regard to the mitotic chromosome condensation, Genes Cells 7 (2002) 11–17.
[45] A.M. Bode, Z. Dong, Inducible covalent posttranslational modification of histone H3, Sci. STKE 2005 (281) (2005) re4.
[46] D. Demidov, D. Van Damme, D. Geelen, F.R. Blattner, A. Houben, Identification and dynamics of two classes of aurora-like kinases in Arabidopsis and other plants, Plant Cell 17 (2005) 836–848.
[47] A. Kawabe, S. Matsunaga, K. Nakagawa, D. Kurihara, A. Yoneda, S. Hasezawa, S. Uchiyama, K. Fukui, Characterization of plant Aurora kinases during mitosis, Plant Mol. Biol. 58 (2005) 1–13.
[48] P. Vagnarelli, W.C. Earnshaw, Chromosomal passengers: the four-dimensional regulation of mitotic events, Chromosoma 113 (2004) 211–222.
[49] P.D. Andrews, E. Knatko, W.J. Moore, J.R. Swedlow, Mitotic mechanics: the auroras come into view, Curr. Opin. Cell Biol. 15 (2003) 672–683.
[50] S.G. Zeitlin, R.D. Shelby, K.F. Sullivan, CENP-A is phosphorylated by Aurora B kinase and plays an unexpected role in completion of cytokinesis, J. Cell Biol. 155 (2001) 1147–1157.
[51] A.H. Osmani, K. O'Donnell, R.T. Pu, S.A. Osmani, Activation of the nimA protein kinase plays a unique role during mitosis that cannot be bypassed by absence of the bimE checkpoint, EMBO J. 10 (1991) 2669–2679.
[52] C.P. De Souza, A.H. Osmani, L.P. Wu, J.L. Spotts, S.A. Osmani, Mitotic histone H3 phosphorylation by the NIMA kinase in *Aspergillus nidulans*, Cell 102 (2000) 293–302.
[53] M.J. Krien, R.R. West, U.P. John, K. Koniaras, J.R. McIntosh, M.J. O'Connell, The fission yeast NIMA kinase Fin1p is required for spindle function and nuclear envelope integrity, EMBO J. 21 (2002) 1713–1722.
[54] Y. Hashimoto, H. Akita, M. Hibino, K. Kohri, M. Nakanishi, Identification and characterization of Nek6 protein kinase, a potential human homolog of NIMA histone H3 kinase, Biochem. Biophys. Res. Commun. 293 (2002) 753–758.
[55] M.J. O'Connell, M.J. Krien, T. Hunter, Never say never. The NIMA-related protein kinases in mitotic control, Trends Cell Biol. 13 (2003) 221–228.

[56] M. Cloutier, F. Vigneault, D. Lachance, A. Seguin, Characterization of a poplar NIMA-related kinase PNek 1 and its potential role in meristematic activity, FEBS Lett. 579 (2005) 4659–4665.
[57] H. Zhang, G. Scofield, P. Fobert, J.H. Doonan, A nimA-like protein kinase transcript is highly expressed in meristems of *Antirrhinum majus*, J. Microsc. (Oxford) 181 (1996) 186–194.
[58] L. Pnueli, T. Gutfinger, D. Hareven, O. Ben-Naim, N. Ron, N. Adir, E. Lifschitz, Tomato SP-interacting proteins define a conserved signaling system that regulates shoot architecture and flowering, Plant Cell 13 (12) (2001) 2687–2702.
[59] H. Tanaka, Y. Yoshimura, M. Nozaki, K. Yomogida, J. Tsuchida, Y. Tosaka, T. Habu, T. Nakanishi, M. Okada, H. Nojima, Y. Nishimune, Identification and characterization of a haploid germ cell-specific nuclear protein kinase (Haspin) in spermatid nuclei and its effects on somatic cells, J. Biol. Chem. 274 (1999) 17049–17057.
[60] J. Dai, S. Sultan, S.S. Taylor, J.M. Higgins, The kinase haspin is required for mitotic histone H3 Thr 3 phosphorylation and normal metaphase chromosome alignment, Genes Dev. 19 (2005) 472–488.
[61] J.M. Higgins, Structure, function and evolution of haspin and haspin-related proteins, a distinctive group of eukaryotic protein kinases, Cell Mol. Life Sci. 60 (2003) 446–462.
[62] M. Menges, L. Hennig, W. Gruissem, J.A.H. Murray, Cell cycle-regulated gene expression in Arabidopsis, J. Biol. Chem. 277 (2002) 41987–42002.
[63] A. Nespoli, R. Vercillo, L. di Nola, L. Diani, M. Giannattasio, P. Plevani, M. Muzi-Falconi, Alk1 and Alk2 are two new cell cycle-regulated haspin-like proteins in budding yeast, Cell Cycle 5 (2006) 1464–1471.
[64] D. Kogel, J.H. Prehn, K.H. Scheidtmann, The DAP kinase family of pro-apoptotic proteins: novel players in the apoptotic game, BioEssays 23 (2001) 352–358.
[65] K.M. Johansen, J. Johansen, Regulation of chromatin structure by histone H3S10 phosphorylation, Chromosome Res. 14 (2006) 393–404.
[66] R. Loury, P. Sassone-Corsi, Analysis of histone phosphorylation: coupling intracellular signaling to chromatin remodelling, Methods Enzymol. 377 (2004) 197–212.
[67] W.S. Lo, E.R. Gamache, K.W. Henry, D. Yang, L. Pillus, S.L. Berger, Histone H3 phosphorylation can promote TBP recruitment through distinct promoter-specific mechanisms, EMBO J. 24 (2005) 997–1008.
[68] T. Reitsema, D. Klokov, J.P. Banath, P.L. Olive, DNA-PK is responsible for enhanced phosphorylation of histone H2AX under hypertonic conditions, DNA Rep. 4 (2005) 1172–1181.
[69] I.S. Strelkov, J.R. Davie, Ser-10 phosphorylation of histone H3 and immediate early gene expression in oncogene-transformed mouse fibroblasts, Cancer Res. 62 (1) (2002) 75–78.
[70] G.F. Li, K.J. Bishop, T.C. Hall, De novo activation of the beta-phaseolin promoter by phosphatase or protein synthesis inhibitors, J. Biol. Chem. 276 (2001) 2062–2068.
[71] T. Mizoguchi, N. Hayashida, K. Yamaguchishinozaki, H. Kamada, K. Shinozaki, 2 genes that encode ribosomal-protein-S6 kinase homologs are induced by Cold or salinity stress in *Arabidopsis thaliana*, FEBS Lett. 358 (1995) 199–204.
[72] A.L. Clayton, L.C. Mahadevan, MAP kinase-mediated phosphoacetylation of histone H-3 and inducible gene regulation, FEBS Lett. 546 (2003) 51–58.
[73] A. Sokol, M. Prymakowska-Bosak, A. Jerzmanowski, Changes in the modifications of core histone H3 after salt stress in the BY-2 tobacco cell line and *Arabidopsis thaliana* cells, Abstract book of the 15th International Conference on Arabidopsis Research Published by: Max Planck Institute of Molecular Plant Physiology, Am Mühlenberg1 14476 Potsdam, T12-020, 2004.
[74] S.J. Nowak, V.G. Corces, Phosphorylation of histone H3 correlates with transcriptionally active loci, Genes Dev. 14 (2000) 3003–3013.
[75] J.P. Th'ng, Histone modifications and apoptosis: cause or consequence? Biochem. Cell. Biol. 79 (2001) 305–311.
[76] B. Sarg, W. Helliger, H. Talasz, B. Forg, H.H. Lindner, Histone H1 phosphorylation occurs site-specifically during interphase and mitosis: identification of a novel phosphorylation site on histone H1, J. Biol. Chem. 281 (2006) 6573–6580.
[77] W.L. Cheung, K. Ajiro, K. Samejima, M. Kloc, P. Cheung, C.A. Mizzen, A. Beeser, L.D. Etkin, B. Chernoff, B. Earnshaw, C.D. Allis, Apoptotic phosphorylation of histone H2B is mediated by mammalian sterile twenty kinase, Cell 113 (2003) 507–517.
[78] E. Lam, Controlled cell death, plant survival and development, Nat. Rev., Mol. Cell Biol. 5 (2004) 305–315.
[79] C. Thiriet, J.J. Hayes, Chromatin in need of a fix: phosphorylation of H2A.X connects chromatin to DNA repair, Mol. Cell 18 (2005) 617–622.
[80] J.D. Friesner, B. Liu, K. Culligan, A.B. Britt, Ionizing radiation-dependent gamma-H2AX focus formation requires ataxia telangiectasia mutated and ataxia telangiectasia mutated and Rad3-related, Mol. Biol. Cell 16 (2005) 2566–2576.
[81] T. Okada, M. Endo, M. Singh, P.L. Balla, Analysis of the histone H3 gene family in Arabidopsis and identification of the male-gamete-specific variant AtMGH3, Plant J. 44 (2005) 557–568.
[82] C.M. Barber, F.B. Turner, Y.M. Wang, K. Hagstrom, S.S. Taverna, S. Mollah, B. Ueberheide, B.J. Meyer, D.F. Hunt, P. Cheung, C.D. Allis, The enhancement of histone H4 and H2A serine 1 phosphorylation during mitosis and S-phase is evolutionarily conserved, Chromosoma 112 (2004) 360–371.
[83] T. Krishnamoorthy, X. Chen, J. Govin, W.L. Cheung, J. Dorsey, K. Schindler, E. Winter, C.D. Allis, V. Guacci, S. Khochbin, M.T. Fuller, S.L. Berger, Phosphorylation of histone H4 Ser1 regulates sporulation in yeast and is conserved in fly and mouse spermatogenesis, Genes Dev. 20 (2006) 2580–2592.
[84] S.H. Ahn, K.A. Henderson, S. Keeney, C.D. Allis, H2B (Ser10) phosphorylation is induced during apoptosis and meiosis in *S. cerevisiae*, Cell Cycle 4 (2005) 780–783.
[85] P. Loidl, A plant dialect of the histone language, Trends Plant Sci. 9 (2004) 84–90.
[86] J. Fuchs, D. Demidov, A. Houben, I. Schubert, Chromosomal histone modification patterns—From conservation to diversity, Trends Plant Sci. 11 (2006) 199–208.
[87] K. Czempinski, J.M. Frachisse, C. Maurel, H. Barbier-Brygoo, B. Mueller-Roeber, Vacuolar membrane localization of the Arabidopsis 'two-pore' K+ channel KCO1, Plant J. 29 (2002) 809–820.

A7 Houben, A., Demidov, D., Rutten, T., and Scheidtmann, K.H. (2005). Novel phosphorylation of histone H3 at threonine 11 that temporally correlates with condensation of mitotic and meiotic chromosomes in plant cells. Cytogenet Genome Res 109, 148-155.

Cytogenet Genome Res 109:148–155 (2005)
DOI: 10.1159/000082394

Cytogenetic and Genome Research

Novel phosphorylation of histone H3 at threonine 11 that temporally correlates with condensation of mitotic and meiotic chromosomes in plant cells

A. Houben,[a] D. Demidov,[a] T. Rutten[a] and K.H. Scheidtmann[b]

[a] Institute of Plant Genetics and Crop Plant Research (IPK), Gatersleben;
[b] Institute of Genetics, University of Bonn, Bonn (Germany)

Abstract. A novel mitosis-specific phosphorylation site in histone H3 at threonine 11 has been described for mammalian cells. This modification is restricted to the centromeric region while phosphorylation at the classical H3 sites, Ser10 and Ser28 occurs along the entire chromosomal arms. Using phosphorylation state-specific antibodies we found that phosphorylation at threonine 11 occurs also in plant cells, during mitosis as well as meiosis. However, in contrast to animal cells, ph(Thr11)H3 was distributed along the entire length of condensed chromosomes, whereas H3 phosphorylated at Ser10 and Ser28 appeared to be restricted to centromeric/pericentromeric chromatin. Phosphorylation at Thr11 started in prophase and ended in telophase, it correlated with the condensation of mitotic and meiotic chromosomes and was independent of the distribution of late replicating heterochromatin and Giemsa-banding positive regions. Interestingly, treatment of cells with the phosphatase inhibitor cantharidin revealed a high level of Thr11 phosphorylation in interphase cells, in this case particularly in pericentromeric regions. These data show that histone modifications are highly dynamic. Moreover, animal and plant organisms may have evolved individual histone codes.

Dynamic changes in the organization of chromatin are emerging as key regulators in nearly every aspect of DNA metabolism in eukaryotes. Histones, the main protein components of chromatin, undergo extensive post-translational modifications, particularly acetylation, methylation, phosphorylation, ubiquitination and ADP-ribosylation. The various modifications of histones serve different functions in the dynamic changes of chromatin during transcription, replication, DNA repair, recombination, and cell division (for review see Fischle et al., 2003).

Phosphorylation of histone H3, at serines 10 and 28 seems to be crucial for cell cycle dependent chromosome condensation and segregation (Thomson et al., 1999; reviewed in Prigent and Dimitrov, 2003), but has also been linked to activation of transcription (Thomson et al., 1999; Prigent and Dimitrov, 2003).

Observations in several eukaryotes have shown that the level of H3 phosphorylation, which is very low in interphase, increases substantially at the beginning of prophase and decreases again during telophase and thus parallels the time of chromosome condensation (Gurtley et al., 1975; Wei and Allis, 1998). The use of site- and phosphorylation state-specific antibodies has greatly facilitated detailed analyses of the spatiotemporal distributions of the various modifications (Hendzel et al., 1997; Goto et al., 1999).

Interestingly, although histone H3 and most of its post-translational modifications are highly conserved, a number of significant differences exist between animals and plants. In

Supported by the Deutsche Forschungsgemeinschaft (Ho 1779/2-3).

Received 21 October 2003; manuscript accepted 6 February 2004.

Request reprints from Dr. Andreas Houben
Institute of Plant Genetics and Crop Plant Research (IPK)
DE–06466 Gatersleben (Germany); telephone: +49 394825486
fax: +49 394825137; e-mail: houben@ipk-gatersleben.de

0301–0171/05/1093–0148$22.00/0

Accessible online at:
www.karger.com/cgr

non-plant eukaryotes phosphorylation of H3 at serine 10 (Hendzel et al., 1997) and serine 28 (Goto et al., 1999) starts in late G2 phase in the pericentromeric region from where it is distributed homogeneously throughout the chromosomes. In contrast, in plants, H3 phosphorylation levels at both serine positions are high in pericentromeric regions but very low along the chromosome arms (Houben et al., 1999; Kaszas and Cande, 2000; Manzanero et al., 2000; Pedrosa et al., 2001; Gernand et al., 2003; Schroeder-Reiter et al., 2003). Interestingly, during meiosis in plants the distribution of Ser10 and Ser28 phosphorylation varies between the two meiotic divisions (Manzanero et al., 2000; Gernand et al., 2003). During the first division, the entire chromosomes are highly phosphorylated, while in the second division the H3 phosphorylation is restricted to the pericentromeric regions, similar to mitotic chromosomes. At the same time single chromatids, resulting from equational division of univalents at anaphase I, show low levels of phosphorylation all over. These results led to the hypothesis that in plants H3 phosphorylation at both serine positions is involved in sister chromatid cohesion (Manzanero et al., 2000; Gernand et al., 2003). This assumption is supported by the observation of Kaszas and Cande (2000) who showed that in a maize mutant defective in sister chromatid cohesion, univalents at metaphase I showed high (Ser10)H3 phosphorylation only in the pericentromeric regions.

Recently, a novel phosphorylation site in H3 at Thr11 was reported for mammalian cells. This modification was temporally as well as spatially distinct from the classical modifications at Ser10 and Ser28 in that phosphorylation at Thr11 occurred between prophase and anaphase and was largely restricted to centromeres (Preuss et al., 2003). This site can be phosphorylated by serine/threonine-specific DAP-like protein kinase (Dlk) in vitro. Moreover, Dlk associated with centromeres during mitosis suggesting that this kinase is responsible for phosphorylation of Thr11 in vivo. The significance of (Thr11)H3 phosphorylation in mammals is not clear yet. However, a role as a recognition code for kinetochore assembly has been proposed (Preuss et al., 2003).

In the present study we identified this novel phosphorylation site of H3 in plants and compared the chromosomal distribution of phosphorylated histone H3 at Thr11 and Ser28 during mitotic and meiotic divisions. To elucidate possible correlations between the chromosomal patterns of constitutive heterochromatin and late DNA replication on one side and (Thr11)H3 phosphorylation on the other, different plant species *(Arabidopsis thaliana, Secale cereale, Triticum aestivum, Hordeum vulgare* and *Vicia faba)* with well characterized but different heterochromatin and late replication patterns were investigated. The antibodies used against phosphorylated (Ser28)H3 (Goto et al., 1999) and (Thr11)H3 (Preuss et al., 2003) are likely to recognize the same peptide in plants since a striking sequence similarity for histone H3 exists between animals and plants (Waterborg and Robertson, 1996). Furthermore, the histone H3 amino acid sequences of many plant species are identical to the synthetic peptide sequence used for immunization. In addition, we employed the protein phosphatase inhibitor cantharidin to compare the response of dividing plant cells with regard to H3 phosphorylation at Thr11. Our study revealed striking differences in the chromosomal patterns of H3 phosphorylation between animal and plant cells. Moreover, H3 modifications appear to be highly dynamic.

Materials and methods

Plant material

The following plant species have been used: *Arabidopsis thaliana*, field bean *(Vicia faba)*, barley *(Hordeum vulgare)*, wheat *(Triticum aestivum)*, and rye *(Secale cereale)*.

Cantharidin treatment

Seedlings of barley, field bean and *A. thaliana* were transferred to filter paper soaked in 50 µM cantharidin (Calbiochem) dissolved in 0.1 % dimethyl sulfoxide (DMSO) in water, for 3 h, prior to fixation (Manzanero et al., 2002).

Chromosome preparation and indirect immunofluorescence

Preparation of mitotic and meiotic chromosomes and immunostaining were carried out following the method described by Manzanero et al. (2000). To avoid non-specific antibody binding, slides were blocked for 30 min in 4 % (w/v) bovine serum albumin (BSA), 0.1 % Triton X-100 in phosphate-buffered saline (PBS) at room temperature (RT) prior to two washes in PBS for 5 min each, and incubated with the primary antibodies in a humid chamber. Polyclonal affinity purified rabbit antibody against histone H3 phosphorylated at threonine 11 (Preuss et al., 2003) and a rat monoclonal antibody against H3 phosphorylated at serine 28 [ph(Ser28)H3] (Goto et al., 1999), were diluted 1:400 in PBS with 3 % BSA. After 12 h incubation at 4 ° C and washing for 15 min in PBS, the slides were incubated in rhodamine-conjugated anti-rabbit IgG (Dianova) and FITC-conjugated anti-rat IgG (Dianova) diluted 1:200 in PBS, 3 % BSA for 1 h at 37 ° C. After final washes in PBS, the preparations were mounted in antifade containing 4′,6-diamidino-2-phenylindole (DAPI) as counterstain.

Imaging of immunofluorescence was recorded with an Olympus BX61 microscope equipped with an ORCA-ER CCD camera (Hamamatsu). Deconvolution microscopy was employed for superior optical resolution of globular structures. Thus each photograph was collected as sequential image along the Z-axis with approximately 11 slices per specimen. All images were collected in gray scale and pseudocolored with Adobe Photoshop, and projections (maximum intensity) were done with the program AnalySIS (Soft Imaging System).

Immunogold electron microscopy

Suspensions of metaphase chromosomes were prepared from partially synchronized root tip meristems of seedlings of a field bean (translocation line: ACB) according to Schubert and coworkers (1993). For a better preservation of chromatin structure 0.5 % glutaraldehyde was included in the fixation solution. After washing in PBS, the chromosome suspension was centrifuged onto 11-mm diameter poly-L-lysine coated cover slips at 5,000 *g* for 25 min. The next steps were performed at room temperature unless otherwise stated. Samples were dehydrated in an ethanol series and infiltrated with HM20 resin. Polymerization was performed under UV light in a Reichert-Jung AFS at –35 ° C for 72 h. Ultrathin sections of 95 nm were cut on a Reichert Ultracut S and collected on formvar-coated 75-mesh hexagonal copper grids. Non-specific binding of antibodies was blocked with 3 % BSA in PBS for 15 min. Sections were incubated with primary antibody for 60 min, washed with 0.1 % BSA in PBS and then incubated for 45 min with 1.4-nm gold-conjugated goat anti-rabbit IgG (H+L) antibody (Nanoprobes, Yaphank, NY, USA) diluted 1:50 in 0.1 % BSA in PBS. After extensive washes in PBS and water, the probes were incubated in a gold enhancement solution (Nanoprobes, USA) according to the manufacturer's instructions. After 5 min, the reaction was stopped in water. Sections were contrasted with 4 % aqueous uranyl acetate and observed with an electron microscope (Zeiss 902 EM) at 80 kV. Controls were prepared avoiding the first antibody.

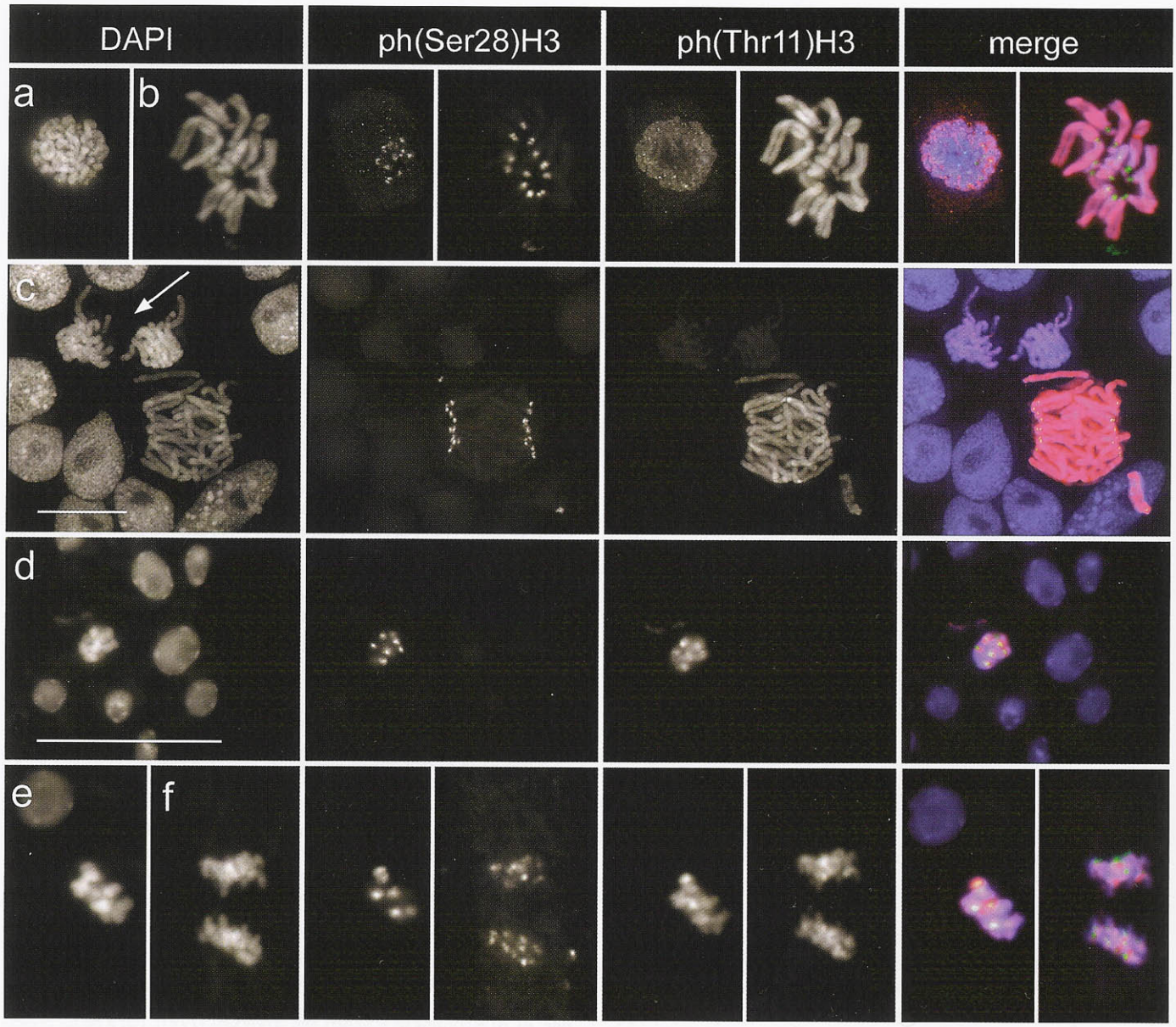

Fig. 1. Immunolabeling of phosphorylated histone H3 at threonine 11 [ph(Thr11)H3] or serine 28 [ph(Ser28)H3] during mitosis of *Vicia faba* (**a–c**) and *Arabidopsis thaliana* (**d–f**). The merged photographs show DNA counterstained with DAPI in blue, phosphorylated (Thr11)H3 in red, and phosphorylated (Ser28)H3 in green. Bars represent 10 μm. Only chromosomes at prophase (**a**, **d**), metaphase (**b**, **e**), anaphase (**c**, **f**) and the onset of telophase (**c**, arrowed) are phosphorylated at (Thr11)H3. Note: No immunostaining of interphase nuclei is detectable (**c**, **d**).

Results

Phosphorylation of histone H3 at threonine 11 is coupled with the process of chromosome condensation at mitosis and meiosis

Mitotic cells of the large genome species *V. faba* (Fig. 1a–c) and the small genome species *A. thaliana* (Fig. 1d–f) were simultaneously labeled with antibodies recognizing histone H3 phosphorylated at threonine 11 and serine 28. In both species, no immunostaining of interphase nuclei was observed (Fig. 1c, d). Distinct ph(Ser28)H3-immunofluorescence signal clusters became first visible at the beginning of chromosome condensation at early prophase. At this stage ph(Thr11)H3 distribution was more diffuse (Fig. 1a, d). In meta- and anaphase the entire chromosomes are hyperphosphorylated at (Thr11)H3, whereas ph(Ser28)H3-signals were confined strictly to the pericentromeric regions (Fig. 1b, c, e, f). Occasionally, the pericentromeric chromatin revealed the highest level of (Thr11)H3 phosphorylation in metaphase chromosomes of *H. vulgare* (data not shown). While in *A. thaliana* the late replicating constitutive heterochromatin is predominantly located close to the centromeres (Jasencakova et al., 2003), the late-replicating consti-

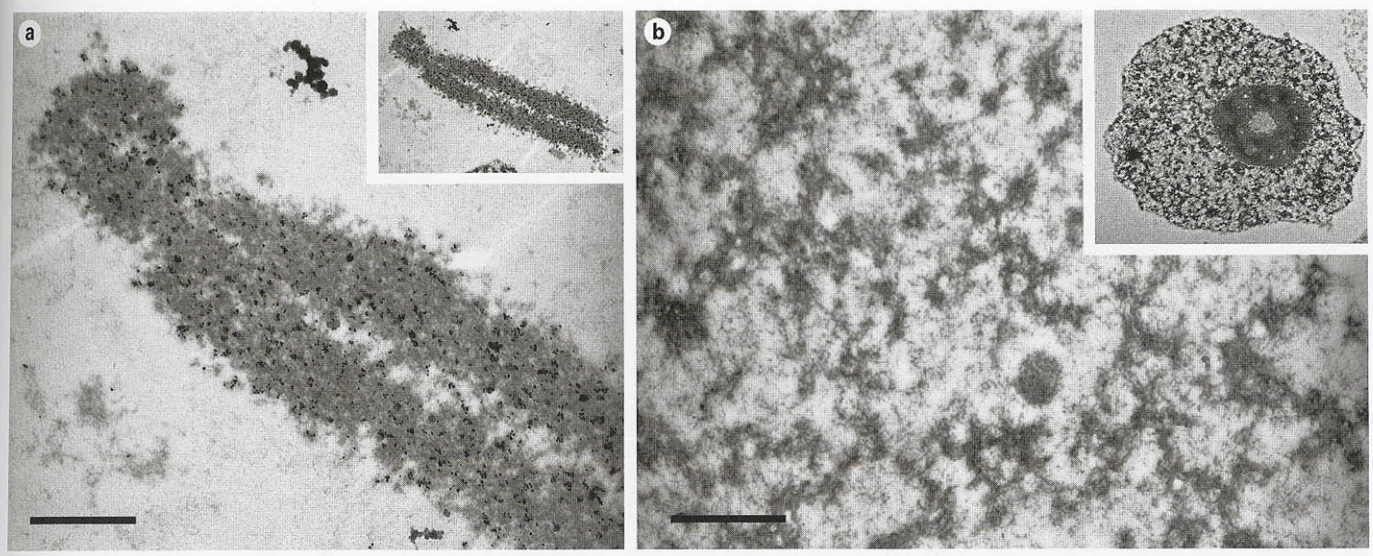

Fig. 2. Transmission electron micrographs of a *Vicia faba* metaphase chromosome (**a**) and nucleus (**b**) stained with primary antibody against phosphorylated (Thr11)H3, followed by secondary gold-labeled anti-rabbit IgG and subsequent gold enhancement. Only the metaphase chromosome shows evenly distributed immunosignals over the entire region. Inserted pictures show images of the corresponding chromosome and nucleus at lower magnification. Bars represent 1.5 μm.

tutive heterochromatin of *Vicia faba* (Döbel et al., 1978) is mainly located at intercalary positions. In both species heterochromatic regions were not differentially immunostained with the occasional exception of the pericentromeric region. With decondensation of the chromosomes at telophase, the phosphorylated Ser28 and Thr11 immunoreactivity disappeared (Fig. 1c).

Immuno-electron microscope studies on isolated mitotic *V. faba* chromosomes and nuclei following incubation with specific antibodies underlined the uniform distribution of ph(Thr11)H3 in condensed chromatin of metaphase chromosomes (Fig. 2a). No label was found in interphase nuclei indicating the absence of ph(Thr11)H3 at this stage (Fig. 2b).

We next investigated whether phosphorylation at Thr11 occurred during meiosis as well. Different stages of meiosis were analyzed in the species *S. cereale* and *T. aestivum,* two species with different distribution of constitutive heterochromatin (Schlegel and Gill, 1984). The immunolabeling patterns obtained with both antibodies were similar for the chromosomes of both species. Immunostaining of interphase cells was hardly observed. The first diffuse ph(Ser28 and Thr11)H3 immunosignals were detectable from diplotene to diakinesis (Fig. 3a). With further compaction of chromosomes during diakinesis, immunosignals were scattered over the chromosomes (Fig. 3b). At this stage ph(Ser28)H3 appeared to be much more abundant in the centromeric regions as compared to the rest of the chromosomes. At metaphase I, congressed bivalents were entirely and strongly ph(Thr11 and Ser28)H3-immunolabeled (Fig. 3c). At telophase I (not shown), the phosphorylation of histone H3 at both serine positions gradually disappeared towards interkinesis. During the second meiotic division the phosphorylation patterns were similar to those observed during mitosis, with (Thr11)H3 phosphorylation distributed over the entire chromosomes and (Ser28)H3 phosphorylation mainly restricted to the pericentromeric regions (Fig. 3d).

In contrast to (Ser28)H3 and (Ser10)H3 (Manzanero et al., 2000; Gernand et al., 2003), which appear hyperphosphorylated only in pericentromeric chromatin during mitosis and second meiosis, the phosphorylated (Thr11)H3 was uniformly distributed along the entire length of condensed chromosomes. These results suggest that the temporal and spatial phosphorylation pattern of H3 at threonine 11 correlates with the condensation of mitotic and meiotic chromosomes and is independent of the distribution of late replicating constitutive heterochromatin. The fact that (Thr11)H3 becomes dephosphorylated at interkinesis and phosphorylated again during prophase II, indicates that this post-translational modification is reversible and can occur independent of the DNA replication process.

The phosphatase inhibitor cantharidin induces histone H3 phosphorylation at threonine 11 in pericentromeric regions at interphase

The phosphatase inhibitor cantharidin perturbs the balance between phosphorylation and dephosphorylation of histone H3 at Ser10 (Manzanero et al., 2002) and Ser28 (Gernand et al., 2003). To assess the effects of cantharidin on the phosphorylation of histone H3 at threonine 11, we treated seedlings of *H. vulgare*, *V. faba* and *A. thaliana* for 3 h with 50 μM cantharidin. In all species analyzed, cantharidin-treated metaphase cells were uniformly immunolabeled, comparable to untreated cells (Fig. 4d). However, in interphase cantharidin clearly altered the phosphorylation status of histone H3 at Thr11. Inter-

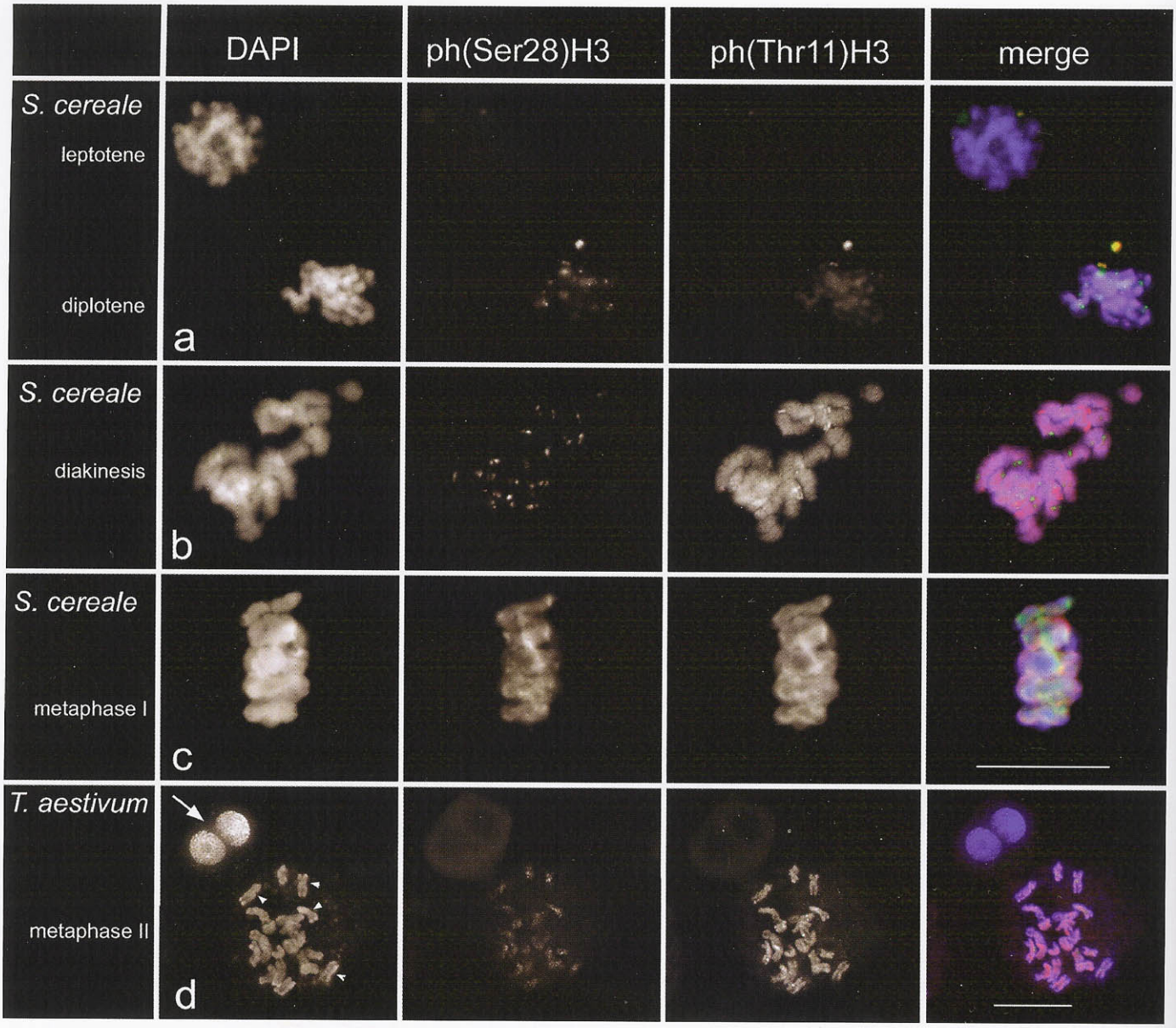

Fig. 3. Immunolocalization of phosphorylated histone H3 at serine 28 [ph(Ser28)H3] or threonine 11 [ph(Thr11)H3] during meiosis of *Secale cereale* (**a**, **b**, **c**) and *Triticum aestivum* (**d**). Leptotene and diplotene (**a**), diakinesis (**b**), metaphase I (**c**), metaphase II (**d**). A binucleated tapetal cell is indicated by an arrow (**d**). The merged photographs show DNA counterstained with DAPI in blue, phosphorylated (Thr11)H3 in red, and phosphorylated (Ser28)H3 in green. A number of centromeres are indicated by arrowheads. Bars represent 10 μm.

phase nuclei of cantharidin treated meristematic (Fig. 4c, e) or differentiated tissue (Fig. 4a) displayed distinct immunofluorescence spots in all species analyzed. The highest number of immunosignals counted was consistent with the number of chromosomes per cell. A signal distribution typical for the Rabl orientation (Rabl, 1885) was observed for *V. faba* and *H. vulgare* interphase nuclei (Fig. 4c, e), with signals positioned at one pole of the nucleus. Similar observations were reported for the distribution of prekinetochores in interphase nuclei of *V. faba* (Houben et al., 1995). Because at prophase only pericentromeres were immunoreactive and distinct signal gaps colocalized with the regions between the pericentromeric sister chromatids (Fig. 4b), it was concluded that the signals at interphase colocalized with the pericentromeres too. Thus, cantharidin may disturb directly or indirectly an ordered sequence of phosphorylation and dephosphorylation of threonine 11 of histone H3 at interphase. Due to the fact that also the pericentromeres in nuclei of differentiated (Fig. 4a) and non-dividing cells were de novo (Thr11)H3 phosphorylated, cantharidin induced phosphorylation must be S-phase independent.

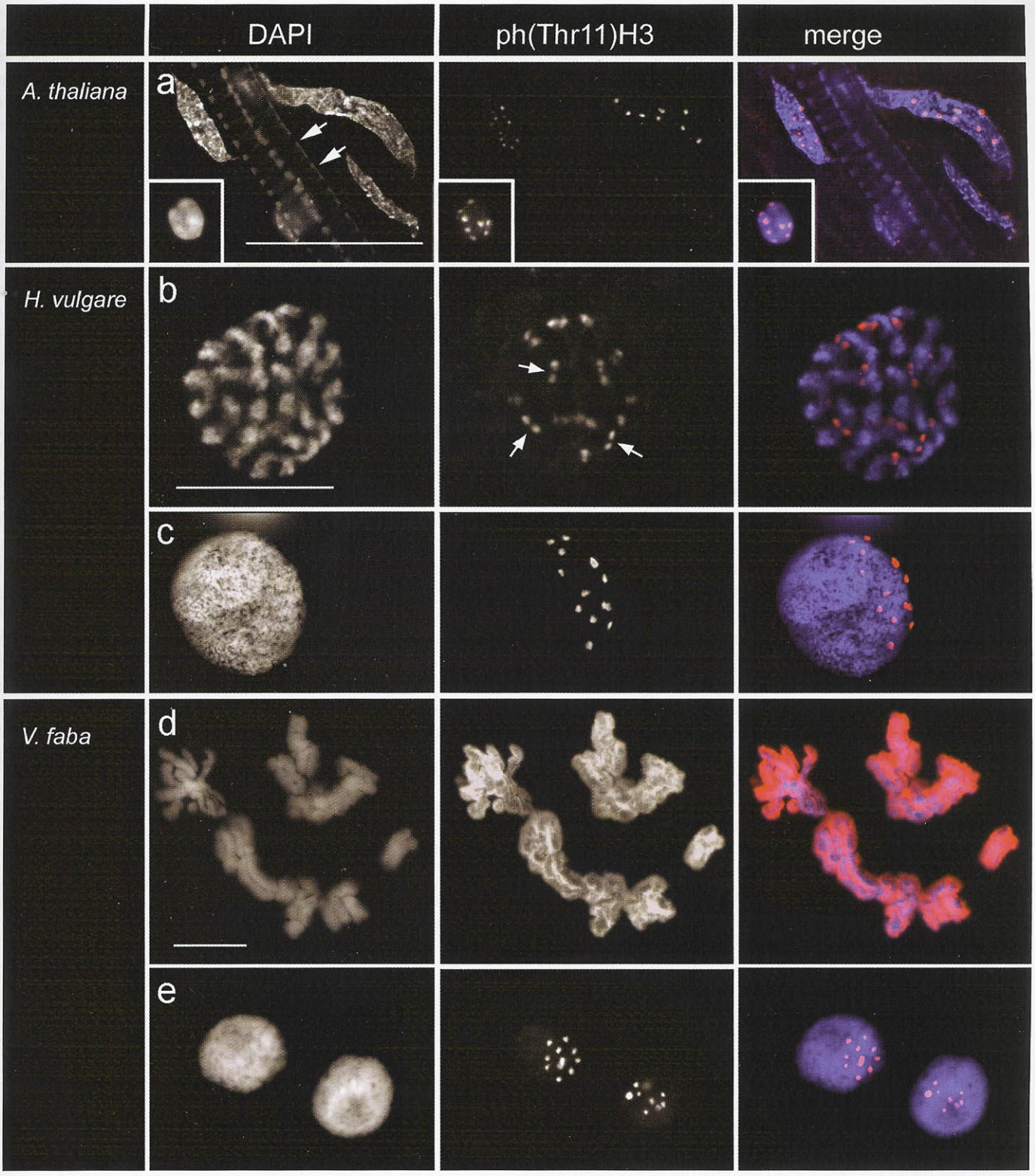

Fig. 4. Immunolabeling of phosphorylated (Thr11)H3 in *A. thaliana* (**a**), *H. vulgare* (**b**, **c**), and *V. faba* (**d**, **e**) nuclei (**a**, **c**, **e**), mitotic prophase (**b**) and metaphase (**d**) after 3 h treatment with 50 µM cantharidin. (**a**) Spindle-shaped nuclei of differentiated cells (tracheary element is arrowed); inserted picture shows a typical nucleus of meristematic tissue. The number of signal patches is consistent with the number of chromosomes per cell and with the position of the centromeres. Distinct signal gaps in the middle of each labeled domain are detectable at the prophase of *H. vulgare* (arrowed in **b**). Bar represents 10 µm.

Discussion

The novel finding of this study is that during cell division of plants histone H3 is phosphorylated not only at serine 10 (Houben et al., 1999; Kaszas and Cande, 2000; Manzanero et al., 2000) and serine 28 (Gernand et al., 2003), but also at threonine 11, thus extending previous observations in mammalian cells (Preuss et al., 2003) to plants. However, the immunolabeling patterns show remarkable differences in the chromosomal distribution of H3 phosphorylated at either the serine positions or at Thr11. Whereas H3 phosphorylated at Ser10 and Ser28 was confined to the centromeric/pericentromeric region, phosphorylation at Thr11 was discernable along the entire chromosomes. This was seen in all plant species investigated. Moreover, the uniform distribution of Thr11-phosphorylated H3 along chromosomes was independent of their heterochromatin composition and late-replication status. Therefore anti-ph(Thr11)H3 represents a robust marker for identifying mitotic and meiotic plant cells.

Remarkably, although the cell cycle-dependent process of histone H3 phosphorylation at serines 10 and 28 and at threonine 11 seems to be highly conserved during evolution of plants and animals, the distribution of H3 carrying these individual modifications is opposite. Thus, in mammalian chromosomes, it is Thr11 phosphorylation which is confined to centromeric chromatin (Preuss et al., 2003), whereas phoshorylated Ser10 and 28 is distributed along the chromosomal arms (Hendzel et al., 1997; Goto et al., 1999; Crosio et al., 2002).

The kinase(s) involved in phosphorylation of (Thr11)H3 in plants remains to be identified. In mammals Dlk/ZIP kinase seems to be a likely candidate since it phosphorylates H3 at Thr11 in vitro and its association with centromeres parallels precisely the appearance of Thr11 phosphorylation (Preuss et al., 2003). A BLAST search in the *A. thaliana* genomic databank for homologs of DAP kinase family members (Kogel et al., 2001) revealed only protein kinases with low similarity.

Generally, phosphorylation of H3 is not detectable during interphase, neither at Thr11 nor at Ser10 or Ser28. However, using the protein phosphatase inhibitor cantharidin revealed clear detection of Thr11 phosphorylation in interphase. Previous studies on plant cells showed that cantharidin did not have a severe effect on interphase, but affected the distribution of H3 phosphorylation at both Ser10 and 28 in mitotic cells, causing high H3 phosphorylation on the whole chromosome, as opposed to just the pericentric area in control cells (Manzanero et al., 2002; Gernand et al., 2003). For Thr11, we observed a different response to cantharidin. It became phosphorylated during interphase but this phosphorylation was restricted to pericentromeric regions. The simplest explanation for this finding is that phosphorylation of Thr11 takes place in interphase as well but remained undetected because the rate of dephosphorylation exceeds that of phosphorylation. Alternatively, the kinase phosphorylating Thr11 may be inactivated by dephosphorylation during interphase. Thus, inhibition of phosphatase activity could result in activation of this kinase. Since cantharidin affects a number of different PP2A and PP1 phosphatases (MacKintosh and MacKintosh, 1994) the specific enzyme involved cannot be deduced. It might be however, that the artificially induced (Thr11)H3 phosphorylation of the pericentric interphase chromatin and the phosphorylation of the chromosome arms is controlled by different kinases/phosphatases. In any case, ph(Thr11)H3-specific immunostaining after cantharidin treatment of cells could be used as a method to visualize the position of centromeres at interphase for plant species for which no centromere marker is available.

What might be the function(s) of H3 Thr11 phosphorylation in plants? Our data suggest that Thr11 phosphorylation correlates with the process of chromosome condensation during mitosis and meiosis. We propose that this modification may serve as a recognition code for other proteins involved in chromosome condensation. In contrast, in mammals, where phosphorylation of Thr11 is restricted to the centromere, it may, together with phosphorylated CENP-A (Zeitlin et al., 2001), serve as a recognition code for kinetochore assembly (Preuss et al., 2003). The reverse may be true for Ser10/28 modifications, which may provide a label for the centromere region in plants but serve in chromosome condensation in animals. Our data may thus resolve a long lasting controversy about the significance of mitotic H3 phosphorylation. The coincidence of H3 phosphorylation (at Ser10/28) with chromosome condensation in animal cells had led to the proposal that both are causally related (Hendzel et al., 1997; Goto et al., 1999). However, since for plants and other organisms this correlation did not exist, this proposal was modified to the "ready production hypothesis" (Hans and Dimitrov, 2001; Prigent and Dimitrov, 2003) meaning that H3 phosphorylation during mitosis simply serves as a record that chromosomes are ready for separation. With our finding that in plant cells phosphorylation at Thr11 rather than Ser10/28 correlates with chromosome condensation, the original proposal by Hendzel et al. (1997) may very well be valid due to species-specific differences in the biological significance of the histone code.

Acknowledgements

We are grateful to Margit Hantschmann, Katrin Kumke and Achim Bruder for excellent technical assistance. The antibody against H3 phosphorylated at serine 28 was kindly provided by Dr. M. Inagaki.

References

Crosio C, Fimia GM, Loury R, Kimura M, Okano Y, Zhou H, Sen S, Allis CD, Sassone-Corsi P: Mitotic phosphorylation of histone H3: spatio-temporal regulation by mammalian Aurora kinases. Mol Cell Biol 22:874–885 (2002).

Döbel P, Schubert I, Rieger R: Distribution of heterochromatin in a reconstructed karyotype of *Vicia faba* as identified by banding and DNA-late replication patterns. Chromosoma 69:193–209 (1978).

Fischle W, Wang Y, Allis CD: Histone and chromatin cross-talk. Curr Opin Cell Biol 15:172–183 (2003).

Gernand D, Demidov D, Houben A: The temporal and spatial pattern of histone H3 phosphorylation at serine 28 and serine 10 is similar in plants but differs between mono- and polycentric chromosomes. Cytogenet Genome Res 101:172–176 (2003).

Goto H, Tomono Y, Ajiro K, Kosako H, Fujita M, Sakurai M, Okawa K, Iwamatsu A, Okigaki T, Takahashi T, Inagaki M: Identification of a novel phosphorylation site on histone H3 coupled with mitotic chromosome condensation. J Biol Chem 274:25543–25549 (1999).

Gurtley LR, Walters RA, Tobey RA: Sequential phosphorylation of histone subfractions in the Chinese hamster cell cycle. J Biol Chem 250:3936–3944 (1975).

Hans F, Dimitrov S: Histone H3 phosphorylation and cell division. Oncogene 20:3021–3027 (2001).

Hendzel MJ, Wei Y, Mancini MA, Van Hooser A, Ranalli T, Brinkley BR, Bazett-Jones DP, Allis CD: Mitosis-specific phosphorylation of histone H3 initiates primarily within pericentromeric heterochromatin during G2 and spreads in an ordered fashion coincident with mitotic chromosome condensation. Chromosoma 106:348–360 (1997).

Houben A, Guttenbach M, Kress W, Pich U, Schubert I, Schmid M: Immunostaining and interphase arrangement of field bean kinetochores. Chromosome Res 3:27–31 (1995).

Houben A, Wako T, Furushima-Shimogawara R, Presting G, Künzel G, Schubert I, Fukui K: The cell cycle dependent phosphorylation of histone H3 is correlated with the condensation of plant mitotic chromosomes. Plant J 18:675–679 (1999).

Jasencakova Z, Soppe WJ, Meister A, Gernand D, Turner BM, Schubert I: Histone modifications in *Arabidopsis* – high methylation of H3 lysine 9 is dispensable for constitutive heterochromatin. Plant J 33:471–480 (2003).

Kaszas E, Cande WZ: Phosphorylation of histone H3 is correlated with changes in the maintenance of sister chromatid cohesion during meiosis in maize, rather than the condensation of the chromatin. J Cell Sci 113:3217–3226 (2000).

Kogel D, Prehn JH, Scheidtmann KH: The DAP kinase family of pro-apoptotic proteins: novel players in the apoptotic game. Bioessays 23:352–358 (2001).

MacKintosh C, MacKintosh RM: Inhibitors of protein kinases and phosphatases. Trends Biochem Sci 19:444–448 (1994).

Manzanero S, Arana P, Puertas MJ, Houben A: The chromosomal distribution of phosphorylated histone H3 differs between plants and animals at meiosis. Chromosoma 109:308–317 (2000).

Manzanero S, Rutten T, Kotseruba V, Houben A: Alterations in the distribution of histone H3 phosphorylation in mitotic plant chromosomes in response to cold treatment and the protein phosphatase inhibitor cantharidin. Chromosome Res 10: 467–476 (2002).

Pedrosa A, Jantsch MF, Moscone EA, Ambros PF, Schweizer D: Characterisation of pericentrometric and sticky intercalary heterochromatin in *Ornithogalum longibracteatum* (Hyacinthaceae). Chromosoma 110:203–213 (2001).

Preuss U, Landsberg G, Scheidtmann KH: Novel mitosis-specific phosphorylation of histone H3 at Thr11 mediated by Dlk/ZIP kinase. Nucleic Acids Res 31:878–885 (2003).

Prigent C, Dimitrov S: Phosphorylation of serine 10 in histone H3, what for? J Cell Sci 116:3677–3685 (2003).

Rabl C: Zellteilung. Morphol Jahrb 10:214–330 (1885).

Schlegel R, Gill BS: N-banding analysis of rye chromosomes and the relationship between N-banded and C-banded heterochromatin. Can J Genet Cytol 26:765–769 (1984).

Schroeder-Reiter E, Houben A, Wanner G: Immunogold labeling of chromosomes for scanning electron microscopy: A closer look at phosphorylated histone H3 in mitotic metaphase chromosomes of *Hordeum vulgare*. Chromosome Res 11:585–596 (2003).

Schubert I, Dolezel J, Houben A, Scherthan H, Wanner G: Refined examination of plant metaphase chromosome structure at different levels made feasible by new isolation methods. Chromosoma 102:96–101 (1993).

Thomson S, Clayton AL, Hazzalin CA, Rose S, Barratt MJ, Mahadevan LC: The nucleosomal response associated with immediate-early gene induction is mediated via alternative MAP kinase cascades: MSK1 as a potential histone H3/HMG-14 kinase. EMBO J 18:4779–4793 (1999).

Waterborg JH, Robertson AJ: Common features of analogous replacement histone H3 genes in animals and plants. J Mol Evol 43:194–206 (1996).

Wei Y, Allis CD: A new marker for mitosis. Trends Cell Biol 8:266 (1998).

Zeitlin SG, Barber CM, Allis CD, Sullivan KF, Sullivan K: Differential regulation of CENP-A and histone H3 phosphorylation in G2/M. J Cell Sci 114:653–661 (2001).

A8 Houben, A., Demidov, D., Gernand, D., Meister, A., Leach, C.R., and Schubert, I. (2003). Methylation of histone H3 in euchromatin of plant chromosomes depends on basic nuclear DNA content. Plant Journal 33, 967-973.

The Plant Journal (2003) **33**, 967–973

Methylation of histone H3 in euchromatin of plant chromosomes depends on basic nuclear DNA content

Andreas Houben*, Dmitri Demidov, Dorota Gernand, Armin Meister, Carolyn R. Leach† and Ingo Schubert
Institute of Plant Genetics and Crop Plant Research (IPK), 06466 Gatersleben, Germany

Received 23 October 2002; revised 10 December 2002; accepted 17 December 2002.
*For correspondence (fax +49 394825137; e-mail houben@ipk-gatersleben.de).
†Present address: Molecular Biosciences (Genetics), The University of Adelaide, SA 5005, Australia.

Summary

Strong methylation of lysine 4 (K4) and low methylation of lysine 9 (K9) have been proposed as modifications of histone H3, typical for transcriptionally active euchromatin and the opposite for inactive heterochromatin. We have analysed the correlation between the global distribution of histone H3, methylated at either lysine 4 or lysine 9, and of microscopically detectable euchromatic or heterochromatic regions in relation to genome size for 24 plant species. Two different distribution patterns of methylated (K9)H3 (Met(K9)H3) were found that depend on genome size. For most species with small genomes (1C <500 Mbp), including *Arabidopsis thaliana,* strong methylation of (K9)H3 was restricted to constitutive heterochromatin. Species with larger genomes showed a uniform distribution of Met(K9)H3. Contrary to this and regardless of the genome size, methylated (K4)H3 (Met(K4)H3) was found to be enriched within the euchromatin of all species. Transcriptionally less active B chromosomes showed the same patterns as basic A chromosomes. We thus propose that large genomes with high amounts of dispersed repetitive sequences (mainly retroelements) have to silence these sequences and therefore display epigenetic modifications such as methylation of DNA and (K9)H3 also within euchromatic regions.

Keywords: euchromatin, heterochromatin, genome size, histone H3 methylation, silencing.

Introduction

The genome size of plant species may differ by several orders of magnitude. Polyploidization-independent enlargement of genome size is mainly due to an increase in repetitive sequences (SanMiguel *et al.*, 1996). Such genome increases require an epigenetic mechanism for heterochromatinization of repetitive sequences to ensure genome stability by inactivating mobile elements (Richards and Elgin, 2002). Methylated (K9)H3 (Met(K9)H3) serves as a binding site for recruitment of the heterochromatin protein HP1/Swi6 during heterochromatin assembly (Bannister *et al.*, 2001; Lachner *et al.*, 2001; Nakayama *et al.*, 2001). In contrast to this, methylation at (K4)H3 has been associated with transcriptionally active chromatin that is specific for euchromatin in several non-plant species (Litt *et al.*, 2001; Noma *et al.*, 2001; Reuben and Lin, 2002; Strahl *et al.*, 1999).

Here we show that cytological investigations may broaden our insight into the large-scale organization and epigenetic re-modelling of chromatin and provide a testable hypothesis to the relationship between genome size and histone modification in euchromatin and constitutive heterochromatin. We have analysed the distribution of histone H3 isoforms, methylated at either K4 or K9, between microscopically detectable heterochromatic and euchromatic chromosome regions for one moss, 10 monocot and 13 dicot plant species of different genome size. Furthermore, species possessing B chromosomes were analysed to compare the levels of methylated histone H3 in transcriptionally active versus transcriptionally poor chromosomes.

Results

The chromosomal distribution pattern of methylated (K9)H3 is influenced by the size of the nuclear genome

The antibodies against methylated histone H3 at either lysine 4 or lysine 9 recognized a protein of the H3-type, molecular mass of 15 kDa on Western blots of barley and

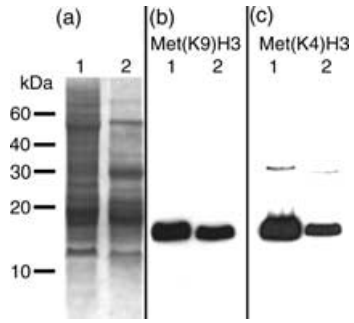

Figure 1. Protein gel blot analysis using antibodies specific to histone H3 dimethylated at either lysine 4 or lysine 9.
(a) Coomassie blue-stained SDS–PAGE gel from protein extracts of *Nicotiana tabacum* (lane 1) and *Hordeum vulgare* (lane 2).
(b) Antidimethylated (K9)H3 antibodies and (c) antidimethylated (K4)H3 antibodies detect a 15-kDa protein of *Nicotiana tabacum* and *Hordeum vulgare* in lanes 1 and 2, respectively.

tobacco protein extracts (Figure 1). The antibodies are likely to recognize the same peptide in plants because the histone H3 amino acid sequences of many plant species are identical to the synthetic peptide sequence used for immunization.

We first determined the distribution of antibodies specific for methylated (K4)H3 (Met(K4)H3) or Met(K9)H3 in mitotic cells of *Arabidopsis thaliana* and *Vicia faba*. *Arabidopsis thaliana* has an extremely small genome (approximately 170 Mbp) and only about 15% of the nuclear genome consists of repetitive sequences (Leutwiler *et al*., 1984), mainly located within the pericentromeric heterochromatin and nucleolus-organizing regions (Bauwens *et al*., 1991; Maluszynska and Heslop-Harrison, 1991). In contrast, *V. faba* possesses a relatively large genome (approximately 12 810 Mbp) and contains at least 85% repetitive sequences (Flavell *et al*., 1974), which are present in heterochromatic as well as euchromatic regions (Fuchs *et al*., 1998).

In *A. thaliana*, the Giemsa-banding positive (Ambros and Schweizer, 1976) corresponding to brightly 4′,6-diamidino-2-phenylindole (DAPI)-stained heterochromatin showed strong Met(K9)H3-specific immunofluorescence during interphase and nuclear division (Figure 2). Very few signals were seen in the less intensely DAPI-stained euchromatin (Figure 2). In contrast, immunosignals for H3 methylated at K4 were enriched in euchromatin, while nucleoli and heterochromatic chromocentres remained unlabelled. Therefore, extensive methylation of K9 and, reciprocally, rare methylation of K4 of histone H3 appear to be specific features of heterochromatin in *A. thaliana*. In *V. faba,* all chromosomes revealed a more or less uniform distribution of Met(K9)H3. Only occasionally were prominent heterochromatic regions in interphase nuclei found to be more intensely labelled (Figure 3a). Methylated (K4)H3 was not detectable in constitutive heterochromatin during interphase or in metaphase chromosomes (Figure 3b,c). Thus, Met(K4)H3 is located within cytologically defined euchromatin while Met(K9)H3 is concentrated within cytologically defined heterochromatin only in *A. thaliana*.

This difference raised the question as to whether the distribution of Met(K9)H3 depends on basic genome size. Accordingly, we analysed the distribution of Met(K9)H3 and Met(K4)H3 for 22 additional plant species, including monocots, dicots and a moss, with genome sizes ranging from 170 to 44 500 Mbp (Table 1). As in *A. thaliana*, signals for Met(K9)H3 occurred almost exclusively within the microscopically detectable heterochromatin of species with a DNA content of approximately 500 Mbp or less. These signals correlate with Giemsa-banding positive heterochromatic regions so far described. The contrasting dispersed and nearly uniform labelling of the entire chromatin, as observed in *V. faba,* was found for rice (approximately 500 Mbp) and all species with a genome size clearly above 500 Mbp (Table 1). Nucleoli showed an average labelling with anti-Met(K9)H3 in most cases.

This result suggests that genome size is a factor that significantly influences the global distribution of Met(K9)H3. Nevertheless, the nuclear DNA content may not be the only determinant of the chromosomal distribution of Met(K9)H3 because species with a genome size close to 500 Mbp showed either clustered (*Ricinus communis* (Figure 4c), *Cardaminopsis arenosa*) or uniform distribution of Met(K9)H3 (*Oryza sativa* (Figure 4d), *Brachypodium sylvaticum*). DAPI-staining of *C. arenosa* and *R. communis* nuclei revealed pronounced heterochromatic chromocentres, whereas in *O. sativa* (Figure 4d) and *B. sylvaticum*, the heterochromatin appeared to be more dispersed. Thus, at a genome size of approximately 500 Mbp $1C^{-1}$, the distribution of Met(K9)H3 apparently depends on the genomic distribution (clustered versus dispersed) of repetitive sequences. Although monocots with genomes smaller than rice were not available, we propose that the genome size-dependence of Met(K9)H3 distribution is similar for all plants because the large genomes of monocots and dicots showed the same Met(K9)H3 pattern.

The euchromatin-specific methylation of (K4)H3 is independent of the genome size

Regardless of the genome size, immunostaining with antibodies against Met(K4)H3 resulted in an exclusive labelling of euchromatic regions of interphase and mitotic nuclei. This correlates with Giemsa-banding negative regions as far as described. In rice (Figure 5a), maize (Figure 5b), barley (Figure 5c), oat (Figure 5d), *Ornithogalum longibracteatum* (Figure 5e), *Trillium camschatcense* (Figure 5f), rye (Figure 6c,d) and *Crepis capillaris* (Figure 6a), Met(K4)H3 occupies preferentially euchromatic regions in distal positions (Figure 5a–d, f) and outside DAPI-bright

Table 1 Distribution patterns of methylated (K9)H3 (Met(K9)H3)

Plant species	1C values (in Mbp)	Distribution patterns of Met(K9)H3
*Arabidopsis thaliana** (di)	170	1
Cardamine amara (di)	290	1
Arabidopsis lyrata ssp. *petraea* (di)	300	1
Arabidopsis pumila (di)	330	1
Arabidopsis wallichii (di)	390	1
Cardaminopsis arenosa (di)	490	1
*Oryza sativa** (mo)	490	2
Ricinus communis (di)	510	1
Brachypodium sylvaticum (mo)	530	2
Brachypodium distachyon (mo)	770	2
Brachycome dichromosomatica (di)	1510	2
Zingeria biebersteiniana (mo)	1810	2
Crepis capillaris (di)	2200	2
Pellia epiphylla (m)	2450	2
*Zea mays** (mo)	2670	2
*Gossypium hirsutum** (di)	3160	2
*Hordeum vulgare** (mo)	5440	2
*Nicotiana tabacum** (di)	5730	2
Ornithogalum longibracteatum (mo)	7760	2
*Secale cereale** (mo)	8110	2
*Avena sativa** (mo)	12961	2
*Vicia faba** (di)	12810	2
*Triticum aestivum** (mo)	16660	2
Trillium camschatcense (mo)	43410	2

*Indicates the 1C values taken from a genome size database (http://www.rbgkew.org.uk/cval/homepage.html) (Bennett and Leitch, 1995).
mo: monocot; di: dicot; m: moss.
1: Labelling confined to microscopically detectable heterochromatin.
2: Disperse labelling of entire chromatin.

chromocentres (Figure 5e), respectively. Furthermore, in nuclei of barley and rye, two species showing a typical Rabl-orientation at interphase (Dong and Jiang, 1998), the Met(K4)H3 chromatin occupies the poles opposite to centromeres (Figure 5c) around which heterochromatin is clustered in these species. Nucleoli remained unlabelled. This agrees with observations of Briggs *et al.* (2001) on yeast showing that methylation of (K4)H3 is required for silencing of rDNA.

The euchromatin-specific distribution of methylated (K4)H3 is similar between A and B chromosomes

The methylation status of lysine 4 and 9 of histone H3 on supernumerary B chromosomes and basic A chromosomes of *C. capillaris*, *Brachycome dichromosomatica* and *Secale cereale* were determined. The B chromosomes of these species are morphologically distinguishable after DAPI-staining (Figure 6). A comparison of the immunofluorescence intensity of A and B chromosomes indicated that both chromosome types show similar patterns of (K9)H3 methylation (data not shown). A comparable degree of methylation was found for (K4)H3 of transcriptionally active A chromosomes and transcriptionally less active B chromosomes of *C. capillaris* (Figure 6a) and *S. cereale* (Figure 6c,d). The pericentromeric regions of the metacentric B chromosome, as well as other heterochromatic A chromosome regions of *C. capillaris* (Maluszynska, 1990), showed a lower degree of (K4)H3 methylation (Figure 6a). The same was true for A and B chromosomes of rye (Figure 6d). Only micro B chromosomes of *B. dichromosomatica*, which are entirely heterochromatic and mainly composed of tandem-repeats (Houben *et al.*, 1997, 2001), were free of signals (Figure 6b). This suggests that euchromatin and heterochromatin of B chromosomes are subject to histone H3 methylation at lysines 4 and 9 in a similar way as the standard set of A chromosomes.

Discussion

To explain the discrepancy between cytologically defined heterochromatin and the uniform distribution of Met(K9)H3 along the chromosomes of large genomes, it must be considered that the amount of disperse repetitive sequences within cytologically euchromatic regions increases with the genome size. The cytologically detectable euchromatin within large genomes is interspersed with different families of mobile elements (together approximately 70–85% of the nuclear genome) (Kumar and Bennetzen, 1999) which, although silenced by 'heterochromatinization', are not detectable microscopically as heterochromatin. Their interspersion with potentially active genes is presumably responsible for a chromatin organization that differs from that of constitutive heterochromatin. While cytosine-methylated, dispersed repetitive sequences may be associated with Met(K9)H3 within the euchromatin of large genomes, such sequences and the corresponding modifications are mainly confined to the constitutive heterochromatin of small genomes like that of *A. thaliana* (Mittelsten Scheid *et al.*, 2002; Soppe *et al.*, 2002). Methylated (K9)H3 within euchromatin might theoretically associate with (sufficient amounts of) proteins that establish heterochromatin. However, euchromatin-specific (K4)H3 methylation and the maintenance of high levels of histone acetylation in potentially active chromatin after replication (Houben *et al.*, 1996; Jasencakova *et al.*, 2000, 2001) might prevent this process within euchromatin of large plant genomes. Therefore, this 'incomplete' heterochromatin formation within large genomes yields a structure less condensed than that of constitutive heterochromatin but more dense than euchromatin of small genomes (see model, Figure 7). Indeed it was reported that for plant species with low nuclear DNA contents the amount of

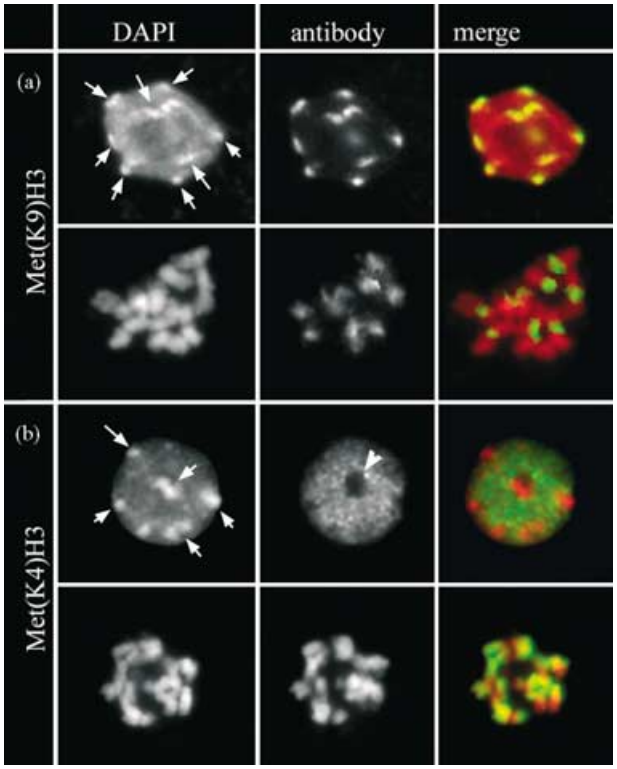

Figure 2. Immunolocalization of histone H3 methylated at either lysine position 9 (a) or 4 (b) on interphase and metaphase chromosomes of *Arabidopsis thaliana*.
The positions of chromocentres and of the nucleolus are indicated by arrows and an arrowhead, respectively.

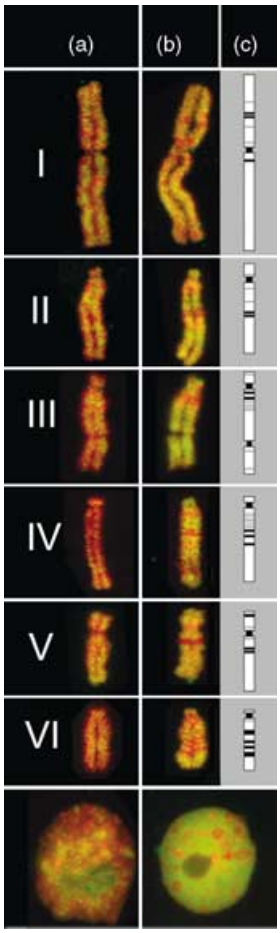

Figure 3. Immunolocalization of histone H3 methylated at either lysine position 4 (b) or 9 (a) on metaphase chromosomes and nuclei of the field bean karyotype ACB. Scheme of Giemsa-banded chromosomes (c).

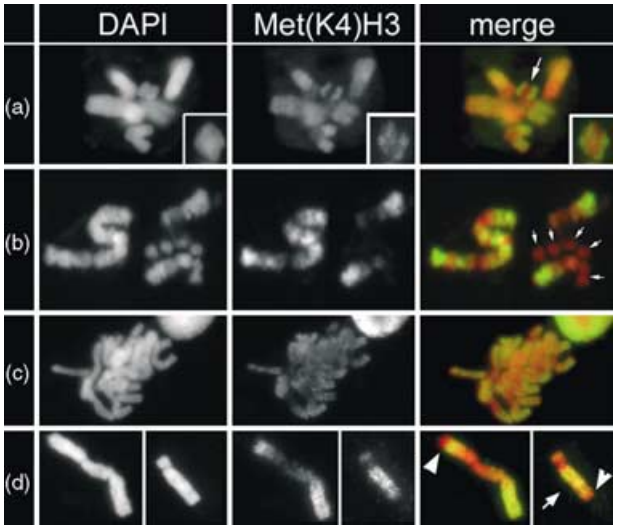

Figure 6. Immunolocalization of histone H3 methylated at lysine position 4 on A and B chromosomes of (a) *Crepis capillaris*, (b) *Brachycome dichromosomatica* and (c,d) *Secale cereale*.
The B chromosomes of *C. capillaris* and *B. dichromosomatica* are indicated by arrows. Single A and B chromosomes of *S. cereale* are shown in (d). The positions free of methylated (K4)H3 (Met(K4)H3) and Giemsa-banding positive regions are indicated by arrowheads. B chromosomes of *C. capillaris* are further enlarged in the inserts of (a).

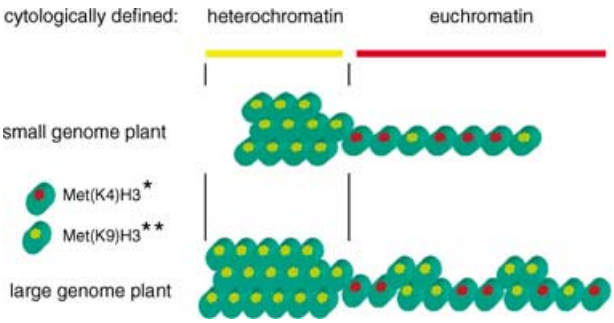

Figure 7. Model on the distribution of histone H3 methylated at either lysine position 4 or 9 and the positions of cytologically defined euchromatic and heterochromatic regions in relation to the genome size.
(*) representing mainly coding/unique sequences, (**) representing mainly non-coding/repetitive sequences.

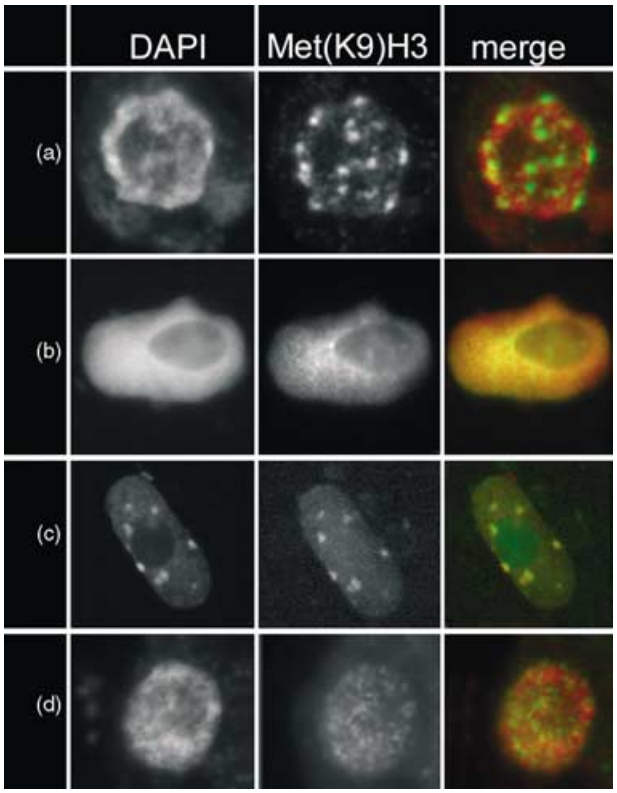

Figure 4. Immunolocalization of histone H3 methylated at lysine position 9 on interphase nuclei of (a) *Cardamine amara* (1C = 290 Mbp), (b) *Triticum aestivum* (1C = 16 660 Mbp), (c) *Ricinus communis* (1C = 515 Mbp) and (d) *Oryza sativa* (1C = 490 Mbp).

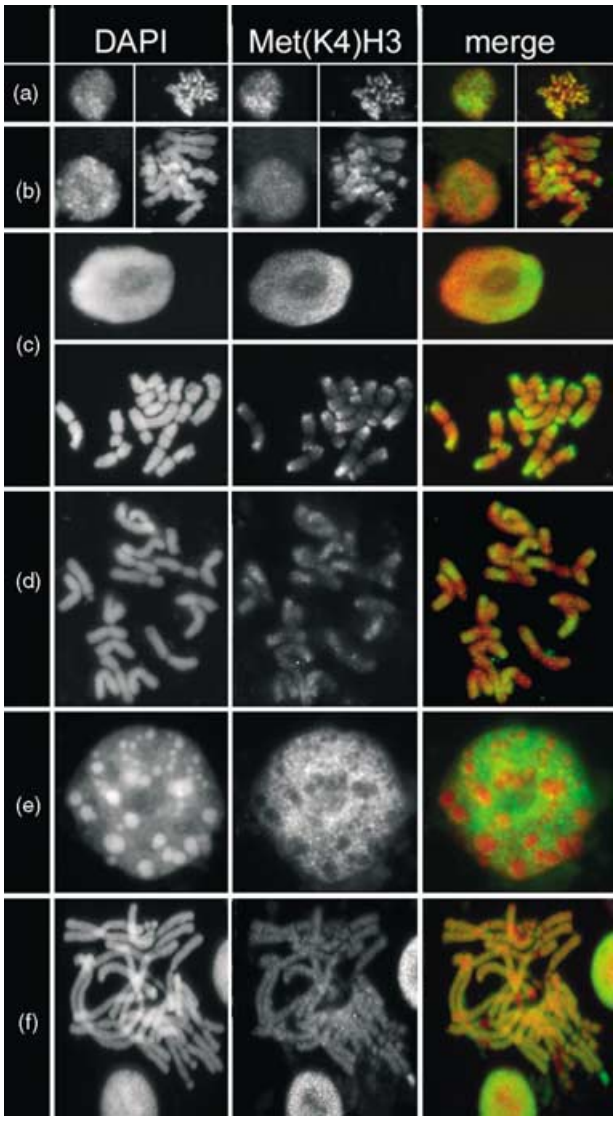

Figure 5. Immunolocalization of histone H3 methylated at lysine position 4 on interphase and metaphase chromosomes of (a) *Oryza sativa*, (b) *Zea mays*, (c) *Hordeum vulgare*, (d) *Avena sativa*, (e) *Ornithogalum longibracteatum* and (f) *Trillium camschatcense*.

DNA per unit of nuclear volume is lower than for plants with high DNA contents (Barlow, 1977; Raina and Bisht, 1988). It remains to be seen whether Met(K9)H3 in plants serves as a binding site for the recently identified LHP1 of *A. thaliana* (Gaudin *et al.*, 2001), the first plant homologue of *Drosophila* heterochromatin protein 1.

In order to test whether the euchromatin-specific methylation of (K4)H3 correlates with transcriptionally competent chromatin, different types of B chromosomes were included in this study. B chromosomes are generally assumed to be genetically inactive because no major genes with specific phenotypic effects necessary for normal development are known (Camacho *et al.*, 2000; Jones, 1995). The similar global (K4)H3 methylation patterns between A and B chromosomes of three different species raise the question whether the methylation of (K4)H3 is a reliable diagnostic feature of transcriptionally potent euchromatin in plants, the more so as the Met(K4)H3-specific labelling of euchromatic A chromosome regions does not reflect the actual number of genes which is independent of genome size. In addition, the absence of Met(K4)H3 seems to be more significant in defining constitutive heterochromatin than the presence of Met(K9)H3 which, in large genomes, also occurs in euchromatin and may even become reduced to the level of euchromatin within DAPI-positive heterochromatin of mutants defective in (K9)H3-specific histone methylases (Jasencakova *et al.*, 2003; Peters *et al.*, 2001; Schotta *et al.*, 2002).

Experimental procedures

Plant material

The 24 plant species analysed are listed in Table 1.

Isolation of proteins and Western blot analysis

Approximately 200 mg leaf tissue of barley and tobacco was powdered in a mortar and pestle using liquid nitrogen and treated with 800 μl ice-cold lysis buffer (20 mM Hepes (pH 7.9), 400 mM sucrose, 1.5 mM $MgCl_2$, 10 mM KCl, 0.1% Triton X-100, 0.02% NaN_3, 1.5 mM PMSF, 1 mM DTT). After a short ultrasonic treatment, 800 μl 0.4 M H_2SO_4 was added and samples were incubated on ice for 1 h. Extracted proteins were centrifuged at 1400 ***g*** for 10 min. Proteins were precipitated with 250 μl each of methanol and chloroform by incubating on ice for 10 min. After centrifugation at 1400 ***g*** for 10 min, the interface was recovered. The sample was washed with 1 ml of ice-cold 80% acetone, incubated on ice for 5 min and centrifuged at 1400 ***g*** for 10 min. All centrifugation steps were performed at 4°C. The protein pellet was dried at room temperature for 15 min and re-suspended in loading buffer.

Proteins were analysed by SDS 15% polyacrylamide gels and visualized by Coomassie Brilliant Blue staining or transferred to nitrocellulose membranes. Membranes containing the proteins were used for immunodetection of Met(K4)H3 or Met(K9)H3 with antibodies against histone H3, dimethylated at either lysine 4 or 9 (Upstate Biotechnology, USA) and peroxidase-conjugated goat antirabbit antibodies (Sigma), using SuperSignal West Pico detection (Pierce). The specificity of the antibodies against Met(K4)H3 and Met(K9)H3 has been shown by the supplier and for plants by Gendrel *et al*. (2002).

Chromosome preparation and in situ *immunostaining*

Leaflets of the moss *Pellia epiphylla* and root meristems of the other plants studied were fixed for 30 min in freshly prepared 4% (w/v) formaldehyde solution containing phosphate buffered saline (PBS, pH 7.3), washed for 45 min in PBS and digested at 37°C for 25 min in a mixture of 2.5% pectinase, 2.5% cellulase Onozuka R-10 and 2.5% pectolyase Y-23 (w/v) dissolved in PBS. Meristems were then washed for 15 min in PBS and squashed between a glass slide and coverslip in PBS. After freezing in liquid nitrogen, the coverslips were removed and the slides were transferred immediately into PBS. To avoid non-specific antibody binding, slides were incubated for 30 min in 8% BSA (w/v), 0.1% Triton X-100 in PBS at room temperature prior to two washes in PBS for 5 min each, and incubated with the primary antibody in a humidified chamber. The primary antibodies were diluted 1 : 300 in PBS, 1% BSA. After 12 h incubation at 4°C and washing for 15 min in PBS, the slides were incubated in rhodamine-conjugated antirabbit IgG (Dianova) diluted 1 : 100 in PBS, 1% BSA for 1 h at 37°C. After final washes in PBS, the preparations were mounted in antifade containing DAPI as counterstain. Fluorescence signals were observed using an epifluorescence microscope. The images recorded with a cooled CCD camera were pseudo-coloured and merged with the program Adobe Photoshop 6.0.

Determination of genomic DNA content

The genomic DNA content (1C) was determined by flow cytometry as described by Barow and Meister (2002) on propidium iodide-stained nuclei. *Allium cepa* and *V. faba* served as reference plants for species with large and *Glycine max* and *Raphanus sativus* for species with small genomes.

Acknowledgements

A.H., D.D., D.G., A.M. and I.S. were supported by the DFG, the BMFT and the Fonds der Chemischen Industrie and the Land Sachsen-Anhalt. We are grateful to V. Kotseruba for supplying plant material and helping with immunostaining and to E. Richards, D. Schweizer, R. N. Jones, G. Jenkins, J. N. Timmis, M. Schmid and R. Rieger for critical reading and comments.

References

Ambros, P. and Schweizer, D. (1976) The Giemsa C-banded karyotype of *Arabidopsis thaliana* (L.) Heynh. *Arabidopsis Information Service*, **13**, 167–171.

Bannister, A.J., Zegerman, P., Partridge, J.F., Miska, E.A., Thomas, J.O., Allshire, R.C. and Kouzarides, T. (2001) Selective recognition of methylated lysine 9 on histone H3 by the HP1 chromodomain. *Nature*, **410**, 120–124.

Barlow, P.W. (1977) Determinants of nuclear chromatin structure in angiosperms. *Annales des Sciences Naturelles*, **12**, 193–206.

Barow, M. and Meister, A. (2002) Lack of correlation between AT frequency and genome size in higher plants and the effect of non-randomness of base sequences on dye binding. *Cytometry*, **47**, 1–7.

Bauwens, S., Van Oostveldt, P., Engler, G. and Van Montagu, M. (1991) Distribution of the rDNA and three classes of highly repetitive DNA in the chromatin of interphase nuclei of *Arabidopsis thaliana*. *Chromosoma*, **101**, 41–48.

Bennett, M.D. and Leitch, I.L. (1995) Nuclear DNA amounts in angiosperms. *Ann. Bot.* **76**, 113–176.

Briggs, S.D., Bryk, M., Strahl, B.D., Cheung, W.L., Davie, J.K., Dent, S.Y.R., Winston, F. and Allis, C.D. (2001) Histone H3 lysine 4 methylation is mediated by Set1 and required for cell growth and rDNA silencing in *Saccharomyces cerevisiae*. *Genes Dev.* **15**, 3286–3295.

Camacho, J.P.M., Sharbel, T.F. and Beukeboom, L.W. (2000) B-chromosome evolution. *Philos. Trans. R. Soc. Lond. B*, **355**, 163–178.

Dong, F. and Jiang, J. (1998) Non-Rabl patterns of centromere and telomere distribution in the interphase nuclei of plant cells. *Chromosome Res.* **6**, 551–558.

Flavell, R.B., Bennett, M.D., Smith, J.B. and Smith, D.B. (1974) Genome size and the proportion of repeated nucleotide sequence DNA in plants. *Biochem. Genet.* **12**, 257–279.

Fuchs, J., Strehl, S., Brandes, A., Schweizer, D. and Schubert, I. (1998) Molecular cytogenetic characterization of the *Vicia faba* genome – heterochromatin differentiation, replication patterns and sequence localization. *Chromosome Res.* **6**, 219–230.

Gaudin, V., Libault, M., Pouteau, S., Juul, T., Zhao, G., Lefebvre, D. and Grandjean, O. (2001) Mutations in LIKE HETEROCHROMATIN PROTEIN 1 affect flowering time and plant architecture in *Arabidopsis*. *Development*, **128**, 4847–4858.

Gendrel, A.V., Lippman, Z., Yordan, C., Colot, V. and Martienssen, R. (2002) Dependence of heterochromatic histone H3 methylation patterns on the *Arabidopsis* gene DDM1. *Science*, **297**, 1871–1873.

Houben, A., Belyaev, N.D., Turner, B.M. and Schubert, I. (1996) Differential immunostaining of plant chromosomes by antibodies recognizing acetylated histone H4 variants. *Chromosome Res.* **4**, 191–194.

Houben, A., Leach, C.R., Verlin, D., Rofe, R. and Timmis, J.N. (1997) A repetitive DNA sequence common to the different B chromosomes of the genus *Brachycome*. *Chromosoma*, **106**, 513–519.

Houben, A., Verlin, D., Leach, C.R. and Timmis, J.N. (2001) The genomic complexity of micro B chromosomes of *Brachycome dichromosomatica*. *Chromosoma*, **110**, 451–459.

Jasencakova, Z., Meister, A., Walter, J., Turner, B.M. and Schubert, I. (2000) Histone H4 acetylation of euchromatin and heterochro-

matin is cell cycle dependent and correlated with replication rather than with transcription. *Plant Cell*, **12**, 2087–2100.

Jasencakova, Z., Meister, A., Walter, J., Turner, B.M. and Schubert, I. (2001) Chromatin organization and its relation to replication and histone acetylation during the cell cycle in barley. *Chromosoma*, **110**, 83–92.

Jasencakova, Z., Soppe, W., Meister, A., Gernand, D., Turner, B.M. and Schubert, I. (2003) Histone modifications in *Arabidopsis* – high methylation of H3 lysine 9 is dispensable for constitutive heterochromatin. *Plant J.* (in press).

Jones, R.N. (1995) Tansley Review No. 85. B chromosomes in plants. *New Phytol.* **103**, 411–434.

Kumar, A. and Bennetzen, J.L. (1999) Plant retrotransposons. *Ann. Rev. Genet.* **33**, 479–532.

Lachner, M., O'Carroll, D., Rea, S., Mechtler, K. and Jenuwein, T. (2001) Methylation of histone H3 lysine 9 creates a binding site for HP1 proteins. *Nature*, **410**, 116–120.

Leutwiler, L.S., Hough-Evans, B.R. and Meyerowitz, E.M. (1984) The DNA of *Arabidopsis thailiana*. *Mol. Gen. Genet.* **194**, 15–23.

Litt, M.D., Simpson, M., Gaszner, M., Allis, C.D. and Felsenfeld, G. (2001) Correlation between histone lysine methylation and developmental changes at the chicken beta-globin locus. *Science*, **293**, 2453–2455.

Maluszynska, L. (1990) *B Chromosomes of Crepis capillaris (L.) Waller, In vivo and In vitro.* Katowice: Uniwersytet Slaski 92 pp.

Maluszynska, J. and Heslop-Harrison, J.S. (1991) Localization of tandemly repeated sequences of *Arabidopsis thaliana*. *Plant J.* **1**, 159–166.

Mittelsten Scheid, O.M., Probst, A.V., Afsar, K. and Paszkowski, J. (2002) Two regulatory levels of transcriptional gene silencing in *Arabidopsis*. *Proc. Natl. Acad. Sci. USA*, **99**, 13659–13662.

Nakayama, J., Rice, J.C., Strahl, B.D., Allis, C.D. and Grewal, S.I. (2001) Role of histone H3 lysine 9 methylation in epigenetic control of heterochromatin assembly. *Science*, **292**, 110–113.

Noma, K., Allis, C.D. and Grewal, S.I.S. (2001) Transitions in distinct histone H3 methylation patterns at the heterochromatin domain boundaries. *Science*, **293**, 1150–1155.

Peters, A.H., O'Carroll, D., Scherthan, H. *et al.* (2001) Loss of the Suv39h histone methyltransferases impairs mammalian heterochromatin and genome stability. *Cell*, **107**, 323–337.

Raina, S.N. and Bisht, M.S. (1988) DNA amounts and chromatin compactness in *Vicia*. *Genetica*, **77**, 65–77.

Reuben, M. and Lin, R. (2002) Germline X chromosome exhibit contrasting patterns of histone H3 methylation in *Caenorhabditis elegans*. *Dev. Biol.* **245**, 71–82.

Richards, E.J. and Elgin, S.C. (2002) Epigenetic codes for heterochromatin formation and silencing: rounding up the usual suspects. *Cell*, **108**, 489–500.

SanMiguel, P., Tikhonov, A., Jin, Y.K. *et al.* (1996) Nested retrotransposons in the intergenic regions of the maize genome. *Science*, **274**, 765–768.

Schotta, G., Ebert, A., Krauss, V., Fischer, A., Hoffmann, J., Rea, S., Jenuwein, T., Dorn, R. and Reuter, G. (2002) Central role of *Drosophila* SU (VAR) 3–9 in histone H3–K9 methylation and heterochromatic gene silencing. *EMBO J.* **21**, 1121–1131.

Soppe, W.J.J., Jasencakova, Z., Houben, A., Kakutani, T., Meister, A., Huang, M.S., Jacobsen, S.E., Schubert, I. and Fransz, P.F. (2002) DNA methylation controls histone H3 lysine 9 methylation and heterochromatin assembly in *Arabidopsis*. *EMBO J.* **21**, 6549–6559.

Strahl, B.D., Ohba, R., Cook, R.G. and Allis, C.D. (1999) Methylation of histone H3 at lysine 4 is highly conserved and correlates with transcriptionally active nuclei in *Tetrahymena*. *Proc. Natl. Acad. Sci. USA*, **96**, 14967–14972.

A9 Houben, A., Verlin, D., Leach, C.R., and Timmis, J.N. (2001). The genomic complexity of micro B chromosomes of *Brachycome dichromosomatica*. Chromosoma 110, 451-459.

Chromosoma (2001) 110:451–459
DOI 10.1007/s00412-001-0173-1

ORIGINAL ARTICLE

Andreas Houben · Dawn Verlin · Carolyn R. Leach
Jeremy N. Timmis

The genomic complexity of micro B chromosomes of *Brachycome dichromosomatica*

Received: 30 January 2001 / In revised form: 25 August 2001 / Accepted: 25 September 2001 / Published online: 1 November 2001

Abstract A major sequence component of the micro B chromosome of *Brachycome dichromosomatic*a (2*n*=4) is the tandem repeat Bdm29, which was found by in situ hybridisation to be distributed along the entire length of the chromosome. A high copy number of this sequence does not occur as a regular feature of the A chromosomes in this species but it was found in infrequent individuals in two wild populations that were analysed. In these instances Bdm29 is localised within heterochromatic, polymorphic segments on the long arm of chromosome 1. The origin of the micro B chromosomes was investigated by determining whether they are related to this A chromosome polymorphism by simple excision and/or integration. Results obtained by using Bdm29, together with a newly isolated repeat sequence, Bdm54, and a number of other sequences known to occur on the micro B chromosome, as probes in in situ hybridisation and Southern analysis demonstrated that the formation of micro B chromosomes is a complex multistep process. The observation that the genomic organisation of the micro B chromosome is unlike anything found on the A chromosomes precludes their origin by simple excision and also indicates that micro Bs do not integrate directly into the A complement to form polymorphic heterochromatic segments.

Introduction

B chromosomes (Bs), which are supernumerary to the basic (A) chromosome set, are capable of generating one of the most obvious genome size polymorphisms within a species. They differ from the A chromosomes in morphology and pairing behaviour and are not required for normal growth and development (reviewed by Jones and Rees 1982; Beukeboom 1994; Jones 1995; Camacho et al. 2000). Little is known about the origin of B chromosomes but it is likely that those of different organisms arose in different ways. It is widely accepted that Bs could be derived from A chromosomes (e.g. *Crepis capillaris*, Jamilena et al. 1994; *Zea mays*, Stark et al. 1996) or from sex chromosomes (e.g. *Eyprepocnemis plorans*, López-León et al. 1994; *Leiopelma hochstetteri*, Sharbel et al. 1998). The spontaneous generation of Bs following interspecific crosses has been reported in hybrids of *Coix aquaticus* and *Coix gigantea* (Sapre and Deshpande 1987), in *Nasonia vitripennis* (McAllister and Werren 1997) and in the progeny of the fish Amazon Molly and Black Molly (Schartl et al. 1994). The de novo formation of Bs is most likely a rare process, as analyses of different B chromosome variants within species suggest a close relationship between different variants (Cabrero et al. 1999; Houben et al. 1999).

Studies have revealed that the plant genome is more dynamic than originally supposed (Meyerowitz 1999) and some genomic changes, once thought to be long-term evolutionary events, may occur rapidly. In addition to DNA transposition, translocation and deletion, the selective amplification of particular DNA sequences is a hallmark of genomic instability (Flavell 1985). One species with extraordinary genome plasticity is *Brachycome dichromosomatica* (synonym *Brachyscome dichromosomatica*), an Australian member of the Asteraceae, which is an annual outbreeder with only two pairs of A chromosomes. This species occurs in four karyotypically distinct cytodemes, A1, A2, A3 and A4 (Watanabe et al. 1975), and two different types of B chromosome may be found within populations and, rarely, within a single plant. These are the somatically stable large B chromosomes and the somatically unstable dot-like micro B chromosomes (Carter and Smith-White 1972). The observed variation in number of micro Bs within plants is caused by nondisjunction of sister chromatids during

Edited by: D. Schweizer
Accession number: Bdm54, AJ276463

A. Houben (✉) · D. Verlin · C.R. Leach · J.N. Timmis
Molecular Biosciences (Genetics), Adelaide University, SA, Australia 5005
e-mail: houben@ipk-gatersleben.de

Present address:
A. Houben, IPK, 06466 Gatersleben, Germany

anaphase, suggesting that the centromere is not fully functional (Houben et al., unpublished results).

Genome size variability between different plants of *B. dichromosomatica* may also occur due to the presence or absence of heterochromatic A chromosome segments (Houben et al. 1997a). In some species such segments have been called 'supernumerary segments' by analogy with supernumerary (B) chromosomes as they are usually heterochromatic and dispensable, although some polymorphic euchromatic segments have also been reported. One polymorphic segment type of *B. dichromosomatica* is composed mainly of the short tandem repeat Bds1 (Houben et al. 2000). Almost half of cytodeme A2 plants analysed by fluorescence in situ hybridisation (FISH) were hemizygous or homozygous at one, two or three different Bds1-positive loci on A chromosomes. In addition, a Bds1 cluster was always present on micro B chromosomes (Houben et al. 2000). Another tandem repeat sequence called Bdm29 was identified as a component of the micro B of *B. dichromosomatica*, as were telomere and ribosomal DNA sequences (Houben et al. 1997b). After FISH using Bdm29, the entire micro B was labelled, suggesting that a high proportion of the micro B consists of this sequence with an even distribution along the chromosome. Only very low copy numbers of Bdm29-like sequences were found on the A chromosomes of plants tested by Southern hybridisation (Houben et al. 1997b).

Multiple copies of Bdm29-like sequences were found in the larger Bs of *B. dichromosomatica* and in other Bs within the genus *Brachycome* (Houben et al. 1997b). This suggested that Bdm29 is a highly conserved sequence that may be important in the formation and behaviour of the B chromosomes, as it may have appeared early in the evolution of *Brachycome* Bs and persisted during subsequent speciation. Alternatively, the sequence may have evolved independently several times in different lineages of the genus.

In order to study the evolutionary relationship between the micro Bs and the polymorphic A chromosome segments, we investigated whether the micro B major component, repeat Bdm29, could form an A chromosome segment polymorphism similar to that demonstrated for Bds1. To do this, members of different *B. dichromosomatica* populations without any Bs were screened for the presence of a high copy number of Bdm29 and a few rare plants were found with heterochromatic Bdm29-positive A segments. To test whether or not the micro B chromosome could originate from a single excised Bdm29-positive A segment, the detailed genomic organisation of this polymorphic A segment was examined in different genotypes with a range of micro B chromosome localised probes.

Materials and methods

Plant material

B. dichromosomatica (2*n*=4) is a member of the *Brachycome linearioba* complex (Watanabe et al. 1975). Seeds of *B. dichromosomatica* were collected from two different wild populations in South Australia (18.3 km south of Wild Dog Glen, 17.5 km north of Hawker) and from laboratory lines from adjacent areas cultivated over several years. The cytodemes (A2 and A4) were characterised on the basis of their chromosome morphology as described by Watanabe et al. (1975).

Cloning and selection of micro B chromosome sequences

Degenerate oligonucleotide-primed polymerase chain reaction (DOP-PCR) amplified DNA of 20 microdissected micro B chromosomes (Houben et al. 1997b) was ligated into the vector pGEM-T Easy (Promega) and propagated in the *Escherichia coli* strain DH5α. DNA from the resulting colonies was successively hybridised with ^{32}P-labelled total genomic DNA of plants with and without micro B chromosomes and colonies showing differential hybridisation were selected for further study.

Sequencing and sequence data analysis

Sequence analysis of the clones was performed by the automated dideoxynucleotide-dye termination method (Perkin-Elmer). Searches for sequence similarity in the Genbank database were performed using FASTA and BLASTA services (Australian National Genomic Information Service).

Southern hybridisation

Genomic DNA was isolated from leaf material (Wienand and Feix 1980) and digested with different restriction enzymes according to the manufacturer's recommendations. DNA fragments were resolved on 0.8% agarose gels and transferred to Hybond N+ nylon membranes (Amersham) for hybridisation. The DNA probes were labelled with [^{32}P]dCTP by random-primed DNA synthesis. Hybridisation was carried out overnight at 65°C in 5×SSPE, 0.2% SDS, 5×Denhardt's reagent and 100 µg/ml salmon sperm DNA. After hybridisation, blots were washed twice in 0.5×SSC with 0.1% SDS at 65°C (1×SSC is 0.15 M NaCl, 0.015 M sodium citrate). They were then exposed at –70°C to X-ray film with enhancing screens or to phospho imager plates (Fuji) for appropriate periods.

DNA probe preparation

Plasmid VER17 (Yakura and Tanifuji 1983), encoding part of the 18S, the 5.8S, most of the 25S and the internal transcribed spacers of *Vicia faba* 45S rRNA, was used as an rDNA-specific probe. A 5S rDNA-specific probe was amplified from genomic DNA of *B. dichromosomatica* using primers designed to the 5S rDNA sequence of *Glycine* species (Gottlub-McHugh et al. 1990). An *Arabidopsis*-type telomere probe was synthesised by PCR according to Ijdo et al. (1991). The inserts of the clones pBdm29, pBdm54 and pBds1 were used as *Brachycome*-specific probes.

Preparation of mitotic chromosomes and extended DNA fibres

Mitotic preparations for in situ hybridisation were obtained from root tips according to Donald et al. (1997). The preparation of the extended DNA fibres was modified from Fransz et al. (1996). Isolated leaf nuclei were collected in PBS and 3 µl of suspension were pipetted onto a glass slide and air-dried. Nuclei were disrupted for 3 min at room temperature in 20 µl of STE buffer (0.5% SDS, 100 mM TRIS, pH 7.0, 0.5 mM EDTA). The fibres were stretched by dropping 200 µl of freshly prepared, ice-cold ethanol:acetic acid (3:1) onto the slides which were then air dried, immersed in ethanol:acetic acid (3:1) for 2 min, air-dried again and baked at 60°C for 1 h.

Fluorescence in situ hybridisation

The probes were labelled with digoxigenin (DIG)-11-dUTP or biotin-17-dUTP by nick translation or PCR. Hybridisation sites of the DIG- or biotin-labelled probes were detected using sheep anti-DIG-rhodamine/rhodamine anti-sheep antibody or streptavidin-fluorescein isothiocyanate (FITC)/anti-streptavidin-FITC, respectively. Epifluorescence signals were recorded on Fuji 400 film or electronically with a cooled CCD camera. The image manipulations including pseudo-colouring were performed with the program Adobe Photoshop.

Results

Detection of heterochromatic A chromosome segments containing high copies of Bdm29

To find high copy numbers of the micro B repeat Bdm29 in plants without B chromosomes, three different plant populations were screened by dot-blot or Southern hybridisation with labelled Bdm29 sequences. The copy number of Bdm29 was very low in all 55 plants analysed from the laboratory population, but 1 of 19 and 4 of 14 plants from two wild populations showed a high copy number of this sequence. After in situ hybridisation of metaphase chromosomes, clustered Bdm29-specific signals were identified in all these plants on only one of the four chromosomes present. Copy number differences of Bdm29-like sequences between the different plants analysed were indicated by consistent differences in the size and intensity of the hybridisation signal (Figs. 1a, 2d, i, j, k). The site of hybridisation coincided with an interstitial polymorphic heterochromatic segment on the long arm of chromosome 1 of cytodeme A2 (Fig. 1c) and cytodeme A4 (Fig. 2d, f). This region remains highly condensed at all stages of the cell cycle in the same way as do the micro Bs and it can be observed during interphase as a chromocentre (Figs. 1a, 2l). Because the Bdm29 cluster co-locates with the condensed chromatin of micro Bs and the polymorphic A segments, it appears that this repeat unit contains DNA that has a propensity to form heterochromatin.

The karyotype of all mitotic root cells analysed was stable within each single plant and Mendelian inheritance was demonstrated for the Bdm29-positive A segments by analyses of progeny from crosses between heterozygous plants. Plants homozygous for the Bdm29 A segment were observed in the progeny (Fig. 2e, f, g) at the expected frequency, although no homozygotes were found in the wild population.

To determine the organisation of Bdm29 in these heterochromatic A segments, Southern blots of genomic DNA partially digested with EcoRI were hybridised with labelled Bdm29. Ladders characteristic of multiples of a 0.3 kb monomer arranged in tandem arrays were observed (Fig. 3). Complete digestion with EcoRI yielded the 0.3 kb monomer, showing that the restriction site was conserved on all copies of the sequence, consistent with a recent evolutionary amplification event.

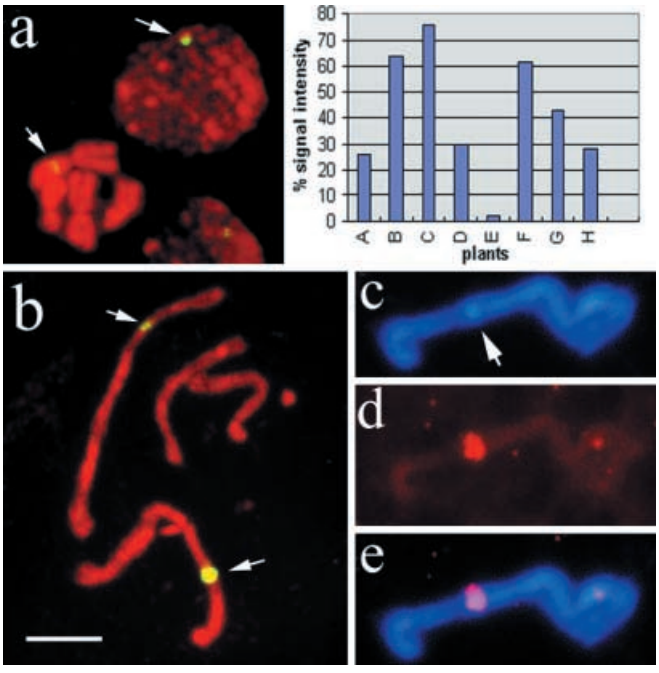

Fig. 1 Fluorescence in situ hybridisation (FISH) of Bdm29 to mitotic metaphase cells of different *Brachycome dichromosomatica* (2*n*=4, cytodeme A2) plants heterozygous (**a**) and homozygous (**b**) for a polymorphic Bdm29-positive segment on A chromosome 1. Note the differences in the hybridisation signal size and intensity between the different Bdm29 loci. Enlarged (**c**) 4′, 6-diamidino-2-phenylindole (DAPI)-stained prometaphase chromosome 1 (heterochromatic region is *arrowed*) before (**c**) and after (**d**) FISH with Bdm29. In **e** the pictures **c** and **d** were merged. The *bar* in **b** represents 5 µm. The histogram shows the relative signal intensity (% of 5S control) of Bdm29-like sequences to the genomic DNA of plants *A–H* after Southern hybridisation with labelled Bdm29

The copy number of Bdm29-like sequences at the A chromosome sites varies between different plants

Comparative Southern hybridisation experiments were performed in order to quantify the copy number of Bdm29-like sequences in individual plants containing A chromosome repeat clusters. To obtain comparability between different DNA loadings, 5S ribosomal DNA of *B. dichromosomatica* was selected as an internal standard. Southern hybridisations of EcoRI-digested genomic DNA, isolated from eight plants (Fig. 1, plants A–H), with simultaneously labelled Bdm29 and 5S rDNA probes revealed two distinct hybridising bands of size 0.3 and 21 kb. Setting the intensity of the 21 kb 5S rDNA signal at 100% for each sample allowed estimates of the relative abundance of Bdm29 (0.3 kb band) in different plants. The histogram (Fig. 1) shows the relative intensity of the Bdm29 signal obtained from different DNA samples from plants that were heterozygous for the Bdm29-positive heterochromatic segment. The Bdm29 signal intensity differed by 32-fold between plants C and E and the copy number varied more than twofold within the group when plant E was excluded.

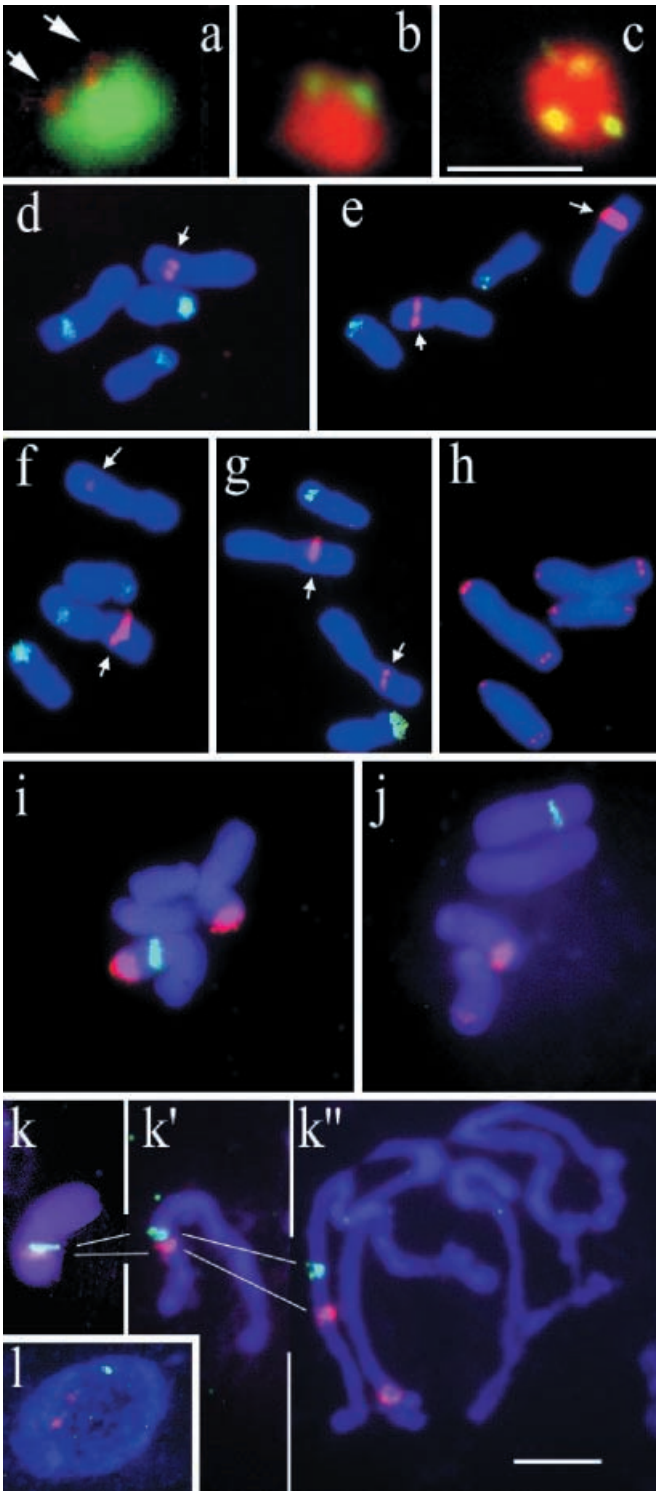

Fig. 2 Fluorescence in situ hybridisation (FISH) with different micro B chromosome and A chromosome sequences to single micro B chromosomes (**a–c**) and mitotic cells (**d–k**) of *B. dichromosomatica* (2*n*=4). *Bar* in **c** represents 1 µm for **a–c**. **a–c** Single micro B chromosomes of *B. dichromosomatica* are hybridised in situ with **a** Bdm29 (*green*) and 18S/25S rDNA (*red, arrowed*), **b** polymorphic A chromosome segment sequence Bds1 (in *yellow*) and **c** *Arabidopsis*-type telomere sequences (*yellow*). **d–l** Metaphase A chromosomes of *B. dichromosomatica* cytodeme A2 (**e, g–k**) and a cytodeme A4/A2 hybrid (**d, f**) carrying a polymorphic Bdm29-positive A chromosome segment after FISH with **d–g** differentially labelled Bdm29 (*red* signals) and 18S/25S rDNA (*green* signals). **h** FISH with an *Arabidopsis*-type telomere sequence. **i–j** Mitotic cells of different plants carrying polymorphic Bdm29-positive A chromosome segments and polymorphic Bds1-positive A segments after FISH with differentially labelled Bdm29 (*green*) and Bds1 (*red*) sequences. **k** One of the three possible polymorphic Bds1 A chromosome sites is adjacent to the Bdm29 segment site at metaphase. Note, these two heterochromatic regions are clearly separated in less condensed prometaphase (**k′, k″**) or interphase chromosomes (**l**). *Bar* in **k″** is representative for **d–l** and indicates 5 µm

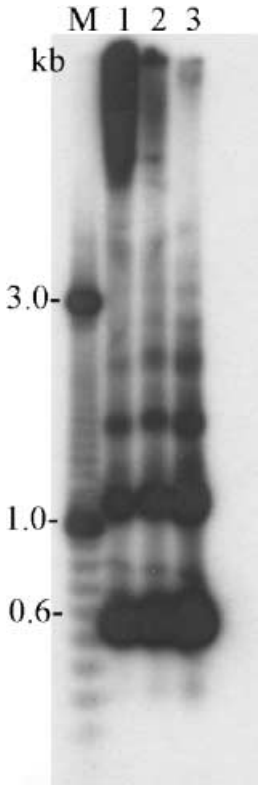

Fig. 3 Partial and complete digests of genomic DNA isolated from a plant with a Bdm29-positive polymorphic A chromosome segment. The DNA samples were digested with 0.5 *lane 1*, 1.5 *lane 2* or 6 units *lane 3* of EcoRI and Southern hybridised with Bdm29

The sequence composition of micro Bs and Bdm29-positive A chromosome segments

The detailed genomic organisation of the Bdm29-positive A segments was probed with a range of known micro B sequences to determine whether the A and B chromosome structures are directly related by excision/integration. The chromosome positions of the relevant in situ hybridisation probes used (Table 1) are shown in the schematic karyotype of *B. dichromosomatica* (Fig. 4). The micro B chromosome localised rDNA (Fig. 2a), Bds1 (Fig. 2b) and telomere (Fig. 2c) sequences were hybridised together with labeled Bdm29 sequences (Fig. 2d–g, i–l) to metaphase chromosomes of different genotypes carrying Bdm29-positive A segments. After FISH with rDNA and Bdm29 sequences, no rDNA signals apart from those already reported on the A chromosomes (Houben et al. 1999) were detected (Fig. 2d–g). One of the three possible polymorphic Bds1 A chromosome sites of cytodeme A2 (Houben et al. 2000) was detected next to the Bdm29 segment in two plants

Table 1 List of relevant sequences tested on A and micro B chromosomes of *B. dichromosomatica*, cytodeme A2

Sequence, reference	Presence on:	
	A chromosome	Micro B
Bdm29 repeat (accession number Y13091), Houben et al. (1997b)	Forms a rare polymorphic heterochromatic region on chromosome 1	High copy number detected
Bds1 repeat (accession number AJ130940), Houben et al. (2000)	Forms up to three polymorphic heterochromatic regions on chromosomes 1 and 2	Detected
Bdm54 repeat (accession number AJ276463), this paper	Not detected	High copy number detected
18S/25S rDNA (VER17), Yakura and Tanifuji (1983)	Detected	Detected
Arabidopsis-type telomere	Detected	Detected

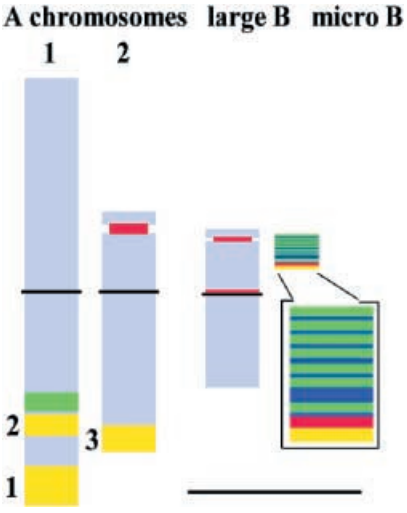

Fig. 4 Schematic karyotype of *B. dichromosomatica* (cytodeme A2, *n*=2 A chromosomes + large B chromosome + micro B chromosome) shows the positions of Bdm29 (*green*), Bds1 (*yellow*), rDNA (*red*) and Bdm54 and other unidentified sequences (*dark blue*). Bds1 forms up to three different polymorphic regions on A chromosomes 1 and 2. The physical order of Bds1 and rDNA sequences at the distal end of the micro B is uncertain. The micro B is enlarged in the *inset*. *Bar* represents 5 µm

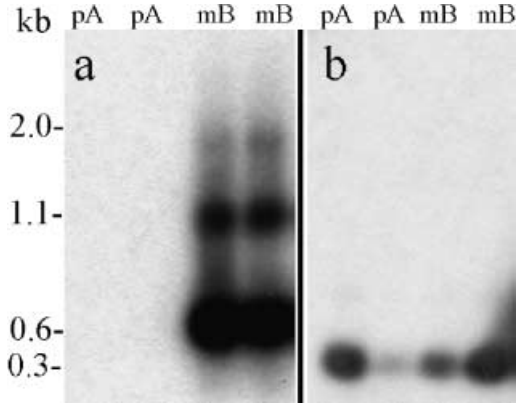

Fig. 5a, b Southern hybridisation of Bdm54 and Bdm29 to AluI-digested genomic DNA of genotypes with micro B chromosomes (*lanes mB*) or Bdm29-positive A chromosome segments (*lanes pA*). **a** After hybridisation with Bdm54, **b** after hybridisation with Bdm29

(Fig. 2k). However, these two heterochromatic regions were clearly separated in less condensed prometaphase (Fig. 2k', k") or interphase chromosomes (Fig. 2l). This arrangement contrasts with that in the micro B, where the larger Bdm29 region is closely juxtaposed to the Bds1-positive region at all stages of mitosis studied (Fig. 2b). In addition, Bdm29-positive genotypes without any, or with distantly located, Bds1 segments were also found (Fig. 2i, j). No interstitial signals were detected on any A chromosome after in situ hybridisation with *Arabidopsis*-type telomere sequences (Fig. 2h).

Since none of the micro B chromosome probes (rDNA, telomeres, Bds1) were detected in proximity to the Bdm29-positive A segment, we conclude that the micro B and the A segment are not related to each other by simple excision or integration. However, the Bdm29-positive A region could be formed by an integrated micro B chromosome fragment lacking rDNA, telomeres and Bds1 sequences. Additional micro B sequences were therefore sought in order to test this possibility.

To obtain other diagnostic probes, a partial micro B DNA library was screened with total genomic DNA of plants with and without micro Bs. After Southern hybridisation, in addition to clones showing only minor levels of differential hybridisation, one clone (Bdm54) with a strong and almost exclusive micro B specificity was identified. Southern analysis of AluI-digested genomic DNA probed with Bdm54 showed intense signals characteristic of another tandem repeat in all plant genotypes containing micro Bs (Fig. 5a). No such hybridisation was obtained with DNA from plants containing a Bdm29-positive A chromosome region (Fig. 5a) or large B chromosomes (not shown). However, weak hybridising bands were detectable after extended exposure in DNA from *B. dichromosomatica* without micro Bs and the related *B. lineariloba* (2*n*=10, 12 or 16) species (result not shown). Reprobing the same Southern filter with Bdm29 gave strongly hybridising bands in DNA from

Fig. 6 Sequence of the 477 bp tandem repeat Bdm54 (EMBL accession number AJ276463). The repeat units of TCGAAAAGTTCGAAG are *underlined*; the perfect and degenerate repeat units AGTTCGAA are *boxed*

TCCGACTCGAGGCTGTGATGTGGGTGGGTTCGAAAGTTTCGAAGGTGGATTTTTGAAGGTGGGCTC
GAAGGTGAGATCGAAAAGTTCGAAGATGAAAGTTCGAGGATGAGTTCGAAAAGTTCGAAGATGAAA
GTTTTCGAAAAGTTCGAAGTGGTTTCCGTTAGAAGGTTCAAAAATGTCGAACGTAATTTATAATGT
TTTTTTGTTAAATTGATGATATGTGTGTAAGTATTGTATTTGAACTTTGTTATATTAGGGGGTTTT
GCAAAACCCTAATTTGGAATTAGGAAAATGGTGAAATGGAATGTTAGTGGTTATATTATGTATTAC
CTTTAGCTATACGTTAATTATGTTTGGTGTATTGGTGACTCCAAAGGTACTAAATATTTTGATCTA
CCATAATAAAAAGTTATCAATgCAACTACTTCATTAACTGCAGGGTTCACAAAAATATCCACATGC
CAAACTCGAGTCGGA

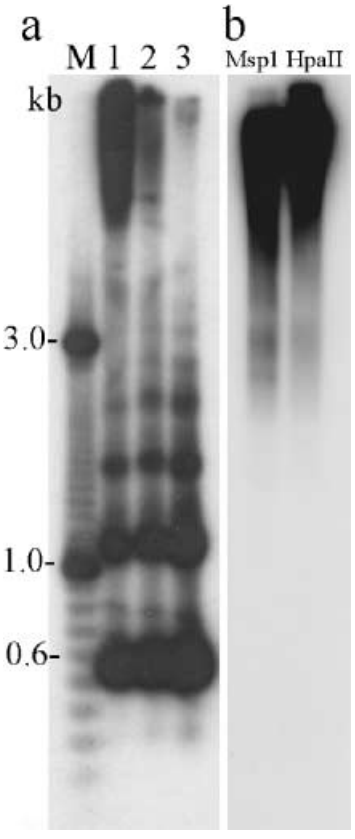

Fig. 7a, b Genomic organisation and methylation of Bdm54. **a** A partial digest of genomic DNA isolated from a plant with micro B chromosomes. The DNA samples were digested with 0.5 *lane 1*, 1.5 *lane 2* or 6 units *lane 3* of AluI. **b** Genomic DNA isolated from a plant with micro B chromosomes was digested with MspI or HpaII. Both Southern blots were hybridised with Bdm54

genotypes with micro Bs and Bdm29-positive A regions (Fig. 5b). Since no Bdm54-specific signals were found in genotypes carrying Bdm29-positive A regions, the DNA composition of the micro Bs differs from that of the Bdm29-positive A chromosome segment. We conclude that the Bdm29-positive A chromosome region did not originate by integration or excision of whole micro B chromosomes or chromosome fragments.

The AT-rich (61%) insert of Bdm54 is 477 bp long and contains four copies of a subrepeat unit (TCGAAAAGTTCGAAG) as well as three perfect and

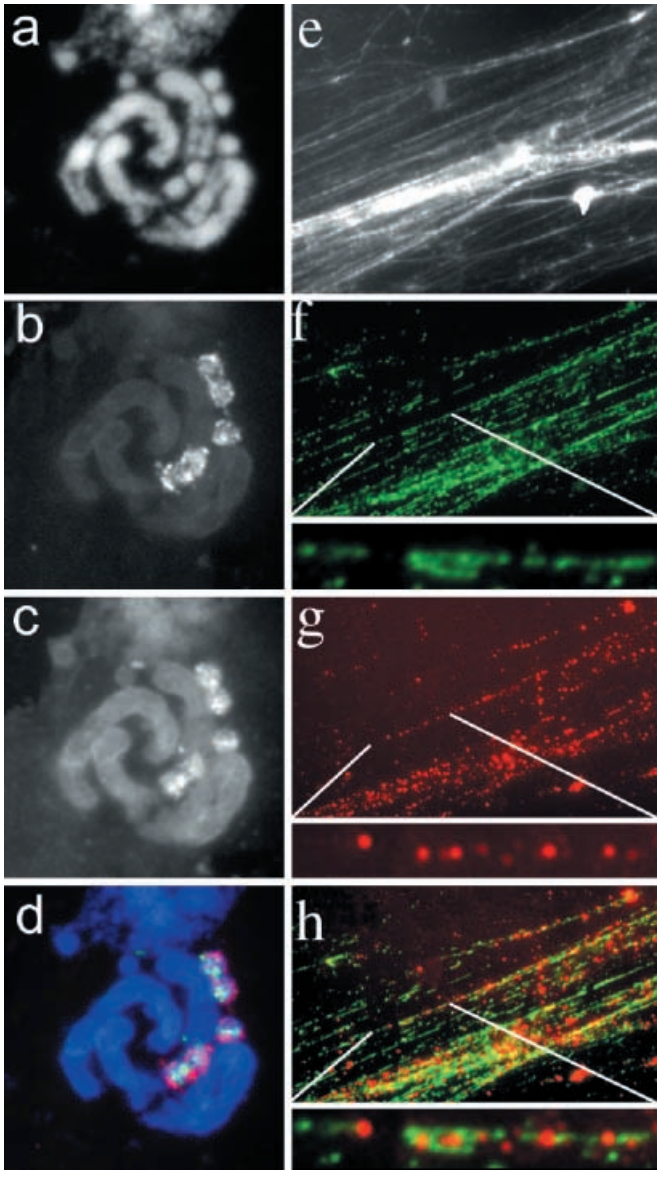

Fig. 8a–h Fluorescence in situ hybridisation (FISH) of tandem repeats Bdm29 and Bdm54 to mitotic chromosomes and extended DNA fibres prepared from *B. dichromosomatica* with micro B chromosomes. DAPI-counterstained **a** mitotic metaphase chromosomes and **e** extended DNA fibres after FISH with differentially labelled Bdm29 (**b, f**) and Bdm54 sequences (**c, g**). The pictures were pseudo-coloured (**a** *blue*, **b** *green*, **c** *red*) and merged (**d**). In **h** pictures **f** and **g** are merged. Fibres are further enlarged in the *insets* of **f–h**

four degenerate copies of a second short repeat (AGTTCGAA) that are embedded in the first unit (Fig. 6). The sequence (EMBL, Genbank accession number AJ276463) was compared with the Genbank database and no significant sequence homology was found. To confirm the sequence organisation of Bdm54, it was used as a probe to genomic DNA from a plant with micro B chromosomes partially digested with AluI. The result showed a pattern characteristic of tandem repetitive sequences (Fig. 7a). Southern analysis suggested a medium degree of methylation of genomic Bdm54 sequences at C^{m}CGG sites recognised by HpaII compared with ^{m}CCGG sites recognised by MspI (Fig. 7b).

Tandem repeat clusters of Bdm29, Bdm54 and other sequences are interspersed in micro B chromosomes

Multicolour in situ hybridisation with Bdm54 and Bdm29 sequences revealed labelling of the entire micro Bs (Fig. 8a–d), suggesting that both sequences are dispersed and interspersed along the chromosome. To investigate the arrangement of the two repeats in individual DNA molecules, extended DNA fibre-FISH was performed with differentially labelled Bdm29 and Bdm54 probes. Figure 8h shows individual fibres with pseudocoloured Bdm29 (Fig. 8f) and Bdm54 signals (Fig. 8g), showing that the two repeat clusters are interspersed irregularly with each other along the fibres. Generally, stretches of fibres hybridised with Bdm29 were longer than those with Bdm54. Non-hybridising DNA fibre stretches were also detected, which must contain undiscovered micro B sequences. Therefore, the micro B-localised Bdm29-like sequence is not organised as an extended and uninterrupted tandem array but rather as clusters that vary in size along the micro B. Since no internal size marker was available, the degree of DNA fibre extension could not be estimated.

Discussion

The DNA composition and cytological appearance of the A heterochromatic segment is similar to the Bds1-positive segments of *B. dichromosomatica* recently described by Houben et al. (2000) and the polymorphic heterochromatic knobs of maize (Peacock et al. 1981). In maize (Peacock et al. 1981; Ananiev et al. 1998) and in *B. dichromosomatica*, the heterochromatic segments appear to be predominantly composed of tandem sequence arrays. In both species, these sequences are also related to high copy sequences located in B chromosomes (Alfenito and Birchler 1993; Houben et al. 2000). However, the frequency of appearance of Bdm29-positive A segments is lower than the frequency of Bds1-positive A segments. Furthermore, Bds1 segments were found at three different possible A chromosome sites (Houben et al. 2000), whereas the Bdm29-positive segments were found only at a single A chromosome site. Therefore, the Bdm29-positive A chromosome segment polymorphism represents a new type of chromosome feature in *B. dichromosomatica*.

The question remains as to the nature of the mechanism responsible for the formation and maintenance of the Bdm29-positive segment polymorphism in natural populations and its relationship to the micro B chromosomes. There are a number of possible evolutionary interpretations of this situation. One explanation for the polymorphic status of the A segments in *B. dichromosomatica* populations is that they are advantageous or disadvantageous for plants within the population under specific environmental conditions. If Bdm29-positive A segments are a recent addition to the genome then homogenisation/stabilisation of the chromosome distribution may be expected later. However, as all cytodemes analysed carry a small number of Bdm29-like sequences on the large B chromosomes (Houben et al. 1997b), it is likely that Bdm29 was already present before the cytodemes diverged.

Rapid and ongoing spontaneous amplification/deletion processes may explain the Bdm29 copy number differences detected between genotypes with Bdm29-positive A segments. Differential DNA amplification, in vitro, has been reported for high copy sequences in plants (Arnhold-Schmitt 1993) and repeats arranged in tandem arrays are particularly prone to molecular events that alter their number (Flavell 1985).

It is striking that the major component of the micro B is composed of a tandem repeat (Bdm29) that is also able to form a heterochromatic A chromosome segment. The Bdm29-positive A segment shows similar structures to those described as interchromosomal “homogeneously staining regions” (HSRs) in mammalian cells (Cowell 1982). As in *Brachycome*, repeated sequences are found in these condensed HSR chromosome segments (Smith et al. 1990) and the amplified sequences are often variable in repeat number and organised as tandem arrays (Ma et al. 1993). However, it must be noted that the HSR regions observed in mammalian karyotypes are a result of strong selective pressure (i.e. for drug resistance), which, although it may exist, is not identifiable in these wild populations.

There is clearly an evolutionary relationship between the polymorphic A chromosome sites of Bdm29 and the micro B chromosomes and this relationship has been rigorously scrutinised in this paper. The approach was to determine the sequence architecture of Bdm29 at the two sites with respect to other sequences known to occur on the micro B chromosome. The results indicate that the relationship between the A and micro B sites is complex and cannot be explained by simple integration and/or excision. Since no ribosomal DNA, telomeres or Bds1 segments were detected in proximity to the Bdm29-positive A segment (Fig. 4), it is unlikely that any of the plants analysed showing a Bdm29-positive A segment represents a direct forerunner or integration product of the particular micro Bs that were characterised. Furthermore, it is only in micro Bs that the Bdm29 tandem arrays are

intermingled with the tandem repetitive sequence Bdm54, such that the Bdm29-like sequences of the micro B do not consist entirely of an extended and uninterrupted tandem array of the repeat unit. Nevertheless the sequence blocks are quite long, as Southern analysis of partially digested DNA of genotypes with micro Bs shows a ladder with large numbers of rungs (Houben et al. 1997b). Interspersion of this nature appears to be a rare feature of tandemly repeated DNA. In most plant and animal species, long uninterrupted single repeat-type arrays of several hundred kilobases to several megabases in length are most commonly described (examples compiled in Zinic et al. 2000) but mosaic structures have been observed among tandem arrays of A chromosome satellite DNA (Zinic et al. 2000) and B chromosome-specific repeats (Franks et al. 1996; McAllister and Werren 1999; Langdon et al. 2000).

It is not clear how the interspersion of arrays of different sequences has occurred. Although Bdm54 shows no sequence similarity to known transposable DNA elements, we cannot exclude the possibility that the flanking sequences form part of a transposable element and that the Bdm54 sequences associated with the flanking sequences have been inserted by a transposition mechanism. Under the selfish DNA hypothesis, Bdm54 elements would accumulate in micro Bs because they are less likely to be deleterious to the host genome. A rapid accumulation of Bdm54-like sequences on a de novo micro B may have been under initial strong selection because of the necessity to reduce the sequence similarity to the Bdm29-positive. These changes would reduce the competence of meiotic pairing between the ancestral and derived segments, such that the newly formed B may survive and begin its independent evolution. The chromosome-specific accumulation of Bdm54 elements may represent a crucial step in a ratchet-like (Green 1990) chromosome evolution mechanism.

Because evolutionary processes cannot be reproduced experimentally, the course of B chromosome formation can only be tentatively reconstructed. However, considering that high copy numbers of Bdm29 are conserved on other types of B chromosomes of *Brachycome* (Houben et al. 1997b) and the Bdm29-positive A segments appear to be in constant flux, it is still feasible that this repeat may represent one of the micro B founder sequences. Our data are consistent with the hypothesis that the *B. dichromosomatica* micro B originated from the standard genome but did not derive from a simple chromosome excision of part of one of the A chromosomes.

The findings presented here highlight that caution needs to be exercised when analysing karyotype evolution with a low number of chromosomal probes and also reinforce the point that it is vital to consider a sufficient number of plants to ensure that the full range of genome variation present is detected. The experiments also demonstrate that laboratory collections must be expected to be seriously unrepresentative of the level of genomic variation and dynamic structure present in wild populations.

Acknowledgements A.H. was supported by the Australian Research Council and this research was funded by ARC grants to A.H., C.R.L. and J.N.T.

References

Alfenito MR, Birchler JA (1993) Molecular characterisation of a maize B chromosome centric sequence. Genetics 135:589–597

Ananiev EV, Phillips RL, Rines HW (1998) Complex structure of knob DNA on maize chromosome 9: retrotransposon invasion into heterochromatin. Genetics 149:2025–2037

Arnhold-Schmitt B (1993) Rapid changes in amplification and methylation pattern of genomic DNA in cultured carrot root explants (*Daucus carota* L.). Theor Appl Genet 85:793–800

Beukeboom LW (1994) Bewildering Bs: an impression of the 1st B-chromosome conference. Heredity 73:328–336

Cabrero J, López-León MD, Bakkali M, Camacho JPM (1999) Common origin of B chromosome variants in the grasshopper *Eyprepocnemis plorans*. Heredity 83:435–439

Camacho JPM, Sharbel TF, Beukeboom LW (2000) B-chromosome evolution. Philos Trans R Soc Lond B Biol Sci 355:163–178

Carter CR, Smith-White S (1972) The cytology of *Brachycome lineariloba* 3. Accessory chromosomes. Chromosoma 39:361–379

Cowell JK (1982) Double minutes and homogeneously staining regions: gene amplification in mammalian cells. Annu Rev Genet 16:21–59

Donald TM, Houben A, Leach CR, Timmis JN (1997) Ribosomal RNA genes specific to the B chromosome in *Brachycome dichromosomatica* are not transcribed in leaf tissue. Genome 40:674–681

Flavell RB (1985) Repeated sequences and genome change. In: Hohn B, Dennis ES (eds) Genetic flux in plants. Springer, Vienna, New York, pp 139–156

Franks TK, Houben A, Leach CR, Timmis JN (1996) The molecular organisation of a B chromosome tandem repeat sequence from *Brachycome dichromosomatica*. Chromosoma 105:223–230

Fransz PF, Alonso-Blanco C, Liharska TP, Peeters AJM, Zabel P, de Jong H (1996) High resolution physical mapping in *Arabidopsis thaliana* and tomato by fluorescence in situ hybridisation to extended DNA fibres. Plant J 9:421–430

Gottlub-McHugh SG, Levesque M, MacKenzie K, Olson M, Yarosh O, Johnson DA (1990) Organisation of the 5S rDNA genes in the soybean (*Glycine max* L. Merrill) and conservation of the 5S rDNA repeat structure in higher plants. Genome 33:486–494

Green DM (1990) Muller's Ratchet and the evolution of supernumerary chromosomes. Genome 33:818–824

Houben A, Belyaev ND, Leach CR, Timmis JN (1997a) Differences of histone H4 acetylation and replication timing between A and B chromosomes of *Brachycome dichromosomatica*. Chromosome Res 5:233–237

Houben A, Leach CR, Verlin D, Rofe R, Timmis JN (1997b) A repetitive DNA sequence common to the different B chromosomes of the genus *Brachycome*. Chromosoma 106:513–519

Houben A, Thompson N, Ahne R, Leach CR, Verlin D, Timmis JN (1999) A monophyletic origin of the B chromosomes of *Brachycome dichromosomatica* (Asteraceae). Plant Syst Evol 219:127–135

Houben A, Wanner G, Hanson L, Verlin D, Leach CR, Timmis JN (2000) Cloning and characterisation of polymorphic heterochromatic segments of *Brachycome dichromosomatica*. Chromosoma 109:206–213

Ijdo JW, Wells RA, Baldini A, Reeders ST (1991) Improved telomere detection using a telomere repeat probe $(TTAGGG)_n$ generated by PCR. Nucleic Acids Res 19:4780

Jamilena M, Ruiz Rejón C, Ruiz Rejón M (1994) A molecular analysis of the origin of the *Crepis capillaris* B chromosome. J Cell Sci 107:703–708

Jones RN (1995) Tansley Review No. 85, B chromosomes in plants. New Phytol 131:411–434
Jones RN, Rees H (1982) B chromosomes, 1st edn. Academic Press, London, New York
Langdon T, Seago C, Jones RN, Ougham H, Thomas H, Forster JW, Jenkins G (2000) De novo evolution of satellite DNA on the rye B chromosome. Genetics 154:869–884
López-León MD, Neves N, Schwarzacher T, Heslop-Harrison TS, Hewitt GM, Camacho JPM (1994) Possible origin of a B chromosome deducted from its DNA composition using double FISH technique. Chromosome Res 2:87–92
Ma C, Martin S, Trask B, Hamlin JL (1993) Sister chromatid fusion initiates amplification of the dihydrofolate reductase gene in Chinese hamster cells. Genes Dev 7:605–620
McAllister BF, Werren JH (1997) Hybrid origin of a B chromosome (PSR) in the parasitic wasp *Nasonia vitripennis*. Chromosoma 106:243–253
McAllister BF, Werren JH (1999) Evolution of tandemly repeated sequences: what happens at the end of an array? J Mol Evol 48:469–481
Meyerowitz EM (1999) Today we have naming of parts. Nature 402:731–732
Peacock WJ, Dennis ES, Rhoades MM, Pryor AJ (1981) Highly repeated DNA sequence limited to knob heterochromatin in maize. Proc Natl Acad Sci U S A 78:4490–4491
Sapre B, Deshpande S (1987) Origin of B chromosomes in *Coix* L. through spontaneous interspecific hybridisation. J Hered 78:191–196
Schartl M, Nanda I, Schlupp I, Wilde B, Epplen JT, Schmid M, Parzefall J (1994) Incorporation of subgenomic amounts of DNA as compensation for mutational load in a gynogenetic fish. Nature 373:68–71
Sharbel TF, Green DM, Houben A (1998) B chromosome origin in the endemic New Zealand frog *Leiopelma hochstetteri* through sex chromosome devolution. Genome 41:14–22
Smith KA, Gorman PA, Stark MB, Groves RP, Stark GR (1990) Distinctive chromosomal structures are formed very early in the amplification of CAD genes in Syrian hamster cells. Cell 63:1219–1227
Stark EA, Connerton I, Bennett ST, Barnes SR, Parker JS, Forster JW (1996) Molecular analysis of the structure of the maize B-chromosome. Chromosome Res 4:15–23
Watanabe K, Carter CR, Smith-White S (1975) The cytology of *Brachycome lineariloba* 5. Chromosome relationships and phylogeny of the race A cytodemes (n=2). Chromosoma 52:383–397
Wienand U, Feix G (1980) Zein-specific restriction enzyme fragments of maize DNA. FEBS Lett 116:14–16
Yakura K, Tanifuji S (1983) Molecular cloning and restriction analysis of EcoRI-fragments of *Vicia faba* rDNA. Plant Cell Physiol 24:1327–1330
Zinic SD, Ugarkovic D, Cornudella L, Plohl M (2000) A novel interspersed type of organisation of satellite DNAs in *Tribolium madens* heterochromatin. Chromosome Res 8:201–212

A10 Houben, A., Wanner, G., Hanson, L., Verlin, D., Leach, C.R., and Timmis, J.N. (2000). Cloning and characterisation of polymorphic heterochromatic segments of *Brachycome dichromosomatica*. Chromosoma 109, 433-433.

Chromosoma (2000) 109:206–213

CHROMOSOMA

Cloning and characterisation of polymorphic heterochromatic segments of *Brachycome dichromosomatica*

Andreas Houben[1], **Gerhard Wanner**[2], **Lynda Hanson**[3], **Dawn Verlin**[1], **Carolyn R. Leach**[1], **Jeremy N. Timmis**[1]

[1] Department of Genetics, The University of Adelaide, Adelaide, South Australia 5005, Australia
[2] Botanisches Institut der Universität München, Menzingerstrasse 67, 80638 München, Germany
[3] Jodrell Laboratory, Royal Botanic Gardens, Kew, Richmond, Surrey, TW9 3AB, UK

Received: 16 March 1999; in revised form: 28 September 1999 / Accepted: 11 November 1999

Abstract. After selective enrichment and differential hybridisation of C_0t-1 DNA fractions of plants with and without polymorphic heterochromatic segments, a repetitive sequence (called Bds1) specific to the polymorphic chromosome segments of *Brachycome dichromosomatica* (*Brachyscome dichromosomatica*) was isolated. A single repeat unit of Bds1 is 92 bp long and is organised in tandem arrays at three different polymorphic segment sites on the chromosomes of cytodeme A2. Although all three sites showed extensive polymorphism between plants, the karyotypes of all analysed mitotic root cells were stable within a single plant. Electron microscopy revealed heavily condensed chromatin structures at the most obvious polymorphic site. The mechanisms that generate and maintain the observed chromosome structure polymorphisms are discussed.

Introduction

Most eukaryotic chromosomes consist of both euchromatic and heterochromatic segments, which are generally identical between homologous chromosomes. With differential chromosome staining methods it is possible to visualize the different chromatin types and to use the resulting lengthwise chromosome differentiation as a tool to distinguish homologous pairs of chromosomes. The expectation is that the succession of positive- and negative-staining chromosome bands will be essentially identical between homologous chromosomes in a population. However, intraspecific variations in size and number of the bands between homologous chromosomes have frequently been found in animals, e.g. *Eyprepocnemis* (Martin-Alganza et al. 1997); and plant species, e.g. *Alstroemeria* (Buitendijk et al. 1998), *Scilla* (Vosa 1973), (Greilhuber and Speta 1976), *Triticum araraticum* (Badaeva et al. 1994), *Tulipa australis* (Ruiz Rejon et al. 1985), *Secale cereale* (Vinikka and Kavander 1986) and *Allium subvillosum* (Jamilena et al. 1990). In some species such bands are also called 'supernumerary segments', e.g. *Rumex* (Wilby and Parker 1988), grasshopper (Hewitt 1979; Camacho et al. 1984), by analogy with supernumerary (B) chromosomes, with which they share several characteristics, i.e. they are often heterochromatic and dispensable, although some polymorphic euchromatic segments have also been found (e.g. Ainsworth et al. 1983; Camacho et al. 1984). Individuals possessing them are phenotypically indistinguishable from those lacking the segments. In maize, variable heterochromatic segments (called 'knobs') have been found in 23 possible locations on the 10 maize chromosomes (Rhoades and Dempsey 1966).

Chromosome band polymorphisms range from changes in the size of pre-existing bands (Vosa 1973) to the addition of truly supernumerary segments (Hewitt 1979). Different patterns of inheritance have been determined for these polymorphic segments. In some species meiotic drive was shown to play a role in their maintenance (Ainsworth et al. 1983; Wilby and Parker 1988), while in another species the segments were found to be inherited in a normal Mendelian fashion (Ruiz Rejon et al. 1985). In addition different patterns of inheritance have been reported for different polymorphic segments of the same species (Wilby and Parker 1988; Lopez-Leon et al. 1992). In maize, the knobs are centromerically inactive under normal conditions, but in the presence of an abnormal chromosome 10, they acquire centromeric functions during meiosis and override the function of normal centromeres (Rhoades and Vilkomerson 1942). The reported band polymorphisms will also generate intraspecific variation in nuclear DNA amount as already reported in numerous other angiosperm species (reviewed by Bennett and Leitch 1995).

Recently a striking chromosome structure polymorphism in the plant *Brachycome dichromosomatica* was described (Houben et al. 1997a). C-banding revealed

EMBL accession number: AJ130940

Edited by: J.M. Graves

Correspondence to: A. Houben
e-mail: andreas.houben@adelaide.edu.au

one or two additional terminal heterochromatic segments on a single chromosome of one homologous pair in a number of plants analysed. *Brachycome dichromosomatica* is an outbreeder with only two pairs of A chromosomes. Within the species there are four different cytodemes (A1, A2, A3 and A4) each of which contains large B chromosomes (Bs) and dot-like micro B chromosomes (micro Bs) (Carter and Smith-White 1972).

The aim of the present investigation was to characterise the structure and DNA composition of the highly polymorphic heterochromatic segments of *B. dichromosomatica*.

Materials and methods

Plant material and cytogenetic preparation

Brachycome dichromosomatica (also called *Brachyscome dichromosomatica*) (2*n*=4) is a member of the *Brachycome lineariloba* complex (Watanabe et al. 1994). Plants of the cytodemes A1 and A2 of *B. dichromosomatica* were characterised on the basis of their chromosome morphology as described by Watanabe et al. (1975). Mitotic preparations for in situ hybridisation were obtained from root tips according to Houben et al. (1997b).

Isolation, cloning and selection of C_ot-1 DNA

Genomic DNA was isolated from leaf material using the procedure described by Wienand and Feix (1980). The C_ot-1 fraction of *B. dichromosomatica* DNA was prepared using the procedure described by Zwick et al. (1997). In brief, DNA was sheared to a length of between 0.1 and 1 kb and dissolved in 0.3 M NaCl at a concentration of 0.5 mg/ml. The resulting DNA was denatured for 10 min at 95°C and immediately chilled in an ice bath for 10 s. For reannealing the single-stranded DNA was incubated for 11.2 min at 65°C. Unannealed, single-stranded DNA was digested by adding 1 U S1 nuclease (Boehringer) per 1 µg DNA in the appropriate buffer. The samples were gently mixed and incubated at 37°C for 8 min and the DNA was purified by phenol/chloroform extraction. After ethanol precipitation and centrifugation, the DNA was resuspended in TE buffer. For cloning, the 3' termini of the C_ot-1 DNA fragments were end-filled by using the Klenow fragment of *Escherichia coli* DNA polymerase I. The blunt-ended DNA fragments were ligated into the SmaI restriction site of the plasmid pBluescript (Stratagene) and propagated in the *E. coli* DH5α strain. The resulting transformants were successively colony hybridised with ^{32}P-labelled total C_ot-1 DNA of plants with and without polymorphic segments.

Sequencing and sequence data analysis

Sequence analysis of the clones was performed by the automated dideoxynucleotide-dye termination method (Perkin-Elmer). Searches for sequence similarity in the Genbank database were performed using FASTA and BLASTA services (Australian National Genomic Information Service).

Polymerase chain reaction (PCR) with Bds1-specific primers

The PCR was performed in a 25 µl volume using 20 ng of genomic DNA as the template. The other components of the reaction were 0.2 mM dNTPs, 0.3 U Taq polymerase (Bresatec), 0.2 mM primers (5'-GCTTTATGGAGGCTCGTGTG-3' and 5'-CATTTCGATTCCCATGGTTG-3'), 2 mM $MgCl_2$, 50 mM KCl, 10 mM TRIS-HCl and 0.1% (v/v) Triton X-100. After denaturation for 2 min at 94°C, 20 cycles of amplification were performed under the following conditions: 94°C, 1 min; 45°C, 1 min; 72°C, 1 min followed by a final primer extension step of 5 min at 72°C. The PCR products were ligated into the vector pGEM-T Easy (Promega) and propagated in the *E. coli* DH5α strain.

Southern hybridisation

Genomic DNA was digested with restriction enzymes according to the manufacturer's recommendations. For partial digestions, 5 µg of DNA was cut with successively diluted amounts of the enzyme for 4 h. DNA fragments were resolved on 0.8% agarose gels in TAE buffer and subsequently transferred to Hybond N^+ nylon membranes (Amersham). For hybridisation, the DNA probes were labelled with [α-^{32}P]dCTP by random primed DNA synthesis. Hybridisation was carried out overnight at 65°C in 5×SSPE, 0.2% SDS, 5×Denhardt's reagent, 100 µg/ml single-stranded salmon sperm DNA. Blots were washed successively in 0.1×SSC and 0.1% SDS and then exposed to X-ray film with intensifying screens at –70°C for appropriate periods. (1×SSC is 0.15 M NaCl, 0.015 M sodium citrate.)

Estimation of the genomic DNA content of B. dichromosomatica *and determination of repeat unit copy number*

Feulgen microdensitometry was performed to estimate DNA amounts in *B. dichromosomatica*. Seeds of *B. dichromosomatica* and *Vigna radiata* cv. Berken (the calibration standard) were germinated on moist filter paper. Once germinated, the root tips from each species were simultaneously placed into vials containing freshly prepared fixative (3:1 ethanol:glacial acetic acid). After at least 24 h, but not more than 3 weeks, in fixative, the roots were rinsed in distilled water, then hydrolysed in vials of 5 N HCl for 40 min at 25°C. Once hydrolysed, the root tips were stained, washed and stored in distilled water. On the following day, the slides were prepared and stain absorbency was measured using a Vickers M85a Microdensitometer (all as described in Rudall et al. 1998). To estimate the 4C values of each sample, arbitrary readings of nuclei judged to be at mid-prophase of mitosis were measured from each slide and three integrated values were taken from each nucleus. To estimate the size of the B chromosomes, arbitrary readings of individual standard B and micro B chromosomes were taken from well-spread metaphase cells. The arbitrary values were converted to picograms from the ratio of the mean absorbancy of the nuclei of the test species to that of the calibration standard, which has a known 4C DNA amount (2.12 pg, Bennett and Leitch 1995). Standard deviations and standard errors were then calculated.

The determination of copy number was performed by quantitative slot-blot hybridisation. Genomic DNA was applied in different concentrations together with a dilution series of the DNA of clone Bds1 to Hybond N+ using a slot-blot apparatus. Hybridisation of the filter was performed with ^{32}P-labelled (see above) probe Bds1. After hybridisation the relative radioactivity was measured with a phosphoimager (Fuji) and copy number estimated by comparison of radioactivity, genome size of plant and clone, and slot-blot sample loading.

Fluorescence in situ hybridisation (FISH)

An *Arabidopsis*-type telomeric probe was synthesised using PCR according to Ijdo et al. (1991). The probes (Bds1, telomere) were labelled with digoxigenin-11-dUTP (DIG-11-dUTP) by nick translation. Hybridisation sites of the DIG-labelled probe were detected using sheep anti-digoxigenin-rhodamine/rhodamine anti-sheep antibody. Epifluorescence signals were recorded on Fuji 400 film or electronically with a CCD camera. The image manip-

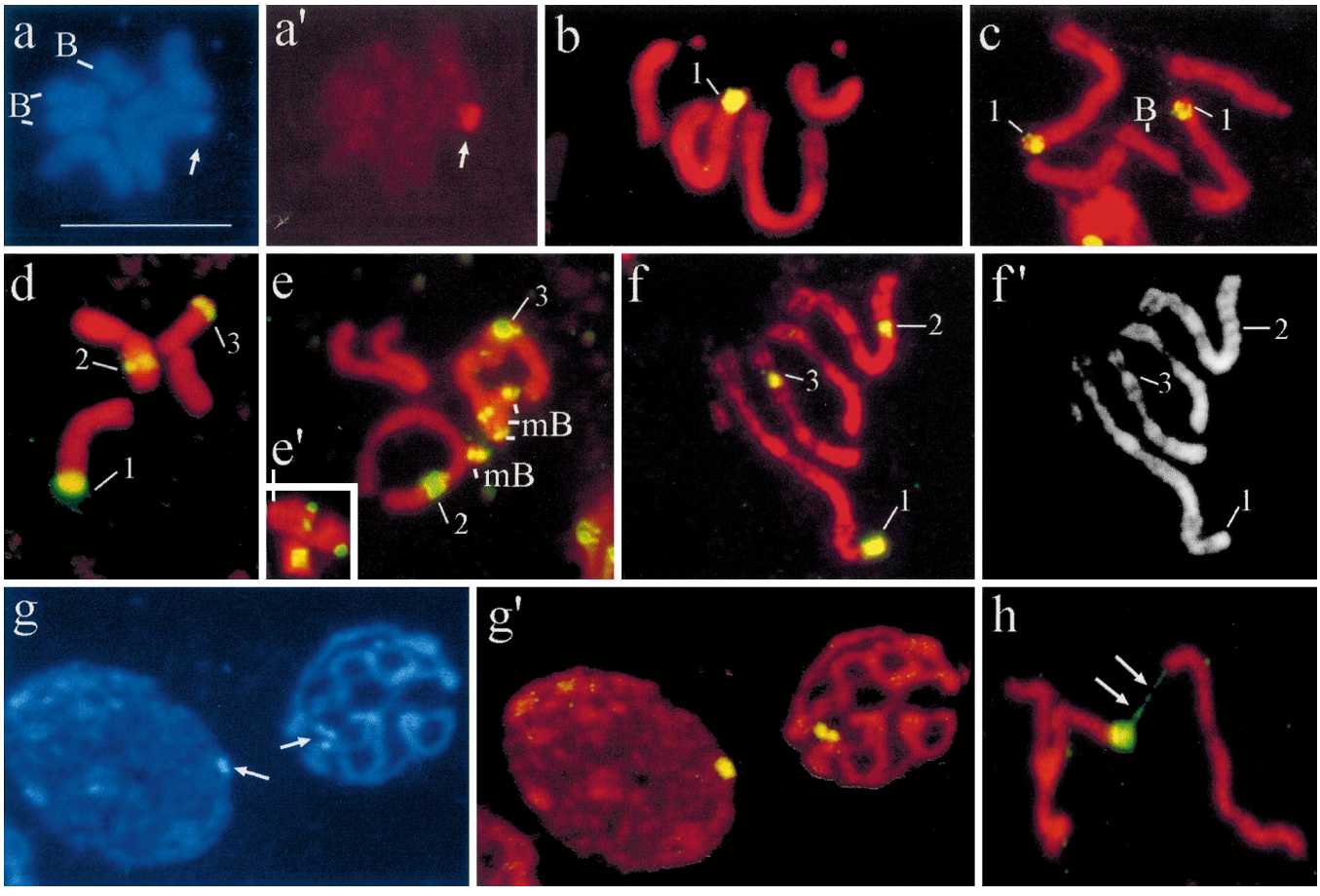

Fig. 1. a Metaphase cell of *Brachycome dichromosomatica* (cytodeme A1, 2*n*=4+3Bs) after 4',6-diamidino-2-phenylindole (DAPI) staining and **a'** after fluorescence in situ hybridisation (FISH) with labelled C_ot-1 DNA isolated from a plant carrying the polymorphic segment 1. The polymorphic segment is indicated with an *arrow*. The metaphase shows a strong hybridisation at the polymorphic segment, the other chromosome regions are faintly labelled. **b–f** Metaphase cells of different plants of cytodeme A2 after FISH with labelled Bds1 sequences. The three different hybridisation sites are numbered *1*, *2* and *3*. In **a, c** and **e** the large B chromosome and micro B chromosomes are labelled *B* and *mB*, respectively. The micro Bs are further enlarged in the inset of **e'**. Interphase, prophase (**g**) and prometaphase (**f'**) cells after DAPI staining and (**g'**) after FISH with Bds1. The position of segment 1 is *arrowed* in **g**. **h** The Bds1-hybridising chromatin fibre between two chromosomes 1 is indicated with *two arrows*. *Bar* in **a** represents 10 µm. All panels are at the same magnification except the inset in **e**

ulations including pseudocolouring were performed with the program Adobe Photoshop.

Electron microscopic studies

Chromosomes for high-resolution scanning electron microscopy were prepared and stained with platinum blue as described by Wanner and Formanek (1995). The preparations were analysed with a Hitachi S-4100 field emission scanning electron microscope. Back-scattered electrons (BSE) were monitored at 15 kV with an Autrata detector (Plano, Germany) of the YAG type.

Results

Isolation and characterisation of the polymorphic heterochromatic segment-specific sequence Bds1

As constitutive heterochromatin is composed mainly of rapidly reannealing, highly repetitive DNA (Rae 1970), it was assumed that the heterochromatic polymorphic regions of *B. dichromosomatica* would be composed of DNA within the C_ot-1 fraction. This DNA fraction was selected from a plant with a polymorphic heterochromatic segment and cloned. The success of the C_ot-1 fractionation was confirmed by in situ hybridisation. After FISH with labelled C_ot-1 DNA, an intensely fluorescent signal was detected specifically at the telomeric polymorphic segment of chromosome 1, while the remaining chromosome regions were weakly labelled with no obvious localisation of the signal (Fig. 1a, a'). The sequence responsible for the segment-specific FISH signals was identified after cloning of the C_ot-1 fraction and sequential hybridisation of individual clones with labelled total C_ot-1 DNA of plants with and without polymorphic segments. One clone (called Bds1), of the 60 clones hybridised, showed strongly preferential hybridisation with labelled C_ot-1 DNA of a plant with polymorphic segments.

After in situ hybridisation with clone Bds1, the site of hybridisation was coincident with the position of the ma-

```
                          20                  40                  60                  80
                  Primer 1    .                   .          Primer 2 .                  .
Bds1      AATAAAGCTTTATGGAGGCTCGTGCGTTGTCATTTTTTGCTTCCTTTGACCCAACCATGGGAATCGAAATGTAAAAAG
Bds1-3    .........C.C...................G.....................................A......AGGGCATAATGTTT
Bds1-6    .........C.C...................G.....................................A......AGGGCATAATGTTG
Bds1-7    .........C.C...................G.....................................A......AGGGCATAATGTTT
Bds1-11   .........C......A.......TA.....G.............A.....................A......AGGGCATAATGTTG
Bds1-12   .........C.C...................G.....................................A......AGGCCATAATGTTT
Consens   AATAAAGCTCTCTGGAGGCTCGTGCGTTGTCGTTTTTTGCTTCCTTTGACCCAACCATGGGAATCGAAATGAAAAAAGAGGGCATAATGTTT
```

Fig. 2. Sequence relationships within the Bds1-like family and the consensus sequence of Bds1. Comparison of Bds1 (cytodeme A2) with polymerase chain reaction (PCR)-derived sequences Bds1-3, -6, -7, -11, -12. The two primer regions are *underlined*. A *dot* indicates identity with Bds1. The potential stem/loop structure-forming sequence is printed in *italics*

jor polymorphic heterochromatic segment in the distal position of the long arm of chromosome 1 (position 1). Two additional polymorphic Bds1 sites were also revealed after FISH analysis of a number of *B. dichromosomatica* (cytodeme A2) plants (Fig. 1b–f). Interstitial minor hybridisation sites were found on the same chromosome arm (position 2) and on the long arm of chromosome 2 (position 3) (Fig. 1d). After 4',6-diamidino-2-phenylindole (DAPI) counterstaining, all polymorphic chromosome regions revealed the typical staining behaviour of heterochromatin (Fig. 1f').

There were no Bds1 hybridisation sites detectable on the larger B chromosomes of cytodemes A1 and A2 (Fig. 1a', c). However, on the micro B chromosomes, weak Bds1 signals were detected on one telomeric end in all instances (Fig. 1e, e').

After Southern hybridisation of genomic DNA of 48 randomly selected plants of cytodeme A2, 48% of the plants analysed showed a strong Bds1-specific hybridisation signal (data not shown). The distribution of the different chromosome positions of Bds1 was analysed for a number of plants by FISH using labelled Bds1 sequences. Plants hemizygous for one (Fig. 1b), two (Fig. 1e) or all three different Bds1 positions (Fig. 1d, f) were observed as well as plants that were homozygous for a chromocentre at position 1 (Fig. 1c) and position 2. Also plants homozygous for position 2 and hemizygous for position 3 were detected. Although all three sites showed extensive polymorphism between plants, the karyotypes of all analysed mitotic root cells were stable within a single plant.

The insert of clone Bds1 is 78 bp long and contains no significant subrepeats (Fig. 2). The imperfect palindromic structure of a 37 bp motif (5'-TTTTGCTTCCTTGACCCAACATGGGAATCGAAA-3') between nucleotides 33 and 69 is the most striking feature of this sequence. This sequence could form dyad intrastrand DNA structures. The sequence (EMBL accession number AJ130940) was compared with the Genbank database and no significant sequence homology was detected. We have found no evidence for the presence of Bds1-like transcripts using blot hybridisation analysis of total RNA prepared from leaf tissue (data not shown).

To determine whether the sequence is organized in a tandem array or whether it is part of a repeat unit with nonhomologous flanking regions, partially AluI-digested genomic DNA from a plant with the polymorphic segment 1 was Southern hybridised with Bds1. The result

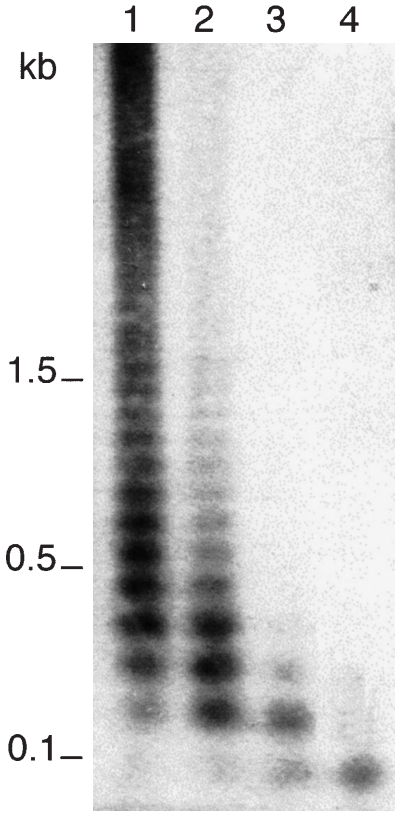

Fig. 3. Partial and complete restriction digest of genomic DNA of a plant with the polymorphic segment 1. The DNA samples were partially (*lanes 1–3*) and completely (*lane 4*) digested with AluI, Southern blotted and probed with Bds1

showed a polymeric ladder characteristic of sequences arranged in tandem arrays (Fig. 3). After complete digestion, AluI yielded a single band of about 92 bp, indicating that the AluI site is conserved in all repeat units.

In order to characterise the missing nucleotides of the entire Bds1 repeat unit and also to compare the repeat organisation of Bds1 at the different chromosome sites, Bds1-specific PCR primers were designed. The PCRs were performed separately with genomic DNA of plants with polymorphic segments at chromosome position 2 or 3, and all three different positions (Fig. 4, lanes 1–3). Equivalent PCRs were also performed with DNA of plants without detectable Bds1-specific in situ hybridisation and slot-blot hybridisation signals (Fig. 4, lanes 4, 5). After gel separation of the PCR-generated

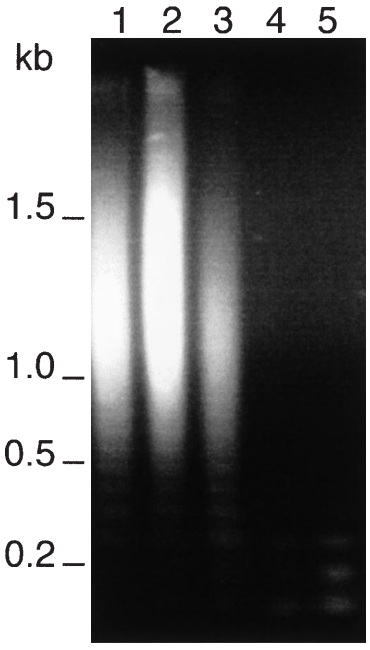

Fig. 4. Separated DNA products of a PCR using Bds1-specific primers and templates of genomic DNA of plants with polymorphic segments 1, 2 and 3 (*lane 1*), segment 2 (*lane 2*), segment 3 (*lane 3*) and without segments detectable by FISH with Bds1 (*lanes 4, 5*)

DNA fragments a typical tandem repeat ladder was seen with bands between 65 bp and several kilobases of DNA (Fig. 4). The resulting DNA fragment patterns of the Bds1 sequences were identical between plants having the repeat at different chromosome positions. A similar tandem organisation of Bds1 sequences was assumed to be present at each of the different chromosome sites. The PCR showed also that, in plants without detectable Bds1 FISH signals, Bds1 is present in low copy number. The PCR with genomic DNA of plants without detectable Bds1 FISH signals resulted in a DNA fragment ladder of between 66 bp and approximately 500 bp (Fig. 4, lanes 4, 5). Hence, Bds1 is organised as a tandem repeat in all *B. dichromosomatica* plants analysed but it is present in very low copy numbers in some individuals.

The PCR product derived from a plant carrying the polymorphic segment 1 was cloned and the inserts of five clones (Bds1-3, -6, -7, -11, -12), with insert sizes between 450 and 800 bp, were sequenced. Multiple tandemly organised Bds1-like units were identified after comparison with the sequence of Bds1. The missing 14 nucleotides of the entire Bds1 repeat unit were identified at the 3' end of the Bds1-like sequences (Fig. 2). Comparison of the aligned sequences of the five PCR-generated clones and Bds1 revealed a low level of heterogeneity between the different Bds1-like sequences (Fig. 2). A small number of single base pair substitutions compared with Bds1 was found for the Bds1-like PCR-generated sequences, suggesting that Bds1-like sequences are a recently amplified portion of the genome.

Characterisation of the structure of the polymorphic heterochromatic segment 1

The polymorphic segment 1 of chromosome 1 is the most obvious heterochromatic region (Fig. 5a). This region remains highly condensed at all stages of the cell cycle and can be identified during interphase as a chromocentre (Fig. 1g, g'). The heteropycnotic character was even more obvious after analysis by scanning electron microscopy (Fig. 5b). In contrast to the rest of the nucleus, it appears that the chromatin of this region is highly condensed and compact at prometaphase and metaphase.

After staining of the chromosomes with the DNA-specific dye platinum blue (Wanner and Formanek 1995), the DNA distribution within the chromosomes was analysed by BSE electron microscopy (Fig. 5c, d). The BSE image of segment 1 appears much brighter than other prometaphase chromosome regions (Fig. 5e), indicating a higher DNA concentration within this region. Differences in DNA concentration are likely to reflect the different degree of condensation of DNA in different types of chromatin.

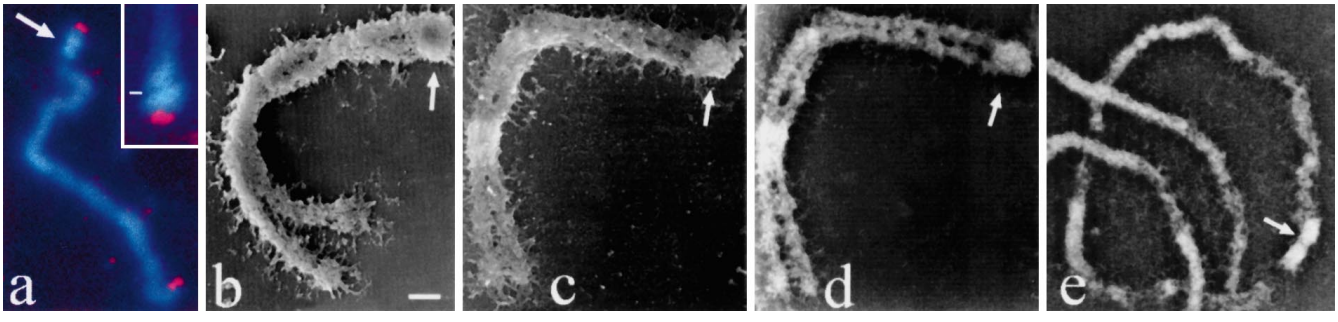

Fig. 5a–e. Structural analysis of the polymorphic heterochromatic segment 1 by FISH and electron microscopy. **a** Chromosome 1 of *Brachycome dichromosomatica* (cytodeme A2) after FISH with telomere-specific sequences (*red signals*). The *inset* shows an enlargement of segment 1. The internal constriction of segment 1 is indicated with a *bar*. **b** Scanning electron micrograph of chromosome 1. The chromatin of segment 1 appears highly condensed. **c** Secondary electron (SE) image (DNA + protein) and **d, e** backscattered electron (BSE) image (only DNA) of the polymorphic segment 1-bearing chromosome 1 stained with the DNA-specific dye platinum blue. The internal constriction of segment 1 is marked with an *arrow* in **e**. In all panels the position of the heterochromatic segment 1 is indicated with an *arrow*. *Bar* in **b** represents 1 µm

In all the polymorphic heterochromatic segments of region 1 analysed, no gaps between sister chromatids were distinguishable at metaphase (Fig. 5b, d). At prometaphase a constriction was visible in the middle of segment 1 after DAPI and platinum blue staining (Fig. 5a, e). Also, at early prophase, in a number of cells analysed, segment 1 showed a connection with the euchromatic telomeric regions of another chromosome (Fig. 1g, g'). Later, in metaphase, both chromosomes were still connected by a thin chromatin fibre (Fig. 1h). However, no chromosome bridges were observed at anaphase. It is likely that the constricted, polymorphic segment 1 is a duplicated band that arose from a chromosome fusion and breakage event between chromosomes, such that the daughter cells gained or lost some or all of segment 1. To test this possibility, in situ hybridisation with a telomere-specific probe was performed. If fusion and breakage had occurred the expection was to find interstitial telomeric signals at the constriction of segment 1. However, telomeric sequences were localised only at the very ends of all the chromosomes observed (Fig. 5a and inset).

After Feulgen microdensitometry of prophase nuclei without B chromosomes of *B. dichromosomatica*, a 4C nuclear DNA content of 4.47 pg (SE=0.12 pg) was estimated. In addition, the DNA amount of a standard B chromosome and a micro B chromosome at metaphase was estimated to be 0.49 pg (SE=0.06 pg) and 0.12 pg (SE=0.008 pg), respectively. This is in reasonable agreement with that of John et al. (1991) who estimated a 4C DNA value of 5.8 pg by chromosome length comparisons of plants without B chromosomes. Quantitative analysis gave estimates of 1.09×10^5 copies of Bds1-related sequences in the diploid genome hemizygous for the Bds1-positive heterochromatic segment 1.

Discussion

The DNA cloning and screening strategy employed in these experiments is simple and efficient and could be adapted for the isolation of polymorphic heterochromatic segment-specific sequences in other species. Due to the preselection of the highly repetitive DNA, the complexity of the hybridising DNA is reduced, and so the differential hybridisation screening approach is more effective.

The sequence Bds1 is the second polymorphic chromosome segment-specific DNA to be reported. The DNA composition of the polymorphic segment of *B. dichromosomatica*, which is composed of a high copy tandem repeat, is similar to the DNA composition of the polymorphic heterochromatic segments (knobs) of maize. Peacock et al. (1981) found that a 180 bp repeating unit arranged in tandem arrays is the major component of maize knob regions. More recently Ananiev et al. (1998) discovered that, in addition to the 180 bp repeat, other types of DNA sequences such as retrotransposons and non-180 bp tandem repeats are also involved in the formation of knob heterochromatin. This could also be true for the DNA composition of the heterochromatic segments of *B. dichromosomatica* since, after FISH with labelled genomic DNA of a plant with only very few copies of the Bds1 repeat, the entire chromosome complement was labelled, including the positions of the polymorphic segments (data not shown).

We propose that the Bds1 repeat unit contains DNA that has a propensity to form heterochromatin. There is a correlation between the size of the detectable heterochromatic regions and the size of in situ regions hybridised with Bds1. Segment 1 is the most obvious heterochromatic region (Fig. 1f'), and because of its high copy number it also shows a strong hybridisation signal after FISH with Bds1 (Fig. 1f). Consistently, the less obvious heterochromatic segments 2 and 3 are weakly labelled after FISH with Bds1 (Fig. 1f, f'). This observation supports the assumption of Kunze et al. (1996) that DNA sequences with heterochromatin-forming capacity must reach a certain threshold amount before they can be recognized as heterochromatin by differential chromosome staining techniques. The potential dyad intrastrand DNA structures of Bds1 could function as protein binding sites that may be involved in heterochromatin formation or other functions. The potential stem-loop structures identified in Bds1 are good candidates for protein binding sites (Sierzputowska-Gracz et al. 1995) and have been shown to be associated with heterochromatin formation in Hymenopteran insects (Bigot et al. 1990). The sister chromatid cohesion of the polymorphic segment 1 (see Fig. 5d) could be caused by its special chromatin topology as suggested for cohesive chromatids observed in other organisms (reviewed in Miyazaki and Orr-Weaver 1994). In a number of prometaphase cells analysed, an interconnection of segment 1 with the telomeric chromosome regions of other chromosomes was observed. The close chromosome association could be a reflection of late-resolved ectopic chromosome pairing (Yoon and Richardson 1978). In *B. dichromosomatica* association of the chromosomes between eu- and heterochromatic segments has been observed, in contrast to the observations in metaphase cells of cereals, where Gustafson et al. (1983) observed somatic chromosome bridges between terminal heterochromatic regions.

In contrast to the Bds1-carrying micro B chromosomes, the larger B chromosomes had no detectable hybridisation after FISH with labelled Bds1 sequences. This suggests that, if the larger B chromosomes originated from the micro B chromosomes as proposed by Houben et al. (1997b), the sequence Bds1 must be lost during subsequent chromosome evolution. Alternatively some micro B chromosomes may not have the sequence and some large B chromosomes might do so as we analysed only limited number of plants of a population.

The question remains concerning the nature of the mechanism that has resulted in the maintenance of chromosome segment polymorphism in natural populations. Different plants showed different combinations of the three polymorphic heterochromatic segments. The Bds1 segment polymorphism could be responsible for the chromosome length polymorphism observed in the different cytodemes (Houben et al. 1999). There appear to

be a number of possible evolutionary interpretations of this situation. One possibility is that the Bds1 tandem repeat sequence is a recent addition to the genome and homogenisation/stabilisation of the chromosome distribution may be expected later. However, as both cytodemes analysed carry Bds1 sequences, it is likely that Bds1 was already present before the differentiation of the cytodemes occurred. It can be also assumed that the cytodemes of *B. dichromosomatica* diverged some considerable time ago since the different cytodemes are characterized by a number of karyotype differences (Houben et al. 1999). The observed patterns of variation suggest that strong selection pressures acting on the chromosome complement in these wild populations are more likely to explain the polymorphisms. We have to consider each population as a balanced genotype/environment interaction with its genetic components in a state of rapid flux influenced by a fluctuating, sometimes extreme, environment. One explanation for the polymorphic status of Bds1 segments in *B. dichromosomatica* populations is that the homozygous state of the Bds1 segments is disadvantageous for plants within the population whereas heterozygotes can survive and are maintained in the population. Alternatively, the polymorphic segments could be of benefit when they occur in specific combinations and under specific environmental conditions. This latter interpretation is likely to apply to maize where heterochromatic knobs in certain chromosomes have been demonstrated to have an influence on the flowering time (Chughtai and Steffensen 1987). The heterochromatin variation may play an indirect role in genome variation through its meiotic effects on chiasma distribution and frequency (Hewitt and John 1968; Jones and Rees 1982; Navas-Castillo et al. 1987; Lopez-Leon et al. 1992). The structural heterozygosity could be maintained by meiotic drive (Jones 1991), pollen-tube competition (Carlson 1969) or assortative gametic fertilization (Hewitt 1979). In *Zea mays* the neocentric activity of K10 leads to an enhanced recovery of the knobbed chromosome in the offspring (Rhoades and Vilkomerson 1942). Finally, there is a distinct possibility that repetitive sequence Bds1 is 'selfish DNA' (Orgel and Crick 1980). In this scenario Bds1 is in constant competition with the 'host' DNA of *B. dichromosomatica*.

Acknowledgements. We acknowledge support from the Australian Research Council and the Deutsche Forschungsgemeinschaft. The technical assistance of S. Steiner is gratefully acknowledged.

References

Ainsworth CC, Parker JS, Horton D (1983) Chromosome variation and evolution in *Scilla autumna*. Kew Chromosome Conference II, pp 261–268

Ananiev EV, Phillips RL, Rines HW (1998) Complex structure of knob DNA on maize chromosome 9: retrotransposon invasion into heterochromatin. Genetics 149:2025–2037

Badaeva ED, Badaev NS, Gill BS, Lilatenko AA (1994) Intraspecific karyotype divergence in *Triticum araraticum* (Poaceae). Plant Syst Evol 192:117–145

Bennett MD, Leitch IJ (1995) Nuclear DNA amounts in angiosperms. Ann Bot 76:113–176

Bigot Y, Hamlin MH, Periquet G (1990) Heterochromatin condensation and evolution of unique satellite-DNA families in two parasitic wasp species: *Diadromus pulchellus* and *Eupelmus vuilletei* (Hymenoptera). Mol Biol Evol 7:351–364

Buitendijk JH, Peters A, Quene RJ, Ramanna MS (1998) Genome size variation and C-band polymorphism in *Alstroemeria aurea*, *A. ligtu*, and *A. magnifica* (Alstroemeriaceae). Plant Syst Evol 212:87–106

Camacho JPM, Viseras E, Navas J, Cabrero J (1984) C-heterochromatin content of supernumerary chromosome segments of grasshoppers: detection of euchromatic extra segment. Heredity 53:157–175

Carlson WR (1969) Factors affecting preferential fertilisation in maize. Genetics 62:543–554

Carter CR, Smith-White S (1972) The cytology of *Brachycome lineariloba* 3. Accessory chromosomes. Chromosoma 39:361–379

Chughtai SR, Steffensen DM (1987) Heterochromatin knob composition of commercial inbred lines of maize. Maydica 32:171–187

Greilhuber J, Speta F (1976) C-banded karyotypes in the *Scilla hohenackeri* group, *S. persica*, and *Poschkinia* (Liliaceae). Plant Syst Evol 126:149–188

Gustafson JP, Lukaszewski AJ, Bennett MD (1983) Somatic deletion and redistribution of telomeric heterochromatin in the genus *Secale* and in *Triticale*. Chromosoma 88:293–298

Hewitt GM (1979) Grasshoppers and crickets. Animal cytogenetics, vol 3. Insecta 1. Othoptera. Borntraeger, Berlin

Hewitt GM, John B (1968) Parallel polymorphism for super numerary segments in *Chorthippus parallelus* (Zetterstedt). I. British populations. Chromosoma 25:319–342

Houben A, Belyaev ND, Leach CR, Timmis JN (1997a) Differences of histone H4 acetylation and replication timing between A and B chromosomes of *Brachycome dichromosomatica*. Chromosome Res 5:233–237

Houben A, Leach CR, Verlin D, Rofe R, Timmis JN (1997b) A repetitive DNA sequence common to the different B chromosomes of the genus *Brachycome*. Chromosoma 106:513–519

Houben A, Thompson N, Ahne R, Leach CR, Verlin D, Timmis JN (1999) A monophyletic origin of the B chromosomes of *Brachycome dichromosomatica*. Plant Syst Evol 219:127–135

Ijdo JW, Wells RA, Baldini A, Reeders ST (1991) Improved telomere detection using a telomere repeat probe $(TTAGGG)_n$ generated by PCR. Nucleic Acids Research 19:4780

Jamilena M, Ruiz Rejon C, Ruiz Rejon M (1990) Variation in the heterochromatin and nucleolar organizing regions of *Allium subvillosum* L. (Lileaceae). Genome 33:779–784

John UP, Leach CR, Timmis JN (1991) A sequence specific to B chromosomes of *Brachycome dichromosomatica*. Genome 34:739–744

Jones RN (1991) B-chromosome drive. Am Nat 135:430–442

Jones RN, Rees H (1982) B-chromosomes. Academic Press, London

Kunze B, Weichenhan D, Virks P, Traut W, Winking H (1996) Copy numbers of a clustered long-range repeat determine C-band staining. Cytogenet Cell Genet 73:86–91

Lopez-Leon MD, Cabrero J, Camacho JPM (1992) Male and female segregation distortion for heterochromatic supernumerary segments on the S_8 chromosome of the grasshopper *Chorthippus jacobsi*. Chromosoma 101:511–516

Martin-Alganza A, Cabrero J, Lopez-Leon MD, Perefectti F, Camacho JPM (1997) Supernumerary heterochromatin does not affect several morphological and physiological traits in the grasshopper *Eyprepocnemis plorans*. Hereditas 126:187–189

Miyazaki WY, Orr-Weaver TL (1994) Sister-chromatid cohesion in mitosis and meiosis. Annu Rev Genet 28:167–187

Navas-Castillo J, Cabrero J, Camacho JPM (1987) Chiasma redistribution in presence of supernumerary chromosome segments in grasshoppers: dependence on the size of the extra segment. Heredity 58:409–412

Orgel LE, Crick FHC (1980) Selfish DNA: the ultimate parasite. Nature 284:604–607

Peacock WJ, Dennis ES, Rhoades MM, Pryor AJ (1981) Highly repeated DNA sequence limited to knob heterochromatin in maize. Proc Natl Acad Sci U S A 78:4490–4491

Rae PMM (1970) Chromosome distribution of rapidly reannealing DNA in *Drosophila melanogaster*. Proc Natl Acad Sci USA 67:1018–1025

Rhoades MM, Dempsey E (1966) The effect of abnormal chromosome 10 on preferential segregation and crossing over in maize. Genetics 53:989–1020

Rhoades MM, Vilkomerson H (1942) On the anaphase movement of chromosomes. Proc Natl Acad Sci U S A 28:433–436

Rudall PJ, Engleman EM, Hanson L, Chase MW (1998) Embryology, cytology and systematics of *Hemiphylacus*, *Asparagus* and *Anemarrhena* (Asparagales). Plant Syst Evol 211:181–199

Ruiz Rejon C, Ruiz Rejon M (1985) Chromosomal polymorphism for a heterochromatic supernumerary segment in a natural population of *Tulipa australis* Link. (Liliaceae). Can J Genet Cytol 27:633–639

Sierzputowska-Gracz H, McKenzie RA, Theil EC (1995) The importance of a single G in the hairpin loop of the iron responsive element (IRE) in ferritin mRNA for structure: an NMR spectroscopy study. Nucleic Acids Res 23:146–153

Vinikka Y, Kavander T (1986) C-band polymorphism in the inbred lines showing neocentric activity in rye. Hereditas 104: 203–207

Vosa CG (1973) Heterochromatin recognition and analysis of chromosome variation in *Scilla sibirica*. Chromosoma 43:269–278

Wanner G, Formanek H (1995) Imaging of DNA in human and plant chromosomes by high-resolution scanning electron microscopy. Chromosome Res 3:368–374

Watanabe K, Carter CR, Smith-White S (1975) The cytology of *Brachycome lineariloba* 5. Chromosome relationships and phylogeny of the race A cytodemes (n=2). Chromosoma 52:383–397

Watanabe K, Denda T, Suzuki Y, Kosuge K, Ito M, Short PS, Yahara T (1994) Chromosomal and molecular evolution in the genus *Brachyscome* (Astereae). In: Hind DJN, Beebtje HJ (eds) Compositae: systematics. Proceedings of the International Compositae Conference, Kew, vol 1, pp 705–722

Wilby AS, Parker JS (1988) The supernumerary segment systems of *Rumex acetosa*. Heredity 60:109–117

Wienand U, Feix C (1980) Zein-specific restriction enzyme fragments of maize DNA. FEBS Lett 116:14–16

Yoon JK, Richardson RH (1978) Mechanisms of chromosomal rearrangements: the role of heterochromatin and ectopic pairing. Genetics 88:305–316

Zwick MS, Hanson RE, McKnight TD, Islam-Faridi MN, Stelly DM, Wing RA, Price HJ (1997) A rapid procedure for the isolation of C_ot-1 DNA from plants. Genome 40:138–142

A11 Houben, A., Thompson, N., Ahne, R., Leach, C.R., Verlin, D., and Timmis, J.N. (1999). A monophyletic origin of the B chromosomes of *Brachycome dichromosomatica* (Asteraceae). Plant Syst Evol 219, 127-135.

Plant Syst. Evol. 219: 127–135 (1999)

Plant Systematics and Evolution

A monophyletic origin of the B chromosomes of *Brachycome dichromosomatica* (Asteraceae)

Andreas Houben[1], **Nicole Thompson**[2], **Richard Ahne**[3], **Carolyn R. Leach**[1], **Dawn Verlin**[1], and **Jeremy N. Timmis**[1]

[1]Department of Genetics, The University of Adelaide, South Australia, Australia
[2]Department of Crop Protection, The University of Adelaide, Waite Campus, Glen Osmond, South Australia, Australia
[3]Bundesanstalt für Züchtungsforschung an Kulturpflanzen, Quedlinburg, Germany

Received July 7, 1998
Accepted October 5, 1998

Abstract. The A and B chromosomes of different karyotype variants (cytodemes A1, A2, A3 and A4) of *Brachycome dichromosomatica* were analysed by computer-aided chromosome image analysis and fluorescence *in situ* hybridisation (FISH). Ribosomal DNA and the B chromosome-specific sequence Bd49 were detected on all B chromosomes. In addition to minor size variation of the Bs, polymorphism of the rDNA and Bd49 position and copy number revealed two major types of B chromosomes. The B chromosomes of all the cytodemes were indistinguishable from each other in length, but that of A3 showed evidence of rearrangements consistent with its long-term geographic isolation. The results presented suggest a monophyletic origin of the B chromosomes of *B. dichromosomatica*.

Key words: Asteraceae, *Brachycome*. B chromosome, polymorphism, evolution, karyotyping, centromere.

B chromosomes (Bs) occur in many organisms as numerically variable chromosomes, extra to the standard complement (A chromosomes). As B chromosomes are mainly transcriptionally inactive, a greater tolerance is expected to deletions and rearrangements of the genetic material within the Bs compared with the A chromosomes. B chromosome structural polymorphism has been reported in a number of different species (see review Jones and Rees 1982). For example thirteen morphologically different types of Bs are known in *Allium schoenoprasum* (Holmes and Bougourd 1991) and 40 different B chromosome variants were described for the B chromosomes of the grasshopper *Eyprepocnemis plorans* (Lopez-Leon et al. 1993, Cabrero et al. 1997). However, there are also species with little structural variation in their B chromosomes (listed in Jones 1995).

The ephemeral daisy, *Brachycome dichromosomatica*, native to the arid regions of Australia, has two pairs of A chromosomes. Within the species there are four different cytodemes (A1, A2, A3 and A4) based on their karyotypes and geographical distribution (Watanabe et al. 1975, Carter 1978). In addition to the A chromosome complement, two different types of B chromosomes have been reported; the large B chromosome

(or "standard" B) and the micro B chromosome. The standard B chromosomes are mitotically stable whereas the micro B chromosomes behave irregularly at mitosis (Carter and Smith-White 1972).

Hitherto the majority of molecular and cytological studies were carried out with the larger B chromosome of cytodeme A1. A high copy number tandem repeat sequence (Bd49), specific to the B chromosome, was described (John et al. 1991, Leach et al. 1995, Franks et al. 1996) and its was also shown that the standard B chromosomes contain rDNA sequences which are transcriptionally inactive (Donald et al. 1995, 1997). However, nothing is known about the molecular organisation of the standard B chromosomes of A2, A3 and A4 cytodemes. In this study the A and B chromosomes of all four cytodemes of *B. dichromosomatica* were analysed by computer-aided image analyses, *in situ* and Southern hybridisation and DNA sequence comparison, in order to determine whether the standard B chromosomes are identical or divergent at the chromosomal and molecular levels.

Materials and methods

Plant material and cytogenetic preparation. *Brachycome dichromosomatica* ($2n = 4$) is a member of the *B. lineariloba* complex (Watanabe et al. 1996). Plants and seeds of *B. dichromosomatica* were collected from wild populations in Australia. The different cytodemes (A1, A2, A3, and A4) of *B. dichromosomatica* were characterised on the basis of their chromosome morphology as described by Watanabe et al. (1975). Mitotic preparations for *in situ* hybridisation were obtained from root tips according to Houben et al. (1997a).

Computer aided image analyses. Feulgen stained metaphase cells were photographed and their images were digitised. For karyotype analysis, chromosome pictures were analysed on a computer using the UNICHRO program (Ahne et al. 1989). The average chromosome lengths were calculated from at least 12 metaphase chromosomes of each cytodeme.

Southern hybridisation. Genomic DNA was isolated from leaf material by the procedure described by Wienand and Feix (1980) and digested with different restriction enzymes according to the manufacturer's recommendations. DNA fragments were resolved on 0.8% agarose gels and transferred to Hybond N+nylon membranes (Amersham) for hybridisation. The DNA probes were labelled with (α-^{32}P)dCTP by random primed DNA synthesis. Hybridisation was carried out overnight at 65 °C in 5 × SSPE, 0.2% SDS, 5 × Denhardts reagent, 100 µg/ml salmon sperm DNA. Blots were washed successively in 0.5 × SSC and 0.1% SDS and then exposed to X-ray film with enhancing screens at −70 °C for appropriate periods.

Amplification, cloning and sequence analysis of Bd49-like sequences from *B. dichromosomatica* cytodemes. Primers used for PCR amplification of the Bd49-like sequences and cloning procedure of PCR fragments were the same as described by Leach et al. (1995). Sequencing was by the Sequenase (Version 2.0) system (United States Biochemical).

Fluorescence *in situ* hybridisation (FISH). A plasmid (VER17, Yakura and Tanifuji 1983) containing part of the 18S, and 5.8S, most of the 25S rRNA sequences and the internal transcribed spacers of the *Vicia faba* 45S rRNA gene, was used as an rDNA-specific probe. A 5S rDNA-specific probe was amplified from genomic DNA of *V. faba* using primers designed according to the 5S rDNA sequence of *Glycine* species (Gottlob-McHugh et al. 1990). The insert of the clone Bd49 (John et al. 1991) was used as B chromosome-specific probe. An *Arabidopsis*-type telomere probe was synthesised using PCR according to Ijdo et al. (1991). Probes (5S, rDNA, Bd49 and telomere) were labelled with biotin-16-dUTP by nick translation. Hybridisation of the biotinylated probes was detected by the use of a streptavidin-FITC-anti-streptavidin-FITC system. Epifluorescence signals were recorded on Fuji 400 film or by confocal microscopy.

Results

To characterise the morphology of the A and B chromosomes of the different cytodemes, mitotic chromosomes were karyotyped with

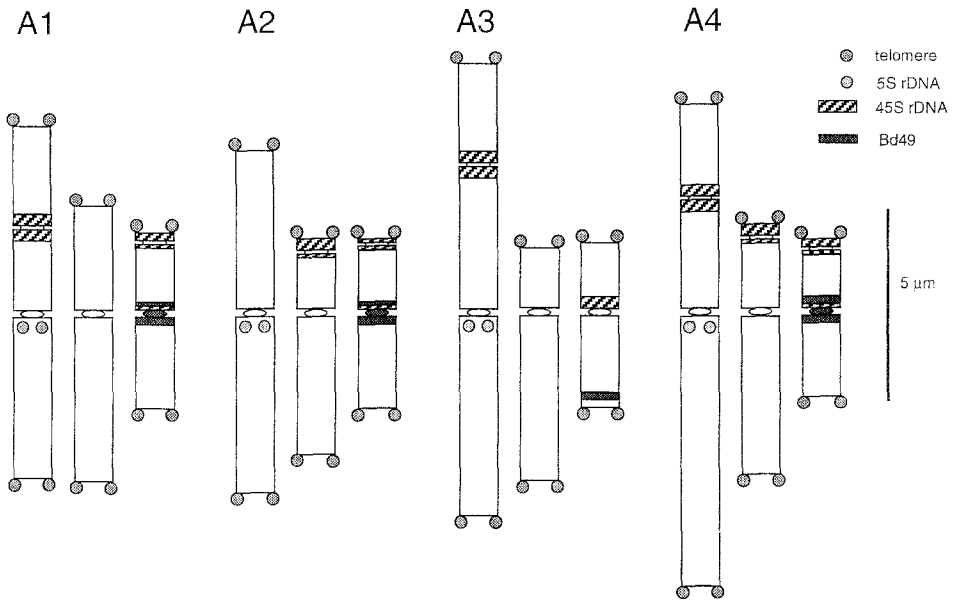

	A1			A2			A3			A4		
	1	2	B	1	2	B	1	2	B	1	2	B
p	2.05	2.71	2.00	4.12	1.84	1.82	3.68	1.54	1.79	2.97	1.74	1.78
s.d.	0.50	0.60	0.33	0.80	0.26	0.28	0.63	0.20	0.22	0.43	0.27	0.25
s	2.59						2.71			2.46		
s.d.	0.86						0.82			0.35		
q	4.16	4.32	2.39	4.65	3.59	2.44	5.20	4.34	2.36	7.14	4.13	2.20
s.d.	1.01	1.09	0.42	0.97	0.73	0.47	0.60	0.45	0.26	0.61	0.49	0.31
n	17	16	14	25	22	12	17	17	12	21	22	16

Fig. 1. Karyotypes of the haploid chromosome set (A and B chromosomes) at mitotic metaphase and the chromosomal location of the centromeres, telomeres, 45S and 5S rDNA and B chromosome-specific sequence Bd49 loci of *Brachycome dichromosomatica* (cytodemes A1, A2, A3 and A4). (*p*) indicates the mean length of the short arm. (*s*) shows the mean length of the "satellite" distal to the NOR (only shown for the satellites of chromosome 1), (*q*) indicates the mean length of the long chromosome arm. (*s.d.*) are the standard deviations. (*n*) is the number of chromosomes measured. The bar represents 5 µm

a computer-aided image analysis program. No significant differences in mean length were observed between the different B chromosomes. In contrast, differences in mean length of the A chromosome types were found within the different cytodemes (mean length comparison of chromosome 1: A4 > A3 > A2 = A1, comparison of chromosome 2: A1 > A2 = A3 = A4) (Fig. 1) which may reflect parallel variation in genome size between the four cytodemes. This suggests that reciprocal translocations considered by Watanabe et al. (1975) contribute to, but are not sufficient to account for, the different chromosome morphologies. The chromosome rearrangements suggested by Watanabe et al. (1975) may be expected to result in interstitial telomeric sequences. To test this possibility, *in situ* hybridisation with a telomere-specific probe was applied to mitotic metaphase chromosomes. Signals were localised on the ends of all the A and B chromosomes but no interstitial telomere signals were observed in any of the cytodemes (Figs. 1, 2).

In addition to the previously-reported intercalary position of rDNA on the larger A chromosome and the end of the shorter arm of the B chromosome of cytodeme A1 (Donald

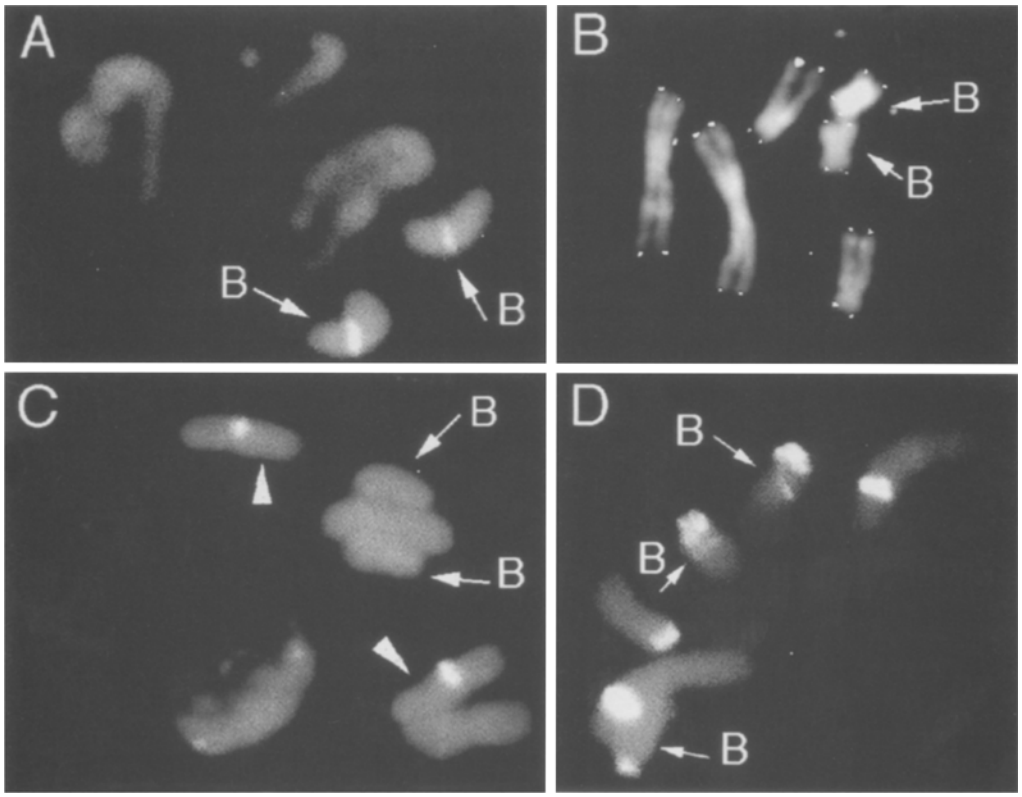

Fig. 2. Fluorescence *in situ* hybridisation of metaphase chromosomes of *Brachycome dichromosomatica* with probes specific for Bd49, telomere sequences and 5S and 45S rDNA. (**A**) cytodeme A2 (2n = 4+2B) showing hybridisation of the B chromosome-specific probe Bd49 specifically to the centromeric region of each of the two B chromosomes. (**B**) cytodeme A4 (2n = 4 + 2B) showing hybridisation signals of the telomere probe on all chromosome ends. (**C**) cytodeme A1 (2n = 4 + 2B) showing hybridisation signals of the 5S rDNA probe on A chromosome 1. The NOR-region of A chromosome 1 is marked with a arrowhead. (**D**) cytodeme A4 (2n = 4 + 3B) showing hybridisation signals specific for 45S rDNA. Note two hybridisation sites on the B chromosomes. All B chromosomes are arrowed

et al. 1995), a minor locus adjacent to the centromere on the short arm of the B chromosome was also detected. Similar rDNA positions were found on B chromosomes of the cytodemes A2 and A4 (Figs. 2, 3), but the B chromosome of cytodeme A3 showed an intense signal near the centromere of the short arm with no evidence of a subterminal rDNA cluster (Fig. 3). The rDNA signals on the A chromosomes were co-located with the NOR-regions on chromosome 2 of cytodeme A2, on chromosome 1 of A3 and on both A chromosomes of cytodeme A4 (Figs. 2, 3). Chromosome 1 of cytodeme A2 showed an ill-defined secondary constriction, visible at prophase at the same position as the rDNA cluster on chromosome 1 of cytodeme A1. This constriction is not visible at metaphase and suppression rather than loss of rDNA sequences was suggested by Watanabe et al. (1975) to account this observation. However, after FISH with rDNA sequences, no signal was detectable at this position. Therefore the constriction on chromosome 1 of cytodeme A2

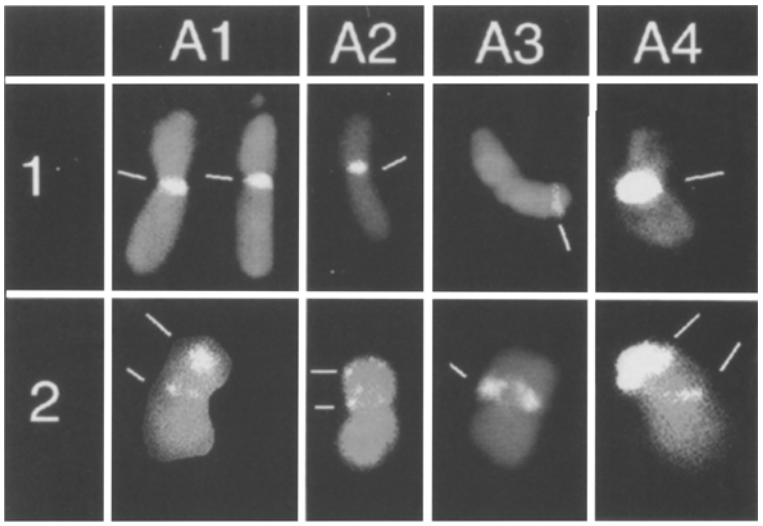

Fig. 3. Fluorescence *in situ* hybridisation of B chromosomes of *Brachycome dichromosomatica* (cytodemes A1, A2, A3 and A4) with the B chromosome-specific probe Bd49 and 45S rDNA analysed conventional epifluorescence microscopy. (1) selected B chromosomes after FISH with Bd49. The B chromosome pictures of cytodeme A1 shows (left) horizontal and (right) longitudinal optical sectioning by methods of the confocal microscopy. Note the entire centromere region is labelled with Bd49-specific signals. (2) selected B chromosomes after FISH with 45S rDNA. The positions of the hybridisation signals are arrowed. After FISH with Bd49 only the B chromosome of cytodeme A1 was analysed by confocal microscopy, all other pictures were examined by conventional epifluorescence microscopy

must be caused by sequences other than rDNA or by a very low copy number of ribosomal sequences that cannot be detected by FISH.

The 5S rDNA-specific probe revealed a cluster of genes on A chromosome 1, on the long arm near the centromere in all four cytodemes (Figs. 1, 2). The position of the 5S rDNA in cytodeme A1 contrasted with that reported in the karyotype analysis of Adachi et al. (1997) where the signal was localised on A chromosome 2. As the 5S rDNA location is consistent in all our experiments, the 5S rDNA location identified by Adachi et al. (1997) may reflect a rare karyotype polymorphism.

The previously-reported centromeric location of the B chromosome-specific tandem repeat, Bd49, (Leach et al. 1995) was confirmed and more closely resolved by confocal microscopy. The repeat was found on both B chromosome arms, overlapping the centromere in cytodeme A1 (Figs. 2, 3). The same intense hybridisation site of Bd49 was found on the Bs of cytodemes A2 and A4, but a faint fluorescence signal only was located on the end of the long arm of the B chromosome in cytodeme A3 with no evidence of proximal hybridisation (Fig. 3).

Consistent with an evolutionary change in the location and amount of Bd49, Southern hybridisation to genomic DNA of plants with and without B chromosomes also revealed significant differences between the cytodemes (Fig. 4). A hybridisation pattern characteristic of a tandem repeat sequence was detected in *Hinf*I partial genomic digestions of cytodeme A1, A2, A3 and A4 DNA. With DNA of cytodeme A1, A2 and A4 also the same ladder pattern of hybridisation was observed after complete digestion with *Msp*I (Fig. 4). Cytodeme A3 showed a weaker hybridisation signal (Fig. 4) and no clear banding pattern, probably because of extensive polymorphism of C-methylation at *Msp*I restriction sites and a lower copy number of the Bd49 repeat

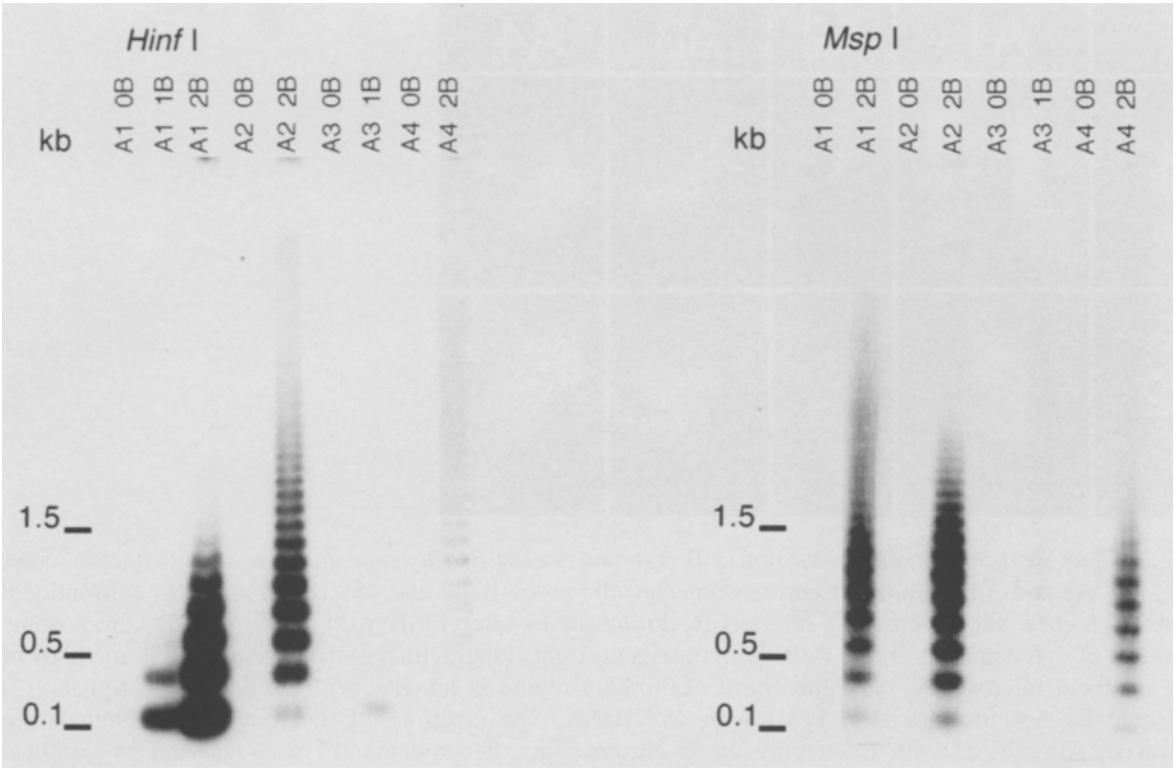

Fig. 4. Restriction analysis of Bd49-homologous sequences. Samples of genomic 0B and +B DNA of *B. dichromosomatica* (cytodemes A1, A2, A3 and A4) were digested with restriction enzymes *Msp*I and *Hinf*I, transferred to a nylon membrane and probed with the labelled insert of clone pBd49 (John et al. 1991)

homologs. The reduced level of hybridisation in A3 is unlikely to be due to sequence divergence because the *Hinf*I site appears relatively conserved (Fig. 4, lane 7).

Comparison of Bd49-like sequences from the different cytodemes could provide clues about the similarity of the different B chromosomes. Sequences were cloned after PCR amplification using a Bd49-specific primer pair. Comparison of two aligned sequences from each cytodeme revealed a level of heterogeneity within and between the different cytodemes (Fig. 5) that was extensive, but no greater than the variation already demonstrated within a single B chromosome from cytodeme A1 (Leach et al. 1995). A minor number of single base pair insertions, deletions and substitutions compared with Bd49 were found for the Bd49-like sequences of cytodeme A2 and A4. In one clone from cytodeme A3 a 10 bp long sequence insertion, predominantly of C residues, was detected in addition to a few sequence modifications.

Discussion

Seeds of the plants in these experiments were collected in the areas reported by Watanabe et al. (1975) and germinated and screened to find karyotypes which matched those of the four cytodemes described by these workers. However during these and other cytogenetic analyses over the last 8 years, many karyotype variants have been observed which do not clearly fit the model of four cytodemes. Whilst some of these plants may be explained as hybrids, polyploids or aneuploids of the A1, A2, A3 and A4 cytodemes, there is certainly no

```
bp       1                              30                                  60
Bd49     ATCAGGAGGTCCGGGATTCGTAAAAAACAAAAAGTCATAGGTATTCCTCACCGTXXXXXXXXXXTTAAxAAATTAA
Bd49A21 ----------T----------------TG----------------------XXXXXXXXXX-----X----*-
Bd49A22 --------------------A-------------------------------XXXXXXXXXX-----X---A--
Bd49A31 ----------------------------------------------T-GATCGACCCCCCCCCCG----X---X-X
Bd49A32 ------------------------------------------------------XXXXXXXXXX-----A------
Bd49A41 ----------------------------------------------T---XXXXXXXXXX----------X-
Bd49A42 -------CC-------------------------------------GT---XXXXXXXXXX-----X---A--

bp                  90                    114
Bd49     CCCTACTTATATTTTCAGTTCGGAATGTATTCXXAXA
Bd49A21 --------------------TAGCATGCAGTTACAT
Bd49A22 ---------------------------------XX---
Bd49A31 --X-----T--A-----*---TCGTCGGTATCATCTG
Bd49A32 ---------------------------------XX---
Bd49A41 --------*G-------A---A-CG------TTC-G-
Bd49A42 --------------*-----------------XX---
```

Fig. 5. Sequence relationships within the Bd49-like family. Comparison of Bd49 (cytodeme A1) with PCR-derived relative sequences from cytodemes A2 (Bd49A21, Bd49A22), A3 (Bd49A31, Bd49A32) and A4 (Bd49A41, Bd49A42) excluding the primer regions. (−) indicates identity with Bd49. (×) and (*) respectively indicate insertions and deletions compared with Bd49

reason to suggest that the chromosome system of *B. dichromosomatica* is fully described. We have already described extensive heterozygousity for a C-band (Houben et al. 1997b) and polymorphic arrangements of Bd49 on individual B chromosomes (Leach et al. 1995) and we suspect that both the A and B chromosomes are very much more variable at the sequence level than has currently been described.

It is uncertain when the four different *B. dichromosomatica* cytodemes diverged. However it is remarkable that the variation between the A chromosomes is more striking than the few structural changes observed in the different B chromosomes. As the Bs are considered to be genetically inert, they have a potential for greater structural polymorphism and it is surprising to find relatively high conservation of structure. One explanation for the observed uniformity is that the A chromosome genotypes have a low genetic tolerance which limits B chromosome variation to only minor changes. This suggests the existence of an A and/or B chromosome-derived control mechanism for the maintenance of a "standard" B chromosome.

Our observations show that the Bs of cytodemes A1, A2 and A4 group into a single class and the B of cytodeme A3 is the only variant. In A3, the B-specific sequence Bd49 is localised outside the centromeric region and probably occurs in a low copy number compared with the other cytodemes. The observed difference is consistent with the geographical locations of the cytodemes: A1, A2 and A4 are found in close proximity to each other, whilst A3 is found in a region 1000 km distant. Cytodeme A4 has been suggested to be the most primitive form. It occurs in the centre of the distribution of the whole species and the other cytodemes have been suggested to be derived from A4 by chromosome rearrangements (Watanabe et al. 1975).

As the B chromosomes in all the cytodemes contain Bd49 and rDNA sequences, it is likely that all types are derived from a common ancestral B chromosome. We have described a highly repetitive micro B chromosome sequence (Bdm 29), which is also present at low copy number on all the standard Bs (Houben et al. 1997a), further suggesting a

common origin for all these supernumerary chromosomes.

It is possible that the B chromosome progenitor initially had a structure similar to that of A1, A2 and A4. After the geographic isolation of cytodeme A3 and B chromosome underwent a rearrangement, such as a paracentric inversion of the long chromosome arm, to give the extant supernumerary B that we have characterised. This scenario is consistent with the relocation of the sequence Bd49 near to the end of the long arm of the B chromosome and a reduction in copy number or elimination on the short arm. However the change is more complex as it must also have included amplification of the proximal rDNA and a reduction in the number of the distal rDNA repeats. Ribosomal DNA has been described as a very dynamic sequence capable of changing in copy number (Cullis 1979, Martinez et al. 1993). An alternative explanation for the evolution of the variant Bs is that those of cytodeme A3 are more primitive and evolved into those found in the other cytodemes. A less likely explanation is that morphologically similar B chromosomes arose independently in different plant populations, driven by common selection pressures on chromosome organisation and behaviour.

We favour a monophyletic origin of the B chromosome at a time prior to the divergence of the cytodemes. A monophyletic origin has also been proposed for the rye B chromosomes of plants from different geographic areas and different taxa (Niwa and Sakamoto 1995).

It is remarkable that the sequence Bd49 is only specific for the B chromosome centromeres of cytodemes A1, A2, and A4. The heterogeneity of the tandem repeat Bd49 within each cytodeme makes this repeat unsuitable for phylogenetic analysis. A comparable high level of heterogeneity has already been described for Bd49-like sequences of cytodeme A1 and of other related *Brachycome* species (Leach et al. 1995). Sequence comparison based on PCR-based strategies for recovering Bd49-like sequences are likely to be unproductive because of selection by the primers of non-random sequences during amplification.

It is not known whether the tandem repeat Bd49 has an important function within the B chromosome centromere. Optical sectioning using methods of the confocal microscopy demonstrated that the B-centromere region of cytodeme A1 is flanked by Bd49 hybridisation signals after FISH with Bd49 (Fig. 2). In many organisms, tandem repeats are localised close to the centromere region, but a true centromere function is not yet demonstrated in any case. If Bd49 has a centromere function, it must have been taken over by another sequence(s) in cytodeme A3, after the rearrangement of the B chromosome. However, the *de novo* formation of a former non-centromeric region into an active centromeric region is already reported for several chromosomes (Choo 1997).

We thank C. R. Carter for providing seed material of cytodeme A3 and P. Kolesik for assistance on the confocal microscope. A. H. was supported by the Deutsche Forschungsgemeinschaft (Ho 1779/1-1) and by the Australian Research Council.

References

Adachi J., Watanabe K., Fukui K., Ohmido N., Kosuge K. (1997) Chromosomal location and reorganisation of the 45S and 5S rDNA in the *Brachycome lineariloba* complex (Asteraceae). J. Plant Res. 110: 371–377.

Ahne R., Huhn P., Laumer N., Zerneke F. (1989) Interaktive rechnergestützte Chromosomenanalyse. Ein Grundsoftwarepaket. Arch. Züchtungsforschung 19: 133–140.

Cabrero J., Lopez-Leon M. D., Gomez R., Castro A. J., Martin-Alganza A., Camacho J. P. M. (1997) Geographical distribution of B chromosomes in the grasshopper *Eyprypocnemis plorans*, along a river basin, is mainly shaped by non-selective historical events. Chromosome Res. 5: 194–198.

Carter C. R., Smith-White S. (1972) The cytology of *Brachycome lineariloba* 3. Accessory chromosomes. Chromosoma 39: 361–379.

Carter C. R. (1978) Taxonomy of the *Brachycome lineariloba* complex (*Asteraceae*). Telopea 1: 387–393.

Choo K. H. A. (1997) Chromatin Dynamics 97 Centromere DNA dynamics: Latent centromeres and neocentromere formation. Am. J. Hum. Genet 61: 1225–1233.

Cullis C. A. (1979) Quantitative variation of ribosomal RNA genes in flax genotrophs. Heredity 42; 237–246.

Donald T. M., Leach C. R., Timmis J. N. (1995) Ribosomal RNA genes and the B chromosome of *Brachycome dichromosomatica*. Heredity 74: 556–561.

Donald T. M., Houben A., Leach C. R., Timmis J. N. (1997) Ribosomal RNA genes specific to the B chromosome in *Brachycome dichromosomatica* are not transcribed in leaf tissue. Genome 40: 674–681.

Franks T. K., Houben A., Leach C. R., Timmis S. J. N. (1996) The molecular organisation of a B chromosome tandem repeat sequence from *Brachycome dichromosomatica*. Chromosoma 105: 223–230.

Gottlob-McHugh S. G., Levesque M., Mackenzie K., Olson M., Yarosh O., Johnson D. A. (1990) Organization of the 5S rDNA genes in the soybean (*Glycine max* (L.)) Merrill and conservation of the 5S rDNA repeat structure in higher plant. Genome 33: 486–494.

Holmes D. S., Bougourd S. M. (1991) b Chromosome selection in *Allium schoenoprasum*. II. Experimental populations. Heredity 67: 117–122.

Houben A., Leach C. R., Verlin D., Rofe R., Timmis J. N. (1997a) A repetitive DNA sequence common to the different B chromosomes of the genus *Brachycome*. Chromosoma 106: 513–519.

Houben A., Belyaev N. D., Leach C. R., Timmis J. N. (1997b) Differences of histone H4 acetylation and replication timing between A and B chromosomes of *Brachycome dichromosomatica*. Chromosome Res 5: 223–237.

Ijdo J. W., Wells R. A., Baldini A., Reeders S. T. (1991) Improved telomere detection using a telomere repeat probe $(TTAGGG)_n$ generated by PCR. Nucleic Acids Research 19: 4780.

John U. P., Leach C. R., Timmis J. N. (1991) A sequence specific to B chromosomes of *Brachycome dichromosomatica*. Genome 34: 739–744.

Jones R. N., Rees H. (1982) B chromosomes, 1st edn. Academic Press, London New York.

Jones R. N. (1995) Tansley Review No. 85, B chromosomes in plants. New Phytol. 131: 411–434.

Leach C. R., Donald T. M., Franks T. K., Spiniello S. S. Hanrahan C. F., Timmis J. N. (1995) Organisation and origin of a B chromosome centromeric sequence from *Brachycome dichromosomatica*. Chromosoma 103: 708–714.

Lopez-Leon M. D., Cabrero J., Pardo M. C., Viseras E., Camacho J. P. M., Santos J. L. (1993) Generating high variability of B chromosomes in the grasshopper *Eyprepocnemis plorans*. Heredity 71: 352–362.

Martinez P., Vinas A., Bouza C., Castro J., Sanchez L. (1993) Quantitative analysis of the variability of nucleolar organizer regions in *Salmo trutta*. Genome 36: 1119–1123.

Niwa K., Sakamoto S. (1995) Origin of B chromosomes in cultivated rye. Genome 38: 307–312.

Watanabe K., Carter C. R., Smith-White S. (1975) the Cytology of *Brachycome lineariloba* 5. Chromosome relationships and phylogeny of the race A cytodemes (n = 2). Chromosoma 52: 383–397.

Watanabe K., Denda T., Suzuki Y., Kosuge K., Ito M., Short P. S., Yahara T. (1994) Chromosomal and molecular evolution in the genus *Brachycome* (Astereae). In: Hind D. J. N., Beebtje H. J. (eds.) Compositae: Systematics. Proceedings of the international Compositae Conference. Kew, Vol. 1, pp. 705–722.

Wienand U., Feix G. (1980) Zein-specific restriction enzyme fragments of maize DNA. FEBS Lett. 116: 14–16.

Yakura K., Tanifuji S. (1983) Molecular cloning and restriction analysis of *Eco*R1-Fragments of *Vicia faba* rDNA. Plant Cell Physio. 24: 1327–1330.

Addresses of the authors: Andreas Houben, Carolyn R. Leach, Dawn Verlin, Jeremy N., Timmis, Department of Genetics, The University of Adelaide, South Australia 5005, Australia. Nicole Thompson, Department of Crop Protection, The University of Adelaide, Waite Campus, PMB1, Glen Osmond, South Australia 5064, Australia. Richard Ahne, Bundesanstalt für Züchtungsforschung an Kulturpflanzen, D-06484 Quedlinburg, Germany.

A12 Houben, A., Belyaev, N.D., Leach, C.R., and Timmis, J.N. (1997a). Differences of histone H4 acetylation and replication timing between A and B chromosomes of *Brachycome dichromosomatica*. Chromosome Res 5, 233-237.

Chromosome Research 1997, 5, 233–237

Differences of histone H4 acetylation and replication timing between A and B chromosomes of *Brachycome dichromosomatica*

Andreas Houben, Nikolai D. Belyaev, Carolyn R. Leach & Jeremy N. Timmis

Received 3 January 1997; received and accepted in revised form by M. Schmid 10 March 1997

Differences are demonstrated between A (transcriptionally active) and B (transcriptionally inactive) chromosomes that are characterized by a different level of histone H4 acetylation and a different timing of DNA replication. These differences between the chromatin of A and B chromosomes were found after immunolabelling of chromsomes of *Brachycome dichromosomatica* with antibodies specific for different acetylated forms (lysine 5, 8, 12 and 16) of histone H4. In contrast to the A chromosomes, which are labelled brightly in their entirety, the transcriptionally inactive B chromosomes are faintly labelled with antibodies against H4Ac5 and H4Ac8. No such difference between the chromosomes is found after immunostaining with the other antibodies H4Ac12 and H4Ac16. Analysis of DNA replication timing in root-tip meristems suggests that B chromosomes are labelled late in S-phase compared with A chromosomes. After C-banding the B chromosome appeared to have a similar amount of heterochromatin to the A chromosomes.

Key words: acetylated histone H4, B chromosome, heterochromatin, plants, replication

Introduction

It is well established that the regulation of gene expression in eukaryotes occurs at the level of chromatin and that transcription requires changes in chromatin structure (Felsenfeld 1992).

The packaging of DNA within chromatin is seen increasingly as having an essential role in the regulation of nuclear processes. It is evident that, besides their structural importance in nucleosome formation, histones are involved in processes of chromatin condensation and decondensation, and in the regulation of gene expression. These functional aspects are apparently connected with various post-translational modifications of the histone proteins (Matthews 1988, Roth & Allis 1996). Histone acetylation is generally believed to play a role in modulating the higher order folding of chromatin (Loidl 1988, 1994). Reversible acetylation of the histones is mediated by several different chromatin-associated acetyltransferase/deacetylase enzymes (Attisano & Lewin 1990, Lopes-Rodas *et al.* 1991). Differential underacetylation of H4 is of particular interest because of its potential role in the mechanism of gene silencing in yeast (Braunstein *et al.* 1993) and mammals (O'Neill & Turner 1995). During S-phase in mammalian systems, H4 lysines become acetylated in an order 16, 12, 8 and 5 (Turner 1993).

In the pericentric heterochromatin of mammals, H4 is underacetylated at all four lysine positions compared with active chromatin. The same is true for the inactive X chromosomes of female mammals. In contrast, the mammalian R-band regions, which are enriched in coding sequences, reveal a high level of H4 acetylation (Jeppesen & Turner 1993, Belyaev *et al.* 1996a&b). Recently, similar differences in acetylation pattern between euchromatin and heterochromatin on plant chromosomes were shown on the basis of indirect immunofluorescence (Houben *et al.* 1996, Idei *et al.* 1996).

B chromosomes, which are supernumerary to the basic (A) chromosome set, occur in many diverse groups of plants and animals. They are somewhat enigmatic; chiefly because their origin is unknown and also because they are maintained in many natural populations, even though they are not essential for normal development – indeed they are mildly deleterious in most cases.

Certain B chromosomes carry rDNA sequences (reviewed by Green 1990) and, to a lesser extent, other genes have been postulated to be located on B chromosomes through correlations with phenotypic traits. The presence of B chromosomes in certain plants has been associated with a number of phenotypic effects (reviewed by Jones 1995), such as in the control of meiotic pairing (Dover & Riley 1972) and increased germination rates in specific environmental conditions (Plowman & Bougourd 1994). Although several studies have compared DNA of A and B chromosomes, with the exception of a few repetitive B chromosome-specific sequences, no differences have been found between the two chromosome types (reviewed by Jones 1995, Hackstein *et al.* 1996).

Andreas Houben (corresponding author), Carolyn R. Leach and Jeremy N. Timmis are at the Department of Genetics, The University of Adelaide, SA 5005, Australia. Email: ahouben@genetics.adelaide.edu.au; Fax: +61 8 303 4399. Nikolai D. Belayev is at the Department of Anatomy, The University of Birmingham, Edgbaston, Birmingham B15 2TT, UK.

There is very little information available on the chromosomal protein composition of B chromosomes and whether it differs in any way to that of the A chromosomes. In the present study, we applied immunolabelling with antibodies against histone H4 acetylated at lysines 5, 8, 12 and 16 to A and B chromosomes of *Brachycome dichromosomatica*, a plant with up to three B chromosomes in natural populations and only two homologous pairs of A chromosomes. The labelling patterns observed were related to C-banding and the timing of DNA replication during S-phase.

Materials and methods

Plant material and antibodies

The origin of seed stocks and methods for germination and propagation of *B. dichromosomatica* (cytodeme A1, Watanabe *et al.* 1975) plants have been described elsewhere (Donald *et al.* 1995).

The antibodies used were polyclonal rabbit antisera, which recognized specifically histone H4 acetylated at lysine positions 5 (R41/5, 8 (R12/8), 12 (R20/12), 16 (R14/16) and non-acetylated H4 (Turner 1989, Turner & Fellows 1989). A rabbit pre-immune serum was used as the control.

Chromosome preparation and indirect immunofluorescence

Root-tip meristems were treated overnight in ice water and fixed in ice-cold, freshly prepared, 12% (w/v) formaldehyde solution containing 10 mM Tris HCl (pH 7.5), 10 mM EDTA and 100 mM NaCl. After washing for 20 min in 10 mM citric acid–sodium citrate buffer (pH 4.5) at room temperature (RT) the root-tip meristems were digested at 37°C for 25 min with 2.5% pectinase, 2.5% cellulase 'Onozuka R-10' and 2.5% 'Pectolyase Y-23' (w/v) dissolved in citric acid–sodium citrate buffer. The root tips were then washed for 10 min in 50 mM phosphate buffer containing 5 mM $MgSO_4$ at RT. For metaphase chromosome preparations, the meristems were squashed on glass slides in phosphate buffer. After freezing in liquid nitrogen, the coverslips were removed and the thawed slides were immediately transferred into phosphate-buffered saline (pH 7.4) (PBS). To minimize non-specific antibody-binding problems, slides were preincubated for 30 min with 3% bovine serum albumin (BSA) (w/v), 5% non-fat milk powder (w/v) and 0.2% Tween 20 (v/v) in PBS at RT.

The chromosome preparations were then incubated for 1 h at 4°C in primary sera (diluted 1:200 in PBS) in a humidified chamber, washed in PBS and incubated for 1 h at 4°C with fluorescein (FITC)-conjugated anti-rabbit IgG (Dianova), diluted 1:40 in PBS with 3% BSA (w/v), 5% (w/v) non-fat dry milk and 0.2% Tween 20. After a further three washes in PBS, the preparations were counter-stained with 4′,6-diamidino-2-phenylindole (DAPI) and mounted in antifade. Drying out of the slides had to be avoided throughout the procedure. Fluorescence was observed using a microscope equipped with epifluorescence optics. The images were recorded on Fuji 400 photographic films.

DAPI C-banding

For C-banding analysis, root-tip meristems were pretreated in ice water and fixed for several days in ethanol–glacial acetic acid (3:1). For metaphase chromosome preparations, root meristems were washed in enzyme buffer (consisting of 0.01 M citric acid-sodium citrate, pH 4.5) for 30 min at RT, enzyme treated with 1% (w/v) cellulase 'Onozuka R10' and 1% (w/v) pectinase in the same buffer at 37°C for 22 min, washed in enzyme buffer, transferred to 45% acetic acid and squashed on glass slides. Prepared slides were dehydrated and used immediately for banding or stored in glycerol at 4°C until use.

The C-banding method was a modified Giemsa C-banding procedure but using the fluochrome DAPI instead of Giemsa according to Bennett *et al.* (1995). Slides were treated in 45% acetic acid at 60°C, washed for 15 min with distilled water, dehydrated in absolute ethanol and dried at 42°C for 30 min. slides were treated with a saturated solution of $Ba(OH)_2$ at 30°C for 10 min and washed as above. Slides were then incubated in 2 × standard saline citrate (SSC) at 60°C for 90 min, washed in water and dried. Finally, slides were stained with DAPI and mounted in antifade. The photographs were taken as described above.

DNA late replication

For autoradiographic determination of the DNA late replication pattern, excised roots were incubated with [3H]-thymidine (5 μCi/ml) for 30 min, washed thoroughly and grown for an additional 5 h in water. The roots were then treated with ice water overnight, fixed in 3:1 (ethanol–acetic acid) and stained in Feulgen. After squashing the root meristems and removal of the cover slips, the slides were dried and coated with photographic emulsion (EM-1, Amersham). The emulsion was exposed at 4°C for 4–7 days in the dark. Silver grains were developed in Kodak D19B developer, fixed in photographic fixative and washed extensively before light microscopy.

Results

The B chromosome is more weakly labelled by antisera against acetylated histone H4

Specific antibodies were used for the first time to study the distribution of acetylated variants of histone H4 in A and B chromosomes. Antibodies against H4Ac5 revealed a bright fluorescence of interphase nuclei and weaker staining of the metaphase chromosomes. A comparison of the intensity of labelling of A and B chromosomes indicated that the B chromosomes were less intensely stained (Figure 1a). This difference was more evident after using serum R12, which specifically recognizes histone H4 acetylated at lysine 8. Comparisons between the DAPI-stained and the anti-histone-labelled images showed that one type of chromosome was very weakly stained by the anti-histone antibody. The B chromosome of *B. dichromosomatica* is the smallest chromosome of the complement (Watanabe *et al.* 1975) and the size of the underacetylated chromosome is therefore consistent with its identification as the B (Figure 1b&c). The antibody stained interphase nuclei and A chromosomes at metaphase with the same intensity.

The distribution of H4 acetylated forms of lysine 12 and 16 was apparently identical on A and B chromosomes. As shown in Figure 1d, the centromeric region of all chromosomes seemed to be depleted of H4Ac16. Antibodies against non-acetylated H4 yielded uniform labelling along all chromosomes (result not shown). Interphase nuclei showed no differential staining features after treatment with any of the five antibodies. When a rabbit pre-immune serum was used instead of the anti-histone antibody, only a low level of background cytoplasmic staining was visible, with no specific staining of the chromosomes (result not shown).

Differences in C-banding and DNA replication timing between A and B chromosomes

After DAPI staining of untreated chromosomes, no banding pattern was visible. Following DAPI C-banding, distinct chromosome regions showed enhanced fluorescence (Figure 1e). Chromosome 1 had an intense band at the NOR region and a more faintly stained region between the NOR region and the centromere.

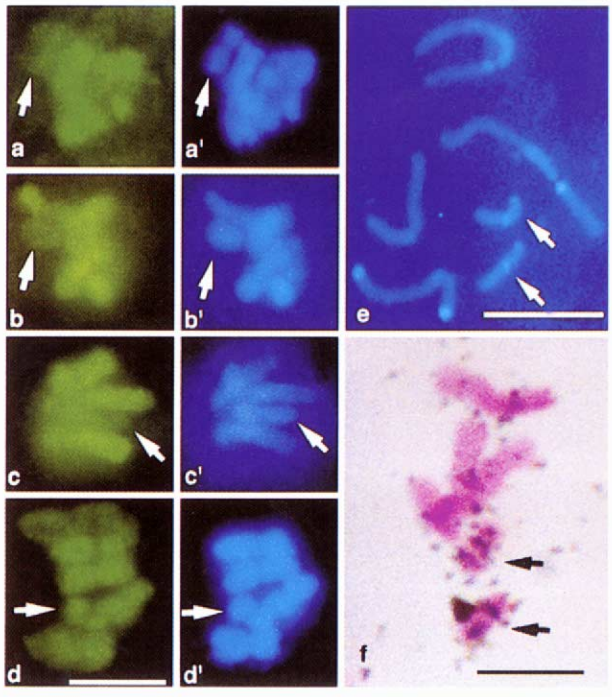

Figure 1. Mitotic metaphase chromosomes of *Brachycome dichromosomatica*. ↑ Immunofluorescence ↑ staining mediated by antibodies against histone H4 acetylated at position **a** lysine 5, **b&c** lysine 8 and **d** lysine 16. B chromosomes (marked by arrows) are more weakly labelled **a–c** compared with the rest of the karyotype. In **d** the B chromosome has the same intensity as the rest of the karyotype. **a′**, **b′**, **c′** and **d′** show the corresponding chromosome spreads after DAPI-staining. **e** Mitotic metaphase after DAPI C-banding. **f** Late replication revealed by tritiated thymidine uptake. The bar represents 10 μm.

Chromosome 2 showed a prominent band on one or both telomeric ends. In 10 plants examined, this band(s) was in all cases visible on only one chromosome of the homologous pair. Karyotype variants for this species have been reported Watanabe *et al.* (1975). The B chromosome was highlighted with faint C-bands near the centromere and NOR region and therefore appeared less heterochromatic than the autosomes.

The earliest metaphases showing silver grains were found 5 h after incubation with [^{3}H]thymidine, at which time the B chromosomes were disproportionately highly labelled (Figure 1f). As would be expected, at times earlier than 5 h, no silver grains were observed over any chromosomes and at later times all the chromosomes showed silver grains. The simplest explanation for this result is that B chromosomes are among the last components of the genome to replicate in S-phase. No reproducible labelling pattern was detectable in interphase nuclei.

Discussion

Immunofluorescence using specific antibodies demonstrated that the chromatin in A and B chromosomes of *B. dichromosomatica* differs markedly in histone H4 acetylation status. The observation that H4Ac5 and H4Ac8 were absent or reduced in Bs, whereas H4Ac12 and H4AC16 were equally present in both chromosome types, can be interpreted as showing that the B chromosome contains less acetylated H4, retaining predominantly the acetylated forms H4Ac12 and H4Ac16. Differences similar to these have been observed in comparisons of autosomes and sex chromosomes in mammals (see review by Turner 1993), except that the inactive X chromosome appeared to be depleted in all four different acetylated forms of H4 (Jeppesen & Turner 1993). In contrast to *V. faba* (Houben *et al.* 1996), immunostaining was not able to differentiate the A chromosomes of *B. dichromosomatica* into euchromatic and heterochromatic regions. This lack of resolution is probably because of the negative influence of cytoplasm on the immunostaining behaviour of squashed metaphase chromosomes. The same problem was noted after comparison of immunostaining behaviour of a pure chromosome suspension and squashed chromosomes of *V. faba* (Idei *et al.* 1996). However, for comparison of both chromosome types in one cell, it was neccessary to use the squashing technique. There is a possibility that the differential immunostaining with antibodies H4Ac5 and H4Ac8 in earlier condensing B chromosomes (Carter 1979) is due to a change in chromatin conformation accompanied by reduced antibody accessibility rather than underacetylation. This appears unlikely because the other antibodies labelled A and B chromosomes with equal intensity.

After C-banding, the B chromosomes appeared less heterochromatic than the A chromosomes. There are cases known in which the B chromosomes are less heterochromtic than the A chromosomes, such as those

of *Scilla vvedenskyi* (Greilhuber & Septa 1976) or more heterochromatic (*Chortoicetes terminifera*, Webb & Neuhauss 1979; *Heteracris littoralis*, Cano & Santos 1988). In the present study, the B chromosome of *B. dichromosomatica* was significantly later replicating than most segments of the A chromosomes. However the correlation between heterochromatin and late replication is not complete and the same apparent contradiction was noted earlier for B chromosomes of other organisms, such as *Crepis capillaris* (Araham *et al.* 1968) and the plague locust *Chortoicetes terminifera* (Webb & Neuhaus 1979). In this context, it is interesting to note that a delayed start of replication in late S-phase has been observed for the inactivated second X chromosome of female mammals (Takagi *et al.* 1982) and in the dioecious plant *Melandrium album* (Siroky *et al.* 1994).

These results suggest that underacetylation and late replication of DNA may play complementary, and possibly interacting, roles in the formation of B chromosome chromatin and that these features may be significant in controlling the genetic inactivity of the supernumerary chromosome. The mechanism by which H4 acetylation and late replication might control the transcriptional activity of chromatin of B chromosomes remains to be established. There may be parallels to be drawn between the forms of genetic inactivation characteristic of B chromosome and that associated with sex chromosome inertia in mammals.

The mechanisms by which the H4 proteins of B chromosomes are differentially acetylated and the way in which histone acetylation effects the transcriptional status of the B chromosomes are yet to be determined. Few potentially active genes are known to be located on B chromosomes in plants. However, rDNA clusters have been detected in many species using silver staining or *in situ* hybridization and the former method is assumed to indicate transcriptional activity. *In situ* hybridization shows the presence of rDNA on the *B. dichromosomatica* B chromosome of cytodeme Al (Donald *et al.* 1996). Sensitive molecular experiments using reverse transcription polymerase chain reaction (RT-PCR) with primers specific for the B chromosome rDNA indicate that the B genes are not transcribed (Donald *et al.* 1997, in press).

In further experiments, it would be worthwhile blocking histone deacetylase and analysing whether the immunolabelling behaviour of B chromosomes has changed or even whether there are any genes carried on B chromosomes that can be reactivated.

Acknowledgements

This work was supported in part by grants from the Deutsche Forschungsgemeinschaft (Ho1779/1-1) and the Department of Industry, Science and Tourism (Australian Bilateral Science & Technology Collaboration Program).

References

Abraham S, Ames IH, Smith HH (1968) Autoradiographic studies of DNA synthesis in the B chromosomes of *Crepis capillaris*. *Heredity* **59**: 297–299.

Attisano L, Newis PN (1990) Purification and characterization of the porcine liver nuclear histone acetyltransferase. *J Biol Chem* **265**: 3949–3955.

Belyaev ND, Keohane AM, Turner BM (1996a) Histone H4 acetylation and replication timing in Chinese hamster chromosomes. *Exp Cell Res* **225**: 277–285.

Belyaev ND, Keohane AM, Turner BM (1996b) Differential underacetylation of histones H2A, H3 and H4 on the inactive X chromosome in human female cells. *Hum Genet* **97**: 573–378.

Bennett ST, Leitch IJ, Bennett MD (1995) Chromosome identification and mapping in the grass *Zingeria biebersteiniana* (2n = 4) using fluorochromes. *Chrom Res* **3**: 101–108.

Braunstein M, Rose AB, Holmes SG, Allis CD, Broach JR (1993) Transcriptional silencing in yeast is associated with reduced nucleosome acetylation. *Genes Dev* **7**: 592–604.

Cano MI, Santos JL (1988) B chromosomes of the grasshopper *Heteracris littoralis:* meiotic behaviour and endophenotypic effects in both sexes. *Genome* **30**: 797–801.

Carter CR (1978) The cytology of *Brachycome*. 8. The inheritance, frequency and distribution of B chromosomes on *B. dichromosomatica* (n = 2), formerly included in *B. lineariloba*. *Chromosoma* **67**: 109–121.

Donald TM, Leach CR, Clough A, Timmis JN (1995) Ribosomal RNA genes and the B chromosome of *Brachycome dichromosomatica*. *Heredity* **74**: 556–561.

Donald TM, Houben A, Leach CR, Timmis JN (1997) Ribosomal RNA genes specific to the B chromosomes in *Brachycome dichromosomatica* are not transcribed. *Genome* (in press).

Dover GA, Riley R (1972) The prevention of pairing of homeologous meiotic chromosomes of wheat by a genetic activity of supernumerary chromosomes of *Aegilops*. *Nature* **240**: 159–161.

Felsenfeld G (1992) Chromatin as an essential part of the transcriptional mechanism. *Nature* **355**: 219–224.

Green DM (1990) Muller's ratchet and the evolution of supernumerary chromosomes. *Genome* **33**: 818–824.

Greilhuber J, Septa F (1976) C-banded karyotypes in the *Scale hohenackeri* group, *S. persica*, and *Puschkinia* (Liliaceae). *Plant System Evol* **126**: 149–188.

Hackstein JHP, Hochstenbach R, Hauschtek-Jungen E, Beukeboom WL (1996) Is the Y chromosome of *Drosophila* an evolved supernumerary chromosome? *BioEssays* **18**: 317–323.

Houben A, Belyaev ND, Turner BM, Schubert I (1996) Differential immunostaining of plant chromosomes by antibodies recognizing acetylated histone H4 variants. *Chrom Res* **4**: 191–194.

Idei S, Kondon K, Turner BM, Fukui K (1996) Tomographic distribution of acetylated histone H4 in plant chromosomes, nuclei and nucleoli. *Chromosoma* **105**: 293–302.

Jeppesen P, Turner BM (1993) The inactive X chromosome in female mammals is distinguished by a lack of histone H4 acetylation, a cytogenetic marker for gene expression. *Cell* **74**: 281–289.

Jones RN (1995) Tansley Review No. 85. B chromosomes in plants. *New Phytol* **103**: 411–434.

Loidl P (1988) Towards an understanding of the biological function of histone acetylation. *FEBS Lett* **227**: 91–95.

Loidl P (1994) Histone acetylation: facts and questions. *Chromosoma* **103**: 441–449.

Lopez-Rodas G, Georgieva EI, Sendra R, Loidl, P (1991) Histone acetylation in *Zea mays L. J Biol Chem* **266**: 18745–18750.

Matthews HR (1988) Histone modifications and chromatin structure. In: Adolph K, ed. *Chromosomes and Chromatin 1*. Boca Raton: CRC Press, pp 3–32.

O'Neill LP, Turner BM (1995) Histone H4 acetylation distinguishes coding regions of the human genome from heterochromatin in a differentiation-dependent by transcriptions-independent manner. *EMBO J* **14**: 3946–3957.

Plowman AB, Bougourd SM (1994) Selectively advantageous effects of B chromosomes on germination behaviour in *Allium scheonoprasum* L. *Heredity* **72**: 589–593.

Roth SY, Allis, CD (1996) Histone acetylation and chromatin assembly: a single escort, multiple dances? *Cell* **87**: 5–8.

Siroky J, Janousek B, Mouras A, Vyskot B (1994) Replication patterns of sex chromosomes in *Melandrium album* female cells. *Hereditas* **120**: 175–181.

Takagi M, Sugawara O, Sasaki M (1982) Regional and temporal changes in the pattern of X-chromosome replication during the early postimplantation of the female mouse. *Chromosoma* **85**: 275–286.

Turner BM (1989) Acetylation and deacetylation of histone H4 continue through metaphase with depletion of more-acetylated isoforms and altered site usage. *Exp Cell Res* **182**: 206–214.

Turner BM (1993) Decoding the nucleosome. *Cell* **75**: 5–8.

Turner BM, Fellows G (1989) Specific antibodies reveal ordered and cell-cycle-related use of histone-H4 acetylation sites in mammalian cells. *Eur J Biochem* **179**: 131–139.

Watanabe K, Carter CR, Smith-White S (1975) The cytology of *Brachycome lineariloba*. 5. Chromosome relationships and phylogeny of the race A cytodemes (n = 2). *Chromosoma* **52**: 383–397.

Webb GC, Neuhaus P (1979) Chromosome organisation in the Australian plague locust *Chortoicetes terminifera*. 2. Banding variants of the B-chromosome. *Chromosoma* **70**: 205–238.

A13 Houben, A., Leach, C.R., Verlin, D., Rofe, R., and Timmis, J.N. (1997b). A repetitive DNA sequence common to the different B chromosomes of the genus *Brachycome*. Chromosoma 106, 513-519.

Chromosoma (1997) 106:513–519

CHROMOSOMA

A repetitive DNA sequence common to the different B chromosomes of the genus *Brachycome*

Andreas Houben, Carolyn R. Leach, Dawn Verlin, Ruth Rofe, Jeremy N. Timmis

Department of Genetics, The University of Adelaide, SA 5005, Australia

Received: 30 May 1997; in revised form: 20 August 1997 / Accepted: 20 August 1997

Abstract. Dot-like micro B chromosomes of *Brachycome dichromosomatica* were analysed for their sequence composition. Southern hybridization patterns of a total micro B probe to genomic DNA from plants with and without micro Bs demonstrated that the micro Bs shared sequences with the A chromosomes. In addition to telomere, rDNA and common A and B chromosome sequences, a new B-specific, highly methylated tandem repeat (Bdm29) was detected. After in situ hybridization with Bdm29 the entire micro B chromosome was labelled and clustering of the condensed micro Bs could be observed at interphase. A high number of Bdm29-like sequences were also found in the larger B chromosomes of *B. dichromosomatica* and in other Bs within the genus *Brachycome.*

Introduction

B chromosomes (Bs), which are supernumerary to the basic (A) chromosome set, are common in many groups of plants and animals. They differ from the A chromosomes in morphology and pairing behaviour and are fully dispensable, indicating that they are not required for normal growth and development. In most cases, a small number of Bs are selectively neutral in their effect on phenotype, but they are deleterious in high numbers. To date little is known about the origin and biological significance of B chromosomes. It is generally accepted that B chromosomes arise from the A chromosomes because of the large number of shared sequences (for reviews see Beukeboom 1994; Jones 1995). In general only one type of B chromosome is found in a given species, but two or more morphological forms of Bs are known in at least 65 plant species (Jones 1995).

EMBL Genbank Accession no: Y 13091

Edited by: R. Appels

Correspondence to: A. Houben
(e-mail: ahouben@genetics.adelaide.edu.au)

In the plant *Brachycome dichromosomatica,* in addition to the large B chromosome (4 μm in length), dot-like micro B chromosomes (micro Bs) less than 1 μm in diameter have been described (Carter and Smith-White 1972). In contrast to the larger Bs, the micro Bs are mitotically unstable. They can vary in number in somatic tissues of a plant and they do not pair with other micro Bs or with the A or B chromosomes at meiosis (Carter and Smith-White 1972). Irregular chromosome segregation at mitotic anaphase is probably responsible for the variation in number of B chromosomes in different cells. A sequence (Bd49) specific to the larger B chromosome of *B. dichromosomatica*, has been described (John et al. 1991; Leach et al. 1995; Franks et al. 1996). It has been shown that these chromosomes contain rDNA sequences that are transcriptionally inactive (Donald et al. 1997), consistent with the observation that the chromatin composition is different between As and Bs (Houben et al. 1997).

In this study, we used a number of molecular and cytogenetic techniques to investigate the sequences composition and organisation of the micro B chromosomes. Our results indicate that the micro B contains a number of DNA sequences that are also present on the A chromosomes. From amongst these, we have isolated a sequence that is highly repeated on the micro B chromosome, and also present in lower copy number on the larger B chromosome, but that is found only in very low numbers on the A chromosomes of the plants tested.

Materials and methods

Plant material and cytogenetic preparation. Brachycome dichromosomatica (2*n*=4) is a member of the *B. lineariloba* complex with the other members *B. breviscapis* (2*n*=8), *B. lineariloba* E (2*n*=10), B (2*n*=12) and *C* (2*n*=16) (Watanabe et al. 1994). Plants and seeds of *B. dichromosomatica, B. lineariloba, B. dentata* and *B. curvicarpa* were collected from wild populations in Australia. The different cytodemes (A1, A2, A3, and A4) of *B. dichromosomatica* were characterised on the basis of their chromosome morphology as described by Watanabe et al. (1975). Mitotic preparations for in situ hybridization and chromosome microdissection were obtained from root tips according to Donald et al. (1997).

Microdissection and DOP-PCR. B chromosomes were microisolated from mitotic preparations using an inverted microscope with a micromanipulation system. The DNA of 20 microisolated Bs was amplified by the polymerase chain reaction (PCR) according to Pich et al. (1994) using the degenerate oligonucleotide primer (DOP) 6-MW (Telenius et al. 1992). This primer has a random hexamer sequence in between defined sequences at the 5' and 3' ends. The first cycles of the DOP-PCR consist of low stringency annealing, followed by cycles with more stringent annealing conditions. It cannot be assumed that the DOP-PCR-amplified DNA is a full representation of the chromosome region isolated by microdissection. The size of the PCR products was monitored by gel electrophoresis, and after Southern transfer, hybridized with labelled total genomic DNA of plants with micro Bs.

Southern hybridization. Genomic DNA was isolated from leaf material by the procedure described by Wienand and Feix (1980) and digested with different restriction enzymes according to the manufacturer's recommendations. For partial digestions, 5 µg of DNA was cut with decreasing amounts of the enzyme for 4 h. DNA fragments were resolved on 0.8% agarose gels in TAE buffer and subsequently transferred to Hybond N+ nylon membranes (Amersham). For hybridization, the DNA probes were labelled with (α-^{32}P)dCTP by random-primed DNA synthesis. Hybridization was carried out overnight at 65° C in 5×SSPE, 0.2% SDS, 5×Denhardt's reagent, 100 µg/ml salmon sperm DNA. Blots were washed successively in 0.1×SSC (1×SSC is 0.15 M NaCl, 0.015 M sodium citrate) and 0.1% SDS and then exposed to X-ray film at −70° C for appropriate periods.

Sequencing and sequence analysis. Sequencing was done by the Sequenase (Version 2.0) system (United States Biochemical). Searches for sequence similarity in the Genbank database were performed using FASTA and BLASTA services (Australian National Genomic Information Service).

Fluorescence in situ hybridization (FISH). A clone VER17 (Yakura and Tanifuji 1983) containing part of the 18S, the 5.8S, most of the 25S rDNA sequence and the internal transcribed spacer of *Vicia faba*, was used as a nucleolus organiser (NOR)-specific probe. An *Arabidopsis*-type telomere probe was synthesised using PCR according to Ijdo et al. (1991). Probes (18S/25S rDNA, telomere, micro B DOP-PCR product) were labelled with biotin-16-dUTP by nick translation. Probe Bdm29 was labelled with digoxigenin-(DIG)-11-dUTP by PCR with vector pBluescript (Stratagene) specific primers. FISH was carried out as described by Fuchs and Schubert (1995). Hybridization of the biotinylated probes was detected by the use of a streptavidin-FITC/anti-streptavidin-FITC (fluorescein isothiocynate) system. Hybridization sites of the DIG-labelled probe were detected using anti-digoxigenin-rhodamine/rhodamine anti-sheep antibody. Epifluorescence signals were recorded by Fuji 400 film.

Results

The micro B chromosomes contain specific and common repeats

The configurations of mitotic micro B chromosomes of *B. dichromosomatica* (cytodeme A2) at different stages of mitosis are shown in Fig. 1a–c. Doublet associations of micro Bs and, to a lesser extent, chain-like formations of several micro Bs were regularly found (Fig. 1). A fine chromatin fibre was often observed between the micro Bs (Fig. 1b, c). In contrast to the A chromosomes, which showed specific condensation patterns during the different stages of the mitotic cell cycle, the dot-like micro Bs always appeared highly condensed. Differential chromatin condensation behaviour has also been reported for the larger B chromosome of *B. dichromosomatica* (Watanabe et al. 1976). After reciprocal crosses of plants with and without micro Bs we found that the micro B can be consistently inherited by male or female gametes. Further

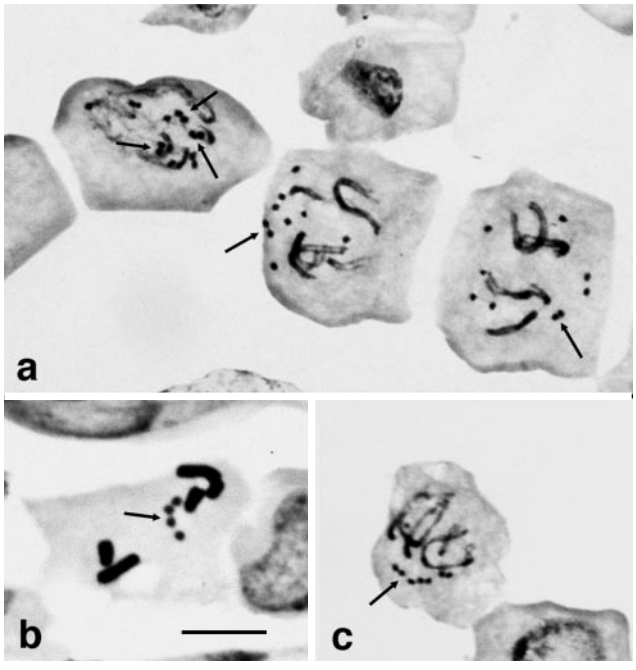

Fig. 1a–c. Feulgen-stained mitotic chromosomes of *Brachycome dichromosomatica* (2*n*=4 plus micro B chromosomes). The micro B chromosomes are very condensed at all stages of the cell cycle and able to form double micro B chromosomes (**a** *arrows*) or chain-like formations (**b, c** *arrows*) at mitotic metaphase. *Bar* represents 10 µm

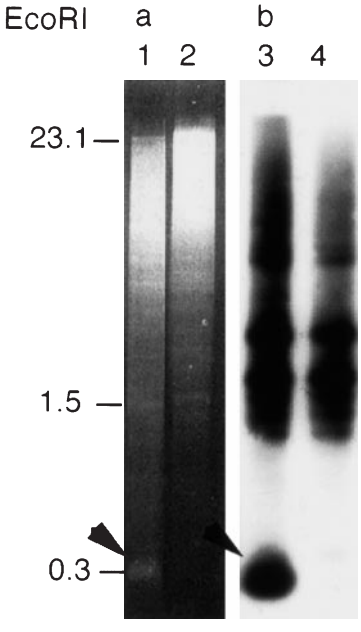

Fig. 2a, b. Visualisation of a micro B chromosome-specific DNA fragment. **a** Ethidium bromide-stained gel of 5 µg *Eco*RI-digested genomic DNA from a plant with (*lane 2*) and without (*lane 2*) micro B chromosomes **b** Southern hybridization of *Eco*RI-digested DNA with labelled degenerate oligonucleotide-primed polymerase chain reaction (DOP-PCR)-amplified micro B chromosome DNA. The micro B-specific bands are marked with *arrowheads*

crosses showed that micro Bs and the larger B chromosomes are able to coexist in a single plant.

To obtaine DNA from micro Bs, microdissection and DOP-PCR were carried out. The amplified DNA from the isolated chromosomes showed a smear ranging in size from 0.1 to 1.8 kb after gel electrophoresis and Southern hybridization probed with total genomic DNA from a plant with micro Bs (data not shown). To examine the similarity between the DNA of micro Bs and that of A chromosomes, labelled DNA from the DOP-PCR-amplified micro Bs was used for Southern hybridization and FISH experiments. The Southern hybridization of *Eco*RI-digested DNA from 0B and +micro B plants resulted in a specific hybridization pattern for each genotype but with a prominent band of 0.3 kb in +micro B genotypes (Fig. 2b, arrowed). This band was also visible on the ethidium bromide-stained gels of *Eco*RI-digested DNA of +micro B genotypes (Fig. 2a, arrowed). No B chromosome-specific band was obvious after Southern hybridization of the DOP-PCR-micro B probe to genomic DNA of plants with the larger B chromosome (data not shown).

The presence, in the microdissected DNA, of a high copy micro B-specific sequence and sequences that are also shared with the A chromosome complement was confirmed by in situ hybridization. After FISH using the labelled DOP-PCR product on metaphase spreads of +micro B genotypes, the micro Bs showed preferential hybridization compared with a weak dispersed signal along the entire length of the two A chromosome pairs (Fig. 3a).

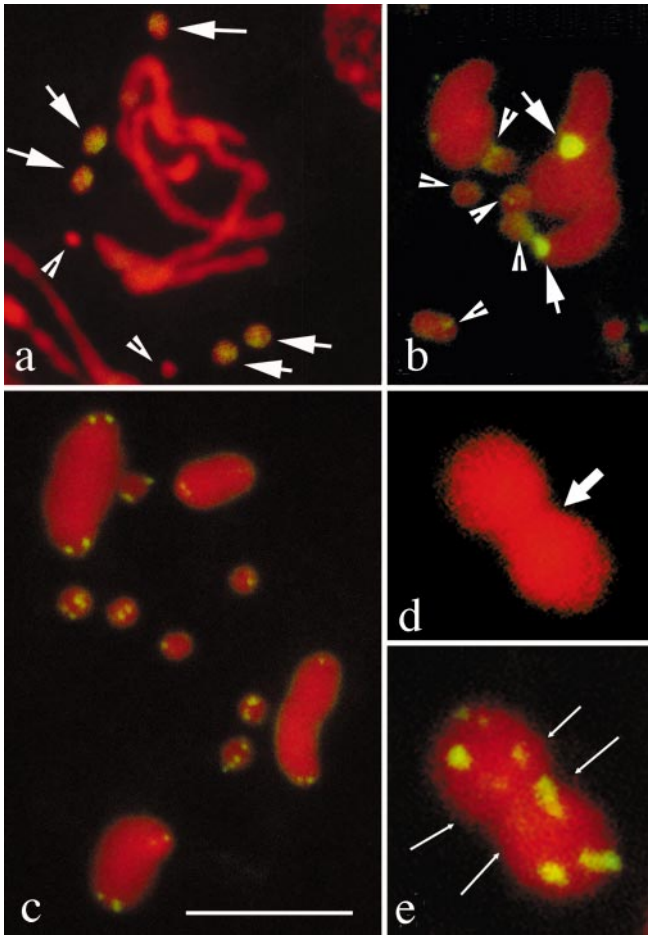

Fig. 3a–e. Characterisation of micro B chromosomes by fluorescence in situ hybridization (FISH) with different probes. **a** FISH of the labelled DOP-PCR products to a mitotic metaphase spread of *B. dichromosomatica*, cytodeme A2 (2*n*=4 plus 5 micro Bs) showing preferential hybridization to the micro Bs (*arrows*) and additional signals of lower intensity on the A chromosomes. Unlabelled satellites of the smaller A chromosome pair, separated during the squash preparation, are marked with *arrowheads*. **b** FISH with an 18S/25S rDNA clone to mitotic metaphase chromosomes. The nucleolus organiser regions of the smaller A chromosome pair are strongly labelled (*arrows*) and signals of weaker intensity appear on the micro B chromosomes (*arrowheads*). **c** Hybridization with an *Arabidopsis* telomere-specific sequence showing two signals on each end of the A and micro B chromosomes. The *bar* in **c** represents 10 μm for **a, b** and **c**. **d** Physically associated micro B chromosomes stained with propidium iodide showing the connection site (indicated with an *arrow*). **e** Telomere signals for each micro B chromatid are indicated with *arrows*. The chromosomes of **d** and **e** are at a greater magnification

The micro B contains a high proportion of a specific tandem repeat sequence

To isolate the micro B-specific sequence, the 0.3 kb *Eco*RI fragment was eluted from a preparative gel and ligated into pBluescript (Stratagene) and the inserts were hybridized sequentially with genomic DNA of 0B and +micro B genotypes. A number of clones (Bdm5, 14, 22, 23, 29, 55) that hybridized only with +micro B genomic DNA were sequenced and aligned (Fig. 4). The sequences showed a high degree of similarity and were thus considered as members of a single repeat family. The clone Bdm29 was chosen for further investigation. The AT-rich (62%) insert of Bdm29 is 290 bp long and contains no significant subrepeats. The sequence (EMBL, Genbank accession number, Y13091) was compared with the Genbank database and no sequence homology was found.

Hybridization of Bdm29 with *Eco*RI-digested genomic DNA of genotypes with micro Bs revealed a strongly hybridizing band of 0.3 kb after only a few hours exposure of the film (Fig. 5, lane 12 U). Faint bands of 0.3 kb and 5 kb were also detected in material with no micro B chromosomes after exposing the film for 10 days (data not shown). To determine whether the sequence is organised in a randem array or whether it is part of a repeat unit with nonhomologous flanking regions, we hybridized *Eco*RI partially digested genomic micro B DNA with Bdm29. The result showed a ladder characteristic of multiples of the 0.3 kb monomer arranged in tandem arrays (Fig. 5). Since many repetitive DNA sequences are known to be subject to hypermethylation, we investigated the methylation status of these repeats at the sequenc CCGG. Genomic DNA of plants with micro Bs was digested with the differentially methylation-sensitive enzymes *Msp*I or *Hpa*II and Southern blots were hybridized with labelled Bdm29. MspI digests from +micro B genomic DNA showed a hybridization ladder ranging from 0.3 to 23 kb in length. In contrast *Hpa*II showed little or no digestion, indicative of a high degree of methylation of genomic DNA at C^{m}CGG sites recognised by *Hpa*II com-

```
                    20                  40                  60                  80                 100
Bdm29 GAATTCAAGAACTGAGGTATGGAGGCCATTTATGGAGCTGGxACACGCCTACTGGGxxACGAGCxxTAGCAxCCTAAACAAGAAGAATAGTGAAGATTTAGAAGAATTATATTA
Bdm14 ............x.GGG..T........T.........CGx.......T.CAGGGxx..ATG.xx.....x.AT...C........TA.........xAG.AG.ATT...AG
Bdm23 ............x.AAG..A........T.........AGG.......T.TTGGGxx..ATG.xx.....x.AT...C........TA.........TAG.AG.ATT...AT
Bdm55 ............x.GGG..T........G.........CCx.......A.CTGGGxx..TTA.xx.....x.AT...G........Cx.........TAG.AT.ATT...AG
Bdm5  ............x.GGx..T........T.........CCx.......A.CATATTT..TTG.GC.....G.AA...G........CA.........TAG.AT.ATT...AG

         120                 140                 160                 180                 200                 220
Bdm29GCGAGTTACAGTACTGGGAGTAAxxxxAGAGTTTAGTATCATTCTGTGTTCTTATCTTAAAGTCGACCGAAAxTCCTTxGTGTACTAGxCAAAATGATTAGxxTTTTCAAAACAAA
Bdm14..TA......A...GGxxAGTA.xxxx......xA..Tx.....GTxG..Txx....AT..xxx.G.....Ax.....x......ATGG.....T.....AGT.T..T........
Bdm23..xx......G...GGGxAGTA.xxxx......TA..xA.....GTCG..TTC....AT..xxx.G.....AA.....A......TAGC.....T.....AGT.T..T........
Bdm55..Tx......A...ATACCATG.GTAA......TA..AT.....ATxG..CTT....AT..xxx.G.....xx.....x......ATGx.....C.....AGT.C..T........
Bdm05..Tx......A...ATGxTGTA.xxxA......CA..xT.....xTxG..CTT....AT..xxx.G.....xx.....x......ATGx.....T.....AGT.T..T........

            240                 260                 280                 300
Bdm29 TAACCTACTCGxATCGATTTTGGAAxTTCCGGGAAGCTTGTTTTTGCAATTATCAAATTCAGTGAATTCAGxxxxxxGAATTC
Bdm14 AT.C....xxxxGCG..........A.C.C.............................CxxxxxxxxxxxxxxxAG......
Bdm23 AT.C....CTACGCA......  ..x.C.C.............................CxxxxxxxxxxxxxxxAG......
Bdm55 AT.T....xxxxGAC.......  .A.T.C.............................TATCAAATTCAxxxxxxG......
Bdm5  AT.C....xxxxGCG......  ..A.T.T.............................CxTGAAATTCTGAAGTTC......
```

Fig. 4. Comparison of Bdm29-like sequences of *B. dichromosomatica.* Differences from the Bdm29 sequence (*top line*) are shown for the other four clones. *Asterisks* indicate gaps introduced for maximum alignment

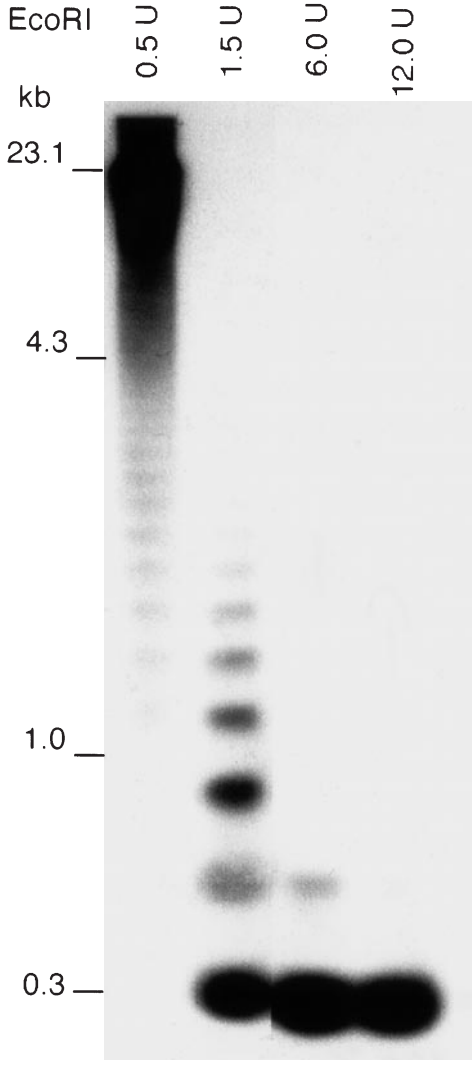

Fig. 5. Partial and complete restriction digest of genomic DNA with micro Bs. The DNA samples (5 µg) were partially (0.5, 1.5, 6 U of enzyme) or completely (12 U of enzyme) digested with *Eco*RI and Southern blots probed with Bdm29. The autoradiograph was exposed for 5 h

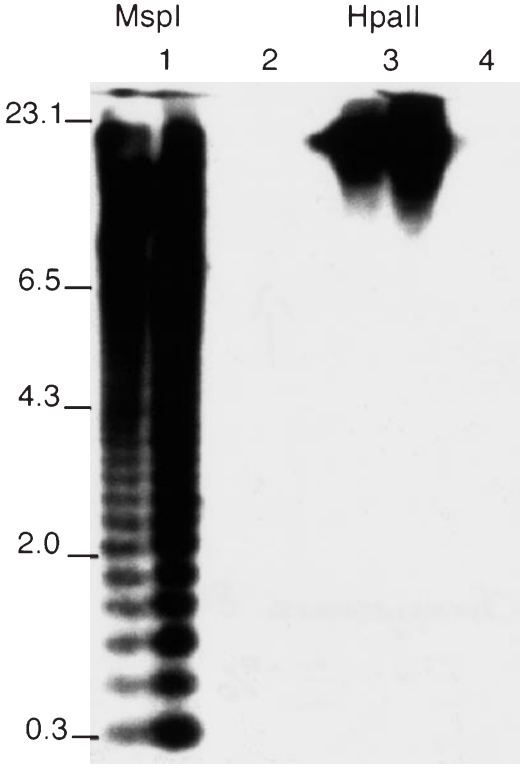

Fig. 6. Methylation status of Bdm29. Genomic DNA was prepared from duplicate plants with (*lanes 1, 3*) and without micro Bs (*lanes 2, 4*). Samples of DNA (5 µg) were digested with *Msp*I (*lanes 1, 2*) or *Hpa*II (*lanes 3, 4*). Southern blots were hybridized with Bdm29 and autoradiographed with an exposure time of 5 h

pared with ^{m}CCGG sites recognised by *Msp*I (Fig. 6). Lanes 2 and 4 show no hybridization, confirming that the A chromosomes contain no high copy number repeats of Bdm29.

After in situ hybridization of metaphase spreads from plants with micro B chromosomes with Bdm2, the entire micro Bs were strongly labelled (Fig. 7a, b). The whole micro B metaphase chromosomes were labelled with Bdm29, suggesting that the sequence was dispersed along

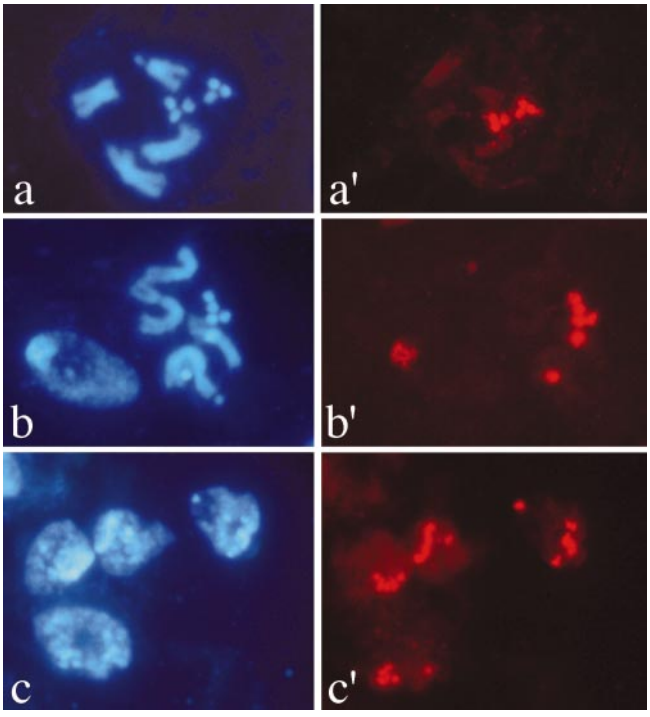

Fig. 7a–c'. Mitotic interphase and metaphase nuclei of *B. dichromosomatica*, 2*n*=4 plus micro B chromosomes, after staining with 4',6-diamidino-2-phenylindole (**a–c**). In situ hybridization of a tandem repeat (Bdm29) to the corresponding chromosome preparations (**a', b'**). The metaphase cells show hybridization of the probe specifically to the entire micro B chromosomes and no detectable hybridization to the two pairs of A chromosomes. **c** Interphase cells showing condensed and clustered hybridization foci after FISH with Bdm29

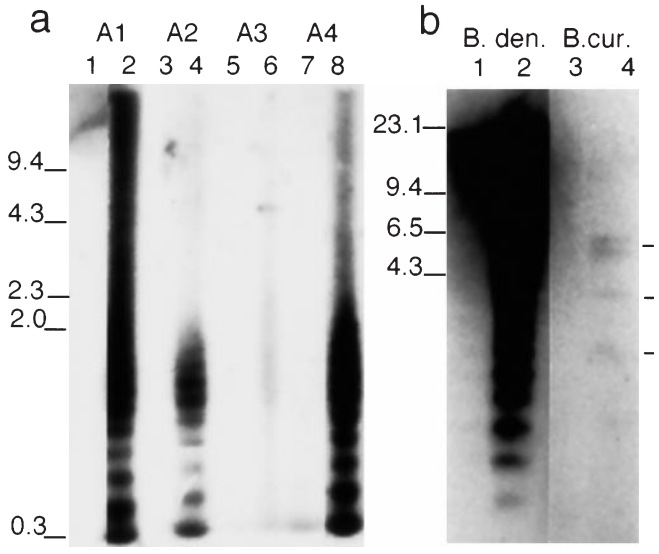

Fig. 8a, b. Southern hybridization of Bdm29 to genomic DNA of various species within the genus *Brachycome* with and without B chromosomes. **a** *Msp*I-digested DNA of the different cytodemes (A1, A2, A3, and A4) of *B. dichromosomatica* with (*lanes 2, 4, 6, 8*) and without B chromosomes (*lanes 1, 3, 5, 7*). **b** *Eco*RI-digested DNA of *B. dentata* (*lanes 1, 2*) and *B. curvicarpa* (*lanes 3, 4)* with *(lanes 2, 4*) and without B chromosomes (*lanes 1, 3*). The autoradiographs were exposed for 2 days

the chromosome, making it feasible to characterise the organisation of the micro Bs at interphase with Bdm29. Figure 7c shows compact foci of hybridization that were clearly seen at all stages of the cell cycle. Observation of 200 different labelled interphase cells indicated that 85% of the micro Bs in squash preparations were clustered and 15% were arranged in a more random distribution within the nucleus.

Bdm29 is also present on other B chromosomes

To determine whether the sequence of Bdm29 is present on other larger B chromosome types in the genus *Brachycome,* we examined the 0B and B-containing genomes of *B. dichromosomatica* (cytodemes A1, A2, A3 and A4), *B. dentata* and *B. curvicarpa* in Southern hybridization experiments with Bdm29. B chromosome-specific hybridization of Bdm29 was found for each of these (Fig. 8). *Msp*I digestion (Fig. 8a) of DNA from A1, A2, and A4 cytodemes of *B. dichromosomatica* with and without B chromosomes showed evidence of an array of tandem repeats similar in size of Bdm29 but not as repetitious as on the micro B. Cytodeme A3 (lanes 5, 6) showed a very much reduced degree of hybridization at 300 bp. Hybridization of Bdm29 to *Eco*RI-digested DNA from plants of *B. dentata* with and without B chromosomes indicated the presence of a large population of Bdm29-like tandem repeats on the B chromosome and evidence of some hybridization to the A chromosomes. Corresponding experiments with *B. curvicarpa* showed reduced hybridization to four bands between 2 and 5 kb in size that appeared to be confined to the B chromosomes of this species (Fig. 8b).

Since it is known that *B. lineariloba* (2*n*=10, 12 or 16) and *B. eriogona* form hybrids with *B. dichromosomatica* (Smith-White and Carter 1970), we included these closely related species in Southern hybridization experiments but no cross hybridization of Bdm29 was observed (result not shown). However a small amount of cross hybridization of Bdm29 was found between genomic DNA of the more distantly related species *B. ciliaris* (result not shown).

The micro B chromosome carries 18S/25S rDNA and telomere sequences

In order to obtain more information about the structure of the micro Bs, in situ hybridization experiments were carried out with telomere and rDNA probes. The in situ hybridization of *Arabidopsis*-type telomeric sequences, to A and micro B chromosomes revealed two signals on each end (Fig. 3c). The finding of four hybridization signals per micro B indicates the presence of normally replicated sister chromatids at metaphase (Fig. 3c, e), although these are not resolved by light microscopy analysis prior to in situ hybridization (Fig. 1). The hybridization signal on A and micro B chromosomes appeared to be of the same intensity, suggesting that the number of telomere repeat

units is similar. This is in contrast to the situation in *Crepis capillaris*, where the B chromosome appears to have a higher telomere repeat copy number than the As (Jamilena et al. 1994).

Using the 18S/25S rDNA probe, FISH signals were detected on the short arms of the smaller A chromosomes in cytodeme A2 and on one end of the micro Bs (Fig. 3b). No association of the interphase micro Bs with the nucleolus was observed, suggesting that the micro B rDNA sequence is not transcriptionally active.

Discussion

In this study we describe the isolation and characterisation of a repetitive element that is present on the micro B chromosome of *B. dichromosomatica*. The Southern hybridization experiments showed that Bdm29 is present in low copy number on the A chromosomes and in very high copy number on the micro Bs. The other known B chromosome-localised sequence (Bd49) is likewise present in low copy number on the A chromosome complement (Leach et al. 1995). Analogous high copy, tandemly repeated B-specific sequences have been found on B chromosomes of various other species, including rye (Sandery et al. 1990; Blunden et al. 1993; Houben et al. 1996) wasp (Eickbush et al. 1992) and maize (Alfenito and Birchler 1993).

How and why the amplification of Bdm29 on B chromosomes occurred is unknown. Generally DNA amplification occurs during periods of genomic instability and several amplification mechanisms have been suggested (for review see Wintersberger 1994). Because of the dispensable nature of Bs, sequences unconstrained by selection are likely to be prone to particularly rapid sequence evolution, as predicted by Muller's Ratchet (Green 1990).

The finding of rDNA sequences on micro Bs (Fig. 3b) may be significant in a consideration of the origin of B chromosomes as ribosomal sequences are also present on the larger B of *B. dichromosomatica* (Donald et al. 1995). As assessed by the intensity of the fluorescence signal the rDNA copy number was lower on the micro B than on the larger B chromosome. Ribosomal DNA is known to be carried on B chromosomes of many species (Green 1990; Jones 1995) but it is uncertain whether rDNA is involved in the formation of B chromosomes or if they are incorporated into the chromosome later in evolution. The ability of rDNA to move into other genomic regions has been discussed (Schubert and Wobus 1985; Dubcovsky and Dvorak 1995). Nevertheless, the chromosomes of *B. dichromosomatica* are in a period of rapid evolution to the extent that the species is characterised by different cytodemes (Watanabe et a. 1975), probably differing from one another by several structural rearrangements of the A chromosomes. Different positions of the NOR can be observed in the different cytodemes (Houben et al. in preparation) and it is therefore tempting to speculate on the origin of the rDNA-carrying micro Bs as fragmentation products of convoluted meiotic pairing in structural hybrids. On the other hand an rDNA transcription event may itself generate chromosomal breaks that may play a role in the origin of micro Bs.

It is generally accepted that the chromatin of transcriptionally inactive chromosome domains is more condensed than active chromatin at interphase. After chromosome painting of the micro Bs with Bdm29 we found very condensed signal clusters in interphase cells (Fig. 7c). Although condensed interphase Bs (or chromocentres) were also found in a number of other plants, this is not a general characteristic of B chromosomes (for review see Jones 1995). Furthermore, Morais-Cecilio et al. (1996) suggested, from interphase in situ hybridization experiments, that rye B chromosome chromatin is organised in an extended string-like form and concluded that their interphase organisation was similar to the cereal A chromosomes. Grouping of micro B chromosomes was also found in metaphase cells. Contiguous pairs of micro Bs and, to a lesser extent, chain-like formations of several micro Bs were regularly found (Fig. 1b, c).

Unlike the end-to-end association of chromosomes in the sperm heads of monotreme mammals (Watson et al. 1996), separate telomere signals were seen on each of the associated micro Bs after FISH with a telomere-specific probe (Fig. 3d, e). The optical appearance of paired micro Bs is very similar to double minutes (DMs) in drug-resistant mammalian cells in culture (see review by Hahn 1993). However micro Bs have telomeric sequences, whereas there is none on the circular chromatin bodies of the DMs (Furuya et al. 1993).

Another possible explanation for the adhesive behaviour and heteropycnotic character of micro B is the methylated state of Bdm29. Miniou et al. (1994) demonstrated that hyerpmethylation of a human satellite sequence correlates with a condensed chromatin structure, presumably via differential binding of proteins. Hypermethylation is also considered to be an important mechanism of transcription inactivation (Finnegan et al. 1996) and we have found no evidence for the presence of Bdm29-like transcripts using Northern blot hybridization analysis of total RNA prepared from leaf and young flower bud tissue (data not shown).

Bdm29 showed hybridization to the large B chromosome DNA of *B. dichromosomatica, B. dentata* and to a lesser extent, *B. curvicarpa.* This indicates that the Bdm29 sequence is highly conserved and high numbers correlate with B chromosomes of both types. Southern emphasising 20- to 30-fold difference between micro B and large Bs. Perhaps this sequence is important for the function of the B chromosome itself and was independently involved several times in the formation of different B chromosomes. Alternatively the sequence evolved early in the evolution of *Brachycome* B chromosomes and has been maintained in several lineages, with or without any functional significance. As both, the micro B and the larger B chromosomes contain Bdm29 and rDNA sequences, it is possible that both types of Bs were derived from a common ancestral B chromosome. Alternatively the micro B may represent a forerunner of the larger B chromosome into which it evolved by the amplification and addition of more DNA. During this process the sequence Bd49 (John et al. 1991) presumably accumulated on the larger B chromosome of *B. dichromosomatica* but not on other B chromosomes within the genus *Brachycome*.

Micro and larger B chromosomes have been also reported for other species. The micro Bs of *Calyadenia multiglandulosa* (Carr and Carr 1982) appear to be similarly mitotically unstable with numbers ranging from 0 to about 10 in different cells, whereas the larger B is stable. Parallels can also be drawn between the micro Bs of *B. dichromosomatica* and the dot-like B chromosomes of *Drosophila subsilvestris* described by Gutknecht et al. (1995). These authors have also suggested that the larger B chromosome of *Drosophila* may have originated from a dot-like B chromosome, since FISH with a specific satellite sequence (pSsP216) from the dot-like B chromosome showed signals on the large B chromosomes. It was concluded that these sequences carry information necessary for establishing a chromosome-like structure (Gutknecht et al. 1995).

Acknowledgements. We thank C.R. Carter, K. Watanabe and P.S. Short for providing some of the seed material. A.H. was supported by the Deutsche Forschungsgemeinschaft (Ho 1779/1-1).

References

Alfenito MR, Birchler JA (1993) Molecular characterization of a maize B chromosome centric sequence. Genetics 135:589–597

Beukeboom LW (1994) Bewildering Bs: an impression of the 1st B-chromosome conference. Heredity 73:328–336

Blunden R, Wilkes TJ, Forster JW, Jimenez MM, Sandery MJ, Jarp A, Jones RN (1993) Identification of the E3900 family, second family of rye B chromosome specific repeated sequences. Genome 36:706–711

Carr GD, Carr RL (1982) Micro- and nucleolar-organising B-chromosomes in *Calycadenia* (Asteraceae). Cytologica 47:79–87

Carter CR, Smith-White S (1972) The cytology of *Brachycome lineariloba* 3. Accessory chromosomes. Chromosoma 39:361–379

Donald TM, Leach CR, Timmis JN (1995) Ribosomal RNA genes and the B chromosome of *Brachycome dichromosomatica.* Heredity 74:556–561

Donald TM, Houben A, Leach CR, Timmis JN (1997) Ribosomal RNA genes specific to the B chromosomes in *Brachycome dichromosomatica* are not transcribed in leaf tissue. Genome (in press)

Dubcovsky J, Dvorak J (1995) Ribosomal RNA multigene loci – nomads of the triticeae genomes. Genetics 140:1367–1377

Eickbush DG, Eickbush TH, Werren JH (1992) Molecular characterization of repetitive DNA sequences from a B chromosome. Chromosoma 101:575–583

Finnegan EJ, Peacock WJ, Dennis E (1996) Reduced DNA methylation in *Arabidopsis thaliana* results in abnormal plant development. Proc Natl Acad Sci USA 93:8449–8454

Franks TK, Houben A, Leach CR, Timmis JN (1996) The molecular organisation of a B chromosome tandem repeat sequence from *Brachycome dichromosomatica.* Chromosoma 105:223–230

Fuchs J, Schubert I (1995) Localisation of seed protein genes on metaphase chromosomes in *Vicia faba* via fluorescent in situ hybridisation. Chromosome Res 3:94–100

Furuya T, Morgan R, Berger CS, Sandberg AA (1993) Presence of telomeric sequences on deleted chromosomes and their absence on double minutes in cell line HL-60. Cancer Genet Cytogenet 70:132–135

Green DM (1990) Muller's Ratchet and the evolution of supernumerary chromosomes. Genome 33:818–824

Gutknecht J, Sperlich D, Bachmann L (1995) A species specific satellite DNA family of *Drosophila subsilvestris* appearing predominantly in B chromosomes. Chromosoma 103:539–544

Hahn PJ (1993) Molecular biology of double minute chromosomes. BioEssays 5:477–484

Houben A, Kynast RG, Heim U, Hermann H, Jones RN, Forster JW (1996) Molecular cytogenetic characterisation of the terminal heterochromatic segment of the B-chromosome of rye (*Secale cereale*). Chromosoma 105:97–103

Houben A, Belyaev ND, Leach CR, Timmis JN (1997) Differences of histone H4 acetylation and replication timing between A and B chromosomes of *Brachycome dichromosomatica.* Chromosome Res 5:233–237

Ijdo JW, Wells RA, Baldini A, Reeders ST (1991) Improved telomere detection using a telomere repeat probe $(TTAGGG)_n$ generated by PCR. Nucleic Acids Res 19:4780

Jamilena M, Garrido-Ramos M, Ruiz Rejon C, Ruiz Rejon M (1994) A molecular analysis of the origin of the *Crepis capillaris* B chromosome. J Cell Sci 107:703–708

John UP, Leach CR, Timmis JN (1991) A sequence specific to B chromosomes of *Brachycome dichromosomatica*. Genome 34: 739–744

Jones RN (1995) Tansley Review No. 85, B chromosomes in plants. New Phytol 131:411–434

Leach CR, Donald TM, Franks TK, Spiniello SS, Hanrahan CF, Timmis JN (1995) Organisation and origin of a B-chromosome centromeric sequence from *Brachycome dichromosomatica*. Chromosoma 103:708–714

Miniou P, Jeanpierre M, Blanquet V, Sibilla V, Bonneau D, Herbelin C, Fisher A, Niveleau A, Viegas-Pequignot E (1994) Abnormal methylation pattern in constitutive and facultative (X inactive chromosome) heterochromatin of ICF syndrome. Hum Mol Genet 3:2093–2102

Morais-Cecilio L, Delgado M, Jones RN, Viegas W (1996) Painting rye B chromosomes in wheat: interphase chromatin organization, nuclear disposition and association in plants with two, three or four Bs. Chromosome Res 4:195–200

Pich U, Houben A, Fuchs J, Meister A, Schubert I (1994) Utility of DNA amplified by degenerate oligonucleotide-primed PCR (DOP-PCR) from the total genome and defined chromosomal regions of field bean. Mol Gen Genet 243:173–177

Sandery MJ, Forster JW, Blunden R, Jones RN (1990) Identification of a family of repeated sequences on the rye B chromosome. Genomce 33:908–913

Schubert I, Wobus U (1985) In situ hybridization confirms jumping nucleolus organizing regions in *Allium.* Chromosoma 92:143–148

Smith-White S, Carter CR (1970) The cytology of *Brachycome lineariloba*. 2. The chromosome species and their relationships. Chromosoma 30:129–153

Telenius H, Carter NP, Bebb CE, Nordenskjold A, Ponder BAJ, Tunnacliffe A (1992) Degenerate oligonucleotide-primed PCR: general amplification of target DNA by a single degenerate primer. Genomics 13:718–725

Watanabe K, Carter CR, Smith-White S (1975) The cytology of *Brachycome lineariloba* 5. Chromosome relationships and phylogeny of the race A cytodemes (n=2). Chromosoma 52:383–397

Watanabe K, Carter CR, Smith-White S (1976) The cytology of *Brachycome lineariloba.* 6. Asynchronous chromosome condensation and meiotic behaviour of *B. lineariloba* A (n=2)×*B. campylocarpa* A (n=4). Chromosoma 57:319–331

Watanabe K, Denda T, Suzuki Y, Kosuge K, Ito M, Short PS, Yahara T (1994) Chromosomal and molecular evolution in the genus *Brachycome* (Astereae). In: Hind DJN, Beebtje HJ (eds) Compositae: systematics. Proceedings of the International Compositae Conference, Royal Botanic Gardens, Kew, vol 1. pp 705–722

Watson JM, Meyne J, Graves JM (1986) Ordered tandem arrangements of chromosomes in the sperm heads of monotreme mammals. Proc Natl Acad Sci USA 93:10200-10205

Wienand U, Feix C (1980) Zein-specific restriction enzyme fragments of maize DNA. FEBS Lett 116:14–16

Wintersberger E (1994) DNA amplification: new insights into its mechanism. Chromosoma 103:73–81

Yakura K, Tanifuji S (1983) Molecular cloning and restriction analysis of *Eco* R1-fragments of *Vicia faba* rDNA. Plant Cell Physiol 24:1327–1330

A14 Houben, A., Kynast, R.G., Heim, U., Hermann, H., Jones, R.N., and Forster, J.W. (1996). Molecular cytogenetic characterisation of the terminal heterochromatic segment of the B-chromosome of rye (*Secale cereale*). Chromosoma 105, 97-103.

Chromosoma (1996) 105:97–103

CHROMOSOMA

Molecular cytogenetic characterisation of the terminal heterochromatic segment of the B-chromosome of rye (*Secale cereale*)

Andreas Houben[1,*], **Ralf G. Kynast**[1], **Ute Heim**[1], **Hanno Hermann**[1], **R. Neil Jones**[2], **John W. Forster**[2]

[1] Institut fur Pflanzengenetik und Kulturpflanzenforschung, D-06466 Gatersleben, Germany
[2] Genetics Group, Institute of Biological Sciences, University of Wales, Aberystwyth, Dyfed SY23 3DD, Wales, UK

Received: 31 December 1995; in revised form: 13 March 1996 / Accepted: 1 May 1996

Abstract. The terminal heterochromatic segments of the long arms of 20 rye B-chromosomes were isolated by means of laser microdissection technology. Also the remaining portions of the long arms, along with the short arms of the same chromosomes were isolated. Each sample was used for degenerate oligonucleotide primer-polymerase chain reaction (DOP-PCR) amplification reactions. The resulting products were used as probes for chromosome in situ hybridisation experiments, and in Southern hybridisation to digests of 0B and +B DNA. Competition hybridisation of these probes with 0B DNA allowed the detection of B-specific sequences. The terminal heterochromatin of the rye B-chromosome contains both B-specific sequences and sequences also present on the A-chromosomes of rye. The B-specific D1100 family is the major repeat species located in the terminal heterochromatin. Primers designed to the cloned sequence (E1100) were used to search for related low copy sequences in 0B DNA. The sequences of the PCR products revealed no similarities to that of the clone E1100 except for the primer sequences. The possible origin of this sequence is discussed in the context of models for the evolution of the rye B-chromosome.

Introduction

B-chromosomes (Bs) occur in many species of higher plants and animals over a wide geographical distribution (Jones and Rees 1982; Jones 1995). Although Bs have been well described cytologically, the origin and mode of evolution of these supernumerary chromosomes remains unknown. They differ from the normal (A-chromosome) nuclear complement in morphology and pairing behaviour, and are fully dispensable for growth and development. In most cases, the phenotypic effects of Bs are either selectively neutral or deleterious in high numbers. However, in the wild chive species *Allium schoenoprasum* they may show some adaptive functions (Plowman and Bougourd 1994).

Rye provides one of the best examples of studies of B-chromosome polymorphisms. On the basis of pairing studies in F_1 hybrids between Bs of rye lines of different origin, Niwa and Sakamoto (1995) suggested a monophyletic origin for the Bs of rye. The DNA composition of rye Bs has been extensively investigated in recent years, in order to explain their origin and genetic properties. Timmis et al. (1975) demonstrated identical GC content and reassociation kinetics of DNA from plants with and without Bs. Rimpau and Flavell (1975) observed similar quantities and complexity of repetitive DNA in As and Bs of rye. However, in situ hybridisation studies (Appels et al. 1978; Cuadrado and Jouve 1994; Wilkes et al. 1995) have demonstrated that certain repetitive sequence families, which are characteristic of the rye As, are not regularly present on the Bs. Specific sequences for the rye B were identified as intense bands in restriction digests of DNA from B-carrying genotypes, and are designated as D1100 (Sandery et al. 1990) and E3900 repetitive families (Blunden et al. 1993).

A direct approach to the isolation of sequences from the rye B is by microdissection. This technique, linked to microcloning into phage vectors, allowed the isolation of a sequence common to As and Bs (Sandery et al. 1991). More recently, microdissection followed by linker-adaptor polymerase chain reaction (PCR) amplification generated a small library of B-derived sequences, which is substantially composed of A+B sequences (A. Houben, R.N. Jones, R. Schlegel, R. Blunden, H.M. Williams, J.W. Forster, unpublished). Therefore, the available molecular evidence suggests that the rye Bs are predominantly composed of sequences shared with the As, but also contain some specific sequences.

**Present address:* Department of Genetics, The University of Adelaide, South Australia 5005, Australia

EMBL and Genbank accession numbers: Z54196 (E1199); Z54278 (B1)

Edited by: R. Appels

Correspondence to: A. Houben, U. Heim

Several studies have used the genomic in situ hybridisation (GISH) technique to probe B-chromosome preparations with labelled 0B genomic DNA (Tsujimoto and Niwa 1992; Wilkes et al. 1995). The majority of the Bs is labelled by this approach except for the terminal heterochromatic region, which is the known location of the D1100 and E3900 family sequences. For this reason, we have targetted this chromosomal region by microisolation in order to determine the presence of both B-specific and A+B sequences. To explore the origin of B-specific sequences, PCR amplification products recovered from genomic 0B DNA using specific primers for the E1100 clone were sequenced.

Materials and methods

Plant material and cytological analysis. The plant material was derived from the Aberystwyth experimental rye B population. Plants carrying 0, 2 and 4 Bs were identified by cytological analysis and cultivated in the greenhouse. The distribution and intensity of Giemsa bands on C-banded chromosomes were determined with an interactive computer-assisted image processing system (UNICHRO; Ahne et al. 1989) as described by Houben et al. (1990).

Laser microdissection, degenerate oligonucleotide primed PCR (DOP-PCR) and DNA cloning. In order to arrest cell divisions in root tip meristems, mitoses were synchronised according to the method of Pan et al. (1993). After fixation for 5 min in 45% acetic acid, root tips were rinsed in water and the meristematic tips were removed and digested using an enzyme mixture of 2.5% (w/v) pectolyase Y-23 and 2.5% (w/v) cellulase Onozuka R10 in 75 mM KCl, 7.5 mM EDTA, pH 4.0 at room temperature (Kakeda et al. 1991). After maceration for 30 min, the root tips were briefly washed in 45% acetic acid and squashed on coverslips using the dry ice technique. Air-dried preparations were used immediately or stored in 98% ethanol at –70°C for up to several weeks.

A Zeiss Axiovert 35 inverted microscope equipped with a micromanipulator (5170, Eppendorf), a stepping motor driven x, y stage (Maerzhauser), a pulsed nitrogen laser with adaptation optics (SL Microtest) and an image analysis control unit (CUT and RUB; Tech. Hand.) was used for chromosome microdissection (Houben et al. 1996). The terminal heterochromatic part (Fig. 1) was dissected from 20 Bs to generate DNA pool I, while the complementary portions of the Bs formed DNA pool II.

Both pools were collected in a 1 ml droplet containing proteinase K (Boehringer, 0.5 mg/ml) in 10 mM TRIS-HCl, pH 8.0, 10 mM NaCl, 0.1% (w/v) SDS and overlaid with water-saturated paraffin oil (Schondelmaier et al. 1993). The DNA was amplified according to Pich et al. (1994) using the degenerate oligonucleotide primer MW-6 (Telenius et al. 1992).

The PCR amplification products of pools I and II were separated by electrophoresis on 1.2% (w/v) agarose gels and transferred by alkaline blotting (Reed 1986) to Hybond N+ nylon membranes (Amersham). The remaining PCR products of pool I were digested with *Sau*3A and purified using a QIAquick-spin column (QIAGEN). The digested PCR products were cloned into the *Bam*HI site of the vector Bluescript KS+ (Stratagene) and propagated in the *Escherichia coli* strain DH5a.

Eighty colonies were selected for the isolation of recombinant clones. The sizes of the inserts were determined on agarose gels. Two milligrams of DNA from each undigested recombinant plasmid was dot-blotted onto membranes using the alkaline method. To estimate the ratio of relative abundance of high and low copy sequences and the presence of B-specific repetitive sequences, the membranes were sequentially probed with 0B and 2B rye genomic DNA oligo-labelled in the presence of [^{32}P]dCTP (Feinberg and Vogelstein 1984).

Genomic DNA isolation and Southern blotting. Genomic DNA was isolated from leaf tissue. DNA samples from rye plants with 0, 2 and 4 Bs were digested with the restriction endonucleases *Hin*dIII, *Dra*I, *Rsa*I, *Eco*RI and *Eco*RV, electrophoresed in a 0.8% (w/v) agarose gel and transferred by alkaline transfer to Hybond N+ membranes.

Competition hybridisation. In order to detect B-specific DNA sequences among blotted total genomic DNA, labelled DNA from the entire microisolated B was hybridised together with unlabelled total 0B rye DNA to the 0B/+B digests. The unlabelled DNA was present in a 25-fold excess over the labelled DNA. For labelling and detection the ECL-direct system (Amersham) was used according to the manufacturer's instructions, with the following modifications:

a. The B-chromosome DNA was labelled for 20 min at 37°C.
b. The filters were treated with 250 ml/cm^2 of ready-to-use gold buffer (Amersham) supplemented with Na^+ for 30 min at 42°C to fix the stringency at 85% (Meinkoth and Wahl 1984).
c. The filter bound DNA was hybridised with unlabelled rye 0B DNA (250 ng/cm^2) for 30 min at 42°C in the same buffer.
d. Hybridisation was overnight at 42°C in the same buffer with the additional presence of 10 ng/cm^2 labelled probe DNA.
e. The filters were washed at 42°C in the presence of 6 M urea to a stringency of 92%.
f. Luminography was performed by exposure for 80 min to ECL-Hyperfilm.

PCR with E1100-specific primers. The PCR was performed in a 50 µl volume using 20 ng of genomic DNA (0B or +B) as the template. The other components of the reaction were 0.2 mM dNTPs, 0.2 µM primers (5′-GCTTGCACCGGCTTCGTCCCG-3′ and 5′-GTGTACTTGAGACACGCAAGC-3′), 2 mM $MgCl_2$, 50 mM KCl, 10 mM TRIS-HCl and 0.1% (v/v) Triton X-100. After denaturation 2.5 U *Taq* DNA polymerase (Promega) was added and five cycles of amplification were performed under the following conditions: 94°C, 0.5 min; 57°C, 1.2 min; 72°C, 1.2 min. Subsequently, 25 cycles at 94°C, 0.2 min; 60°C, 1 min; 72°C, 0.25 min were followed by a final primer extension step for 5 min.

The blunt-ended PCR products from 0B DNA were ligated into the *Sma*I site of the Bluescript KS+ vector and sequenced.

Sequence analysis. DNA clones were sequenced using an Automated Laser Fluorescent (A.L.F.) DNA Sequencer (Pharmacia LKB Biotechnology). The nucleotide sequences appeared in the EMBL, GenBank databases under the accession numbers Z54196 (E1100) and Z54278 (B1). The EMBL database was screened for homology to other sequences. The computer program PC/Gene (Release 6.8, IntelliGenetics) was used for sequence comparison.

Fluorescence in situ hybridisation (FISH). The B-chromosome DNAs of pools I and II were labelled separately by PCR using MW-6 primers and biotin-16-dUTP according to the method of Fuchs et al. (1994). The insert of clone B1, obtained from pool I DNA, was biotinylated by nick-translation. FISH was carried out as described by Fuchs and Schubert (1995). Hybridisation of the biotinylated probes was detected by the use of a streptavidin-FITC-antistreptavidin-FITC system (Camon). (ATC is fluorescein isothiocyanate.) Epifluorescence signals were recorded on Kodak Ektachrome 400 film.

Results and discussion

Isolation and characterisation of microclones

The distal part of the long arm of the rye B (pool I), corresponding to the large Giemsa C-band (Fig. 1) and the

complementary part of this chromosome (pool II) were reciprocally isolated by microdissection (Fig. 2). The DNA of the isolated chromosome segments was amplified by DOP-PCR, which provides a simpler alternative to other microcloning methods. The amplification products from both pools formed smears of 0.1–1.8 kb after gel electrophoresis. The B-specific clones E1100 (Sandery et al. 1990) and E3900 (Blunden et al. 1993; Blunden 1994) hybridised to the pool I PCR products, indicating that representative B-terminal DNA amplification has occurred.

A selected set of approximately 1000 microclones derived from pool I PCR products were analysed to determine the average insert size, which was 340 bp. Sequential dot-blot hybridisation with labelled total genomic rye DNA was performed to analyse further the composition of this clone collection.

Although the sequence families D1100 and E3900 occur in this chromosomal region , after sequential hybridisation with genomic 0B and +B DNA all these microclones hybridised with comparable intensity. This indicates that, even in this microclone library, the sequences D1100 and E3900 are less than l% representative.

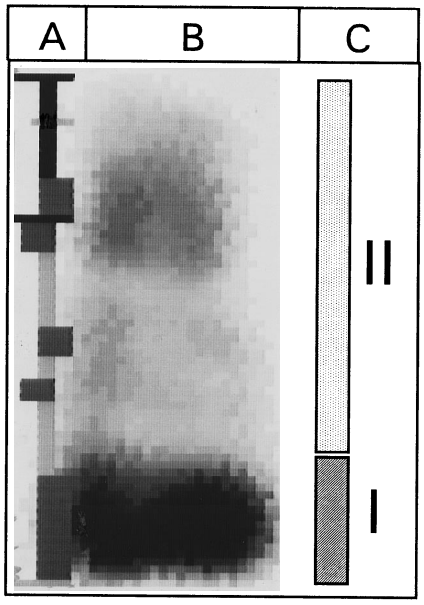

Fig. 1A–C. The Giemsa C-banded rye B-chromosome. **A** The distribution of bands after analysis of a digitised picture **B** of a single B-chromosome using the programme UNICHRO. **C** Scheme of the microisolated parts (pools I and II) of the chromosome

After 1 day of exposure, 96% of the plasmids showed medium to strong signals due to the presence of repetitive sequences. This is in contrast to the behaviour of a whole B-chromosome microclone library, in which 49% of the clones showed weak or no signals, and 51% a moderate to strong signal when hybridised with labelled genomic 0B/+B rye DNA (Houben 1993). The higher proportion of microclones with moderate to strong signals indicates that the distal portion of the long arm is almost exclusively composed of repetitive sequences, but there is no evidence of B-chromosome specificity.

Hybridisation of DOP-PCR products to 0B/+B genomic digests

The labelled DNA probes derived from PCR-amplified DNAs of pools I and II were used to probe digested 0B/+ B rye genomic DNA. As the probes contain sequence mixtures of varying copy number, the resulting hybridisation patterns are dominated by the highly repeated sequences. Hybridisation of labelled pool I PCR products to *Dra*I and *Eco*RI digests revealed hybridisation to 0B and +B DNA, but with additional B-specific sites of hybridisation (Fig. 3B). *Rsa*I- and *Hin*dIII-digested genomic DNA failed to show such differences. With both *Dra*I and *Eco*RI, specific bands of 1–2 kb in size were apparent. The intensity of these bands is positively correlated with the number of Bs, especially in the *Eco*RI digests. Hybridisation of the B-specific clones E1100 (Fig. 3C) and E3900 (Fig. 3D) to the same filters shows B-specific bands, which in some cases correspond to those seen with the pool I probe. The pool II PCR products also produce some specific bands in the 1.0–1.2 kb region in *Eco*RI and *Dra*I digests, although the overall hybridisation pattern show greater similarity between 0B and +B digests (Fig. 3A). This may indicate that copies of the known B-specific repeat families are present at locations on the B other than the terminal heterochromatin, but are not detectable by FISH.

Detection of B-specific sequences by competition hybridisation

PCR amplification products from both pools were mixed and labelled using the ECL system and hybridised to 0B/+B digests in the presence of a 25-fold excess of unlabelled 0B genomic rye DNA. The resulting luminograph (Fig. 4) showed prominent bands with greater intensity at approximately 0.8, 0.9 and 1.6 kb in *Dra*I di-

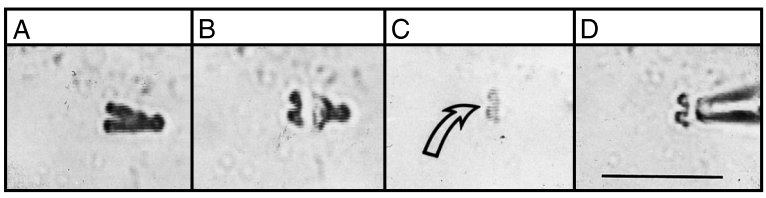

Fig. 2A–D. Microdissection of the distal end of the long arm of the rye B-chromosome to generate pool I DNA. **A** Before, **B** during and **C** after the oblation of the remaining portion of the chromosome by the UV-microlaser beam and **D** the isolation of the remaining chromosome segment using a microneedle. Bar represents 10 μm

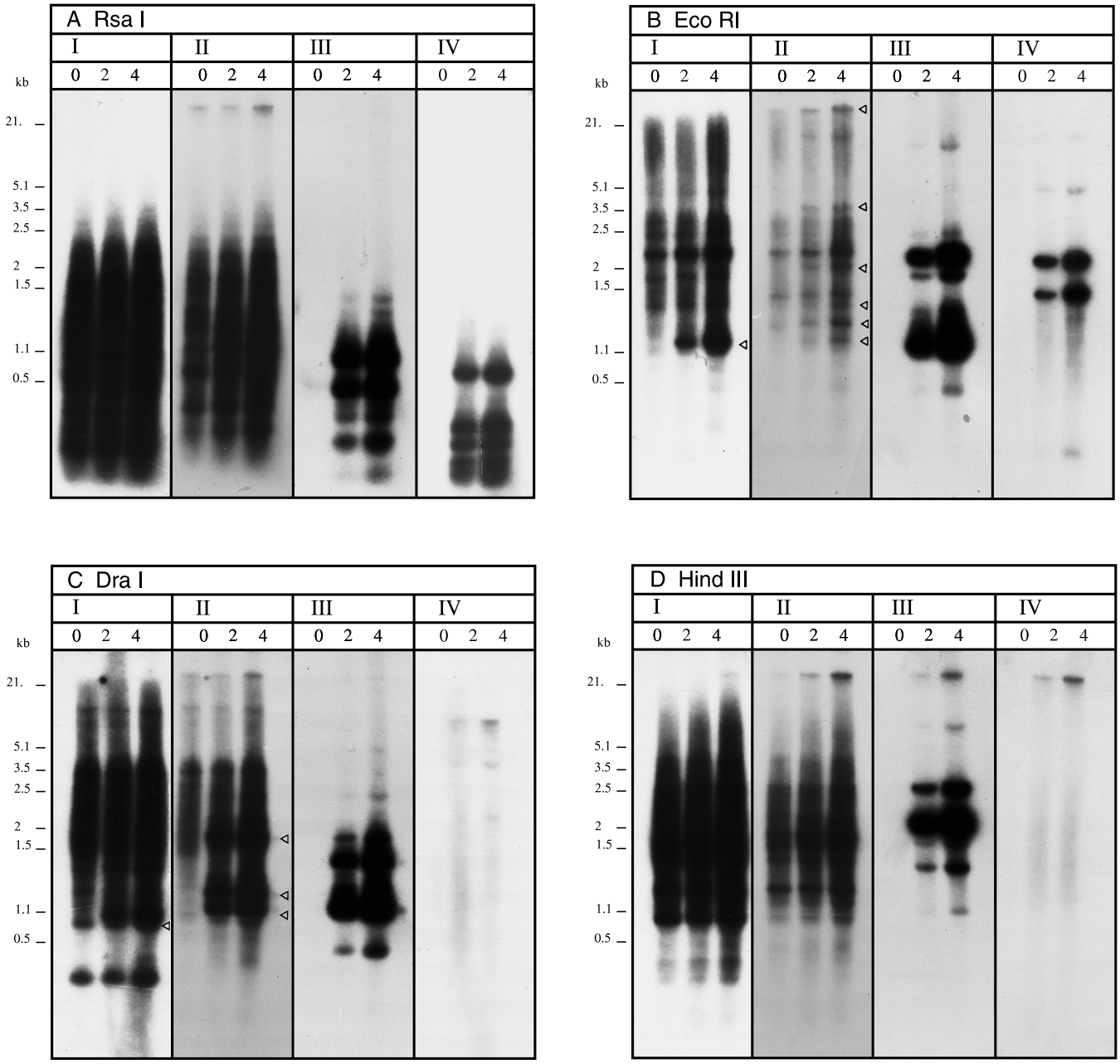

Fig. 3A–D. Sequential Southern hybridisation of 0B, 2B and 4B DNA digested with **A** *Rsa*I, **B** *Eco*RI, **C** *Dra*I and **D** *Hin*dIII with labelled *I* pool II PCR (polymerase chain reaction) DNA, (*arrow heads* mark B-chromosome specific fragments), *II* pool I PCR DNA (*arrow heads* mark B-chromosome specific fragments), *III* E1100 DNA and *IV* E3900 DNA

gests, and 1.6 kb in *Hin*dIII digests, with higher number of Bs. These fragments correspond to B-specific fragments probed by pool I PCR products, and possibly to fragments detected by the E1100 clone. In the *Hin*dIII digests were apparently revealed a small amount of 1.6 kb sequence present in 0B DNA, although such sequences are not detected in the other digests. Weak signals are also detected between 0.9 kb and 3.5 kb on hybridisation of 2B as well as 4B DNA digested by *Eco*RI and *Eco*RV, apparently indicating lower copy number. The fragment sizes obtained are not clearly attributable to the D1100 or E3900 family sequence.

The experiments with direct and competition hybridisation demonstrate the feasibility of identifying chromosome-specific sequences directly by the use of PCR-amplified microisolated DNA as a probe. In the terminal heterochromatin of the B-chromosome, some of the specific sequences seem to correspond in part to the known D1100 and E3900 families. The distal portion of the long arm of the B may also contain other B-specific repeat familes, and microdissection may be employed to identify and isolate them in due course. At the same time, it is clear that the pool I microisolated DNA contains substantial numbers of A+B repetitive sequences,

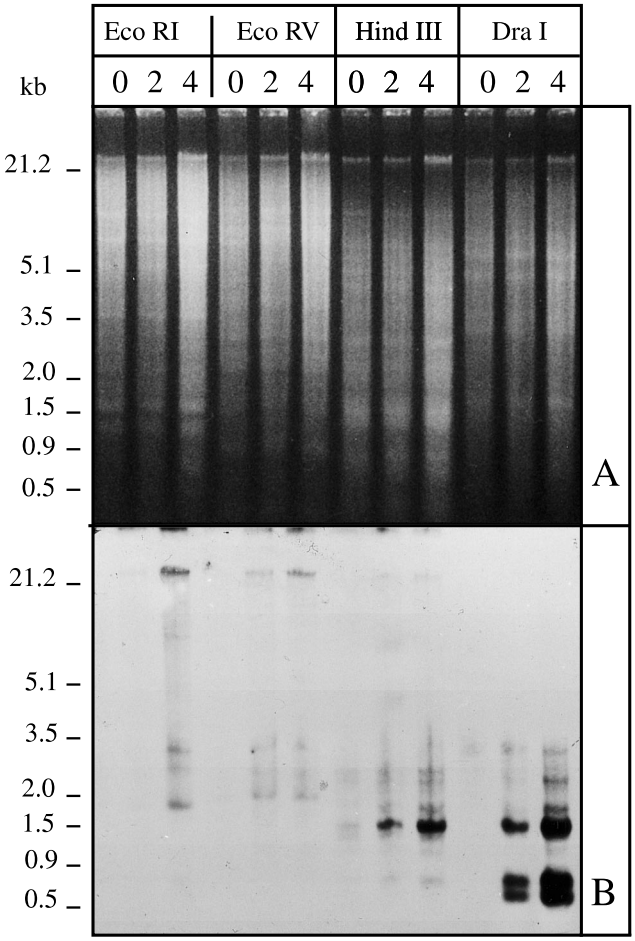

Fig. 4. A Electrophoretogram of 0B, 2B and 4B rye genomic DNA digested with *Eco*RI, *Eco*RV, *Hin*dIII and *Dra*I. **B** Southern hybridisation of the digests using the ECL system. Labelled PCR-amplified DNA from the entire B-chromosome was used as the probe, after pre-hybridisation of the filter with 0B rye genomic DNA

despite the exclusion of this region during GISH using 0B DNA (Tsujimoto and Niwa 1992). Shared repeated sequences may be interspersed among the B-specific sequences.

FISH using complex probes derived from different parts of the rye Bs

The pool I PCR product was used as a probe for in situ hybridisation to metaphase spreads from root tips of +B plants and it shows preferential hybridisation to the heterochromatic end of the long arm of the Bs (Fig. 5). Additional signals of lower intensity were also detected in As in Giemsa C-band positive regions. These regions, both on the As and Bs, correspond to sites of highly repetitive DNA content (Cuadrado and Jouve 1994). In situ hybridisation of pool II PCR product produced a dispersed signal on all As and Bs (data not shown). This confirms that high copy B-specific sequences are confined to the terminal locus only.

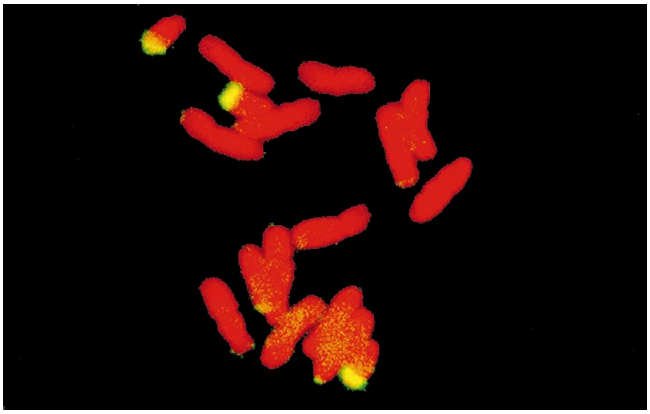

Fig. 5. In situ hybridisation of labelled pool I PCR products to a mitotic metaphase spread from a rye plant with 14 A-chromosomes plus 3 B-chromosomes. Metaphase cell showing preferential hybridisation to the heterochromatic end of the long arm of the B-chromosomes and additional signals of lower intensity to the Giemsa C-band positive regions of the A-chromosomes. Bar represents 10 μm

Characterisation of B-derived cloned sequences

The sequences of two B-derived clones were determined. Clone B1 was randomly selected from the pool I microlibrary. It shows an A+T content of 53%, and no significant match to known sequences in the EMBL database. Southern hybridisation of this cloned sequence to 0B/+B DNA digests shows a pattern consistent with an A+B dispersed repetitive sequence. This was further confirmed by using in situ hybridisation, in which both As and Bs showed a faint homogenous signal (data not shown).

The B-specific clone E1100 (Sandery et al. 1990) was also sequenced. The 1047 bp insert contained one direct repeat and two inverted repeats longer than 10 bp. No known transposable genetic elements are associated with the sequence. No sequence similarity to other B-specific sequences of plants (John et al. 1991; Alfenito and Birchler 1993) or to other sequences in the EMBL database was detected.

Search for E1100-related sequences in As

Although the D1100 and E3900 repeat families show B specificity in Southern hybridisations, it is possible that related sequences are present at low copy number in the As of rye. Primers were designed using the E1100 sequence, and used to perform PCR on 0B DNA in order to detect E1100-related sequences in As. A faint band at 1.2 kb was obtained (Fig. 6I), and filter hybridisation of labelled 0B DNA to the same PCR products revealed bands of 1.2 kb and larger.

PCR amplification of +B DNA using the same primers produced amplification products of 0.4 and 1.8 kb. The signals after filter hybridisation with rye 0B DNA showed a size distribution of 1.2 kb and larger (Fig. 6II). The hybridisation of the labelled E1100 clone insert to the +B PCR products produced a different hybridisation

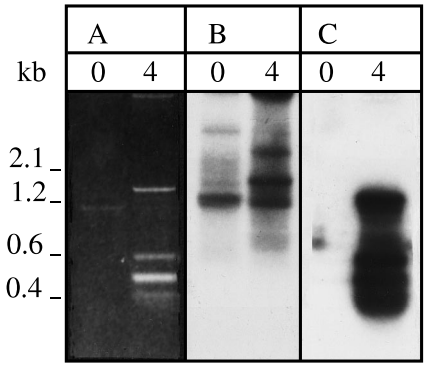

Fig. 6. A PCR products obtained with primers specific for the sequence of the clone E1100 using 0B and +B genomic DNA as templates. **B** Southern hybridisation to the PCR products using labelled 0B DNA as a probe. **C** Southern hybridisation to the PCR products using labelled E1100 clone DNA as a probe

pattern with strong signals between 0.2 and 1.2 kb, while the PCR products obtained with 0B DNA showed no signals after hybridisation with the clone (Fig. 6III).

The PCR products obtained from E1100 primer - specific amplification of 0B rye DNA were cloned and four of the resulting clones, designated 0B-2, 0B-6, 0B-8 and 0B-9, were sequenced. The sequence of a representative clone was compared with that of E1100. The sequence similarity was less than 50%, suggesting that no direct ancestral sequence to the D1100 family was detectable in A-chromosome DNA with the chosen primer combination.

Most models for the origin of supernumerary chromosomes are based on an origin from within the genome, perhaps through chromosome fragmentation (Wiebe et al. 1974) . This is compatible with the observation of the high level of sequence identity between the rye As and Bs. However, these models present a problem when explaining the evolution of B-specific sequences such as the D1100 family. One possibility is that the D1100 family is descended from an ancient ancestral sequence that was present on the As, but has diverged on both As and Bs since the origin of the B. Because of the dispensable nature of Bs, sequences are likely to be prone to particularly rapid sequence evolution unconstrained by selection, as predicted by Muller's Ratchet (Green 1990). In the case of the D1100 family, divergence may have been accelerated by a combination of mutation, replication slippage and unequal sister chromatid exchange. The latter process could account for the amplification of these sequence families from their putative low copy precursors, to generate the existing tandem arrays at the terminal heterochromatic locus (Smith 1973). Alternatively, saltatory amplification may have arisen through mechanisms such as 'rolling circle' replication (Hourcade et al. 1973). Another possible source of Bs is interspecific hybridisation (Leach et al. 1995).

In summary, the results presented here demonstrate the value of the microisolation technique for the identification of chromosome-specific sequences in particular cytological locations, along with the sequence characteristics of both B-specific and common cloned sequences. Future work in this area will concentrate on the identification of further elements of B-chromosome structure, in particular low copy sequences that may be used to deduce the detailed origin of the B.

Acknowledgements. We are grateful to I. Schubert for discussion and for critical reading of the manuscript. The skilful technical assistance of Birgit Fischer and Barbara Hildebrandt is gratefully acknowledged. Parts of this work were supported by grants from the Deutsche Forschungsgemeinschaft (Schu 951/2-1, Ho 1779/1-1).

References

Ahne R, Huhn P, Laumer N, Zernecke, F (1989) Interactive computer assisted chromosome analysis: a basic software package. Arch Züchtungsforsch 19:133–140

Alfenito MR, Birchler JA (1993) Molecular characterisation of a maize B-chromosome centric sequence. Genetics 135:389–397

Appels R, Driscoll C, Peacock WJ (1978) Heterochromatin and highly repeated DNA sequences in rye (*Secale cereale*). Chromosoma 70:67–89

Blunden R (1994) Molecular analysis of the rye B-chromosome. Ph.D. Thesis, University of Wales

Blunden R, Wilkes TJ, Forster JW, Jimenez MM, Sandery MJ, Karp A, Jones RN (1993) Identification of the E3900 family, a second family of rye B-chromosome specific sequences. Genome 36:706–711

Cuadrado A, Jouve N (1994) Highly repetitive sequences in B-chromosomes of *Secale cereale* revealed by fluorescence in situ hybridisation. Genome 37:709–712

Feinberg AP, Vogelstein B (1984) A technique for radiolabelling DNA restriction fragments to high specific activity. Anal Biochem 137:266–267 (Addendum)

Fuchs J, Schubert I (1995) Localisation of seed protein genes on metaphase chromosomes of *Vicia faba* via fluorescent in situ hybridisation. Chromosome Res 3:94–100

Fuchs J, Pich U, Meister A, Schubert I (1994) Differentiation of field bean heterochromatin by in situ hybridisation with a repeated *Fok*I sequence. Chromosome Res 2:25–28

Green DM (1990) Muller's ratchet and the evolution of supernumerary chromosomes. Genome 33:818–824

Houben A (1993) Experimentelle Untersuchungen zur Isolierung individueller Pflanzenchromosomen and deren Nutzungsmöglichkeiten. PhD Thesis, Martin Luther University, Halle-Wittenberg

Houben A, Schlegel R, Ahne R, Huhn P (1990) C-banding and computer assisted chromosomal analysis of wheat (*Triticum aestivum* L. cv 'Chinese Spring'). Arch Züchtungsforsch 20: 133–143

Houben A, Franke J, Ahne R (1996) A computer assisted system combining image analysis and chromosome microdissection. Microsc Res Tech (in press)

Hourcade D, Dressler D, Wolfson J (1973) The amplification of ribosomal RNA genes involving a rolling circle intermediate. Proc Natl Acad Sci USA 70:2926–2930

John UP, Leach CR, Timmis JN (1991) A sequence specific to B-chromosomes of *Brachycome dichromosomatica*. Genome 34: 739–744

Jones RN (1995) Tansley review no. 85. B chromosomes in plants. New Phytol 131:411–434

Jones RN, Rees H (1982) B-chromosomes. Academic Press, London

Kakeda K, Fukui K, Yamagata H (1991) Heterochromatic differentiation in barley chromosomes revealed by C- and N-banding techniques. Theor Appl Genet 81:144–150

Leach CR, Donald TD, Franks TK, Spiniello SS, Hanrahan CF, Timmis JN (1995) Organisation and origin of a B chromo-

some centromeric sequence from *Brachycome dichromosomatica*. Chromosoma 103:708–714
Meinkoth J, Wahl G (1984) Hybridisation of nucleic acids immobilised on solid supports. Anal Biochem 138:267–284
Niwa K, Sakamoto S (1995) Origin of B-chromosomes in cultivated rye. Genome 38: 307–312
Pan WH, Houben A, Schlegel R (1993) Highly effective cell synchronisation in plant roots by hydroxyurea and amiprophosmethyl or colchicine. Genome 36:387–390
Pich U, Houben A, Fuchs J, Meister A, Schubert I (1994) Utility of DNA amplified by degenerate oligonucleotide-primed PCR (DOP-PCR) from the total genome and defined chromosomal regions of field bean. Mol Gen Genet 243:173–177
Plowman AB, Bougourd SM (1994) Selectively advantageous effects of B-chromosomes on germination behaviour in *Allium schoenoprasum* L. Heredity 72:587–593
Rimpau J, Flavell RB (1975) Characterisation of rye B-chromosome DNA by DNA/DNA hybridisation. Chromosoma 52: 207–217
Sandery MJ, Forster JW, Blunden R, Jones RN (1990) Identification of a family of repeated sequences on the rye B-chromosome. Genome 33:908–913
Sandery MJ, Forster J, Macadam SR, Blunden R, Jones RN, Brown SDM (1991) Isolation of a sequence common to A- and B-chromosomes of rye (*Secale cereale*) by microcloning. Plant Mol Biol Rep 9:21–30
Schondelmaier RM, Jahoor A, Houben A, Graner A, Koop HU, Herrmann RG, Jung C (1993) Microdissection and microcloning of the barley (*Hordeum vulgare* L.) chromosome 1HS. Theor Appl Genet 86:629–636
Smith UP (1973) Unequal crossing over and the evolution of multigene families. Cold Spring Harbor Symp Quant Biol 38: 507–514
Telenius H, Nigel PC, Bebb CE, Nordenskjold M, Ponder B, Tunnacliffe AJ (1992) Degenerate oligonucleotide-primed PCR: general amplification of target DNA by a single degenerate primer. Genomics 13:718–725
Timmis JN, Ingle J, Sinclair J (1975) The genomic quality of rye B-chromosomes. J Exp Bot 26:367–378
Tsujimoto H, Niwa K (1992) DNA structure of the B-chromosome of rye revealed by in situ hybridisation using repetitive sequences. Jpn J Genet 67:233–241
Wiebe GA, Ramage RT, Eslick RF (1974) Eight paired barley lines. Barley Genet Newslett 4:93–95
Wilkes TM, Francki MJ, Langridge P, Karp A, Jones RN, Forster JW (1995) Analysis of rye B-chromosome structure using fluorescence in situ hybridisation (FISH). Chromosome Res 3: 466–472

A15 Jones, N., and Houben, A. (2003). B chromosomes in plants: escapees from the A chromosome genome? Trends Plant Sci 8, 417-423.

B chromosomes in plants: escapees from the A chromosome genome?

Neil Jones[1] and Andreas Houben[2]

[1]The Institute of Biological Sciences, The University of Wales Aberystwyth, Cledwyn Building, Aberystwyth, UK SY23 3DD
[2]The Institute of Plant Genetics and Crop Plant Research (IPK), 06466 Gatersleben, Germany

B chromosomes are dispensable elements that do not recombine with the A chromosomes of the regular complement and that follow their own evolutionary track. In some cases, they are known to be nuclear parasites with autonomous modes of inheritance, exploiting 'drive' to ensure their survival in populations. Their 'selfishness' brings them into conflict with their host nuclear genome and generates a host–parasite relationship, with anti-B-chromosome genes working to ameliorate the worst of their excesses in depriving their hosts of genetic resources. Molecular studies are homing in on their sequence organization to give us an insight into the origin and evolution of these enigmatic chromosomes, which are, with rare exceptions, without active genes.

Supernumerary B chromosomes are recognized by three criteria: (i) they are dispensable and can be present or absent from individuals within a population; (ii) they do not pair or recombine with any members of the standard diploid (or polyploid) set of A chromosomes at meiosis; and (iii) their inheritance is non-mendelian and irregular. These criteria were embodied into the definition of a B chromosome as a 'dispensable supernumerary chromosome that does not recombine with the A chromosomes and which follows its own evolutionary pathway', which arose out of the First B-Chromosome Conference, held in Madrid in 1993 [1]. The simplicity of the definition belies the complexity of a diverse range of B-chromosome systems, which are found in many of the major groups of plants and animals. Earlier reviews (Table 1) contain the full story from the 1920s to the present but, to give this article some context, we profile the properties of B chromosomes, with their many generalities and exceptions (Box 1), and then deal with the more recent work that focuses on the question of the origin of B chromosomes and on aspects of their transmission and population dynamics.

Significance of B chromosomes

The significance of B chromosomes is to be found in their widespread occurrence in hundreds of flowering plants, and also in gymnosperms and in some lower forms such as ferns, bryophytes and fungi (they are also common in animals, including mammals) [2]. Owing to their particular properties, B chromosomes have been used to elucidate the function of post-translational histone modifications, such as histone H3 phosphorylation [3] and methylation [4]. They are of particular interest in maize (*Zea mays*), in which they have been extensively used in genetic analysis involving A–B translocations for mapping [5,6] and for the identification of centromere structure and size [7,8]. In other species, there is interest in their capacity to behave as diploidizing agents for chromosome pairing in certain allopolyploid hybrids [9,10] and their influence on recombination through the modulation of chiasma frequency and distribution in the A chromosomes (e.g. in rye) [2].

The question of their adaptive significance in natural populations has been argued over for decades, with the final position showing little if any substantial evidence to support such a role, with the possible exception of chives (*Allium schoenoprasum*) [11–13] and the fungal pathogen *Nectria haematococca* [14]. The emerging view in plants, principally from rye and maize, is that the B chromosomes are parasitic elements that maintain their polymorphism by DRIVE (see Glossary) and that there is a host–parasite relationship between the A and B chromosomes. The idea that B chromosomes are nuclear parasites is fascinating. It places them in the arena with other forms of selfish DNA

Table 1. Chronological list of selected reviews of B chromosomes

Date	Content of review
1982	Research monograph based on the world literature in plants and animals up to 1980, including references to all earlier reviews and an atlas of species with B chromosomes [2]
1982	B chromosomes in plants, particularly good on effects on chiasma frequency and chromosome pairing in hybrids [9]
1986	General review of the B chromosome of maize [59]
1988	The maize B chromosome as a model system for nondisjunction [60]
1990	Muller's Ratchet and the evolution of B chromosomes [61]
1990	Review of the Red Queen theory in the context of B chromosomes as parasites that induce changes in host recombination [62]
1991	Cytogenetics and plant breeding applications of B–A translocations in maize [5]
1991	B–A translocations and chromosome manipulations in maize [6]
1991	Cytogenetics of B chromosomes in crop plants, including species hybrids [63]
1991	Review of B chromosome 'drive' [64]
1993	B chromosomes of rye, Secale cereale [65]
1995	B chromosomes in plants [48]
2000	B chromosome evolution [32]
2002	Recent advances and insights on origin and evolution [26]

Corresponding author: Neil Jones (rnj@aber.ac.uk).

 1360-1385/$ - see front matter doi:10.1016/S1360-1385(03)00187-0

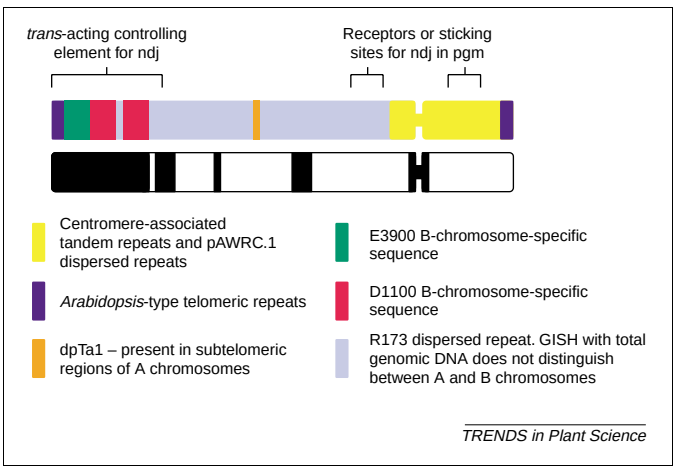

Fig. 1. The sequence, genetic and chromatin organization of the B chromosome of rye. The lower chromatid indicates C-band heterochromatic regions [65]. References: E3900 C-chromosome-specific sequence [45]; centromere-associated tandem repeats and pAWRC.1 dispersed repeats [66]. Abbreviations: ndj, nondisjunction; pgm, pollen grain mitosis.

in A-chromosome genomes (e.g. retro-elements), the difference being that they are autonomous in their inheritance and not constrained by the normal rules of chromosome behaviour. Little wonder, then, that interest is now focusing on 'transmission genes' and that a cocktail of molecular technologies is being thrown at B chromosomes in an attempt to make sense of them, especially their structure, origin and evolution.

Transmission genotypes

Östergren [15] first proposed that B chromosomes in plants could be viewed as parasitic chromosomes, based on his observations that progeny had more B chromosomes than their parents in crossing experiments. This idea did not meet with enthusiasm and much energy was invested in trying to show that their population polymorphisms could be explained in terms of Darwinian fitness and selection based on phenotypic effects. Much later, Kimura and Kayano [16] proposed an elegant model of the selfish nature of the B chromosomes of *Lillium callosum* based on meiotic drive in the female, and Nur provided convincing evidence of their parasitic nature in the grasshopper *Melanoplus femur-rubrum* [17] and the mealy bug *Pseudococcus affinis* [18,19]. Studies of the genetic control of transmission properties are best developed in rye and maize. In rye, the drive mechanism based on directed nondisjunction in gametophytes is strong and is under the control of the B chromosome itself (Figs 1,2). A computer

Glossary

Electrophoretic karyotypes: Descriptions of chromosome number and size produced by pulse-field gel electrophoresis in species with chromosomes that are too small to be seen by light microscopy (e.g. fungi).
Isochromosome: A chromosome with two genetically identical arms that are mirror images of each other.
Drive: With reference to B chromosomes, drive occurs when chromosome number in the gametes is greater than mendelian expectations (i.e. >0.5). In some cases, this can occur at meiosis, when the B chromosomes can migrate to one pole of the spindle during the first anaphase and then pass preferentially into the nucleus that is destined to form the egg cell (particularly where the spindle is asymmetrical). Alternatively, drive can occur in the first pollen grain mitosis, when the B-chromatids fail to separate and both pass into the generative nucleus. Nondisjunction at the second pollen mitosis followed by preferential fertilization of the egg by the B-containing sperm is another drive mechanism.
Microchromosomes: Tiny dot-like chromosomes that are too small for their centromeres and individual arms to be resolved under the light microscope (Fig. 2).
Telocentrics: Chromosomes that have their centromere at one end.

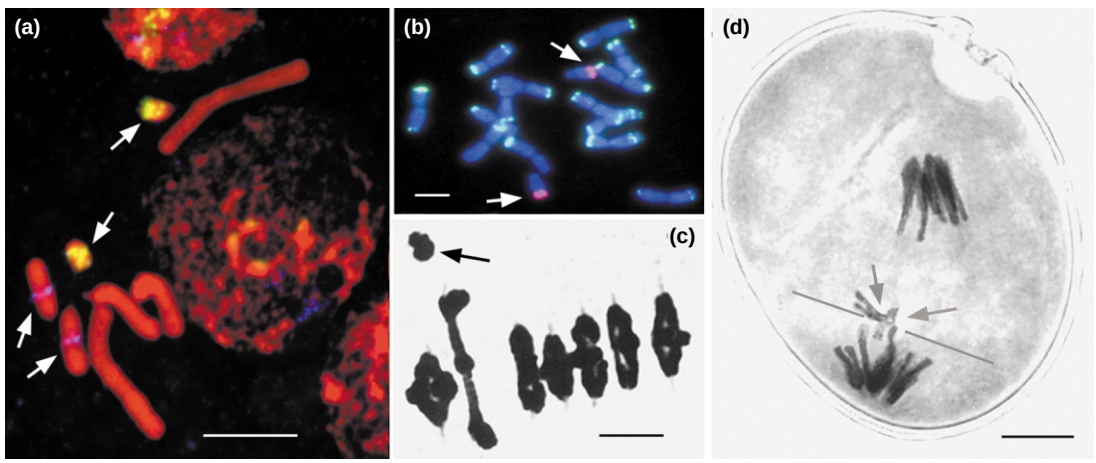

Fig. 2. B chromosomes in rye and in an Australian member of the Asteraceae, *Brachycome dichromosomatica* (synonym *Brachyscome dichromosomatica*), which has extraordinary genome plasticity. *B. dichromosomatica* is an annual outbreeder with only two pairs of A chromosomes, and it occurs in four karyotypically distinct cytodemes. In some cases, supernumerary A chromosome fragments can be present as well as different types of B chromosomes within a single plant; these are the somatically stable large B chromosomes and the somatically unstable dot-like micro-B chromosomes. (a) A mitotic cell of *B. dichromosomatica* ($2n$ = four A chromosomes + two standard B chromosomes + two iso-micro-B chromosomes) after fluorescence *in situ* hybridization performed with a micro-B-chromosome-specific probe {Bdm29 [67], yellow (arrowed)} and a standard B-chromosome centromere-specific probe {Bd49 [68], blue (arrowed)}. (b) C metaphase in a root meristem cell of rye with two B chromosomes (arrowed) and 14 normal A chromosomes, after fluorescence *in situ* hybridization using the pSc200 probe for subtelomeric repeats, which marks the ends of the A chromosomes, and the B-chromosome-specific probe D1100 (red), which marks the end of the long arm of the B chromosomes. Notice the absence of the A chromosome subtelomeric sequences on the B chromosomes (photographs courtesy of Robert Hasterok, and reproduced, with permission, of Ref. [56]). (c) Metaphase I of meiosis in a rye plant with single B chromosome (arrowed) and seven A chromosome bivalents. (d) First pollen grain mitosis in rye, showing directed nondisjunction of a single B chromosome towards the generative nucleus. The two chromatids of the B are held together at two sensitive sticking sites, one on each side of the centromere, and the centromeres are being pulled towards the poles. The spindle is asymmetrical and B chromatids are transiently held together in such a way that they become passively included in the generative nucleus. Because the same process happens on the female side in rye, the progeny will carry four B chromosomes in a 2B × 2B cross. The broken line represents the equator of the spindle. Arrows indicate sticking sites. Scale bars = 5 μm.

Box 1. General properties of B chromosomes and exceptions to them

Form and size
B chromosomes are smaller than A chromosomes (Fig. 2) except in a few cases, in which they are of equal size. They often have distinct centromere positions and can be readily identified at mitosis. Variants include B chromosomes as ISOCHROMOSOMES or TELOCENTRICS, and, in a few species, they appear as MICROCHROMOSOMES.

Structural polymorphism
The normal situation is for only one form of a B chromosome, with variants arising at mutation frequency. However, in at least 65 plant species, two or more polymorphic forms are known.

Chromatin
B chromosomes are described as heterochromatic in about half of plants that carry them [e.g. maize (*Zea mays*)]. In general, their heterochromatic content is similar to that of their A chromosomes (Figs 1,3–5).

Gene content and sequence organization
No B-chromosome-localized gene has been isolated in plants yet but they might have ribosomal DNA, some organize nucleoli and some have genetic information controlling their own transmission (e.g. in rye and maize). The strongest evidence to date for genes on B chromosomes comes from the fungal plant pathogen *Nectria haematococca*, which infects peas. Several genes determining pathogenicity have been identified and located to the 1.6 Mb supernumerary B chromosome in this fungus [14], and ELECTROPHORETIC KARYOTYPES indicate that several fungal species carry dispensable supernumerary B chromosomes [71]. The chromosomes of these fungi are too small to be resolved by light microscopy and so we have no information about how they behave at meiosis.

Mitotic stability
B chromosomes show a constant number in all somatic tissues in about a third of species for which information is available (i.e. 60 out of 180 species). Where there is instability, this can take the form of cell-to-cell variation in number or of absence from certain tissues (e.g. as in *Aegilops mutica*, in which there are no B chromosomes in the roots).

Meiotic behaviour
The only fixed rule is that, by definition, B chromosomes never pair or recombine with A chromosomes (Fig. 2c). Where they do pair, it is among themselves, forming multivalents when more than two are present. Two B chromosomes can have a regular meiotic process but, as univalents, they suffer elimination. There are more than 20 cases known in which B chromosomes are described as nonpairing (e.g. *Allium cernuum* and *Centauria scabiosa*) and, surprisingly, this does not lead to their loss from the populations. The meiotic properties of some B chromosomes endow them with 'drive', which is the case in female meiosis in *Lillium callosum*.

Inheritance
The inheritance of B chromosomes is non-mendelian and irregular owing to vagaries in the levels of paring, to degrees of meiotic elimination and to various drive processes. Drive is mostly caused by directed nondisjunction of sister chromatids at the first pollen mitosis, such that the generative nucleus carries the unreduced number, which then forms the sperm (e.g. many species of Gramineae). In rye, unusually, this drive happens on both the male (Fig. 2d) and the female side, and, in maize, the nondisjunction happens at the second pollen mitosis, followed by preferential fertilization by the B-chromosome-containing sperm. Meiotic drive and accumulation at earlier developmental stages in the germ line operate in a few cases. These irregularities in transmission generate a numerical polymorphism in populations, with a spectrum of B chromosome numbers including individuals with none. There is usually a modal number and an equilibrium frequency based on a balance between drive and the harmful effects caused by high numbers. Drive is by no means a universal process: it is known in ~60% of species for which transmission data are available. In the others, there is no known drive and no real understanding of how the population equilibrium frequencies are maintained.

Phenotypic effects
B chromosomes tend to be neutral in their phenotypic effects in low numbers and harmful in high numbers, affecting a wide range of nuclear [72] and exophenotypic characters. They are particularly detrimental to fertility and also have the enigmatic effect of influencing phenotype in certain cases according to their presence in odd or even-numbered combinations. Visualizing rye B chromosomes carried as an additional line in a wheat background with *in situ* hybridization probes indicates that they have a dose-dependent association at interphase, with even numbers (2B, 4B) having a greater preference for being physically associated than odd ones [72]. There might therefore be some relationship between their nuclear disposition and their phenotypic effects.

simulation of B-chromosome transmission in rye suggested that the main factor contributing to equilibrium B-chromosome frequencies in populations is the level of meiotic pairing among B chromosomes themselves, and is not determined solely by their negative phenotypic effects [20,21]. Subsequently, Puertas and colleagues identified high and low transmission lines from different rye populations, and developed the concept of 'high' and 'low' transmission genotypes [22]. An elegant set of experiments confirmed that the level of meiotic pairing was indeed the main factor influencing equilibrium B-chromosome frequencies in populations [23,24] and that the 'genes' controlling B-transmission rate are located on the B chromosomes themselves and that such 'genes' are the sites for chiasma formation [25,26].

The B chromosome of maize has a more complex genetic organization than that of rye, with at least four different regions (Fig. 3) that influence the nondisjunction process, which happens on the male side only. In addition, unpaired univalent B chromosomes can suppress their meiotic loss and enhance their transmission potential [27]. Transmission genotypes were first demonstrated by Rosato *et al.* [28], and it was later suggested that the genetic elements

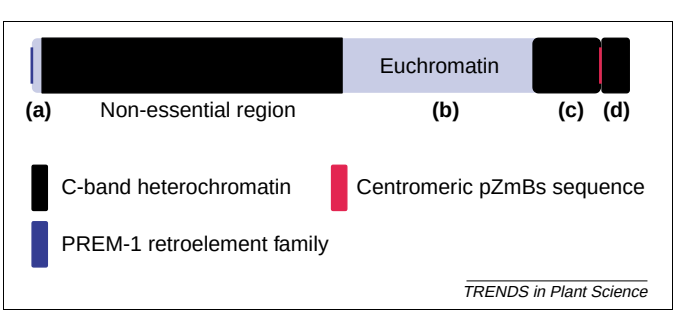

Fig. 3. The genetic, sequence and chromatin organization of the B chromosome of maize. (a) Distal euchromatic tip is *trans*-acting and essential for nondisjunction. (b) Proximal euchromatin is *trans*-acting and essential for nondisjunction. (c) Centromeric chromatin is a *cis*-acting receptor for nondisjunction. (d) Short arm and centromere region enhances nondisjunction. Loss of short arm reduces the rate of nondisjunction but does not prevent it. Regions controlling nondisjunction were identified by deletion studies [60]. References: PREM-1 retroelement family [37]; centromeric pZmBs sequence [53,54].

controlling transmission rate are located on the A chromosomes [29]. Subsequent experiments [30] determined that a single major gene in an A chromosome controls B-chromosome transmission rate in maize, and that it acts in the haploid egg cell at the time of fertilization. In high transmission lines, the *H* (high transmission) allele allows the B chromosome opportunistically to use the fertilization process to promote its own accumulation within populations, and the *L* allele works in the opposite direction to reduce B-chromosome transmission and to serve essentially as an anti-B-chromosome gene. The way that the maize B chromosome interacts with its host genome therefore constitutes a co-evolutionary host–parasite system [31]. A wider view of this topic, including some interesting animal systems, is found in two reviews [32,33].

A patchwork of A-chromosome sequences?

The origin of B chromosomes has remained a mystery since their description in the early part of the past century but the B chromosomes of different organisms probably arose in various ways. The *de novo* formation of B chromosomes must be a rare process because analyses of different B-chromosome variants within a species suggests a common origin of different B-chromosome forms [34,35]. It is widely accepted that B chromosomes could be derived from the A chromosomes (e.g. *Crepis capillaries* [36], *Z. mays* [37]) and/or from sex chromosomes in animals (e.g. *Eyprepocnemis plorans* [38]). However, there is also evidence suggesting that B chromosomes can be generated spontaneously in response to the new genome conditions following interspecific hybridization (e.g. *Coix aquaticus* and *Coix gigantea* [39], and in the parasitic wasp *Nasonia vitripennis* [40]). This view derives from new knowledge that allopolyploidization induces structural rearrangements at the chromosome level, as well as the elimination, reorganization or amplification of sequences [41,42], and there is every reason to believe that this restructuring of the genome could generate sequences that have the potential to form B chromosomes. In addition, spontaneous amplification of coding and noncoding tandem repeat sequences derived from A chromosomes seem to be strongly associated with the origin and evolution of plant B chromosomes [43–45]. Repeats arranged in tandem arrays are particularly prone to molecular events that alter the number of repeats [46], such as unequal crossing over between the sister chromatids, replication slippage and replication on a rolling circle [47].

The involvement of ribosomal RNA coding repeats does not appear to be accidental because ribosomal DNA (rDNA) loci have been detected on B chromosomes of many species [48]. In the herb *Plantago lagopus*, the origin of a B chromosome seems to be associated with massive amplification of 5S rDNA sequences after chromosome fragmentation of an aneuploid A chromosome [43]. Alternatively, but less likely, B-chromosome-localized rDNA sites could be a consequence of the reported mobile nature of rDNA [49,50], with B chromosomes as the preferred 'landing sites' owing to their neutral character.

The origin of the dot-like micro-B chromosomes of *Brachycome dichromosomatica* has also been linked to rapidly evolving tandem repeat sequences [44] (Figs 2,4). In *Brachycome*, there is an evolutionary relationship between different types of polymorphic and heterochromatic A-chromosome regions ('supernumerary segments') and B chromosomes. The supernumerary segments are often heterochromatic and dispensable, and provide a natural platform from which B chromosomes could be formed. However, because the genomic organization of the micro-B chromosome is a patchwork or conglomerate of repetitive sequences from different polymorphic A-chromosome sites, the present micro-B chromosomes could not have originated by simple excision of an A-chromosome fragment. We propose instead that B-chromosome founder sequences were 'released' from a polymorphic A-chromosome region and were then stabilized by the addition of telomeric repeats and other sequences. The rapid accumulation of other sequences on a *de novo* micro-B chromosome would present a barrier to the similarity between the 'parent' homologous chromosome regions and thus interfere with the competence for meiotic pairing between the 'parental' and derived segments. The newly formed B chromosome can then start its independent evolution. This, of course, begs the question of how a centromere appears in a newly formed chromosome. Transposition or activation of a cryptic

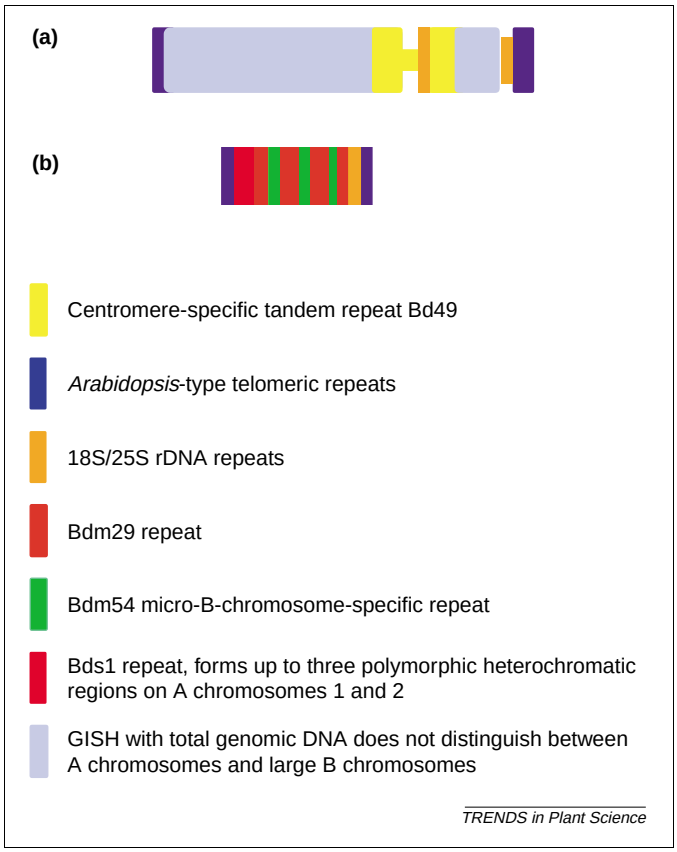

Fig. 4. The sequence and chromatin organization of the B chromosomes of *Brachycome dichromosomatica*. (a) Large B-chromosomes contain euchromatic and heterochromatic DNA, and are late replicating and hypoacetylated on histone H4 [69]. (b) Micro-B chromosomes contain heterochromatic DNA, replicate throughout S-phase, and are hypomethylated on histone H3 Lys4 and hypermethylated on H3 Lys9 [4]. The Bdm29 repeat forms a rare polymorphic heterochromatic region on A chromosome 1 [44]. 18S/25S ribosomal DNA repeats on the large B chromosomes are transcriptionally inactive [70]. Reference: centromere-specific tandem repeat Bd49 [68]. Abbreviation: GISH, genome *in situ* hybridization.

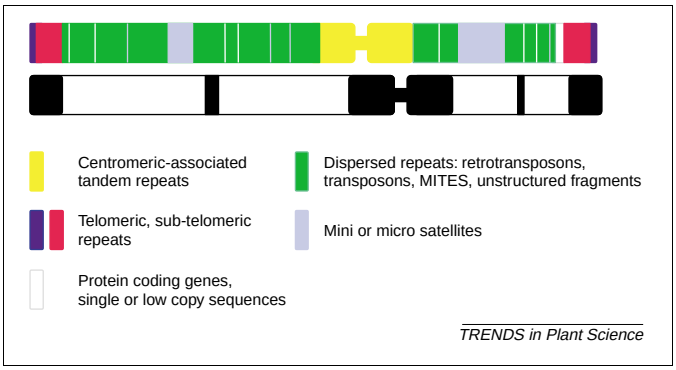

Fig. 5. The sequence organization of a representative plant A chromosome for comparison with the B chromosomes in Figs 1, 3 and 4. Abbreviation: MITES, miniature inverted-repeat transposable elements.

centromere sequence is possible, but it is more likely that an epigenetic event induced centromere activity [51].

The genetic and sequence organization of the maize B chromosome has been intensively studied (Fig. 3), as indicated earlier. Interestingly, the maize B chromosome has many sequences that originate from different A chromosomes [52,53], and also from polymorphic and heterochromatic A chromosome regions (often called 'knobs') [54] (Fig. 3). Because no such knobs are found adjacent to centromeres of A chromosomes in any karyotype of maize or its relatives [55], the B chromosome of maize could also be an amalgamation of sequences from several A chromosomes. The sequence organization of the B chromosomes of rye (Fig. 1), maize (Fig. 3) and *Brachycome dichromosomatica* (Fig. 4) can be usefully compared with the sequence organization of a representative plant A chromosome (Fig. 5).

B chromosomes are mainly transcriptionally inactive, so a greater tolerance is expected to modifications of the B chromosomes than of the A chromosomes, and B-chromosome structural polymorphisms have been reported in several different species [2]. However, there are also species (e.g. *B. dichromosomatica* [35]) with little structural variation in their B chromosomes [48]. One explanation for the observed uniformity is that the A chromosome genotypes have a low tolerance, which limits B chromosome variation to only minor changes. This suggests the existence of an A- and/or B-chromosome-derived control mechanism for the maintenance of 'suitable' B chromosomes. Also, stable B–A translocations seldom occur and it seems that there can be no crossing of the chromosome-type barrier in rye [56]. By contrast, stable B–A translocations in maize are widely used for experimental mapping purposes [57] and also to manipulate the dosage of chromosomal segments on gene expression [58], but we do not know of the existence of any such translocations in natural maize populations.

The B-chromosome centromere of maize has also been used as a model to study the DNA organization of a functional centromere. Changes in the physical structure of the B-chromosome repeat array are correlated with altered meiotic transmission [7]. There is a correlation between the size of a centromere and meiotic transmission. It is proposed that at least 55 kb is crucial for full meiotic transmission, and that the surrounding DNA, which leads to a larger fragment of 370 kb, provides additional stabilizing DNA. Healing of broken centromeres can be achieved through the addition or fusion of telomeric repeats to the broken chromosome [8]. The elegant studies of the centromere structure of maize B chromosomes provide a convincing example of the usefulness of B chromosomes for research into genome organization.

Afterthoughts

The thrust of current research on the biology of plant B chromosomes has a sharp point. It penetrates only a handful of species and we do not know whether they are widely representative. Nonetheless, some truths are evident. We are confident that B chromosomes arise because of errors during meiosis that generate A-chromosome fragments, and that interspecific hybridization and allopolyploidization cause a plethora of genome rearrangements that provide the platform from which autonomous selfish elements can emerge. We know, too, that there are methods of sequence amplification and rearrangement that can affect A as well as B chromosomes, and that these activities can inflate genome size and provide sequence resources to make some B chromosomes 'grow'. When a B chromosome is born complete with a centromere (e.g. from a trisomic), we are confident of its developmental progression. Beyond this level, there are uncertainties yet to be resolved. How does the capacity for mitotic and meiotic drive arise, as it must do in the early post-natal phase, and what sequence information encodes such processes? What is the meaning of a 'genetic element' or a 'region of a chromosome' that controls nondisjunction? Transmission genotypes have 'genes' controlling rates of transmission, but there is still much to be learned about these 'genes' and how they act to determine the various processes that they control and how they interact and co-evolve with their A-chromosome counterparts. There is a good story unfolding here (albeit told briefly), and not just about B chromosomes themselves but also about how we might use them as tools to investigate wider issues of genome organization and evolution in plants.

References

1 Beukeboom, L.W. (1994) Bewildering Bs: an impression of the 1st B-chromosome conference. *Heredity* 73, 328–336
2 Jones, R.N. and Rees, H. (1982) *B Chromosomes*, 1st edn, Academic Press
3 Manzanero, S. *et al.* (2000) The chromosomal distribution of phosphorylated histone H3 differs between plants and animals at meiosis. *Chromosoma* 109, 308–317
4 Houben, A. *et al.* (2003) Methylation of histone H3 in euchromatin of plant chromosomes depends on basic nuclear DNA content. *Plant J.* 33, 967–973
5 Beckett, J.B. (1991) Cytogenetic, genetic and plant breeding applications of B–A translocations in maize. In *Chromosome Engineering in Plants: Genetics, Breeding, Evolution* (Part A) (Gupta, P.K. and Tsuchiya, T., eds), pp. 493–529, Elsevier
6 Birchler, J.A. (1991) Chromosome manipulation in maize. In *Chromosome Engineering in Plants: Genetics, Breeding, Evolution* (Part A) (Gupta, P.K. and Tsuchiya, T., eds), pp. 531–559, Elsevier
7 Kaszas, E. and Birchler, J.A. (1998) Meiotic transmission rates correlate with physical features of rearranged centromeres in maize. *Genetics* 150, 1683–1692
8 Kaszas, E. *et al.* (2002) Cytological and molecular analysis of centromere misdivision in maize. *Genome* 45, 759–768

9 Tanaka, M. and Kawahara, T. (1982) Cytogenetical effects of B chromosomes in plants – a review. *Report of the Plant Germplasm Institute, Kyoto University* 5, 1–18, Plant Germplasm Institute, Kyoto University, Japan
10 Jenkins, G. (1986) Synaptonemal complex formation in hybrids of *Lolium temulentum* × *Lolium perenne* (L.) III. Tetraploid. *Chromosoma* 93, 413–419
11 Holmes, D.S. and Bougourd, S.M. (1991) B chromosome selection in *Allium schoenoprasum* II. Experimental populations. *Heredity* 67, 117–122
12 Plowman, A.B. and Bougourd, S.M. (1994) Selectively advantageous effects of B-chromosomes on germination behavior in *Allium schoenoprasum* L. *Heredity* 72, 587–593
13 Bougourd, S.M. and Plowman, A.B. (1996) The inheritance of B chromosomes in *Allium schoenoprasum* L. *Chromosome Res.* 4, 151–158
14 Han, Y. *et al.* (2001) Genes determining pathogenicity to pea are clustered on a supernumerary chromosome in the fungal plant pathogen *Nectria haematococca*. *Plant J.* 25, 305–314
15 Östergren, G. (1947) Heterochromatic B chromosomes in *Anthoxanthum*. *Hereditas* 33, 261–296
16 Kimura, M. and Kayano, H. (1961) The maintenance of supernumerary chromosomes in wild populations of *Lillium callosum* by preferential segregation. *Genetics* 46, 1699–1712
17 Nur, U. (1977) Maintenance of a 'parasitic' B chromosome in the grasshopper *Melanoplus femur-rubrum*. *Genetics* 87, 499–512
18 Nur, U. and Brett, B.L.H. (1988) Genotypes affecting the condensation and transmission of heterochromatic B chromosomes in the mealy bug *Pseudococcus affinis*. *Chromosoma* 96, 205–212
19 Nur, U. and Brett, B.L.H. (1987) Control of meiotic drive of B chromosomes in the mealy bug *Pseudococcus affinis (obscurus)*. *Genetics* 115, 499–510
20 Matthews, R.B. and Jones, R.N. (1982) Dynamics of the B chromosome polymorphism in rye. I. Simulated populations. *Heredity* 48, 345–369
21 Matthews, R.B. and Jones, R.N. (1983) Dynamics of the B chromosome polymorphism in rye. II. Estimates of parameters. *Heredity* 50, 119–137
22 Jimenez, M.M. *et al.* (1995) Genetic control of the rate of transmission of rye B-chromosomes. 2. 0B × 2B crosses. *Heredity* 74, 518–523
23 Jimenez, M.M. *et al.* (1997) Genetic control of the rate of transmission of rye B chromosomes. 3. Male meiosis and gametogenesis. *Heredity* 78, 636–644
24 Jimenez, G. *et al.* (2000) Relationship between pachytene synapsis, metaphase I associations, and transmission of 2B and 4B chromosomes in rye. *Genome* 43, 232–239
25 Puertas, M.J. *et al.* (1998) Genetic control of the rate of transmission of rye B chromosomes. IV. Localization of the genes controlling B transmission rate. *Heredity* 80, 209–213
26 Puertas, M.J. (2002) Nature and evolution of B chromosomes in plants: a non-coding but information-rich part of plant genomes. *Cytogenet. Genome Res.* 96, 198–205
27 Carlson, W.R. and Roseman, R.R. (1992) A new property of the maize B-chromosome. *Genetics* 131, 211–223
28 Rosato, M. *et al.* (1996) Genetic control of B chromosome transmission rate in *Zea mays* ssp *mays (Poaceae)*. *Am. J. Bot.* 83, 1107–1112
29 Chiavarino, A.M. *et al.* (1998) Localization of the genes controlling B chromosome transmission rate in maize (*Zea mays* ssp. *mays*, Poaceae). *Am. J. Bot.* 85, 1581–1585
30 Chiavarino, A.M. *et al.* (2001) Is maize B chromosome preferential fertilization controlled by a single gene? *Heredity* 86, 743–748
31 Gonzalez-Sanchez, M. *et al.* (2003) One gene determines maize B chromosome accumulation by preferential fertilization; another gene(s) determines their meiotic loss. *Heredity* 90, 122–129
32 Camacho, J.P.M. *et al.* (2000) B-chromosome evolution. *Philos. Trans. R. Soc. London Ser. B* 355, 163–178
33 Frank, S.A. (2000) Polymorphism of attack and defense. *Trends Ecol. Evol.* 15, 167–171
34 Cabrero, J. *et al.* (1999) Common origin of B chromosome variants in the grasshopper *Eyprepocnemis plorans*. *Heredity* 83, 435–439
35 Houben, A. *et al.* (1999) A monophyletic origin of the B chromosomes of *Brachycome dichromosomatica* (Asteraceae). *Plant Syst. Evol.* 219, 127–135
36 Jamilena, M. *et al.* (1994) A molecular analysis of the origin of the *Crepis capillaris* B chromosome. *J. Cell Sci.* 107, 703–708
37 Stark, E.A. *et al.* (1996) Molecular analysis of the structure of the maize B-chromosome. *Chromosome Res.* 4, 15–23
38 Lopez-Leon, M.D. *et al.* (1994) Possible origin of a B chromosome deduced from its DNA composition using double FISH technique. *Chromosome Res.* 2, 87–92
39 Sapre, B. and Deshpande, S. (1987) Origin of B chromosomes in *Coix* L. through spontaneous interspecific hybridization. *J. Hered.* 78, 191–196
40 McAllister, B.F. and Werren, J.H. (1997) Hybrid origin of a B chromosome (PSR) in the parasitic wasp *Nasonia vitripennis*. *Chromosoma* 106, 243–253
41 Ozkan, H. *et al.* (2001) Allopolyploidy-induced rapid genome evolution in the wheat (*Aegilops–Triticum*) group. *Plant Cell* 13, 1735–1747
42 Liu, B. and Wendel, J.F. (2002) Non-mendelian phenomena in allopolyploid genome evolution. *Curr. Genom.* 3, 489–505
43 Dhar, M.K. *et al.* (2002) Origin of an apparent B chromosome by mutation, chromosome fragmentation and specific DNA sequence amplification. *Chromosoma* 111, 332–340
44 Houben, A. *et al.* (2001) The genomic complexity of micro B chromosomes of *Brachycome dichromosomatica*. *Chromosoma* 110, 451–459
45 Langdon, T. *et al.* (2000) *De novo* evolution of satellite DNA on the rye B chromosome. *Genetics* 154, 869–884
46 Flavell, R.B. (1985) Repeated sequences and genome change. In *Genetic Flux in Plants* (Hohn, B. and Dennis, E.S., eds) pp. 139–156, Springer
47 Wintersberger, E. (1994) DNA amplification: new insights into its mechanism. *Chromosoma* 103, 73–81
48 Jones, R.N. (1995) B chromosomes in plants. *New Phytol.* 131, 411–434
49 Schubert, I. and Wobus, U. (1985) *In situ* hybridization confirms jumping nucleolus organizing regions in *Allium*. *Chromosoma* 92, 143–148
50 Dubcovsky, J. and Dvorak, J. (1995) Ribosomal RNA multigene loci: nomads of the Triticeae genomes. *Genetics* 140, 1367–1377
51 Karpen, G.H. and Allshire, R.C. (1997) The case for epigenetic effects on centromere identity and function. *Trends Genet.* 13, 489–496
52 Page, B.T. *et al.* (2001) Characterization of a maize chromosome 4 centromeric sequence: evidence for an evolutionary relationship with the B chromosome centromere. *Genetics* 159, 291–302
53 Cheng, Y.M. and Lin, B.Y. (2003) Cloning and characterization of maize B chromosome sequences derived from microdissection. *Genetics* 164, 299–310
54 Alfenito, M.R. and Birchler, J.A. (1993) Molecular characterization of a maize B chromosome centric sequence. *Genetics* 135, 589–597
55 Buckler, E.S. *et al.* (1999) Meiotic drive of chromosomal knobs reshaped the maize genome. *Genetics* 153, 415–426
56 Hasterok, R. *et al.* (2002) The nature and destiny of translocated B-chromosome-specific satellite DNA of rye. *Chromosome Res.* 10, 83–86
57 Beckett, J.B. (1978) B–A translocations in maize. I. Use in locating genes by chromosome arms. *J. Hered.* 93, 135–138
58 Auger, D.L. and Birchler, J.A. (2002) Maize tertiary trisomic stocks derived from B–A translocations. *J. Hered.* 93, 42–47
59 Carlson, W.R. (1986) The B chromosome of maize. *CRC Crit. Rev. Plant Sci.* 3, 201–206
60 Carlson, W.R. (1988) B chromosomes as a model system for nondisjunction. In *Aneuploidy: Induction and Test Systems* (Part B) (Vig, B.K. and Sandberg, A.A., eds), pp. 199–207, Alan R. Liss, New York, NY, USA
61 Green, D.M. (1990) Muller's ratchet and the evolution of supernumerary chromosomes. *Genome* 33, 818–824
62 Bell, G. and Burt, A. (1990) B-chromosomes: germ-line parasites which induce changes in host recombination. *Parasitology* 100, S19–S26
63 Jones, R.N. (1991) Cytogenetics of B chromosomes in crops. In *Chromosome Engineering in Plants: Genetics, Breeding, Evolution* (Part A) (Gupta, P.K. and Tsuchiya, T., eds), pp. 141–157, Elsevier
64 Jones, R.N. (1991) B-chromosome drive. *Am. Nat.* 137, 430–442
65 Jones, R.N. and Puertas, M.J. (1993) The B-chromosomes of rye (*Secale cereale* L.). In *Frontiers in Plant Science Research* (Dhir, K.K. and Sareen, T.S., eds) pp. 81–112, Bhagwati Enterprises, Delhi, India
66 Wilkes, T.M. *et al.* (1995) Analysis of rye B-chromosome structure using fluorescence *in situ* hybridization (FISH). *Chromosome Res.* 3, 466–472

67 Houben, A. *et al.* (1997) A repetitive DNA sequence common to the different B chromosomes of the genus *Brachycome*. *Chromosoma* 106, 513–519
68 Leach, C.R. *et al.* (1995) Organization and origin of a B chromosome centromeric sequence from *Brachycome dichromosomatica*. *Chromosoma* 103, 708–714
69 Houben, A. *et al.* (1997) Differences of histone H4 acetylation and replication timing between A and B chromosomes of *Brachycome dichromosomatica*. *Chromosome Res.* 5, 233–237
70 Donald, T.M. *et al.* (1997) Ribosomal RNA genes specific to the B chromosomes in *Brachycome dichromosomatica* are not transcribed in leaf tissue. *Genome* 40, 674–681
71 Covert, S.F. (1998) Supernumerary chromosomes in filamentous fungi. *Curr. Genet.* 33, 311–319
72 Morais-Cecilio, L. *et al.* (1996) Painting rye B chromosomes in wheat: interphase chromatin organization, nuclear disposition and association in plants with two, three or four Bs. *Chromosome Res.* 4, 195–200

A16 Kumke, K., Jones, R.N., and Houben, A. (2008). B chromosomes of *Puschkinia libanotica* are characterized by a reduced level of euchromatic histone H3 methylation marks. Cytogenet Genome Res 121, 266-270.

Original Article

Cytogenet Genome Res 121:266–270 (2008)
DOI: 10.1159/000138895

Cytogenetic and Genome Research

B chromosomes of *Puschkinia libanotica* are characterized by a reduced level of euchromatic histone H3 methylation marks

K. Kumke[a] R.N. Jones[b] A. Houben[a]

[a]Leibniz-Institute of Plant Genetics and Crop Plant Research (IPK), Gatersleben (Germany)
[b]Aberystwyth University, Institute of Biological Sciences, Edward Llywd Building, Aberystwyth, Wales (UK)

Accepted in revised form for publication by M. Schmid, 29 February 2008.

Abstract. Epigenetic marks in the chromosome complement of the liliaceous plant *Puschkinia libanotica* were studied using immunofluorescence to detect histone modifications. In particular, a comparison was made between the euchromatic and heterochromatic components of supernumerary B chromosomes (Bs) relative to the A chromosomes of the basic diploid set, in order to provide further insights into the enigmatic properties of these 'genetically silent' Bs. No differences were found between A and B chromosomes for the heterochromatic dimethylation marks of histone H3 at lysine positions 9 and 27. However, distinctions between A and B chromosomes were revealed for the euchromatic di- and trimethylation marks of histone H3 at lysine 4. The results indicate that the less-transcriptionally active Bs are not marked by an enriched level of heterochromatic histone marks, but rather by a low level of euchromatin-associated histone modifications.

Chromosomes that are dispensable, separate in their inheritance from those of the regular set, occur in hundreds or even thousands of species, and are lacking genes and adaptive significance constitute a genetic paradox, the B chromosome paradox. This puzzle has several intriguing components like the origin, molecular composition and survival of the B chromosomes in natural populations. B chromosomes impose a burden on their hosts in terms of the competitive demands they make on the physiology of the nucleus and the A chromosome genome with which they co-habit and we are baffled by their power of survival and widespread occurrence. There are some recent clues to their origin and escape from the A chromosome set (Dhar et al., 2002; Jones et al., 2007), some plausible hypotheses for the selfish nature of their drive processes in relatively few plant and animal species (Jones and Rees, 1982; Camacho, 2005; Burt and Trivers, 2006; Jones et al., 2008), and some detailed observations on their molecular organisation (Puertas, 2002; Jones and Houben, 2003; Jones et al., 2008). The molecular studies on Bs of plants are largely confined to just a few species, namely maize (Alfenito and Birchler, 1993; Kaszás and Birchler, 1996; Stark et al., 1996; Cheng and Lin, 2003, 2004; Lamb et al., 2005, 2007), rye (Langdon et al., 2000; Jones et al., 2008), *Brachycome dichromosomatica* (Leach et al., 2004) and *Crepis capillaris* (Leach et al., 2005). Except for the B-located 45S rRNA gene of *C. capillaris*, in which one of two B-specific members of the rRNA gene family is weakly transcribed and the bulk of the repetitive DNA is identical with that of the A chromosomes (Leach et al., 2005), we only know that B chromosomes are most likely lacking genes. We are also bedevilled by questions about the chromatin status of Bs, and whether they are heterochromatic or not. The general notion from classical cytological observations that their genetic inertness is based on heterochromatin was found to be plausible for only about the half of several hundred species that were surveyed (Jones, 1975). The reality is that heterochromatin is not the answer to the silence of the Bs since many Bs comprised a large amount of euchromatin.

AH was supported by a grant of the DFG (HO1179/10-1)

Request reprints from Andreas Houben
Leibniz-Institute of Plant Genetics and Crop Plant Research (IPK)
DE–06466 Gatersleben (Germany)
telephone: +49 (0) 39482 5486; fax: +49 (0) 39482 5137
e-mail: houben@ipk-gatersleben.de

KARGER
Fax +41 61 306 12 34
E-Mail karger@karger.ch
www.karger.com

1424–8581/08/1214–0266$24.50/0

Accessible online at:
www.karger.com/cgr

Although chromatin structure is increasingly believed to play an essential role in different aspects of chromosome function, little information is available on the chromatin composition of Bs, and whether it differs from that of the standard A chromosomes. Recent advances in chromatin characterisation in terms of epigenetic marks have shown the involvement of DNA methylation and post-translational histone modifications in various aspects of chromosome biology (reviewed in Kouzarides, 2007). The N-terminal tails of the nucleosomal core histones, extending from the nucleosome surface, are subjected to post-translational modifications such as acetylation, methylation, phosphorylation, ubiquitination, glycosylation, ADP-ribosylation, carbonylation and sumoylation. Several studies have shown that modification of the histone H3 tail by methylation of lysine residues 9 and 27 negatively regulates transcription by causing a compact chromatin structure. In contrast, euchromatin is marked by methylation of lysine residues 4 and 36 (reviewed by Martin and Zhang, 2005). Whereas euchromatin-specific methylation of H3K4 is highly conserved among eukaryotes, heterochromatin indexing by methylation marks at H3K9, H3K27 and H4K20 is more variable (reviewed by Fuchs et al., 2006).

The use of highly specific antibodies against various lysine residues of histone H3 has shown that in *Brachycome dichromosomatica*, which carries both large and micro Bs, although chromosome banding results suggest a similar eu- and heterochromatin composition of B and A chromosomes, the large Bs are characterised by a low level of euchromatic histone marks. Heteropycnotic tandem-repeat enriched micro Bs revealed only traces of these histone modifications. No differences between As and Bs were found for the heterochromatic marks H3K9me1,2 and H3K27me1,2 indicating that Bs are not marked by an enriched level of heterochromatic histone marks, but rather marked by a low level of euchromatin-associated histone modifications (Marschner et al., 2007). A comparable distribution of histone marks was also found for the B chromosomes of *Crepis capillaris* (Houben et al., 2003).

In rye, the subterminal heterochromatic domain of the B is characterised by a unique combination of histone methylation marks (Carchilan et al., 2007). Contrary to the heterochromatic regions of A chromosomes this domain is simultaneously marked by trimethylated histone H3K4 and by trimethylated H3K27. In addition this domain shows a dark Giemsa band at mitosis, but undergoes decondensation during interphase and reveals transcription of B-specific high copy repeat families. The distribution patterns along A and B chromosomes observed for the heterochromatin marks H3K9me1,2 were mainly uniform. The terminal heterochromatic regions of As and Bs showed little H3K27me1 but were enriched in di- and trimethylated H3K27 (Carchilan et al., 2007). In addition to a distinct methylation of histone H3, B chromosomes are marked by a reduced level of histone H3 and H4 acetylation as shown for the Bs of the grasshopper *Eyprepocnemis plorans* (Cabrero et al., 2007) and of *B. dichromosomatica* (Houben et al., 1997), respectively.

Given this paucity of knowledge and the conflicting and intriguing nature of the signals from rye, there is a need to build a stronger base of comparative studies before any general B-specific patterns of histone modifications can be established, if such even exists. Accordingly we made a comparative analysis of the chromosomal distribution of epigenetic marks of a further plant species with B chromosomes.

Puschkinia libanotica (Liliaceae) is a native species of Asia Minor in the Caucasus Mountains and Afghanistan. It has a basic diploid chromosome number of 2n = 2x = 10, plus 1–7 Bs. The Bs are regularly found in the coloured form of ornamental bulbs purchased from garden centres and seed companies, and they occur in 73–84% of the plants (Vosa, 1969). The number of Bs is constant between cells within a root tip, and between different root tips and pollen mother cells (Vernon and Witkus, 1970). The B chromosomes are completely heterochromatic in their long arm (Fig. 1A), which replicates its DNA, later than the rest of the nuclear chromatin, at the end of the S-phase (Barlow and Vosa, 1969a). The number of heterochromatic bodies visible in interphase nuclei represents the heterochromatic long arm of the B (Fig. 1), and corresponds to the number of Bs at metaphase, although there is a small level of fusion of interphase bodies in plants with two or more Bs (Barlow and Vosa, 1969b; Vernon and Witkus, 1970). The DNA condensation of the Bs at metaphase is identical with that of the A chromosomes (Barlow and Vosa, 1969b). They do not have obvious phenotypic effects on the morphology or growth of the plants which carry them, but influence the pattern of chiasma formation at metaphase of meiosis (Barlow and Vosa, 1970) by raising the chiasma frequency of each of the five A chromosome pairs in an additive way. They also modify the pattern of chiasma distribution by causing additional chiasmata to form in more proximal regions of the A bivalents. The submetacentric Bs are all homologous with one another and form multivalents among themselves at meiosis.

Materials and methods

Plant material

Puschkinia libanotica (Liliaceae) bulbs which were purchased from a garden centre were grown in moist vermiculite to obtain growing root tips.

Giemsa C-banding and indirect immunostaining

For Giemsa C-banding root tips were pre-treated with 0.2% colchicine for 2 h at room temperature, and then fixed in 3:1 alcohol:acetic acid overnight. Fixed meristems were macerated in acetic acid and squashed. Cover slips were removed after freezing with dry ice. Slides were air dried, incubated in a saturated solution of barium hydroxide at room temperature for 10 min, rinsed in distilled water and incubated in 2× SSC at 60°C for 1.5 h and then stained in Giemsa solution for about 30 min before mounting in Euparal.

Preparation of chromosomes and indirect immunostaining using the primary antibodies anti-histone H3K4me2, H3K4me3, H3K9me2 and H3K27me2 (Abcam Ltd, UK and Upstate Biotechnology, USA) were performed as described by Carchilan et al. (2007).

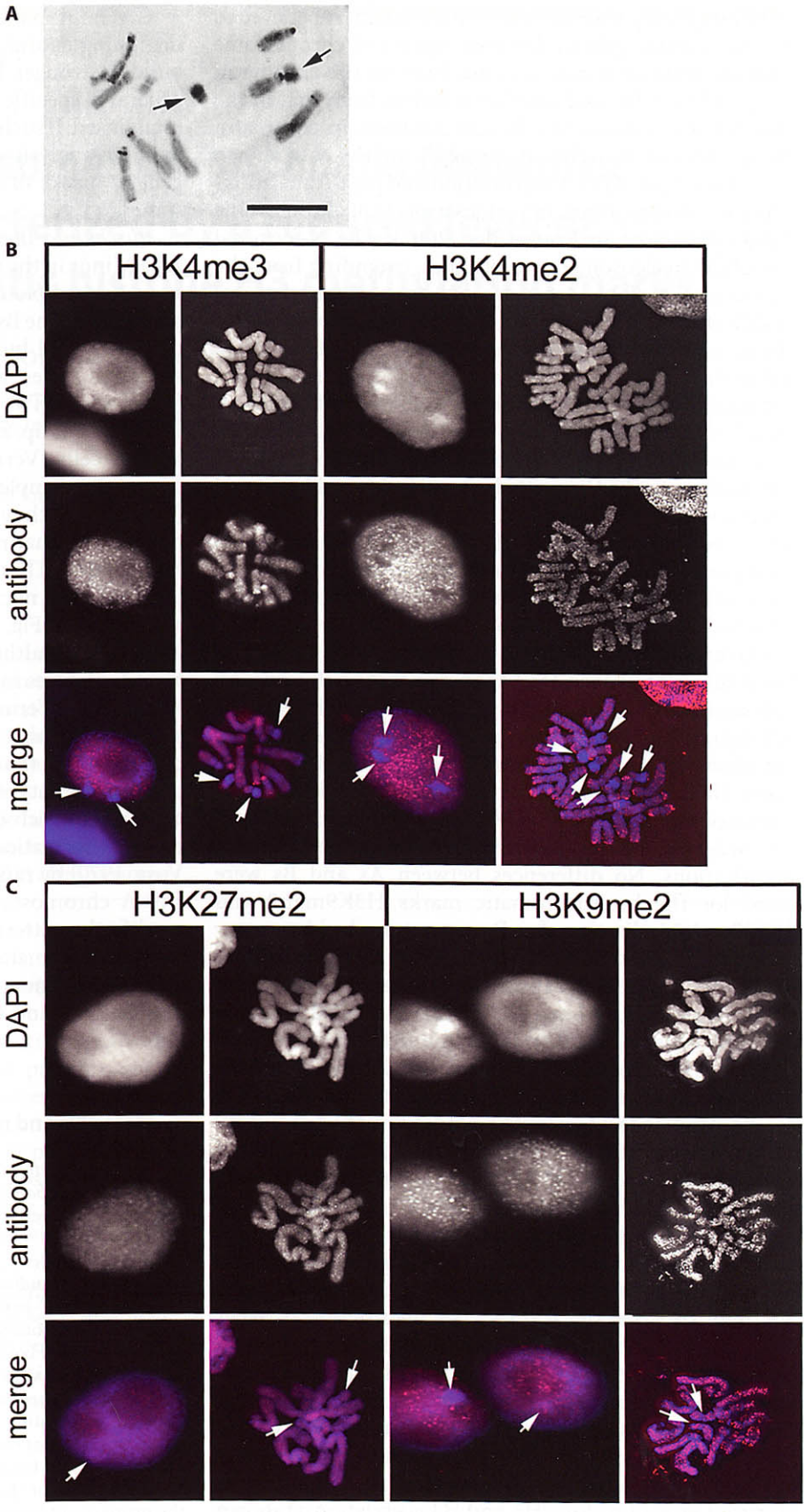

Fig. 1. Characterisation of A and B chromosome chromatin of *Puschkinia libanotica*. (**A**) Giemsa C-banding of a somatic metaphase cell with two B chromosomes (arrows). Bar represents 10 μm. (**B**, **C**) Somatic cells of *P. libanotica* with B chromosomes (arrows) after immunostaining with antibodies specific for (**B**) the euchromatin-specific modification H3K4me2,3 and (**C**) the heterochromatin-specific modifications H3K9me2 and H3K27me2. Note the B chromosome-specific heterochromatic interphase regions (arrows).

Results and discussion

A number of the *Puschkinia libanotica* plants were found to possess Bs, and as described previously (Barlow and Vosa, 1969b; Vernon and Witkus, 1970) one of the B chromosome arms revealed a pronounced Giemsa C-banding-positive region (Fig. 1A), suggesting that this B-region is completely heterochromatic. The Giemsa staining intensity of the other chromosome arm was comparable with that of A chromosomes.

For each type of antibody a reproducible distribution of histone marks was detected. The euchromatic di- and trimethylation marks of histone H3K4 revealed differences between transcriptionally active A chromosomes and less-transcriptionally active B chromosomes (Fig. 1B). Except for the distal chromosome ends and the euchromatic B chromosome arm, the heterochromatic B arm revealed the weakest H3K4me2,3-specific immunosignals of the entire chromosome complement. Also, immunostaining of interphase nuclei revealed that the brightly DAPI-stained B chromosome-specific heterochromatic bodies are only slightly labelled with both types of antibodies.

The chromosomal distribution patterns observed for the heterochromatin marks H3K9me2 on As and Bs (Fig. 1C) were as reported for plants with large genomes (Houben et al., 2003), having a uniform distribution throughout chromosomes of the same immunofluorescence intensity. A comparable distribution was found for H3K27me2-specific signals. Notably, the highly condensed B-specific interphase regions did not show any pronounced labelling specific for these heterochromatin marks.

Our observation confirms that cytologically detectable eu- and heterochromatin of B chromosomes of *P. libanotica* are subject to histone H3 methylation at lysines 4, 9 and 27 as is the standard set of A chromosomes. No differences between A and B chromosomes were found for the heterochromatic marks H3K9me2 and H3K27me2, indicating that Bs are not marked by an enriched level of heterochromatic histone marks, as previously reported for Bs of other species, but specifically marked by a reduced level of euchromatin-associated histone modifications (Houben et al., 2003; Carchilan et al., 2007; Marschner et al., 2007). The reduced level of histone H3K4 di/trimethylation, a modification that has been linked to transcriptionally active chromatin, corresponds with the observation that B chromosomes are generally transcriptionally inactive.

The discussion about the gene content of B chromosomes has thus far revolved around the fact that at least in plants there is no evidence from phenotypes or known sequence data for any coding sequence except for rDNA (Leach et al., 2005).

The best we have to date are the findings from rye (Carchilan et al., 2007) and maize (Lamb et al., 2007) where B-specific noncoding RNA is transcribed, and the basis of this phenomenon is currently being further investigated. The present work on *Puschkinia* and on *B. dichromosomatica* and on *Crepis* does however raise some interesting questions about the control of the methyltransferases which are responsible for the post-transcriptional modification of histone H3 at various lysine residues. How do the H3K4 methyltransferase(s) distinguish the intensity with which they modify the histone tails in the euchromatin of the A and B chromosomes? It is also noteworthy, though rarely mentioned (Camacho, pers. communication), that in addition to histone modifications other properties of B chromosomes (existence of drive mechanisms, predominant heterochromatic nature, frequent presence of ribosomal RNA genes and effects on chiasma frequency and distribution) have a lot of similarities in both plants and animals.

Acknowledgements

We are grateful to J. Fuchs for helpful discussions.

References

Alfenito MR, Birchler JA: Molecular characterization of a maize B chromosome centric sequence. Genetics 135:589–597 (1993).

Barlow PW, Vosa CG: Pattern of DNA replication in chromosomes of *Puschkinia libanotica*. Chromosoma 28:457–467 (1969a).

Barlow PW, Vosa CG: The chromosomes of *Puschkinia libanotica* during mitosis. Chromosoma 27:436–447 (1969b).

Barlow PW, Vosa CG: Effect of supernumerary chromosomes on meiosis in *Puschkinia libanotica* (Liliaceae). Chromosoma 30:344–355 (1970).

Burt A, Trivers R: B chromosomes, in Genes in Conflict: The Biology of Selfish Genetic Elements, pp 325–380 (Harvard University Press, Cambridge 2006).

Cabrero J, Teruel M, Carmona FD, Jimenez R, Camacho JP: Histone H3 lysine 9 acetylation pattern suggests that X and B chromosomes are silenced during entire male meiosis in a grasshopper. Cytogenet Genome Res 119:135–142 (2007).

Camacho JPM: B chromosomes, in Gregory TR (ed): The Evolution of the Genome, pp 223–286 (Elsevier, San Diego 2005).

Carchilan M, Delgado M, Ribeiro T, Costa-Nunes P, Caperta A, et al: Transcriptionally active heterochromatin in rye B chromosomes. Plant Cell 19:1738–1749 (2007).

Cheng YM, Lin BY: Cloning and characterization of maize B chromosome sequences derived from microdissection. Genetics 164:299–310 (2003).

Cheng YM, Lin BY: Molecular organization of large fragments in the maize B chromosome: indication of a novel repeat. Genetics 166:1947–1961 (2004).

Dhar MK, Friebe B, Koul AK, Gill BS: Origin of an apparent B chromosome by mutation, chromosome fragmentation and specific DNA sequence amplification. Chromosoma 111:332–340 (2002).

Fuchs J, Demidov D, Houben A, Schubert I: Chromosomal histone modification patterns – from conservation to diversity. Trends Plant Sci 11: 199–208 (2006).

Houben A, Belyaev ND, Leach CR, Timmis JN: Differences of histone H4 acetylation and replication timing between A and B chromosomes of *Brachycome dichromosomatica*. Chromosome Res 5:233–237 (1997).

Houben A, Demidov D, Gernand D, Meister A, Leach CR, Schubert I: Methylation of histone H3 in euchromatin of plant chromosomes depends on basic nuclear DNA content. Plant J 33: 967–973 (2003).

Jones RN: B chromosome systems in flowering plants and animal species. Int Rev Cytol 40:1–100 (1975).
Jones RN: Tansley Review – B chromosomes in plants. New Phytol 131:411–434 (1995).
Jones RN, Houben A: B chromosomes in plants: escapees from the A chromosome genome? Trends Plant Sci 8:417–423 (2003).
Jones RN, Rees H: B-Chromosomes (Academic Press, London 1982).
Jones RN, Viegas W, Houben A: A century of B chromosomes in plants: so what? Ann Bot 101: 767–775 (2008).
Jones RN, González-Sánchez M, González-García M, Vega JM, Puertas MJ: Chromosomes with a life of their own. Cytogenet Genome Res 120: 265–280 (2008).
Kaszás E, Birchler JA: Misdivision analysis of centromere structure in maize. EMBO J 15:5246–5255 (1996).
Kouzarides T: Chromatin modifications and their function. Cell 128:693–705 (2007).
Lamb JC, Kato A, Birchler JA: Sequences associated with A chromosome centromeres are present throughout the maize B chromosome. Chromosoma 113:337–349 (2005).
Lamb JC, Riddle NC, Cheng YM, Theuri J, Birchler JA: Localization and transcription of a retrotransposon-derived element on the maize B chromosome. Chromosome Res 15:383–398 (2007).
Langdon T, Seago C, Jones RN, Ougham H, Thomas H, et al: De novo evolution of satellite DNA on the rye B chromosome. Genetics 154:869–884 (2000).
Leach CR, Houben A, Timmis JN: The B chromosomes in Brachycome. Cytogenet Genome Res 106:199–209 (2004).
Leach CR, Houben A, Field B, Pistrick K, Demidov D, Timmis JN: Molecular evidence for transcription of genes on a B chromosome in *Crepis capillaris*. Genetics 171:269–278 (2005).
Marschner S, Kumke K, Houben A: B chromosomes of *B. dichromosomatica* show a reduced level of euchromatic histone H3 methylation marks. Chromosome Res 15:215–222 (2007).
Martin C, Zhang Y: The diverse functions of histone lysine methylation. Nat Rev Mol Cell Biol 6:838–849 (2005).
Puertas MJ: Nature and evolution of B chromosomes in plants: A non-coding but information-rich part of plant genomes. Cytogenet Genome Res 96:198–205 (2002).
Stark EA, Connerton I, Bennett ST, Barnes SR, Parker JS, Forster JW: Molecular analysis of the structure of the maize B-chromosome. Chromosome Res 4:15–23 (1996).
Vernon GM, Witkus ER: Behavior of supernumerary chromosomes in *Puschkinia libanotica*. B Torrey Bot Club 97:289–295 (1970).
Vosa CG: Heterochromatic B chromosomes in *Puschkinia libanotica*. Chromosomes Today 2: 189–191 (1969).

A17 Leach, C.R., Houben, A., Field, B., Pistrick, K., Demidov, D., Timmis, J.N. (2005). Molecular evidence for transcription of genes on a B chromosome in *Crepis capillaris*. Genetics 171, 269-278.

DOI: 10.1534/genetics.105.043273

Molecular Evidence for Transcription of Genes on a B Chromosome in *Crepis capillaris*

Carolyn R. Leach,* Andreas Houben,† Bruce Field,* Klaus Pistrick,† Dmitri Demidov† and Jeremy N. Timmis*,[1]

**School of Molecular and Biomedical Science (Genetics), The University of Adelaide, Adelaide, South Australia 5005, Australia and* †*Institute of Plant Genetics and Crop Plant Research (IPK), 06466 Gatersleben, Germany*

Manuscript received March 14, 2005
Accepted for publication May 10, 2005

ABSTRACT

Dispensable, supernumerary (B) chromosomes are found in diverse eukaryotic species. The origin and genetic consequences of B chromosomes have been the subjects of speculation for more than a century. Until now, there has been no molecular evidence that B chromosome DNA is transcribed and there is no unequivocal evidence as to their origin. B chromosomes are considered to be genetically inert although they appear to cause a variety of phenotypic effects. We report that members of one of two ribosomal RNA gene families that are confined to the B chromosomes of a plant, *Crepis capillaris*, are transcribed—thus providing the first molecular evidence of gene activity on B chromosomes. Sequence analysis of part of the A and B chromosome rRNA genes, together with comparisons with related species, indicates that the B chromosome rRNA genes originate from the A chromosome.

B chromosomes (B's) are among the oldest conundrums in genetics and evolution (Wilson 1907). These chromosomes are supernumerary to the basic (A chromosome) set and variation in their numbers produces major intraspecific genome size polymorphism. B chromosomes differ from A chromosomes in morphology and pairing behavior and are not required for normal growth and development (reviewed by Jones and Rees 1982; Jones 1995; Jones and Houben 2003). The origin of B chromosomes remains obscure but it is likely that they arose in different ways in different organisms. It has been argued that B's could be derived from A chromosomes in, *e.g.*, *Crepis capillaris* (Jamilena *et al.* 1994), or from sex chromosomes in, *e.g.*, *Leiopelma hochstetteri* (Sharbel *et al.* 1998). The spontaneous generation of B's following interspecific crosses has been reported in, *e.g.*, hybrids of *Coix aquaticus* and *C. gigantea* (Sapre and Deshpande 1987). The *de novo* formation of B's is most likely a rare event, as analyses of different B chromosome variants within species suggest a close relationship among different variants (Houben *et al.* 1999).

Most supposed B-specific sequences have been found subsequently, at least in low copy numbers, on the A's of the host species or in a close relative and probably it would be more accurate to describe these as B-amplified sequences. One possible exception to this generality comes from a recent detailed study using amplified fragment length polymorphism analyses (AFLP) and fluorescence *in situ* hybridization (FISH) in the cyprinid fish *Alburnus alburnus* which has one of the largest supernumerary chromosomes in vertebrates. This B chromosome contains specific sequences with strong homology to a retrotransposon from Drosophila and medaka (*Oryzias latipes*). The sequence is highly abundant on the B chromosome but undetectable in the normal A chromosome complement or in the B chromosome of the closely related species, *Rutilus rutilus*. These results suggest that the supernumerary chromosome of *A. alburnus* is not derived from the normal chromosome complement (Ziegler *et al.* 2003). In contrast, Page *et al.* (2001), investigating sequences isolated from the maize B chromosome (Alfenito and Birchler 1993), found that homologous sequences were confined to the centromere of chromosome 4 in the A genome. This indicates that a diversity of sequences compose centromeric regions in maize and also suggests that the centromere of chromosome 4 is related to that of the B chromosome (Page *et al.* 2001).

B chromosomes appear to carry very few identified genes other than commonly occurring clusters of 18S, 5.8S, and 25S ribosomal RNA (rRNA) genes (here referred to as 45S rDNA as this is the size of the unprocessed RNA transcript). These genes have been

Sequence data from this article have been deposited with EMBL/GenBank Data libraries under the following accession numbers: *C. capillaris* ITS-B2 (AJ876602), *C. capillaris* ITS-A (AJ876603), *C. capillaris* ITS-B1 (AJ876604), *C. alpestris* (AJ876605), *C. tectorum* (AJ876606), *C. nicaeensis* (AJ876607), *C. taraxacifolia* (AJ876608), *C. aspera* (AJ876609), *C. rhoeadifolia* (AJ876610), *C. foetida* (AJ876611), *C. rubra* (AJ876612), *C. praemorsa* (AJ876613), *C. paludosa* (AJ876614), *C. dioscoridis* (AJ876615), *C. setosa* (AJ876616), and *C. mollis* (AJ876617).

[1]*Corresponding author:* School of Molecular and Biomedical Science (Genetics), The University of Adelaide, Adelaide, SA 5005, Australia. E-mail: jeremy.timmis@adelaide.edu.au

recognized on B's by their capacity to organize extra nucleoli (Green 1990), by *in situ* hybridization, and, in a few instances, their activity has been inferred from positive silver nitrate staining (Jones 1995). It has been argued that active nucleolus organizing regions (NORs) are visualized by silver staining (*e.g.*, Hubbell 1985) and more recently Sirri *et al.* (2000) identified subunits of RNA polymerase I and a transcription factor (UBF) as the silver-staining proteins that remain associated with NORs at the metaphase of mitosis. Until now there has been no direct molecular evidence of transcription of B chromosome DNA in any species.

In situ hybridization demonstrated the presence of ribosomal genes dispersed throughout the B chromosomes of *Rattus rattus* but despite the clear demonstration of silver-staining NORs on the A chromosomes, no signal is apparent on the B chromosomes. The authors suggest that the accessory chromosomes of this species originated from one of the smaller NOR-carrying chromosome pairs and that, in the course of evolution, repetitive sequences invaded this supernumerary element. They suggest that its ribosomal DNA content was dispersed throughout the chromosome where it was inactivated by heterochromatinization that precluded access by transcription factors (Stitou *et al.* 2000).

The B chromosomes of the Australian daisy *Brachycome dichromosomatica* C. R. Carter have a clear secondary constriction and a cluster of rRNA genes detectable by FISH that is often seen associated with a nucleolus at mitotic prophase (Donald *et al.* 1995). These loci do not silver stain and Donald *et al.* (1997) were unable to detect a transcription product using PCR, of reverse-transcribed total RNA from leaf tissue of plants containing B chromosomes, with primers specific to the internal transcribed spacer 2 (ITS2) of the B chromosome rRNA gene.

The B chromosomes of *C. capillaris* (L.) Wallr ($2n = 6$) were first described and investigated by Rutishauser (1960), who recognized two B types termed monocentric and dicentric. An accession derived from the original collection contains only one type of B, a small metacentric chromosome (Małuszyńska and Schweizer 1989), which is morphologically identical to the B chromosome present in natural populations in Britain (Parker *et al.* 1989). Jones *et al.* (1989) studied synaptonemal complexes in *C. capillaris* plants derived from two British populations and found that single B chromosomes showed predominantly foldback meiotic pairing resulting in a symmetrical univalent hairpin loop, which suggests that the B is an isochromosome. The B chromosomes paired freely and extensively within and among themselves but there was no indication of pairing with the A chromosomes (Jones *et al.* 1989). The *C. capillaris* B may have originated from the standard genome because any repeated DNA sequences that they contain are also present on the A chromosomes (Jamilena *et al.* 1994, 1995). Histochemical silver staining and *in situ* hybridization of mitotic chromosomes suggested the presence of active rDNA on both ends of the B chromosomes of *C. capillaris*, as well as the major functional NORs located on chromosome 3 (Małuszyńska and Schweizer 1989; Małuszyńska 1990).

In this article we report two *C. capillaris* B-chromosome-specific rRNA gene types that differ substantially in sequence from those located on the A chromosomes. We present the first evidence that some of these rRNA genes are transcribed in leaf and flower bud tissues. We also report the outcome of an extensive search for a possible donor species for this unique B chromosome rDNA.

MATERIALS AND METHODS

Plant material: Achene samples of *C. capillaris* that originated from a *C. capillaris* population near Schaffhausen, Switzerland, in which B chromosomes were first identified (Rutishauser 1960; D. Schweizer, personal communication) were provided by J. Małuszyńska (Poland). Leaf tissue of living plants was collected directly from sites in the northeastern Harz region of Germany and documented by voucher specimens (Table 1). Herbarium material was selected from the collection of the Institute of Plant Genetics and Crop Plant Research Gatersleben (GAT), including those species naturally occurring in the surroundings of Schaffhausen, northernmost Switzerland (Hess *et al.* 1972). The classification follows Babcock (1947a,b), Sell (1976), and Jäger and Werner (2002).

Isolation of RNA and DNA: Total cellular RNA and DNA of *C. capillaris* were prepared from young leaves and flower buds as previously described (Donald *et al.* 1997). DNA of herbarium specimens of Crepis species was isolated by using a DNeasy plant kit (QIAGEN, Chatsworth, CA).

Chromosome microdissection, PCR isolation, and cloning of rRNA gene sequences: DNA was prepared from 15 microdissected B chromosomes according to Houben *et al.* (2001). PCR was used to amplify the ITS1-5.8S-ITS2 region (the two internal transcribed spacers and the 5.8S encoding region of the rRNA gene) from microisolated B chromosome DNA and from total genomic DNA of 0B *C. capillaris* plants using the primers ITS4 (5′-TCC TCC GCT TAT TGA TAT GC) and ITS5 (5′-GGA AGT AAA AGT CGT AAC AAG G) (White *et al.* 1990). PCR products were ligated into pGEM-T Easy (Promega, Madison, WI) and propagated in *Escherichia coli* strain DH5α. PCR was used to amplify the *C. capillaris* ITS1 region. Primer P1 (5′-GGA AGG ATC ATT GTC GAA CCC TGC) spanned the junction of 18S and ITS1 and primer P2 (5′-GGG ATT CTG CAA TTC ACA CCA G) was located in the central region of the 5.8S sequence (see Figure 2). The PCR conditions for primers P1 and P2 were 94°, 2 min (94°, 30 sec; 59°, 1 min; 72°, 5 min) for 30 cycles.

Primers were designed to be specific for ITS-B1 (5′-ACA CCA AAA CAA ACC GTT AGG ATG) (see Figure 2 and the text for explanation) and ITS-A (5′-A-CC CTA GCA GCT CAC AAC ACA CGG C) (see Figure 2 and the text for explanation) sequences when used in conjunction with P1 above (see Figure 2). The PCR conditions for these primers were 94°, 2 min (94°, 30 sec; 61°, 1 min; 72°, 5 min) for 30 cycles.

The ITS2 region was PCR amplified using the primers XF58S (5′-CTT CTA GAG CCT GGG CGT CAC G) and ER25S (5′-CGG AAT TCT GAC CTG GGG TCG C) for heterologous comparisons within the genus Crepis. The PCR conditions were 94°, 2 min (94°, 30 sec; 59°, 1 min; 72°, 5 min) for 30 cycles. The primer positions are shown in Figure 2.

TABLE 1

Crepis specimens from the herbarium of the Institute of Plant Genetics and Crop Plant Research (GAT) of which dry leaf material has been analyzed and the voucher specimens of the living material from the northeastern Harz region investigated in 2004

C. alpestris (Jacq.) Tausch	GAT 3686 Alpbach (Tirol): Gratspitz, leg. N. Reich 20.6.1934 (8.10.2004:11)
C. aspera L.	GAT 3667 Jerusalem: Mt. Scopus, leg. I. Amdurski 30.4.1931 (10.12.2004)
C. biennis L.	GAT 3636, 3637, 3638 northeastern Harz foreland: Gatersleben, railway station, leg. K. Pistrick (K.P.), A. Houben (A.H.) et J. Timmis (J.T.) 30.9.2004 (l, 30.9.2004:3, 4, 5)
	GAT 3646, 3647, 3648 northeastern Harz foreland: Schadeleben, leg. K.P., A.H. et J.T. 30.9.2004 (l, 30.9.2004:11, 12, 13)
	GAT 3654, 3655, 3656 northeastern Harz foreland: Warnstedt, leg. K.P., A.H. et J.T. 30.9.2004 (l, 30.9.2004:19, 20, 21)
	GAT 3664 Harz: Kreuztal, leg. K.P., A.H. et J.T. 30.9.2004 (l, 30.9.2004:29)
C. capillaris (L.) Wallr.	GAT 3634, 3635 northeastern Harz foreland: Gatersleben, Gutspark, leg. K.P., A.H. et J.T. 30.9.2004 (l, 30.9.2004:1, 2)
	GAT 3639, 3640, 3641/3642 northeastern Harz foreland: Gatersleben, cemetery, leg. K.P., A.H. et J.T. 30.9.2004 (l, 30.9.2004:6, 7, 8)
	GAT 3643, 3644/3645 northeastern Harz foreland: Concordia-lake, leg. K.P., A.H. et J.T. 30.9.2004 (l, 30.9.2004:9, 10)
	GAT 3649, 3650 northeastern Harz foreland: Cochstedt, leg. K.P., A.H. et J.T. 30.9.2004 (l, 30.9.2004:14, 15)
	GAT 3651, 3652, 3653 northeastern Harz foreland: Westerhausen, Königstein, leg. K.P., A.H. et J.T. 30.9.2004 (l, 30.9.2004:16, 17, 18)
	GAT 3660 Harz: Neuwerk, Krockstein, leg. K.P., A.H. et J.T. 30.9.2004 (l, 30.9.2004:25)
C. dioscoridis L.	GAT 3674 Genbank Gatersleben: CRE 2 (D 2544/79) leg. H. Ohle 23.7.1979 (8.10.2004:20)
C. foetida L. subsp. *foetida*	GAT 3676 Könnern, leg. P. Schuster 23.7.1952 (8.10.2004:1)
C. foetida subsp. *rhoeadifolia* (M. Bieb.) Celak.	GAT 3688 Ungarn: Bács. Kysáč, leg. S. Kupčok 7.1909 (8.10.2004:15)
C. mollis (Jacq.) Asch.	GAT 3680 Altvater mountains: Grosser Kessel, leg. H. Laus 7.1930 (8.10.2004:6)
C. nicaeensis Balb.	GAT 3665 Aveyron: St. Paul les Fonto, leg. A. Bec 20.6.1910 (4.1.2005)
C. paludosa (L.) Moench	GAT 3658, 3659 Harz: Treseburg, leg. K.P., A.H. et J.T. 30.9.2004 (l, 30.9.2004:23, 24)
C. praemorsa (L.) Walther	GAT 3683 Wiener Wald: Mödling, leg. O. Schwarz 21.5.1944 (8.10.2004:8)
C. rubra L.	GAT 3691 Italien, leg. V. Engelhardt 15.5.1935 (8.10.2004:16)
C. setosa Haller f.	GAT 3692 Slowakei: Nová Baňa, leg. K. Hammer (K.H.), P. Hanelt (P.H.) et F. Kühn (F.K.) 1.8.1974 (8.10.2004:17)
C. taraxacifolia Thuill.	GAT 3694 Rheinland: Bingen, leg. P. Schuster 22.6.1938 (8.10.2004:19)
C. tectorum L.	GAT 3679 Spremberg: Slamener Heide, leg. R. Fritsch 8.7.1971 (8.10.2004:4)
Hieracium spec.	GAT 3685 Taunus: Eggenheim, leg. M. Schuster 8.1956 (8.10.2004:10)

Dates (DD.MM.YYYY) when the material was collected and sample number are in parentheses.

Sequencing and sequence data analysis: Sequence analysis of the clones was performed by the dideoxynucleotide-dye termination method. A neighbor-joining tree was calculated with maximum-likelihood distances (corresponding to the HKY85 + G + I model of sequence evolution) in PAUP*4.0 (Swofford 2002). Bootstrap values were calculated from 200 resamples using identical settings as in the initial neighbor-joining analysis.

RT-PCR: Total RNA isolated from leaves and young flower buds was DNased with electrophoretically pure DNase (Ambion, Austin, TX) and 60 ng of RNA was reverse transcribed with random primers. Primers P1 and A and primers P1 and B1 were used to amplify the reverse-transcribed RNA as described above.

FISH: The plasmid VER17 (Yakura and Tanifuji 1983) containing part of the 18S, the 5.8S, most of the 25S, and the internal transcribed spacers of the *Vicia faba* rRNA gene was used as an rDNA-specific probe. An Arabidopsis-type telomere probe was synthesized using PCR according to Ijdo *et al.* (1991). *In situ* hybridization probes were labeled by PCR with biotin-16-dUTP or digeoxigenin-11-dUTP. Young seedlings were pretreated in iced water for 16 hr, fixed in ethanol-glacial acetic acid (3:1, v/v) for 4 days at 4°, and stored at 4° in 70% ethanol. Preparation of mitotic chromosomes and FISH were performed as described by Leach *et al.* (1995) and Houben *et al.* (2001). Hybridization sites of digeoxigenin-labeled or biotin-labeled probes were detected using sheep antidigeoxigenin-rhodamine-rhodamine anti-sheep antibody or the streptavidin-Alexa 488 system, respectively. Epifluorescence signals were recorded with a cooled CCD camera and image manipulations were performed using Adobe Photoshop software.

RESULTS

Fluorescence *in situ* hybridization confirmed clusters of 45S rRNA genes on both ends of the B chromosomes as well on chromosome 3 of *C. capillaris* (Figure 1). The B chromosome signal strength was considerably lower than that on chromosome 3, suggesting that the B's contribute a minority of additional rRNA genes to the cell. The rDNA signals were immediately proximal to telomere signals on the B chromosomes, which were consistently brighter than those seen on the A's, indicating a higher number of $(AGGGTTT)_n$ repeats on B's (Figure 1).

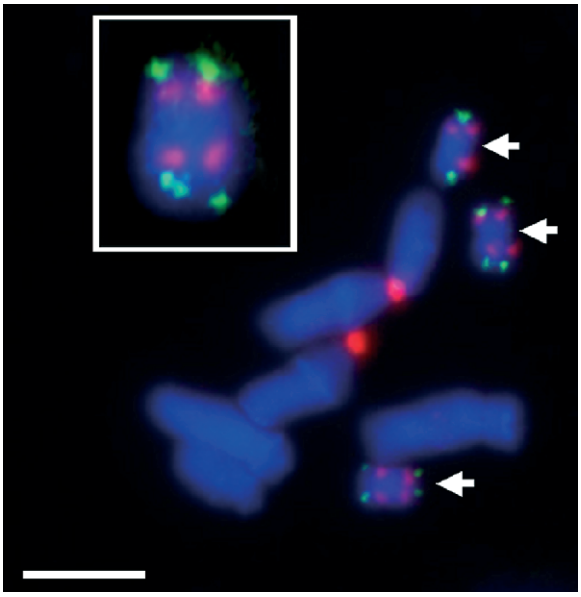

FIGURE 1.—The location of rDNA and telomeres on the A and B chromosomes of *C. capillaris*. Telomeres are labeled in green and 45S rRNA gene clusters in red. The chromosomal DNA is stained with DAPI. Bar, 5 μm. The inset shows an enlarged B chromosome.

The ITS1, 5.8S, and ITS2 rDNA regions differ between A and B chromosomes: One type of rDNA sequence, derived from the A chromosomes, was recovered from plants without B chromosomes, while two additional types of sequences were recovered from microcloned B chromosome DNA. The nucleotide sequences of the ITS1, 5.8S, and ITS2 regions from 11 cloned inserts derived by PCR from DNA of microdissected B chromosomes of *C. capillaris* were determined and compared with four comparable A chromosome sequences isolated from plants that did not contain B chromosomes. A single type of rDNA sequence was found on the A chromosomes and two different ones were identified on the B chromosomes. The A chromosome sequences (called ITS-A) contained 643 bp, of which 265 bp were in ITS1, 152 encoded the 5.8S rRNA, and 226 bp were in ITS2. The corresponding consensus B chromosome sequences were 1 bp shorter, and one cloned insert was 676 bp long. Alignment revealed considerable sequence polymorphism between the ITS-A rDNA and the two distinct B sequences. Nine of the B chromosome clones were of one type, named ITS-B1, and the other two were a second type that was designated ITS-B2. Consensus sequences were determined for the three distinct types of sequences (Figure 2).

The ITS-A consensus sequence was 94.4% similar to ITS-B1, differing by 20 nucleotides in ITS1 and 18 in ITS2, and 95.6% similar to ITS-B2, differing by 13 nucleotides in ITS1 and 12 in ITS2. The 5.8S regions were identical in ITS-A and ITS-B1 and differed in this region from ITS-B2 by three nucleotides. The two B chromosome consensus sequences showed only 91.3% sequence identity. In addition to the three differences in 5.8S, ITS-B1 and ITS-B2 sequences differed by 26 nucleotides in ITS1 and 27 nucleotides in ITS2. An *Nsi*I restriction site was unique to ITS1 of ITS-B1. We analyzed the mutational profile of these clones assuming the B chromosome rDNA is derived from that on the A chromosome. Among the 12 possible kinds of point mutations, C → T and G → T substitutions were the most prevalent types in A/B1 comparisons, accounting for almost half of all the mutations. They are significantly ($P < 0.001$) more frequent than any other types of substitution, including the reverse transitions T → C and T → G. C → T transitions (and G → A transitions on the opposite strand) are the hallmark of spontaneous deamination of 5-methylcytosine (5^mC), which produces a G-T mismatch at the deaminated site. The mismatch can be restored to the G-C pair in one direction, but creates an A-T pair in the other direction (HOLLIDAY and GRIGG 1993; FINNEGAN *et al.* 1998), resulting in T → C transitions (and A → G on the opposite strand). This observation is consistent with the known high level of C methylation in plant nuclear DNA (AYLIFFE *et al.* 1998) and with assuming no purifying selection on the sequence of ITS2 as may be expected if the ITS-B1-type genes do not contribute to the ribosome population. The origin of the G → T substitutions is not clear and G → A is not overrepresented. Nonetheless, these distortions suggest that some nucleotides in the rDNA of the B chromosome are modified and have been subject to hypermutation—assuming that they are derived from the A chromosome copies. Comparison of the ITS-A and ITS-B2 sequences indicates that the mutations are more randomly distributed among the 12 possible types.

Specific PCR amplification of B chromosome rDNA: Primer P1 was used with primer B1 or primer A to determine specificity for their target sequences (Figure 3). Primers P1 and B1 amplified the expected product of 476 bp only from templates containing B chromosome DNA from either positive control clones of microdissected B rDNA (Figure 3, lanes 14 and 16) or total cellular DNA isolated from plants with two B chromosomes (lanes 6 and 8). This primer pair was unable to amplify any product from cloned A chromosome rDNA (lanes 2 and 4) or from total DNA isolated from plants lacking B chromosomes (lanes 10 and 12). It was concluded that primer B1 was specific for the ITS-B1-type ribosomal repeats that contribute the majority of rDNA that is present on the B chromosome. In contrast, the primer pair P1 and A amplified a product of 608 bp from all the plant DNA samples (odd-numbered lanes), including all the control plasmid DNAs (lanes 9, 11, 13, and 15), indicating that the 3′ mismatch incorporated into primer A was insufficient, at the stringency of annealing used here, to differentiate the two types of sequence. The reliability and universality of the specific

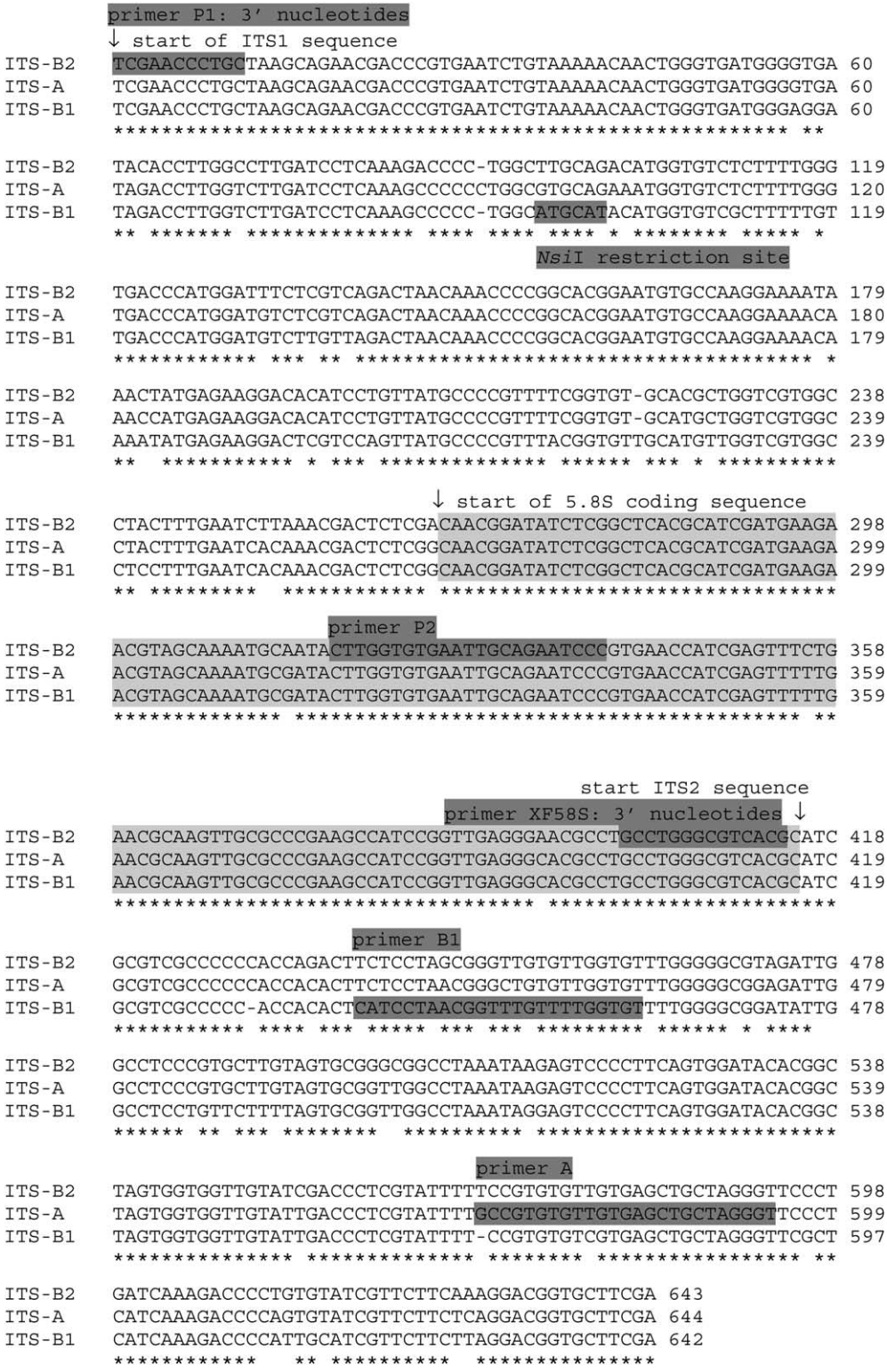

Figure 2.—Alignment of the consensus sequences of part of the A and B chromosome rRNA genes. The dark shading indicates the *Nsi*I restriction site and the primer sequences and their corresponding labels. The light shading indicates the 5.8S rRNA encoding sequence. Asterisks (*) indicate conservation of the sequence in the three gene types.

amplification of B chromosome rDNA was confirmed when the P1 and B1 primers were applied to four independently isolated samples of DNA from 0B plants (*i.e.*, plants containing no B chromosomes) and four plants containing two B chromosomes (2B plants) as well as positive and negative controls of cloned B chromosome and A chromosome rDNA sequences. In all cases complete specificity of the B1 primer for B chromosome rDNA was confirmed (data not shown).

The B chromosome rDNA is transcriptionally active in leaves and flower buds: The availability of specific primers made possible a sensitive assay for transcription of the B-chromosome-located rRNA genes by probing total reverse-transcribed cellular RNA for the 45S

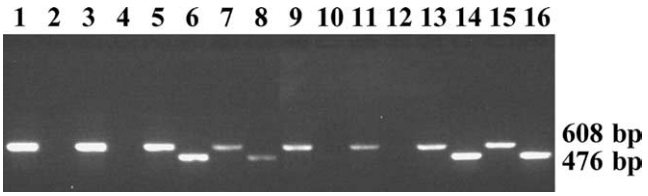

FIGURE 3.—Gel electrophoresis of PCR-amplified DNA testing the specificity of the A and B1 primers. PCR products were amplified using P1 and A as primers from 0B total plant DNA (lanes 1 and 3), 2B total plant DNA (lanes 5 and 7), clones derived from 0B total plant DNA (lanes 9 and 11), and clones derived from microdissected B chromosome DNA (lanes 13 and 15) and using P1 and B1 as primers from 0B total plant DNA (lanes 2 and 4), 2B total plant DNA (lanes 6 and 8), clones derived from 0B total plant DNA (lanes 10 and12), and clones derived from microdissected B chromosome DNA (lanes 14 and 16). Fragment sizes are indicated in base pairs.

precursor rRNA, which is the initial product of plant rRNA genes by RNA polymerase I (KAVANAGH and TIMMIS 1988). Total RNA was isolated from leaves and young flower buds of individual 0B (Figure 4, lanes 5–12) and 2B (lanes 13–20) plants. The samples were DNased with electrophoretically pure DNase and 60 ng of RNA was reverse transcribed with random primers. Primers P1 and A (Figure 4, odd-numbered lanes) and primers P1 and B1 (Figure 4, even-numbered lanes) were used to amplify the reverse-transcribed RNA. In each sample derived from RNA of B-chromosome-containing plants, a product was amplified by primers P1 and B1 that was not present in any sample derived from the RNA of plants lacking B chromosomes. This result indicates that the B chromosome rDNA is transcribed because the 45S precursor is detectable in the total RNA of leaf and flower bud tissue.

Control experiments with and without DNase treatment, and with and without an initial reverse transcription step, confirmed that the PCR products in Figure 4 (lanes 14, 16, 18, and 20) are unequivocally dependent upon reverse transcription of RNA molecules originating from rRNA genes on B chromosomes (results not shown).

Having established that the B chromosome rRNA genes are transcribed, we determined the level of transcript relative to the number of ITS-B1 sequences present in the genomes. This was achieved by PCR amplification using primers P1 and P2 to amplify 353 bp spanning ITS1 and part of the 5.8S gene, followed by digestion of the products with *Nsi*I for which there is a recognition site in ITS-B1 that is lacking in ITS-A. Figure 5 shows the PCR products before (odd-numbered lanes) and after (even-numbered lanes) complete *Nsi*I digestion. The primers were applied to genomic DNA templates of 0B (Figure 6, lanes 1 and 2) and two independent 2B (lanes 3–6) plants. The product of the 0B plant is not digested by *Nsi*I whereas a proportion of those of the two 2B plants is cleaved into the predicted fragments of 241 and 112 bp. Quantitative analysis of the Gel Doc (Bio-Rad, Hercules, CA) data file of Figure 5 (lanes 4 and 6) with the software Quantity One (Bio-Rad) indicated that 20.8 and 22.1% of the total product derived from the B-chromosome-containing genomes was digested by *Nsi*I, consistent with each B chromosome contributing ~10% of ITS-B1-type rRNA genes to the composite genome, assuming that the primers amplify the A and B chromosome sequences with equal efficiency. As controls to ensure that *Nsi*I digestion was complete and specific, DNA from an ITS-A clone (lane 7) and an ITS-B1 clone (lane 9) was amplified and digested. As predicted, the products from the former were undigested by *Nsi*I (lane 8) and those from the latter were completely digested into the expected fragments (lane 10). Similar experiments were performed with three of the DNased and reverse-transcribed RNA samples used in Figure 4 and the results are shown in Figure 5 (lanes 11–16). In no case was any *Nsi*I digestion of the products observable. We conclude that, while there is demonstrable transcription of the B chromosome rDNA, the transcripts are present in the final 45S precursor pool at undetectable levels that are therefore disproportionately low compared with the number of genes present on the supernumerary B (~10% of the total gene number per cell). Therefore, in the cellular RNA of leaves and flower buds of a 2B plant, nearly all the pre-rRNA molecules are derived from the A chromosome NOR.

A search for a donor of the B chromosome rDNA: The observation that the B1 and B2 ITS regions were very significantly different from those of the A chromosome NOR suggested a search of species in central Europe that may have hybridized with *C. capillaris* and donated these rDNA types. The assumption was that, as in Hordeum interspecies (KASHA and KAO 1970) and some Poaceae (LAURIE and BENNETT 1989) or other intergeneric crosses, the chromosomes of one parent may be eliminated during embryogenesis. In most systems this leads to the formation of haploids containing only

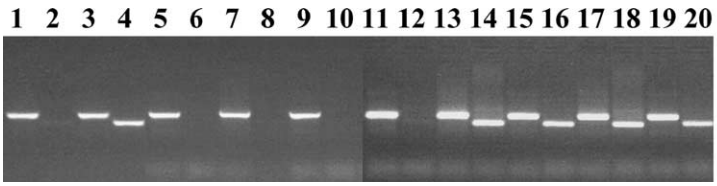

FIGURE 4.—Gel electrophoresis of PCR-amplified products testing for transcription of rRNA genes from A and B chromosome DNA. PCR products were amplified using P1 and A as primers from 0B total plant DNA (lane 1), 2B total plant DNA (lane 3), 0B total flower bud RNA (lanes 5 and 9), 0B total leaf RNA (lanes 7 and 11), 2B total flower bud RNA (lanes 13 and 17), and 2B total leaf RNA (lanes 15 and 19) and using P1 and B1 as primers from 0B total plant DNA (lane 2), 0B total flower bud RNA (lanes 6 and 10), 0B total leaf RNA (lanes 8 and 12), 2B total flower bud RNA (lanes 14 and 18), and 2B total leaf RNA (lanes 16 and 20). Fragment sizes are indicated in base pairs.

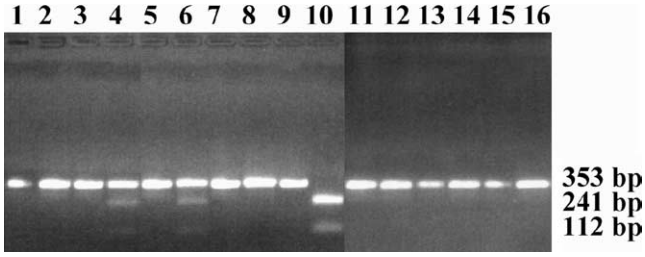

Figure 5.—Gel electrophoresis of PCR-amplified products to quantify the level of transcription from the B chromosome. All PCR products were amplified using P1 and P2 with the reverse transcriptase step included for samples in lanes 11–16 and all RNA samples digested with DNase. All samples are in pairs not digested (odd numbers) and digested with *Nsi*I (even numbers). Total plant DNA from 0B (lanes 1 and 2), 2B (lanes 3–6), clone 10 DNA from 0B (lanes 7 and 8), clone 3 from microdissected B chromosome DNA (lanes 9 and 10), total flower bud RNA from 2B plant (lanes 11 and 12), and total leaf RNA from 2B plant (lanes 13–16). Fragment sizes are indicated in base pairs.

the chromosomes of one parent, but the process of elimination takes some time (Thomas and Pickering 1983; Pickering 1985) and some chromatin may survive provided that it becomes mitotically stable. If this event is followed by spontaneous chromosome doubling or backcrossing to one of the parents, then diploids may result in the formation of supernumerary chromosomes that may be genetically suppressed (Sapre and Deshpande 1987). We prepared DNA from herbarium specimens of 10 species and fresh tissue from 3 additional species collected in the northeastern Harz region in Germany, from which we amplified ITS2, which was sequenced and compared

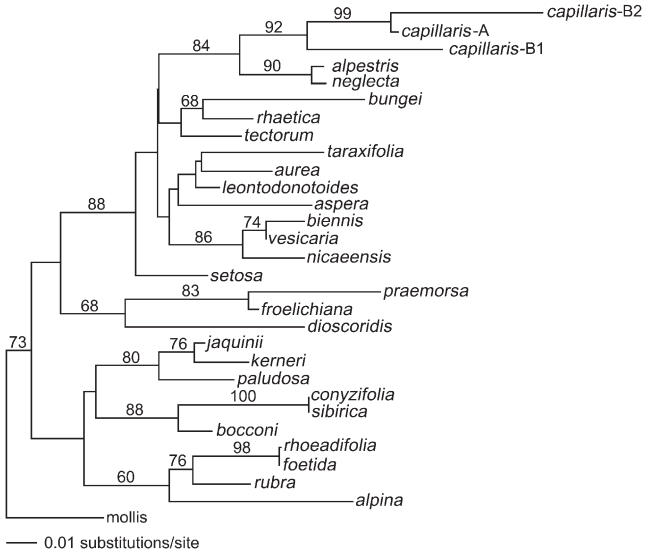

Figure 6.—The phylogenetic relationships between the ITS2 sequences of 29 species within the genus Crepis and the corresponding sequences on the B chromosome of *C. capillaris*. The tree was prepared using neighbor-joining analysis. Numbers depict bootstrap values (>50%) derived from 200 bootstrap resamples.

with ITS2 sequences of 18 additional Crepis species, available from the EMBL databases. In particular, we included those species occurring in the vicinity of Schaffhausen, in northernmost Switzerland (Hess *et al.* 1972), where the B-chromosome-positive *C. capillaris* population was first identified (Rutishauser 1960). We focused particularly on *C. dioscoridis*, *C. tectorum*, *C. nicaeensis*, *C. leontodontoides*, and *C. aspera* because chromosome fragments in artificially induced species hybrids have been described in crosses with *C. capillaris* (Navashin 1927; Avery 1930; Hollingshead 1930; Grob 1966; Doerschug and Miksche 1976).

Neighbor-joining phylogenetic analyses (Swofford 2002) of the sequence data (Figure 6) did not identify a species that contained an ITS2 sequence that was more similar to either of the B chromosome sequences than that of the *C. capillaris* A chromosomes. This reinforces the mutational analysis and suggests strongly that the B chromosome rDNA was derived from the A chromosome followed by divergence over time into major (ITS-B1) and minor (ITS-B2) gene clusters. A parsimony analysis of the ITS sequences resulted in identical taxon groups as found in the neighbor-joining tree (data not shown).

DISCUSSION

These experiments provide the first molecular demonstration of the transcription of B chromosome DNA. These chromosomes, which have the capacity to accumulate through generations or during mitosis, have generally been considered to be genetically, although not functionally, inert. There is ample evidence that they have a great variety of exo- and endo-phenotypic effects (Jones and Rees 1982; Puertas 2002).

Here we have shown that B chromosomes are not genetically inert but it appears unlikely, in the case of these rDNA clusters, that they make a *pro rata* contribution to the functional ribosome population. We cannot distinguish whether all the ITS-B1-type genes are transcribed at a low level or whether a few are transcribed and others are inactive. Of course, this same uncertainty applies for the A chromosome NOR, and it appears that most plants have a large excess of rRNA genes above the number that is capable of producing the amount of RNA required by somatic cells (Kavanagh and Timmis 1986).

Togby (1943) described the evolution of *C. fuliginosa* Sibth. & Sm. (*C. neglecta* subsp. *fuliginosa* (Sibth. & Sm.) Vierh. ($2n = 6$) from *C. neglecta* L. ($2n = 8$) as a result of unequal interchange and loss, subsequently, of a small dispensable centric fragment. If this centric fragment is retained rather than lost, it could evolve into a B chromosome. Babcock (1942) presented an extensive analysis of the systematics, cytogenetics, and evolution in Crepis species and argued that species with lower chromosome numbers appeared to be derived from species with higher numbers. *C. fuliginosa* and *C. capillaris* are both

species with the lowest diploid number found in the genus: $2n = 6$.

If a similar kind of chromosome rearrangement was responsible for the evolution of the B chromosome in *C. capillaris*, it is still necessary to provide an explanation for the source, location, and activity of the rRNA genes found on the B chromosomes. First, it possible that the NOR-bearing chromosome was involved in the interchange and that the remaining centric fragment carried rRNA genes. This chromosome would have to undergo a misdivision of the centromere to generate the isochromosome now found in *C. capillaris* and such centromeric misdivisions are not uncommon in B chromosomes (see Jones and Rees 1982 for numerous examples). Second, most, if not all, Crepis species have distal rRNA gene clusters (see Jones 1995 for list) so that the position of this locus is not unusual. Finally, as the rRNA genes probably derive from the A genome, nucleolar dominance as seen, if only cytologically, in Crepis hybrids (Navashin 1934; Doerschug and Miksche 1976) would not be predicted in the nascent B chromosome. Sequence divergence may occur due to the relaxation of the constraints of concerted evolution due to lack of pairing of the B chromosome with the A's. However, there are a number of examples of either concerted evolution of different arrays of rRNA genes (Joly *et al.* 2004; Kovarik *et al.* 2004) or maintenance of different arrays (Rauscher *et al.* 2004) in various polyploid species. Thus either maintenance of sequence identity or sequence divergence is equally likely even in the absence of detectable pairing.

Jamilena *et al.* (1994) endeavored to determine the origin of the B chromosome of *C. capillaris* using *in situ* hybridization with a range of probes. Genomic *in situ* hybridization with DNA from plants with and without B's as probe indicated that the B chromosome had many DNA sequences in common with the A chromosomes, but showed no region rich in B-specific sequences. Additional DNA probes derived from the NOR chromosome (chromosome 3) were also used to test the possible origin of the B from this chromosome and only the 18S + 25S rDNA and the telomeric sequences were found to hybridize to the B's. Jamilena *et al.* (1994, p. 703) concluded that "the entire B of *C. capillaris*, although possibly having originated from the standard genome, did not derive directly from the NOR chromosome."

If the B was derived from a centric fragment lacking rRNA genes, it is possible that the latter relocated as a result of a transposition event (Schubert and Wobus 1985). B chromosomes carry many transposable elements and numerous reports of variation in NOR location within individuals (Hall and Parker 1995) suggest that rRNA genes are mobile.

Babcock (1942) also reports that many variations from the typical diploid number are found in Crepis, including both trisomics and polyploids in *C. capillaris* and *C. tectorum*. Furthermore, Babcock and Navashin (1930) described a trisomic plant in *C. tectorum* in which the extra member was an atypical satellited chromosome. It is possible that this chromosome was in fact a B chromosome, although not recognized as such. The cohabitation of diploids and tetraploids of the same or closely related species provides an ideal environment for a scenario similar to that described by Sapre and Deshpande (1987) in *Coix* L. where a B chromosome was generated spontaneously as a result of the crossing of two allopatric species, *C. gigantica* ($2n = 20$) and *C. aquatica* ($2n = 10$), followed by natural backcrossing of the hybrid yielding a *C. aquatica* ($2n = 10 + 1B$) where the B was derived as a relic from *C. gigantica*. Crossing of diploid and tetraploid *C. capillaris* plants or crosses with *C. tectorum* (with which it forms hybrids; Babcock 1942) plants followed by natural backcrossing to the diploid could readily lead to the formation of a B chromosome. However, the phylogenetic analysis of the ITS2 regions from 28 other Crepis species, including *C. nicaeensis* (Grob 1966), *C. leontodontoides* (Avery 1930), *C. aspera* (Navashin 1927), *C. tectorum*, and *C. dioscoridis* (Doerschug and Miksche 1976) with which *C. capillaris* forms hybrids, did not indicate that any of them was a more likely donor of the B chromosome rRNA genes than was the A genome of *C. capillaris*.

As suggested above, a possible explanation for the extensive sequence variation between the ITS1 and ITS2 regions of the A and B chromosomes is that lack of meiotic pairing of the A's and B's and the stability of B's as univalents releases them from concerted evolution with the A chromosome rDNA (Liao 1999). This is further supported by the lack of identification of a donor species for the very different rRNA gene types that are present on the B chromosome, suggesting that the B genes have evolved from those on the A chromosome under different selection pressures and/or homogenizing mechanisms.

The presence of a transcript from the B chromosome rRNA genes indicates that these genes at least are not completely suppressed. However, transcripts are rare when compared with the number of rRNA genes on the B, suggesting that transcription is suppressed or the transcripts are quickly degraded compared with those arising from the A chromosomes. The lack of any detectable association of the B's with a nucleolus may be attributable to the low level of transcription or, consistent with intermittent silver staining, the fact that transcription is confined to a few cells. The search for a possible donor of the B chromosome did not identify any candidate species. Rather, the phylogenetic analysis shows that the B's are more closely related to the *C. capillaris* A's than to those of any other species tested and this is consistent with mutational analyses of the A and B rDNA.

We are grateful to Margit Hantschmann and Katrin Kumke for excellent technical assistance and to Frank Blattner for his valuable advice on the phylogenic analysis. A.H. was supported by a grant of the

Land Saxony-Anhalt. J.N.T. thanks the Australian-German Joint Research Co-operation Scheme for financial assistance.

LITERATURE CITED

Alfenito, M. R., and J. A. Birchler, 1993 Molecular characterization of a maize B chromosome centric sequence. Genetics **135:** 589–597.

Avery, P., 1930 Cytological studies of five interspecific hybrids of *Crepis leontodontoides*. Univ. Calif. Publ. Calif. Publ. Ag. Sci. **6:** 135–167.

Ayliffe, M. A., N. S. Scott and J. N. Timmis, 1998 Analysis of plastid DNA-like sequences within the nuclear genomes of higher plants. Mol. Biol. Evol. **15:** 738–745.

Babcock, E. B., 1942 Systematics, cytogenetics and evolution in *Crepis*. Bot. Rev. **8:** 139–190.

Babcock, E. B., 1947a The genus *Crepis*. Part 1: the taxonomy, phylogeny, distribution and evolution of *Crepis*. Univ. Calif. Publ. Bot. **21:** 1–198.

Babcock, E. B., 1947b The genus *Crepis*. Part 2: systematic treatment. Univ. Calif. Publ. Bot. **22:** 199–1030.

Babcock, E. B., and M. Navashin, 1930 The genus *Crepis*. Bib. Genet. **6:** 1–90.

Doerschug, E. B., and J. P. Miksche, 1976 DNA variation and ribosomal-DNA constancy in two *Crepis* species and the interspecific hybrid exhibiting nucleolar-organiser suppression. Heredity **37:** 441–450.

Donald, T. M., C. R. Leach, A. Clough and J. N. Timmis, 1995 Ribosomal RNA genes and the B chromosome of *Brachycome dichromosomatica*. Heredity **74:** 556–561.

Donald, T. M., A. Houben, C. R. Leach and J. N. Timmis, 1997 Ribosomal RNA genes specific to the B chromosomes in *Brachycome dichromosomatica* are not transcribed in leaf tissue. Genome **40:** 674–681.

Finnegan, E. J., R. K. Genger, W. J. Peacock and E. S. Dennis, 1998 DNA methylation in plants. Annu. Rev. Plant Physiol. Plant Mol. Biol. **49:** 223–247.

Green, D. M., 1990 Muller's rachet and the evolution of supernumerary chromosomes. Genome **33:** 818–824.

Grob, R., 1966 Zytotaxonomische Untersuchen an *Crepis capillaris* und *Crepis nicaneensis* und ihren F1-Bastarden. Ber. Schweiz. Bot. Ges. **76:** 306–351.

Hall, K. J., and J. S. Parker, 1995 Stable chromosome fission associated with rDNA mobility. Chromosome Res. **3:** 417–422.

Hess, H. E., E. Landolt and R. Hirzel, 1972 *Flora der Schweiz. Bd. 3.* Birkhäuser Basel, Stuttgart, Germany.

Holliday, R., and G. W. Grigg, 1993 DNA methylation and mutation. Mutat. Res. **285:** 61–67.

Hollingshead, L., 1930 Cytological investigations of hybrids and hybrid derivatives of *Crepis capillaris* and *Crepis tectorum*. Univ. Calif. Publ. Calif. Publ. Ag. Sci. **6:** 55–94.

Houben, A., N. Thompson, R. Ahne, C. R. Leach, D. Verlin *et al.*, 1999 A monophyletic origin of the B chromosomes of Brachycome dichromosomatica (Asteraceae). Plant Syst. Evol. **219:** 127–135.

Houben, A., B. L. Field and V. Saunders, 2001 Micro-dissection and chromosome painting of plant B chromosomes. Methods Cell Sci. **23:** 115–124.

Hubbell, H. R., 1985 Silver staining as an indicator of active ribosomal genes. Stain Technol. **60:** 258–294.

Ijdo, J. W., R. A. Wells, A. Baldini and S. T. Reeders, 1991 Improved telomere detection using a telomere repeat probe (TTAGGG)n generated by PCR. Nucleic Acids Res. **19:** 4780.

Jäger, E. J., and K. Werner (Editors), 2002 *Rothmaler. Exkursionsflora von Deutschland. Bd.4. Gefässpflanzen: Kritischer Band.* Spektrum Heidelberg, Berlin.

Jamilena, M., C. Ruiz Rejón and M. Ruiz Rejón, 1994 A molecular analysis of the origin of the *Crepis capillaris* B chromosome. J. Cell Sci. **107:** 703–708.

Jamilena, M., M. Garridoramos, C. Ruiz Rejón, M. Ruiz Rejón and J. S. Parker, 1995 Characterisation of repeated sequences from micro-dissected B chromosomes of *Crepis capillaris*. Chromosoma **104:** 103–120.

Joly, S., J. T. Rauscher, S. L. Sherman-Broyles, A. H. D. Brown and J. J. Doyle, 2004 Evolutionary dynamics and preferential expression of homeologous 18S–5.8S–26S nuclear ribosomal genes in natural and artificial *Glycine* allopolyploids. Mol. Biol. Evol. **21:** 1409–1421.

Jones, G. H., J. A. F. Whitehorn and S. M. Albini, 1989 Ultrastructure of meiotic pairing in B chromosomes of *Crepis capillaris*. I. One-B and two-B pollen mother cells. Genome **32:** 611–621.

Jones, N., and A. Houben, 2003 B chromosomes in plants: Escapees from the A chromosome genome? Trends Plant Sci. **8:** 417–423.

Jones, R. N., 1995 Tansley review no. 85: B chromosomes in plants. New Phytol. **131:** 411–423.

Jones, R. N., and H. Rees, 1982 *B Chromosomes*. Academic Press, London/New York.

Kasha, K. J., and K. N. Kao, 1970 High frequency haploid production in barley (*Hordeum vulgare* L.). Nature **225:** 874–876.

Kavanagh, T. A., and J. N. Timmis, 1986 Heterogeneity in cucumber ribosomal DNA. Theor. Appl. Genet. **72:** 337–345.

Kavanagh, T. A., and J. N. Timmis, 1988 Structure of melon rDNA and nucleotide sequence of the 17–25S spacer region. Theor. Appl. Genet. **75:** 673–680.

Kovarik, A., R. Matyasek, K. Y. Lim, K. Skalická, B. Koukalová *et al.*, 2004 Concerted evolution of 18–5.8–26S rDNA repeats in *Nicotiana* allotetraploids. Biol. J. Linn. Soc. **82:** 615–625.

Laurie, D. A., and M. D. Bennett, 1989 The timing of chromosome elimination in hexaploid wheat × maize crosses. Genome **32:** 953–961.

Leach, C. R., T. M. Donald, T. K. Franks, S. S. Spiniello, C. F. Hanrahan *et al.*, 1995 Organisation and origin of a B chromosome centromeric sequence from *Brachycome dichromosomatica*. Chromosoma **103:** 708–714.

Liao, D., 1999 Concerted evolution: molecular mechanism and biological implications. Am. J. Hum. Genet. **64:** 24–30.

Małuszyńska, J., 1990 B chromosomes of *Crepis capillaris* (L.) Wallr. *in vivo* and in *vitro*. Ph.D. Thesis, Uniwersytet Sląski, Katowice, Poland.

Małuszyńska, J., and D. Schweizer, 1989 Ribosomal RNA genes in B chromosomes of *Crepis capillaris* detected by non-radioactive in situ hybridization. Heredity **62:** 59–66.

Navashin, M., 1927 Über die Veränderung von Zhal und der Chromosomen infolge der Hybridisierung. Zeitschr. Zellforschung Mikroskopische Anatomie **19:** 195–233.

Navashin, M., 1934 Chromosomal alterations caused by hybridisation and their bearing upon certain general genetic problems. Cytologia **5:** 169–203.

Page, B. T., M. K. Wanous and J. A. Birchler, 2001 Characterization of a maize chromosome 4 centromeric sequence: evidence for an evolutionary relationship with the B chromosome centromere. Genetics **159:** 291–302.

Parker, J. S., G. H. Jones, L. A. Edgar and C. L. Whitehouse, 1989 The population cytogenetics of *Crepis capillaris*. II. The stability and inheritance of B chromosomes. Heredity **63:** 19–27.

Pickering, R. A., 1985 Partial control of chromosome elimination by temperature in immature embryos of *Hordeum vulgare* L. × *H. bulbosum*. Euphytica **14:** 869–874.

Puertas, M. J., 2002 Nature and evolution of B chromosomes in plants: a non-coding but information-rich part of plant genomes. Cytogenet. Genome Res. **198:** 198–205.

Rauscher, J. T., J. J. Doyle and A. H. D. Brown, 2004 Multiple origins and rDNA internal transcribed spacer homeologue evolution in the *Glycine tomentella* (Leguminosae) allopolyploid complex. Genetics **166:** 987–998.

Rutishauser, A., 1960 Fragmentchromosomen bei *Crepis capillaris*. Beih. Z. Schweiz. Forstvereins **30:** 93–106.

Sapre, A. B., and D. Deshpande, 1987 Origin of B chromosomes in *Coix* L. through spontaneous interspecific hybridisation. J. Hered. **78:** 191–196.

Schubert, I., and U. Wobus, 1985 In situ hybridization confirms jumping nucleolus organizing regions in *Allium*. Chromosoma **92:** 143–148.

Sell, P. D., 1976 *Crepis*, pp. 344–357 in *Flora Europaea*, Vol. 4, edited by T. G. Tutin, V. H. Heywood, N. A. Burges, D. M. Moore, D. H. Valentine *et al.* Cambridge University Press, Cambridge, UK/London/New York.

Sharbel, T. F., D. M. Green and A. Houben, 1998 B-chromosome origin in the endemic New Zealand frog Leiopelma hochstetteri through sex chromosome devolution. Genome **41:** 14–22.

Sirri, V., P. Roussel and D. Hernandez-Verdun, 2000 The AgNOR proteins: qualitative and quantitative changes during the cell cycle. Micron **31:** 121–126.

Stitou, S., R. Jimenez, R. D. de la Guardia and M. Burgos, 2000 Sex-chromosome pairing through heterochromatin in the African rodent Lemniscomys barbarus (Rodentia, Muridae). A synaptonemal complex study. Chromosome Res. **8:** 277–283.

Swofford, D., 2002 *PAUP* Phylogenetic Analysis Using Parsimony (*and Other Methods)*. Version 4. Sinauer Associates, Sunderland, MA.

Thomas, H. M., and R. A. Pickering, 1983 Chromosome elimination in *Hordeum vulgare* × *Hordeum bulbosum* hybrids. 2. Chromosome behaviour in secondary hybrids. Theor. Appl. Genet. **66:** 141–146.

Togby, H.A., 1943 A cytological study of *Crepis fuliginosa*, *C. neglecta* and their F_1 hybrids and its bearing on a mechanism of phytogenetic reduction in chromosome number. J. Genet. **45:** 67–111.

White, T. J., T. Bruns, S. Lee and J. Taylor, 1990 Amplification and direct sequencing of fungal ribosomal RNA genes for phylogenetics, pp. 315–322 in *PCR Protocols: A Guide to Methods and Applications*, edited by M. A. Innis, D. H. Gelfand, J. J. Sninsky and T. J. White. Academic Press, San Diego.

Wilson, E. B., 1907 The supernumerary chromosomes of *Hemiptera*. Science **26:** 870.

Yakura, K., and S. Tanifuji, 1983 Molecular cloning and restriction analysis of *Eco R*I fragments from *Vicia faba* rDNA. Plant Cell Physiol. **24:** 1327–1330.

Ziegler, C. G., D. K. Lamatsch, C. Steinlein, W. Engel, M. Schartl *et al.*, 2003 The giant B chromosome of the cyprinid fish Alburnus alburnus harbours a retrotransposon-derived repetitive DNA sequence. Chromosome Res. **11:** 23–35.

Communicating editor: J. Birchler

A18 Manzanero, S., Arana, P., Puertas, M.J., and Houben, A. (2000). The chromosomal distribution of phosphorylated histone H3 differs between plants and animals at meiosis. Chromosoma 109, 308-317.

Chromosoma (2000) 109:308–317
DOI 10.1007/s004120000087

ORIGINAL ARTICLE

Silvia Manzanero · Pilar Arana · María J. Puertas
Andreas Houben

The chromosomal distribution of phosphorylated histone H3 differs between plants and animals at meiosis

Received: 4 February 2000 / in revised form: 5 April 2000 / Accepted: 6 April 2000 / Published online: 29 June 2000

Abstract Plant (*Secale cereale*, *Triticum aestivum*) and animal (*Eyprepocnemis plorans*) meiocytes were analyzed by indirect immunostaining with an antibody recognizing histone H3 phosphorylated at serine 10, to study the relationship between H3 phosphorylation and chromosome condensation at meiosis. To investigate whether the dynamics of histone H3 phosphorylation differs between chromosomes with a different mode of segregation, we included in this study mitotic cells and also meiotic cells of individuals forming bivalents plus three different types of univalents (A chromosomes, B chromosomes and X chromosome). During the first meiotic division, the H3 phosphorylation of the entire chromosomes initiates at the transition from leptotene to zygotene in rye and wheat, whereas in *E. plorans* it does so at diplotene. In all species analyzed H3 phosphorylation terminates toward interkinesis. The immunosignals at first meiotic division are identical in bivalents and univalents of A and B chromosomes, irrespective of their equational or reductional segregation at anaphase I. The grasshopper X chromosome, which always segregates reductionally, also shows the same pattern. Remarkable differences were found at second meiotic division between plant and animal material. In *E. plorans* H3 phosphorylation occurred all along the chromosomes, whereas in plants only the pericentromeric regions showed strong immunosignals from prophase II until telophase II. In addition, no immunolabeling was detectable on single chromatids resulting from equational segregation of plant A or B chromosome univalents during the preceding anaphase I. Simultaneous immunostaining with anti-tubulin and anti-phosphorylated H3 antibodies demonstrated that the kinetochores of all chromosomes interact with microtubules, even in the absence of detectable phosphorylated H3 immunosignals. The different pattern of H3 phosphorylation in plant and animal meiocytes suggests that this evolutionarily conserved post-translational chromatin modification might be involved in different roles in both types of organisms. The possibility that in plants H3 phosphorylation is related to sister chromatid cohesion is discussed.

Edited by: W. Hennig

S. Manzanero · P. Arana · M.J. Puertas (✉)
Departamento de Genética, Facultad de Biología,
Universidad Complutense, 28040 Madrid, Spain
e-mail: majetas@eucmax.sim.ucm.es

A. Houben
Department of Genetics, The University of Adelaide, SA 5005,
Australia

Introduction

During mitotic and meiotic cell division, the chromatin becomes remarkably condensed to facilitate chromosome segregation. In order to accomplish the structural and functional requirements for alignment, pairing and recombination of homologous chromosomes, the chromosome condensation process at meiosis most likely differs from that at mitosis.

One of the phenomena that correlates with the initiation and maintenance of mitotic chromosome condensation is the phosphorylation of the core histone H3 at Ser10 (Gurtley et al. 1975; Ajiro et al. 1983, 1996), close to its flexible N-terminal end (Paulson and Taylor 1982). While only a few H3 molecules are phosphorylated at interphase, nearly all become phosphorylated during mitosis (Gurtley et al. 1987). The interrelation of H3 phosphorylation and chromatin condensation is not understood. It has been proposed that phosphorylation of the H3 N-terminal tail might reduce its affinity for DNA, facilitating the movement of nucleosomes and the access of condensation factors to the chromatin (Roth and Allis 1992; Hendzel et al. 1997; Sauvé et al. 1999). With an antiserum against phosphorylated H3, Hendzel et al. (1997) demonstrated H3 phosphorylation of mammalian mitotic chromosomes initiating in pericentromeric heterochromatin in late G2 interphase cells, spreading throughout the condensing chromatin, and completing just prior to the formation of prophase chromosomes. Coincidence of H3 phosphorylation and mitotic chromo-

some condensation has meanwhile been reported for a broad spectrum of eukaryotes, such as protozoa (*Tetrahymena thermophila*; Wei et al. 1998), fungi, worms and insects (*Aspergillus nidulans, Caenorhabditis elegans, Drosophila melanogaster;* Wei and Allis 1998), as well as mono- and dicot plants (*Hordeum vulgare, Secale cereale, Vicia faba*; Houben et al. 1999).

Recently, H3 phosphorylation has also been described for meiotic chromosomes of *Tetrahymena* (Wei et al. 1998, 1999) and mice (Cobb et al. 1999a, b). In *Tetrahymena* mutants with unphosphorylatable histone H3, Wei et al. (1999) observed disturbed chromosome segregation during micronuclear mitosis and meiosis. This was interpreted as a consequence of impaired chromosome condensation.

The present study describes the chromosomal distribution of phosphorylated histone H3 during both meiotic divisions in various types of plant and animal bivalents and univalents: (1) bivalent-forming chromosomes with normal meiotic behavior, such as the chromosomes of the normal set (A chromosomes, As) or pairs of supernumerary B chromosomes (Bs); (2) chromosomes forming natural univalents such as the X chromosome or non-associated Bs at metaphase I; (3) univalents in haploids or monosomic addition lines, and (4) artificially induced autosomal univalents. The univalents may show either unipolar (syntelic) or bipolar (amphitelic) orientation at metaphase I and, consequently, reductional or equational segregation at anaphase I. Plant and animal materials are compared and the relationship between histone H3 phosphorylation, meiotic chromosome condensation and sister chromatid cohesion is discussed.

Materials and methods

The following materials were used: (1) Rye (*S. cereale*) 2*n*=14+Bs, from the Korean population Paldang, which contains B chromosomes in 20% of the individuals. (2) Haploid plants of wheat (*Triticum aestivum*, 2*n*=6*x*=42, var. Chinese Spring). (3) A monotelosomic addition line consisting of the 42 chromosomes of wheat plus the long arm of chromosome 5 of rye (5RL). (4) The grasshopper *Eyprepocnemis plorans* (2*n*=22+XX-X0).

All these materials share the feature of forming univalents: two types of natural univalents, such as the X chromosome in the male grasshopper and the rye B chromosomes; univalents produced by lack of homologous pairing, such as those in the haploids or in the monosomic addition line; and artificially induced autosomal univalents as is explained below.

Living spermatocyte cultures and univalent induction in *E. plorans*

Living spermatocyte cultures were made following the technique described by Nicklas et al. (1982) from testicular follicles obtained by biopsy from young adult males of the grasshopper *E. plorans*. In the testicular follicles of grasshoppers, cells are arranged in cysts of rather synchronous cells, in various stages of meiosis and spermatogenesis. Cysts from premeiotic mitosis to mature sperm can be found. In this species, the X chromosome appears as a univalent in male meiosis and shows regular behavior, migrating undivided to one pole at anaphase I and separating chromatids at anaphase II.

Autosomal univalents were induced by heat treatment of young adult males at 44°C for 4 days, followed by recovery in normal laboratory conditions (Rebollo and Arana 1995). The meiotic behavior of autosomal univalents is highly irregular (Rebollo and Arana 1995, 1997; Rebollo et al. 1998), showing a great variety of segregation abnormalities.

Plant chromosome preparation

Anthers were fixed for 30 min in freshly prepared 4% (w/v) paraformaldehyde solution containing phosphate-buffered saline (PBS, pH 7.3), washed for 45 min in PBS and digested at 37°C for 25 min in a mixture of 2.5% pectinase, 2.5% cellulase Onozuka R-10 and 2.5% pectolyase Y-23 (w/v) dissolved in PBS. Anthers were then washed for 15 min in PBS and squashed between a glass slide and coverslip in PBS. After freezing in liquid nitrogen, the coverslips were removed and the slides were transferred immediately into PBS.

For routine controls and quantitative estimations of configuration frequencies, anther squashes were made in 1% acetocarmine.

Mitotic chromosomes of rye were prepared from root tips according to Houben et al. (1999).

Plant immunostaining techniques

To avoid nonspecific antibody binding, slides were incubated for 30 min in 8% BSA (w/v), 0.1% Triton X100 in PBS at room temperature prior to two washes in PBS for 5 min each, and incubated with the primary antibody in a humidified chamber. The primary antibodies of a polyclonal rabbit antiserum that specifically recognized histone H3 phosphorylated at Ser 10 (Upstate Biotechnology, USA) were diluted 1:500 in PBS, 3% BSA. After 12 h incubation at 4°C and washing for 15 min in PBS, the slides were incubated in rhodamine-conjugated anti-rabbit IgG (Dianova) diluted 1:200 in PBS, 3% BSA for 3 h at room temperature. After final washes in PBS, the preparations were mounted in antifade containing 4′,6-diamidino-2-phenylindole (DAPI) as counterstain.

For simultaneous immunostaining with anti-α-tubulin, a microtubule stabilizing buffer (50 mM PIPES, 5 mM $MgSO_4$, 5 mM EGTA, pH 6.9) was used instead of PBS. The anti-α-tubulin antibody (N356, Amersham) diluted 1:50 was detected after incubation with fluorescein isothiocyanate (FITC)-conjugated anti-mouse antibody (Dianova) diluted 1:100. Fluorescent signals were observed using a microscope equipped with epifluorescence optics. The images, recorded with a cooled CCD camera, were pseudo-colored and merged with the program Adobe Photoshop 4.0.

Animal immunostaining techniques

Immunostaining was carried out on cultured spermatocytes previously tracked in vivo. Cells were labeled following the technique employed by Nicklas et al. (1995) for kinetochore staining with 3F3/2 antibody (Gorbsky and Ricketts 1993), without microcystin LR in the lysis/fixative buffer. A monoclonal anti-α-tubulin antibody (Boehringer) and the anti-phosphorylated H3 serum were used as primary antibodies at 1:50 and 1:100 dilutions in PBS, 1% BSA, respectively. FITC-conjugated anti-mouse (Boehringer) for tubulin, and rhodamine-conjugated anti-rabbit (Dianova) for phosphorylated H3 were used as secondary antibodies at 1:25 and 1:50 dilutions, respectively. Preparations were counterstained with DAPI before mounting in Vectashield. Cells were examined in an Olympus BX-60 epifluorescence microscope, photographed on 400 ISO color negative film, and the negatives scanned at 1340 dpi. The images were optimized for best contrast and brightness with Adobe Photoshop 4.0.

Table 1 Chromosomal distribution of phosphorylated histone H3 at mitosis and meiosis. (P, pericentromeric distribution of the immunolabeling; +, immunolabeling visible along the entire chromosome; –, immunolabeling not detectable; R, reductional segregation; E, equational segregation; L, leptotene; Z, zygotene; P, pachytene; D-Dk, diplotene-diakinesis; MI, metaphase I; AI, anaphase I; I, interkinesis; PII, prophase II; MII, metaphase II; AII, anaphase II; TII/In, telophase II/interphase transition)

Material	Type of chromosome	Mitosis	First meiotic division								Second meiotic division			
					L	Z	P	D–DK	MI	AI	I	PII	MII	AII	TII/In
Rye	As	P	Bivalents	R	–	+	+	+	+	+	–	P	P	P	–
	Bs	P	Bivalents	R	–	+	+	+	+	+	–	P	P	P	–
Univalents	R	–	+	+	+	+	+	–	P	P	P	–			
				E	–	+	+	+	+	+	–	–	–	–	–
Haploid wheat	As	P	Bivalents	R	–	+	+	+	+	+	–	P	P	P	–
			Univalents	R	–	+	+	+	+	+	–	P	P	P	–
				E	–	+	+	+	+	+	–	–	–	–	–
Wheat-5RL addition line	Mono 5RL	P	Univalent	R	–	+	+	+	+	+	–	P	P	P	–
				E	–	+	+	+	+	+	–	–	–	–	–
Eyprepocnemis plorans	As	+	Bivalents	R	–	–	–	+	+	+	–	+	+	+	–
			Univalents	R	–	–	–	+	+	+	–	+	+	+	–
				E	–	–	–	+	+	+	–	+	+	+	–
	X	+	Univalent	R	–	–	–	+	+	+	–	+	+	+	–

Results

A summary of the immunolabeling patterns obtained with antibodies against phosphorylated H3 during the different stages of meiosis in plant and animal meiocytes is presented in Table 1.

In plants the phosphorylation pattern of chromosomal histone H3 alters during meiosis

The immunolabeling patterns obtained with antibodies against phosphorylated H3 during the different stages of meiosis were similar for the chromosomes of the monocot species *S. cereale* and *T. aestivum*. Immunostaining of interphase cells was hardly observed. The first diffuse immunosignals were detectable during the transition from leptotene to zygotene (Fig. 1A, B). Strong immunosignals appeared to be dispersed randomly throughout the nuclei from zygotene to diplotene (Fig. 1C, D). With the further compaction of chromosomes during diakinesis, immunosignals were scattered over the chromosomes (Fig. 1E). At metaphase I, congressed rye and wheat bivalents (Figs. 1F, 2A), rye Bs (not shown) and wheat univalents (Fig. 2A, B) were entirely and strongly immunolabeled. During diakinesis and metaphase I, the histone H3 of the centromeric regions appeared slightly more strongly phosphorylated than the rest of the chromosomes (Fig. 1E, F, arrowed). At metaphase I, all bivalents were syntelically oriented, and the chromosomes migrated reductionally to the poles at anaphase I (Fig. 1G), still homogeneously labeled.

At telophase I (Fig. 1H), the phosphorylation of histone H3 gradually disappeared. At interkinesis, the short stage between the first and second meiotic divisions, in which no DNA replication occurs, the chromatin displayed only faint immunostaining (Fig. 1I). At the light microscopy level, it seems that the degree of chromatin condensation at interkinesis is higher than at mitotic interphase (Fig. 1O).

The H3 phosphorylation pattern at second meiotic division was similar to that observed in mitotic cells (Houben et al. 1999), where mainly the pericentromeric regions are immunolabeled at metaphase and anaphase (Fig. 1P, Q). At early prophase II, the recondensation of the chromosomes coincided with renewed phosphorylation of histone H3. The phosphorylation initiated in discrete areas and pronounced immunofluorescent spots became visible, while other areas were less intense and more diffusely labeled (Figs. 1J, 3A, upper cell). At late prophase II and metaphase II, the centromeric regions were phosphorylated, whereas the chromatid arms were very weakly labeled (Figs. 1K; 3A, lower cell, B, C).

The status of phosphorylation remained unchanged after the separation of the sister chromatids at anaphase II (Fig. 1L). At telophase II (Fig. 1M), the phosphorylation of histone H3 disappeared gradually with the decondensation of the chromosomes (Fig. 1N).

Histone H3 phosphorylation patterns differ between formerly reductionally and equationally divided plant univalents during the second meiotic division

At metaphase I, most chromosomes in the haploid wheat (Fig. 2A, B), and 66% of rye B chromosomes, form univalents. A high proportion of wheat univalents, 50% of B univalents and 75.2% of rye univalent 5RL of the wheat-rye addition line were syntelically oriented and migrated reductionally to the poles at anaphase I, still homogeneously labeled. The amphitelically oriented univalents divided equationally at anaphase I, their sister chromatids separating to different poles (Fig. 2C, one chromatid arrowed). Phosphorylation of H3 at first mei-

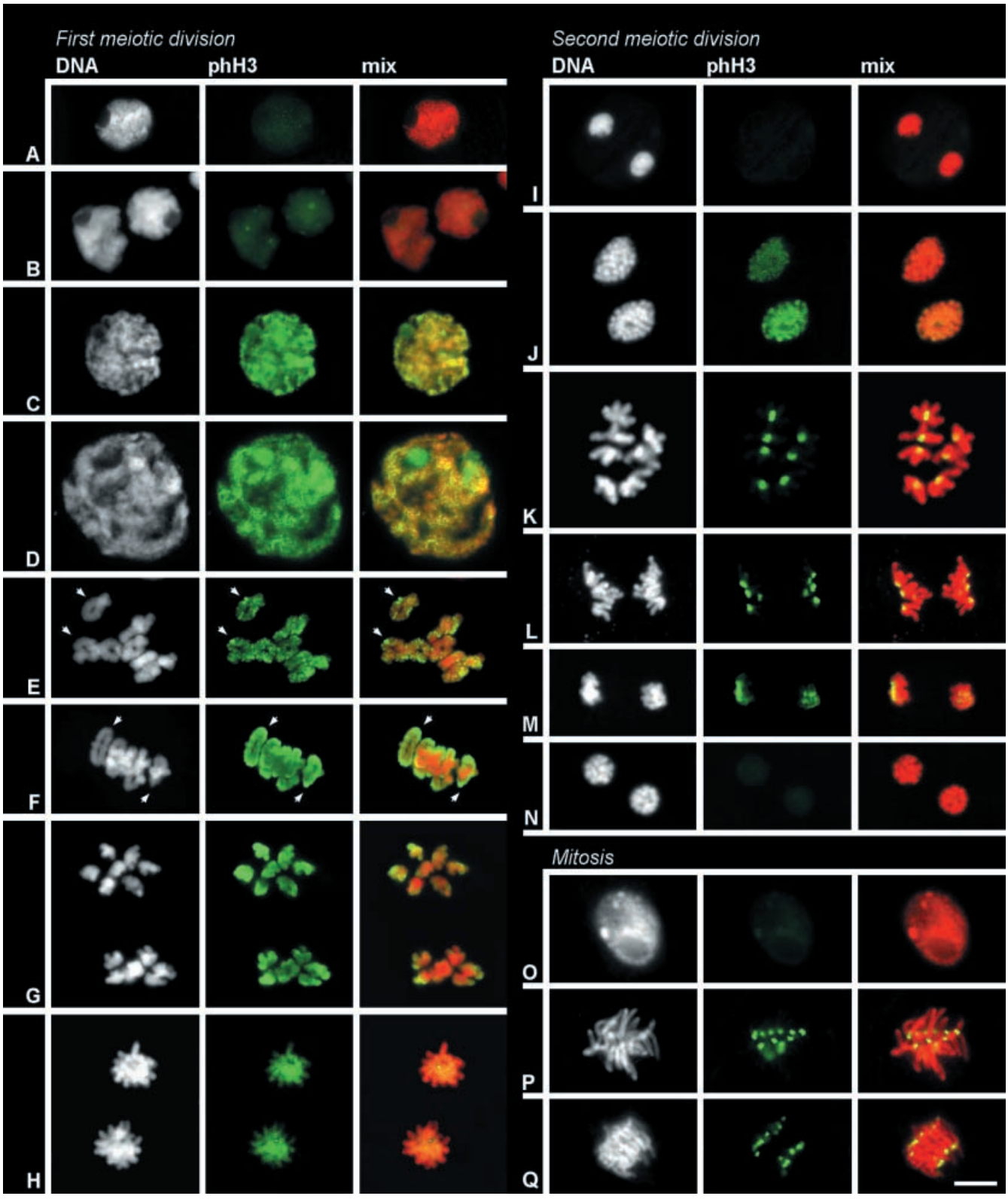

Fig. 1 Immunolocalization of phosphorylated histone H3 during meiosis (**A–N**) and mitosis (**O–Q**) of *Secale cereale* without B chromosomes. The different meiotic and mitotic stages were distinguished according to the morphology of the chromosomes. First meiotic division: **A** preleptotene-leptotene, **B** leptotene, **C** zygotene-pachytene, **D** diplotene, **E** diakinesis, **F** metaphase I, **G** anaphase I, **H** telophase I, **I** interkinesis. Second meiotic division: **J** prophase II, **K** metaphase II, **L** anaphase II, **M** telophase II, **N** interphase (tetrads). Mitosis: **O** interphase, **P** metaphase, **Q** anaphase. *DNA column* DAPI staining; *phH3 column* phosphorylated H3 labeling; in the *mix column*, the images of the DNA stained (*red*) and immunolabeled (*green*) cells are merged. *Bar* represents 5 µm (**Q**)

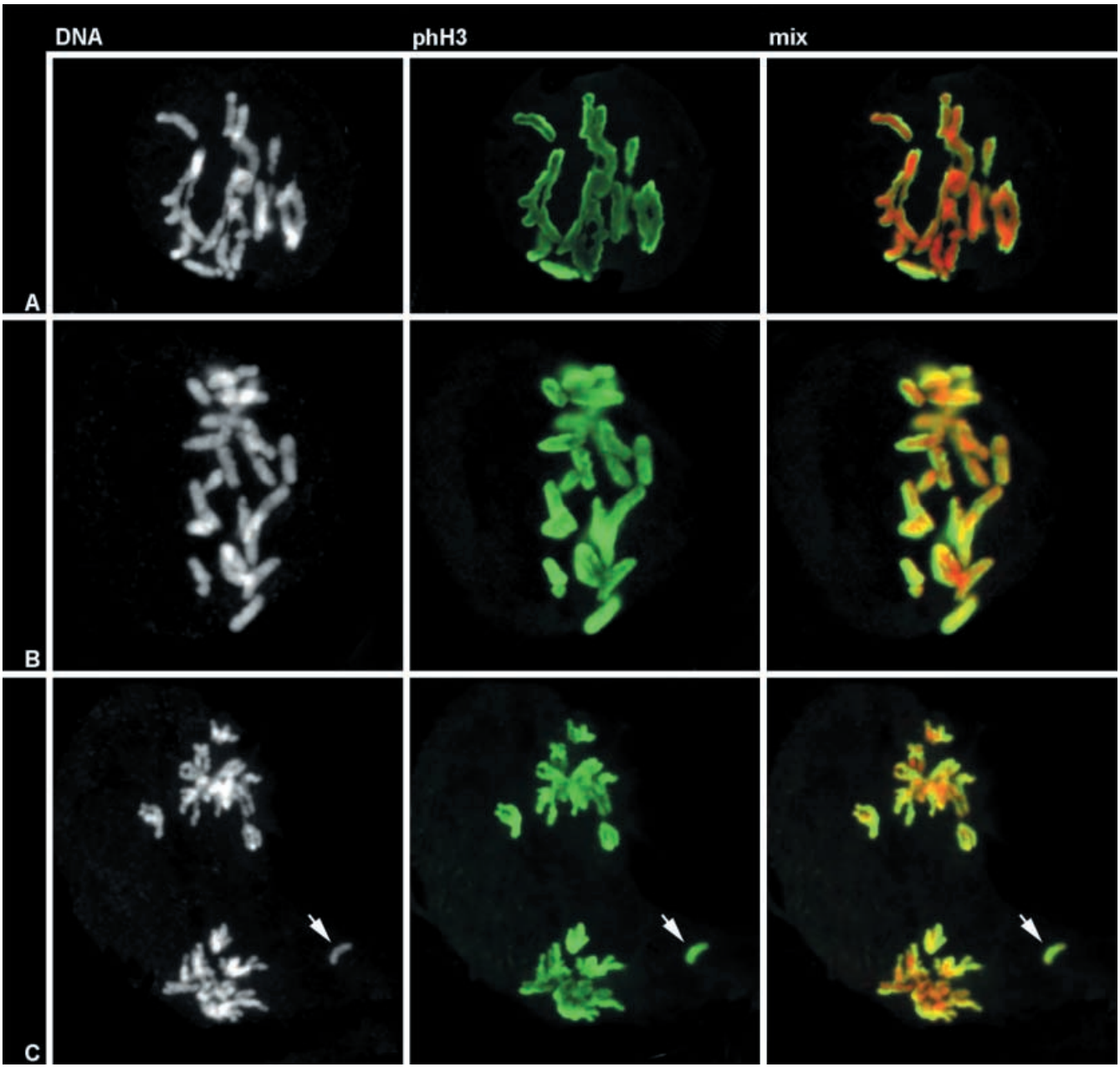

otic division was identical for equationally and reductionally dividing chromosomes.

To ascertain the fate of the equationally divided univalents, the frequency of cells with equationally dividing rye B univalents at anaphase I, the frequency of cells with uncoupled B chromatids at metaphase II and the frequency of cells with laggards at anaphase II were scored in 100 cells of ten rye anthers stained with acetocarmine. The frequencies coincided (33%), indicating that single chromatids at metaphase II and chromatid laggards at anaphase II are products of equational division of univalents at first meiotic division.

The frequency of cells with uncoupled chromatids at metaphase II was 25% for rye A chromosomes in the addition line, and more than 95% for haploid wheat. As in the case of rye Bs, single chromatids are easily detected

Fig. 2 Immunolocalization of phosphorylated histone H3 on meiocytes of haploid *Triticum aestivum* at metaphase I (**A**, **B**), and anaphase I (**C**). In **A** bivalents as well as univalents are shown, whereas in **B** there are only univalents. Note the prematurely separated sister chromatid *arrowed* in **C**. *DNA column* DAPI staining; *phH3 column* phosphorylated H3 labeling; *mix column* merged DNA staining (*red*) and immunolabeling (*green*) images

Fig. 3A–E Simultaneous immunostaining of phosphorylated histone H3 and α-tubulin on meiocytes of haploid *Triticum aestivum* during the second meiotic division. **A** Prophase II, **B, C** metaphase II, **D** early anaphase II, **E** late anaphase II. Single chromatids are *arrowed*. **C** The interaction between tubulin fibers and the kinetochore of a single chromatid is illustrated. *DNA column* DAPI staining; *phH3 column* phosphorylated H3 labeling; *tubulin column* α-tubulin labeling; *mix column* merged DNA (*blue*), phH3 (*red*) and tubulin (*green*) images ▶

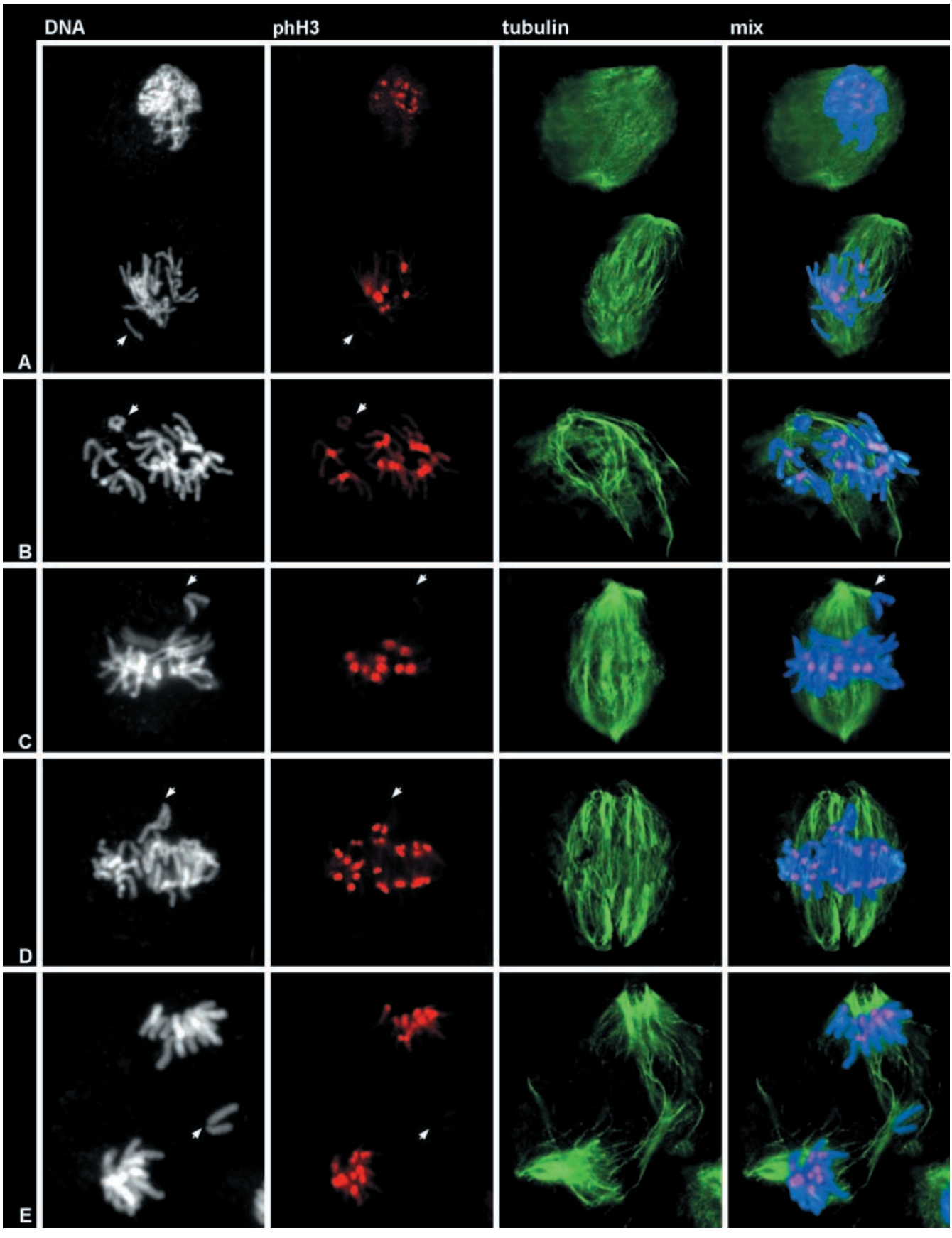
DNA
phH3
tubulin
mix
A
B
C
D
E

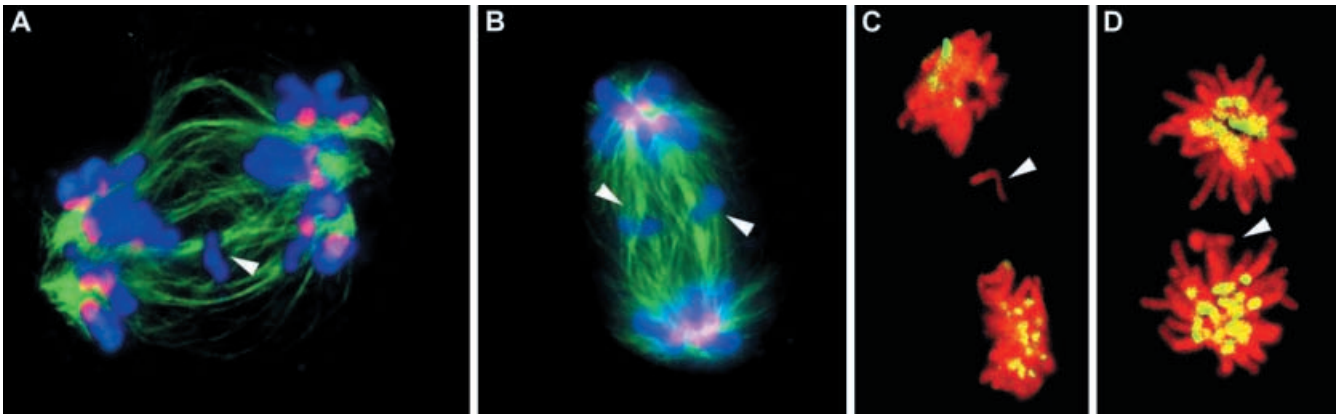

Fig. 4A–D Histone H3 of condensed prematurely separated A or B chromatids is not phosphorylated at the centromeric region. **A, B** Anaphase II cells of rye showing lagging B chromatids (*arrowed*); DNA *blue*, phosphorylated H3 labeling *red*, α-tubulin labeling *green*. **C, D** Anaphase II chromosomes (*red*) of a wheat 5RL monosomic addition line after immunostaining of phosphorylated H3 (*yellow*). The lagging rye chromatids are *arrowed*

by their faulty congression at the metaphase II plate (Fig. 3C) or by their impaired segregation at anaphase II, where they often appear as laggards (Figs. 3E; 4). They were condensed in a similar manner to the sister chromatids of reductionally divided chromosomes (Fig. 3, 4). However, the immunostaining revealed that, within the same metaphase II cell, only chromosomes consisting of two sister chromatids had strong signals at their pericentromeric regions, whereas single chromatids showed no immunosignal (Fig. 3A, B, C, arrowed). At anaphase II, these single A and B chromatids also revealed unphosphorylated H3 (Figs. 3D, E; 4, arrowed).

To analyze whether the different H3 phosphorylation status of the pericentromeric chromatin affects the ability of the kinetochore to attach to spindle microtubules, triple-staining with anti-phosphorylated H3, anti-tubulin antibodies and DAPI was performed (Figs. 3; 4A, B). Anti-tubulin staining also confirmed the affiliation of single chromatids lacking phosphorylated H3 to the cells analyzed. The triple-staining experiment demonstrated that the kinetochores interact with microtubules, irrespective of their level of H3 phosphorylation. Figures 3C, E and 4A, B show single A and B chromatids without phosphorylated H3 at the pericentromeric chromatin, in interaction with apparently normal chromosomal fibers. The centromeric regions of such single chromatids appear to have a normal degree of condensation.

Histone H3 phosphorylation patterns in *E. plorans* at meiosis and mitosis

In *E. plorans*, the meiotic H3 phosphorylation pattern obtained (Fig. 5) coincided with that previously reported by Cobb et al. (1999a, b) for *Mus musculus*. The onset of phosphorylation was detected at diplotene (Fig. 5C, C′, D, D′, a) and the immunosignals were distributed all over the condensed chromosomes. At metaphase I, both the autosomal bivalents and the X univalent were strongly immunolabeled (Fig. 5D, D′, b, X arrowed).

At anaphase I the condensed chromosomes showed strong immunolabeling, which gradually disappeared during telophase I, and was not observed at interkinesis (Fig. 5D, D′, c, d, e). The immunosignals reappeared at prophase II, and were distributed over the entire length of the condensed chromosomes during the second meiotic division.

This behavior was the same for all types of chromosomes studied, i.e., the autosomal bivalents, the X chromosome, and the induced autosomal univalents, irrespective of their reductional or equational segregation at anaphase I (Fig. 5E, E′, F, F′, G, G′, G″). Also, in the case of *E. plorans*, there is evidence that the single chromatids at metaphase II or lagging chromosomes at anaphase II are the result of equationally dividing univalents at first division (Rebollo and Arana 1997).

The mitotic H3 phosphorylation pattern was observed in mitosis in those testicular follicles where spermatogonial cells were dividing. The immunosignals appeared not at the initiation of chromosome condensation, but at mid-prophase (Fig. 5A, A′). It was not possible to determine whether the H3 phosphorylation initiates on the pericentromeric regions or scattered along the chromosomes. At metaphase and anaphase, the whole chromosome showed strong immunolabeling, which disappeared during telophase (Fig. 5B, B′).

Discussion

Histone H3 phosphorylation at Ser10, associated with chromatin condensation in mitosis and meiosis, has been described in species ranging from *Tetrahymena* (Wei et al. 1998) to mammals (Hendzel et al. 1997; Cobb et al. 1999a, b), indicating that H3 phosphorylation during nuclear division is a highly conserved process among eukaryotes. However, the immunolabeling patterns obtained with antibodies against phosphorylated H3 in the present work show that there are remarkable differences in the chromosomal distribution of phosphorylated H3

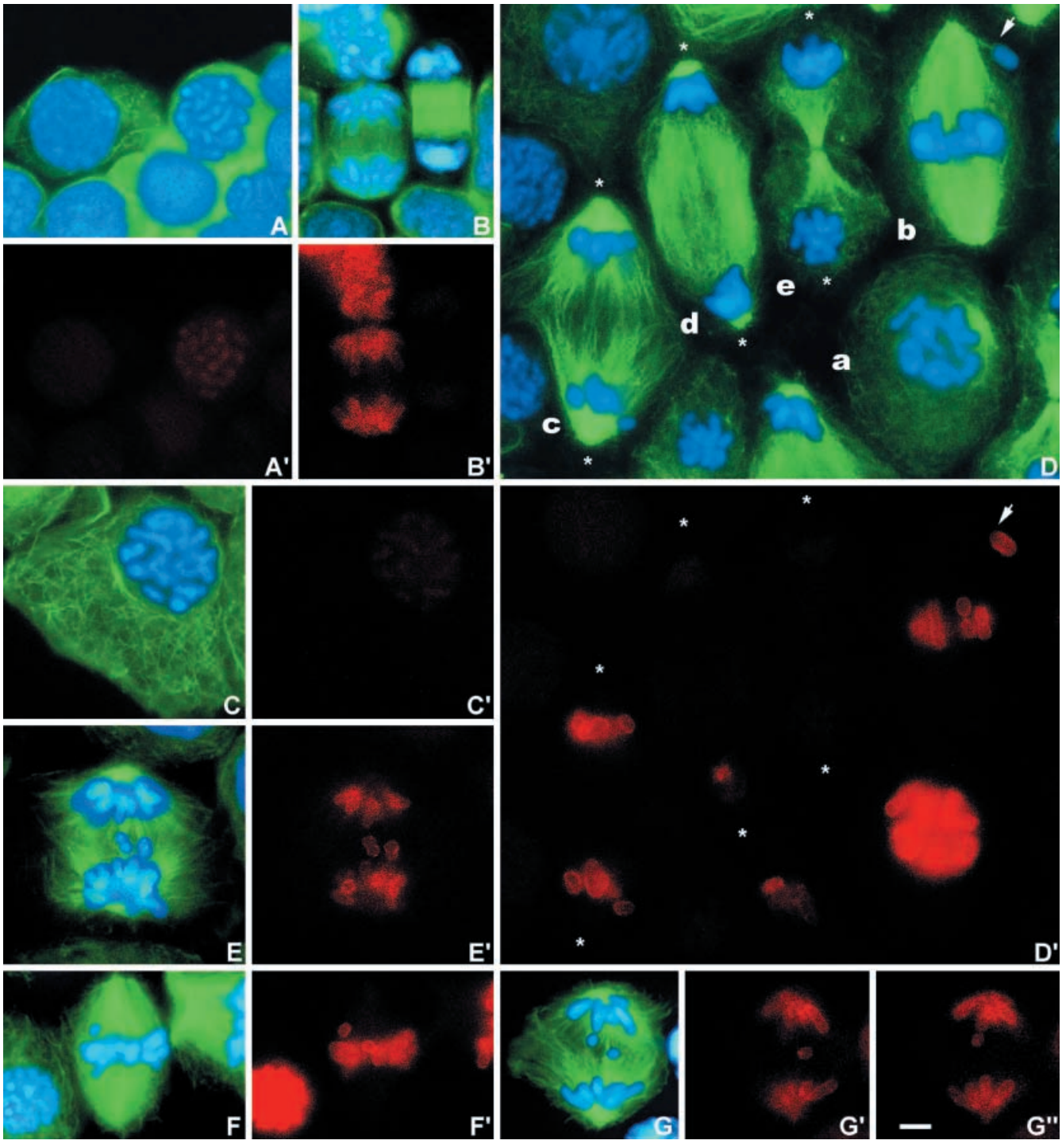

Fig. 5A–G Immunostaining of phosphorylated H3 and α-tubulin during mitosis and meiosis of *Eyprepocnemis plorans*. **A–G** DAPI and α-tubulin staining; **A′–G′** phosphorylated H3 labeling. **A, A′** early (*left*) and late (*right*) mitotic prophase; **B, B′** mitotic anaphase (*left*) and telophase (*right*); **C, C′** diplotene; **D, D′** *a* diakinesis, *b* metaphase I (X *arrowed*), *c* anaphase I, *d* telophase I, *e* cytokinesis; *asterisks* indicate the poles; **E, E′** anaphase I with two lagging univalents amphitelically oriented; **F, F′** metaphase II with a single chromatid out of the plate; **G, G′, G″** anaphase II with two lagging chromatids (**G′** and **G″** are two focal planes of the same cell). **E–G** Cells from heat-treated individuals. *Bar* represents 5 μm (**G″**)

between animal and plant cells, and between mitosis and the first and second meiotic divisions.

Unlike mitosis, where the phosphorylation of H3 starts distinctly in the pericentromeric chromatin of mammals (Hendzel et al. 1997) and plants (Houben et al. 1999), at first meiotic division the phosphorylation of H3 initiates, and remains uniform, along the chromosomes. In plants, the first immunosignals were observed when the initiation of chromosome condensation began during the transition from leptotene to zygotene. At this stage, chromosomes undergo a global structural reorganization,

the chromatids separate slightly and the chromosome volume increases (Dawe et al. 1994). By contrast, in *E. plorans*, the onset of phosphorylation was detected at diplotene, as it was in *M. musculus* (Cobb et al. 1999a, b).

From metaphase I to interkinesis, the H3 phosphorylation patterns were similar in *E. plorans* and plant meiocytes. In both cases, the condensed chromosomes showed strong immunolabeling that gradually disappeared during telophase I. At the light microscopy level, it seems that the degree of chromatin condensation at interkinesis is higher than at mitotic interphase for the species analyzed. In most animals, telophase I and interkinesis are absent, and the anaphase chromosomes pass directly to late prophase II. The contraction of chromosomes is retained; in fact, it persists until the whole meiotic cycle is completed (Swanson et al. 1981). The fact that histone H3 becomes dephosphorylated at interkinesis and phosphorylated again during prophase II, indicates that this post-translational modification is reversible and can occur independently of the DNA replication process.

The spatial and temporal course of H3 phosphorylation during the second meiotic division resembles that of mitosis of the same species. In rye and wheat the immunolabeling was restricted to pericentromeric positions, whereas in *E. plorans*, the chromosomes or chromatids were labeled throughout their length.

Surprisingly, the single chromatids of equationally segregated A or B chromosome univalents, of both grass species analyzed, revealed no detectable phosphorylated histone H3 during the entire second meiotic division. In *E. plorans*, however, this phenomenon was not observed, and the single chromatids, resulting from heat-induced univalents, showed the same immunolabeling as the normally dividing chromosomes.

It should be noted that normal plant chromosome arms were condensed at second meiotic division in the absence of detectable levels of phosphorylated H3. Furthermore, those single chromatids lacking immunosignals even at the pericentromeric region, were equally condensed. These observations prompt the question of whether or not phosphorylation of histone H3 is an absolute requirement for the initiation and/or maintenance of chromosome condensation. Van Hooser et al. (1998) have already observed that hypotonic treatment of mitotic mammalian cells can cause H3 dephosphorylation without chromosome decondensation, and suggested that H3 phosphorylation is not required for the maintenance of high levels of chromosome condensation. Also, in *Tetrahymena* mutants with unphosphorylatable H3, the condensation of chromosomes during mitosis and meiosis did not fail completely (Wei et al. 1999). At mitosis, such cells exhibited difficulty in passing out of anaphase, and some chromosomes could not segregate properly and lagged between the two daughter nuclei (Wei et al. 1999). Also, the condensation status of early prophase chromosomes of mice spermatocytes was unaffected after artificial induction of precocious histone H3 phosphorylation by okadaic acid treatment. Further histone H3 phosphorylation was not inhibited, even though chromosome condensation was artificially inhibited, demonstrating that the phosphorylation of histone H3 can be uncoupled from meiotic chromosome condensation (Cobb et al. 1999a, b). Thus, histone H3 phosphorylation is not sufficient for the condensation of mitotic and meiotic chromosomes. Perhaps the phosphorylation at Ser10 of histone H3 is not necessary at all for the condensation of meiotic plant chromosomes, and other chromosomal components are more important in this process.

Alternatively, the phosphorylation of H3 might be necessary for condensation, but only a few phosphorylated H3 molecules, not detectable by epifluorescence microscopy, would be sufficient to initiate the condensation of chromosomes during the second meiotic division. In any case, the different longitudinal phosphorylation of the chromosomes remains unexplained. Also, it cannot be ruled out that in plant chromosomes the pericentromeric regions and chromosome arms use different condensation mechanisms.

Since, in our experiments, H3 phosphorylated and nonphosphorylated chromatids showed a normal degree of condensation during the second meiotic division, it is tempting to speculate that the phosphorylation of H3 may play different roles affecting chromatin structure in plants and animals. One possible assumption would be that the pattern of phosphorylated histone H3 found in plant cells is closer to that of sister chromatid cohesion than to chromosome condensation in both meiotic divisions. At first meiotic division, the condensed sister chromatids are entirely H3 phosphorylated and closely associated along their entire length (Fig. 1C–F). Cohesion along the chromatid arms serves to keep the bivalents intact by counteracting the spindle forces that act at the kinetochores. This association along the chromosome arms disappears at anaphase I, allowing the homologs to segregate to opposite poles (Bickel and Orr-Weaver 1996).

At second meiotic division, as in mitosis, the phosphorylation of histone H3 occurs only at the pericentromeric regions (Fig. 1K–M), where sister chromatids cohere until the onset of anaphase II. The situation is different for chromatids already separated by equational segregation of univalents during the first division. Since no chromosome reduplication occurs at interkinesis, such chromatids lack a sister to cohere with and therefore need not, or cannot, get H3 phosphorylated at the pericentromeric chromatin. Since the kinetochores of such chromatids interact with microtubules, it can also be concluded that the phosphorylation of H3 of the pericentromeric chromatin is not essential for the successful interaction between microtubules and kinetochores.

However, the correlation between sister chromatid cohesion and phosphorylation of H3 is not perfect because the processes do not begin or end simultaneously. Firstly, it is generally assumed that sister chromatid cohesion is already established during S-phase (Uhlmann and Nasmyth 1998) and is maintained during interkinesis (Bickel and Orr-Weaver 1996). Secondly, sister chromatids eventually separate at the arm region at anaphase I, and along the entire chromatid length during anaphase of

mitosis and second meiotic division, without observable dephosphorylation of histone H3 until telophase.

It is possible that the phosphorylation of histone H3 has a more complex role, including both condensation and sister chromatid cohesion. A mechanistic link between cohesion and condensation has been proposed recently (Biggins and Murray 1999). Guacci et al. (1997) have demonstrated that the product of the *MCD1* gene physically links sister chromatids, and also recruits condensation proteins to condense the chromosomes of budding yeast. The evolutionarily conserved SMC family, with the related but distinct condensin and cohesin protein complexes, is apparently also involved in sister chromatid cohesion and chromosome condensation (Hirano 1999), as is topoisomerase II (Rose et al. 1990; Anderson and Roberge 1996; Cobb et al. 1999b).

Taken together, our results indicate that the changes in chromosome structure during the cell mitotic and meiotic cycles are not universal. Further research will be needed to reach a deeper understanding of the mechanisms governing these complex changes.

Acknowledgements Our thanks go to A.K.M.R. Islam and K. Shepherd (Adelaide, Australia) for providing haploid wheat, and to I. Schubert (Gatersleben, Germany) for helpful comments on the manuscript. A.H. was supported by the Australian Research Council. S.M., P.A. and M.J.P. were supported by research project PB98-0678 of the DGICYT of Spain; S.M. was also supported by the Consejería de Cultura de la Comunidad de Madrid.

References

Ajiro K, Nishimoto T, Takahashi T (1983) Histone H1 and H3 phosphorylation during premature chromosome condensation in a temperature-sensitive mutant (tsBN2) of baby hamster kidney cells. J Biol Chem 258:4534–4538

Ajiro K, Yasuda H, Tsuji H (1996) Vanadate triggers the transition from chromosome condensation to decondensation in a mitotic mutant (tsTM13). Inactivation of $p34^{cdc2}$/H1 kinase and dephosphorylation of mitosis-specific histone H3. Eur J Biochem 241:923–930

Anderson H, Roberge M (1996) Topoisomerase II inhibitors affect entry into mitosis and chromosome condensation in BHK cells. Cell Growth Differ 7:83–90

Bickel SE, Orr-Weaver TL (1996) Holding chromatids together to ensure they go their separate ways. BioEssays 18:293–300

Biggins S, Murray AW (1999) Sister chromatid cohesion in mitosis. Curr Opin Genet Dev 9:230–236

Cobb J, Cargile B, Handel MA (1999a) Acquisition of competence to condense metaphase I chromosomes during spermatogenesis. Dev Biol 205:49–64

Cobb J, Miyaike M, Kikuchi A, Handel MA (1999b) Meiotic events at the centromeric heterochromatin: histone H3 phosphorylation, topoisomerase IIα localization and chromosome condensation. Chromosoma 108:412–425

Dawe RK, Sedat JW, Agar DA, Cande WZ (1994) Meiotic chromosome pairing in maize is associated with a novel chromatin organization. Cell 76:901–912

Gorbsky GJ, Ricketts WA (1993) Differential expression of a phosphoepitope at the kinetochores of moving chromosomes. J Cell Biol 122:1311–1321

Guacci V, Koshland D, Strunnikov A (1997) A direct link between sister chromatid cohesion and chromosome condensation revealed through the analysis of MCD1 in *S. cerevisiae*. Cell 91:47–57

Gurtley LR, Walters RA, Tobey RA (1975) Sequential phosphorylation of histone subfractions in the Chinese hamster cell cycle. J Biol Chem 250:3936–3944

Gurtley LR, D'Anna JA, Barham SS, Deaven LI, Tobey RA (1987) Histone phosphorylation and chromatin structure during mitosis in Chinese hamster cells. Eur J Biochem 84:1–15

Hendzel MJ, Wei Y, Mancini MA, Van Hooser A, Ranalli T, Brinkley BR, Bazett-Jones DP, Allis CD (1997) Mitosis-specific phosphorylation of histone H3 initiates primarily within pericentromeric heterochromatin during G2 and spreads in an ordered fashion coincident with mitotic chromosome condensation. Chromosoma 106:348–360

Hirano T (1999) SMC-mediated chromosome mechanics: a conserved scheme from bacteria to vertebrates? Genes Dev 13:11–19

Houben A, Wako T, Furushima-Shimogawara R, Presting G, Künzel G, Schubert I, Fukui K (1999) The cell cycle dependent phosphorylation of histone H3 is correlated with the condensation of plant mitotic chromosomes. Plant J 19:1–5

Nicklas RB, Kubai DF, Hays TS (1982) Spindle microtubules and the mechanical associations after micromanipulation in anaphase. J Cell Biol 95:91–104

Nicklas RB, Ward SC, Gorbsky GJ (1995) Kinetochore chemistry is sensitive to tension and may link mitotic forces to a cell cycle checkpoint. J Cell Biol 130:929–939

Paulson JR, Taylor SS (1982) Phosphorylation of histones 1 and 3 and nonhistone high mobility group 14 by an endogenous kinase in HeLa metaphase chromosomes. J Biol Chem 257:6064–6072

Rebollo E, Arana P (1995) A comparative study of orientation at behavior of univalent in living grasshopper spermatocytes. Chromosoma 104:56–67

Rebollo E, Arana P (1997) Univalent orientation in living meiocytes. In: Henriques-Gil N, Parker JS, Puertas MJ (eds) Chromosomes today 12, Chapman & Hall, London, pp 249–269

Rebollo E, Martín S, Manzanero S, Arana P (1998) Chromosomal strategies for adaptation to univalency. Chromosome Res 6:515–531

Rose D, Thomas W, Holm C (1990) Segregation of recombined chromosomes in meiosis I requires DNA topoisomerase II. Cell 60:1009–1017

Roth SY, Allis CD (1992) Chromatin condensation: does histone H1 phosphorylation play a role? Trends Biochem Sci 17:93–98

Sauvé DM, Anderson HJ, Ray JM, James WM, Rohberge M (1999) Phosphorylation-induced rearrangement of the histone H3 NH_2-terminal domain during mitotic chromosome condensation. J Cell Biol 145:225–235

Swanson CP, Merz T, Young WJ (1981) Cytogenetics. The chromosome in division, inheritance, and evolution. Prentice Hall, Englewood Cliffs, NJ

Uhlmann F, Nasmyth K (1998) Cohesion between sister chromatids must be established during DNA replication. Curr Biol 8:1095–1101

Van Hooser A, Goodrich DW, Allis CD, Brinkley BR, Mancini MA (1998) Histone H3 phosphorylation is required for the initiation, but not maintenance, of mammalian chromosome condensation. J Cell Sci 111:3497–3506

Wei Y, Allis CD (1998) A new marker for mitosis. Trends Cell Biol 8:266

Wei Y, Mizzen CA, Cook RG, Gorovsky MA, Allis CD (1998) Phosphorylation of histone H3 at serine 10 is correlated with chromosome condensation during mitosis and meiosis in *Tetrahymena*. Proc Natl Acad Sci USA 95:7480–7484

Wei Y, Yu L, Bowen J, Gorovsky MA, Allis CD (1999) Phosphorylation of histone H3 is required for proper chromosome condensation and segregation. Cell 97:99–109

A19 Marschner, S., Kumke, K., and Houben, A. (2007a). B chromosomes of *B. dichromosomatica* show a reduced level of euchromatic histone H3 methylation marks. Chromosome Res 15, 215-222.

Chromosome Research (2007) 15:215–222
DOI: 10.1007/s10577-006-1114-x

B chromosomes of *B. dichromosomatica* show a reduced level of euchromatic histone H3 methylation marks

Sylvia Marschner, Katrin Kumke & Andreas Houben*
Leibniz Institute of Plant Genetics and Crop Plant Research (IPK), 06466, Gatersleben, Germany;
Tel: +49-039482-5486; Fax: +49-039482-5137; E-mail: houben@ipk-gatersleben.de
**Correspondence*

Received 1 November 2006. Received in revised form and accepted for publication by Herbert Macgregor 27 November 2006

Key words: B chromosomes, euchromatin, heterochromatin, histone H3 methylation

Abstract

B chromosomes (Bs) are dispensable, less-transcriptionally active components of the genomes of numerous species. Little information is available on the chromatin composition of Bs and whether it differs in any way from that of the A chromosomes. Methylated isoforms of histone H3 are of particular interest because of their role in eu/heterochromatin formation. Immunofluorescence using site-specific antibodies demonstrates that the chromatin in A and both types of Bs of *B. dichromosomatica* differs markedly in euchromatic histone H3 methylation marks. While A chromosomes are labelled brightly, the micro B and large B chromosomes are faintly labelled with antibodies against H3K4me2/3, H3K9me3 and H3K27me2/3. The heteropycnotic, tandem-repeat enriched micro Bs were even less labelled with euchromatic histone H3 methylation marks than large Bs, most probably due to different DNA composition. No differences in immunolabelling intensity between A and B chromosomes were found as to the heterochromatic marks H3K9me1/2 and H3K27me1, indicating that Bs are not additionally labelled by heterochromatin typical histone H3 modifications. Analysis of DNA replication timing suggests that micro Bs are replicating throughout S-phase.

Introduction

B chromosomes (Bs) are dispensable components of the genomes of numerous species of both plants and animals. They do not pair with any of the standard A chromosomes at meiosis, by definition, and have irregular modes of inheritance. Bs are generally assumed to be genetically inactive, because no major genes with specific phenotypic effects, necessary for normal development, are known. Except for the B chromosome-located 45s rRNA gene of *Crepis capillaris*, there has been no direct molecular evidence of transcription of B chromosome DNA in any plant species (Leach *et al*. 1995). Little is known about the origin of Bs, but it is most likely that those of different organisms arise in various ways. It is widely accepted that Bs could be derived from A chromosomes and/or from sex chromosomes (reviewed in Jones & Rees 1982, Jones 1995, Camacho *et al*. 2000, Jones & Houben 2003). Due to the fact that the Bs of maize (Page *et al*. 2001, Cheng & Lin 2003) and *Brachycome dichromosomatica* (Houben *et al*. 2001) have a major representation of sequences that originate from different A chromosomes, Bs could represent an amalgamation of sequences coming from several chromosomes. Bs are of particular interest in maize where they have been used in genetic analysis involving A/B translocations for mapping and A chromosome segment dosage analyses (Birchler *et al*. 1990).

Most of the molecular studies have been focused on the DNA composition of Bs and with the exception of mainly repetitive B chromosome-specific sequences, no major differences have been found between A and B chromosomes at the DNA level. On the other hand, there is little information available on the chromatin composition of Bs. Based on classical cytological observations an early survey suggested that the Bs in about half of plant species which carry them are described as being heterochromatic (Jones 1975). Heterochromatin was recognized, in Bs as in other chromosomes, by its intensely compacted state during interphase and early prophase of mitosis and meiosis and/or after applying a Giemsa C-banding method. Because no genes with specific phenotypic effects, necessary for normal development are known for Bs, the finding of non-heterochromatic Bs is puzzling.

More recent advances in chromatin characterization, in terms of epigenetic marks, showed the involvement of DNA methylation and post-translational histone modifications (reviewed in Richards & Elgin 2002, Craig 2005). Methylation of histone H3 at lysine residues 4, 9 and 27 has become the best-studied epigenetic (reviewed by Martin & Zhang 2005). Whereas euchromatin-specific methylation of H3K4 is highly conserved among eukaryotes, heterochromatin indexing by methylation marks at H3K9/27 and H4K20 is more variable (Fuchs *et al.* 2006). Several studies have shown that modification of the histone H3 tail by methylation of lysine residues 9 and 27 negatively regulates transcription by promoting a compact chromatin structure (Bannister *et al.* 2001, Jacobs *et al.* 2001, Cao *et al.* 2002, Czermin *et al.* 2002, Francis *et al.* 2004). In contrast, euchromatin is marked by methylation of lysine residue 4 (Noma *et al.* 2001, Santos-Rosa *et al.* 2002, Zegerman *et al.* 2002). The identification of a H3K4-specific histone demethylase (Shi *et al.* 2004) challenged the view that histone methylations are permanent and non-reversible.

In order to test whether genetically active A chromosomes and genetically inactive Bs differ as to their content of euchromatin and heterochromatin-specific histone marks, A chromosomes and two different types of Bs of the plant *Brachycome dichromosomatica* (synonym *Brachyscome*) were comparatively analysed in this study.

Bs of *B. dichromosomatica* ($2n = 4$) are among the most extensively studied Bs of higher plants (Leach *et al.* 2004). In the central localities of the species distribution the frequency of Bs tends to be higher in populations in marginal environments, suggesting that under these conditions plus B plants have an increased fitness (Carter 1978). Plants of *B. dichromosomatica* cytodeme A2 may carry large Bs and micro Bs. Large Bs have a similar amount of heterochromatin as A chromosomes, are mitotically stable, show meiotic irregularity and replicate later in S-phase than A chromosomes (Houben *et al.* 1997a). The dot-like accessory chromosomes, called micro Bs are highly heterochromatic and show extreme irregularity in both mitotic and meiotic behavior (Houben *et al.* 1997b). In terms of DNA organization, large Bs of *B. dichromosomatica* are composed of high-copy B chromosome-specific DNA sequences and of sequences in common with the A chromosomes. The genomic organization of the micro B is a conglomerate, of different types of repetitive repeats coming from different polymorphic A chromosome sites. Therefore an evolutionary relationship exists between different types of polymorphic A chromosome regions and micro Bs (Houben *et al.* 2001). The tandem repeat Bd49 has been mapped to the centromere of the large B chromosome (John *et al.* 1991, Leach *et al.* 1995). Except for the 45S rDNA of micro Bs (Houben *et al.* 1997b) and the large Bs of all four cytodemes (Donald *et al.* 1995, 1997, Houben *et al.* 1999) no other genes were found on Bs of *B. dichromosomatica*. The rRNA genes of this species are inactive, because reverse transcriptase-PCR failed to detect any transcripts originated from 45S rDNA of large Bs (Donald *et al.* 1997).

Large Bs of *B. dichromosomatica* are characterized by a different level of histone H4 acetylation (Houben *et al.* 1997a). In contrast to the A chromosomes, which are labelled brightly in their entirety, the large Bs are faintly labelled with antibodies against acetylated histone H4 at lysine positions 5 and 8. No difference between the two types of chromosomes was found for the acetylated histone H4 at lysine positions 12 and 16. Association of histone acetylation with transcriptional activation of promoters and of deacetylation with silencing of repetitive transgenes and rDNA has been confirmed for plants (Probst *et al.* 2004, Tian *et al.* 2005), but no correlation was observed between the distribution of immunosignals for acetylated H4 isoforms and transcriptional activity at the chromosomal level. At

the chromosomal level, DNA replication associated stronger with H4 acetylation and this post-translational modification might be required for post-replicational repair (reviewed in Fuchs *et al*. 2006). The euchromatin–heterochromatin-specific distribution of histone H3K4me2 and H3K9me2 is similar between A and B chromosomes of *Crepis capillaris*, *Secale cereale* and *B. dichromosomatica*, suggesting, that eu- and heterochromatin of Bs are subject to dimethylation at lysines 4 and 9 of histone H3 in a similar way as the standard set of A chromosomes (Houben *et al*. 2003).

In the present study we extend our comparative study of epigenetic marks on Bs and we disclose that the histone H3 methylation pattern partly differs between A and B chromosomes as well as between different types of Bs. Furthermore, we show that the heterochromatic micro Bs replicate throughout the S-phase.

Materials and methods

Plant material, chromosome preparation and immunostaining

The methods for germination of *B. dichromosomatica* (cytodeme A2) were as described (Donald *et al*. 1995). Root meristems were fixed for 30 min in freshly prepared 4% (w/v) formaldehyde solution containing phosphate-buffered saline (PBS, pH 7.3), washed for 45 min in PBS and digested at 37°C for 25 min in a mixture of 2.5% pectinase, 2.5% cellulase 'Onozuka R-10' and 2.5% pectolyase Y-23 (w/v) dissolved in PBS. Meristems were then washed for 15 min in PBS and squashed between a glass slide and coverslip in PBS. After freezing in liquid nitrogen the coverslips were removed and the slides were transferred immediately into PBS. To avoid non-specific antibody-binding, slides were incubated for 30 min in 8% BSA (w/v), 0.1% Triton X100 in PBS at room temperature prior to two washes in PBS for 5 min each, and incubated with the primary antibody in a humidified chamber. The primary antibodies (Abcam Ltd, UK and Upstate Biotechnology, USA) were used in the following dilutions: 1:2000 (anti-H3K4me3), 1:500 (anti-H3K9me2), 1:200 (anti-H3K4me1,2; anti-H3K9me1,3; anti-H3K27me1,2,3) and 1:100 (anti-H4K20me1,2,3) in PBS, 1% BSA. After 12 h incubation at 4°C and washing for 15 min in PBS, the slides were incubated in Cy3-conjugated anti-rabbit IgG (Dianova) diluted 1:100 in PBS, 1% BSA for 1 h at 37°C. After final washes in PBS, the preparations were mounted in antifade containing 4′,6-diamidino-2-phenylindole DAPI as counterstain.

DNA replication banding by in-vivo *pulse-labelling with 5-bromo-2′-deoxyuridine*

Roots were incubated with 1 μg/ml 5-bromo-2′-deoxyuridine (BrdU) in aerated water for 10 min, washed thoroughly and then grown for 1–8 h in aerated water. After this the roots were fixed in 3:1 (ethanol:acetic acid) and chromosomes were prepared. To denature chromosomal DNA the slides were treated with 70% formamide in 2× SSC for 5 min at 70°C and air-dried. For detection of incorporated BrdU the slides were incubated with a FITC-conjugated anti-BrdU (Becton Dickinson) diluted 1:3 in PBS, 1% BSA for 1 h at 37°C. After final washes in PBS the preparations were mounted in antifade containing DAPI as counterstain.

Microscopic analysis

Fluorescence signals were observed using an epi-fluorescence microscope BX61 (Olympus). The images, recorded with a cooled CCD camera, were pseudo-coloured and merged using the program Adobe Photoshop 6.0.

Results and discussion

B chromosomes are characterized by a reduced level of euchromatic histone H3 methylation marks

Mitotic metaphase cells of several plants were stained with antisera that discriminate between mono-, di- and trimethylated lysines at position K4, K9 and K27 of histone H3 and for each type of antibody a reproducible distribution of histone marks was detected (Figure 1, summarized in Table 1). Both types of Bs of *B. dichromosomatica* are morphologically distinguishable after DAPI staining. The euchromatic mono-, di- and trimethylation marks of H3K4 revealed differences between transcriptionally active A chromosomes and less-transcriptionally active Bs. Large Bs are weaker labelled than A chromosomes. Micro Bs, which are heteropycnotic and mainly composed of tandem-repeats (Houben *et al*. 2001), were free of signals.

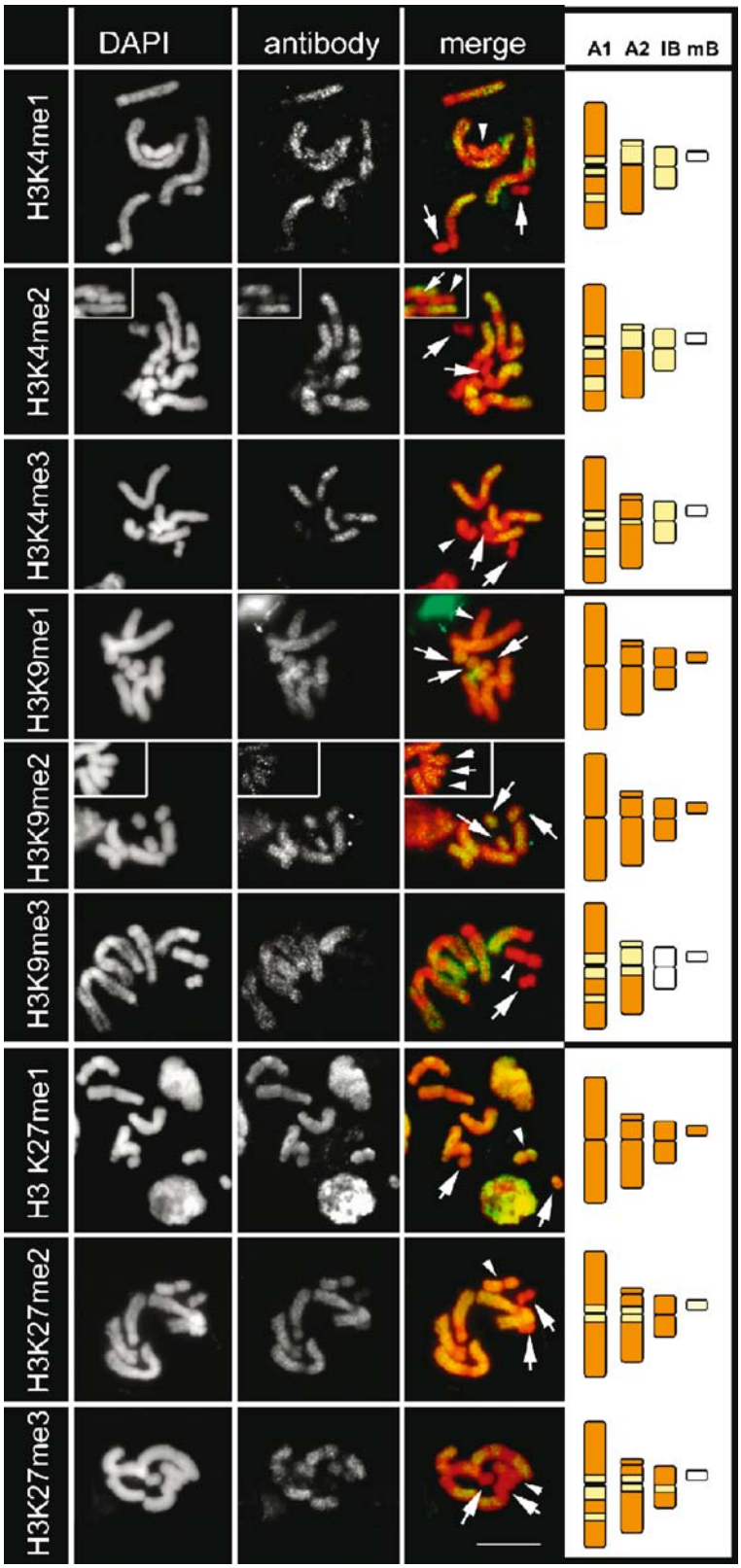

Figure 1. Comparative analysis of chromosomal histone H3 methylation marks. Metaphase cells of *B. dichromosomatica* with micro Bs (arrows) and large Bs (arrow heads) after immunostaining with antibodies specific for H3K4me1,2,3; H3K9me1,2,3 and H3K27me1,2,3. Note, sporadically micro Bs form metacentric isochromosomes. Bar represents 5 µm. Ideograms indicate the distribution of immunosignals at A (A1, A2), large Bs (lB) and micro Bs (mB).

Table 1. Distribution of methylated histone H3 marks along A chromosomes, large Bs and micro Bs of *B. dichromosomatica*

	A chromosomes	Large Bs	Micro Bs
H3K4me1	Clustered	Weak disperse	Very weak disperse
H3K4me2	Clustered	Weak disperse	Unlabelled
H3K4me3	Clustered	Weak disperse	Unlabelled
H3K9me1	Disperse	Disperse	Disperse
H3K9me2	Disperse	Disperse	Disperse
H3K9me3	Disperse	Very weak disperse	Unlabelled
H3K27me1	Disperse	Disperse	Disperse
H3K27me2	Disperse except pericentromere	Disperse except pericentromere	Very weak disperse
H3K27me3	Disperse except pericentromere	Disperse except pericentromere	Unlabelled

The chromosomal distribution patterns observed for the heterochromatin marks H3K9me1 and 2 on A chromosomes, large Bs and micro Bs were as reported for plants with large genomes (Houben *et al*. 2003), having a uniform distribution throughout chromosomes of the same immunofluorescence intensity. The trimethylation mark at lysine 9 of H3 revealed a B chromosome-specific distribution pattern. Micro Bs revealed no, and large Bs displayed very weak immunosignals for H3K9me3, while strong, disperse signals were detected along the A chromosomes except at the brightly DAPI-stained heterochromatic regions around the centromeres. This modification is a typical mark for euchromatin of *Arabidopsis* (Naumann *et al*. 2005) and barley (Fuchs *et al*. 2006), but labels constitutive heterochromatin in mammals (Peters *et al*. 2003).

A similar degree of H3K27 monomethylation was found along A and both B type chromosomes. A heterochromatin-specific distribution was reported for other plant species with large genomes (Fuchs *et al*. 2006). The level of dimethylated H3K27 differs between large Bs and micro Bs. Micro Bs are weakly labelled, large Bs, like A chromosomes, are uniformly labelled except at pericentromeric regions. Immunodetection of histone H3 trimethylated at lysine 27 revealed the same distribution pattern of signals for the A chromosomes and large Bs. There is a decrease of labelling in pericentromeric regions. No H3K27me3-labelling was found for micro Bs.

The micro B chromosome replicates throughout S-phase

To test whether the DNA replication behaviour differs between the different types of chromosomes, BrdU incorporation experiments were conducted. The BrdU incorporation of non-synchronized cells resulted in chromosomes with different replication patterns (Figure 2). The DNA replication pattern could be classified into three main types according to the distribution and intensity of the anti-BrdU signals along the A chromosomes. A chromosomes with the type 1 replication pattern were intensely labelled throughout their length, the type 2 pattern was characterized by intense bands at interstitial regions and the type 3 pattern revealed bands visible in defined regions including the pericentromeres. The replication pattern type 1 most probably reflects chromosomal regions undergoing early replication. The type 3 pattern mainly overlaps with the position of pericentromeric heterochromatin and should therefore be typical for late-replicating regions. The type 2 pattern is in between the other two patterns and therefore indicates a region replicating in mid S-phase. A similar sequence of replication patterns has been described for other plant species (e.g. Fujishige & Taniguchi 1998). Remarkably, although heterochromatic regions are generally late-replicating (Dimitri *et al*. 2005), the heterochromatic micro Bs were replicating not only during late S-phase but throughout S-phase. However, the anti-BrdU signal intensity was strongest during late S-phase. This observation suggests the presence of micro B sequences which undergo replication at different phases of the S-phase. A similar uncommon DNA replication behaviour has been observed for the heterochromatic regions of *Allium fistulosum* chromosomes (Fujishige & Taniguchi 1998). Contrary to micro Bs, large Bs of *B. dichromosomatica* undergo replication during late S-phase (Houben *et al*. 1997a).

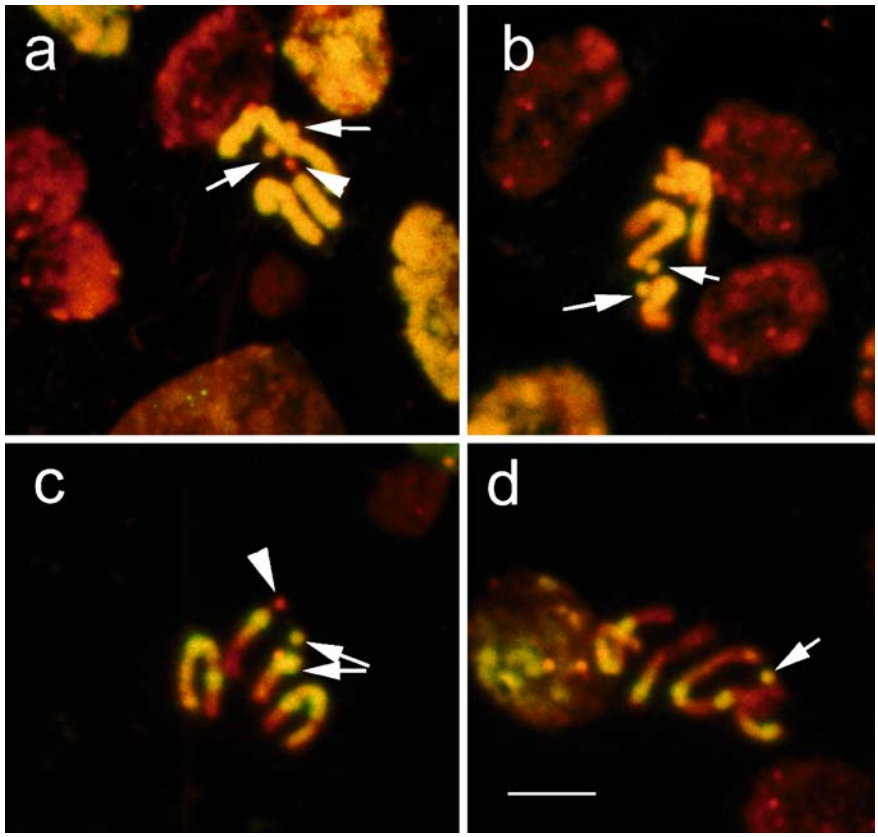

Figure 2. Micro B chromosomes replicate throughout S-phase. (**a**) A chromosomes labelled with dense anti-BrdU signals (in yellow) throughout their length (replication pattern type 1). (**b, c**) A chromosomes with medium signal intensity and same intensely labelled bands (replication pattern type 2). (**d**) Signal bands mainly near the centromeres (replication pattern type 3 pattern). Micro Bs (arrows) are labelled at all stages of the S-phase. The satellite of NOR-bearing chromosome 2 is indicated with an arrow head. Bar represents 5 μm.

Conclusion

Our observation indicates that eu- and heterochromatin of Bs are subject to histone H3 methylation at lysines 4, 9 and 27 as the standard set of A chromosomes. Although C-banding and DAPI staining results suggest a similar eu- and heterochromatin composition of large B and A chromosomes of *B. dichromosomatica* (Houben *et al*. 1997a), large Bs are characterized by a reduced level of the euchromatic histone marks H3K4me1,2,3 and H3K9me3. As expected, heteropycnotic, tandem-repeat enriched micro Bs revealed only traces of these histone modifications. No differences of immunolabelling intensity between A and B chromosomes were found for the heterochromatic marks H3K9me1/2 and H3K27me1, indicating that Bs are not marked by an enriched level of heterochromatic histone marks, but specifically marked by a reduced level of euchromatin-associated histone modifications. The reduced level of histone H3K4 di/trimethylation, a modification that has been linked to transcriptionally active chromatin, corresponds with the observation that Bs are generally transcriptionally inactive. Although the biology of B and sex chromosomes differs, in this context, it is interesting to note that sex chromosome inactivation in mammals is associated with heterochromatin-specific histone modifications, e.g. dimethylation of H3K9 and H3K27 (reviewed in Heard 2005). Probably, because of the general absence of functional genes on Bs, the chromatin of Bs does not need to be enriched with heterochromatin-specific histone modifications, which are involved in gene inactivation.

Our results suggest that H4 underacetylation (Houben *et al*. 1997a), and H3 undermethylation at

certain lysine positions and late or throughout S-phase replication of DNA may play complementary, and possibly interacting, roles in the formation of B chromosome chromatin of *B. dichromosomatica*, and that these features may be significant in controlling the behaviour of supernumerary chromosomes. More comparative studies are needed before a general B chromosome-specific pattern of histone modifications can been concluded.

The analysis of species in which the Bs are less heterochromatic than the A chromosomes, e.g. *Scilla vvedenskyi* (Greilhuber & Septa 1976), would help to analyse the relationship between post-translational histone marks and the chromatin composition of B chromosomes.

Acknowledgements

We thank Jörg Fuchs and Ingo Schubert (IPK, Germany) for critical reading of the manuscript. S.M. and A.H. were supported by grants from the Land Sachsen-Anhalt and the IPK (Gatersleben).

References

Bannister AJ, Zegerman P, Partridge JF *et al.* (2001) Selective recognition of methylated lysine 9 on histone H3 by the HP1 chromo domain. *Nature* **410**: 120–124.

Birchler JA, Chalfoun DJ, Levin DM (1990) Recombination in the B chromosome of maize to produce A-B-A chromosomes. *Genetics* **126**: 723–733.

Camacho JPM, Sharbel TF, Beukeboom, LW (2000) B-chromosome evolution. *Phil Trans R Soc B* **355**: 163–178.

Cao R, Wang LJ, Wang HB *et al.* (2002) Role of histone H3 lysine 27 methylation in polycomb-group silencing. *Science* **298**: 1039–1043.

Carter CR (1978) Cytology of *Brachycome*. 8. Inheritance, frequency and distribution of B chromosomes in *Brachyome dichromosomatica* (N = 2), formerly included in *Brachycome lineariloba*. *Chromosoma* **67**: 109–121.

Cheng YM, Lin BY (2003) Cloning and characterization of maize B chromosome sequences derived from microdissection. *Genetics* **164**: 299–310.

Craig JM (2005) Heterochromatin – many flavours, common themes. *Bioessays* **27**: 17–28.

Czermin B, Melfi R, McCabe D, Seitz V, Imhof A, Pirrotta V (2002) *Drosophila* enhancer of Zeste/ESC complexes have a histone H3 methyltransferase activity that marks chromosomal polycomb sites. *Cell* **111**: 185–196.

Dimitri P, Corradini N, Rossi F, Verni F (2005) The paradox of functional heterochromatin. *Bioessays* **27**: 29–41.

Donald TM, Houben A, Leach CR, Timmis JN (1997) Ribosomal RNA genes specific to the B chromosomes in *Brachycome dichromosomatica* are not transcribed in leaf tissue. *Genome* **40**: 674–681.

Donald TM, Leach CR, Clough A, Timmis JN (1995) Ribosomal RNA genes and the B chromosome of *Brachycome dichromosomatica*. *Heredity* **74**: 556–561.

Francis NJ, Kingston RE, Woodcock CL (2004) Chromatin compaction by a polycomb group protein complex. *Science* **306**: 1574–1577.

Fuchs J, Demidov D, Houben A, Schubert I (2006) Chromosomal histone modification patterns – from conservation to diversity. *Trends Plant Sci* **11**: 199–208.

Fujishige I, Taniguchi K (1998) Sequence of DNA replication in *Allium fistulosum* chromosomes during S-phase. *Chromosome Res* **6**: 611–619.

Greilhuber J, Septa F (1976) C-banded karyotypes in the *Scale hohenackeri* group, *S. persica*, and *Puschkinia* (*Liliaceae*). *Plant Syst Evol* **126**: 149–188.

Heard E, (2005) Delving into the diversity of facultative heterochromatin: the epigenetics of the inactive X chromosome. *Curr Opin Genet Dev* **15**: 482–489.

Houben A, Belyaev ND, Leach CR, Timmis JN (1997a) Differences of histone H4 acetylation and replication timing between A and B chromosomes of *Brachycome dichromosomatica*. *Chromosome Res* **5**: 233–237.

Houben A, Demidov D, Gernand D, Meister A, Leach CR, Schubert I (2003) Methylation of histone H3 in euchromatin of plant chromosomes depends on basic nuclear DNA content. *Plant J* **33**, 967–973.

Houben A, Leach CR, Verlin D, Rofe R, Timmis JN (1997b) A repetitive DNA sequence common to the different B chromosomes of the genus *Brachycome*. *Chromosoma* **106**: 513–519.

Houben A, Thompson N, Ahne R, Leach CR, Verlin D, Timmis JN (1999) A monophyletic origin of the B chromosomes of *Brachycome dichromosomatica* (Asteraceae). *Plant Syst Evol* **219**: 127–135.

Houben A, Verlin D, Leach CR, Timmis JN (2001) The genomic complexity of micro B chromosomes of *Brachycome dichromosomatica*. *Chromosoma* **110**: 451–459.

Jacobs SA, Taverna SD, Zhang YN *et al.* (2001) Specificity of the HP1 chromo domain for the methylated N-terminus of histone H3. *EMBO Journal* **20**: 5232–5241.

John UP, Leach CR, Timmis JN (1991) A sequence specific to B chromosomes of *Brachycome dichromosomatica*. *Genome* **34**: 739–744.

Jones RN (1975) B chromosome systems in flowering plants and animal species. *Int Rev Cytol* **40**: 1–100.

Jones RN (1995) Tansley Review No. 85, B chromosomes in plants. *New Phytol* **131**: 411–434.

Jones RN, Houben A (2003) B chromosomes in plants: escapees from the A chromosome genome? *Trends Plant Sci* **8**: 417–423.

Jones RN, Rees H (1982) *B Chromosomes*, 1st edn. London: Academic Press.

Leach CR, Donald TM, Franks TK, Spiniello SS, Hanrahan CF, Timmis JN (1995) Organization and origin of a B chromosome centromeric sequence from *Brachycome dichromosomatica*. *Chromosoma* **103**: 708–714.

Leach CR, Houben A, Field B, Pistrick K, Demidov D, Timmis JN (2005) Molecular evidence for transcription of B chromosome ribosomal RNA genes in *Crepis capillaris*. *Genetics* **171**: 269–278.

Leach CR, Houben A, Timmis JN (2004) The B chromosomes in *Brachycome*. *Cytogenet Genome Res* **106**: 199–209.

Martin C, Zhang Y (2005) The diverse functions of histone lysine methylation. *Nat Rev Mol Cell Biol* **6**: 838–849.

Naumann K, Fischer A, Hofmann I *et al*. (2005) Pivotal role of AtSUVH2 in heterochromatic histone methylation and gene silencing in *Arabidopsis*. *EMBO J* **24**: 1418–1429.

Noma K, Allis CD, Grewal SIS (2001) Transitions in distinct histone H3 methylation patterns at the heterochromatin domain boundaries. *Science* **293**: 1150–1155.

Page BT, Wanous MK, Birchler JA (2001) Characterization of a maize chromosome 4 centromeric sequence: evidence for an evolutionary relationship with the B chromosome centromere. *Genetics* **159**: 291–302.

Peters AH, Kubicek S, Mechtler K *et al*. (2003) Partitioning and plasticity of repressive histone methylation states in mammalian chromatin. *Mol Cell* **12**: 1577–1589.

Probst AV, Fagard M, Proux F *et al*. (2004) *Arabidopsis* histone deacetylase HDA6 is required for maintenance of transcriptional gene silencing and determines nuclear organization of rDNA repeats. *Plant Cell* **16**: 1021–1034.

Richards EJ, Elgin SCR (2002) Epigenetic codes for heterochromatin formation and silencing: rounding up the usual suspects. *Cell* **108**: 489–500.

Santos-Rosa H, Schneider R, Bannister AJ *et al*. (2002) Active genes are tri-methylated at K4 of histone H3. *Nature* **419**: 407–411.

Shi YJ, Lan F, Matson C, *et al*. (2004) Histone demethylation mediated by the nuclear arnine oxidase homolog LSD1. *Cell* **119**: 941–953.

Tian L, Fong MP, Wang JYJ *et al*. (2005) Reversible histone acetylation and deacetylation mediate genome-wide, promoter-dependent and locus-specific changes in gene expression during plant development. *Genetics* **169**: 337–345.

Zegerman P, Canas B, Pappin D, Kouzarides T (2002) Histone H3 lysine 4 methylation disrupts binding of nucleosome remodeling and deacetylase (NuRD) repressor complex. *J Biol Chem* **277**: 11621–11624.

A20 Marschner, S., Meister, A., Blattner, F.R., and Houben, A. (2007b). Evolution and function of B chromosome 45S rDNA sequences in *Brachycome dichromosomatica*. Genome 50, 638-644.

Evolution and function of B chromosome 45S rDNA sequences in *Brachycome dichromosomatica*

Sylvia Marschner, Armin Meister, Frank R. Blattner, and Andreas Houben

Abstract: The origin and activity of 45S rDNA located on micro B chromosomes of the daisy *Brachycome dichromosomatica* were analysed. The internal transcribed spacer 2 (ITS2) of the 45S rRNA gene was sequenced for micro B, large B, and A chromosomes of *B. dichromosomatica* cytodeme A2, and conserved differences were identified between sequences originating from A and both types of B chromosomes. Phylogenetic analysis did not identify a species containing an ITS2 sequence more similar to either of the B chromosome sequences than the *B. dichromosomatica* A chromosome sequences. Thus, an origin of the B chromosomes from A chromosomes at a time prior to the divergence of the 4 cytodemes of *B. dichromosomatica* is suggested. The frequent (70%) nucleolar non-association of micro B chromosomes suggests inactivity of micro B 45S rDNA.

Key words: B chromosome, 45S rDNA, evolution, nucleolus.

Résumé : L'origine et l'activité des ADNr 45S situés sur le microchromosome B chez la marguerite *Brachycome dichromosomatica* ont été analysées. L'espaceur interne transcrit 2 (« ITS2 ») du gène codant pour l'ARNr 45S a été séquencé chez les chromosomes micro B, grand B et A chez le *B. dichromosomatica* du cytodème A2. Les différences conservées entre les séquences provenant des chromosomes A et des deux types de chromosomes B ont été identifiées. Une analyse phylogénétique n'a permis de trouver aucune espèce contenant une séquence ITS2 plus semblable aux séquences présentes chez l'un ou l'autre des chromosomes B qu'à la séquence présente sur les chromosomes A du *B. dichromosomatica*. Ainsi, les auteurs suggèrent que les chromosomes B ont été dérivés des chromosomes A avant la divergences des 4 cytodèmes du *B. dichromosomatica*. La fréquente (70 %) absence d'association nucléolaire des microchromosomes B suggère l'absence d'activité de l'ADNr 45S des microchromosomes B.

Mots-clés : chromosome B, ADNr 45S, évolution, nucléole.

[Traduit par la Rédaction]

Introduction

B chromosomes (B's) are dispensable components of the genomes of numerous plant and animal species. They do not pair with any of the standard A chromosomes at meiosis, by definition, and have irregular modes of inheritance. B's are generally assumed to be genetically inactive because no major genes with specific phenotypic effects necessary for normal development are known to occur on these chromosomes (reviewed by Camacho et al. 2000; Puertas 2002; Jones and Houben 2003). Except for the B chromosome 45S rRNA gene of *Crepis capillaris*, there has been no direct molecular evidence for transcription of B chromosome DNA in any plant species (Leach et al. 2005).

The origin of B chromosomes remains obscure but it is likely that those of different organisms arose in different ways. It has been argued that B's could be derived from A chromosomes in, for example, *Crepis capillaris* (Jamilena et al. 1994), or from sex chromosomes in *Leiopelma hochstetteri* (Sharbel et al. 1998). Since B chromosomes of maize and *Brachycome dichromosomatica* contain sequences that originate from different A chromosomes (Alfenito and Birchler 1993; Houben et al. 2001*b*; Cheng and Lin 2003), B chromosomes could also represent an amalgamation of sequences coming from several A chromosomes. However, there is also evidence suggesting that B chromosomes can be spontaneously generated in response to new genome conditions following interspecific hybridization in, for example, *Coix aquaticus* and *Coix gigantea* (Sapre and Deshpande 1987) and the parasitic wasp *Nasonia vitripennis* (McAllister and Werren 1997). The de novo formation of B's is most likely a rare event, as analyses of different B chromosome variants within species suggest a close relationship between different variants (Houben et al. 1999).

The involvement of rRNA-coding repeats in the evolution of B chromosomes does not appear to be accidental, because rDNA loci have been detected on B's of many species (e.g., *C. capillaris* (Maluszynska and Schweizer 1989), *Rattus rattus* (Stitou et al. 2000), *Trichogramma kaykai* (van Vugt et al. 2005), and others; for review, see Green 1990; Jones 1995). In the herb *Plantago lagopus* the origin of a B chromosome seems to be associated with massive amplification

Received 13 February 2007. Accepted 8 May 2007. Published on the NRC Research Press Web site at genome.nrc.ca on 24 July 2007.

Corresponding Editor: G. Jenkins.

S. Marschner, A. Meister, F.R. Blattner, and A. Houben.[1] Leibniz Institute of Plant Genetics and Crop Plant Research (IPK), 06466 Gatersleben, Germany.

[1]Corresponding author (e-mail: houben@ipk-gatersleben.de).

 doi:10.1139/G07-048

of 5S rDNA sequences after fragmentation of an aneuploid A chromosome (Dhar et al. 2002). Alternatively, but less likely, B chromosome rDNA sites could be a consequence of the reportedly mobile nature of rDNA (Schubert and Wobus 1985), with B chromosomes being the preferred "landing sites" because of their neutral character.

In the present study, we extend our analyses of the origin and function of B chromosome 45S rDNA of the Australian daisy *Brachycome dichromosomatica* (synonym *Brachyscome dichromosomatica*). The species includes 4 cytodemes, designated A1, A2, A3, and A4, that differ in distribution and karyotype (Watanabe et al. 1975). Plants of cytodeme A2 may carry both large and micro B chromosomes. Large B chromosomes are mitotically stable and show meiotic irregularity. The dot-like accessory chromosomes, called micro B's, are highly heterochromatic and show extreme irregularity in both mitotic and meiotic behavior (Houben et al. 1997). Except for the 45S rDNA of the micro B's and large B's of all 4 cytodemes, no other coding sequence has been found on B's of *B. dichromosomatica* (Leach et al. 2004). The internal transcribed spacer 2 (ITS2) of nuclear rDNA revealed 2 consistent differences between the A and large B chromosomes of *B. dichromosomatica* cytodeme A1. One of these differences concerned an *Sfc*I restriction enzyme recognition site that was present only in large B chromosome rDNA. Using reverse transcriptase PCR of the equivalent region within the 40–45S precursor rRNA, Donald et al. (1997) were unable to detect transcripts from the large B chromosome 45S rDNA of cytodeme A1. For unknown reasons the NOR activity could not be indirectly demonstrated by silver staining of metaphase chromosomes of *B. dichromosomatica*, although the nucleoli stained well with silver nitrate in interphase nuclei.

We aimed to investigate the likely origin of 45S rDNA of the micro B and large B chromosomes of *B. dichromosomatica* by determining the relatedness of the ITS2 between the different chromosome types. The internal transcribed spacers 1 and 2 (ITS1 and ITS2) separate nuclear ribosomal genes and have proved to be useful for analyzing genetic relationships among species (Baldwin 1992). Sequence analysis of part of the A, large B, and micro B chromosome rRNA genes, together with comparisons with related species, indicates that the B chromosome rRNA genes are derived from those of A chromosomes. The limited association of micro B's with nucleoli suggests inactivity of micro B 45S rDNA.

Materials and methods

Plant material and preparation of size-fractionated nuclei

The methods for germination of *B. dichromosomatica* (cytodeme A2) and chromosome number determination have been described by Donald et al. (1995). To isolate nuclei, young flower buds were fixed for 20 min under vacuum in 4% formaldehyde in Tris buffer (100 mmol/L Tris-HCl, pH 7.0, 5 mmol/L $MgCl_2$, 85 mmol/L NaCl, 0.1% Triton® X-100) and then homogenized in Tris buffer. Suspended nuclei were stained with 4′,6-diamidino-2-phenylindole (DAPI) and flow-sorted onto glass slides according to their ploidy (2C, 4C) level using a FACStar™ Plus flow cytometer (BD Biosciences) as described by Pecinka et al. (2004).

Fig. 1. The location of 45S rDNA (in yellow) on the A, micro B (mB), and large B chromosomes (lB) of *Brachycome dichromosomatica* cytodeme A2. Note that micro B's sporadically form metacentric isochromosomes. Scale bar = 5 μm.

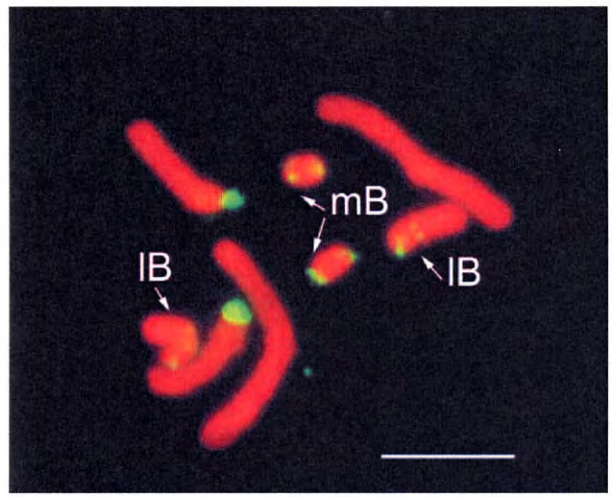

Fluorescence in situ hybridization (FISH)

The inserts of the plasmids VER17 (Yakura and Tanifuji 1983) and pBdm29 (Houben et al. 1997) were used as 45S rDNA–specific and micro B–specific probes, respectively. In situ hybridization probes were labelled by PCR with biotin-16-dUTP or digoxigenin-11-dUTP. Preparation of mitotic chromosomes and FISH were performed as described by Houben et al. (2006). Hybridization sites of digoxigenin- or biotin-labelled probes were detected using anti-digoxigenin–Cy3 antibody or the streptavidin – Alexa Fluor® 488 system (Invitrogen).

Combination of nucleolus silver staining and fluorescence in situ hybridization

Flow-sorted nuclei were incubated with 0.01 mol/L borate buffer for 10 min at room temperature. A few drops of freshly prepared 50% $AgNO_3$ solution (pH 4–5) were added and the slides were incubated for up to 1.5 h at 60 °C in a humid chamber (Hizume et al. 1980). Finally the slides were rinsed in distilled water, air-dried, and hybridized with the micro B–specific tandem repeat Bdm29 (Houben et al. 1997). Fluorescence and $AgNO_3$ signals were observed using a microscope (BX61, Olympus). The images, recorded with a cooled CCD camera, were pseudo-colored and merged using the program Adobe® Photoshop® 6.0.

Computer simulation of interphase positions

The geometrical random spatial distribution model (Pecinka et al. 2004) was used to simulate random association of micro B's and the nucleolus. The coordinates of 2 spheres representing micro B's and nucleolus regions were randomly determined in virtual 2C and 4C nuclei. Micro B's and the nucleolus were considered to be associated when they overlapped or when the distance between their edges was <100 nm (i.e., below the resolution of conventional optical

Fig. 2. Alignment of ITS2 sequences from A (A2-A1 to A2-A4), micro B (A2-mB1 to A2-mB4), and large B chromosomes (A2-lB1 to A2-1B5) of *B. dichromosomatica* cytodeme A2 and consensus ITS2 sequences of A (A1-A1) and large B (A1-lB1) chromosomes of *B. dichromosomatica* cytodeme A1 and *B. lineariloba* race C (Blin1) (Donald et al. 1997). Base changes consistently found between A- and B-chromosome-derived sequences are shaded.

```
                142              *              175
A2-A1  : CTACGGAATCGTGTCGTGTGTCTTTTCAAAAAGGTGCATCTTAATAGACCCA
A2-A2  : CTACGGAATCGTGTCGTGTGTCTTTTCAAAAAGGTGCATCTTAATAGACCCA
A2-A3  : CTACGGAATCGTGTCGTGTGTCTTTTCAAAAAGGTGCATCTTAATAGACCCA
A2-A4  : CTACGGAATCGTGTCGTGTGTCTTTTCAAAAAGGTGCATCTTAATAGACCCA
A2-lB1 : CTACAGAATCGTGTCGTGTGTCTTTTAAAAAAGGTGCATCTTAATAGACCCA
A2-lB2 : CTACAGAATCGTGTCGTGTGTCTTTTCAAAAAGGTGCATCTTAATAGACCCA
A2-lB3 : CTACGGAATCGTGTCGTGTGTCTTTTCAAAAAGGTGCATCTTAATAGACCCA
A2-lB4 : CTACGGAATCGTGTCGTGTGTCTTTTCAAAAAGGTGCTTCTTAATAGACCCA
A2-lB5 : CTACGGAATCGTGTCGTGTGTCTTTTCAAAAAGGTGCTTCTTAAGAGACCCA
A2-mB1 : CTACGGAATCGTGTCGTGTGTCTTTTCAAAAAGGTGCTTCTTAATAGACTCA
A2-mB2 : CTACGGAATCGTGTCGTGTGTCTTTTCAAAAATGTGCTTCTTAATAGACCCA
A2-mB3 : CTACGGAATCGTGTCGTGTGTCTTTTCAATAAGGTGCATCTTAATAGACCCA
A2-mB4 : CTACGGAATCGTGTCGTGTGTCTTTACAAAAAGGTGCATCTTAATAGACCCA
A1-A1  : CTACGGAATCGTGTCGTGTGTCTTTTCAAAAAGGTGCTTCTTAATAGACCCA
A1-lB1 : CTACAGAATCGTGTCGTGTGTCTTTTCAAAAAGGTGCATCTTAATAGACCCA
Blin1  : CTACAGAATCGTGTCGCGTGTCTTTTATAAAAGGTGCATCTTAATAGACCCA
```

microscopy). The random occurrence of association was calculated using a simulation program written in Visual Basic 5.0 (Microsoft). The differences between the experimentally obtained values and the simulated ones were analyzed by the χ^2 test and considered significant at the $P < 0.001$ level. The χ^2 test was based on the absolute number of counted nuclei ($n = 300$).

Chromosome microdissection, PCR amplification, and cloning of rRNA gene sequences

DNA was prepared from 5 and 8 microdissected micro B and large B chromosomes according to Houben et al. (2001*a*). PCR was used to amplify the ITS2 region from microisolated B chromosome DNA and from total genomic DNA of 0B *B. dichromosomatica* plants (plants with no B chromosomes) using the primers XF58s (5′-CTTCTAGAGCCTGGGCGTCACG-3′) and ER25s (5′-CGGAATTCTGACCTGGGGTCGC-3′) (White et al. 1990). PCR products were ligated into the pGEM®-T Easy vector (Promega) and propagated in *E. coli* strain DH5α.

Sequencing and phylogenetic analysis

Sequence analysis was performed by the automated dideoxynucleotide dye termination method. A neighbor-joining tree of the ITS2 sequences was calculated with maximum-likelihood distances (corresponding to the HKY85+G+I model of sequence evolution) in PAUP*4.0 (Swofford 2002) to define relationships of the B chromosome ITS regions with their putative progenitors within *Brachycome*. Bootstrap values were calculated from 500 re-samples using settings identical to those in the initial neighbor-joining analysis.

Results

High sequence similarity indicates an A-chromosome-derived origin of large B and micro B 45S rDNA

Fluorescence in situ hybridization confirmed clusters of 45S rRNA genes on micro B and large B chromosomes and on A chromosome 2 of *B. dichromosomatica* cytodeme A2 (Fig. 1). The signal strength on the B chromosomes was considerably lower than that on A chromosome 2, suggesting that the B's may contribute a minority of additional rRNA genes to the cell.

The nucleotide sequences of the 217 bp long ITS2 regions of cloned inserts derived by PCR from DNA of microdissected micro B and large B chromosomes of *B. dichromosomatica* were determined and compared with the A chromosome sequences isolated from plants that did not contain B chromosomes. There were differences between the A chromosome sequences and 2 distinct types of sequences for each type of B chromosomes. Significantly, there were 2 invariable differences between A, micro B, and large B sequences. At base 142, adenine is present in 2 of the large B ITS2 sequences, whereas guanine is present in all A, micro B, and remaining large B clones. In addition, at base 175, thymine is present in 2 of the large B sequences and 2 of the micro B sequences, whereas adenine is present in all A and remaining B chromosome clones (Fig. 2). In contrast to the ITS2 sequence derived from the large B chromosome of cytodeme A1 (Donald et al. 1997), ITS2 sequences of cytodeme A2 revealed heterogeneity within and between the different types of B chromosomes. In addition, a minor number of inconsistent single base pair insertions, deletions, and substitutions, compared with A chromosome ITS2 sequences, were found for both types of B chromo-

Fig. 3. Phylogenetic tree constructed by a neighbor-joining analysis of consensus ITS2 sequences isolated from *Brachycome* species. Bootstrap values (%) shown at nodes are based on 500 re-samples of the original data set. The B chromosome ITS2 sequences of *B. dichromosomatica* all fall in a cluster with sequences from A chromosomes of *B. dichromosomatica*. The A chromosome (A2.A4, EF194069; A2.A3, EF194068; A2.A2, EF194067; A2.A1, EF194066), large B (A2.1B5, EF194074; A2.1B4, EF194073; A2.lB3, EF194072; A2.lB2, EF194071; A2.lB1, EF194070), and micro B (A2.mB4, EF194078; A2.mB3, EF194077; A2.mB2, EF194076; A2.mB1, EF194075) sequences of *B. dichromosomatica* cytodeme A2 and the A chromosome (A1.A1) and large B chromosome (A1.lB1) sequences of cytodeme A1 were characterized by Donald et al. (1997). All other *Brachycome* sequences have been described by Field et al. (2006).

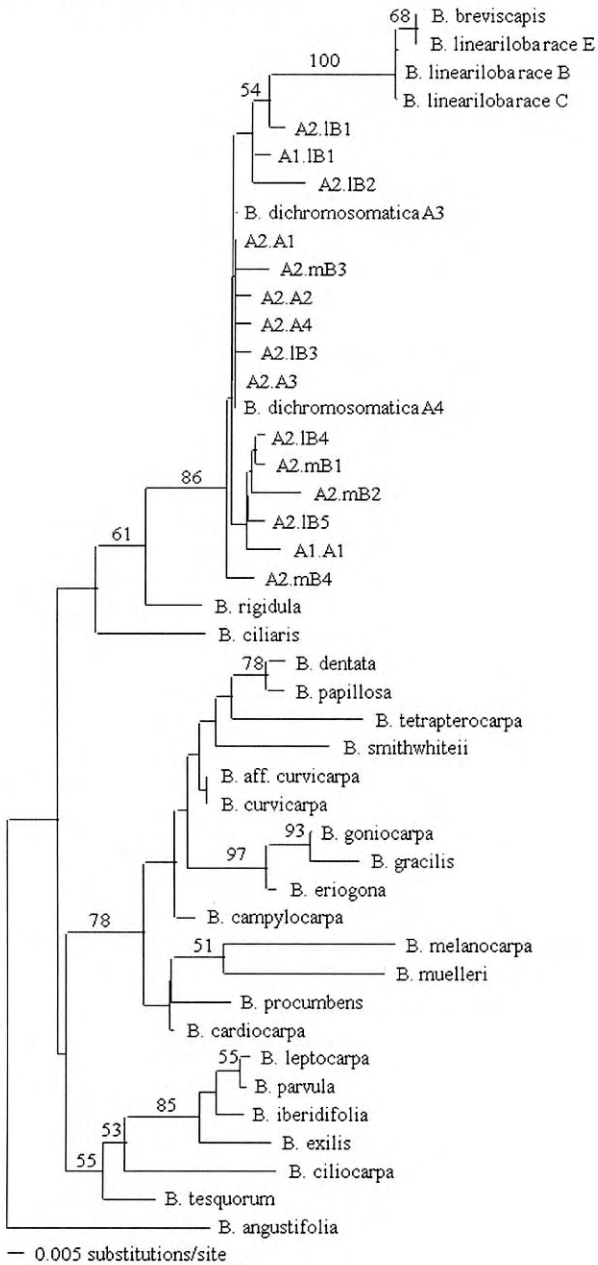

somes. The existence of multiple ITS2 sequences on the B chromosomes suggests the absence of or a delay in sequence homogenization. Because a similar sequence variation was found also for A and large B chromosomes of cytodeme A1 (Donald et al. 1997), it is likely that B chromosome 45S rDNA of cytodeme A1 and B chromosome 45S rDNA of cytodeme A2 are derived from a common ancestral B chromosome.

To investigate the likely origin of the B-located 45S rDNA in *B. dichromosomatica*, phylogenetic relationships were determined between both types of B's and other members of the *Brachycome* genus (Fig. 3). A neighbor-joining analysis of the sequence data did not identify a species that contained an ITS2 sequence more closely related to either of the B chromosome sequences than the *B. dichromosomatica* A chromosome sequences (86% bootstrap support). The B chromosome and A chromosome sequences of the *B. dichromosomatica* cytodemes shared 7 bases that were not present in *B. breviscapis* and the *B. lineariloba* races, and *B. breviscapis* and *B. lineariloba* race E also differed by an additional base.

Limited association of micro B's with nucleoli suggests inactivity of micro B 45S rDNA

To indirectly analyse the transcriptional status of micro B 45S rDNA, we analysed the position of micro B's relative to the position of the nucleolus in 2C and 4C nuclei. Since the nucleolus is the site of rDNA transcription during interphase, it is generally assumed that silent NORs are excluded from the nucleolus (Ochs et al. 1985).

First, to visualize the position of the nucleolus within the nucleus, we performed silver staining on size-fractionated 2C and 4C nuclei (Fig. 4*a*). As cells progress through the cycle, multiple nucleoli appear to fuse into one nucleolus. As a consequence of at least 2 A-chromosome-located rDNA loci, multiple nucleoli were found within a single nucleus. Eighty-four percent of nuclei displayed 1 nucleolus, 15% had 2 nucleoli, and 1% contained 3 or more nucleoli in 2C nuclei. Almost the same values were found for 4C nuclei. Next, the positions of the micro B's and 45S rDNA were determined by multicolor FISH using the whole micro B–specific probe Bdm29 (Houben et al. 1997) together with the 45S rDNA–specific probe VER17. The nuclear positioning of micro B's, 45S rDNA, and nucleoli was determined for 300 2C nuclei and 300 4C nuclei. A micro B chromosome territory was scored as being co-localized with the silver-stained nucleolus if the hybridization signal was found to overlap or abut the silver signal (Figs. 4*b*–4*d*). The flatness of nuclei (average depth 0.5 μm) did not allow a three-dimensional analysis of chromosome positions. Thirty percent of micro B's revealed an association with the nucleolus in 2C and 4C nuclei. Owing to the low copy number of micro B rDNA, these signals were not detectable in all nuclei analysed. The random association frequency between micro B's and the nucleoli was calculated as a weighted average of the predicted association values for nuclei according to the proportion of evaluated nuclei. The observed association frequency was significantly higher ($P < 0.001$) than the prediction of 15% for 1×10^6 simulated nuclei. In contrast, almost all nuclei (2C, 95%; 4C, 97%) revealed an association between the nucle-

Fig. 4. Relative positions of micro B chromosomes, 45S rDNA, and the nucleolus within a nucleus. After nucleolus silver staining (*a*), multicolor FISH (*b–d*) was performed using the whole micro B–specific probe Bdm29 (red) and the 45S rDNA–specific probe VER17 (green). To co-localize nucleolus (arrows in *a*) and FISH signals, the silver-stained image was combined with the FISH images showing the positions of micro B's (*b*) and 45S rDNA signals (*d*). The nucleus in (*c*) is counterstained with DAPI (blue). Scale bar = 5 μm.

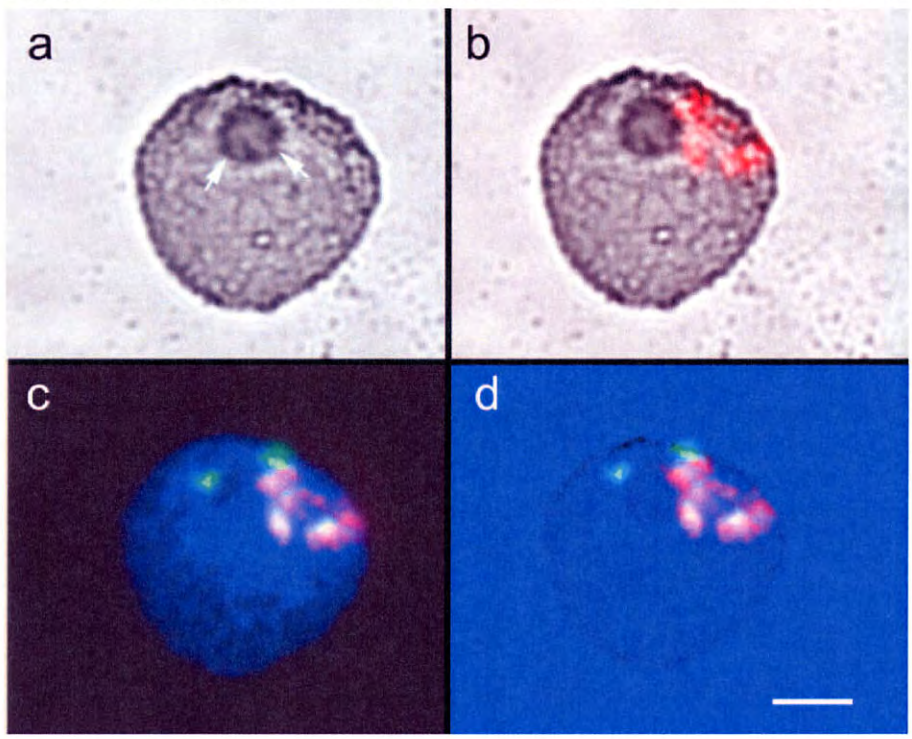

olus and at least 1 A chromosome NOR region. Nuclei (2C, 5%; 4C, 3%) without nucleolus-associated A chromosome 45S rDNA signals are most likely results of technical artifacts. Because 70% of micro B's did not co-localize with the nucleolus, we conclude that micro B 45S rDNA is not constitutively transcribed.

Discussion

The B chromosome ITS2 sequences of *B. dichromosomatica* cytodemes A1 (Donald et al. 1997; Field et al. 2006) and A2 grouped with the *B. lineariloba* complex rather than with another group of *Brachycome* species, and within the *B. dichromosomatica* subclade, supporting the proposal of a monophyletic origin of the B chromosome at a time prior to the divergence of the cytodemes (Houben et al. 1999). The presence of sequence polymorphism at base 142 of the large B chromosomes of cytodemes A1 and A2 and the members of the *B. lineariloba* subclade, but not *B. dichromosomatica*, suggests an association of the large B chromosomes with a common ancestor of *B. lineariloba*, which perhaps had already diverged in this respect from other members of the genus (Field et al. 2006). The polymorphism at base 175 of the large and micro B's of cytodeme A2 further demonstrates an evolutionary link between large and micro B's.

RT-PCR using B-specific rDNA primer pairs did not result in the unambiguous identification of B-derived transcripts. Therefore, an indirect method was selected for determining the transcription status of micro B rRNA genes. The non-association of 70% of micro B's with the nucleolus suggests that the majority of micro B 45S rDNA is transcriptionally inactive. An association of 30% of micro B's with the nucleus is not a strong indication of rDNA transcription, because transcriptionally inactive NORs can associate with a nucleolus, as demonstrated for mouse–human cell hybrids (Sullivan et al. 2001). In addition, a grouping between B chromosomes and the nucleolus has been noted for the large B chromosome of cytodeme A1 in anther tissue (Donald et al. 1995), although RT-PCR demonstrated inactivity of B-located 45S rRNA genes in leaf tissue of the same genotype (Donald et al. 1997). The reason(s) why B chromosome rDNA is not or only weakly transcribed is not yet clear. Differences in histone H3 methylation between A and B chromosomes that may be responsible for differences in gene activity have been demonstrated in *B. dichromosomatica* (Marschner et al. 2007). Immunofluorescence demonstrated that the chromatin in A chromosomes and both types of B chromosomes of *B. dichromosomatica* differs markedly as to euchromatic histone H3 methylation marks. Another possibility is that suppression may occur because of nucleolar dominance, so that the rRNA genes on the A chromosomes are active at the expense of those on the B chromosomes (Donald et al. 1997).

The postulated inactivity of B chromosome rDNA might explain the presence of multiple ITS2 sequences, since homogenization of rDNA spacers is thought to occur only in transcribed regions. Concerted evolution is a feature of rDNA repeats (Dover 1994), but mechanisms that control it

may not include non-transcribed rDNA sequences (Lim et al. 2000). Since no sequence homogenization occurs between A and B chromosome rDNA, and B chromosomes are not constitutively active, one might expect further sequence drift of B-located rDNA sequences. An increase in the number of different members of the already heterogeneous population of ITS2 sequences on both types of B chromosomes could be the evolutionary consequence, as has been postulated for the B-chromosome-like paternal sex ratio chromosome of the wasp *Trichogramma kaykai* (van Vugt et al. 2005).

Acknowledgements

We are grateful to Katrin Kumke for excellent technical assistance and to Jörg Fuchs (IPK, Gatersleben) for flow-sorting of nuclei. We also thank Ingo Schubert (IPK, Germany) for reading the manuscript. S.M. and A.H. were supported by a grant of the Land Sachsen Anhalt and the IPK (Gatersleben).

References

Alfenito, M.R., and Birchler, J.A. 1993. Molecular characterization of a maize B chromosome centric sequence. Genetics, **135**: 589–597. PMID:8244015.

Baldwin, B.G. 1992. Phylogenetic utility of the internal transcribed spacers of nuclear ribosomal DNA in plants: an example from the compositae. Mol. Phylogenet. Evol. **1**: 3–16. doi:10.1016/1055-7903(92)90030-K. PMID:1342921.

Camacho, J.P.M., Sharbel, T.F., and Beukeboom, L.W. 2000. B-chromosome evolution. Philos. Trans. R. Soc. Lond. B, **355**: 163–178. doi:10.1098/rstb.2000.0556.

Cheng, Y.M., and Lin, B.Y. 2003. Cloning and characterization of maize B chromosome sequences derived from microdissection. Genetics, **164**: 299–310. PMID:12750341.

Dhar, M.K., Friebe, B., Koul, A.K., and Gill, B.S. 2002. Origin of an apparent B chromosome by mutation, chromosome fragmentation and specific DNA sequence amplification. Chromosoma, **111**: 332–340. PMID:12474062.

Donald, T.M., Leach, C.R., Clough, A., and Timmis, J.N. 1995. Ribosomal RNA genes and the B chromosome of *Brachycome dichromosomatica*. Heredity, **74**: 556–561. PMID:7759291.

Donald, T.M., Houben, A., Leach, C.R., and Timmis, J.N. 1997. Ribosomal RNA genes specific to the B chromosomes in *Brachycome dichromosomatica* are not transcribed in leaf tissue. Genome, **40**: 674–681. PMID:9352646.

Dover, G. 1994. Concerted evolution, molecular drive and natural selection. Curr. Biol. **4**: 1165–1166. doi:10.1016/S0960-9822(00)00265-7. PMID:7704590.

Field, B.L., Houben, A., Timmis, J.N., and Leach, C.R. 2006. Internal transcribed spacer sequence analyses indicate cytoevolutionary patterns within *Brachycome* Cass. (Asteraceae). Plant Syst. Evol. **259**: 39–51. doi:10.1007/s00606-005-0400-y.

Green, D.M. 1990. Muller's rachet and the evolution of supernumerary chromosomes. Genome, **33**: 818–824.

Hizume, M., Sato, S., and Tanaka, A. 1980. A highly reproducible method of nucleolus organizing regions staining in plants. Stain Technol. **55**: 87–90. PMID:6157230.

Houben, A., Leach, C.R., Verlin, D., Rofe, R., and Timmis, J.N. 1997. A repetitive DNA sequence common to the different B chromosomes of the genus *Brachycome*. Chromosoma, **106**: 513–519. PMID:9426283.

Houben, A., Thompson, N., Ahne, R., Leach, C.R., Verlin, D., and Timmis, J.N. 1999. A monophyletic origin of the B chromosomes of *Brachycome dichromosomatica* (Asteraceae). Plant Syst. Evol. **219**: 127–135. doi:10.1007/BF01090304.

Houben, A., Field, B.L., and Saunders, V. 2001*a*. Microdissection and chromosome painting of plant B chromosomes. Methods Cell Sci. **23**: 115–124. PMID:11741148.

Houben, A., Verlin, D., Leach, C.R., and Timmis, J.N. 2001*b*. The genomic complexity of micro B chromosomes of *Brachycome dichromosomatica*. Chromosoma, **110**: 451–459. doi:10.1007/s00412-001-0173-1. PMID:11862452.

Houben, A., Orford, S.J., and Timmis, J.N. 2006. In situ hybridization to plant tissues and chromosomes. Methods Mol. Biol. **326**: 203–218. PMID:16780203.

Jamilena, M., Ruiz Rejon, C., and Ruiz Rejon, M. 1994. A molecular analysis of the origin of the *Crepis capillaris* B chromosome. J. Cell Sci. **107**: 703–708. PMID:8006083.

Jones, R.N. 1995. B chromosomes in plants. New Phytol. **131**: 411–434. doi:10.1111/j.1469-8137.1995.tb03079.x.

Jones, R.N., and Houben, A. 2003. B chromosomes in plants: escapees from the A chromosome genome? Trends Plant Sci. **8**: 417–423. doi:10.1016/S1360-1385(03)00187-0. PMID:13678908.

Leach, C.R., Houben, A., and Timmis, J.N. 2004. The B chromosomes in *Brachycome*. Cytogenet. Genome Res. **106**: 199–209. doi:10.1159/000079288. PMID:15292592.

Leach, C.R., Houben, A., Field, B., Pistrick, K., Demidov, D., and Timmis, J.N. 2005. Molecular evidence for transcription of genes on a B chromosome in *Crepis capillaris*. Genetics, **171**: 269–278. doi:10.1534/genetics.105.043273. PMID:15956665.

Lim, K.Y., Kovarik, A., Matyasek, R., Bezdek, M., Lichtenstein, C.P., and Leitch, A.R. 2000. Gene conversion of ribosomal DNA in *Nicotiana tabacum* is associated with undermethylated, decondensed and probably active gene units. Chromosoma, **109**: 161–172. PMID:10929194.

Maluszynska, J., and Schweizer, D. 1989. Ribosomal RNA genes in B chromosomes of *Crepis capillaris* detected by non-radioactive in situ hybridization. Heredity, **62**: 59–65. PMID:2732088.

Marschner, S., Kumke, K., and Houben, A. 2007. B chromosomes of *B. dichromosomatica* show a reduced level of euchromatic histone H3 methylation marks. Chromosome Res. **15**: 214–222. doi:10.1007/s10577-006-1114-x.

McAllister, B.F., and Werren, J.H. 1997. Hybrid origin of a B chromosome (PSR) in the parasitic wasp *Nasonia vitripennis*. Chromosoma, **106**: 243–253. doi:10.1007/s004120050245. PMID:9254726.

Ochs, R.L., Lischwe, M.A., Shen, E., Carroll, R.E., and Busch, H. 1985. Nucleologenesis: composition and fate of prenucleolar bodies. Chromosoma, **92**: 330–336. doi:10.1007/BF00327463. PMID:3902398.

Pecinka, A., Schubert, V., Meister, A., Kreth, G., Klatte, M., Lysak, M.A., Fuchs, J., and Schubert, I. 2004. Chromosome territory arrangement and homologous pairing in nuclei of *Arabidopsis thaliana* are predominantly random except for NOR-bearing chromosomes. Chromosoma, **113**: 258–269. doi:10.1007/s00412-004-0316-2. PMID:15480725.

Puertas, M.J. 2002. Nature and evolution of B chromosomes in plants: a non-coding but information-rich part of plant genomes. Cytogenet. Genome Res. **96**: 198–205. doi:10.1159/000063047. PMID:12438799.

Sapre, B., and Deshpande, S. 1987. Origin of B chromosomes in *Coix* L. through spontaneous interspecific hybridization. J. Hered. **78**: 191–196.

Schubert, I., and Wobus, U. 1985. In situ hybridization confirms jumping nucleolus organizing regions in *Allium*. Chromosoma, **92**: 143–148. doi:10.1007/BF00328466.

Sharbel, T.F., Green, D.M., and Houben, A. 1998. B-chromosome

origin in the endemic New Zealand frog *Leiopelma hochstetteri* through sex chromosome devolution. Genome, **41**: 14–22. doi: 10.1139/gen-41-1-14. PMID:9549055.

Stitou, S., Diaz de La Guardia, R., Jimenez, R., and Burgos, M. 2000. Inactive ribosomal cistrons are spread throughout the B chromosomes of *Rattus rattus* (Rodentia, Muridae). Implications for their origin and evolution. Chromosome Res. **8**: 305–311. doi:10.1023/A:1009227427575. PMID:10919721.

Sullivan, G.J., Bridger, J.M., Cuthbert, A.P., Newbold, R.F., Bickmore, W.A., and McStay, B. 2001. Human acrocentric chromosomes with transcriptionally silent nucleolar organizer regions associate with nucleoli. EMBO J. **20**: 2867–2877. doi:10.1093/emboj/20.11.2867. PMID:11387219.

Swofford, D. 2002. PAUP*. Phylogenetic analysis using parsimony (*and other methods). Version 4. Sinauer Associates, Sunderland, Mass.

van Vugt, J.J., de Nooijer, S., Stouthamer, R., and de Jong, H. 2005. NOR activity and repeat sequences of the paternal sex ratio chromosome of the parasitoid wasp *Trichogramma kaykai*. Chromosoma, **114**: 410–419. doi:10.1007/s00412-005-0026-4. PMID:16179988.

Watanabe, K., Carter, C.R., and Smithwhite, S. 1975. Cytology of *Brachycome lineariloba*. 5. Chromosome relationships and phylogeny of race-A cytodemes ($n = 2$). Chromosoma, **52**: 383–397. doi:10.1007/BF00364021.

White, T.J., Burns, T., Lee, S., and Taylor, J. 1990. Amplification and direct sequencing of fungal ribosomal RNA genes for phylogenetics. *In* PCR protocols: a guide to methods and applications. *Edited by* M. Innis, D. Gelfand, J. Sninsky, and T. White. Academic Press, San Diego, Calif. pp. 315–322.

Yakura, K., and Tanifuji, S. 1983. Molecular cloning and restriction analysis of *Eco*RI-fragments of *Vicia faba* rDNA. Plant Cell Physiol. **24**: 1327–1330.

3. Zusammenfassende Diskussion

In den nachfolgenden Abschnitten werden die wichtigsten Ergebnisse der eigenen Arbeiten (**A1-A20**) zusammenfassend dargestellt und deren Relevanz im übergeordneten Kontext diskutiert. Auf eine detaillierte Diskussion der Ergebnisse sei an dieser Stelle verzichtet. Hierfür wird auf die entsprechenden Originalarbeiten verwiesen. Ebenso sind Hintergrund bzw. Zielstellung, Material und Methoden sowie die ausführliche Beschreibung der Ergebnisse den entsprechenden Originalarbeiten zu entnehmen.

3.1. Ursprung und Evolution von B-Chromosomen

Der Ursprung der B-Chromosomen ist noch nicht vollständig geklärt, aber es ist wahrscheinlich, dass sie in den unterschiedlichen Organismen über verschiedene Mechanismen entstehen (Camacho et al., 2000; Jones and Houben, 2003). Eine Möglichkeit besteht darin, dass B-Chromosomen von den A-Chromosomen der gleichen Art abstammen und das Ergebnis duplizierter oder fragmentierter A-Chromosomenteile darstellen, wie z. B. postuliert für *Crepis capillaris* (Jamilena et al., 1994). Beim Vergleich der Sequenzen der A- und B-Chromosomen von Mais wurde festgestellt, dass deren B-Chromosomen viele Sequenzen besitzen, die auch auf unterschiedlichen A-Chromosomen und polymorphen heterochromatischen A-Chromosomenregionen vorliegen (Alfenito and Birchler, 1993; Cheng and Lin, 2003). Es wird angenommen, dass B-Chromosomen in Mais Fusionsprodukte von Sequenzen mehrerer A-Chromosomen darstellen (Buckler et al., 1999; Page et al., 2001). Für *B. dichromosomatica* gibt es ebenfalls eine Ähnlichkeit zwischen polymorphen und heterochromatischen A-Chromosomenregionen und den B-Chromosomen. Die genomische Organisation der Mikro-B-Chromosomen dieser Art wird als ein Konglomerat aus repetetiven Sequenzen von unterschiedlichen polymorphen A-Chromosomensegmenten und anderen A-Chromosomensequenzen betrachtet (Houben et al., 2001). Eine hohe Sequenzähnlichkeit zwischen A- and B-Chromosomen konnte gleichfalls für den Roggen nachgewiesen werden. Nur die heterochromatische Domäne am Ende des langen B-Chromosomenarms zeigte eine Anreicherung von B-spezifischen repetetiven Sequenzen (Houben et al., 1996b).

Unlängst wurde in der Nachkommenschaft einer triploiden Reispflanze ein neugebildetes B-Chromosom nachgewiesen. Der Einsatz von 72 unterschiedlichen Chromosomenarm-spezifischen *single copy* Markern demonstrierte, dass auch

dieses B-Chromosom sich nicht aus einem einzelnen A-Chromosom entwickelt haben kann (Cheng et al., 2000).

Für einige nicht-pflanzliche Organismen, wie für den Frosch *Leiopelma hochstetteri*, wurde die Abstammung der B-Chromosomen von Sexchromosomen postuliert (Sharbel et al., 1998). Eine weitere Möglichkeit ist die spontane Bildung von B-Chromosomen als Folge interspezifischer Kreuzungen, wie sie z. B. in Hybriden von *Coix aquaticus* und *C. gigantea* beobachtet wurde (Sapre and Deshpande, 1987). So konnte in embryonalen Weizen x Hirse-Hybridzellen neben der Eliminierung von Hirse-Chromosomen beobachtet werden, dass zentromerische Fragmente der Hirse erst am Ende der Genomeliminierung abgebaut werden. Nach Stabilisierung der Enden durch Telomersequenzen könnte ein derartiges Zentromerfragment den Ausgangspunkt für die Entstehung eines B-Chromosoms darstellen (Gernand et al., 2005). Die Entstehung von B-Chromosomen ist höchstwahrscheinlich ein seltener Vorgang, da in engverwandten Arten, z. B. unterschiedliche *Brachycome*-Arten (Houben et al., 1999), oder Roggen-Arten (Jones and Puertas, 1993) ähnliche B-Chromosomen nachgewiesen werden konnten.

Der molekulare Prozess der B-Chromosomen-spezifischen Sequenzakkumulation ist erst wenig verstanden. Es kann aber davon ausgegangen werden, dass der Transfer von transposablen Elementen eine Rolle spielt. So konnte für Mais ein transkriptionsaktives *Prem-1* Retroelement (Stark et al., 1996; Lamb et al., 2007) auf den B-Chromosomen nachgewiesen werden. Basierend auf LTR-Sequenzdaten konnte für das Mais B-Chromosom ein Alter von zumindest 2 Millionen Jahren abgeleitet werden (Lamb et al., 2007). Eine Anreicherung von mobilen Elementen wie für Sexchromosomen beschrieben (Steinemann and Steinemann, 2005) konnte nur für einige Roggen B-lokalisierte mobile Elemente (Carchilan et al., in Vorbereitung) nachgewiesen werden. Green (1990) macht die Akkumulation von mobilen Elementen und Mutationen auf B-Chromosomen in einem Prozess analog zu „*Muller's ratchet*" für die Evolution der B-Chromosomen mitverantwortlich. Da eine der Haupteigenschaften von B-Chromosomen ist, nicht mit den Chromosomen des A-Komplementes zu paaren, ist eine Korrektur von Mutationen durch Rekombination wenig wahrscheinlich, so dass die B-Chromosomen insgesamt dem „*Muller's ratchet*"-Mechanismus unterliegen könnten.

Für eine Reihe von B-Chromosomen konnten 45S rDNA-Sequenzen wie z. B. beschrieben für *C. capillaris* (Maluszynska and Schweizer, 1989; Leach et al., 2005), *Plantago lagopus* (Dhar et al., 2002) und *B. dichromosomatica* (Houben et al., 1997b; Marschner et al., 2007b) nachgewiesen werden. 45S rDNA kann zufällig und/oder als Resultat interchromosomaler Transposition auf B-Chromosomen gelangen (Jones and Houben, 2003). Da die Nukleolus-organisierende Regionen relativ leicht mit Hilfe der *in situ* Hybridisierung und der Silberfärbung nachgewiesen werden können, wurden diese Untersuchungen oft zur Analyse von B-Chromosomen eingesetzt und rDNA somit entsprechend häufig nachgewiesen. Eine andere Möglichkeit ist, dass der Ursprung eines rDNA tragenden B-Chromosomes aus einem A-Chromosomenfragment, das rDNA-Gene enthielt hervorging, oder nach der Fragmentierung eine massive Akkumulation von rDNA erfolgte. Bei *P. lagopus* wurde neben der 45S rDNA eine massive Akkumulation von 5S rDNA auf den B-Chromosomen nachgewiesen (Dhar et al., 2002).

Der Vergleich der ribosomalen ITS2-Sequenzen der A- und B-Chromosomen von *C. capillaris* (Leach et al., 2005) und *B. dichromosomatica* (Donald et al., 1997; Field et al., 2006; Marschner et al., 2007b) demonstrierte eine relativ hohe Ähnlichkeit dieser Sequenzen zueinander innerhalb der entsprechenden Art. Damit konnte gefolgert werden, dass die ribosomale DNA der B-Chromosomen von der 45S rDNA der A-Chromosomen der gleichen Art abstammt, oder beide Chromosomentypen einen gemeinsamen Vorgänger haben.

Basierend auf neuen Einsichten zur Karyotypevolution (Schubert, 2007) ist die Formierung von B-Chromosomen nach einer Robertsonschen Translokation vorstellbar. Bei dieser Chromosomenmutation werden die langen Arme der beteiligten Chromosomen in einem Translokationsprodukt rekombiniert, während das zweite Translokationsprodukt im wesentlichen aus einem Zentromer, zwei Telomeren und gegebenenfalls aus perizentromerischen repetetiven Sequenzen besteht. Ein derartiges Minichromosom könnte als Ausgangspunkt für die Bildung eines B-Chromosoms dienen. Ergebnisse von Hall et al. (2006), Lysak et al. (2006), Gaut et al. (2007) demonstrierten unlängst, dass (peri)zentromerische Bereiche sich dynamisch verhalten und durch eine hohe Frequenz von Umbauten gekennzeichnet

sind. Ferner tolerieren diese Segmente B-typische Sequenzen wie mobile Elemente oder rDNA. Durch die hohe Reorganisationsfrequenz (peri)zentromerischer Bereiche könnte das meiotische Paarungsvermögen mit den A-Chromosomen verhindert werden und nach Anreicherung anderer Sequenzen, wie z. B. Telomeren könnte sich daraus, wie in der Abbildung 1 dargestellt, ein proto-B-Chromosom formieren.

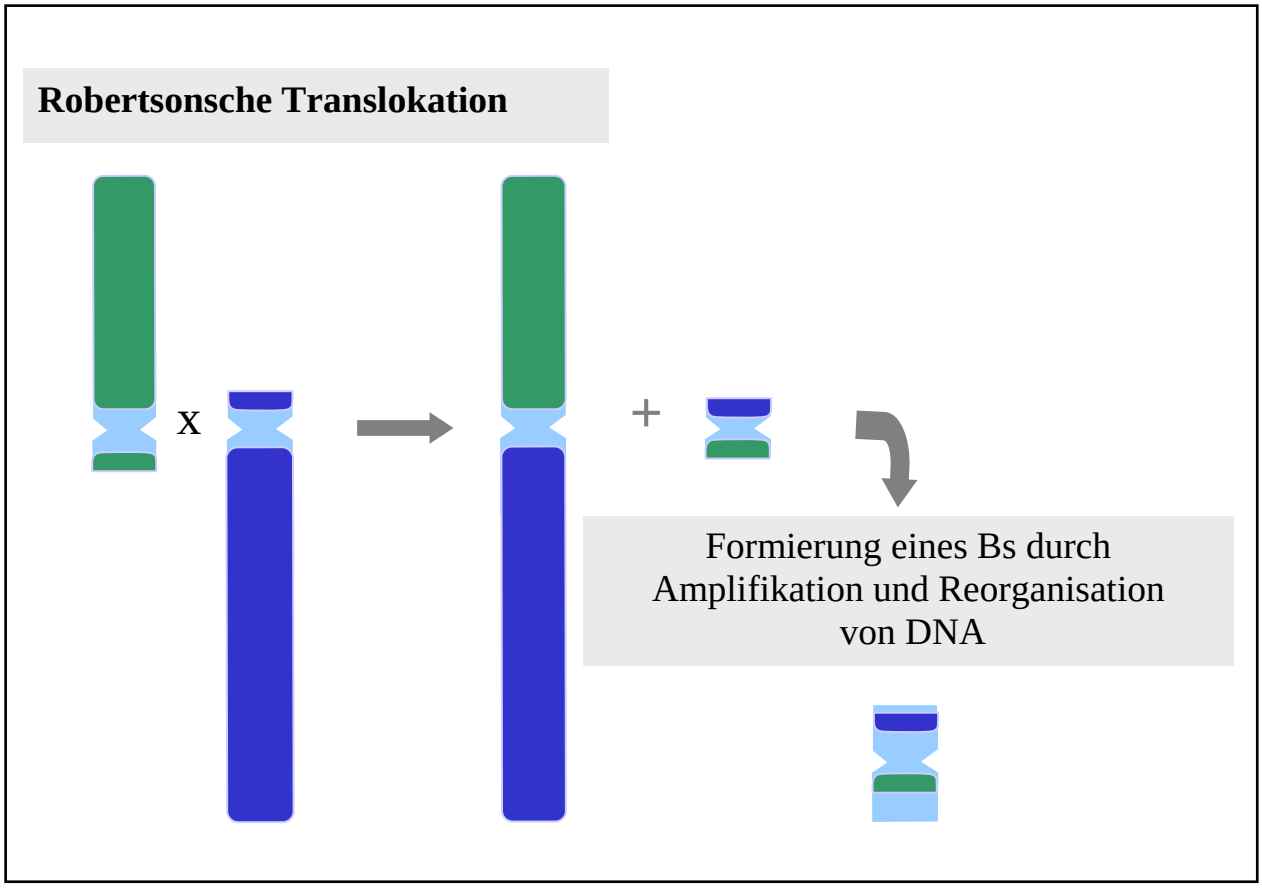

Abbildung 1

Postulierter Mechanismus zur Bildung von proto-B-Chromosomen.

Durch Translokation von zwei Chromosomen mit Bruchpunkt im Zentromerbereich bzw. Chromosomenende entsteht ein großes Chromosom und ein kleines, genarmes Minichromosom welches oftmals verloren geht. Durch die hohe Reorganisationsfrequenz (peri)zentromerischer Bereiche könnte das meiotische Paarungsvermögen mit den A-Chromosomen verhindert werden und nach weiterer Reorganisation und Anreicherung anderer Sequenzen könnte sich daraus ein proto-B-Chromosom bilden.

3.2. A- und B-Chromosomen können sich in der Verteilung von Eu- und Heterochromatin-typischen Histonveränderungen unterscheiden

Obgleich die Erkenntnisse zur Funktion und Struktur von Chromatin sich in den letzten Jahren signifikant erweitert haben, ist unser Wissen zur Chromatinkomposition von B-Chromosomen noch relativ begrenzt. Basierend auf frühen zytologischen Arbeiten werden ca. 50% aller B-Chromosomen als heterochromatisch eingestuft (Jones, 1975). Dieser relativ geringe Prozentsatz ist überraschend, da B-Chromosomen bislang als transkriptionsinaktive Komponenten des Genoms charakterisiert werden. Die Methylierung von Histonen sind in der Ausprägung von Eu- und Heterochromatin involviert. Während die Methylierung von Histon H3 an der Position Lysin 4 (H3K4me) mit einer Aktivierung der Gene in Verbindung gebracht wird und in Eukaryoten hoch konserviert ist, können die Methylierungsfunktionen an den Positionen H3 Lysin 9 (H3K9me), H3 Lysin 27 (H3K27me) und H4 Lysin 20 (H4K20me) in unterschiedlichen Arten variieren (Fuchs et al., 2006).

Unterschiede in der Histonmethylierung an Histon H3K4, H3K9 und H3K27 zwischen A- und B-Chromosomen können Hinweise über die unterschiedliche Transkriptionsaktivität und Chromatinzusammensetzung der jeweiligen Chromosomen liefern. Nach der erstmaligen Etablierung der indirekten Immunfluoreszenz für pflanzliche Chromosomen wurde die Verteilung einzelner Histonmodifizierungen vergleichend beschrieben (Houben et al., 1996a). A- und B-Chromosomen des Roggens (Houben et al., 2003; Carchilan et al., 2007), *C. capillaris* (Houben et al., 2003), *B. dichromosomatica* (Marschner et al., 2007a) und *P. libanotica* (Kumke et al., 2008) zeigten für die Heterochomatin-typischen Histonveränderungen H3K9me1/2 and H3K27me1 keine Unterschiede. Die einheitliche Verteilung der Methylierung von H3K9me2 auf den A- und Standard-B-Chromosomen korreliert mit den Ergebnissen für Pflanzen mit großen Genomen. Untersuchungen an 24 Pflanzenarten mit unterschiedlicher Genomgröße zeigten, dass bei Pflanzen mit einer Genomgröße unter 500 Mbp die Dimethylierung von H3K9 sich auf die heterochromatischen Chromozentren beschränkt. Bei einer Genomgröße von mehr als 500 Mbp verteilt sich die Histon H3K9-Dimethylierung wahrscheinlich auf Grund der hohen Dichte von transposablen Elementen dispers über alle Chromosomen (Houben et al., 2003). Die chromosomale Verteilung von

Histon H3K3me2 ist unabhängig von der Genomgröße und entspricht weitgehend den *Giemsa-banding* negativen Banden.

Die Euchromatin-spezifische Methylierung an Histon H3K4 ergaben für die A-Chromosomen von *B. dichromosomatica* eine disperse Markierung mit Ausnahme des Perizentromers und einer heterochromatischen Region (Abbildung 2). Während an den Standard-B-Chromosomen noch eine sehr schwache Markierung mit den Antikörpern für die drei Methylierungstypen von H3K4 erfolgte, zeigte sich an den Mikro-B-Chromosomen nur noch für H3K4me1 eine schwache disperse Markierung. Di- und Trimethylierungen wurden bei diesem B-Chromosomentyp nicht nachgewiesen (Marschner et al., 2007a). Die Abwesenheit dieser Euchromatin-spezifischen Markierungen ist mit der Mikro-B-Chromosomen-spezifisichen Anreicherung von repetetiven Sequenzen erklärbar.

Die Methylierungen an Histon H4K20 unterschieden sich nicht zwischen A- und B-Chromosomen von *B. dichromosomatica* (Marschner et al., 2007a). Bei *A. thaliana* gelten H4K20me2, 3 als typisch euchromatische Marker, während H4K20me1 sowohl in *A. thaliana* als auch in *H. vulgare* als heterochromatischer Marker auftritt (Naumann et al., 2005; Fuchs et al., 2006). Methylierungen an Histon H4K20 im menschlichen Genom stehen mit der Transkriptionsunterdrückung von Genen in Verbindung (Miao and Natarajan, 2005) sowie in *D. melanogaster* als Kennzeichen für Heterochromatin (Ebert et al., 2006).

Roggen B-Chromosomen sind durch eine unikale Kombination von Histonmodifizierungen gekennzeichnet (Carchilan et al., 2007). Der heterochromatische Bereich des langen B-Chromosomenarms weist sowohl H3K4me3- als auch H3K27me3-Modifikationen auf (Abbildung 2). Da die Methylierung von H3K4 generell mit Transkriptionsaktivität korreliert, wurde der Transkriptionszustand der B-lokalisierten repetetiven Sequenzen E3900 und D1100 evaluiert. Es konnte erstmals eine Expression von nicht-kodierender RNA für B-Chromosomen nachgewiesen werden.

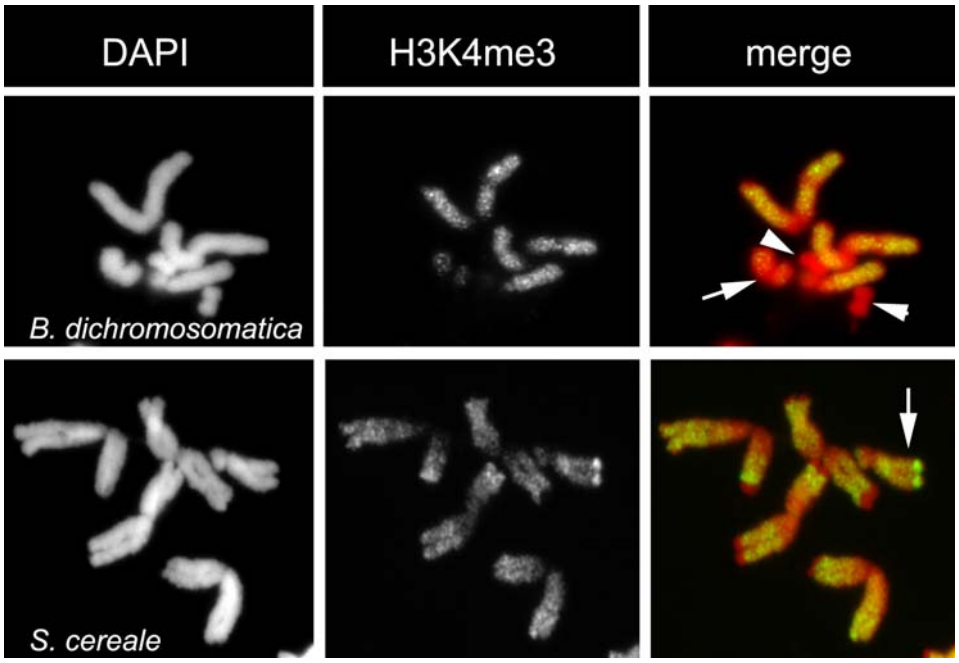

Abbildung 2
Chromosomale Verteilung der Euchromatin-typischen Histonmodifikation H3K4me3 entlang A- und B-Chromosomen. B-Chromosomen von *B. dichromosomatica* zeigen eine reduzierte H3K4me3-Markierung, dagegen zeigt der heterochromatische Bereich des langen B-Chromosomenarms des Roggens eine intensive H3K4me3-Markierung. B-Chromosomen sind mit Pfeilen gekennzeichnet.

Zusätzlich wurde für *B. dichromosomatica* eine reduzierte Acetylierung der Standard-B-Chromosomen an Lysin 5 und Lysin 8 im Histon H4 nachgewiesen (Houben et al., 1997a). Diese Histonmodifikation korreliert mit dem Replikationsverhalten der spät-replizierenden B-Chromosomen. Diese reduzierte Acetylierung von Histon H4 und die schwache Methylierung von H3K4 könnten möglicherweise eine gemeinsame Rolle in der Bildung des B-Chromosomen-Chromatins spielen.

Damit kann gefolgert werden, dass ähnliche epigenetische Markierungen in heterochromatischen Bereichen beider Chromosomentypen auftreten, während Euchromatin-typische Markierungen in den B-Chromosomen (außer Roggen) reduziert auftreten. Ähnliche Beobachtungen gibt es für inaktive X-Chromosomen in Säugern, in denen ebenfalls ein Verlust der Euchromatin-assoziierten Histonmethylierung an H3K4 nachgewiesen wurde. Zusätzlich existiert jedoch eine

Anreicherung von Methylierungen an H3K9 und H3K27, die mit Heterochromatin und Geninaktivierung korrelieren (Cohen and Lee, 2002; Silva et al., 2003; Heard, 2005).

3.3. Meiotische B-Chromosomen zeigen eine veränderte Zellzyklus-abhängige Histon H3-Phosphorylierung

Der Zusammenhang zwischen der Zellzyklus-abhängigen Phosphorylierung von Histon H3 und der Veränderung der Chromosomenstruktur bzw. dem Segregationsverhalten von Chromosomen konnte mit Hilfe von B-Chromosomen demonstriert werden (Houben et al., 2007). Dabei wurde dargestellt, dass das Phosphorylierungsmuster von Histon H3 an den Positionen Serin 10 und 28 sich zwischen der ersten und zweiten meiotischen Teilung unterscheidet. Während der ersten meiotischen Zellteilung ist Histon H3 entlang des Chromosoms phosphoryliert. Die zweite meiotische Zellteilung ähnelt der Mitose, hier zeigt nur der perizentromerische Chromosomenbereich H3S10ph und H3S28ph. Es konnte demonstriert werden, dass Schwesterchromatiden von A- und B-Chromosomen die bereits in der ersten meiotischen Teilung getrennt wurden kein phosphoryliertes Histon H3 mehr aufweisen (Manzanero et al., 2000; Gernand et al., 2003). Der Kondensationszustand von Chromatiden ohne H3S10ph/S28ph-Signalen ist vergleichbar mit dem Kondensationszustand von Chromatiden mit Phosporylierungssignalen in der zweiten meiotischen Teilung. Unabhängig vom Grad der H3-Phosphorylierung erfolgt eine Interaktion zwischen Tubulin-Spindelfasern und dem Zentromer.

Die Dynamik der Histon H3-Phosphorylierung korreliert mit der Etablierung/Auflösung der Schwesterchromatiden-Verklebung kondensierender Chromosomen. Während der ersten meiotischen Teilung bleiben die Schwesterchromatiden über ihre gesamte Länge verbunden. Die H3-Phosphorylierung erfolgt ebenfalls über die gesamte Chromosomenlänge. Im zweiten Abschnitt der Meiose sind die Schwesterchromatiden nur im perizentromerischen Bereich kohäsiv und die H3-Phosphorylierung erfolgt ebenso nur im perizentromerischen Bereich. Somit kann für Pflanzen postuliert werden, dass die Phosphorylierung von Histon H3S10 und S28 mit der Etablierung der Schwesterchromatiden-Verklebung in der Meiose korreliert und eine untergeordnete Rolle in der Kondensation von meiotischen Chromosomen spielt. Diese Annahme wurde durch die Analyse von *afd1*-Mutanten (Mais Mutanten

ohne erste meiotische Teilung) bestätigt (Kaszas and Cande, 2000). Die evolutionär hoch konservierte Aurora-Kinase konnte als Histon H3S10-spezifische Kinase in *A. thaliana* identifiziert werden (Demidov et al., 2005). Die Zellzyklus-abhängige Phosphorylierung von Histon H3 an den Positionen Threonin 3, 11 und 32 korreliert hingegen bei Pflanzen mit dem Kondensationsverhalten mitotischer und meiotischer Chromosomen (Houben et al., 2005; Caperta et al., 2008)

3.4. Segregationsverhalten und Zentromere von B-Chromosomen

Drive ist das Hauptmerkmal von B-Chromosomen. Dieser tritt auf, wenn die Anzahl von B-Chromosomen in den Keimzellen größer ist, als die nach den Mendelschen Gesetzen erwartete Anzahl. Die Regulatoren des *drive*-Prozesses von B-Chromosomen sind unbekannt. *Drive* kann in der Meiose auftreten, wenn die B-Chromosomen während der ersten Anaphase zu einem Spindelpol wandern und dann bevorzugt in den Kern gehen, der für die spätere Bildung der Eizellen bestimmt ist. *Drive* kann auch in der ersten oder zweiten Pollenkorn-Mitose auftreten, wenn die Chromatiden der B-Chromosomen nicht separieren (*nondisjunction*) und beide B-Chromatiden in den generativen Kern wandern (Jones and Houben, 2003). Roggen B-Chromosomen separieren nicht während der ersten Pollenkorn- bzw. Eizellen-Mitose und werden deshalb nur einem Pol zugeteilt (Jones, 1991b; Jones, 2004) (Abbildung 3). In Mais findet *nondisjunction* in der zweiten Pollenkorn-Mitose statt. Es folgt eine bevorzugte Befruchtung von Eizellen durch B-Chromosomen tragende Pollenzellen (Carlson, 1988; Jones, 2004). Der *drive* Mechanismus von B-Chromosomen wurde auch in Weizen (Müntzing, 1970; Niwa et al., 1997; Endo et al., 2008) und Wildroggen *S. vavilovii* (Puertas et al., 1985) mit zusätzlichen Roggen B-Chromosomen beobachtet. Mit Hilfe von B-Chromosomen mit einer Deletion am langen Arm konnte nachgewiesen werden, dass der terminale heterochromatische Bereich des langen B-Chromosomenarms für die Kontrolle des *nondisjunction* Prozesses essentiell ist (Müntzing, 1948; Endo et al., 2008). Wenn dieser heterochromatische Bereich durch chromosomale Umbauten auf ein A-Chromosom gelangt, sind die Faktoren an der Regulation des *nondisjunction* von B-Chromosomen dennoch aktiv (Lima-de-Faria, 1962; Endo et al., 2008).

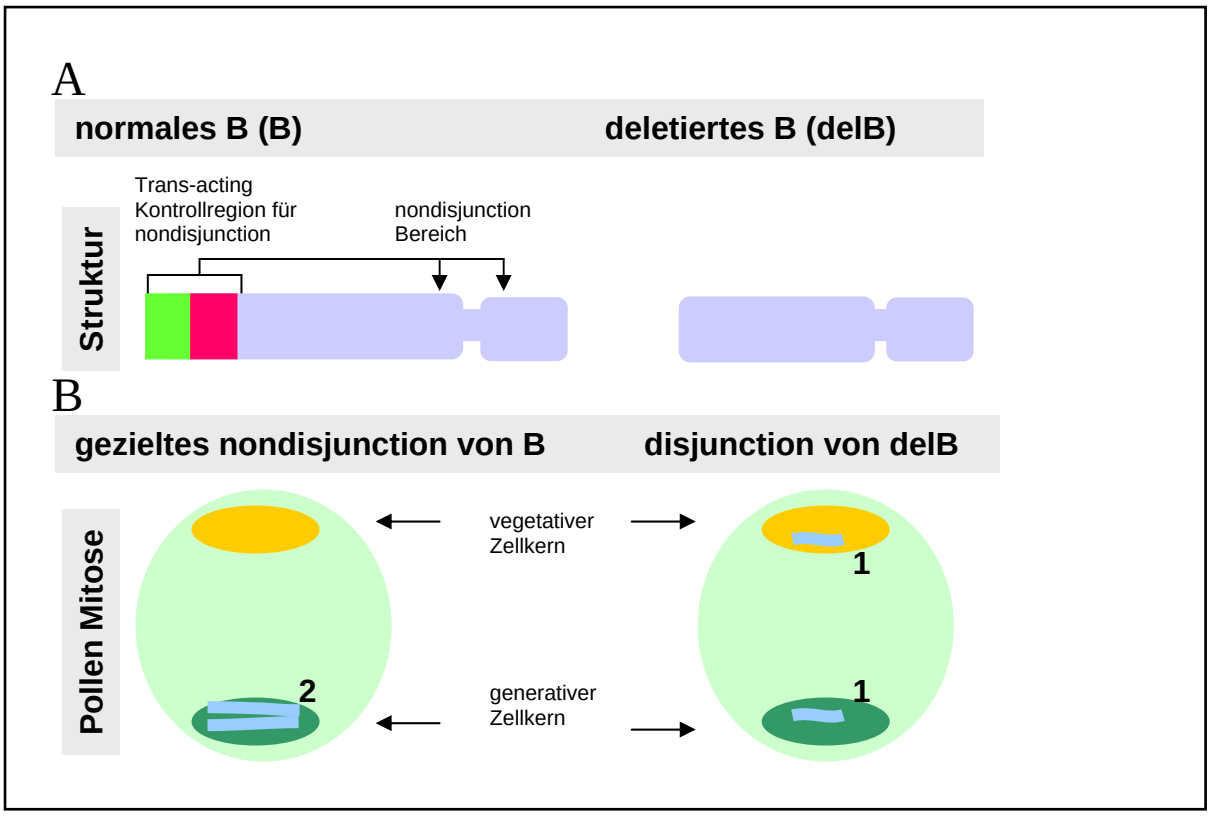

Abbildung 3

Drive Verhalten von Roggen B-Chromosomen. (A) Struktur von normalen und deletierten B-Chromosomen. (B) Schematische Darstellung des *drive* Verhaltens von normalen und deletierten B-Chromosomen während der ersten Pollenmitose.

Die molekularen Mechanismen der *nondisjunction* Kontrolle sind noch unbekannt, aber es ist vorstellbar, dass B-Chromosomen-spezifische nichtkodierende RNA, wie unlängst für Roggen B-Chromosomen identifiziert, an der Regulierung des *drive*-Prozesses involviert ist (Carchilan et al., 2007). Diese Annahme wird unterstützt durch die Beobachtung, dass die Überexpression von nichtkodierender Satelliten DNA mit einem fehlerhaften Separieren von Schwesterchromatiden des Menschen während der Mitose korreliert (Bouzinba-Segard et al., 2006). Die Expression zentromerischer Satelliten DNA konnte auch für *Arabidopsis thaliana* nachgewiesen werden (May et al., 2005). Inwieweit eine Transkriptionsinaktivierung von centromerischen repetetiven Sequenzen in eine fehlerhafte Zellteilung resultiert, ist aber für Pflanzen noch unbekannt.

Ein grundlegendes Verständnis über die Funktion und Organisation von Zentromeren ist notwendig um den *drive* Mechanismus von B-Chromosomen besser zu verstehen. Mais B-Chromosomen besitzen, das bisher am besten untersuchte B-

Zentromer (Alfenito and Birchler, 1993; Kaszas and Birchler, 1996, 1998; Kaszas et al., 2002). So wie die Zentromere der A-Chromosomen, besteht auch diese aus *repeats* wie, ZmBs-, CentC-*repeats* und Zentromer-spezifische Retroelemente. Zirka 700 kb lange DNA Bereiche bestehend aus ZmBs- und CentC-Elementen interagieren mit dem Kinetochorprotein CENH3 (Jin et al., 2005).

Die Aktivität von Zentromeren ist epigenetisch reguliert, da dizentrische A/B-Translokationschromosomen nur ein aktives Zentromer besitzen und somit stabil segregieren (Han et al., 2006). Der (peri)zentromerische Bereich von A- und B-Chromosomen scheint sich in der DNA-Zusammensetzung zu unterscheiden. B-Chromosomen von Mais (Lamb et al., 2005) and Roggen (Wilkes et al., 1995; Francki, 2001) sind durch eine Anreicherung von zentromerischen Sequenzen gekennzeichnet. Im Gegensatz zu Mais B-Chromosomen (Lamb et al., 2005), zeigen Roggen B-Chromosomen keine verstärkten CENH3-spezifischen Immunfluoreszenzsignale (Houben et al. unveröffentlicht).

Die Zentromere der Standard B-Chromosomen von *B. dichromosomatica* (Cytodeme A1, A2 und A4) sind durch B-spezifische Sequenzkluster gekennzeichnet. In diesen Zentromeren wurden die *tandem repeats* Bd49 in hohen Kopiezahlen nachgewiesen (Leach et al., 1995). Ähnliche Fragmente wurden auf den A-Chromosomen der gleichen und verwandter Arten nachgewiesen. Da Bd49 *repeats* auf den B-Chromosomen der *B. dichromosomatica* Cytodeme A3 eine nichtzentromerische Position besitzen ist es fraglich, inwieweit dieses *repeat* einen funktionellen Zentromerbaustein darstellt (Houben et al., 1999).

3.5. B-Chromosomen zeigen eine schwache Transkriptionsaktivität

Obgleich B-Chromosomen als nicht-funktionelle Zusatzchromosomen eingestuft werden, zeigen Individuen mit hoher Anzahl von B-Chromosomen phänotypische Effekte. So sind z. B. Roggenpflanzen mit hoher Anzahl von B-Chromosomen durch geringe Wüchsigkeit und schlechte Fertilität gekennzeichnet (Jimenez et al., 1994; Jones, 1995; Schmitt et al., 1997).

Außer für *C. capillaris*, wurde bisher noch kein transkriptionsaktives Gen auf einem B-Chromosomen nachgewiesen. Anders als in *B. dichromosomatica* (Donald et al.,

1997; Marschner et al., 2007b), ist die B-Chromosomen-lokalisierte 45S rDNA von *C. capillaris* transkriptionsaktiv (Leach et al., 2005). Da bisher für Pflanzen keine generelle Charakterisierung des Transkriptionszustandes von B-Chromosomen durchgeführt wurde, wurde das Transkriptionsverhalten von B-Chromosomen mit Hilfe der cDNA-AFLP Methode an Roggenpflanzen mit und ohne B-Chromosomen bestimmt. Dazu wurden drei semi-isogene Roggenlinien eingesetzt. 63 Primerkombination wurden getestet und 2286 unterschiedliche Transkripte vergleichend analysiert (Carchilan et al., in Vorbereitung). Wie erwartet, unterschieden sich die Transkriptionsprofile von Genotypen mit oder ohne B-Chromosomen minimal. Somit kann die Annahme bestätigt werden, dass B-Chromosomen weitgehend genetisch inaktiv sind. Trotzdem konnten 16 B-Chromosomen-assoziierte Transkripte (0,7% aller Transkripte) identifiziert werden. Für alle B-spezifischen Transkripte konnten ähnliche A-lokalisierte Sequenzen nachgewiesen werden. Die B-spezifischen Transkripte B 1134, B 8149 und B 2465 sind Mitglieder repetetiver Sequenzfamilien. Diese zeigen Ähnlichkeit zu mobilen Sequenzelementen wie, *Gypsy*-Retrotransposons und *LINE*-Elemente. Die hohe Sequenzähnlichkeit zwischen A- und B-lokalisierten Sequenzen bestätigte auch die Annahme, dass Roggen B-Chromosomen aus den A-Chromosomen der gleichen Art entstanden.

3.6. *Brachycome dichromosomatica,* eine Modellart für die Analyse von B-Chromosomen

Die Forschung an B-Chromosomen profitiert von den besonderen Eigenschaften der australischen *Asteraceae Brachycome dichromosomatica* (Synonym: *Brachyscome dichromosomatica*). Diese Art zeichnet sich neben einer geringen A-Chromosomenzahl (2n = 4) durch eine extrem hohe Genomplastizität aus. Zusätzlich zu verschiedenen Cytodemen (A1, A2, A3 und A4, (Houben et al., 1999), existieren zwei B-Chromosomentypen (Standard B-Chromosomen und Mikro B-Chromosomen (Franks et al., 1996; Houben et al., 2001; Leach et al., 2004) und polymorphe, aus Satelliten-DNA bestehende, heterochromatische A-Chromosomensegmente (Houben et al., 2000) siehe Abbildung 4.

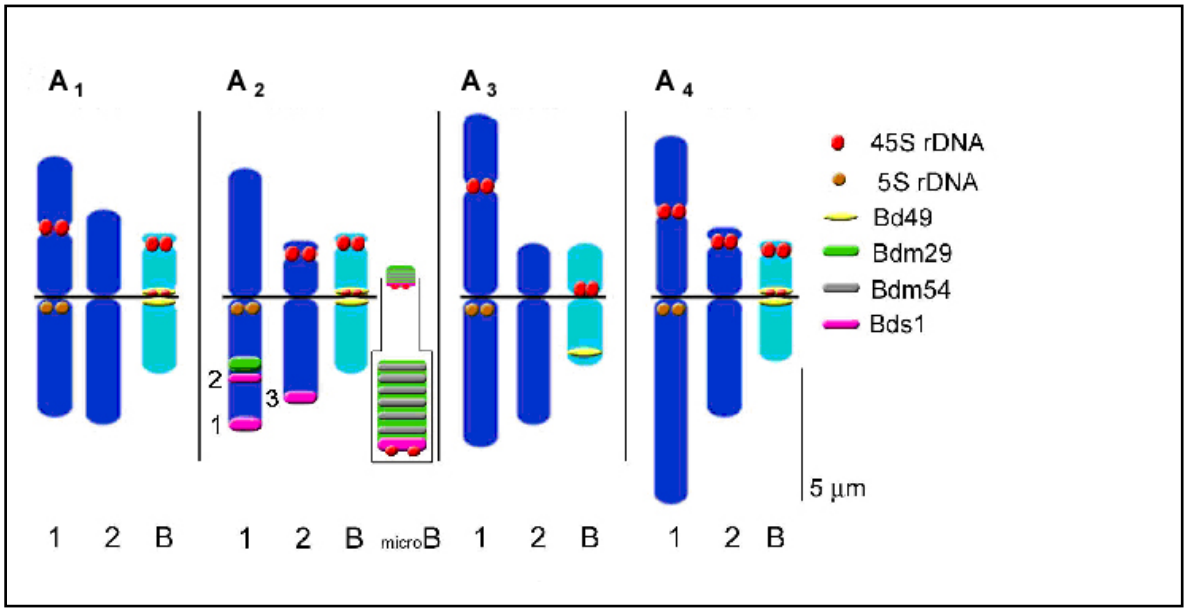

Abbildung 4

Schematische Karyogramme der vier verschiedenen Cytodeme von *B. dichromosomatica* (2n = 4 A-Chromosomen + Standard B-Chromosom (B) + Mikro B-Chromosom (micro B)). Die Positionen verschiedener repetetiver Sequenzen ist farblich gekennzeichnet. Der haploide A-Chromosomensatz der vier Cytodeme ist in dunkelblau dargestellt. Größenmarker = 5 µm.

Ein evolutionärer Zusammenhang zwischen DNA-Amplifikation und der Entstehung von Mikro B-Chromosomen kann postuliert werden. So existieren in *B. dichromosomatica* zwei verschiedene Typen von polymorphen, heterochromatischen, aus Satelliten-DNA bestehende A-Chromosomensegmente (Bds1- und Bdm29-Segmente, siehe Abbildung 4). Bds1-positive A-Chromosomensegmente wurden in ca. 50% aller analysierten Pflanzen an drei möglichen A-Chromosomenpositionen (homozygot und heterozygot) nachgewiesen. Aber auch für Pflanzen ohne mikroskopisch nachweisbare Bds1-Segmente konnte mit Hilfe der PCR diese Sequenz in geringer Kopienzahl detektiert werden (Houben et al. 2000). Das heterochromatische, Bdm29-positive A-Chromosomensegment konnte nur in wenigen Genotypen nachgewiesen werden.

Mikro B-Chromosomen bestehen hauptsächlich aus polymorphen Komponenten der A-Chromosomen (Bdm29, Bds1, (Houben et al., 2001)). Zusätzlich wurden auf beiden B-Chromosomentypen transkriptionsinaktive ribosomale 45S rDNA

Sequenzen nachgewiesen (Donald et al., 1997; Houben et al., 1997b; Marschner et al., 2007b). Trotz morphologisch hoher Ähnlichkeit zwischen Mikro B-Chromosomen und den Bdm29-positiven A-Chromosomensegmenten, konnte demonstriert werden, dass Mikro B-Chromosomen nicht nur aus A-Chromosomen lokalisierten, repetetiven Sequenzen bestehen. So werden die Mikro B-Chromosomen lokalisierten Bdm29-*tandem repeats* von dem Mikro B-spezifischen *tandem repeat* Bdm54 unterbrochen. Damit ist es eher unwahrscheinlich, dass Bdm29-positive A-Chromosomensegmente durch die Integration von Mikro B-Chromosomen entstanden (Houben et al. 2001). Es ist vorstellbar, dass die Gründersequenzen der Mikro B-Chromosomen durch genomischen Stress aus dem Standard-Chromosomenkomplement freigesetzt wurden. Dabei können die in ihren Kopienzahlen variablen *repeats* Bdm29, Bds1 und ribosomale DNA Sequenzen eine ”Gründerrolle” gespielt haben. Solche extrachromosomale DNA könnte durch Kombination mit Telomer- und Zentromersequenzen stabilisiert werden. Es ist möglich, dass durch Mutationen oder epigenetische Ereignisse eine bisher nicht-zentromerische Sequenzen in eine aktive Zentromersequenz umgebildet wird. Extrachromosomale zirkuläre DNA (eccDNA) mit hoher Ähnlichkeit zu A- und B-lokalisierten *tandem repeat* Sequenz konnten nachgewiesen werden (Cohen et al., 2008). Ähnlich wie in nicht-pflanzlichen Organismen (Cohen et al., 1999; Cohen and Mechali, 2001; Cohen et al., 2005) lag die Größe pflanzlicher eccDNA zwischen >2 kb und <20 kb.

Außerdem wurden Bdm29-ähnliche Sequenzen in den Standard B-Chromosomen der Cytodeme A1, A2, A3 und A4 und der verwandten Arten *B. curvicarpa* und *B. dentata* nachgewiesen (Houben et al., 1997b). Somit kann davon ausgegangen werden, dass diese Sequenz für die Entstehung eines B-Chromosoms wichtig ist und evtl. mehrmals unabhängig bei der B-Chromosomenbildung eine Rolle gespielt hat. Es ist aber auch möglich, dass Mikro B- und B-Chromosomen der verschiedenen Cytodeme von *B. dichromosomatica* einen gemeinsamen Ursprung haben oder sich der Standard B-Chromosomentyp aus dem Mikro B-Chromosom entwickelt hat. Die Entstehung von *Brachycome* B-Chromosomen im Rahmen der Artbildung durch Alloployploidisierung kann angenommen werden, da mehrere potentiell allopolyploide Brachycome-Arten (z. B. *B. marginata, B. nivalis*) mit B-Chromsomen existieren.

3.7. Potentielle Anwendung von B-Chromosomen in der Biotechnologie

Neben der Aufklärung von Mechanismen der Genomevolution und Chromosomenbiologie könnten B-Chromosomen eine Rolle in der Biotechnologie spielen. In Zukunft werden effiziente, gezielte und sichere Verfahren der Genübertragung für Züchtungsprozesse unverzichtbar sein. „Künstliche“ Chromosomen u. a. als Vektoren für den Gentransfer werden auch bei Pflanzen in Grundlagenforschung und Biotechnologie eine zunehmende Rolle spielen (Houben and Schubert, 2007). Sie bieten eine nahezu unbegrenzte Aufnahmekapazität für Gene und Genkomplexe und umgehen einige Probleme, die im Falle konventioneller Gentransfertechniken auftreten können und durch DNA-Integration an zufälligen Positionen bedingt sind, z. B. Positionseffekte hinsichtlich der Transgenexpression bzw. Insertionsmutagenese. Minichromosomen können je nach Bedarf stabil von Generation zu Generation übertragen, auf dem Wege der genetischen Segregation entfernt, oder durch Kreuzung in andere Zielorganismen überführt werden. Sie ermöglichen darüber hinaus die Untersuchung der Funktionsweise spezifischer Chromatindomänen (z.B. Zentromerkomponenten). In Kombination mit Kassetten zur wiederholten Zielsequenz-spezifischen Integration von DNA-Fragmenten bieten sie die optimale Strategie zum Transfer komplexer Merkmale. Prinzipiell können Minichromosomen durch konventionelle Gattungskreuzung auch in verwandte, ökonomisch relevante Arten überführt und dort genutzt werden. Trotz international intensiver Bemühungen (z. B. Phan et al. (2007)) konnten im Gegensatz zu Hefen und Säugern bis vor kurzem keine künstlichen Chromosomen für Pflanzen entwickelt werden.

Künstliche Chromosomen können aus einzelnen Komponenten *in vitro* bzw. innerhalb von Zielzellen zusammengesetzt werden. Diese '*bottom up*' Strategie ist schwer zu kontrollieren und wegen der unbekannten Mechanismen zur Bildung von funktionalen Zentromeren für Pflanzen wenig aussichtsreich (Houben and Schubert, 2003). Alternativ können durch die experimentelle Verkürzung von natürlichen Chromosomen *in vivo* Minichromosomen generiert werden, die noch alle Sequenzkomponenten für eine stabile Replikation und Segregation enthalten, aber (weitgehend) frei von endogenen kodierenden Sequenzen sind. Zusätzlich sollen sie über eine Kassette für die gezielte Integration von DNA-Sequenzen verfügen. Eine

Methode hierfür beruht auf der Transformation mit Telomersequenz-haltigen Konstrukten, die am Integrationsort ein neues Chromosomenende für den betroffenen Arm bilden und so Chromosomen verkürzen können. Diese Methode, ursprünglich für Säuger entwickelt (Farr et al., 1991), wurde unlängst als prinzipiell gangbar für die Generierung von potentiell biotechnologisch relevanten Minichromosomen beim Mais beschrieben (Yu et al., 2006; Yu et al., 2007). Zur gezielten nachfolgenden „Beladung“ von Minichromosomen wurden u.a. Sequenzelemente für ein *Cre/loxP*-Rekombinationssystem co-integriert. Solche Systeme erlauben, im Gegensatz zu konventionellen Transformationsmethoden, eine zielgerichtete Integration von DNA-Sequenzen in die Minichromosomen. Die ersten biotechnologisch-relevanten pflanzlichen Minichromosomen wurden aus Mais B-Chromosomen mit Hilfe der „*telomere trunction*“ Technik generiert (Yu et al., 2006). B-Chromosomen sind dafür besonders geeignet, da diese relativ wenige Gene besitzen und die Kopienzahl von B-Chromosomen unter Nutzung des post-meiotischen Akkumulationsmechanismus erhöht werden können. Obgleich B-Chromosomen generell eine geringe Transkriptionsaktivität besitzen, zeigte das im Rahmen der Chromosomenverkürzung co-integrierte GFP-Reporterkonstrukt funktionelle Aktivität. Es ist aber abzuwarten, inwieweit B -lokaliserte Transgene über mehrere Generationen stabil transkribiert werden.

4. Zusammenfassung

B-Chromosomen sind genetische Elemente, welche in manchen Arten zusätzlich zu den A-Chromosomen auftreten. Diese Zusatzchromosomen unterscheiden sich von den A-Chromosomen dadurch, dass diese keine essentiellen Erbinformationen besitzen und ein nicht-mendelndes Segregationsverhalten zeigen. Ihre Anzahl kann innerhalb und zwischen Individuen variieren. Abhängig davon, wie viele zusätzliche Chromosomen eine bestimmte Art tolerieren kann, können B-Chromosomen hohe Zahlen in natürlichen Populationen erreichen. Da in der überwiegenden Mehrzahl die Gegenwart von B-Chromosomen, vor allem in höherer Kopienzahl, sich negativ auf die Vitalität und Fruchtbarkeit des Trägerorganismus auswirken kann, werden B-Chromosomen oftmals als parasitäre Bestandteile des Genoms eingestuft.

Es ist wahrscheinlich, dass B-Chromosomen in den unterschiedlichen Organismen über verschiedene Mechanismen entweder aus A- oder Sex-Chromosomen der

Trägerart entstanden. Beim Vergleich der Sequenzen der A- und B-Chromosomen von *B. dichromosomatica* wurde nachgewiesen, dass deren B-Chromosomen viele Sequenzen besitzen, die auch auf unterschiedlichen A-Chromosomen und polymorphen heterochromatischen A-Chromosomenregionen vorliegen. Die genomische Organisation der Mikro-B-Chromosomen dieser Art wird als ein Konglomerat aus repetetiven Sequenzen von unterschiedlichen polymorphen A-Chromosomensegmenten und anderen A-Chromosomensequenzen betrachtet. Eine hohe Sequenzähnlichkeit zwischen beiden Chromosomentypen konnte gleichfalls für den Roggen nachgewiesen werden. Nur die heterochromatische Domäne am Ende des langen B-Chromosomenarms zeigte eine Anreicherung von B-spezifischen repetetiven Sequenzen.

Eine weitere Möglichkeit besteht in der spontanen Bildung von B-Chromosomen als Folge interspezifischer Kreuzungen und dem Verlust elterlicher Chromosomen, wie sie z. B. in Hybridzellen von Weizen x Hirse Embryonen. So konnten in embryonalen Zellen zentromerische Fragmente der Hirse nachgewiesen werden, obgleich andere Bereiche des Hirsegenoms bereits eliminiert waren. Nach Stabilisierung könnte ein derartiges Zentromerfragment, den Ausgangspunkt für die Entstehung eines B-Chromosoms darstellen.

Die Entstehung von B-Chromosomen ist höchstwahrscheinlich ein seltener Vorgang, da in engverwandten Arten, z. B. unterschiedliche *Brachycome*-Arten ähnliche B-Chromosomen nachgewiesen werden konnten.

Eine Anreicherung von mobilen Elementen auf B-Chromosomen könnte in einem Prozess analog zu „*Muller's ratchet*“ für die Evolution der B-Chromosomen mitverantwortlich sein. Eine *ratchet* oder Sperrklinke lässt sich nur in eine Richtung drehen. Genauso lässt sich die Muller-Rätsche nur in die "Richtung" von zusätzlichen, schädlichen Genmutationen drehen. So wurden für Roggen B-Chromosomen transposable Elemente nachgewiesen. Da eine der Haupteigenschaften von B-Chromosomen ist, nicht mit den Chromosomen des A-Komplementes zu paaren, ist eine Korrektur von Mutationen durch Rekombination wenig wahrscheinlich, so dass die B-Chromosomen insgesamt dem „*Muller's ratchet*“-Mechanismus unterliegt.

Für B-Chromosomen von *C. capillaris* und *B. dichromosomatica* konnten 45S rDNA-Sequenzen nachgewiesen werden. Der Vergleich der ribosomalen ITS2-Sequenzen der A- und B-Chromosomen demonstrierte eine hohe Ähnlichkeit dieser Sequenzen zueinander innerhalb der entsprechenden Art. Damit konnte gefolgert werden, dass die ribosomale DNA der B-Chromosomen von der 45S rDNA der A-Chromosomen der gleichen Art abstammt, oder beide Chromosomentypen einen gemeinsamen Vorgänger haben. Anders als in *B. dichromosomatica*, ist die B- lokalisierte 45S rDNA von *C. capillaris* transkriptionsaktiv.

Nach der Etablierung der indirekten Immunfluoreszenz für pflanzliche Chromosomen wurde die Verteilung einzelner Histonmodifizierungen für A- und B-Chromosomen vergleichend beschrieben. A- und B-Chromosomen des Roggens, *C. capillaris*, *B. dichromosomatica* und *P. libanotica* zeigten für die Heterochomatin-typischen Histonmodifikationen Histon H3K9me1/2 und H3K27me1 keine Unterschiede. Die einheitliche Verteilung der Methylierung von H3K9me2 auf den A- und Standard-B-Chromosomen korreliert mit der Genomgröße dieser Arten. Bei Pflanzen mit einer Genomgröße unter 500 Mbp beschränkt sich die Dimethylierung von H3K9 auf die heterochromatischen Chromozentren. Bei einer Größe von mehr als 500 Mbp verteilt sich die Histon H3K9-Dimethylierung wahrscheinlich auf Grund der hohen Dichte von transposablen Elementen dispers über alle Chromosomen.

Die Euchromatin-spezifische Methylierung an H3K4 ergab für die A-Chromosomen von *B. dichromosomatica* eine disperse Markierung mit Ausnahme des Perizentromers und einer heterochromatischen Region. Während an den Standard-B-Chromosomen noch eine sehr schwache H3K4me1,2,3-Markierung erfolgte, zeigte sich an den Mikro-B-Chromosomen nur noch für H3K4me1 eine schwache Markierung. H3K4 Di- und Trimethylierungen wurden bei diesem B-Chromosomentyp nicht nachgewiesen. Zusätzlich wurde für *B. dichromosomatica* eine reduzierte Acetylierung der Standard-B-Chromosomen an K5 und K8 im Histon H4 detektiert. Diese reduzierte Acetylierung von Histon H4 und die schwache Methylierung von H3K4 könnten eine gemeinsame Rolle in der Bildung des B-Chromosomen-Chromatins spielen.

Der Zusammenhang zwischen der Zellzyklus-abhängigen Phosphorylierung von Histon H3 und der Veränderung der Chromosomenstruktur bzw. dem Segregationsverhalten von Chromosomen wurde mit Hilfe von B-Chromosomen demonstriert. Die Dynamik der H3S10 und H3S28-Phosphorylierung korreliert mit der Etablierung/Auflösung der Schwesterchromatiden-Verklebung kondensierender Chromosomen. Während der ersten meiotischen Teilung bleiben die Schwesterchromatiden über ihre gesamte Länge verbunden. Die H3-Phosphorylierung erfolgt ebenfalls über die gesamte Chromosomenlänge. Im zweiten Abschnitt der Meiose sind die Schwesterchromatiden nur im perizentromerischen Bereich kohäsiv und die H3-Phosphorylierung erfolgt ebenso nur im perizentromerischen Bereich. Es kann postuliert werden, dass die Phosphorylierung von Histon H3S10 und S28 mit der Schwesterchromatiden-Verklebung in der Meiose korreliert und eine untergeordnete Rolle in der Kondensation von meiotischen Chromosomen spielt. Die Zellzyklus-abhängige Phosphorylierung von H3 an den Positionen T3, T11 und T32 korreliert mit dem Kondensationsverhalten mitotischer und meiotischer Chromosomen. Die evolutionär hoch konservierte Aurora-Kinase konnte als Histon H3S10-spezifische Kinase in *A. thaliana* identifiziert werden.

Der heterochromatische Bereich des langen Roggen B-Chromosomenarms weist sowohl H3K4me3- als auch H3K27me3-Modifikationen auf. Da die Methylierung von H3K4 generell mit der Transkriptionsaktivität korreliert, wurde der Transkriptionszustand der B-lokalisierten repetetiven Sequenzen E3900 und D1100 evaluiert. Es konnte eine Expression von nicht-kodierender RNA für B-Chromosomen nachgewiesen werden. Es wird postuliert, dass diese RNA an der Regulierung des B-spezifischen *nondisjunction* Prozesses involviert ist.

Das Transkriptionsverhalten von Roggen B-Chromosomen wurde erstmals molekular charakterisiert. Die Transkriptionsprofile von Genotypen mit oder ohne B-Chromosomen unterscheiden sich minimal, was darauf hindeutet, dass B-Chromosomen weitgehend genetisch inaktiv sind. Für B-spezifische Transkripte konnten ähnliche A-lokalisierte Sequenzen nachgewiesen werden. Die hohe Sequenzähnlichkeit zwischen A- und B-lokalisierten Sequenzen bestätigt die Annahme, dass Roggen B-Chromosomen aus den A-Chromosomen der gleichen Art entstanden.

Summary

B chromosomes (Bs) are accessory chromosomes to the standard number of normal chromosomes (As). The main criteria which distinguish B chromosomes from normal chromosomes are: (i) they are dispensable and can be present or absent from individuals within a population; (ii) they do not pair or recombine with any members of the standard diploid (or polyploid) set of A chromosomes at meiosis; (iii) their inheritance is non-Mendelian and irregular. The upper limit of the B chromosome number within the population is species dependent. The effects of B chromosomes are usually cumulative, depending upon their number and not their presence or absence. Different phenotypic effects were correlated with presence of a high number of Bs. In general, Bs influence negatively the fitness and fertility of the plants. Therefore, often Bs are characterised as a parasitic component of the genome.

It is widely accepted that B chromosomes could be derived from the A chromosomes and/or from sex chromosomes of the host species. The genomic organisation of *B. dichromosomatica* micro Bs could be considered as patchwork, or conglomerate, of repetitive sequences coming from different polymorphic A chromosome sites. Similarly, a high sequence similarity was revealed between As and Bs of rye. Only the terminal heterochromatic regions of the long B chromosome arm is characterized as an accumulation of specific repetitive sequences. However, there is also evidence suggesting that Bs can be spontaneously generated in response to the new genome conditions following interspecific hybridisation. In hybrid cells of wheat x pearl millet embryos which are undergoing elimination of the pollinator genome pearl millet-specific centromeric sequences were detectable. If during elimination of parental chromosomes such a centric fragment is retained rather than lost, a subsequent spontaneous chromosome doubling could provide an ideal prerequisite for the *de novo* formation of supernumerary chromosomes.

The formation of a new B chromosome must be a rare event, as closely related *Brachycome*-species carrying similar B chromosomes. Sequence comparison of A and B chromosome- sequences of *B. dichromosomatica* demonstrate that Bs harbour sequences derived from different polymorphic heterochromatic A chromosome regions.

The accumulation of mobile elements analogues to the process of ‘Muller’s ratchet’ for the evolution of sex chromosomes could play a role in evolution of B chromosomes. Transcription active mobile elements were demonstrated for rye Bs. As Bs do not pair or recombine with any members of the standard diploid (or polyploid) set of A chromosomes at meiosis a correction of mutations is unlikely. The accumulation of irreversible deleterious mutations will drive the evolution of Bs.

B-specific 45SrDNA sequences were identified for *C. capillaris* and *B. dichromosomatica.* Comparison of A- and B-type ribosomal ITS2 sequences revealed high sequence similarity within the species. Therefore, it is concluded that B chromosome-localized 45SrDNA originated from the A chromosome complement of the same species, or both types of chromosomes share a common ancestor. Unlike for *B. dichromosomatica,* B-localized 45S rDNA of *C. capillaris* is transcriptionally active.

The chromosomal distribution patterns of different histone modification marks were studied for A and B chromosomes after the method of indirect immunostaining was established for plant chromosomes. The distribution of the heterochromatin-typical histone marks H3K9me1/2 and H3K27me1 did not differ between A and B chromosomes of rye, *C. capillaris*, *B. dichromosomatica* and *P. libanotica*. The uniform distribution of these histone marks along A and B chromosomes correlate with the genome size of these species. Two different distribution patterns of dimethylated H3K9 were found that depend on genome size. For most species with small genomes (1C<500 Mbp), including *Arabidopsis thaliana,* strong methylation of H3K9me2 was restricted to constitutive heterochromatin. Species with larger genomes showed a uniform distribution of dimethylated H3K9. Contrary to this and regardless of the genome size, dimethylated H3K4 was found to be enriched within the euchromatin of all species. I propose that large genomes with high amounts of dispersed repetitive sequences (mainly retroelements) have to silence these sequences and therefore display epigenetic modifications such as methylation of DNA and H3K9 also within euchromatic regions.

The interrelationship was analysed between the cell cycle-dependent phosphorylation of histone H3 and the segregation and condensation behaviour of chromosomes. The dynamic phosphorylation of H3S10 and H3S28 correlates with the process of sister chromatid cohesion during mitosis and meiosis. Interestingly, during meiosis in monocentric plants the distribution of S10 and S28 phosphorylation varies between the two meiotic divisions. During the first division the chromosomes are highly phosphorylated throughout their entire length, while in the second division the H3 phosphorylation is restricted to the pericentromeric regions, as in mitotic chromosomes. Surprisingly, at the same time, single chromatids resulting from equational division of univalents (e.g. a single B chromosome) at anaphase I show no H3 phosphorylation. Irrespective of their low level of H3 phosphorylation, however, prematurely separated chromatids show normal condensation and their kinetochores interact with the microtubules. These observations led to the hypothesis that in plants pericentromeric H3 phosphorylation at both serine positions is required for cohesion of sister chromatids during metaphase I, and for sister chromatid pericentromeres during mitosis and metaphase II, respectively.

Phosphorylation at T3, T11 and T32 of histone H3 in plants occurs along entire chromosome arms, and correlates with the condensation of mitotic and meiotic chromosomes. In mammals, in contrast, where phosphorylation of T3 and T11 is most abundant in the centromere, it may instead serve as a recognition code for centromere assembly. The reverse may be true for S10/28 modifications, which may provide a label for the pericentromere region in plants, but has a function in chromosome condensation in mammals.

A chromosomes of *B. dichromosomatica* revealed a disperse distribution of methylated histone H3K4 except in pericentromeric regions. In difference, the large B chromosomes of the same species displayed very weak signals specific for H3K4me1,2 or 3. Micro Bs showed only very weak H3K4me1-specific signals and no signals specific for histone di- and trimethylated K4. In addition, B chromosomes are characterized by reduced level of histone H3 lysine 5 and lysine 8 acetylation. Weak acetylation of histone H4 and reduced methylation of H3K4 seems to be involved in the formation of B chromosome chromatin.

The histone H3K4me3-positive B-terminal region of rye is mainly composed of the B chromosome-specific DNA arrays E3900 and D1100. Abundant E3900-specific transcripts were found in somatic and even more often in anther tissue. D1100 displayed activity in anthers only, indicating tissue-specific expression. All subregions of E3900 also revealed cross hybridization with RNAs of small size (<200 bases) derived from anthers with B chromosomes; with the highest level of transcription at the 3'end of the repeat. The majority of D1100 and E3900 transcripts escape processing by the RNAi machinery. The lack of any significant open reading frame and the highly heterogeneous size of mainly polyadenylated transcripts indicate that the non-coding RNA may function as structural or catalytic RNA. It is tempting to hypothesize that these transcripts could serve some structural function in the organization and regulation of B chromosome nondisjunction.

The general transcription behaviour of rye B chromosomes was characterised by molecular means. Despite that the transcription profile of the rye inbred lines with and without B chromosomes is highly similar, sixteen putative B chromosome-associated transcripts were identified. This consists 0.7% of total number of transcripts which is an indication of very low activity of B chromosomes. For all identified B-specific transcripts, similar A chromosome-encoded sequences were found. These results support the hypothesis that the rye B chromosomes are originated from A chromosomes of the same species.

5. Literaturverzeichnis

Alfenito, M.R., and Birchler, J.A. (1993). Molecular characterization of a maize B chromosome centric sequence. Genetics 135, 589-597.

Beukeboom, L.W. (1994). Bewildering Bs: an impression of the 1st B chromosome conference. Heredity 73, 328-336.

Bougourd, S.M., and Jones, R.N. (1997). B chromosomes: a physiological enigma. New Phytol 137, 43-54.

Bouzinba-Segard, H., Guais, A., and Francastel, C. (2006). Accumulation of small murine minor satellite transcripts leads to impaired centromeric architecture and function. Proc. Natl. Acad. Sci. U. S. A. 103, 8709-8714.

Buckler, E.S.t., Phelps-Durr, T.L., Buckler, C.S., Dawe, R.K., Doebley, J.F., and Holtsford, T.P. (1999). Meiotic drive of chromosomal knobs reshaped the maize genome. Genetics 153, 415-426.

Camacho, J.P., Sharbel, T.F., and Beukeboom, L.W. (2000). B chromosome evolution. Philos Trans R Soc Lond B Biol Sci 355, 163-178.

Caperta, A., Rosa, M., Delgado, M., Karimi, R., Demidov, D., Viegas, W., and Houben, A. (2008). Distribution patterns of phosphorylated Thr 3 and Thr 32 of histone H3 in mitosis and meiosis of plants. Cytogenet Genome Res 122, 73-79.

Carchilan, M., Delgado, M., Ribeiro, T., Costa-Nunes, P., Caperta, A., Morais-Cecilio, L., Jones, R.N., Viegas, W., and Houben, A. (2007). Transcriptionally active heterochromatin in rye B chromosomes. Plant Cell 19, 1738-1749.

Carlson, W.R. (1988). B chromosomes as a model system for nondisjunction. aneuploidy, Part B: Induction and Test Systems, Alan R. Liss, Inc., 199-207.

Cheng, Y.M., and Lin, B.Y. (2003). Cloning and characterization of maize B chromosome sequences derived from microdissection. Genetics 164, 299-310.

Cheng, Z.K., Yu, H.X., Yan, H.H., Gu, M.H., and Zhu, L.H. (2000). B chromosome in a rice aneuploid variation. Theoretical and Applied Genetics 101, 564-568.

Cohen, D.E., and Lee, J.T. (2002). X-chromosome inactivation and the search for chromosome-wide silencers. Curr Opin Genet Dev 12, 219-224.

Cohen, S., and Mechali, M. (2001). A novel cell-free system reveals a mechanism of circular DNA formation from tandem repeats. Nucleic Acids Res 29, 2542-2548.

Cohen, S., Menut, S., and Mechali, M. (1999). Regulated formation of extrachromosomal circular DNA molecules during development in *Xenopus laevis*. Mol Cell Biol 19, 6682-6689.

Cohen, S., Houben, A., and Segal, D. (2008). Extrachromosomal circular DNA derived from tandemly repeated genomic sequences in plants. Plant Journal 53, 1027-1034.

Cohen, S., Agmon, N., Yacobi, K., Mislovati, M., and Segal, D. (2005). Evidence for rolling circle replication of tandem genes in *Drosophila*. Nucl. Acids Res. 33, 4519-4526.

Covert, S.F. (1998). Supernumerary chromosomes in filamentous fungi. Current Genetics 33, 311-319.

Demidov, D., Van Damme, D., Geelen, D., Blattner, F.R., and Houben, A. (2005). Identification and dynamics of two classes of aurora-like kinases in *Arabidopsis* and other plants. Plant Cell 17, 836-848.

Dhar, M.K., Friebe, B., Koul, A.K., and Gill, B.S. (2002). Origin of an apparent B chromosome by mutation, chromosome fragmentation and specific DNA sequence amplification. Chromosoma 111, 332-340.

Donald, T.M., Houben, A., Leach, C.R., and Timmis, J.N. (1997). Ribosomal RNA genes specific to the B chromosomes in *Brachycome dichromosomatica* are not transcribed in leaf tissue. Genome 40, 674-681.

Ebert, A., Lein, S., Schotta, G., and Reuter, G. (2006). Histone modification and the control of heterochromatic gene silencing in *Drosophila*. Chromosome Res 14, 377-392.

Endo, T.R., Nasuda, S., Jones, N., Dou, Q., Akahori, A., Wakimoto, M., Tanaka, H., Niwa, K., and Tsujimoto, H. (2008). Dissection of rye B chromosomes, and nondisjunction properties of the dissected segments in a common wheat background. Genes Genet Syst 83, 23-30.

Farr, C., Fantes, J., Goodfellow, P., and Cooke, H. (1991). Functional reintroduction of human telomeres into mammalian cells. Proc Natl Acad Sci U S A 88, 7006-7010.

Field, B.L., Houben, A., Timmis, J.N., and Leach, C.R. (2006). Internal transcribed spacer sequence analyses indicate cytoevolutionary patterns within *Brachycome* Cass. (Asteraceae). Plant Syst Evol 259, 39-51.

Francki, M.G. (2001). Identification of Bilby, a diverged centromeric Ty1-copia retrotransposon family from cereal rye (Secale cereale L.). Genome 44, 266-274.

Franks, T.K., Houben, A., Leach, C.R., and Timmis, J.N. (1996). The molecular organisation of a B chromosome tandem repeat sequence from *Brachycome dichromosomatica*. Chromosoma 105, 223-230.

Fuchs, J., Demidov, D., Houben, A., and Schubert, I. (2006). Chromosomal histone modification patterns - from conservation to diversity. Trends in Plant Science 11, 212-212.

Gaut, B.S., Wright, S.I., Rizzon, C., Dvorak, J., and Anderson, L.K. (2007). Recombination: an underappreciated factor in the evolution of plant genomes. Nat Rev Genet 8, 77-84.

Gernand, D., Demidov, D., and Houben, A. (2003). The temporal and spatial pattern of histone H3 phosphorylation at serine 28 and serine 10 is similar in plants but differs between mono- and polycentric chromosomes. Cytogenet Genome Res 101, 172-176.

Gernand, D., Rutten, T., Varshney, A., Rubtsova, M., Prodanovic, S., Bruss, C., Kumlehn, J., Matzk, F., and Houben, A. (2005). Uniparental chromosome elimination at mitosis and interphase in wheat and pearl millet crosses involves micronucleus formation, progressive heterochromatinization, and DNA fragmentation. Plant Cell 17, 2431-2438.

Green, D.M. (1990). Muller`s rachet and the evolution of supernumerary chromosomes. Genome 33, 818-824.

Hall, A.E., Kettler, G.C., and Preuss, D. (2006). Dynamic evolution at pericentromeres. Genome Research 16, 355-364.

Han, F., Lamb, J.C., and Birchler, J.A. (2006). High frequency of centromere inactivation resulting in stable dicentric chromosomes of maize. Proc Natl Acad Sci U S A 103, 3238-3243.

Heard, E. (2005). Delving into the diversity of facultative heterochromatin: the epigenetics of the inactive X chromosome. Curr Opin Genet Dev 15, 482-489.

Houben, A., and Schubert, I. (2003). DNA and proteins of plant centromeres. Current Opinion in Plant Biology 6, 554-560.

Houben, A., and Schubert, I. (2007). Engineered plant minichromosomes: a resurrection of B chromosomes? Plant Cell 19, 2323-2327.

Houben, A., Belyaev, N.D., Turner, B.M., and Schubert, I. (1996a). Differential immunostaining of plant chromosomes by antibodies recognizing acetylated histone H4 variants. Chromosome Res 4, 191-194.

Houben, A., Belyaev, N.D., Leach, C.R., and Timmis, J.N. (1997a). Differences of histone H4 acetylation and replication timing between A and B chromosomes of *Brachycome dichromosomatica*. Chromosome Res 5, 233-237.

Houben, A., Verlin, D., Leach, C.R., and Timmis, J.N. (2001). The genomic complexity of micro B chromosomes of *Brachycome dichromosomatica*. Chromosoma 110, 451-459.

Houben, A., Demidov, D., Rutten, T., and Scheidtmann, K.H. (2005). Novel phosphorylation of histone H3 at threonine 11 that temporally correlates with condensation of mitotic and meiotic chromosomes in plant cells. Cytogenet Genome Res 109, 148-155.

Houben, A., Leach, C.R., Verlin, D., Rofe, R., and Timmis, J.N. (1997b). A repetitive DNA sequence common to the different B chromosomes of the genus *Brachycome*. Chromosoma 106, 513-519.

Houben, A., Kynast, R.G., Heim, U., Hermann, H., Jones, R.N., and Forster, J.W. (1996b). Molecular cytogenetic characterisation of the terminal heterochromatic segment of the B-chromosome of rye (*Secale cereale*). Chromosoma 105, 97-103.

Houben, A., Thompson, N., Ahne, R., Leach, C.R., Verlin, D., and Timmis, J.N. (1999). A monophyletic origin of the B chromosomes of *Brachycome dichromosomatica* (*Asteraceae*). Plant Syst Evol 219, 127-135.

Houben, A., Wanner, G., Hanson, L., Verlin, D., Leach, C.R., and Timmis, J.N. (2000). Cloning and characterisation of polymorphic heterochromatic segments of *Brachycome dichromosomatica* (Vol 109, pg 206, 2000). Chromosoma 109, 433-433.

Houben, A., Demidov, D., Gernand, D., Meister, A., Leach, C.R., and Schubert, I. (2003). Methylation of histone H3 in euchromatin of plant chromosomes depends on basic nuclear DNA content. Plant Journal 33, 967-973.

Houben, A., Demidov, D., Caperta, A.D., Karimi, R., Agueci, F., and Vlasenko, L. (2007). Phosphorylation of histone H3 in plants - A dynamic affair. Biochim Biophys Acta.

Jamilena, M., Ruiz Rejon, C., and Ruiz Rejon, M. (1994). A molecular analysis of the origin of the *Crepis capillaris* B chromosome. J Cell Sci 107 (Pt 3), 703-708.

Jimenez, M.M., Romera, F., Puertas, M.J., and Jones, R.N. (1994). B chromosomes in inbred lines of rye (*Secale cereale* L) .1. Vigor and fertility. Genetica 92, 149-154.

Jin, W.W., Lamb, J.C., Vega, J.M., Dawe, R.K., Birchler, J.A., and Jiang, J. (2005). Molecular and functional dissection of the maize B chromosome centromere. Plant Cell 17, 1412-1423.

Jones, N., and Houben, A. (2003). B chromosomes in plants: escapees from the A chromosome genome? Trends Plant Sci 8, 417-423.

Jones, R.N. (1975). B chromosome systems in flowering plants and animal species. . International Review of Cytology 40, 1-100.

Jones, R.N. (1991). B-chromosome drive. Am Nat 137, 430-442.

Jones, R.N. (1995). Tansley review no 85 - B chromosomes in plants. New Phytol 131, 411-434.

Jones, R.N. (2004). B Chromosomes. Encyclopedia of Plant und Crop Sience, Marcel Dekker, New York.

Jones, R.N., and Rees, H. (1982). B chromosomes. 1st edn. Academic Press, London New York.

Jones, R.N., and Puertas, M.J. (1993). The B-chromosomes of rye (*Secale cereale* L.). In: Dhir, K.K., Sareen, T.S. eds. Frontiers in Plant Science Research. Dehli (India): Bhagwati Enterprises, 81-112.

Jones, R.N., Gonzalez-Sanchez, M., Gonzalez-Garcia, M., Vega, J.M., and Puertas, M.J. (2008). Chromosomes with a life of their own. Cytogenet Genome Res 120, 265-280.

Kaszas, E., and Birchler, J.A. (1996). Misdivision analysis of centromere structure in maize. Embo J 15, 5246-5255.

Kaszas, E., and Birchler, J.A. (1998). Meiotic transmission rates correlate with physical features of rearranged centromeres in maize. Genetics 150, 1683-1692.

Kaszas, E., and Cande, W.Z. (2000). Phosphorylation of histone H3 is correlated with changes in the maintenance of sister chromatid cohesion during meiosis in maize, rather than the condensation of the chromatin. J Cell Sci 113, 3217-3226.

Kaszas, E., Kato, A., and Birchler, J.A. (2002). Cytological and molecular analysis of centromere misdivision in maize. Genome 45, 759-768.

Kumke, K., Jones, R.N., and Houben, A. (2008). B chromosomes of *Puschkinia libanotica* are characterized by a reduced level of euchromatic histone H3 methylation marks. Cytogenet Genome Res 121, 266-270.

Lamb, J., Kato, A., and Birchler, J. (2005). Sequences associated with A chromosome centromeres are present throughout the maize B chromosome. Chromosoma 113, 337-349.

Lamb, J.C., Riddle, N.C., Cheng, Y.M., Theuri, J., and Birchler, J.A. (2007). Localization and transcription of a retrotransposon-derived element on the maize B chromosome. Chromosome Res 15, 383-398.

Leach, C.R., Houben, A., and Timmis, J.N. (2004). The B chromosomes in *Brachycome*. Cytogenet Genome Res 106, 199-209.

Leach, C.R., Donald, T.M., Franks, T.K., Spiniello, S.S., Hanrahan, C.F., and Timmis, J.N. (1995). Organization and origin of a B chromosome centromeric sequence from *Brachycome dichromosomatica*. Chromosoma 103, 708-714.

Leach, C.R., Houben, A., Field, B., Pistrick, K., Demidov, D., and Timmis, J.N. (2005). Molecular evidence for transcription of genes on a B chromosome in *Crepis capillaris*. Genetics 171, 269-278.

Levin, D.A., Palestris, B.G., Jones, R.N., and Trivers, R. (2005). Phyletic hot spots for B chromosomes in angiosperms. Evolution 59, 962-969.

Lima-de-Faria, A. (1962). Genetic interaction in rye expressed at the chromosome phenotype. Genetics 47, 1455-1462.

Lysak, M.A., Berr, A., Pecinka, A., Schmidt, R., McBreen, K., and Schubert, I. (2006). Mechanisms of chromosome number reduction in *Arabidopsis thaliana* and related *Brassicaceae* species. Proc Natl Acad Sci U S A 103, 5224-5229.

Maluszynska, J., and Schweizer, D. (1989). Ribosomal RNA genes in B chromosomes of *Crepis capillaris* detected by non-radioactive in situ hybridization. Heredity 62 (Pt 1), 59-65.

Manzanero, S., Arana, P., Puertas, M.J., and Houben, A. (2000). The chromosomal distribution of phosphorylated histone H3 differs between plants and animals at meiosis. Chromosoma 109, 308-317.

Marschner, S., Kumke, K., and Houben, A. (2007a). B chromosomes of B. dichromosomatica show a reduced level of euchromatic histone H3 methylation marks. Chromosome Res 15, 215-222.
Marschner, S., Meister, A., Blattner, F.R., and Houben, A. (2007b). Evolution and function of B chromosome 45S rDNA sequences in *Brachycome dichromosomatica*. Genome 50, 638-644.
May, B.P., Lippman, Z.B., Fang, Y., Spector, D.L., and Martienssen, R.A. (2005). Differential regulation of strand-specific transcripts from *Arabidopsis* centromeric satellite repeats. PLoS Genet 1, e79.
Miao, F., and Natarajan, R. (2005). Mapping global histone methylation patterns in the coding regions of human genes. Mol Cell Biol 25, 4650-4661.
Müntzing, A. (1948). Cytological studies of extra fragment chromosomes in rye. V. A new fragment type arisen by deletion. Hereditas 34, 435-442.
Müntzing, A. (1970). Chromosomal variation in the Lindström strain of wheat carrying accessory chromosomes in rye. Hereditas 66, 279-286.
Naumann, K., Fischer, A., Hofmann, I., Krauss, V., Phalke, S., Irmler, K., Hause, G., Aurich, A.C., Dorn, R., Jenuwein, T., and Reuter, G. (2005). Pivotal role of AtSUVH2 in heterochromatic histone methylation and gene silencing in Arabidopsis. Embo J 24, 1418-1429.
Niwa, K., Horiuchi, G., and Hirai, Y. (1997). Production and characterization of common wheat with B chromosomes of rye from Korea. Hereditas 126, 139-146.
Page, B.T., Wanous, M.K., and Birchler, J.A. (2001). Characterization of a maize chromosome 4 centromeric sequence: evidence for an evolutionary relationship with the B chromosome centromere. Genetics 159, 291-302.
Palestis, B.G., Trivers, R., Burt, A., and Jones, R.N. (2004). The distribution of B chromosomes across species. Cytogenetic and Genome Research 106, 151-158.
Phan, B.H., Jin, W., Topp, C.N., Zhong, C.X., Jiang, J., Dawe, R.K., and Parrott, W.A. (2007). Transformation of rice with long DNA-segments consisting of random genomic DNA or centromere-specific DNA. Transgenic Res 16, 341-351.
Puertas, M.J. (2002). Nature and evolution of B chromosomes in plants: A non-coding but information-rich part of plant genomes. Cytogenet Genome Res 96, 198-205.
Puertas, M.J., Romera, F., and Delapena, A. (1985). Comparison of B-chromosome effects on *Secale cereale* and *Secale vavilovii*. Heredity 55, 229-234.
Sapre, A.B., and Deshpande, D.S. (1987). Origin of B chromosomes in *Coix* L through spontaneous interspecific hybridization. Journal of Heredity 78, 191-196.
Schmitt, F., Oakeley, E.J., and Jost, J.P. (1997). Antibiotics induce genome-wide hypermethylation in cultured *Nicotiana tabacum* plants. Journal of Biological Chemistry 272, 1534-1540.
Schubert, I. (2007). Chromosome evolution. Current Opinion in Plant Biology 10, 109-115.
Sharbel, T.F., Green, D.M., and Houben, A. (1998). B-chromosome origin in the endemic New Zealand frog *Leiopelma hochstetteri* through sex chromosome devolution. Genome 41, 14-22.
Silva, J., Mak, W., Zvetkova, I., Appanah, R., Nesterova, T.B., Webster, Z., Peters, A.H., Jenuwein, T., Otte, A.P., and Brockdorff, N. (2003). Establishment of

histone H3 methylation on the inactive X chromosome requires transient recruitment of Eed-Enx1 polycomb group complexes. Dev Cell 4, 481-495.
Stark, E.A., Connerton, I., Bennett, S.T., Barnes, S.R., Parker, J.S., and Forster, J.W. (1996). Molecular analysis of the structure of the maize B-chromosome. Chromosome Res 4, 15-23.
Steinemann, S., and Steinemann, M. (2005). Retroelements: tools for sex chromosome evolution. Cytogenet Genome Res 110, 134-143.
Trivers, R., Burt, A., and Palestis, B.G. (2004). B chromosomes and genome size in flowering plants. Genome 47, 1-8.
Wilkes, T.M., Francki, M.G., Langridge, P., Karp, A., Jones, R.N., and Forster, J.W. (1995). Analysis of rye B-chromosome structure using fluorescence *in situ* hybridization (FISH). Chromosome Res 3, 466-472.
Wilson, E.B. (1907). The supernumerary chromosomes of *Hemiptera*. Science XXVI, 870.
Yu, W., Han, F., and Birchler, J.A. (2007). Engineered minichromosomes in plants. Curr Opin Biotechnol 18, 425-431.
Yu, W., Lamb, J.C., Han, F., and Birchler, J.A. (2006). Telomere-mediated chromosomal truncation in maize. Proc Natl Acad Sci U S A 103, 17331-17336.

Danksagung

Mein erster Dank gilt Herrn Prof. Ingo Schubert für die Möglichkeit zum Aufbau eines eigenen Forschungsgebietes, das er durch großes Interesse und anregende Diskussionen begleitete und ständig unterstützte.

Bei meiner Frau Sabine und meinen Töchtern Sarah und Liesa möchte ich für ihre ständige Unterstützung und Rücksicht bedanken.

Zu großem Dank verpflichtet bin ich auch Frau Dr. Carolyn Leach and Herrn Prof. Jeremy Timmis (Adelaide), die mich in verschiedenen Abschnitten meiner Laufbahn förderten.

Für die jahrelange gute Zusammenarbeit bei der Erforschung pflanzlicher Genome danke ich Prof. Neil Jones (England), Prof. Takashi Endo, Dr. S. Nasuda (Kyoto), Prof. Maria Puertas (Madrid), Dr. Sylvia Manzanero (Perth), Prof. Gerhard Wanner, Elizabeth Schröder-Reiter (München) und Prof. Wanda Vegas (Lissabon).

Bei Herrn Prof. Klaus Pillen bedanke ich mich für die Betreuung meiner Habiliationsarbeit seitens der Martin-Luther-Universität Halle-Wittenberg.

Mein besonderer Dank gilt den jetzigen und früheren Mitgliedern meiner Arbeitsgruppe, für ihre engagierte Arbeit und ihre Begeisterung für die Welt der Chromosomen. Besonders danken möchte ich den ehemaligen bzw. jetzigen Mitarbeitern Francesco Agueci, Ali Banaei, Mariana Carchilan, Dmitri Demidov, Dorota Gernand, Margit Hantschmann, Rahehel Karimi, Katrin Kumke, Sylvia Marschner, Maryam Sanei und Oda Weiß, für ihren Elan und professionelle Mitarbeit.

Bei allen Kollegen und Mitarbeitern des Leibniz-Institutes für Pflanzengenetik und Kulturpflanzenforschung, Gatersleben bedanke ich mich für die vielfältige Unterstützung, die zum Gelingen dieser Arbeit beigetragen hat. Diese Arbeit wurde finanziell von dem Land Sachsen-Anhalt, dem Bundesministerium für Bildung und Forschung und der Deutschen Forschungsgemeinschaft unterstützt.

Lebenslauf

Persönliche Daten

Name: Andreas Houben

Adresse: Augustinern 77, 06484 Quedlinburg

Geburtsdatum:06. Mai 1963 in Magdeburg

Familienstand: verheiratet mit Sabine Houben,

Töchter: Sarah und Liesa

Akademischer Werdegang

1989	Diplom, an der Martin-Luther-Universität Halle-Wittenberg, Pflanzenzüchtung und Saatgutproduktion
1993	Promotion (Dr. agr., *summa cum laude*), an der Martin-Luther-Universität Halle-Wittenberg, Landwirtschaftliche Fakultät
1993 - 1995	Postdoktorand am Institut für Pflanzengenetik und Kulturpflanzenforschung (IPK), Gatersleben in der Gruppe von Prof. I. Schubert
1996 - 1998	DFG-Stipendiat an der Universität Adelaide, Australien
1998 - 2001	Queen Elizabeth II-Stipendiat an der Universität Adelaide, Australien
seit 2001	Leiter der Arbeitsgruppe „Chromosomen Struktur und Funktion“ am Leibniz-Institut für Pflanzengenetik und Kulturpflanzenforschung (IPK), Gatersleben, Deutschland
2005	Gastprofessur, Kyoto Universität, Japan
2008	Innolec Lectureship, Masaryk-Universität, Tschechische Republik

Gatersleben, den 12.01.2009

Andreas Houben

Eidesstattliche Erklärung

Diese Habilitationsschrift wurde selbständig und ohne fremde Hilfe verfasst. Andere als die angegebenen Quellen und Hilfsmittel wurden nicht benutzt. Wörtlich oder inhaltlich übernommene Stellen wurden als Zitate gekennzeichnet.

Gatersleben, den 12.01. 2009

Andreas Houben